Design and synthesis of chiral hyperbranched polymers of cinchona squaramides and their application to asymmetric catalysis

(シンコナスクアラミド骨格を有するハイパーブランチ型高分子の合成と不斉触媒への応用)

July, 2021

Doctor of Philosophy (Engineering)

Sadia Afrin Chhanda

サディア アフリン チョンダ

Toyohashi University of Technology

Dedicated
to
My Husband

ACKNOWLEDGEMENTS

First of all, I would like to thank the Almighty Allah, my creator for His grace and blessings upon me. Without His love and blessings, it is not possible to complete my doctoral research works successfully.

Then I would like to express my sincere gratitude and cordial thanks to my supervisor *Prof. Dr. Shinichi Itsuno* for his continuous support during my doctoral study. His guidance helped me in all the time of my research work and writing of this thesis. I am astonished for his patience, encouragement and immense knowledge. His creativity and great passion for chemistry research have inspired me a lot during my study.

Besides my advisor, I would also like to thank *Prof. Dr. Naoki Haraguchi* for his suggestions, encouragement and valuable discussions throughout my research period. I would also like to thank Prof. Dr. Akihiko Matsumoto and Prof. Dr. Kazutaka Shibatomi for their acceptance for being my thesis examiners. Their insightful comments, suggestions, questions and encouragement contributed to the successful completion of the thesis and my study in general.

My sincere thanks to all respected teachers at TUT whose theoretical courses that have been taken by me during my doctoral study. My sincere thanks also goes to Dr. Ikuhide Fujisawa and all of my former and present labmates for their contributions and being available to help me for experimental works all the time during my study.

I am also thankful to my respected Bachelor and MS supervisors (*Prof. Dr. Md. Azizur Rahman*, *Prof. Dr. Tanvir Muslim*) Department of Chemistry, University of Dhaka for their blessings, suggestions and encouragement.

I am grateful to my respected teacher *Prof. Dr. Abdus Salam*, Department of Chemistry, University of Dhaka, Bangladesh for introducing me to Prof. Itsuno.

I am very much thankful to the Ministry of Education, Culture, Sports, Science and Technology (MEXT), Japan for providing me a prestigious scholarship (Monbukagakusho: MEXT) for the doctoral study. I acknowledge all the staff members of the international and educational affairs divisions at TUT and also Bangladeshi family for their cooperation and help. I am also thankful to my Bangladeshi lab mates Mithun, Azgar and Farhad for their help in experimental work during my pregnancy.

My special thanks go to Rokeya Sharmin Orin, Nina Murata and Nancy Naoko Takekawa for helping me during whole pregnancy time. I want to thank all the faculty members and officials of the Department of Chemistry, University of Dhaka, Bangladesh for all their blessings and cooperation.

Finally, I wish to express my deepest gratitude to my parents, parents-in-law, brother, sister-in-law for their prayers, emotional support and encouragement. My sweet thanks go to my elder daughter *Faiza Ishrar Yashfee* and the huge final thanks go to husband *Abu Saleh Mohammad Rabiul Hasan Chowdhury* for his mental support with endless inspiration and help. I am very much grateful to him for tolerating me.

Sadia Afrin Chhanda
Department of Applied Chemistry and Life Science
Toyohashi University of Technology, Japan

SUMMARY

Chiral hyperbranched polymers (HBPs) containing cinchona derived squaramide moiety have been designed and successfully synthesized. Synthesized HBPs were applied to asymmetric catalysis. Cinchona alkaloids and their derivatives have been widely employed as chiral organocatalysts in diverse asymmetric synthesis, because of their outstanding catalytic activity for several asymmetric reactions. Quinine, quinidine, cinchonidine and cinchonine are the major cinchona alkaloids and this are commonly commercially available. Cinchona alkaloids are useful for suitable modifications to versatile catalysts in asymmetric reactions due to their several functionalities such as secondary alcohols, quinoline rings, and quinuclidine and vinyl groups. Cinchona alkaloids have found part in chiral polymeric organocatalysts design as a privileged class of chirality inducers. The polymeric catalyst design is an essential tool to understand the efficient catalytic process in asymmetric transformations. Thus, several modifications have been already done by different research groups and synthesis of many monomeric and dimeric organocatalysts having cinchona squaramide moieties have also been reported. For this purpose, cinchona derived squaramide were used for the design of chiral polymeric organocatalysts in this work. The acidic NH of the squaramide can act as a H-bond donor, whereas the tertiary nitrogen of the quinuclidine of cinchona alkaloids may acts as both a H-bond acceptor and a base. Thus the cinchona squaramide can act as a bifunctional H-bonding organocatalyst in the asymmetric synthesis.

Cinchona derived squaramides have been proven as an efficient organocatalysts in different asymmetric transformations. Although several works have been reported with the low-molecular-weight squaramide catalysts derived from cinchona alkaloids, limited number of works have been carried out in the synthesis and application of chiral polymeric organocatalyst on the asymmetric transformation. Cinchona squaramide polymeric catalysts can be prepared by the incorporation of low-molecular-weight dimeric squaramide, using suitable polymerization techniques under optimal reaction conditions. In our previous reports, we have established Mizoroki–Heck (MH) polymerization reaction was a reliable C-C bond forming reaction to synthesize chiral linear polymers from cinchona alkaloid derivatives. In this work, we chose to synthesize chiral hyperbranched (HPB) polymers. We noticed that this (MH) methodology is applicable toward the synthesis of chiral HBPs from cinchona alkaloid derivatives. HBPs are highly branched tree-like three-dimensional structures which have drawn a lot of attention in various applications. Chiral HBPs containing chiral catalytic moieties are potential polymer catalysts in asymmetric catalysis. Cinchona-based chiral HBPs have not been reported to date. In this work, we designed and synthesized cinchona-based chiral HBPs containing squaramide moiety by MH polymerization and another new coupling reaction which is called Yamamoto coupling and obtained polymers were successfully applied in the enantioselective Michael addition reactions.

In this thesis, chapter **1** presents the general introduction which includes the structural features of cinchona alkaloids, chiral organocatalysts, polymeric organocatalysts and the background of this thesis work. This chapter also includes the general reviews about low-molecular-weight cinchona alkaloids squaramide catalyzed different asymmetric reactions.

Chapter **2** represents the synthesis of novel chiral cinchona squaramide hyperbranched polymers (HBPs) by the reaction of cinchona squaramide dimer and tri or tetrasubstituted aromatic iodide via a Mizoroki–Heck polycondensation reaction. The Mizoroki-Heck reactions occurred smoothly between the double bonds of the cinchona squaramide and aromatic tri- or tetraiodides to give chiral hyperbranched polymers. Chiral HBPs were then applied in the asymmetric Michael addition reaction and excellent enantioselectivity (>99% ee) was observed with good yield in the Michael

addition reaction of β-ketoesters to *trans*-β-nitrostyrene. Because of insolubility of polymeric catalysts in common organic solvents, the HBPs can be easily separated and reused up to six times without losing their catalytic activity and enantioselectivity. This is the first example of chiral HBP organocatalyst successfully applied to the asymmetric Michael addition reaction.

Chapter **3** describes the synthesis of novel chiral HBPs from cinchona squaramide containing both vinyl (**A**) and iodophenyl (**B**) groups in $\mathbf{AB_2}$ and $\mathbf{A_2B}$ type monomers. These were successfully polymerized by the Mizoroki-Heck (MH) coupling reaction between the vinyl and iodophenyl functionalities to give chiral HBPs. The chiral HBPs prepared by one step MH polymerization were used as catalysts in asymmetric Michael reactions. In case of the reaction between methyl 2-oxocyclopentanecarboxylate and *trans*-β-nitrostyrene, the HBP catalysts showed high catalytic activity with excellent diastereoselectivity and enantioselectivity. Reactions between some other substrate combinations also occurred smoothly with the HBP catalysts. **P1** exhibited superior selectivity in these reactions. Interestingly, the HBP catalysts gave higher diastereoselectivity compared to that obtained with the low-molecular-weight catalyst **4**. Somewhat higher catalytic activity was also observed with HBP catalyst. Precise control of the catalyst conformation may be possible in case of polymer catalyst. These results show that the design of chiral HBP catalyst may lead the development of high performance polymeric catalyst. The HBP catalysts were easily recovered from the reaction mixture and reused several times without any decrease in catalytic activity and stereoselectivity.

Chapter **4** describes the synthesis of cinchona squaramide-based chiral polymers via the Yamamoto coupling reaction. Yamamoto coupling reaction occurs between aromatic halides. This coupling reaction is nickel-catalyzed reaction of organic halides in the presence of neutral ligands. Yamamoto coupling reaction is advantageous because only a single, halogen-functionalized monomer can be used to form polymer. With homopolymers, three copolymers were also synthesized from low molecular weight cinchona squaramide with achiral diiodo or dibromo aromatic compounds. Chiral polymers were applied to the asymmetric Michael addition reactions and afforded good to excellent enantioselectivities. The polymeric catalysts were recovered from the reaction mixture and reused several times without any decrease in catalytic activity.

Chapter **5** presents the general conclusion of this whole thesis works.

[Contents]

List of Figures

List of Schemes

List of Tables

[List of abbreviations]

aq	Aqueous
s	Singlet
br	Broad
d	Doublet
m	Multiplet
Calcd	Calculated
DMF	*N*,*N*-dimethylformamide
ee	enantiomeric excess
dr	diastereomeric ratio
Equiv.	Equivalent
Et	Ethyl
Et_3N	Triethylamine
$Pd(OAc)_2$	palladium acetate
EtOAc	ethyl acetate
MeOH	Methanol
EtOH	Ethanol
$Ni(COD)_2$	bis(1,5-cyclooctadiene)nickel(0)
COD	1,5-cyclo octadiene
PPh3	Triphenyl phosphine
mg	Milligram
h	Hour
HPLC	high performance liquid chromatography
GPC	gel permeation chromatography
^{i}Pr	Isopropyl
IR	Infrared
M	Molar
MHz	Megahertz
mL	Milliliter
mmol	Millimole
mp	melting point
NMR	nuclear magnetic resonance
ppm	parts per million
Ph	Phenyl
R_f	retention factor
rt	room temperature
^{t}Bu	tertiary butyl
temp.	Temperature
THF	Tetrahydrofuran
TLC	thin layer chromatography
t_R	retention time
UV	Ultraviolet

[Notations]

α	Alpha
β	Beta
%	Percentage
J	coupling constant
δ	chemical shift
°C	degrees Celsius
$[\alpha]_D$	specific rotation

Chapter 1

INTRODUCTION

1.1 Research background

Green chemistry is the outline of chemical products and processes that minimize or remove the use or production of hazardous substances. Green chemistry has been known as a methodology for achieving sustainable development.[1] Organocatalysis reports the acceleration of chemical reactions through the addition of a substoichiometric quantity of an organic compound which does not contain metal ion. The catalysis with small organic molecules has become a highly dynamic area in chemical research.[2] Catalysis (enzyme catalysis, organometallic catalysis, and organocatalysis, in particular) is recognized to be at the heart of greening of chemistry, because this branch of science is found to lessen the environmental impact of chemical processes.[3]

Organocatalysis is one of the trending research topics in advanced organic chemistry. The term “organocatalysis" has confirmed to be a useful and attractive tool for the synthesis of enantiomerically enriched molecules. It explained the use of small chiral organic molecules as catalysts. The absence of transition metal in organocatalyst leads an undeniable advantage considering both the economic point of view and the principles of “green chemistry". Due to the novelty of the concept the interest in this field has been increasing spectacularly, and more importantly, the fact that the efficacy and selectivity of many organocatalytic reactions meet the standards of established organic reactions.[4-7]Although, from the beginnings of chemistry, organic molecules have been used as catalysts but their catalytic activity in enantioselective reaction has emerged as a major concept in organic chemistry to date. In conformity with green chemistry practices, organocatalysis is attracting widespread attention and has become an important field of research.[7]

1.2 Importance of organocatalysts and organocatalysis

The term “organocatalyst” is a sequence of the words “organic” and “catalyst.” The definition corresponds to a low molecular weight organic molecule which in substoichiometric amounts catalyzes a chemical reaction.[7] Organocatalysts are often based on nontoxic organic compounds originating from biological materials and could be achiral or chiral and could be composed of C, H, N, S, and P. Organocatalysts can be Lewis bases, Lewis acids, Brønsted bases, and Brønsted acids.[7] Organocatalysts are usually robust, inexpensive, readily available, non-toxic, able to bring about transformations that were not known earlier. Demanding reaction conditions (inert atmospheres, low temperatures, absolute solvents etc.) are usually not required which makes organocatalysts attractive to researchers. Not only because of its synthetic range but also for the economic reasons organocatalysis has several advantages. There are some examples of commonly used known chiral

organocatalysts that have been widely used in different types of asymmetric reactions like MacMillan's catalyst, cinchona alkaloid, Lewis acid/base catalyst etc.

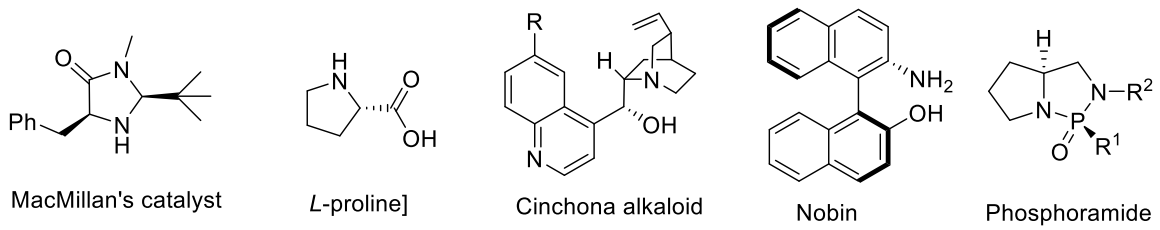

Figure 1.1. Examples of some chiral organocatalysts.

Imidazolidinone-based organocatalysts developed by Professor David MacMillan at Caltech, are designed to serve as general catalysts for a diversity of asymmetric transformations such as Michael addition reaction, Diels-Alder reaction, Friedel-Crafts alkylation, and epoxidation. The first successful highly enantioselective organocatalytic Diels-Alder reaction using (5*S*)-2,2,3-trimethyl-5-phenylmethyl-4-imidazolidinone monohydrochloride was reported by MacMillan in his pioneering work in 2000.[8] (Scheme 1.1a). A great development was made by Pracejus in 1960, in his acetylquinine **4** catalyzed synthesis of optically active methyl esters **5** from ketenes **3** and methanol (Figure 1.1b).[9] In 1960, for the first time, good enantioselectivity levels were achieved in the synthesis of enantioenriched ester where an enantiomeric excess of 74% was obtained, showing for the first time that organocatalysis could be useful in enantioselective synthesis, and not only a curiosity. They can create an asymmetric environment which is responsible for the creation of a new chiral center in the new asymmetric products.

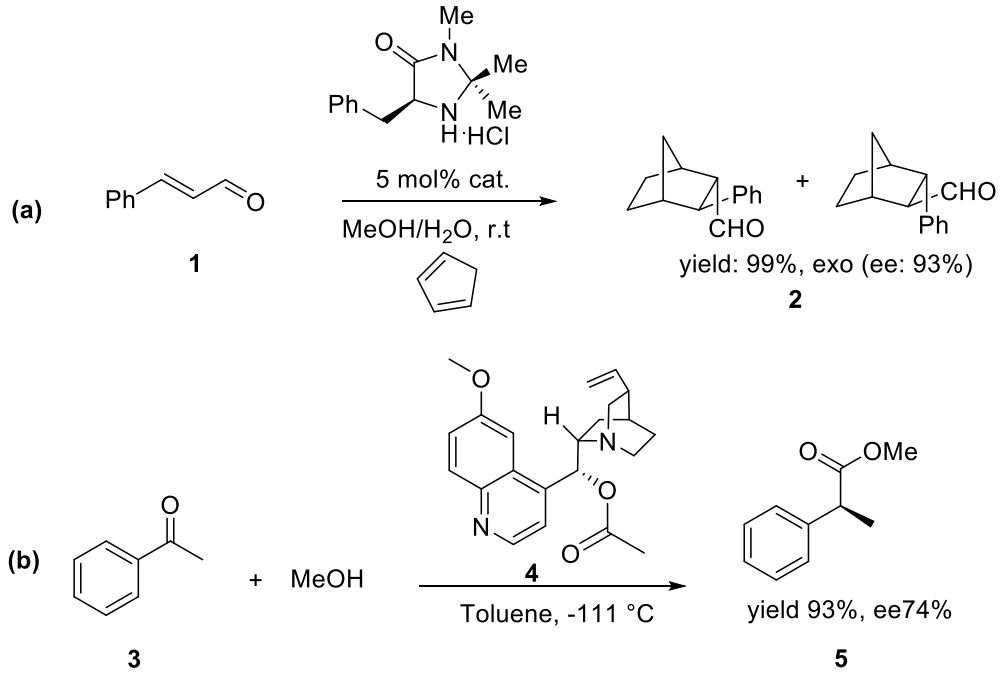

Scheme 1.1. Examples of organocatalytic reaction.

Organocatalysis can be categorized into our different types as follows.

Type-I: Activation of the reaction based on the nucleophilic/electrophilic properties of the. Proline catalysis has now widespread scope of applications. Barbas and List reported an asymmetric, direct, intermolecular aldol reaction of acetones and aldehydes (Scheme 1.1b), presumably *via* enamine formation of proline and acetone.[10] Comparing to its metal-catalyzed alternatives, no preformation of the respective enolate is required, a mode of action that mimics metal-free aldolase enzymes.[11]

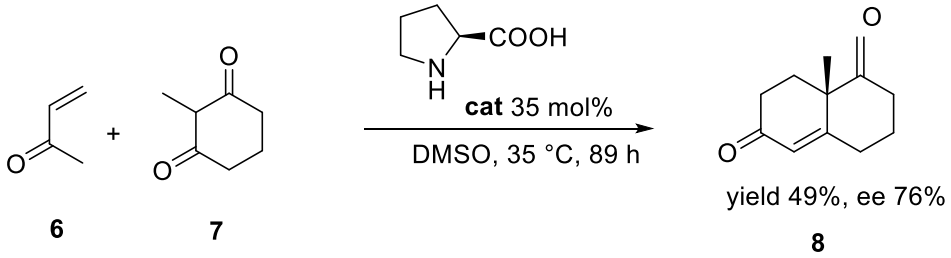

Scheme 1.2. Organocatalytic reaction of proline.

Type-II: Organic molecules form reactive intermediates. The chiral catalyst is consumed in the reaction and requires regeneration in parallel catalytic cycle as it is reported in Scheme 1.3.[12] Di-O-isopropylidene-b-D-erythro-2,3-hexodiulo-2,6-pyranose **9** was used as catalyst for epoxidation**.**

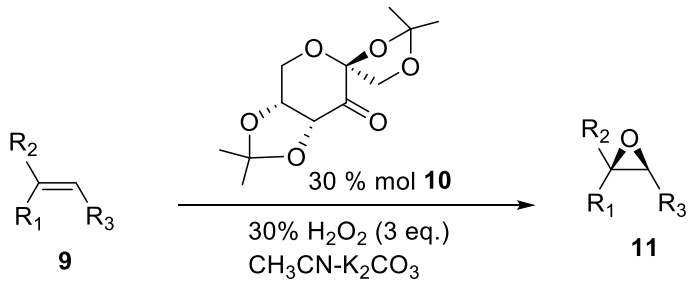

Scheme 1.3. Epoxidation reaction

Type-III: Phase transfer reactions occur. The chiral catalyst forms a host-guest complex with the substrate and shuttles between the standard organic solvent and a second phase. Catalytic enantioselective enolate alkylation of chiral quaternary ammonium salt occurs in Scheme 1.4.[13]

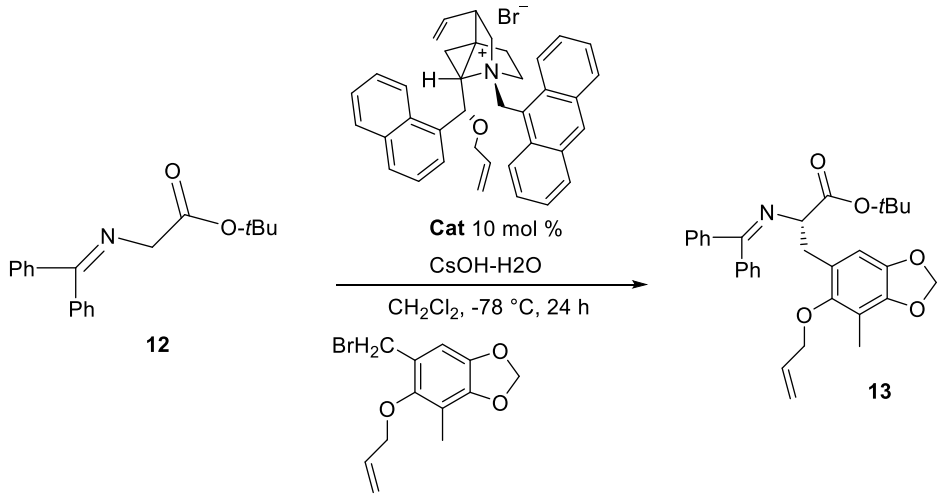

Scheme 1.4. Phase transfer catalysis

Type-IV: molecular-cavity-accelerated asymmetric transformations occur in which the catalyst may select from competing substrates, depending on size and structure criteria (Scheme 1.5).[14]

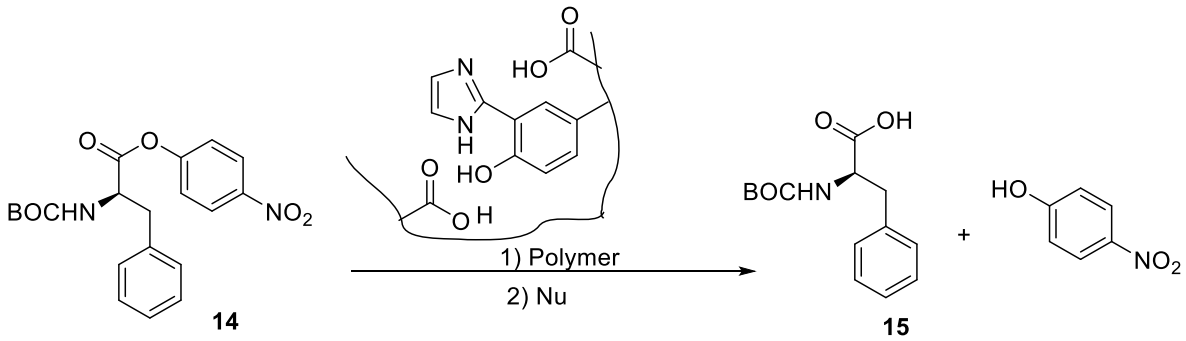

Scheme 1.5. Imidazole ring-based catalyst.

In recent research, asymmetric organocatalysis is very much convenient synthetic pathway to develop highly enantioenriched organic compounds compared to metallic catalysis and enzymatic catalysis. Furthermore, a large number of organocatalysts are easily synthesized, commercially available and stable under extreme conditions and do not need dry or inert environment.

1.3 Objectives of research

The main objective of this research is to study the influence of synthetic chiral polymers in asymmetric reaction processes. Chiral hyperbranched polymers of cinchona squaramides was synthesized for evaluating their catalytic performance in asymmetric synthesis. There are no reports about cinchona-derived hyperbranched polymers prior to this work. For obtaining chiral hyperbranched polymers and linear polymers, the use of cinchona alkaloids derivatives involves with the design stage. Then, Mizoroki-Heck coupling reaction and Yamamoto coupling reaction were used as synthetic methodology to obtain the chiral hyperbranched polymers and chiral linear polymers respectively and finally, the catalytic activity of chiral polymeric catalysts was assessed in asymmetric Michael addition reactions.

1.4 Literature survey

1.4.1 Asymmetric synthesis

Asymmetric synthesis is a special type of chemical synthesis in which one or more new elements of chirality are formed in a new substrate molecule and which produces the enantiomeric or diastereoisomeric products in an unequal amount. Simply, it is the synthesis of a compound by a method that favors the formation of a specific enantiomer or diastereomer under suitable reaction conditions. This is very essential procedure in modern chemistry, basically in the field of pharmaceuticals, as the different enantiomers or diastereomers of a molecule have different biological activities. As the final product does not contain any heavy metals, so it also has the advantage of 'green chemistry.[3,15] The significance of asymmetric synthesis is very much admirable. William S. Knowles and Ryoji Noyori (for their work on chirally catalyzed hydrogenation reactions)

was awarded the Nobel Prize for chemistry in 2001 for the application of chiral catalysts in asymmetric synthesis [16] and also Barry K. Sharpless (for his work on chirally catalyzed oxidation reactions) was awarded.[17] Now the way of further scope for asymmetric synthesis is very much facile. In asymmetric catalysis, at first the chiral catalysts form a complex with achiral substrates. Then the reaction progressed under the control of chiral catalysts to transform achiral substrate to chiral substrate. At the end, desired chiral compound was obtained by separating chiral catalyst and chiral substrate.

1.4.2 Chiral low molecular weight organocatalysts

The enhancement of new chemical modification for systematic and pragmatic synthesis of complex compound has appeared as the main objective in synthetic organic chemistry. Researchers, chemists reported different enantioselective organocatalytic transformation with low molecular weight catalysts,[18-27] which includes C-C bond formation[21-24], C-O bond formation[25,26] as well as desymmetrization[27] asymmetric transformations. L-proline, MacMillan's catalyst, cinchona alkaloids, Lewis acid/base catalyst are the example of commercially available chiral organocatalysts which are the successful synthetic tool in asymmetric transformations.

1.4.3 Cinchona alkaloids

Naturally occurring cinchona alkaloids are important chiral sources with an alluring medicinal history. These are isolated from the bark of cinchona trees. 'Cinchona' is a genus of flowering plants and it belongs to family of Rubiaceae. Before the explosion of organocatalysis,[28] cinchona alkaloids have long been known as very useful and robust catalysts for many kinds of organic reactions. After 1960s, with the enhancement of asymmetric phase transfer catalysts (chiral PTC),[29] cinchona organocatalysts have drawn much more attention and have been widely used in a variety of asymmetric reactions.[30]

Cinchona alkaloids and their derivatives are bifunctional, play an important role as a chiral organocatalysts in different asymmetric synthesis and have been reported as chiral exponents in organic reactions which was described in several review articles.[31] Cinchona squaramide, thiourea, sulfonamide etc are the most popular and important derivatives of cinchona alkaloid (Figure 1.4). Due to numerous availabilities in nature, economic benefit, stability and most important, can easily be structurally modified for various catalytic application purposes, these are unique chiral sources. All cinchona alkaloids contain many stereocenters, C-(3), C-(4), C-(8), C-(9) and N-(1). The absolute configuration of C-(3) and C-(4) is identical in the all naturally occurring cinchona alkaloids, but they occur in pair and configuration differ only at position N-(1), C-(8) and C-(9). The structural feature of cinchona alkaloids (Figure 1.2) and their derivatives show that they have diverse chiral skeleton which conduct their catalytic performance concerning the yields, diastereoselectivity and enantioselectivity of the products which have been reported before.[32-36]

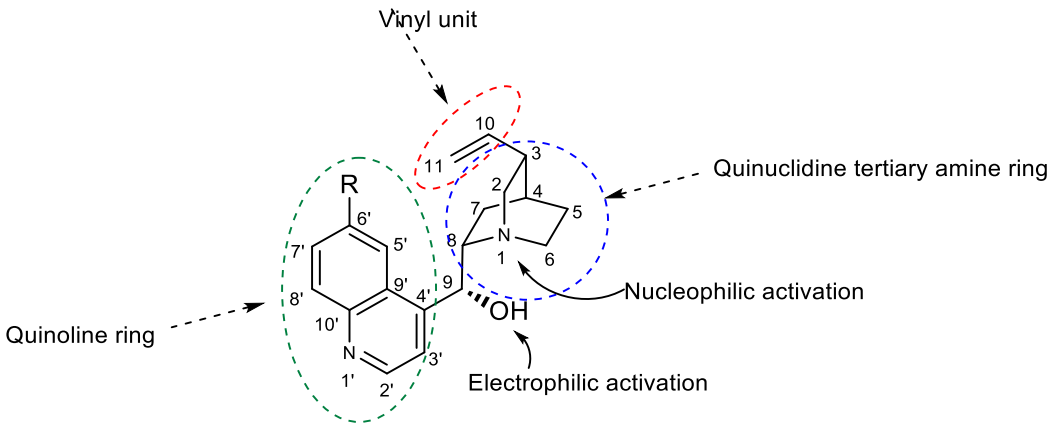

Figure 1.2. Structural feature of cinchona alkaloid with numbering[29]

There are four major cinchona alkaloids, (Figure 1.3) those are related to diastereomeric pairs but are often referred to as 'pseudoenantiomers'. For instance, both quinine and quinidine, cinchonine and cinchonidine are diastereoisomers and also pseudoenantiomeric pairs to each other. Each pair differs in the stereochemistry at C-8 and C-9 position in the structure.

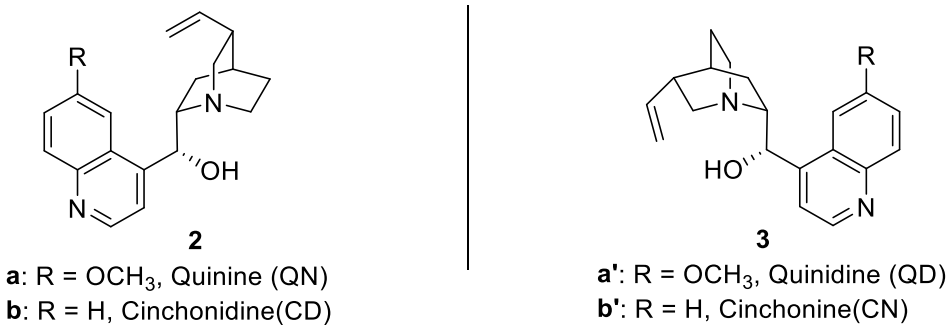

a: R = OCH_3, Quinine (QN)
b: R = H, Cinchonidine(CD)

a': R = OCH_3, Quinidine (QD)
b': R = H, Cinchonine(CN)

Figure 1.3. Structures of major cinchona alkaloids.

The presence of quiniclidine functional group makes them powerful ligands for a diversity of metal catalyzed processes. The metal binding properties of the quinuclidine nitrogen also enable to use cinchona alkaloids as metal surface modifiers. Moreover, the quinuclidine nitrogen can be used as a chiral base or chiral nucleophilic catalyst in various organocatalytic reactions

The C9-hydroxyl group can act as an acid site or hydrogen bond donor. The derivatization of the OH group into ureas, thioureas, amides, esters and so on, with either retention or inversion of the configuration which provides a more acidic site.[37] Moreover, the substitution of C9 into the free amino with the inversion of the configuration enables enantioselective aminocatalysis.

The C6' methoxy group of quinine and quinidine is readily to be derivatized as an effective H-bond donor like free OH group or thiourea moiety. The planar aromatic ring in quinoline aromatic part of cinchona alkaloids has electron-donor capability and in many cases, the catalysis is also supported by a π–π interaction with the aromatic quinoline ring or by its steric hindrance.

By the conformational investigation of the cinchona alkaloids using computational and spectroscopic methods, the chiral induction and discrimination processes could be understood. The dual functionality of cinchona alkaloids in asymmetric reactions was proved by mechanistic studies

of asymmetric catalysis by cinchona alkaloids using computational method.[38] The bifunctional mode of catalysis simultaneously implies the quinuclidine nitrogen to activate the nucleophile using general base catalysis and the hydroxyl group at C-(9) to activate the electrophile via hydrogen bond interactions.

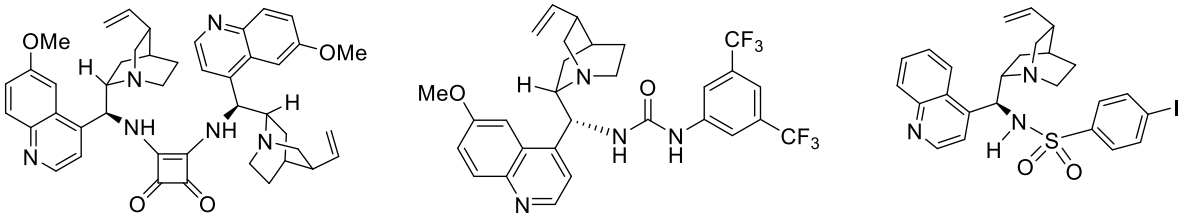

Figure 1.4. Cinchona derivatives

1.4.4 Squaric acid and squaramide

Squaric acid is a dibasic organic acid,which is also called quadratic acid. The conjugate base of squaric acid is hydrogensquarate anion $C_4HO_4^-$; and the conjugate base of hydrogensquarate anion is the divalent squarate anion $C_4O_4^{2-}$.[39] Although it is seemed that its four carbon atoms form a square but actually the structure of squaric acid is not perfectly square, as the carbon–carbon bond lengths are not quite equal. The high acidity of the first proton in comparison of second proton in squaric acid is attributable to resonance stabilization of the anion.[39] The negative charges are equally distributed in between two oxygen atoms and the dianion of squaric acid is completely symmetrical although the squaric acid is not symmetrical. In dianion, all C–O bonds are identical and also all C–C bonds are equal length.

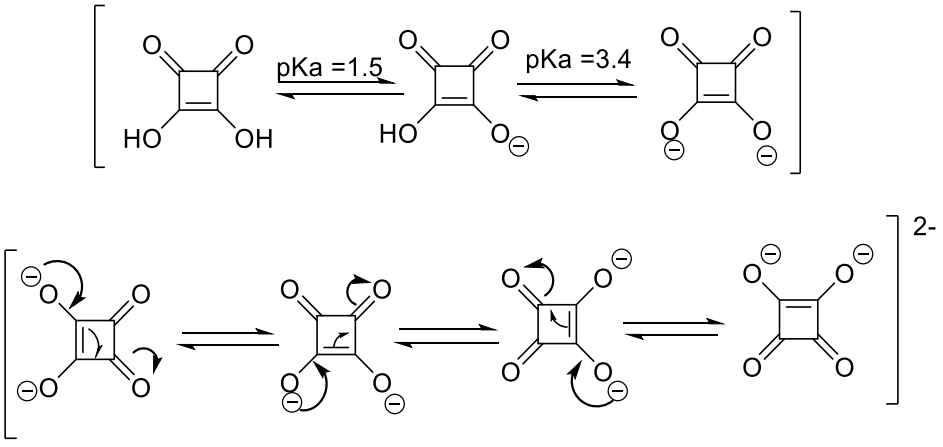

Figure 1.5. Squaric acid dianion resonance forms.

Squaramides are outstanding four-membered ring systems derived from squaric acid that are able to form up to four hydrogen bonds. A high affinity for hydrogen bonding is driven through a consequent increase in aromaticity of the ring. In combination with conformational rigidity, synthetic versatility, and relative stability, this hydrogen bonding and aromatic switching, have been utilized in many research applications as a most useful scaffolds.[40]

In 1959, Cohen et al. synthesized squaramide first via the hydrolysis of dichloro tetrafluorocyclobutene.[41] Different types of squaramides are possible to synthesize from squaric acid. Cinchona alkaloid derived squaramides are one of them that are used in various asymmetric transformations.The NH of squaramide is more acidic than the NH of thiourea and both can act as the bifunctional hydrogen-bonding catalysts.[42] The distance between two donor hydrogens in bisdiaminesquaramides is higher than the distance of two hydrogens in thioureas and it is estimated to be 33% larger than in thioureas.[42]

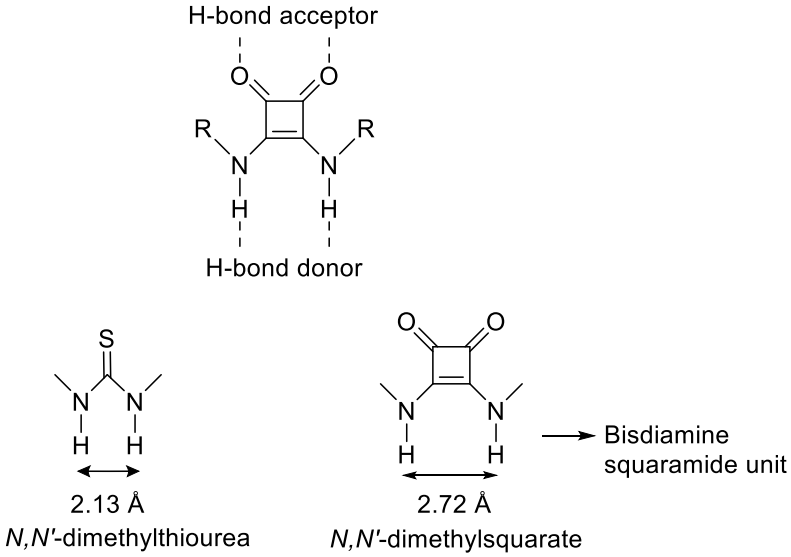

Figure 1. 6. Calculated H–H bond distances in *N,N′*-dimethlythiourea and *N,N′*-dimethlysquaramide.

1.4.5 Dimeric cinchona alkaloids derivatives

Dimeric cinchona alkaloids are products of designed by partial chemical synthesis, not isolated from any species. These synthetic dimers were designed mostly to utilize in the field of asymmetric synthesis.[43,44] Reactivity of the alkaloids at the N1, C3, C6' and C9 are exploited by various synthetic routes. This accessibility of reactive sites, in combination with an abundance of linker molecules, contributes to the diversity of the products obtained. The transition from a monomeric to dimeric alkaloid molecule results in accumulation of functional groups confined within a limited space.

Dimers connected at the C9-position*:* The C9-OH group provides an attractive site for modification by etherification and esterification reactions. On the other hand, the hydroxyl group can be substituted with a few other groups (e.g., NH_2) and subsequently used for dimerization. The C9-amino derivatives of cinchonidine **16**, **17** that were synthesized by Mitsunobu-type azide formation, followed by Staudinger reduction was reported by Itsuno and coworkers.[44,45] These cinchona sulfonamide derivatives have been proven effective catalyst for the asymmetric desymmetrization of cyclic anhydride[44] as well as Michael addition of β-ketoester to β-nitrostyrene.[45] The comparison between monomeric **16** and dimeric **17** cinchona sulfonamide derivatives catalysts in enantioselective synthesis of Michael addition β-ketoester to β-nitrostyrene is shown in Scheme 1.6.

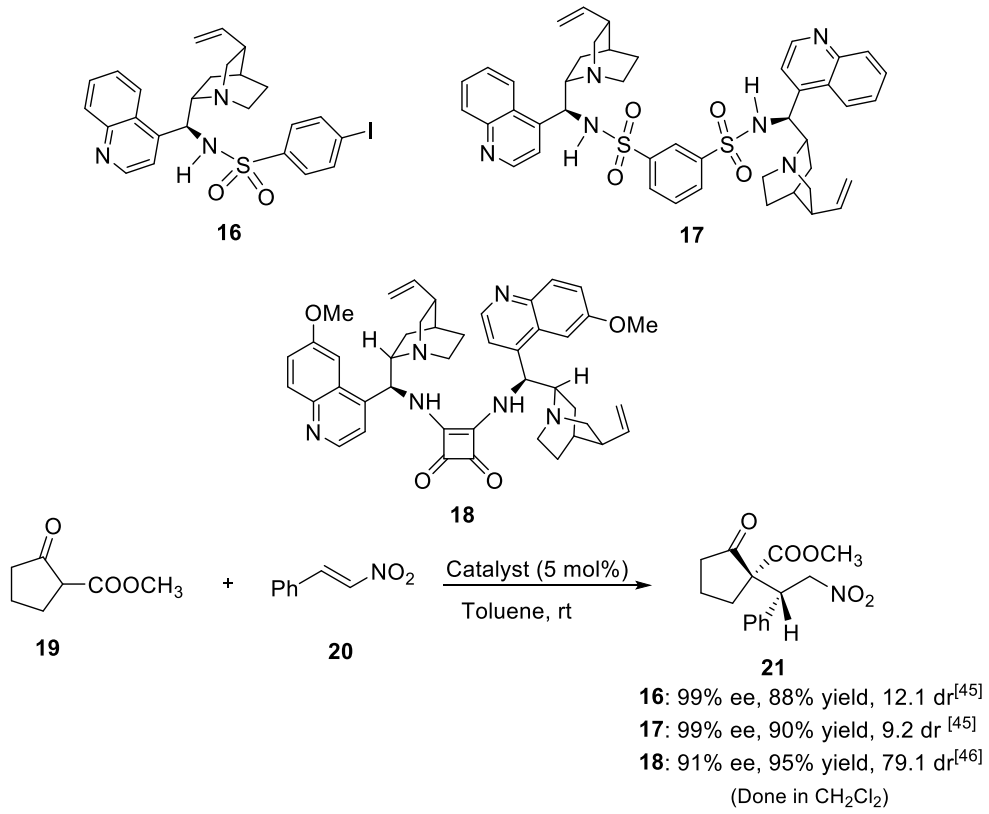

Scheme 1.6. Asymmetric reaction, catalyzed by C9-amino cinchona derivatives.

Another C9-amino cinchona derivative is squaramide dimer **18** which have been reported to be an effective chiral organocatalysts for the same asymmetric Michael addition of β-ketoester to β-nitrostyrene.[46] The acidic NH of squaramide acts as H-bond donor where quinuclidine N1 acts as H-bond acceptor in the asymmetric Michael reaction and catalyze the reaction as a bifunctional catalyst (Scheme 1.6).

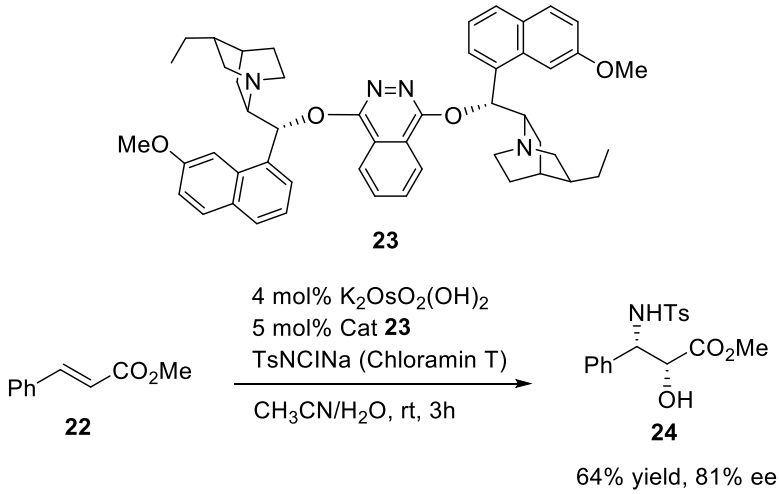

Scheme 1.7. Asymmetric dihydroxylation of olefin catalyzed by C9-cinchona ether derivative.

C9-dimeric alkaloid alkyl ethers were synthesis by the Williamson etherification of an alkali metal alkaloid salt and the respective alkyl dihalide. Their application in different asymmetric reactions also gave good enantioselectivity.[43] An example of C9-ether cinchona alkaloid dimer **23**

have been presented in Scheme 1.7 where 81% ee was achieved for its use as catalyst in Sharpless asymmetric dihydroxylation.[43-47]

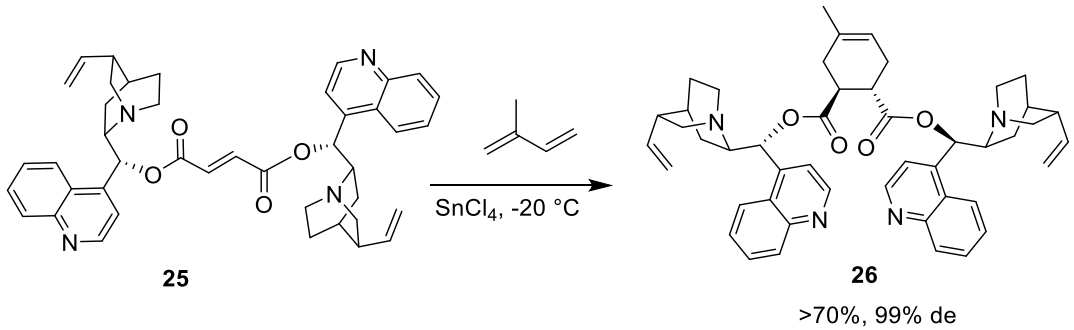

25 **26**

>70%, 99% de

Scheme 1.8. Example of C9-cinchona ester derivative in diastereoselective Diels-Alder reaction.

Alternatively, a few numbers of C9 dimeric ester of cinchona alkaloid have been utilized in asymmetric catalysis. The transformation of alkaloid C9-ester dimer involves the use of a base (usually trimethylamine and sometimes with a catalytic amount of dimethylaminopyridine) and acids dichlorides. C9-cinchona ester dimer could be applied as chiral ancillaries for the Diels-alder reaction. For example, catalytic activity of dimeric ester **25,** prepared from the reaction of cinchonidine and fumaroyl dichloride have been reported by Suzuki H. and coworkers.[48] The reactivity of the activated double bond was further explored in a Diels-Alder reaction with cyclopentadiene and isoprene. As a result, a bicyclic dicarboxylic acid ester **26** was isolated with good diastereoselectivity of 99% de from the reaction of 25 with isoprene (Scheme 1.8).

1.4.6 Cinchona derived chiral polymeric organocatalysts

For the synthesis of different chiral building blocks, polymeric chiral organocatalyst is very much attractive tool, though low-molecular-weight chiral organocatalysts have many advantages in the case of enantioselective synthesis those have some drawbacks also. Immobilization of a chiral organocatalysts (cinchona squaramides, cinchona sulfonamides, quaternary ammonium salt etc.) into a polymer allows for the preparation of a polymeric chiral organocatalyst that can be used in various asymmetric reactions.

Main-chain chiral polymeric organocatalysts contain chiral organocatalysts molecules as their repeating units in the main-chain moiety. Easy separation from the reaction mixture is the primary advantage of polymeric catalysts that allows very efficient recovery, and reusability of the catalysts in asymmetric synthesis.[49] Main-chain chiral polymers have several significant structural advantages in comparison with polymer-immobilized chiral organocatalysts for their applications in asymmetric synthesis, these includes:

- Rigid and sterically defined structure
- Constant repeating unit
- Possesses high catalyst loading
- Creates a precise micro-environment

For the preparation of main-chain chiral polymers various synthetic methodology have been investigated. Some of the reported methods includes ionic polymerization,[50] quaternization polymerization,[51,52] Mizoroki-Heck polymerization,[44,46,52-56] and ADMET polymerization.[57] As for example, Ullah, M. S and Itsuno. S. have reported main-chain type cinchona-based squaramides synthesis.[46] Their design involves the use of cinchona squaramide dimers where the olefinic double bonds in the cinchona squaramide dimer were then used for Mizoroki-Heck (MH) polymerization with aromatic diiodides. The MH polymerization of the cinchona squaramide dimer and aromatic diiodide led the corresponding chiral polymers in good yield.

Some reported examples of main-chain chiral cinchona based polymeric catalysts are described below.

1 Main-chain type polymer of cinchonidium dimer synthesized by Mizoroki-Heck reaction.[58]

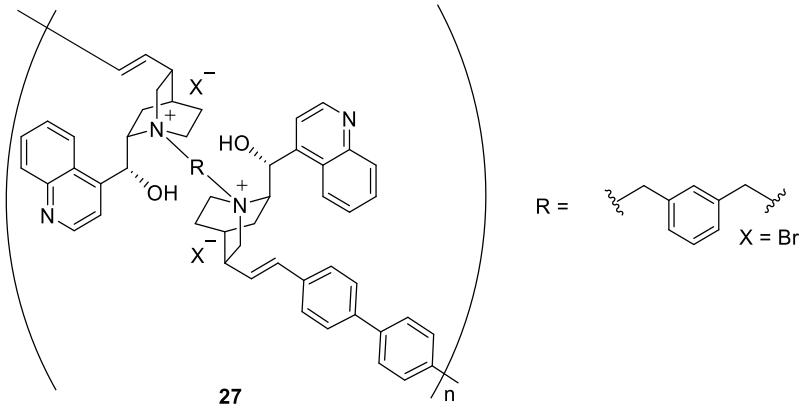

27

The asymmetric benzylation of *N*-diphenylmethylene glycine *tert*-butyl ester was successfully occurred with this above cinchonidine-based polymeric catalyst **21** and high levels of enantioselectivity (up to 95% *ee*) was obtained.

2. Main-chain type polymer of chiral ester. [56]

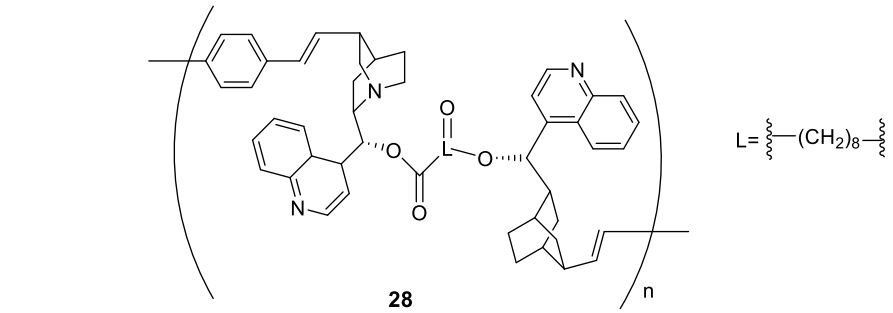

28

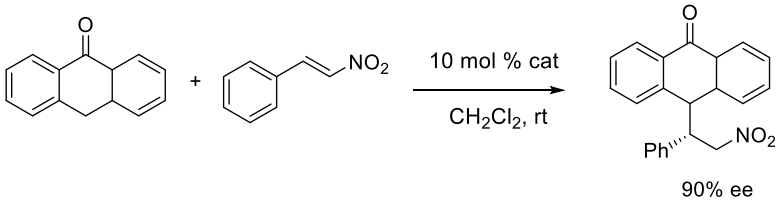

90% ee

Scheme 1.9. Enantioselective Michael addition reaction catalyzed by cinchona ester polymer.

3. Main-chain type cinchona alkaloid sulfonamide polymers.[44]

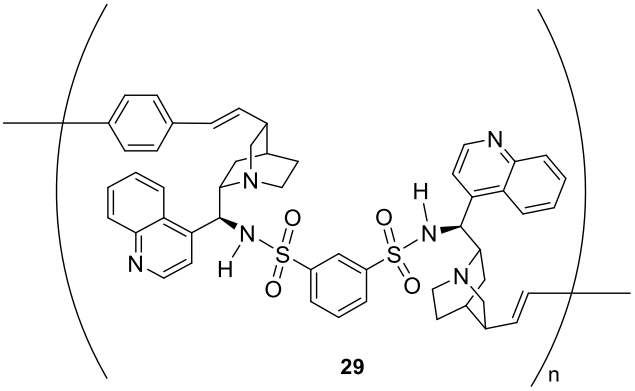

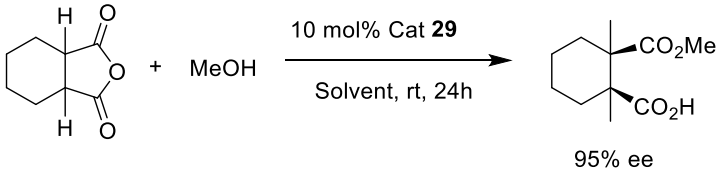

95% ee

Scheme 1.10. Desymmetrization of cyclic anhydride catalyzed by cinchona sulfonamide polymer.

This is the first synthesis of a chiral polymeric catalysts by Mizoroki–Heck polymerization containing a cinchona-based sulfonamide structure in their main chain.

4. Main-chain type cinchona alkaloid squaramide polymer. [46]

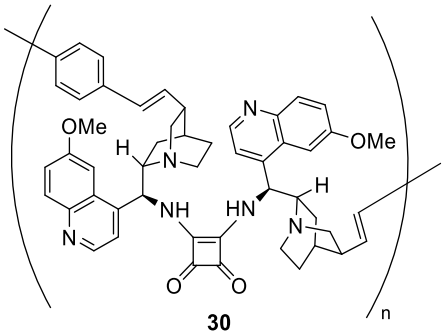

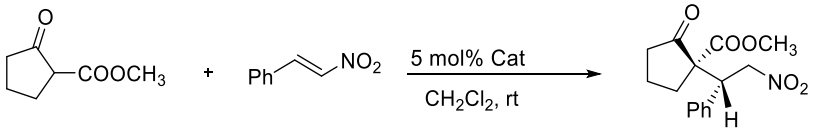

97% ee, 71% yield, 28:1 dr

Scheme 1.11. Asymmetric Michael addition catalyzed by squaramide polymer.

5. Main-chain chiral quaternary ammonium polymers using etherification polymerization.[59]

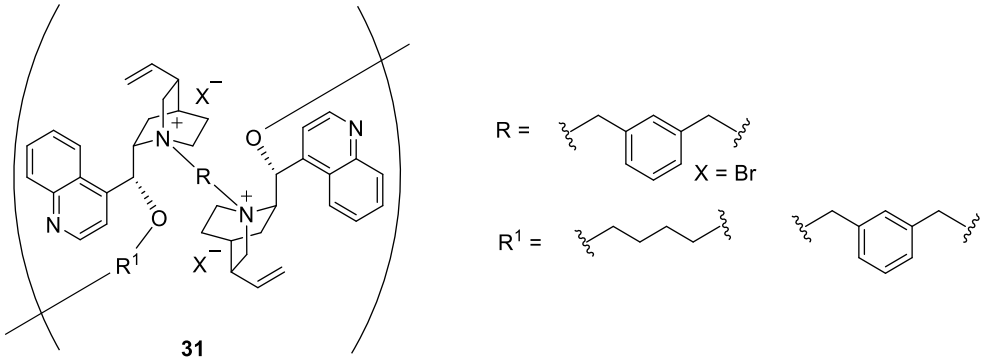

The chiral polymers containing quaternary ammonium salt structure in their main chain have been successfully synthesized by simple polycondensation reaction under *Williamson ether* synthesis conditions. The polymers were used as organocatalyst for the asymmetric alkylation of *N*-diphenylmethylidene glycine *tert*-butyl ester.

6. polymers of chiral imidazolidinone for asymmetric organocatalysis application.[60]

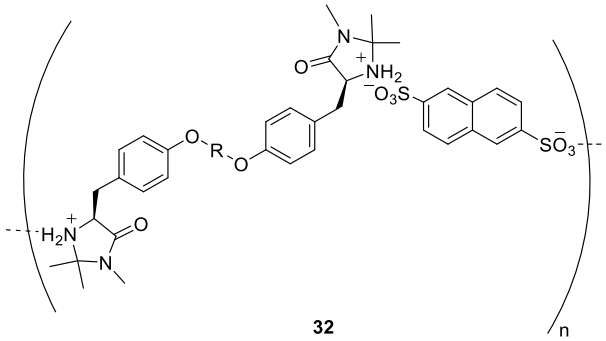

32

In this polymerization, chiral imidazolidinones were incorporated by ionic bonding into the main-chain of the polymer. This type of polymers was successfully synthesized by the reaction of chiral imidazolidinone dimers with disulfonic acid. This polymeric chiral organocatalyst **27** successfully catalyzed the asymmetric Diels–Alder reaction.

1.4.7 Cinchona derived hyperbranched polymeric organocatalysts

Hyperbranched polymers (HBPs), highly branched tree-like macromolecules bearing unique three-dimensional structures, have attracted a lot of attention in various applications.[61-64] Chiral HBPs containing chiral catalytic moieties are potential polymer catalysts in asymmetric catalysis. Their interesting chemical and physical properties, and potential applications have attracted considerable attention. However, only a limited number of chiral HBPs have been synthesized to date.[65] Although chiral dendrimers have precisely controlled structure their synthesis is usually complicated and contain several tedious processes.[66] HBPs are relatively easily to synthesis using a one-step polymerization reaction. The polymerization reactions are classified into three categories: (1) step-growth polycondensation of AB_x monomers; and (2) self-condensing vinyl polymerization of AB^* monomers; (3) multibranching ring-opening polymerization of latent AB_x monomers. Hyperbranched polymers are generally composed of dendritic, linear and terminal units and a degree of branching (DB) helps to describe their structures.[67] Most of the hyperbranched polymers possess some of the unique properties exhibit dendritic macromolecules, such as low viscosity, good solubility, and multi-functionality. Owing to multi-functionality, physical properties such as solubility in solvents and the glass transition temperature can be controlled by the chemical modification of the end functional groups (endcapping reactions).[67] Cinchona-derived hyperbranched polymers are not reported before. Many hyperbranched polymers synthesized previously. For example, in the presence of dicyclohexylcarbodiimide (DCC) and dimethylaminopyridine (DMAP) at room temperature, the reaction of the high molecular weight HBP–SA (M_n = 14 000) with 4-sulfobenzoic acid potassium salt followed by proton exchange

reaction through an acid-type ion exchange resin, gave the hyperbranched polymer with a sulfonic acid group at the periphery (HBP–SA) **34** (scheme 1.12) as a pale yellow rubbery solid with 77% yield.[68] The HBP–SA is soluble in water, methanol and ethanol, and insoluble in chloroform.

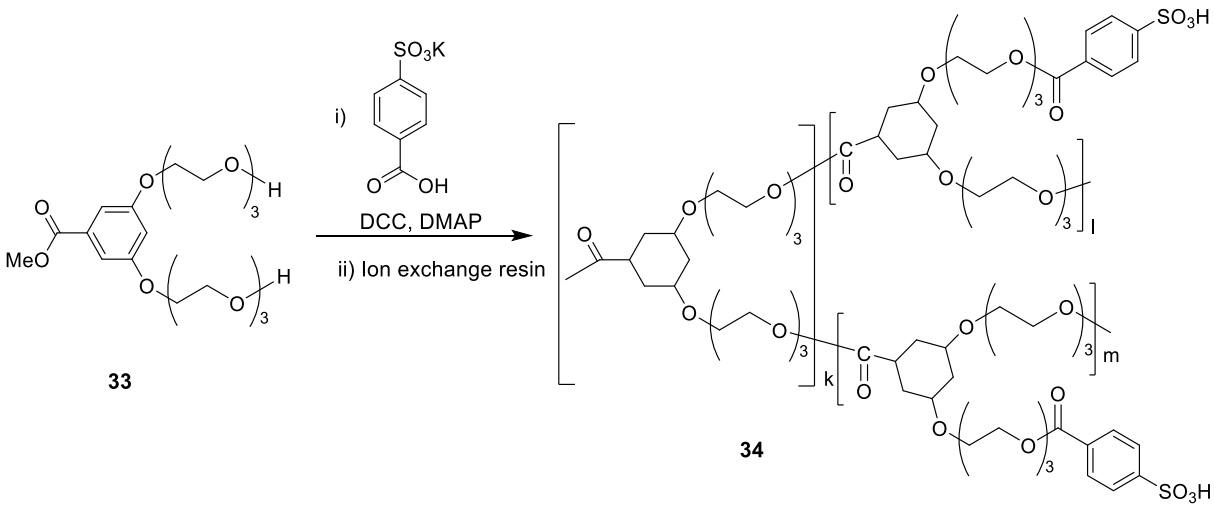

Scheme 1.12. Example of hyperbranched polymer HBP–SA.

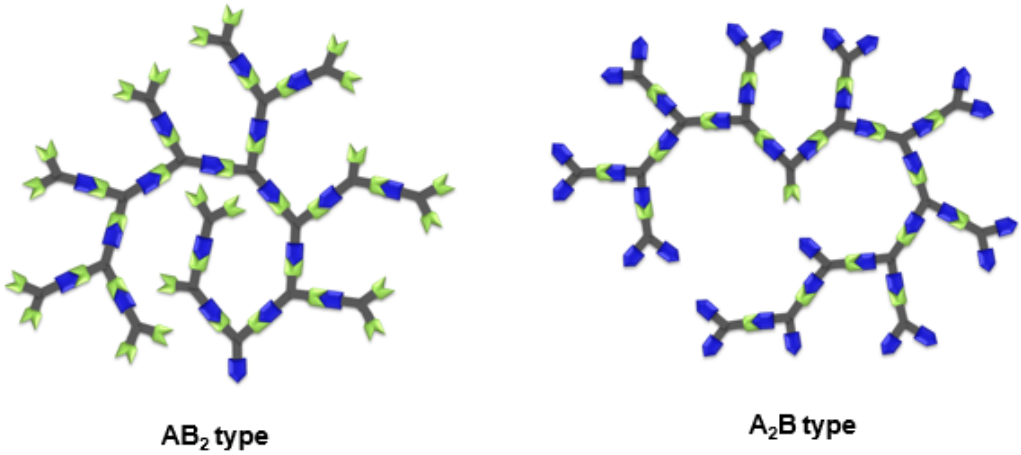

Figure 1.7. Some possible structure of hyperbranched polymer.

1.5 Basic introduction on synthesis methods of polymers

1.5.1 The Mizoroki-Heck reaction

In the early 1970s, Mizoroki T. and Heck R.F. independently discovered that aryl, benzyl and styryl halides react with olefinic compounds at elevated temperatures in the presence of a hindered amine base and catalytic amount of Pd(0) to form aryl-, benzyl-, and styryl-substituted olefins.[69] The Mizoroki-Heck reaction, is the palladium-catalyzed addition of aryl, vinyl, or substituted vinyl groups to organic halides or triflates, commonly known as the Heck reaction. In the presence of a Pd(0) catalyst, the cross coupling reaction occurs between an aryl/alkenyl halide and a terminal olefin to produce a substituted olefin. This coupling reaction has become one of the most widely used catalytic carbon-carbon bond forming tools in organic synthesis, since its discovery.

Scheme 1.13. General scheme of Mizoroki-Heck coupling reaction.

This reaction is highly functional group selective and high yielding. The conditions of MH reaction can be applied on the olefin compounds with a wide range of functional groups: esters, ethers, carboxylic acids, nitriles, phenols, dienes, etc. There is no significant effect of the electronic nature of the substituents of olefin on the formation of product, but the reaction rate is influenced by the degree of substitution of the olefin, usually the slower reaction rate is observed in case of more substituted olefin.

- **Mechanism of Mizoroki-Heck reaction:**

The exact mechanistic pathway of Heck reaction is not fully fixed, it may to vary with the change of reaction conditions. The mechanism proposed by Heck[70] in 1974, when the precursor is $Pd(OAc)_2$ associated with monophosphine ligands, L is described in here. After the formation of a Pd(0) catalyst from the precursor $Pd(OAc)_2$ by a reduction process, the following steps of the catalytic cycle were proposed:

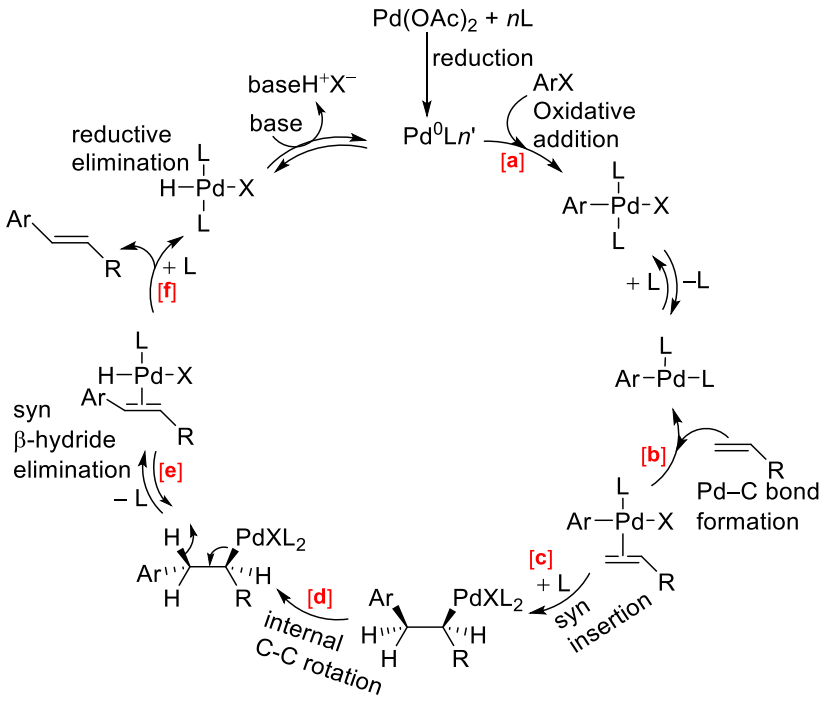

Figure 1.8. Mechanism of Mizoroki-Heck reaction.

i) First step is the oxidative addition of the aryl halide to a Pd(0) complex supported by oxidative addition of aryl halides to $Pd^0(PPh_3)_4$.

ii) σ-aryl-palladium (II) halide ($ArPdXL_2$) from The first step coordinates to the alkene after the dissociation of one phosphine. This reaction is referred to as *organopalladation*, which is the origin of the regioselectivity of Mizoroki-Heck reaction.

iii) Then undergoes a *syn* insertion of the alkene, leading to a σ-alkyl-palladium(II) halide.

iv) The internal C–C bond rotation on the σ-alkyl-palladium(II) halide bring an SP^3-bonded β-hydrogen in a *syn* position relative to the palladium atom.

v) Then a *syn* β-hydride elimination gives a hydridopalladium(II) halide associated with the arylated alkene.

vi) Finally, after the dissociation from arylated alkene, the hydridopalladium(II) halide undergoes a reversible *reductive elimination* to generate the active Pd(0) complex. The base shifts this equilibrium towards the Pd(0) catalyst by quenching the hydrogen halide.

In organic synthesis, Mizoroki–Heck (MH) coupling reaction is one of the easiest ways to form new C–C bond from olefinic double bonds with aromatic iodides. By using MH coupling, polymerization of BINOL like materials is reported[71] but there have been no examples of chiral polymer synthesis from cinchona alkaloids by using this method except for our research group reported works.[41-43,52,53] It has been demonstrated that the double bond of cinchona alkaloids can be altered by Heck coupling reaction. Then we have used Heck coupling reaction for the synthesis of novel chiral cinchona alkaloid derived squaramide polymers from the cinchona squaramide.

For example, when equimolar amount of **35** and diiodo compound reacts to each other under Heck coupling reaction conditions, main-chain chiral squaramide polymer **36** is obtained with quantitative yields.[55]

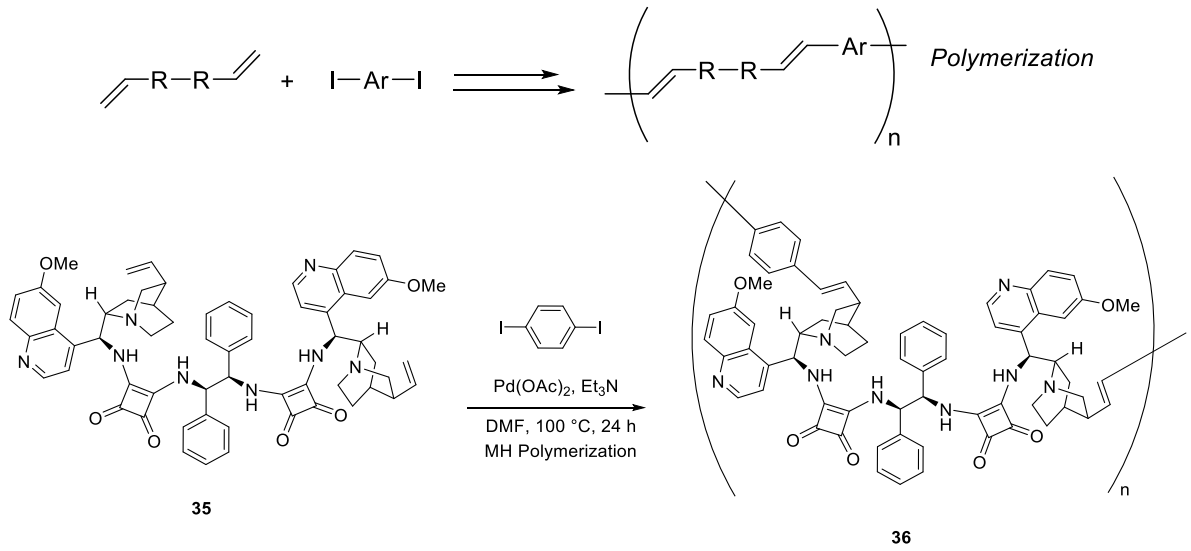

Scheme 1.14. Polymerization of cinchona derived squaramide.

1.5.2 Yamamoto coupling reaction

Yamamoto coupling reaction occurs between aromatic halides. The homopolymerization of aromatic dihalides is possible using this coupling reaction. Yamamoto coupling is the nickel-catalyzed coupling reaction of organic halides in the presence of neutral ligands (e.g., PPh_3 and

bipyridine).[72,73] Carbon-carbon bonds of aryl halogenide compounds are formed via mediation from a transition metal catalyst, in Yamamoto coupling, The most commonly used nickel catalyst for the Yamamoto coupling reaction is bis(cyclooctadiene)nickel(0) ($Ni(COD)_2$). This coupling reaction is particularly interesting when it is applied to polymer synthesis. Yamamoto coupling polymerization proceeds through reductive elimination from a diorganonickel(II) intermediate.[73,74] Aromatic dihalides in the presence of a Ni catalyst simply react to afford π-conjugated polymers.[75] Various types of π-conjugated polymers have been synthesized via Yamamoto coupling polymerization.[76] However, to our knowledge, only one example of chiral polymer synthesis using Yamamoto coupling polymerization has been reported. Onimura et al. reported the Yamamoto coupling polymerization of chiral oxazoline monomers containing a diiodophenyl group (Scheme 1.10).[77] They synthesized optically active poly(*m*-phenylene)s bearing chiral oxazoline at the side chains. The structures and chiroptical properties were characterized using spectroscopic and thermal gravimetric analyses.[77] No application of the chiral polymers to asymmetric catalysis has been reported till date. Only a single halogen functionalized monomer is required, leading to diversity in monomer species, as well as a simple reaction procedure.

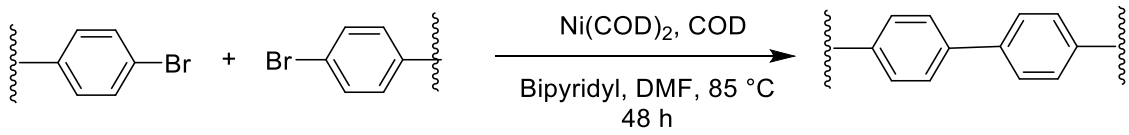

Scheme 1.15. General scheme of Yamamoto coupling reaction.

1.5.3 Michael addition reaction

Cinchona alkaloids and their derivatives have been applied over a several numbers of asymmetric reactions as catalysts. C–C bond forming reactions (Alkylation, Michael addition, Diels-Alder, etc.) is one of them.[78] We focused on Michael addition as the nucleophilic addition of a carbanion or another nucleophile to an α, β-unsaturated carbonyl compound. This type of Michael reaction corresponds to the larger class of conjugate additions, and it is one of the most convenient reaction for the gentle formation of C–C bonds. Michael addition[79] reaction is a nucleophilic addition reaction in which an enolate (a nucleophile) is a Michael donor and a Michael acceptor is a conjugated system with an electron withdrawing group such as nitro, cyano, keto or ester, react to each other to from a new addition product called Michael adduct. The Michael adduct obtained can be chiral or achiral depending on the nature of the catalyst being used for the activation of the reacting substrates. The Michael addition reaction is a thermodynamically controlled reaction; the reaction donors are active methylene such as malonates and nitroalkanes, and the acceptors are activated olefins such as α, β-unsaturated compounds.

In this work, our focus point of interest is enantioselective synthesis. We have prepared chiral organocatalysts derived from cinchona squaramides and utilized them as catalysts in the Michael

addition reactions. Type of base catalyst, reacting substrates and reaction solvent are the general factors that can affects the Michael reaction mechanism.

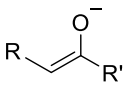

[Michael donor: Nucleophile]

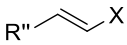

[Michael acceptor: Electrophile]
X= any electron withdrawing groups such as cyano, nitro, keto or ester, etc.

- **Michael reaction: general mechanism**

Step 1

In a Michael donor **i,** R and R' are electron-withdrawing groups such as acyl and cyano making the methylene hydrogen more acidic forming the carbanion on reaction with base. An enolate **ii** is formed in the presence of a base by the removal of alpha hydrogen from the carbonyl containing compound **i**.

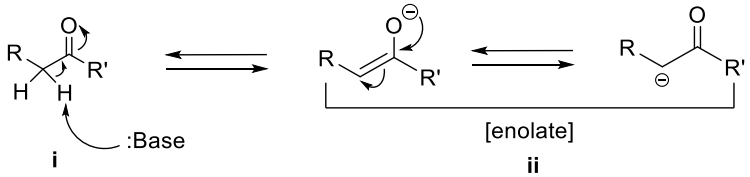

i ii

Step 2

The enolate **ii** acts as a Michael donor which reacts with the Michael acceptor (α, β-unsaturated compound) **iii** to produce the molecule **iv**.

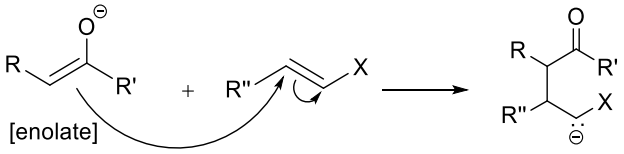

ii iii iv

Step 3

Finally, the base got regenerated from i**v** forming the final product **v**.

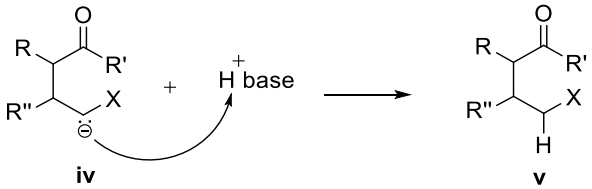

iv v

1.6 Some literature review of cinchona alkaloids-derived squaramides as bifunctional chiral organocatalyst for the asymmetric reactions

1.6.1 Recent application of cinchona alkaloid-based catalysts in asymmetric addition reactions.[80]

The most important aspect of synthetic organic chemistry is the stereocontrol in organic reactions. catalysis is becoming an increasingly popular strategy in asymmetric synthetic endeavors, due to design and development of several natural product-derived chiral molecular frameworks as chiral

oragnocatalysts.[15] *Cinchona* alkaloids, which were once known for the popular antimalarial drug quinine, have appeared as the most powerful class of compounds in the realm of asymmetric organocatalysis during the last two decades.[80] Aside from natural *Cinchona* alkaloids, many derivatives, such as those containing hydroxyl groups, amines, ureas, and thiourea functionalities, especially at the C9 position, either alone or in the presence of an additional catalyst that might be a simple achiral compound or metal salt, have been utilized in divergent types of enantioselective synthesis by asymmetric catalysis. This can be ascribed to the abundance of *Cinchona* alkaloids in nature, their commercial availability at reasonable prices, stability and easy handling in laboratory, and their favorable modification by simple reactions.

Nucleophilic 1,2-addition to the C=O bond

The most enormously investigated reactions of carbonyl compounds is nucleophilic 1,2-additions to the C=O bond. Among them, the aldol reaction constitutes the most common and powerful method for carbon-carbon bond formation.[81] With a new stereocenter, the aldol adducts serve as power-building blocks in organic synthesis. The application of aldol adducts **40**, obtained from asymmetric direct aldol reaction of alkyl azlactones **37** and aliphatic aldehydes **38**, in the synthesis of β-hydroxy-α-amino acids **41**-bearing alkyl substituents was reported by Zheng and Deng.[82] Under optimized conditions *Cinchona* alkaloid **39**, catalyzed the aldol reaction using the 6′-OH as the most efficient catalyst.

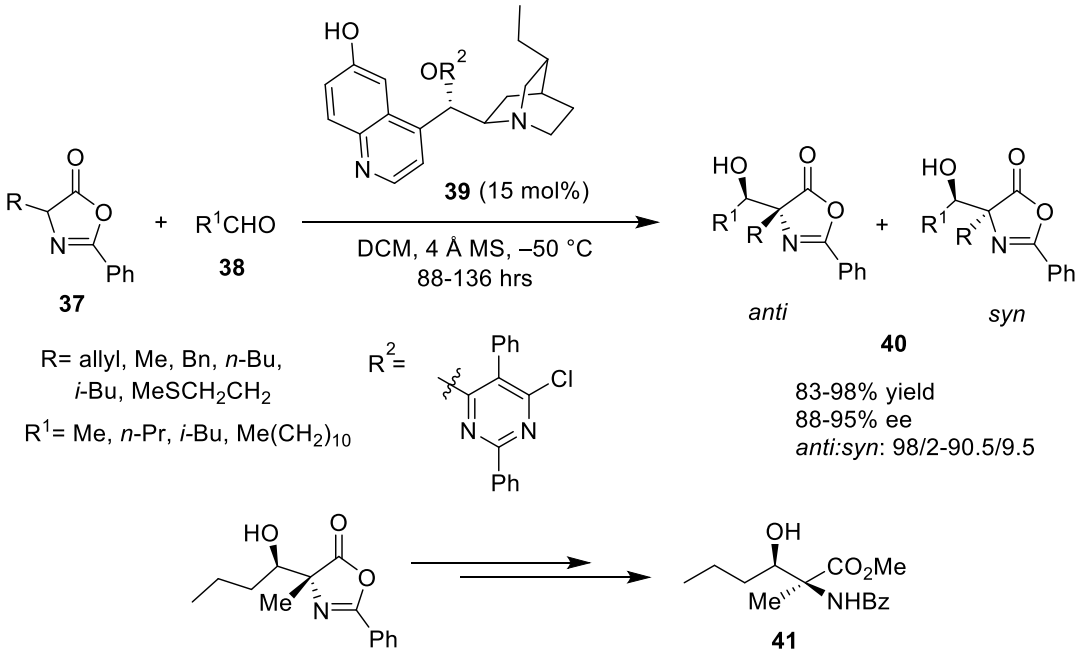

Scheme 1.16 Asymmetric aldol reaction of azalactones with aliphatic aldehyde

Application of C9 primary amine derivatives

Most of the *Cinchona*-alkaloid derivatives employed in inducing chirality in organic reactions include mainly C9 primary amines, C9 ureas and thioureas, C9/C6′ hydroxyl, C9 amides, and C9 squaramides. Asymmetric cross-aldol reaction of enolizable aldehydes **38** and α-ketophosphonates

42 was the first reaction reported by Perera et al.[83] Application of quinine-derived primary amine **43** as an organocatalyst and 4-methoxybenzoic acid as an additive led to the highly enantioselective synthesis of tertiary β-formyl-α-hydroxyphosphonates **44** with anticanceractivity (Scheme 1.17). The reaction worked very well with acetaldehyde, which is a difficult substrate for aldol reaction. The configuration of the product as '*R*' established by the authors on the basis of single crystal X-ray crystallography.

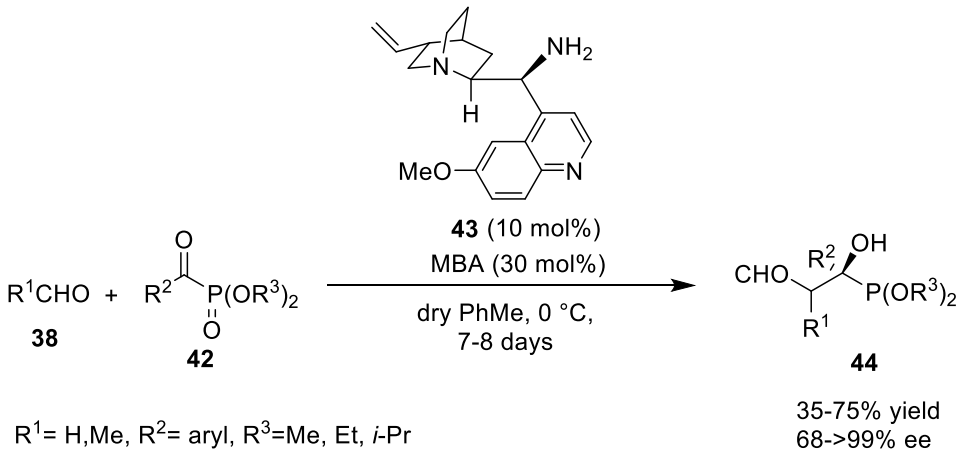

Scheme 1.17. Asymmetric cross aldol reaction of enolizable aldehyde and α-ketophosphonates

Isatins have appeared as one of the most robust classes of compounds, due to the various biological properties of their derivatives and applications in synthesis of spirooxindoles through the last 15 years. The reactions of the C3 ketone group of isatins, including aldol reaction, have been investigated for the synthesis of 3-substituted 3-hydroxy-2-oxindoles and spirooxindoles. The application of quinine-derived primary amine catalyst **46** in asymmetric aldol reaction of isatins **45** with acetaldehyde **38a** was reported by Guo and Zhao.[84] The corresponding adducts were obtained in high yields and with good enantioselectivity. However, they were not very stable and were immediately reduced to diols **47** (Scheme 1.18). According to the proposed mechanism, the primary amino group of the catalyst reacts with aldehyde to form an enamine intermediate. Attack of the enamine to the *Re* face of isatin led to the formation of major *S*-enantiomer.

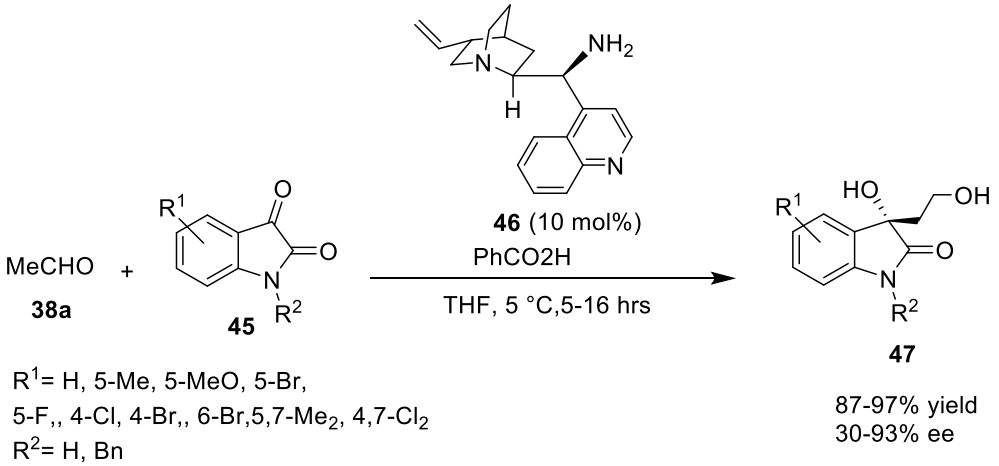

Scheme 1.18. Quinine-derived primary amine catalyzed aldol reaction of Isatins

Application of C9 alkoxy/hydroxyl derivatives

For the phospho-aldol reaction of isatins with diphenyl phosphite, Wang et al screened commercially available quinine **48** as the most effective catalyst in terms of offering enantioselectivity.[85] A variety of *N*-alkylated isatin derivatives **45** undergo asymmetric phospho-aldol reaction with diphenyl phosphite, forming 3-hydroxyisatin-3-phosphonates **49** in good-to-excellent yields and with moderate to good enantioselectivity (Scheme 1.19). Nonpolar solvents gave better enantioselectivity in comparison to polar solvents due to the sensitivity of the reaction towards solvents. A study of electronic effects on the isatin ring showed that electron donating substituents offered better enantioselectivity than electron-withdrawing substituents. Based on this observation, authors proposed a transition state **TS** (Scheme 1.19) involving a ternary complex between the phosphite, the isatin, and the catalyst, in which the isatin's C3 ketone and phosphite were activated by H-bonding with the hydroxyl group of the catalyst.

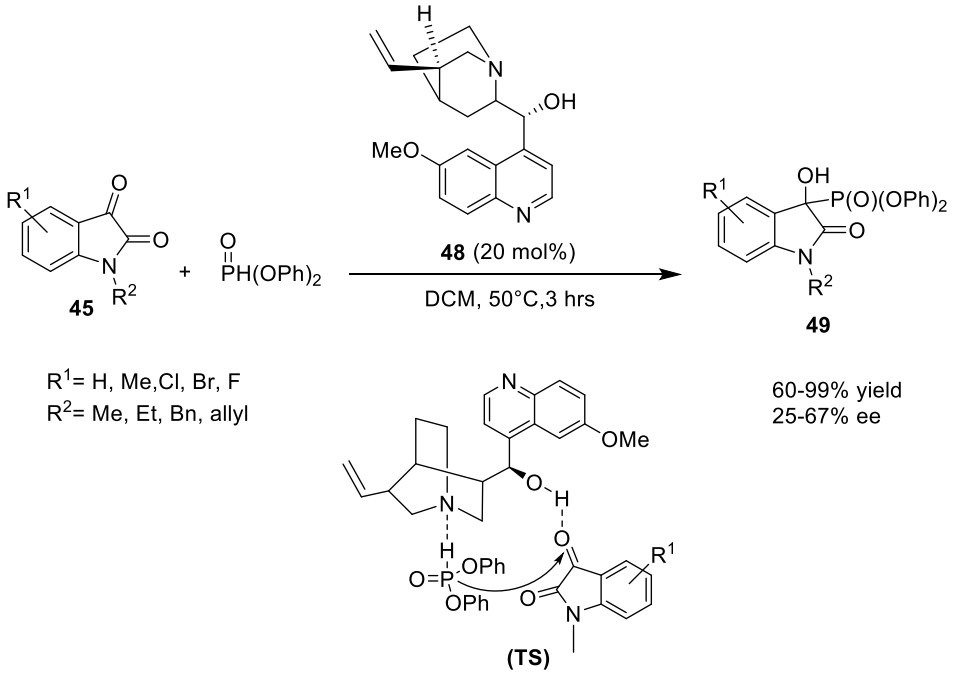

Scheme 1.19. Asymmetric phosphor-aldol reaction of isatins, catalyzed by cinchona-based catalyst bearing C6' methoxy and C9 hydroxyl groups

Application of C9 urea/thiourea derivatives

Isatins and β, γ-unsaturated α-ketoesters have drawn considerable interest among substrates, apart from common aldehydes and ketones. For aldol reactions there are two principal mechanisms. The primary amine catalysts inhibit the reaction through an enamine formation with aldehydes or ketones. The utilization of an acid cocatalyst can enhance the formation of enamine, as well as protonate the quinuclidine nitrogen atom. The urea/thiourea catalysts interfere through an enol/enolate mechanism. The quinuclidine nitrogen abstracts the proton, and the thiourea moiety activates the carbonyl group through H-bonding. The network of H-bonding also creates asymmetry at the reaction center and determines the stereochemical outcome of the reaction. An asymmetric aldol reaction of α-azido ketones **50** with ethyl pyruvate **51** mediated by a *Cinchona*-based

bifunctional urea catalyst **52** reported by Okumus et al (Scheme 1.20).[86] This reaction promoted the first asymmetric synthesis of ethyl 4-aryl-3-azido-2-hydroxy-2-methyl-4-oxobutanoates **53** with high enantioselectivity (up to 91%) and diastereoselectivity (diastereomeric ratio [dr] 95:5 *syn*:*anti*), but in moderate yields.

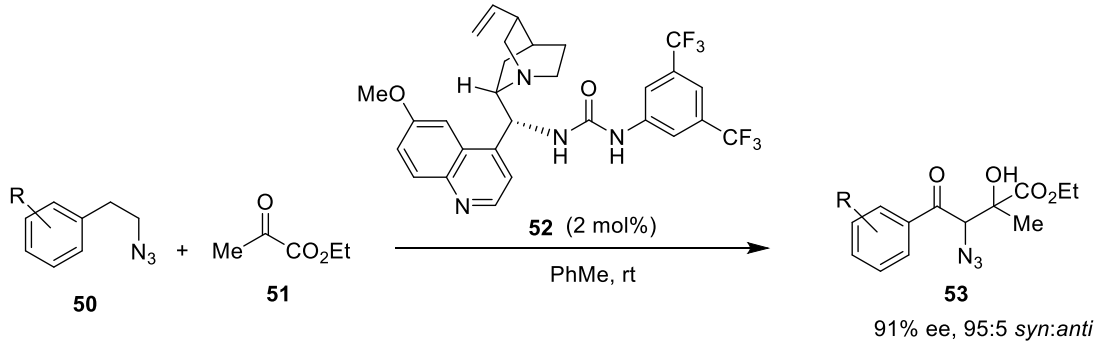

Scheme 1.20. Asymmetric synthesis of **53** using thiourea catalyst

Application of cinchona-derived catalysts in Michael additions to nitroolefins

In the presence of different classes of *Cinchona*-based catalysts, asymmetric Michael additions of diverse Michael donors to nitroolefins have been reported. During 2010, enantioselective Michael additions of cyclohexanones,[87] and aldehydes[88] to nitroolefins catalyzed by various cinchona-based thioureas were reported. In the Michael addition of acetylacetone **54** to nitroolefins **55**, a thiourea catalyst **56** has been employed (Scheme 1.21).[89] Michael-addition reaction of these substrates also reported by Liu et al using a chiral 1,1′-bi-2-naphthol (BINOL)-quinine-squaramide catalyst **57**, affording adducts **58** in good yields and enantioselectivity (Scheme 1.21).[90]

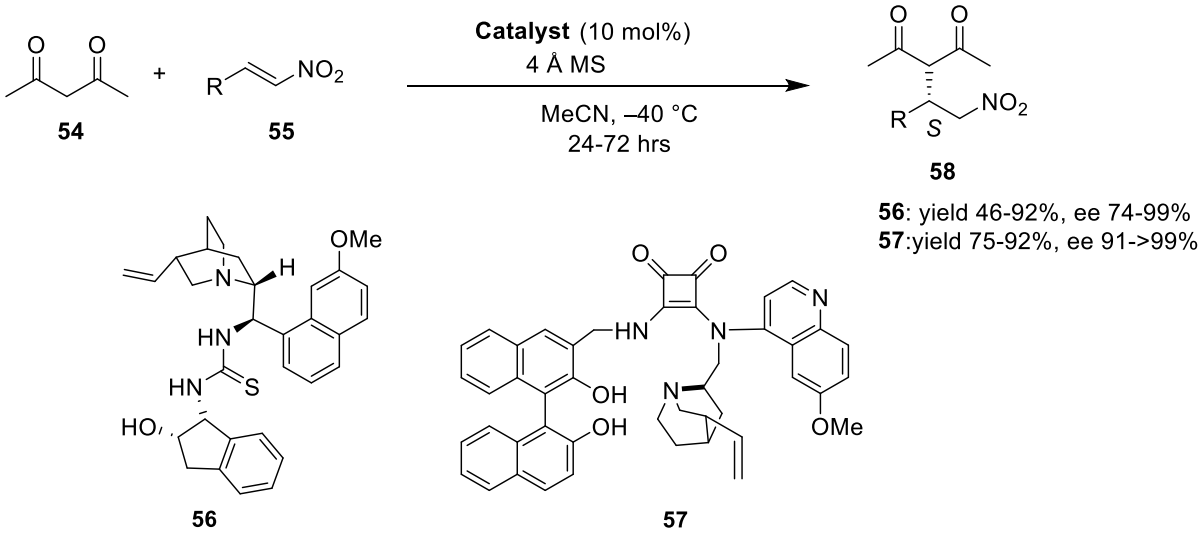

Scheme 1.21. Application of cinchona thiourea and BINOL squaramide catalyst in Michael reaction

Application of cinchona-derived catalysts in oxy- and sulfa-Michael additions

The cinchona-based urea catalyst **60** has been utilized in an intramolecular oxy-Michael addition of phenol derivatives **59** bearing easily available (*E*)-α,β-unsaturated ketones.[91] The reaction promote the formation of asymmetric synthesis of 2-substituted chromans **61** in good yields

(Scheme 1.17). A substrate with the 4-bromophenyl group led the quantitative yield (99%) of the product with 83% ee. A substrate with R = Me offered moderate yield of 64% and low enantioselectivity (36% ee).

The catalytic asymmetric sulfa-Michael addition of thiols to electron deficient olefins defines a straightforward and flexible approach toward obtaining valuable optically active sulfur compounds of biological interest. The enantioselective sulfa-Michael addition of a variety of thiols to *trans*-chalcones was reported by Dai et al.[92] Cinchona alkaloid-derived squaramide catalysts, first developed by Malerich et al,[93] was utilized under mild conditions, getting the corresponding adducts in moderate to excellent yields and high enantioselectivity (up to 99%). A sulfa-Michael addition of thioacids **62** to α, β-unsaturated ketones **63** developed by Rana et al to synthesize the chiral sulfa-containing frameworks, such as **64** (Scheme 1.18), which are common in biologically active natural products and pharmaceutical agents.[94] The reaction was catalyzed by the pseudoenantiomeric quinine/quinidine-derived urea catalysts **60a/b** most efficiently, affording both enantiomers of the desired products equally in high yields and with same level of enantioselectivity.

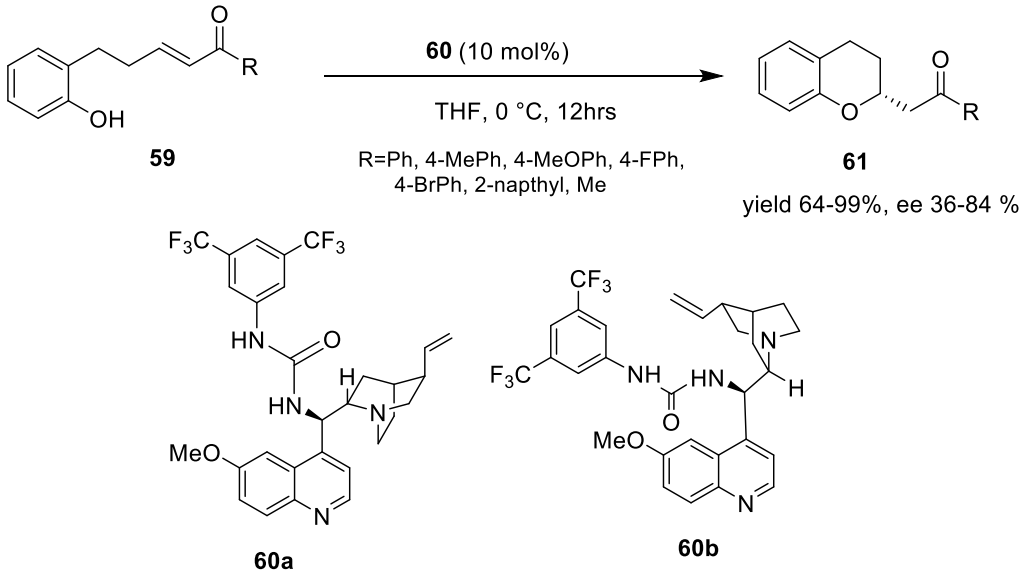

Scheme 1.22 Oxy-Michael addition reaction

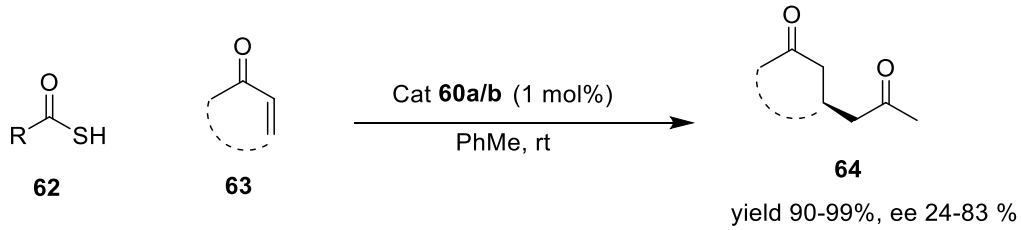

Scheme 1.23 Sulfa-Michael reaction

1.6.2 Cinchona alkaloid derived squaramide catalyzed diastereo and enantioselective Michael addition of isocyanoacetates to 2-enoylpyridines.[95]

A dynamic organocatalytic diastereo- and enantioselective Michael addition of a substituted isocyanoacetates to 2-enoylpyridines catalyzed by cinchona alkaloid-derived squaramide has been

achieved, leading to the corresponding adducts with two adjacent tertiary-quaternary stereocenters in excellent yields (up to 99%) and good to excellent stereoselectivities (up to >20:1 dr, up to 98% ee) under mild conditions. A wide variety of isocyanoacetates and 2- enoylpyridines were tolerated in this reaction. For obtaining best catalyst, the reaction of α-phenyl isocyanoacetate **65** and 2-enoylpyridine **66** was examined in the presence of various cinchona alkaloid-derived thiourea or squaramide catalysts in dichloromethane at room temperature (Table 1.1). Quinine-derived thiourea catalyst **67a** effectively catalyzed this reaction, giving the corresponding Michael adduct **68** in excellent yield, but with moderate enantioselectivity and low diastereoselectivity. Further screening of quinine-derived squaramide catalysts **67b-d** revealed that 3,5-bis(trifluoromethyl)phenyl substituted squaramide **67d** turned out to be a better catalyst for this Michael addition, affording the desired adduct in good yield along with better enantioselectivities for both diastereomers. Moreover, more reactive dihydroquinine derived squaramide **67e** can significantly improve the yield of **68** along with better ee and dr value than **67d**. A pseudo-enantiomer of **67e**, dihydroquinidine-derived squaramide **67f** also boosted this reaction but gave **68** with opposite absolute configuration in much lower stereoselectivities in comparison to **67e**. After finding the squaramide catalyst **67e** as the best catalyst for this reaction, then the screening of solvents and temperature in the Michael reaction were performed. Optimized reaction condition was found in chloroform solvent at 0 °C.

Table 1.1. Catalysts screening.[a]

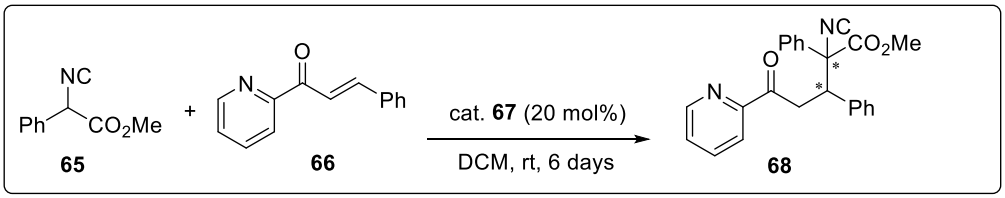

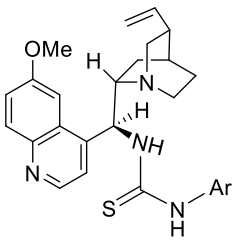

Ar= 3,5-$(CF_3)_2C_6H_3$

67a

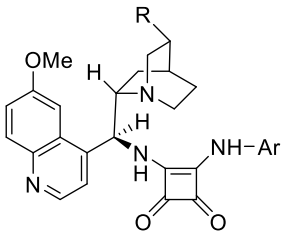

67b: R= vinyl, Ar =4-FC_6H_4
67c: R= vinyl, Ar =4-FC_6H_4
67d: R= vinyl, Ar =4-FC_6H_4
67e: R= Et, Ar =3,5-$(CF_3)_2C_6H_3$

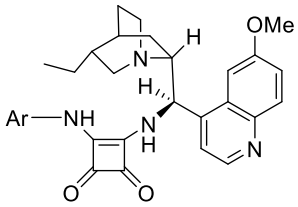

Ar= 3,5-$(CF_3)_2C_6H_3$

67f

Entry	Catalyst	Yield (%)	dr	ee
1	67a	96	1:1	79 (77)
2	67b	99	1:1	85 (78)
3	67c	69	1:1	92 (82)
4	67d	75	1:1	92 (89)
5	67e	99	1:1	94 (91)
6	67f	99	1:1	–91 (–86)

[a] Reactions were carried out on 0.12 mmol of **1a**, 0.1 mmol **2a**, 20% catalyst in DCM at rt for 6 days.

With these optimized reaction conditions, the substrate scope of isocyanoacetates by varying the aryl and ester substituents were investigated. Those bearing an electron-withdrawing substituent afford the Michael adducts with a lower ee value than those having electron donating groups.

A wide range of aryl, heteroaryl, alkyl and ester-substituted 2-enoylpyridines were also evaluated where all of the 2-enoylpyridines, whether bearing electron-withdrawing or electron-donating group on the para, meta or ortho position of the phenyl ring, readily undergo this Michael reaction with isocyanoacetate to afford the desired products in moderate to high yields along with good to excellent diastereo and enantioselectivities.

1.6.3 Squaramide-catalyzed enantioselective Michael addition of masked acyl cyanides to substituted enones.[96]

The Michael addition reaction of masked acyl cyanide (MAC) reagents to enones are efficiently catalyzed by chiral squaramides, affording adducts in high yields (90-99%) and excellent enantioselectivities (85-98%) were reported. This was the first enantioselective reactions of the MAC family of umpolung synthons. Upon unmasking, provided ready access to chiral γ-keto-carboxylic acids, esters, and amides. For the identification of effective catalysts and conditions, the enantioselective Michael reaction between trans-chalcone (**69**) and MOM-MAC (**70**) was examined to afford adduct **72**.

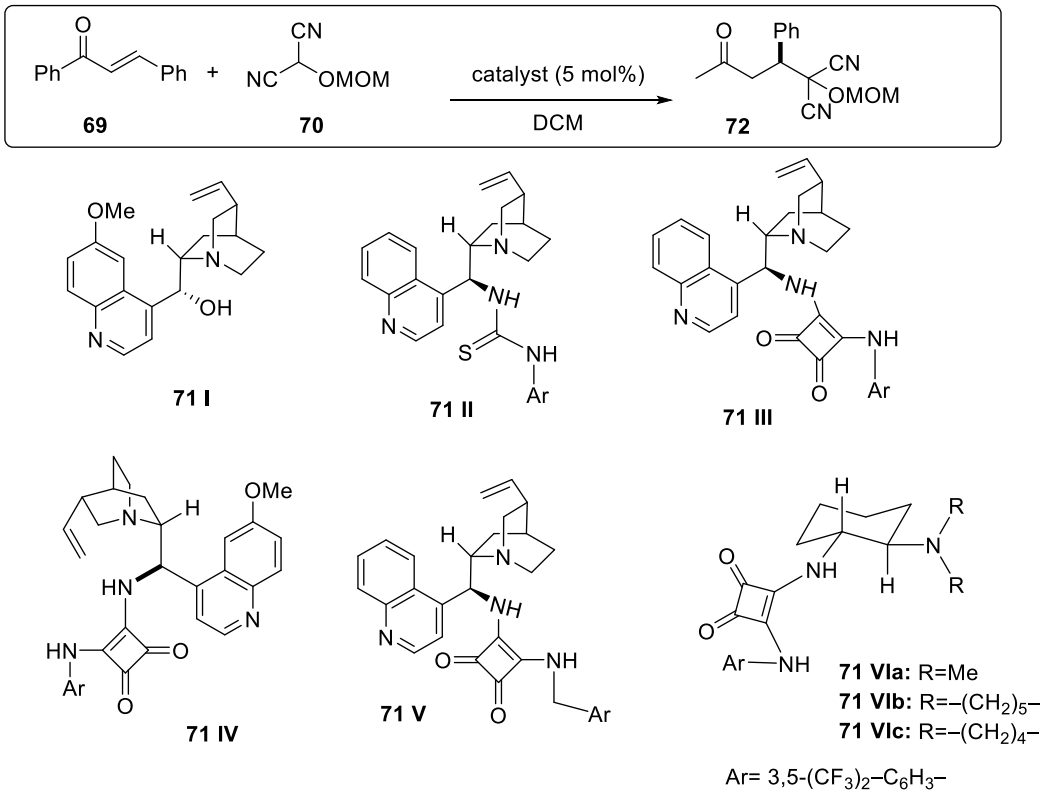

Figure 1.9. Quinine and cinchonidine derived catalysts.

First quinine (**71** I) promoted this reaction affording the adduct with poor enantioselectivity. The cinchonidine-derived thiourea catalyst (**71 II**) gave better enantioselectivity but low conversion. The corresponding squaramide (**71 III**) provided both superior conversion and enantioselectivity. As anticipated, the pseudoenantiomeric, quinidine derived squaramide (**71 IV**) provided the product with comparable selectivity and conversion but enriched in the opposite enantiomer. Among the

other squaramide catalysts examined, those based on 1,2-diaminocyclohexane proved most effective, particularly the pyrrolidine catalyst **71VIc**, which formed **72** at a high rate and with 90% ee. When the reaction was carried out at −30 °C, the enantiomeric excess improved significantly to 97%. Comparable enantioselectivity was observed even at 1 mol % catalyst loading, although with lower conversion. due to the limited solubility of the catalyst, increasing the catalyst loading to 10 mol % did not significantly increase the conversion over the 5 mol % reaction. No improved result was observed with additional solvents investigation.

The practical utility and substrate scope of squaramide-catalyzed enantioselective Michael reactions of MAC reagents was examined. In general, high yields and enantioselectivities were observed for a broad range of enones.

1.6.4 Cinchona squaramide-based chiral polymers as highly eficient catalysts in asymmetric Michael addition reaction.[55]

Novel cinchona squaramide dimers **73Q(a-d)** and **73C(a,b)** were designed that contains two cinchona squaramide units connected by diamines. Then corresponding chiral polymers have been synthesized containing a cinchona-based squaramide in the main chain by applying Mizoroki-Heck polymerization.

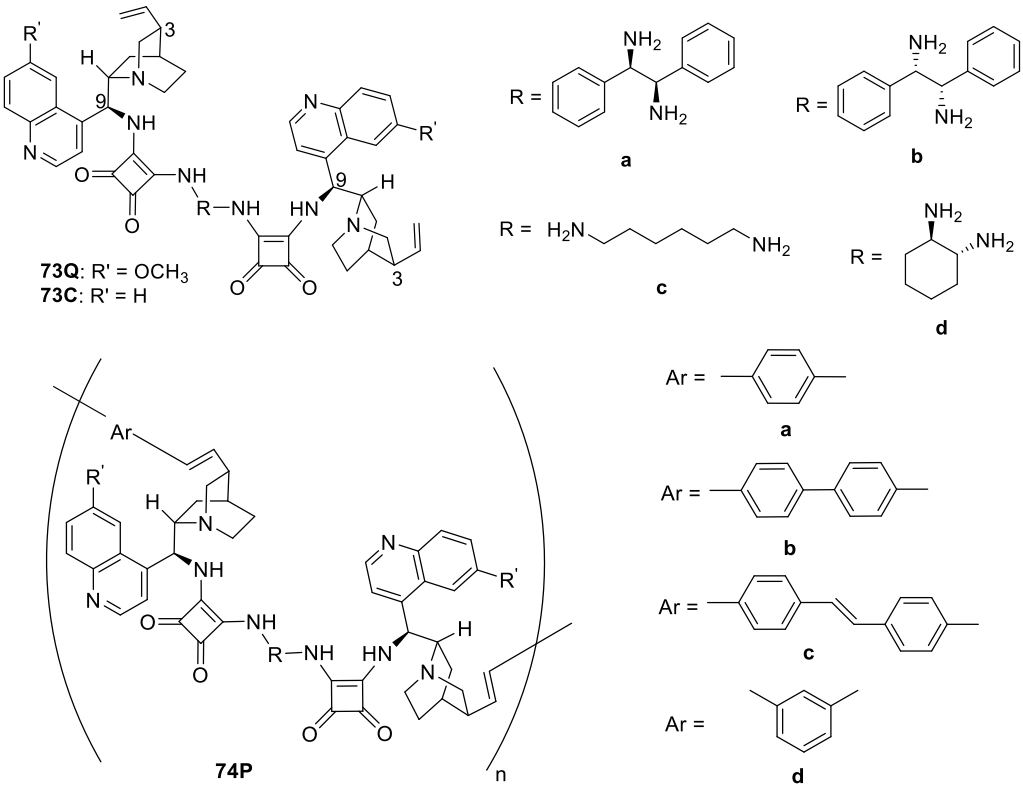

The olefinic double bonds in the cinchona squaramide dimer were used for MH polymerization with aromatic diiodides. to give the corresponding chiral polymers in good yields (73-99%). The catalytic activity of the chiral dimers and polymers was investigated for asymmetric Michael addition reactions of β-ketoesters to nitroolefins.

Table 1.2. Asymmetric Michael addition reaction of β-ketoester **19** to *trans* β-nitrostyrene **20** using squaramide dimers **73** as catalyst.[a]

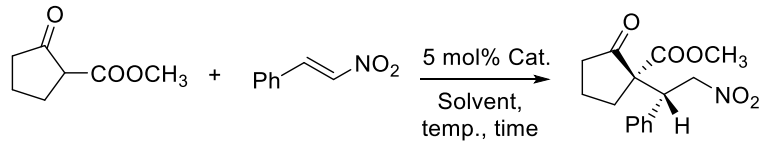

19 **20** **21**

Entry	catalyst	solvent	reaction time, h	yield %	dr	ee %
1	**73Qa**	THF	22	76	>100:1	98
2	**73Qa**	MeOH	24	67	11:1	92
3	**73Qa**	CH_2Cl_2	42	69	52:1	96
4	**73Qb**	THF	26	79	>100:1	94
5	**73Qc**	THF	30	75	35:1	84
6	**73Qd**	THF	16	70	19:1	70
7	**73Ca**	THF	31	45	65:1	90
8	**73Cb**	THF	30	46	>100:1	87

[a]Reactions were carried out with **19** (0.5 mmol), *trans*-β-nitro-styrene **20** (0.55 mmol), and catalyst **73** (5 mol%) in solvent (2.5 mL) at rt.

73Qa promoted the reaction smoothly in THF at room temperature to give the Michael adduct **21** in 76% yield with 98% ee for the major diastereomer (Table 1.2, entry 1). The diastereomeric ratio (*dr*) of the product was also very high (>100:1). Lower stereoselectivity, dr and ee was observed in methanol (entry 2). The effect of the diamine linker (**R** in **73**) was also investigated An appropriate combination of the cinchona moiety and diamine linker in this catalyst is **73Qa** prepared from (*R*,*R*)-amine **a** gave the best result.

Table 1.3. Asymmetric Michael addition reaction of β-ketoester **19** to nitroolefin **20** using polymers **74P** as catalysts at rt in THF.[a]

entry	catalyst	solvent	reaction time, h	yield %	dr	ee %
1	**74PQaa**	THF	22	68	60:1	95
2	**74PQba**	THF	24	71	33:1	97
3	**74PQca**	THF	40	75	46:1	93
4	**74PQda**	THF	50	57	28:1	90
5	**74PCaa**	THF	22	72	68:1	95
6	**74PCba**	THF	22	68	55:1	96

[a]Reactions were carried out with **19** (0.5 mmol), **20** (0.55 mmol) and catalyst **74P** (5 mol%) in 2.5 mL THF at rt.

The chiral polymer **74PQaa** prepared from **73Qa** and 1,4-diiodobenzene was identified as the best polymeric catalyst by applying all polymers in the same reaction. Most of the chiral polymer catalysts **74P** afforded the chiral product **21** with higher enantioselectivities compared to those of the corresponding low-molecular-weight catalysts **73** under the same reaction conditions.

1.6.5 Chiral squaramide-catalyzed asymmetric synthesis of pyranones and pyranonaphthoquinones via cascade reactions of 1,3-dicarbonyls with Morita-Baylis-Hillman acetates of nitroalkenes.[97]

A chiral squaramide-catalyzed cascade reaction of 1,3-dicarbonyl compounds, including 2-hydroxy-1,4-naphthoquinone, with Morita–Baylis–Hillman (MBH) acetates of nitroalkenes affords pyrans and pyranonaphthoquinones (a-lapachones) in high yields and excellent diastereo and enantioselectivities.

Table 1.4 Optimization of catalysts.[a]

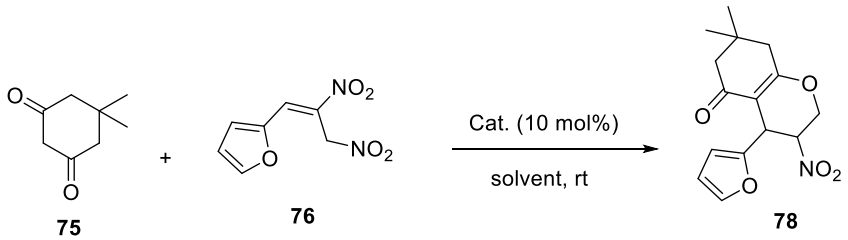

Entry	Catalyst	Solvent	Time	Yield %	ee %
1	**77c1**	THF	1 h	80	0
2	**77c2**	THF	2 h	78	24
3	**77c3**	THF	4 h	89	50
4	**77c3**	THF	7 h	90	57
5	**77c4**	THF	5 h	88	51
6	**77c5**	THF	5 h	85	65
7	**77c6**	THF	3 h	94	69
8[b]	**77c6**	THF	48 h	88	60
9	**77c7**	THF	5 h	87	52
10	**77c8**	THF	5.5 h	85	54
11	**77c9**	THF	15 min	90	92
12	**77c10**	THF	15 min	92	86

[a]Reaction was done with 0.11 mmol **75**, 0.1 mmol **76** and 0.01 mmol of catalyst 77c in 0.5 mL THF under N_2; [b]–40°C.

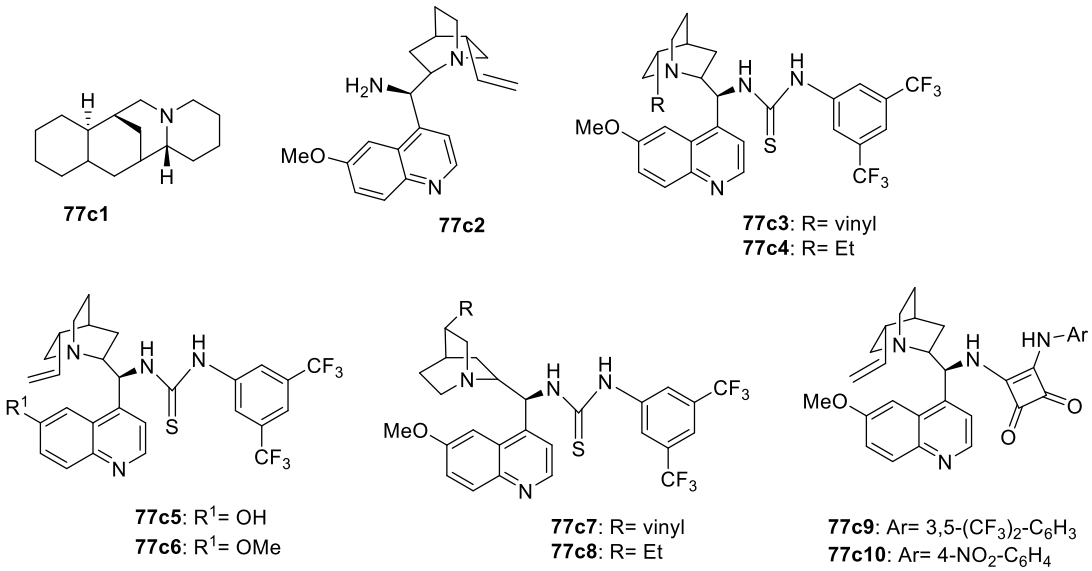

Figure 1.10. Structure of catalysts.

To identify suitable reaction conditions for the asymmetric Michael addition cascade, the reaction of dimedone **75** and MBH-acetate **76** was chosen as the model substrates and 10 mol% of **77c1**–**c10** used as the catalysts (Fig. 1.9 and Table 1.4). When the reaction was carried out in THF using **77c1** as the catalyst, complete conversion was observed in 1 h to give the product in 80% yield, but no selectivity (entry 1). Thus, the product **78** was isolated in good to excellent yield (78–94%), when cinchona-derived thiourea catalysts **77c2**–**c8** were screened (entries 2–10) but the selectivity remained low to moderate (24–69% ee). Then quinine-squaramide catalysts **77c9** and **77c10** were applied which enhanced the selectivities. When squaramide **77c9** was employed 92% ee was obtained with 90% yield and only 15 min required. A slight improvement in the yield with a

marginal drop in the selectivity was observed in the presence of squaramide **77c10**. Several solvents were screened at room temperature with the aim of further improving the selectivity with catalyst **77c9**. Finally, 10 mol% of catalyst **77c9** in 1,4-dioxane at rt was identified as the best condition for further reactions. Cascade reactions of 1,3-dicarbonyls with a variety of Morita–Baylis–Hillman acetates of nitroalkenes using a quinine derived chiral squaramide organocatalyst led to the formation of pyranones and pyrano- naphthoquinones in good to excellent yields and high diastereo and enantioselectivities.

1.6.6 Synthesis of cinchona alkaloid squaramide polymers as bifunctional chiral organocatalysts for the enantioselective Michael addition of β-ketoesters to nitroolefins.[46]

Dimeric cinchona squaramide **18** possesses two terminal double bonds, which is ideal for Mizoroki-Heck (MH) polymerization. The double bonds of **18** were able to react with aromatic diiodides. Repetitive Mizoroki-Heck reactions between dimeric cinchona squaramide **18** and various aromatic diiodides gave chiral polymers **79P**. In order to assess the catalytic activity of the chiral cinchona squaramide polymers **79P**, the asymmetric Michael addition of methyl 2-oxocyclopentanecarboxylate **19** to *trans*-β-nitrostyrene **20** was chosen as a model reaction. Firstly, the dimeric cinchona squaramide **18** was examined as an organocatalyst in the asymmetric Michael reaction. **18** showed excellent performance in the asymmetric reaction. The reaction between **19** and **20** with **18** in CH_2Cl_2 at room temperature proceeded smoothly to give the Michael adduct **21** in 95% yield with 91% ee (Table 1.5, entry 1). A high level of diastereoselectivity (79:1) was also attained with this catalyst. Then the corresponding polymeric catalysts were applied in the same reaction. First, polymeric catalyst **79Pa** was tried. Although **79Pa** was totally insoluble in CH_2Cl_2, the reaction occurred at room temperature to give the corresponding adduct in 71% yield with 97% ee (entry 2). Due to the heterogeneous system, a longer reaction time was required for the polymeric catalyst.

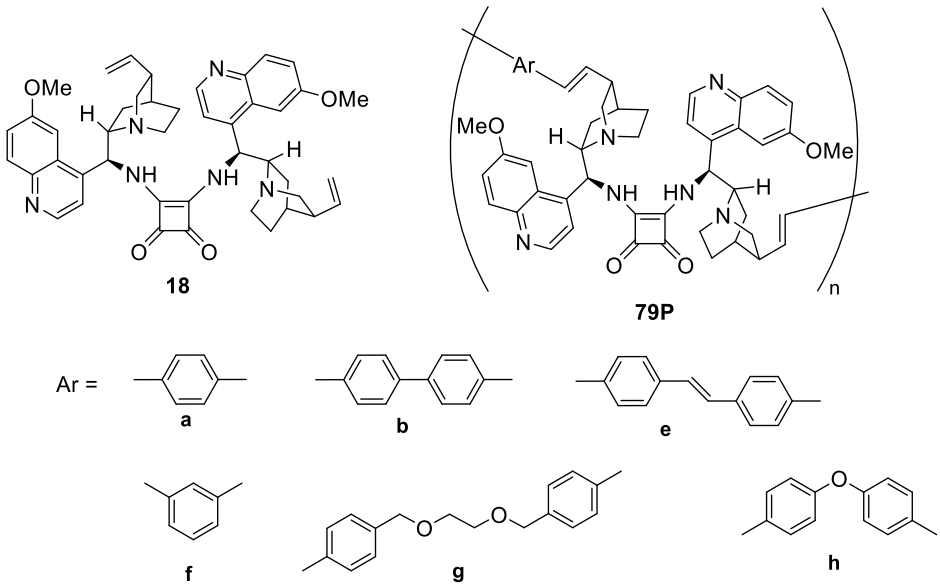

Interestingly, the enantioselectivity obtained with the polymeric catalyst **79Pa** was higher than that obtained with the corresponding low-molecular-weight catalyst **18**. The choice of solvent also influenced the catalytic activity and the enantioselectivity of the reaction, EtOAc was found as a best solvent as shown in Table 1.5. Then polymeric catalysts **79Pb-79Ph** containing differing linker structures were trialed to see the effect of the polymer structure on the stereoselectivity of the reaction. Catalyst **79Pb** (entries 6, 7, and 8), with a biphenyl linker, showed similar performance to that of **79Pa**. Catalyst **79Pf** uses a meta-substituted phenyl linker, which formed the product in a slightly reduced enantioselectivity and diastereoselectivity. A flexible linker structure as in **79Pg** gave no significant influence on the catalytic activity and the stereoselectivity. Using a stilbene linker **79Pe** or a diphenyl ether linker **79Ph** gave the Michael adduct in somewhat lower enantioselectivities. Chiral polymers developed in this study were insoluble in commonly used organic solvents, so after the reaction, the polymers were easily separated and recovered by simple filtration.

Table 1.5. Optimization of reaction conditions: solvent screening for the enantioselective Michael addition of β-ketoester **19** to nitroolefin **20**

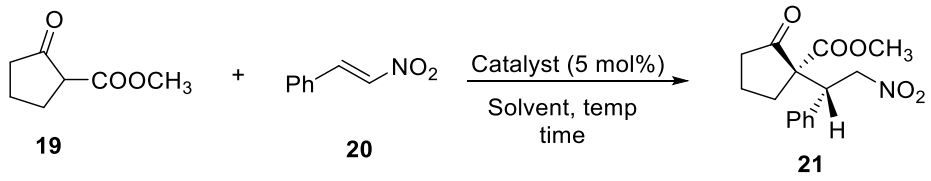

19 **20** **21**

Entry	catalyst	solvent	temp.,°C	reaction time, h	yield ,%[b]	*dr*[c]	*ee*, %[c]
1	**2SQ**	CH_2Cl_2	rt.	2	95	79:1	91
2	**4PaSQ**	CH_2Cl_2	rt.	30	71	28:1	97
3	**4PaSQ**	THF	rt.	36	77	23:1	93
4	**4PaSQ**	Toluene	rt.	43	55	16:1	88
5	**4PaSQ**	EtOAc	rt.	22	66	20:1	96
6	**4PbSQ**	CH_2Cl_2	rt.	30	63	34:1	91
7	**4PbSQ**	MeOH	rt.	16	56	34:1	93
8	**4PbSQ**	EtOAc	rt.	22	76	18:1	95
9	**4PbSQ**	EtOAc	-10	29	54	19:1	96
10	**4PeSQ**	EtOAc	rt.	21	60	17:1	90
11	**4PfSQ**	EtOAc	rt.	30	60	13:1	94
12	**4PgSQ**	EtOAc	rt.	20	63	21:1	95
13	**4PhSQ**	EtOAc	rt.	20	69	22:1	92

[a]Reactions were carried out with **5** (0.50 mmol), *trans*-β-nitrostyrene **6** (0.55 mmol) and the monomeric and polymeric catalyst (5 mol%) in 2.5 mL solvent.

1.6.7 A bifunctional *cinchona* alkaloid-squaramide catalyst for the highly enantioselective conjugate addition of thiols to *trans*-chalcones.[98]

A variety of bifunctional squaramide organocatalysts have prepared. Squaramide-substituted Cinchona alkaloid derivatives **82a–82f** prepared, which were accessed via amination of commercially available dimethyl squarate. The addition of benzyl thiol to trans-chalcone was chosen as a model reaction to determine the catalytic activity of the squaramide catalysts **82a–82f** (Table 1.6).

The catalysts **82a** and **82b** were first examined which had different substituents on the para position of the aromatic rings. Electron-donating groups on the aryl group prolonged the reaction time but did not affect the stereochemistry. Meta position- substituted catalysts **82c–e, 82d** and **82e** showed marked superiority on enantioselectivity. A value of 92% ee was obtained with catalyst **82e**, possessing two CF_3 groups on the aromatic ring which implied that steric hindrance of the aromatic rings and acidity of the squaramide N-H groups were related directly to the stereoselectivity and chemical yield. Catalyst **82f** gave unsatisfactory result. After identification of best catalyst **82e**, a screening of solvents in the Michael reaction of benzyl thiol and trans-chalcone at room temperature was undertaken. Consistent with our speculation, non-polar solvents were more suitable for H-bonding catalysis reactions. Excellent reaction rate and enantiocontrol were obtained when toluene was used as solvent.

Table 1.6. Asymmetric conjugate addition of benzyl thiol **80** to trans-chalcone **81** with squaramide catalysts **82**.[a]

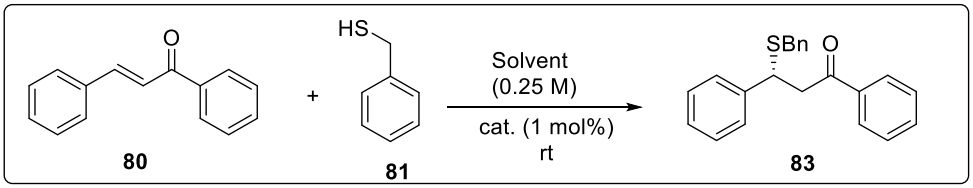

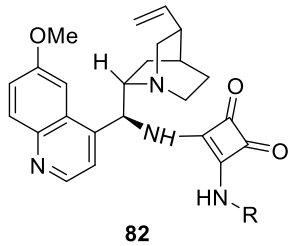

82

82a: R= 4-MeO-C_6H_4
82b: R= 4-CF_3-C_6H_4
82c: R= 3,5-Cl_2-C_6H_3
82d: R= 3,5-Me_2-C_6H_3
82e: R= 3,5-$(CF_3)_2$-C_6H_3
82f: R= cyclohexyl

Entry	Solvent	Catalyst	Reaction time [h]	Yield %	ee %
1	CH_2Cl_2	**82a**	6	81	63
2	CH_2Cl_2	**82b**	3	91	63
3	CH_2Cl_2	**82c**	3	90	62
4	CH_2Cl_2	**82d**	10	81	84
5	CH_2Cl_2	**82e**	3	98	92
6	CH_2Cl_2	**82f**	12	48	33
7	$CHCl_3$	**82e**	3	98	94
8	THF	**82e**	5	92	90
9	Et_2O	**82e**	5	91	94
10	Toluene	**82e**	3	97	96
11	MeCN	**82e**	3	93	33
12	MeOH	**82e**	3	95	10

[a]The reaction between *trans*-chalcone (0.25 mmol) and benzyl thiol (0.375 mmol) was carried out in 1 mL solvent in the presence of 1 mol% catalyst at room temperature.

The absolute configuration of the C-3 position of **83** was determined to be *R* by comparison with the reported optical rotation data. Under these optimized experimental conditions, a range of thiols was surveyed. Moderate to excellent yields and high enantioselectivities (up to 99% ee) were achieved under mild conditions.

1.6.8 Cinchona squaramide-catalyzed intermolecular desymmetrization of 1,3-diketones leading to chiral 1,4-dihydropyridines.[99]

An unprecedented organocatalytic desymmetrization of prochiral 5-substituted 1,3-cyclohexanediones **84** with benzylidene pyruvates **85** applying chiral squaramide catalysts was presented. The reaction of dimedone with benzylidene pyruvate **85** occurs effectively applying various types of catalysts.

Table 1.7. Catalyst screening. The order of organocatalysts refers to acidity of the N-H bond.[a]

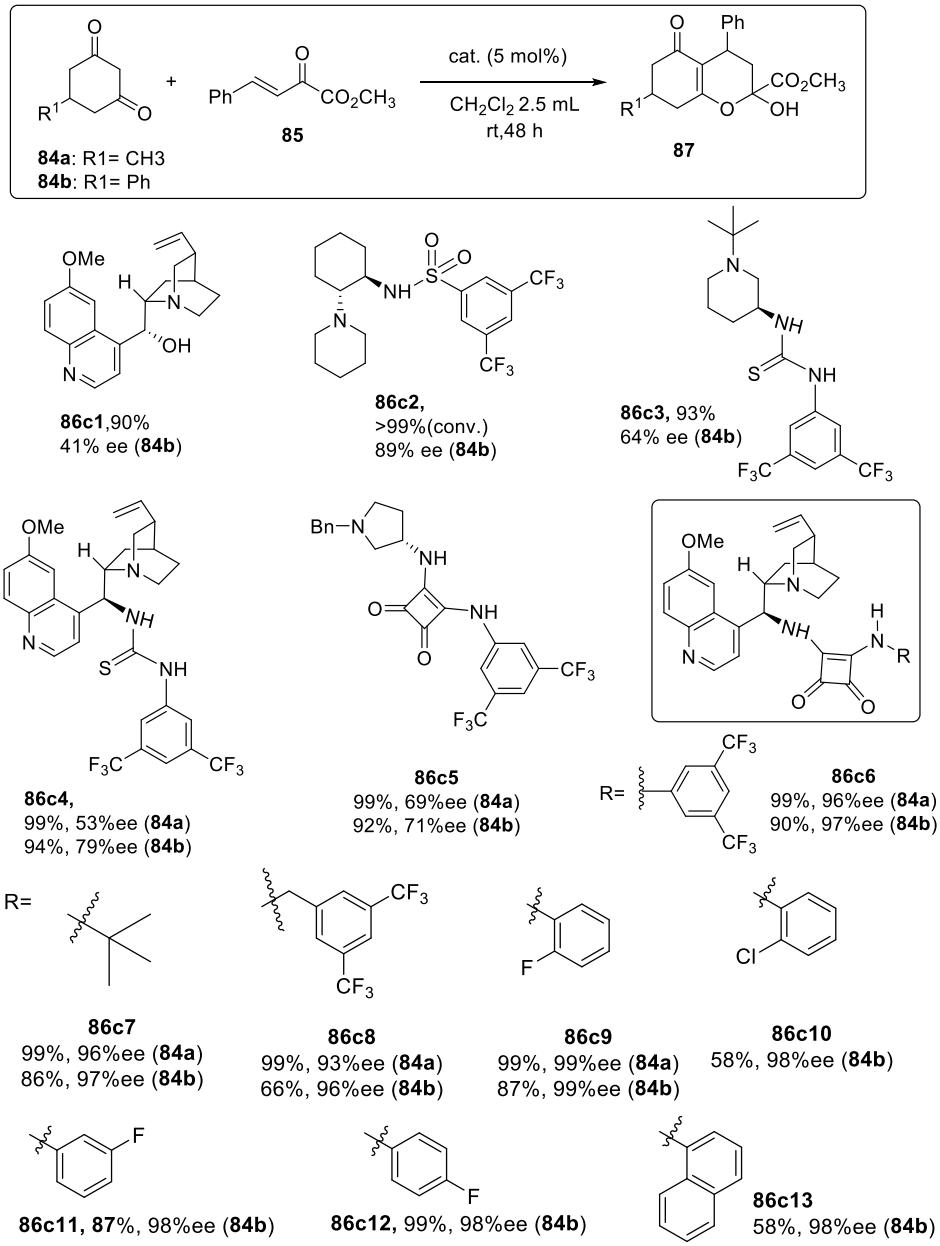

[a]Unless otherwise noted, reactions were performed with **84** (0.5 mmol), **85** (0.55 mmol), catalyst **86c** (5 mol%) in dichloromethane (2.5 mL) at rt for 48 h.

Application of the same reaction conditions for the most effective sulfonamide 86c2 provided a mixture of adduct forms (epimeric hemiacetals and open chain) with only 89% ee for the reaction of 5-phenyl-1,3-cyclohexanedione (84b) (Table 1.7). Further catalyst screening showed that increase of acidity of N- H bonds from quinine (86c1), through sulfonamide (86c2) and thioureas (86c3, 86c4)

to squaramides (86c5, 86c6), resulted in improvement of stereoselectivity of the tested transformation. Catalysts with quinine scaffold 86c6–c13 proved to be superior to pyrrolidine derivative 86c5, but the substitution pattern in squaramide moiety turned out to exert lesser impact on enantioselectivity. 86c9 was found as best catalyst (Table 1.7). Further evaluation of substrate scope applying various 5-aryl-1,3-cyclohexanodiones was performed which gave excellent enantioselectivity (92–>99 % ee). Finally, chiral *Cinchona* alkaloid-based squaramides proved to be effective catalysts in the stereoselective transformations of prochiral 5-substituted 1,3-cyclohexanediones.

1.6.9 Synthesis and applications of cinchona squaramide-modified Poly(glycidyl methacrylate) microspheres as recyclable polymer-grafted enantioselective organocatalysts.[100]

The poly(glycidyl methacrylate) (PGMA) polymer support was prepared by dispersion polymerization in methanol (Scheme 1.19). Obtaining microspheres with narrow size distribution and high reactivity to allow easy chemical modification was the goal.

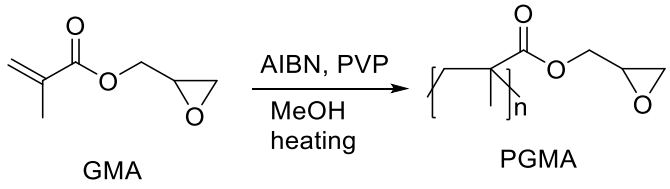

Scheme 1.24 Preparation of PGMA by dispersion radical polymerization of PVP in the presence of AIBN initiator.

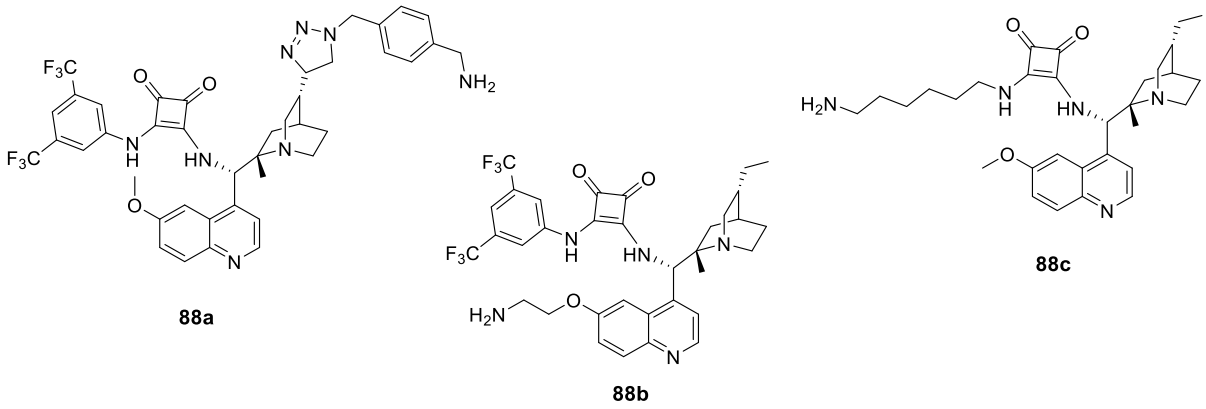

Figure 1.11. Structure of precatalysts

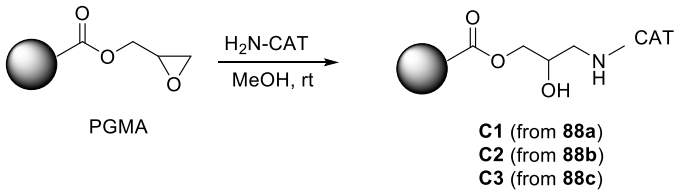

Scheme 1.25 Preparation of the immobilized catalysts C1–C3.

The immobilization of the primary amino group-containing cinchona derivatives **88a**, **88b**, and **88c** on cross-linked PGMA (Scheme 1.20) was carried out in MeOH to gain three new solid-

supported organocatalysts (C1, C2, and C3). The amount of the immobilized precatalysts on the solid support was determined by elemental analysis of the catalysts (C1–C3) by using energy dispersive X-ray analysis (EDX).

Table 1.8. Test of catalysts in the Michael reaction using trans- β-nitro- styrene (**89**) and pentane-2,4-dione (**54**)[a]

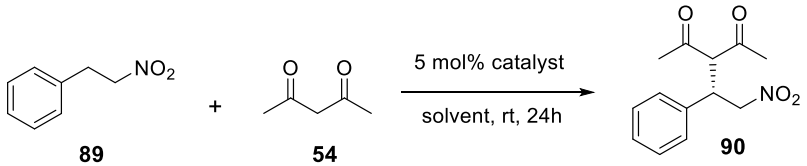

89 **54** **90**

Round	Catalyst	Solvent	Yield [%]	ee [%][b]
1	**C1**	EtOAc	97	6
2	**C1**	EtOAc	98	6
3	**C1**	EtOAc	98	5
4	**C1**	EtOAc	98	4
1	**C1**	CH_2Cl_2	87	29
2	**C1**	CH_2Cl_2	89	31
3	**C1**	CH_2Cl_2	90	21
4	**C1**	CH_2Cl_2	90	21
-	Non modified PGMA[c]	CH_2Cl_2	Not observed	-
-	**88a**	CH_2Cl_2	91	81
-	**88b**	CH_2Cl_2	92	92
-	**88c**	CH_2Cl_2	87	85
1	**C2**	CH_2Cl_2	89	78
2	**C2**	CH_2Cl_2	87	79
3	**C2**	CH_2Cl_2	82	75
4	**C2**	CH_2Cl_2	80	73
1	**C3**	CH_2Cl_2	87	59
2	**C3**	CH_2Cl_2	87	58
3	**C3**	CH_2Cl_2	82	56
4	**C3**	CH_2Cl_2	83	56

[a]Reaction conditions: pentane-2,4-dione (14, 0.407 mmol) was added to the solution of trans-b-nitrostyrene (13, 0.157 mmol) in the presence of 5 mol % catalyst in 0.5 mL of solvent, then the resulting mixture was stirred at r.t. for 24 h. [b]Determined by chiral HPLC (the configuration of the major enantiomer is S). [c]50 mg of non-modified, cross-linked PGMA was used instead of catalysts under the same reaction conditions.

Catalyst **C1** was first applied in a reaction between pentane-2,4-dione (**54**) and trans-β-nitrostyrene (**89**) in two solvents (EtOAc and CH_2Cl_2). After the organocatalytic reaction (Table 1.8), the catalysts were recycled by centrifugation and the recovered catalyst was reused four times in the same reaction. **C1** provided Michael adducts with high yields, but enantiomeric excess values were low. For confirmation that the low ee values are not caused by the PGMA support acting as a competitive catalyst, the Michael reaction was carried out using non-modified PGMA and product formation was not observed. Michael reaction was carried out with the non-immobilized (homogeneous) precatalysts as well. As the ee was significantly higher when using CH_2Cl_2, catalysts **C2** and **C3** were tested only in this solvent. After five cycles, degradation or deformation of any cinchona-modified PGMA catalyst was not observed based on the SEM images. When catalyst **C2** or **C3** was applied, the enantiomeric excess values were higher (up to 79%) than **C1**. Among the immobilized catalysts, the best results were obtained with catalyst **C2**. Regarding the ee, stronger H-bonds could form between the corresponding substrate and the **C2** catalyst containing a

bis(trifluoromethyl)- phenyl modified squaramide moiety. This can result in stronger interaction between the catalyst and substrates, allowing a more definite stereocontrol of the reaction. The selectivities given by these precatalysts (**88a-c**) were higher than those that resulted when the corresponding immobilized ones were applied (**C1**–**C3**). The best results were obtained by the application of recyclable catalyst **C2** at room temperature (and the enantioselectivity may increase by decreasing the temperature). These results show that immobilization of cinchona squaramide organocatalyst on cross-linked PGMA solid support is a feasible method to resolve the inconvenient recycling of the corresponding homogeneous organocatalyst. Finally, the modification of PGMA microspheres with amino functionalized organo- catalysts is a generally applicable approach that could be utilized for a wide variety of organocatalysts.

1.6.10 Cinchonamine squaramide catalyzed asymmetric aza-Michael reaction: dihydroisoquinolines and tetrahydropyridines.[101]

This work describes an efficient intramolecular aza-Michael addition of enamines to a broad class of Michael acceptors, with ketones, esters, thioesters, and Weinreb amides, to produce cyclic enamines with high levels of enantioselectivity by using an amino-squaramide-based bifunctional organocatalyst (**92a-g**). Investigation began by using ortho-homoformyl chalcone **91** as a starting substrate for the synthesis of the dihydroisoquinoline **93** (Table 1.9). Further, a variety of other chiral cinchona-alkaloid-derived (**92a**–**g**) and cyclohexadiamine-derived thiourea/squaramide catalysts were surveyed (entries 1–7). **92g** was found to catalyze the reaction cleanly to furnish **93** in 60 % yield and with excellent enantioselectivity 96% ee.

Table 1.9. Optimization of reaction conditions.[a]

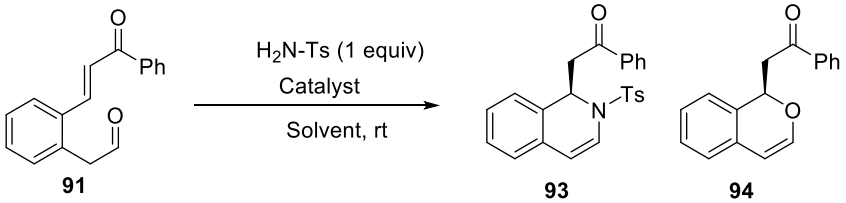

91 **93** **94**

Entry	Catalyst	Solvent	Yield%	ee %
1	2a	1,2-DCE	26	75
2	2b	1,2-DCE	45	80
3	2c	1,2-DCE	43	75
4	2d	1,2-DCE	47	96
5	2e	1,2-DCE	49	66
6	2f	1,2-DCE	56	94
7	2g	1,2-DCE	60	96
8	2g	Toluene	60	96
9	2g	$CHCl_3$	83	96

[a]All reactions were performed on 0.1 mmol scale of aldehyde; DCE = dichloroethane, Ts = 4-toluenesulfonyl.

Further, screening of various organic solvents using **92g** gave the best solvent $CHCl_3$ for this reaction. The substrate scope was explored by using these optimized reaction conditions. Excellent yields and enantioselectivities (average: 97% ee) were obtained with substrates containing various aryl and heteroaryl groups at the terminal position of the enone.

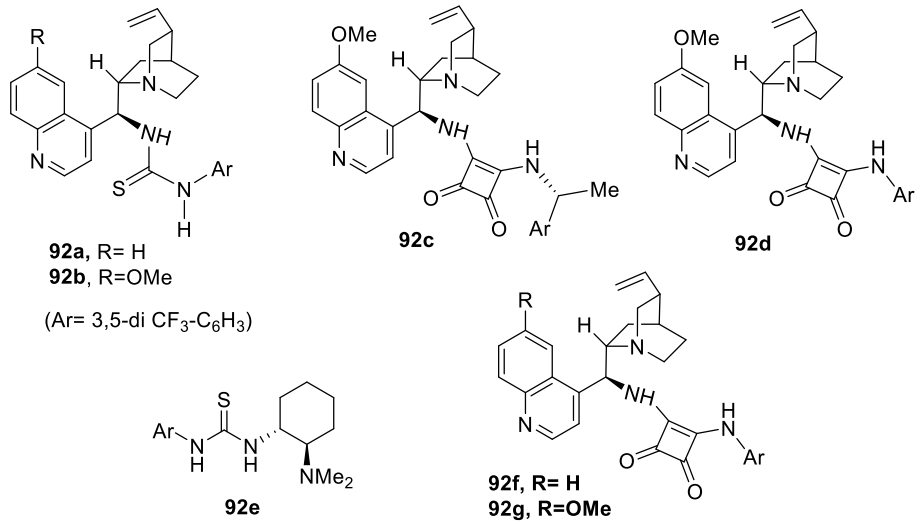

Figure 1.12. Structure of catalysts.

Various amine sources such as Boc-NH_2, Cbz-NH_2, PMB-NH_2, $PhNH_2$, Bn-NH_2, Bz-NH_2 and Ts-NH_2 were examined using the chiral cinchona alkaloid-derived squaramide catalyst **92g** in 1, 2-DCE as a solvent at room temperature only Ts-NH_2 provided the desired **93** in 31 % yield with 96 % enantioselectivity.

1.6.11 Chiral squaramide-catalyzed highly enantioselective Michael addition of 2-hydroxy-1, 4-naphthoquinones to nitroalkenes.[102]

A variety of chiral squaramide-based bifunctional organocatalysts have been synthesized and successfully applied to assist the asymmetric Michael addition of 2-hydroxy-1, 4-naphthoquinones to nitroalkenes. Under mild reaction conditions, very low amount of catalyst loading (0.25 mol %) is highly effective to give good-to-excellent yields and excellent enantioselectivities (95-98% ee).

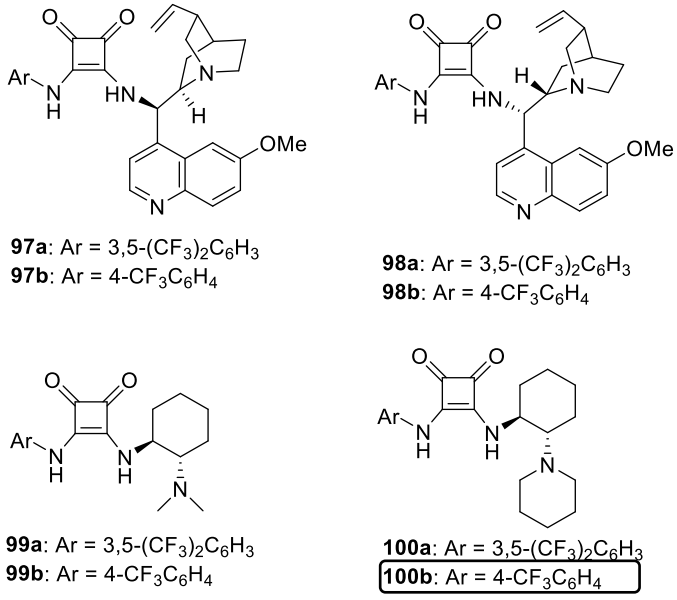

Figure 1.13. Structures of squaramide organocatalysts.

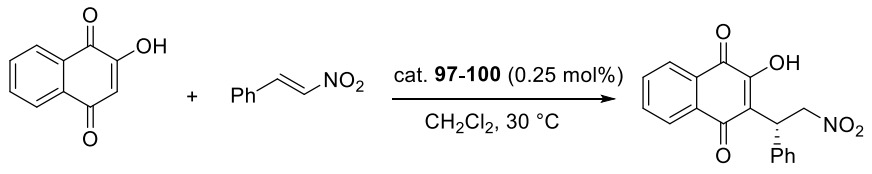

95 96 101

Scheme 1.26. Asymmetric reaction of 2-hydroxy-1,4-naphthoquinone **95** to *trans*-β-nitrostyrene **96.**

Among all squaramide catalysts, catalyst **100b** was selected as the best catalyst for the synthesis of the asymmetric compound **101**. The asymmetric results are summarized in the table **1.10**.

Table 1.10. Screening of organocatalysts for the asymmetric Michael addition of 2-hydroxy-1,4-naphthoquinone **95** to β-nitrostyrene **96**.[a]

entry	catalyst	yield %	ee, %	config.
1	**97a**	94	91	*R*
2	**97b**	96	92	*R*
3	**98a**	96	-87	*S*
4	**98b**	96	-86	*S*
5	**99a**	95	89	*R*
6	**99b**	96	87	*R*
7	**100a**	97	97	*R*
8	**100b**	97	98	*R*

[a]Reactions were carried out with β-nitrostyrene **96** (0.2 mmol) and 2-hydroxy-1,4-naphthoquinone **95** (0.2 mmol) in CH_2Cl_2 (0.5 mL).

This catalytic asymmetric reaction provides a valuable and easy access to chiral naphthoquinone derivatives, which possess the versatile transformation possibilities and potential biological activity. Given the highly modular nature and facile synthesis, chiral squaramides may represent a kind of good hydrogen-bonding organocatalyst.

Reference

1. Lancaster. M. *Green Chemistry: An Introductory Text*, The Royal Society of Chemistry, Cambridge, UK, **2002**, pp 310

2. List. B. *Chem. Rev.* **2007**, *107*, 5413–5415.

3. Dalko, P. I.; Moisan, L. *Angew. Chem. Int. Ed*. **2004**, *43*, 5138–5175.

4. MacMillan, D. W. *Nature* **2008**, *455*, 304–308.

5. Dalko, P. I. *Comprehensive Enantioselective Organocatalysis: Catalysts, Reactions, and Applications, 3 Volume Set*; John Wiley & Sons: 2013.

6. Notz, W.; Tanaka, F.; Barbas, C. F. *Accounts of Chemical Research* **2004**, *37*, 580–591.

7. Shaikh, I. R. *Journal of Catalysts* **2014**, *2014*, 1–35.

8. Ahrendt, K. A.; Borths, C. J.; MacMillan, D. W. C. *J. Am. Chem. Soc*. **2000**, 122, 4243–4244.

9. Pracejus, H. *Justus Liebigs Ann. Chem*., **1960**, *634*, 9–22.

10. List B.; Lerner R. A.; Barbas III C. F. *J. Am. Chem. Soc.*, **2000**, *122*, 2395–2396.

11. Gröger H.; Wilken J. *Angew. Chem. Int. Ed.*, **2001**, *40*, 529–532.

12. Shu, L.; Shi, Y. *J. Org. Chem.* **2000**, *65*, 8807–8810.

13. Corey, E. J.; Xu, F.; Noe, M. C. *J. Am. Chem. Soc.* **1997**, *119*, 12414–12415.

14. Sellergren, B.; Karmalkar, R. N.; Shea, K. J. *J. Org. Chem*, **2000**, *65*, 4009–4027.

15. (a) Dondoni, A.; Masi, A. *Angew. Chem., Int. Ed*. **2008**, *47*, 4638–4660.

(b) Pellissier, H. *Tetrahedron* **2007**, *63*, 9267–9331.

16. Noyori, R.; Hashiguchi, S. *Acc. Chem. Res.,* **1997**, *30*, 97–102.

17. Katsuki, T.; Sharpless, K. B. *J. Am. Chem. Soc*. **1980**, *102*, 5974–5976.

18. Yu, X.; Wang, W. *Organic & Biomolecular Chemistry* **2008**, *6*, 2037–2046.

19. Volla, C. M.; Atodiresei, I.; Rueping, M. *Chemical Reviews* **2013**, *114*, 2390–2431.

20. Nicewicz, D. A.; MacMillan, D. W. *Science* **2008**, *322*, 77–80.

21. Mase, N.; Tanaka, F.; Barbas III, C. F. *Angew. Chem., Int. Ed.* **2004**, *43*, 2420–2423.

22. Hayashi, Y.; Gotoh, H.; Hayashi, T.; Shoji, M. *Angew. Chem., Int. Ed***. 2005**, *117*, 4284–4287.

23. Andrey, O.; Alexakis, A.; Tomassini, A.; Bernardinelli, G. *Adv. Synth. & Catal.* **2004**, *346*, 1147–1168.

24. Zhang, Y.; Wang, W. *Catal Sci & Technol.* **2012**, *2*, 42–53.

25. Marigo, M.; Franzen, J.; Poulsen, T. B.; Zhuang, W.; Jørgensen, K. A. *J. Am. Chem. Soc.* **2005**, *127*, 6964–6965.

26. Wang, X.; Reisinger, C. M.; List B. *J. Am. Chem. Soc.* **2008**, *130*, 6070–6071.

27. Brown, S. P.; Brochu, M. P.; Sinz, C. J.; MacMillan, D. W. *J. Am. Chem. Soc* **2003**, *125*, 10808–10809.

28. Denmark, S. E.; Wynn T. *J. Am. Chem. Soc.* **2001**, *123*, 6199–6200.

29. O'donnell, M. J. *Accounts of Chemical Research* **2004**, *37*, 506–517.

30. Shi, M.; Lei, Z.-Y.; Zhao, M.-X.; Shi, J.-W. *Tetrahedron Letters* **2007**, *48*, 5743– 5746.

31. Tian, S.-K.; Chen, Y.; Hang, J.; Tang, L.; McDaid, P.; Deng, L. *Accounts of Chemical Research* **2004**, *37*, 621–631.

32. Rabe, P.; Ackerman, E.; Schneider, W. *Chem. Ber*. **1907**, *40*, 3655–3658.

33. Yeboah, E. M.; Yeboah, S. O.; Singh, G. S. *Tetrahedron* **2011**, *67*, 1725–1762.

34. Ye, J.; Dixon, D. J.; Hynes, P. S. *Chem. Commun.* **2005**, *322*, 4481–4483.

35. Song, C. E., *Cinchona alkaloids in synthesis and catalysis: ligands, immobilization and organocatalysis*; John Wiley & Sons: **2009.**

36. Ingemann, S.; Hiemstra, H. *Comprehensive Enantioselective Organocatalysis: Catalysts, Reactions, and Applications*, Wiley-VCH: Weinheim*,* **2013**, pp 119–160.

37. Doyle, A. G.; Jacobsen, E.N. *Chem. Rev*., **2007**, *107*, 5713–5743.

38. Cucinotta, C. S.; Kosa, M.; Melchiorre, P.; Cavalli, A.; Gervasio, F. L. *Chem. Eur. J*. **2009**, *15*, 7913–7921.

39. Robert, W.; David L. P. *J. Am. Chem. Soc*. **1963**, *85*, 2577–2579.

40. Storer, R. I.; Aciro, C.; Jones, L. H. *Chem. Soc. Rev* **2011**, *40***,** 2330–2346.

41. Okino, T.; Hoashi, Y.; Furukawa, T.; Xu, X. N.; Takemoto, Y. *J. Am. Chem. Soc.* **2005**, *127*, 119–125.

42. Ni, X.; Li, X.; Wang, Z.; Cheng, J. P. *Org. Lett*. **2014**, *16*, 1786–1789.

43. Boratyński, P. J. *Molecular Diversity* **2015**, *19*, 385–422.
44. Takata, S.; Endo, Y.; Ullah, M. S.; Itsuno, S. *RSC Advances* **2016**, *6*, 72300–72305.
45. Endo, Y.; Takata, S.; Kumpuga, B. T.; Itsuno, S. *ChemistrySelect* **2017**, *2*, 10107– 10111.
46. Ullah, M. S.; Itsuno, S. *Molecular Catalysis* **2017**, *438*, 239–244.
47. Sharpless, K. B.; Amberg, W.; Bennani, Y. L.; Crispino, G. A.; Hartung, J.; Jeong, K. S.; Kwong, H. L.; Morikawa, K.; Wang, Z. M. *J. Org. Chem.* **1992**, *57*, 2768–2771.
48. Suzuki, H.; Mochizuki, K.; Hattori, T.; Takahashi, N.; Tajima, O.; Takiguchi, T. *Bull. Chem. Soc. Jpn.* **1988**, *61*, 1999–2005.
49. Angiolini, L.; Caretti, D.; Giorgini, L.; Salatelli, E. *Polymer* **2001**, *42*, 4005–4016.
50. Itsuno, S.; Paul, D. K.; Salam, M. A.; Haraguchi, N., *J. Am. Chem. Soc.* **2010**, *132*, 2864–2865.
51. Ahamed, P.; Haque, M. A.; Ishimoto, M.; Parvez, M. M.; Haraguchi, N.; Itsuno, S. *Tetrahedron* **2013**, *69*, 3978–3983.
52. Haraguchi, N.; Ahamed, P.; Parvez, M. M.; Itsuno, S. *Macromolecules* **2012**, *17*, 7569–7583.
53. Kumpuga, B. T.; Itsuno, S. *Catalysis Communications* **2019**, *118*, 5–9.
54. Itsuno, S.; Hassan, M. M. *RSC Advances* **2014**, *4*, 52023–52043.
55. Ullah, M. S.; Itsuno, S. *ACS Omega* **2018**, *3*, 4573–4582.
56. Kumpuga, B. T.; Itsuno, S. *Journal of Catalysis* **2018**, *361*, 398–406.
57. Ullah, M. S.; Itsuno, S. *Chemistry Letters* **2018**, *47*, 1220–1223.
58. Parvez, M. M.; Haraguchi, N.; Itsuno, S. *Macromolecules* **2014**, *47*, 1922–1928.
59. Itsuno, S.; Paul, D. K.; Ishimoto, M.; Haraguchi, N. *Chem. Lett*. **2010**, *39*, 86–87.
60. Haraguchi, N.; Kiyono, H.; Takemura, Y.; Itsuno, S. *Chem. Commun*. **2012**, *48*, 4011–4013.
61. Gao, C.; Yan, D. *Progr. Polymer Sci.* **2004**, *29*, 183–275.
62. Yates, C.R.; Hayes, W. *Eur. Polymer J.* **2004**, *40*, 1257–1281.
63. Yamanaka, K.; Jikei, M.; Kakimoto, M. *Macromolecules* **2000**, *33*, 6937–6944.
64. Zheng, Y.; Li, S.; Weng, Z.; Gao, C. *Chem. Soc. Rev*. **2015**, *44*, 4091–4130.
65. Slagt, M.Q.; Stiriba, S.E.; Kautz, H. H.; Gebbink, R.J.M.K.; Frey, H. H.; Koten, G. *Organometallics* **2004,** *23*, 1525–1532.
66. Astruc, D.; Chardac, F. *Chem. Rev*. **2001**, *101*, 2991–3023.
67. Jikei, M.; Kakimoto, M. *Prog. Polym. Sci*. **2001**, *26*, 1233–1285.
68. Itoh, T. *Polymer electrolytes* **2010**, 524–549.
69. Mizoroki, T.; Mori, K.; Ozaki, A. *Bull. Chem. Soc. Jpn*. **1971**, *44*, 581–581.
70. Dieck, H. A.; Heck, R. F. *J. Am. Chem. Soc*. **1974**, *96*, 1133–1136.
71. Can, L.; Kunbing, O.; Nianfa, Y. *Chem. Res. Chin. Univ*. **2017**, *33*, 742–745.
72. Powell, D. A.; Maki, T.; Fu, G. C. *J. Am. Chem. Soc.* **2005**, *127*, 510–511.
73. Yamamoto, T.; Koizumi, T. *Polymer* **2007**, *48*, 5449–5472.
74. Yamamoto, T.; Yamamoto, A.; Ikeda, S. *J. Am. Chem. Soc*. **1971**, *93*, 3350–3359.
75. Yamamoto, T.; Morita, T.; Miyazaki, Y.; Maruyama, T.; Wakayama, H.; Zhou, Z. H.; Nakamura, Y.; Kanbara, T.; Sasaki, S.; Kubota, K. *Macromolecules* **1992**, *25*, 1214–1223.

76. Yamamoto, T. *Chem. Soc. Jpn*. **2010**, *83*, 43–455.
77. Rattanatraicharoen, P.; Tanaka, Y.; Shintaku, K.; Kawaguchi, T.; Yamabuki, K.; Oishi, T.; Onimura, K. *J. Polym. Sci. part A Polym. Chem*. **2013**, *51*, 1315–1322.
78. Marcelli, T.; Hiemstra, H. *Synthesis* **2010**, *2010*, 1229–1279.
79. (a) Michael, A. *J. Prakt. Chem*. **1887**, *35*, 349–356.
(b) Michael, A.; Freer, P. C. *J. Prakt. Chem*. **1891**, *43*, 390–395.
(c) Michael, A.; Schulthess, O. *J. Prakt. Chem*. **1892**, *45*, 55–63.
(d) Michael, A. *J. Prakt. Chem*. **1894**, *49*, 20–25.
80. Singh, G.S.; Eboah, E. M. Dove press, *Reports in org*. *Chem*. **2016**, *6*, 47–75.
81. Bisai, V.; Bisai, A.; Singh V. K. *Tetrahedron* **2012**, *68*, 4541–4580.
82. Zheng, Y.; Deng, L. *Chem Sci*. **2015**, *6*, 6510–6514.
83. Perera, S.; Naganaboina, V.K.; Wang, L.; Zhang, B.; Guo, Q.; Rout, L.; Zhao, C. G. *Adv Synth Catal*. **2011**, *353*, 1729–1734.
84. Guo, Q, Zhao, C.G. *Tetrahedron Lett*. **2012**, *13*, 1768–1771.
85. Peng, L.; Wang, L.L.; Bai, J. F. et al. *Tetrahedron Lett*. **2011**, *52*, 1157–1160.
86. Okumus, S.; Tanyeli, C.; Demir, A.S. *Tetrahedron Lett*. **2014**, *55*, 4302–4305.
87. Chen, J.R.; Cao, Y.J.; Zou, Y.Q. et al. *Org Biomol Chem*. **2010**, *8*, 1275–1279.
88. Chen, J.R.; Zou, Y. Q.; Fu, L.; Ren, F.; Tan, F.; Xiao, W. J. *Tetrahedron*. **2010**, *66*, 5367–5372.
89. Shi, X.; He, W.; Li, H.; Zhang, X.; Zhang, S. *Tetrahedron Lett*. **2011**, *52*, 3204–3207.
90. Liu, B.; Han, X.; Dong, Z.; Lv, H.; Zhou, H.B.; Dong, C. *Tetrahedron Asymmetry*, **2013**, *24*, 1276–1280.
91. Miyaji, R.; Asano, K.; Matsubara, S. *Org Biomol Chem*. **2014**, *12*, 119–122.
92. Dai, L.; Wang, S.X.; Chen, F. E. *Adv Synth Catal*. **2010**, *352*, 2137–2141.
93. Malerich, J. P.; Hagithara, Rawal, V. H. *J Am Chem Soc*. **2008**, *130*, 14416–14417.
94. Rana, K.; Unhale, R.; Singh V.K. *Tetrahedron Lett*. **2012**, *53*, 2121–2124.
95. Zhao, M.-X.; Zhu, G.-Y.; Zhao, X. -L.; Shi, M. *Tetrahedron* **2019**, *75*, 1171–1179.
96. Yang, K. S.; Nibbs, A. E.; Türkmen, Y. E.; Rawal V. H. *J. Am. Chem. Soc.* **2013**, *135*, 16050–16053.
97. Nair, D. K.; Menna-Barreto, R. F. S.; da Silva Ju´nior, E. N.; Mobin, S. M.; Namboothiri, I. N. N. *Chem.Commun.,* **2014**, *50*, 6973–6976.
98. Dai, L. Wang, S.-X. Chen, F.-E. Adv. Synth. Catal. **2010**, *352*, 2137–2141.
99. Dajek, M.; Pruszczynska, A.; Konieczny, K.A.; Kowalczyk. R. *Adv. Synth. Catal.* **2020**, *362*, 3613–3620.
100. Nagy, S.; Feher, Z.; Karpati, L.; Bagi, P.; Kisszekelyi, P.; Koczka, B.; Huszthy, P.; Pukanszky, B.; Kupai, J. *Chem. Eur. J.* **2020**, *26*, 13513–13522.
101. Roy, T. K.; Biswajit Parhi, B.; Prasanta Ghorai, P. *Angew. Chem. Int. Ed.* **2018**, *57*, 9397–9401.
102. Yang, W.; Du, D.-M. *Adv. Synth. Catal*. **2011**, *353*, 1241–1246.

Chapter 2

SYNTHESIS OF CHIRAL HYPERBRANCHED POLYMERS CONTAINING CINCHONA SQUARAMIDE MOITIES BY MIZOROKI-HECK POLYMERIZATION AND THEIR CATALYTIC ACTIVITY IN THE ASYMMETRIC MICHAEL ADDITION REACTION

2.1 Introduction

Cinchona alkaloids isolated from the bark of the cinchona tree, have numerous functionalities including a secondary alcohol, a quinoline ring, a quinuclidine tertiary nitrogen and a terminal vinyl group in their structure. In the various kinds of chiral organocatalysts available for asymmetric catalysis, cinchona alkaloid derivatives[1,2] have shown very successful applications in asymmetric synthesis[3-7]. As a privileged class of chiral catalysts, cinchona alkaloid-derived catalysts exhibit outstanding catalytic activity in various enantioselective reactions[8]. Due to presence of Lewis acidic and basic sites, cinchona alkaloids act as bifunctional catalysts. Both the tertiary amine of quinuclidine and hydroxyl moiety are able to activate and align a nucleophile and an electrophile repectively.[9] Cinchona alkaloids and their derivatives can be utilized as chiral catalysts in four types of reactions, involving; C–C bond formation, C-O bond formation, C-Heteroatom bond formation, and miscellaneous reactions such as desymmetrization and hydrogenation.

Cinchona-substituted squaramides have been proven to be highly efficient chiral bifunctional organocatalysts in asymmetric Michael-type reactions because of their acidic NH and tertiary nitrogen of the quinuclidine.[10-23] These can be easily synthesized from 9-amino derivatives of cinchona alkaloids.[24] The asymmetric Michael reaction is an essential C–C bond forming reaction, High catalytic activity was observed by applying cinchona squaramide derivatives in the asymmetric Michael reactions. Recently, chiral polymeric catalysts have received much attention to the researcher due to their easy separation from the reaction mixture and their recyclability.[25-27] Due to heterogeneity of polymeric catalyst in the reaction mixture, reactivity of polymer can be suppressed, while sometimes a well-designed polymetic catalyst may show higher selectivity with adequate reactivity in asymmetric reactions.[28]

In our previous reports, synthesis of main chain type chiral polymers containing cinchona moiety have been developed by using a variety of polymerization techniques.[29-33] We have established a Mizoroki–Heck (MH) polymerization reaction was a reliable C-C bond forming reaction to synthesize chiral linear polymers from cinchona alkaloid derivatives.[34-36] In this work, we chose to synthesize chiral hyperbranched (HPB) polymers. We noticed that this (MH) methodology is applicable toward the synthesis of chiral HBPs from cinchona alkaloid derivatives. HBPs are usually easily prepared when compared to dendrimers, which requires a multi-step synthesis.[37] HBPs are highly branched tree-like three-dimensional structures which have drawn a lot of attention in various

applications.[38-40] Chiral HBPs containing chiral catalytic moieties are potential polymer catalysts in asymmetric catalysis. Their interesting chemical and physical properties, and potential applications have attracted considerable attention.

Cinchona-based chiral HBPs have not been reported to date. In this chapter we designed and synthesized cinchona-based chiral HBPs containing squaramide moiety. Cinchona squaramides[41,42] and their dimers,[34] such as **3,** show high stereoselectivity in asymmetric reactions. Therefore, we used dimer **3** for the synthesis of three chiral HBPs. Then, we applied these chiral HBPs in asymmetric catalysis and evaluated their catalytic performance in the asymmetric Michael addition reaction. One of the simple HBPs can be prepared via the combination of bifunctionalized (**A2**) and trifunctionalized (**B3**) compounds, as shown in Scheme 1. A quantitative reaction between functionalities **A** and **B** is necessary to prepare HBPs. We have used the Mizoroki–Heck reaction as an efficient C-C bond forming reaction between an olefinic double bond (**A**) and aromatic iodide (**B**). Cinchona alkaloid possesses an olefinic double bond at the C3 position, therefore the reaction between cinchona alkaloid dimer (**A2**) and trisubstituted aromatic iodide (**B3**) may give rise to chiral hyperbranched polymers.

2.2 Results and discussions

Novel chiral HBPs containing cinchona-based squaramides were designed and synthesized using a combination of bifunctional compound **A2** and trifunctional compound **B3,** as shown in Scheme 2.1.

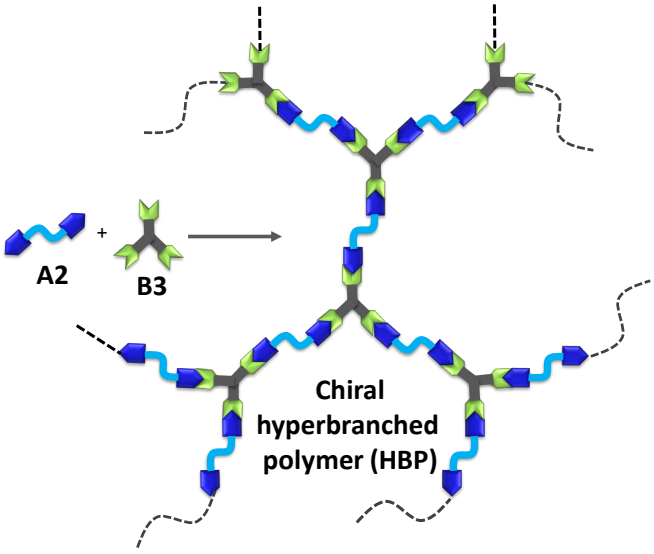

Scheme 2.1. Synthesis of chiral hyperbranched polymers (HBPs).

2.2.1. Synthesis of cinchona dimeric squaramides and triiodides

As bifunctional compounds, cinchona squaramide dimers **3a** and **3b** were synthesized from C9-aminated cinchona alkaloid and dimethyl squarate according to a literature procedure (Scheme 2.2).[34,36,43] C'6-OH compound **3c** was obtained via demethylation of **3b** with BBr_3 (Scheme 2.2). Trifunctional compound **6a** containing three iodophenyl groups was easily prepared from trisphenol

4 and iodobenzylbromide **5** (Scheme 2.2).[44] Another trifunctional compound, **6b**, was prepared from trihydroxybenzene **7** and iodobenzoylchloride **8** (Scheme 2.3).[45] Tetrafunctional compound **6c** was prepared via a two-step synthesis from 1-bromoadamantane **9** according to a literature procedure (Scheme 2.4).[46] Using these components, the novel chiral HBPs containing cinchona-based squaramides were designed and synthesized.

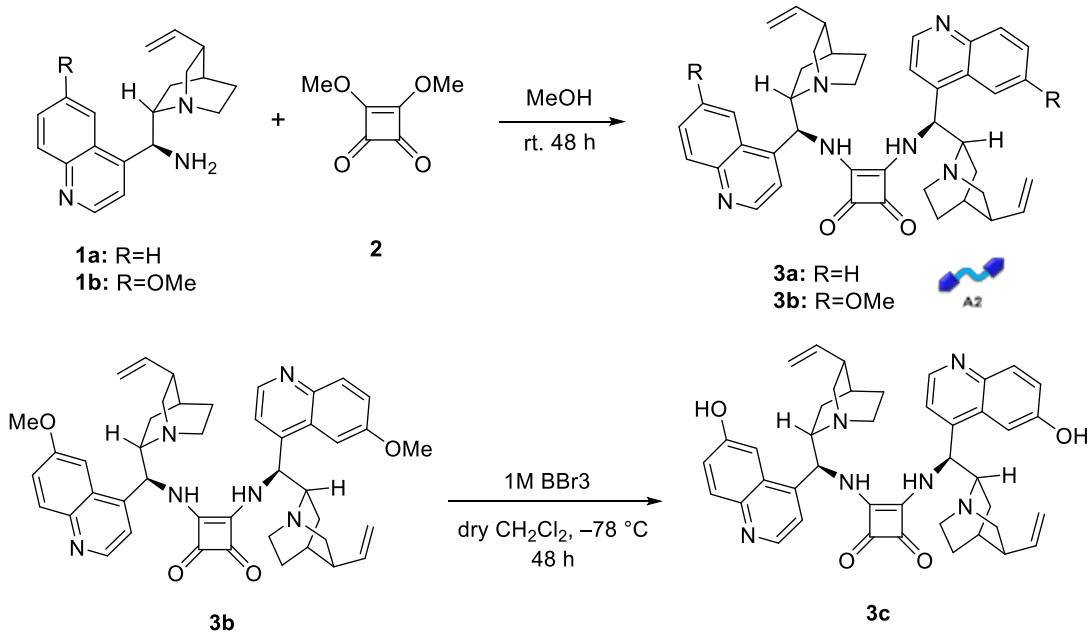

Scheme 2.2. Synthesis of compound **3a**, **3b** and **3c**

2.2.2. Synthesis of cinchona-derived chiral hyperbranched polymers

As illustrated in Scheme 1, the repetitive reaction between components **A2** and **B3** may give chiral HBPs. Linear polymers of **3b** by using Mizoroki-Heck polymerization technique have been synthesized by our lab group.[34] We applied this methodology to the synthesis of chiral HBP. In the presence of $Pd(OAc)_2$, repetitive Mizoroki–Heck reactions take place between cinchona squaramide dimers **3** and various aromatic iodides **6** to give the corresponding chiral HBPs (**P1**) in good yield. In most cases, the as-obtained chiral HBPs were soluble in DMF and DMSO, and partly soluble in other commonly used organic solvents, such as CH_2Cl_2, $CHCl_3$, MeOH, EtOAc, and THF. Typical structure of chiral HBPs were presented in Scheme 2.5 and Figure 2.1. Table 2.1 summarizes the yield and molecular weight of the obtained HBPs.

Table 2.1. Synthesis of chiral HBPs **P1**–**P3** from cinchona squaramide dimers **3a–c** and aromatic iodides **6a–c**

Entry	Dimer **A2**	Iodides **B3**	Chiral HBP	Yield [%]	M_n [a]	M_w [a]	M_w/M_n [a]
1	**3a**	**6a**	**P1aa**	62	34000	72000	2.10
2	**3b**	**6a**	**P1ba**	60	37000	46000	1.66
3	**3c**	**6a**	**P1ca**	60	14000	27000	1.92
5	**3a**	**6b**	**P2ab**	61	16000	28000	1.69
4	**3a**	**6c**	**P3ac**	41	27000	46000	1.72

[a] Determined by SEC using DMF as solvent at a flow rate of 1.0 mL min^{-1} at 40 °C (polystyrene standard).

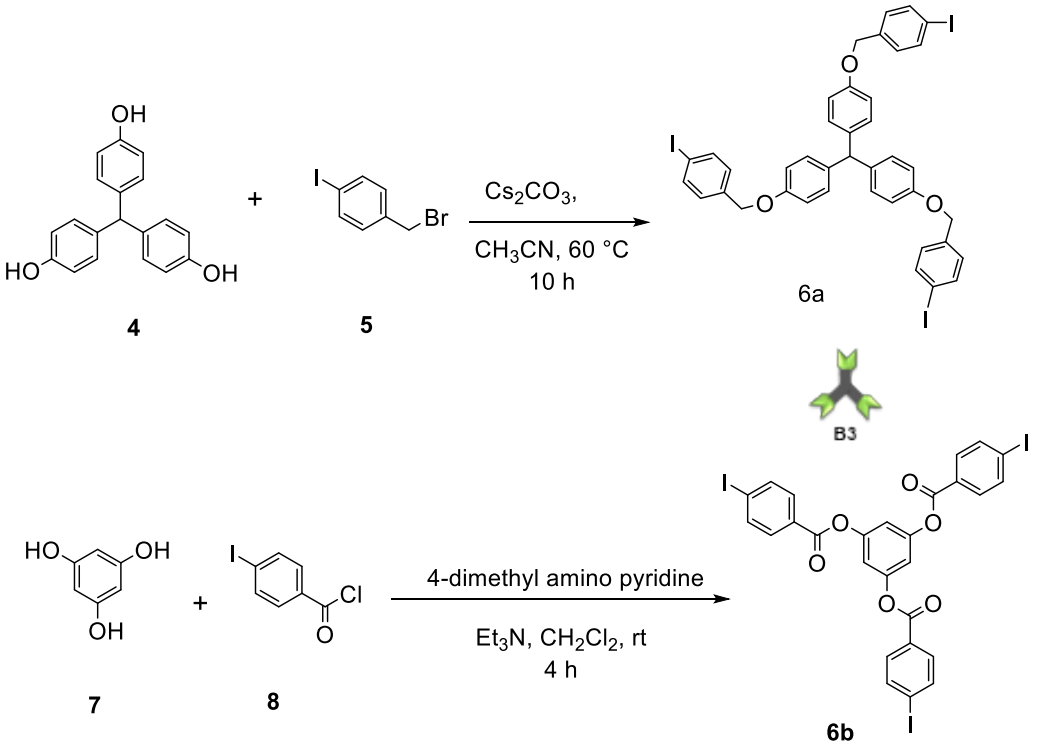

Scheme 2.3. Synthesis of triiodide **6a** and **6b**

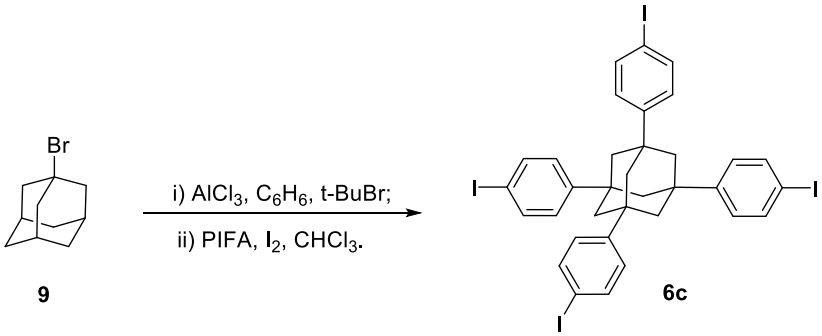

Scheme 2.4. Synthesis of of 1,3,5,7-tetrakis(4-iodophenyl) adamantane **6c**

2.2.3. Catalytic performance of the cinchona squaramide dimer and hyperbranched polymers

2.2.3.1 Asymmetric Michael addition reaction of β-ketoesters to *trans* β-nitrostyrene

Dimeric cinchona squaramide **3a** was first examined as an organocatalyst in the asymmetric Michael addition reaction of methyl 2-oxocyclopentanecarboxylate **11** and *trans*-β-nitrostyrene **12** (Scheme 2.7). In the presence of **3a**, the asymmetric reaction smoothly occurred to give chiral product **13** in 95% yield and 98% ee (Table 2.2, entry 1). High diastereoselectivity (>100:1) was also obtained with **3a**. In our previous report, we synthesized chiral linear polymer **PLb** from quinine squaramide.[34] We also prepared cinchonidine derived linear polymer **PLa**. These polymers showed the similar enantioselectivities compared with the results obtained with dimeric catalyst **1a** (entries 4, 5). We then applied the corresponding chiral HBPs (**P1**–**P3**) as organocatalysts in the same reaction. These chiral HBP catalysts showed excellent performance in the asymmetric reaction. When **P1aa** was used as a catalyst in CH_2Cl_2, chiral product **13** was obtained in 90% yield

even under heterogeneous conditions. Although the diastereoselectivity decreased to some extent, the enantioselectivity of the major diastereomer was almost perfect with **P1aa** (entry 6). The enantioselectivity obtained by the chiral HBP was even higher than that obtained with the corresponding dimeric catalyst. A suitable microenvironment for the asymmetric reaction was created in the chiral polymer network. The other chiral HBPs showed excellent enantioselectivity (>99% ee) except for the result obtained using **P1ca** bearing a C6'-OH group (entry 8). The corresponding dimeric catalyst **3c** also gave lower stereoselectivity (entry 3). The structural difference between iodides **6a**, **6b**, and **6c** had almost no effect on the catalytic activity of their corresponding chiral HBPs (entries 6, 9, 10). Next, the solvent effect on the asymmetric reaction was examined using **P1aa** (Table 2.3). Except for hexane as a solvent (entry 9), high levels of enantioselectivity (>99% ee) were found for the major diastereomer. The diastereoselectivity varied with the solvent used. The reaction of **P1aa** in dichloromethane gave the desired product with the highest diastereoselectivity (entry 1).

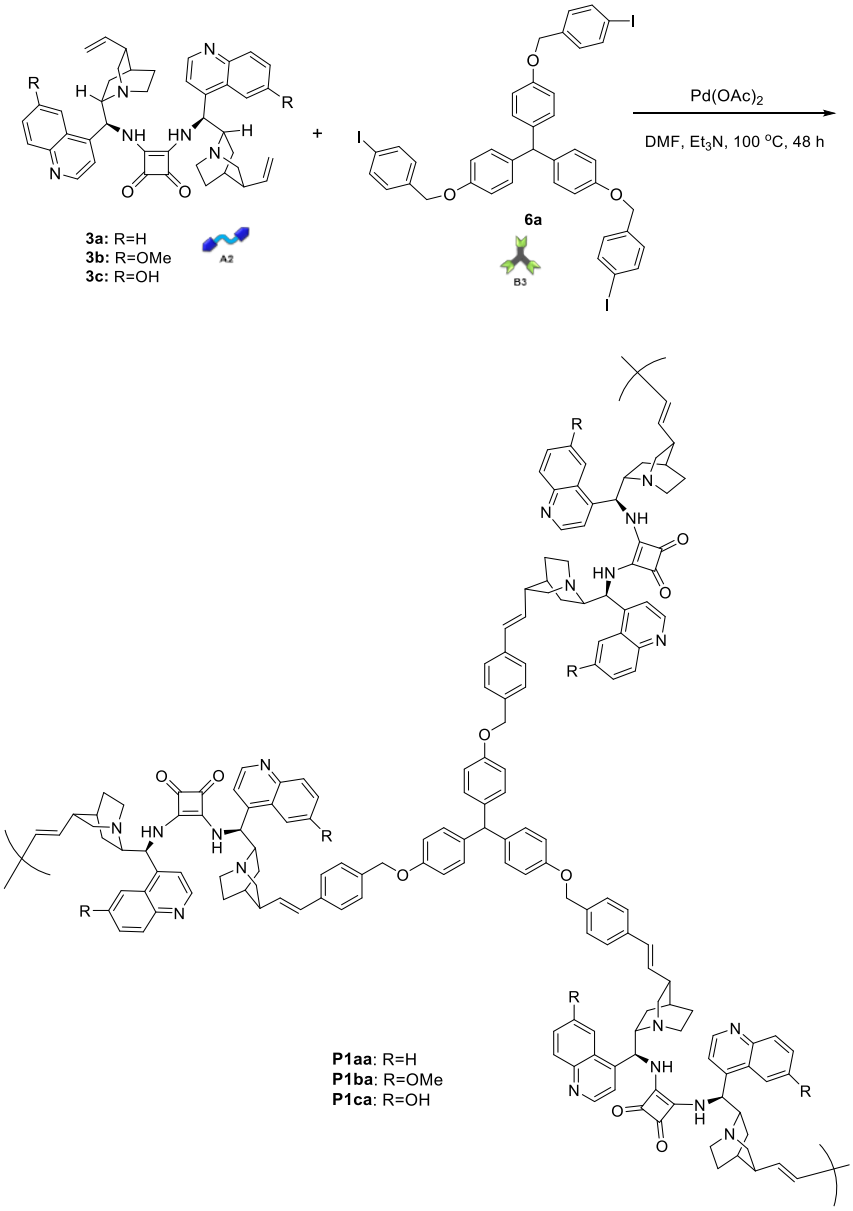

Scheme 2.5. Synthesis of HBP **P1** by MH coupling reaction.

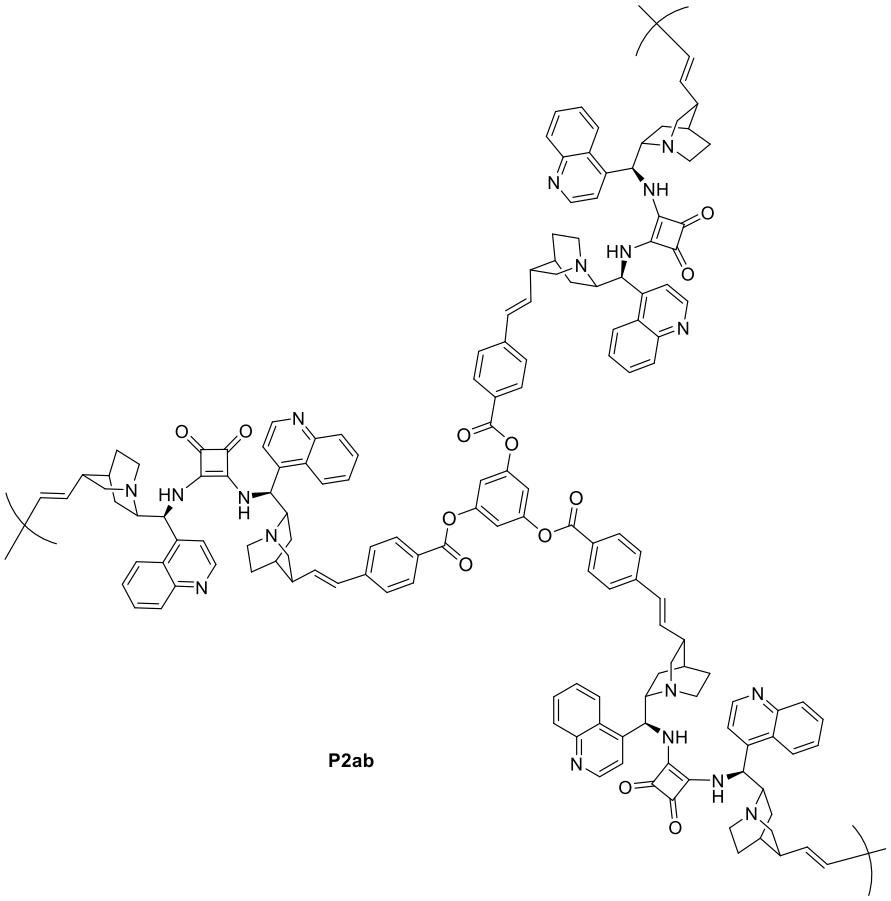

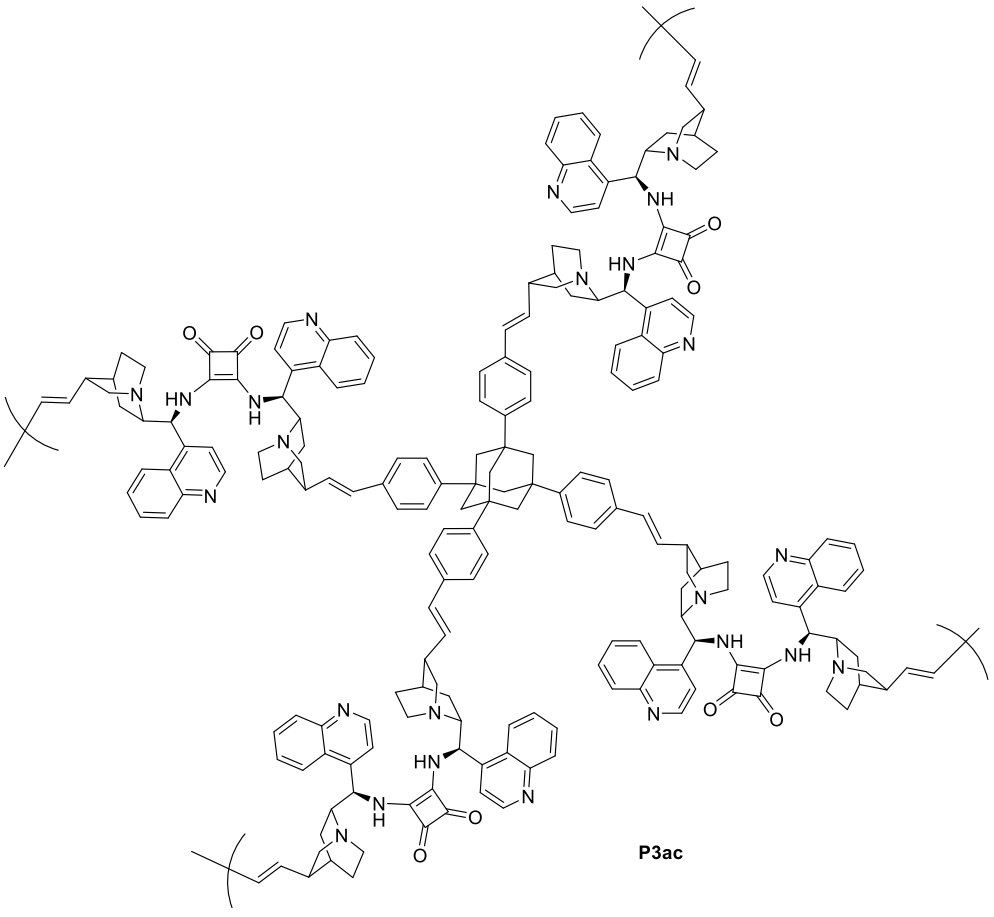

Figure 2.1. Structure of polymers **P2ab** and **P3ac**

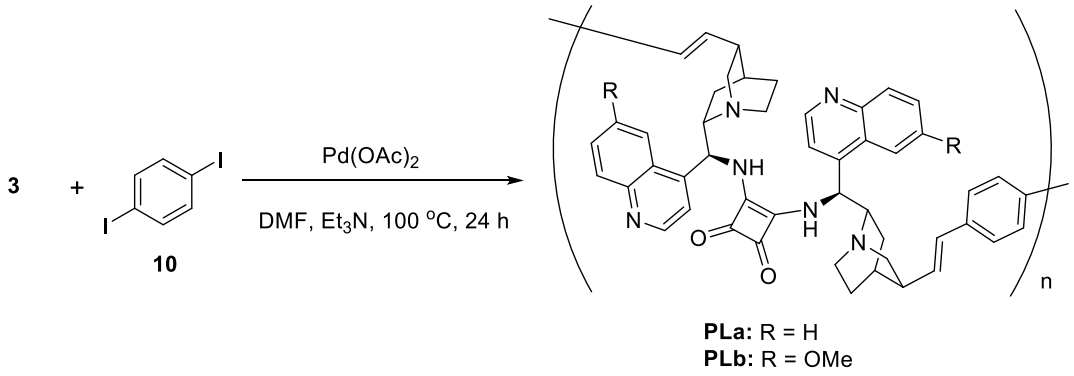

Scheme 2.6. Synthesis of linear polymer **PL** by MH polymerization

2.2.3.2 Recyclability of chiral HBPs

Chiral HBP catalysts **P1**–**P3** were insoluble in dichloromethane and formed a suspension. The asymmetric reaction occurred in this heterogeneous system. After completion of the reaction, the chiral HBPs can be easily separated and recovered via simple filtration. Recovered polymeric catalysts **P1aa** and **P3ac** were reused in the same reaction to examine their recyclability. **P1aa** was recycled six times and **P3ac** four times, and the results of the recycling experiments summarized in Table 2.4 and 2.5, respectively. Both these chiral HBP catalysts maintained a high level of catalytic activity without any decrease in the diastereoselectivity and enantioselectivity.

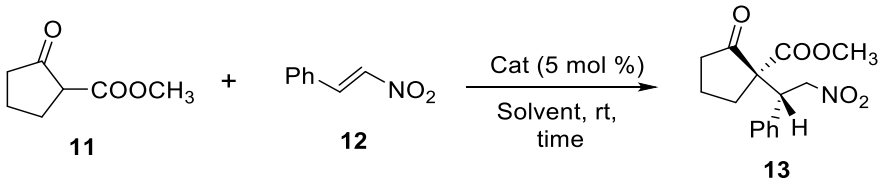

Scheme 2.7. Enantioselective Michael addition reaction of methyl 2-oxocyclopentanecarboxylate **11** to *trans*-β-nitrostyrene **12.**

Table 2.2. Asymmetric Michael addition reaction of methyl 2-oxocyclopentanecarboxylate **11** to *trans*-β-nitrostyrene **12** using dimeric and HBP catalysts.[a]

Entry	Catalyst	Reaction time [h]	Yield[b] [%]	*dr*[c] [%]	*ee*[c] [%]
1	**3a**	4	95	>100:1	98
2[d]	**3b**	2	95	79:1	91
3	**3c**	18	89	2:1	71
4	**PLa**	24	88	32:1	98
5[d]	**PLb**	30	71	28:1	97
6	**P1aa**	24	90	27:1	>99
7	**P1ba**	24	88	18:1	99
8	**P1ca**	21	83	2:1	40
9	**P2ab**	24	84	20:1	>99
10	**P3ac**	24	88	26:1	99
11[e]	**P1aa**	24	90	24:1	>99

[a] The asymmetric reactions were carried out at rt with **11** (0.50 mmol), ***12*** (0.55 mmol), and the polymeric catalyst (5 mol%) in 2.5 mL of CH_2Cl_2.
[b] Isolated yield of the product after column chromatography.
[c] The enantioselectivity (ee) was determined using HPLC (CHIRALCEL OD-H column at a flow rate of 1.0 mL/min)
[d] See ref 34
[e] 2.5 mol% P1aa was used.

Table 2.3. Solvent effect for the asymmetric Michael addition reaction of methyl 2-oxocyclopentanecarboxylate **11** to *trans*-β-nitrostyrene **12** in the presence of chiral HBP **P1aa**.[a]

Entry	Solvent	Reaction time [h]	Yield[b] [%]	*dr*[c] [%]	*ee*[c] [%]
1	CH_2Cl_2	24	90	27:1	>99
2	Ethyl acetate	48	74	12:1	99
3	Acetone	28	79	21:1	>99
4	Methanol	18	78	12:1	>99
5	Acetonitrile	32	72	20:1	99
6	THF	35	83	16:1	99
7	Diethyl ether	38	80	7:1	>99
8	Toluene	39	89	9:1	99
9	Hexane	48	64	15:1	97

[a] The asymmetric reactions were carried out at rt with **11** (0.50 mmol), ***12*** (0.55 mmol), and the monomeric or polymeric catalyst (5 mol%) in 2.5 mL of solvent.
[b] Isolated yield of the product after column chromatography.
[c] The enantioselectivity (ee) was determined using HPLC (CHIRALCEL OD-H column at a flow rate of 1.0 mL/min)

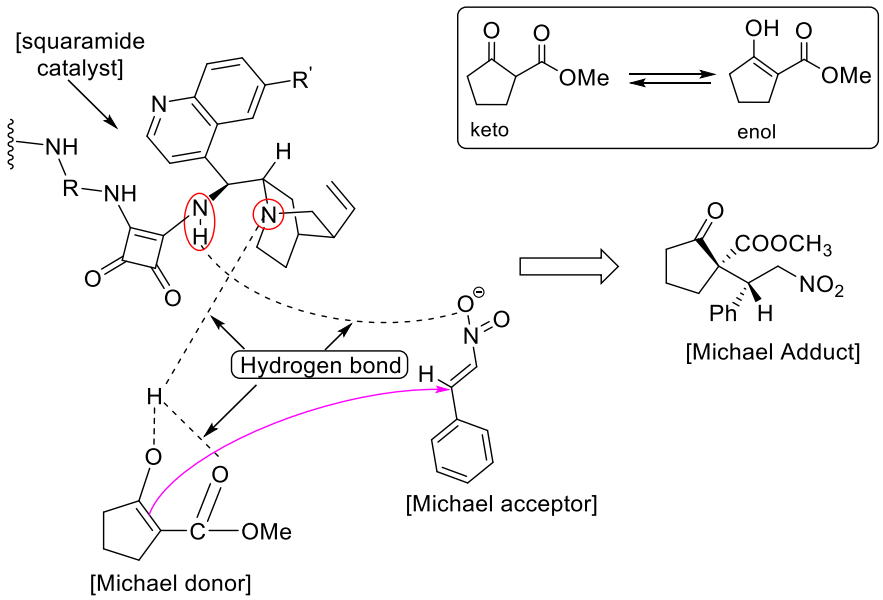

Figure 2.2. Plausible reaction pathway for squaramide catalyzed asymmetric Michael Addition of methyl 2-oxocyclopentanecarboxylate **11** to *trans*-β-nitrostyrene **12**.

Four possible isomers are formed in the asymmetric Michael addition reaction of methyl 2-oxocyclopentanecarboxylate **11** to *trans*-β-nitrostyrene **12**. The transition state leading to **13a** may be the most stable among them.

1. Major diastereomer (major enantiomer)

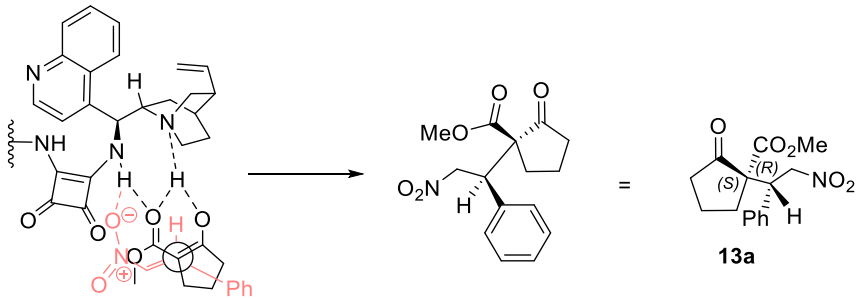

2. Major diastereomer (minor enantiomer)

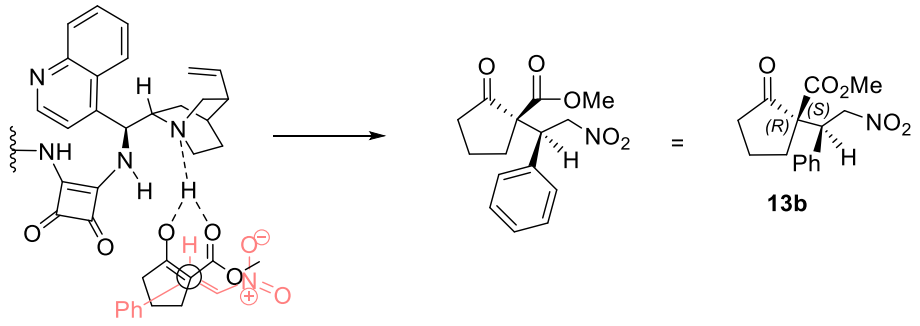

3. Minor diastereomer (major enantiomer)

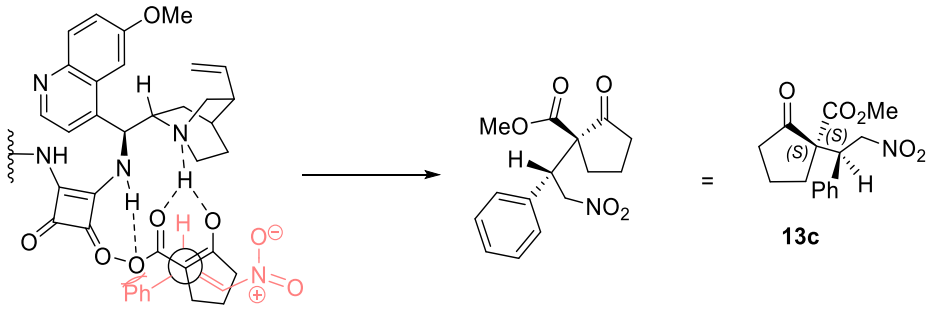

4. Minor diastereomer (minor enantiomer)

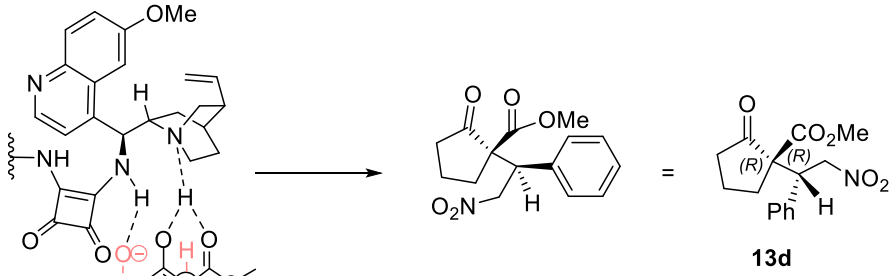

Table 2.4. Recyclability examination of chiral HBP **P1aa** in the asymmetric Michael addition reaction of methyl 2-oxocyclopentane carboxylate **11** and *trans*-β-nitrostyrene.[a]

Entry	Reaction time [h]	Yield[b] [%]	*dr*[c] [%]	*ee*[c] [%]
Fresh polymer	24	90	27:1	>99
Cycle 1	31	85	31:1	>99
Cycle 2	32	80	13:1	99
Cycle 3	32	81	28:1	>99
Cycle 4	32	86	32:1	99
Cycle 5	32	85	30:1	>99
Cycle 6	32	84	29:1	>99

[a] The asymmetric reactions were carried out at *r*t with **11** (0.50 mmol), ***12*** (0.55 mmol), and the polymeric catalyst (5 mol%) in 2.5 mL of CH_2Cl_2.
[b] Isolated yield of the product after column chromatography.
[c] The enantioselectivity (ee) was determined using HPLC (CHIRALCEL OD-H column at a flow rate of 1.0 mL/min)

Table 2.5. Recyclability examination for chiral HBP **P3ac** in enantioselective Michael addition reaction[a] of β-ketoester and *trans*-β-nitrostyrene.

Entry	Reaction time [h]	Yield[b] [%]	*dr*[c] [%]	*ee*[c] [%]
Fresh polymer	24	88	26:1	99
Cycle 1	33	84	17:1	99
Cycle 2	33	82	41:1	99
Cycle 3	33	82	46:1	>99
Cycle 4	33	80	40:1	99

[a] The asymmetric reactions were carried out at *r*t with **11** (0.50 mmol), ***12*** (0.55 mmol), and the polymeric catalyst (5 mol%) in 2.5 mL of CH_2Cl_2.
[b] Isolated yield of the product after column chromatography.
[c] The enantioselectivity (ee) was determined using HPLC (CHIRALCEL OD-H column at a flow rate of 1.0 mL/min)

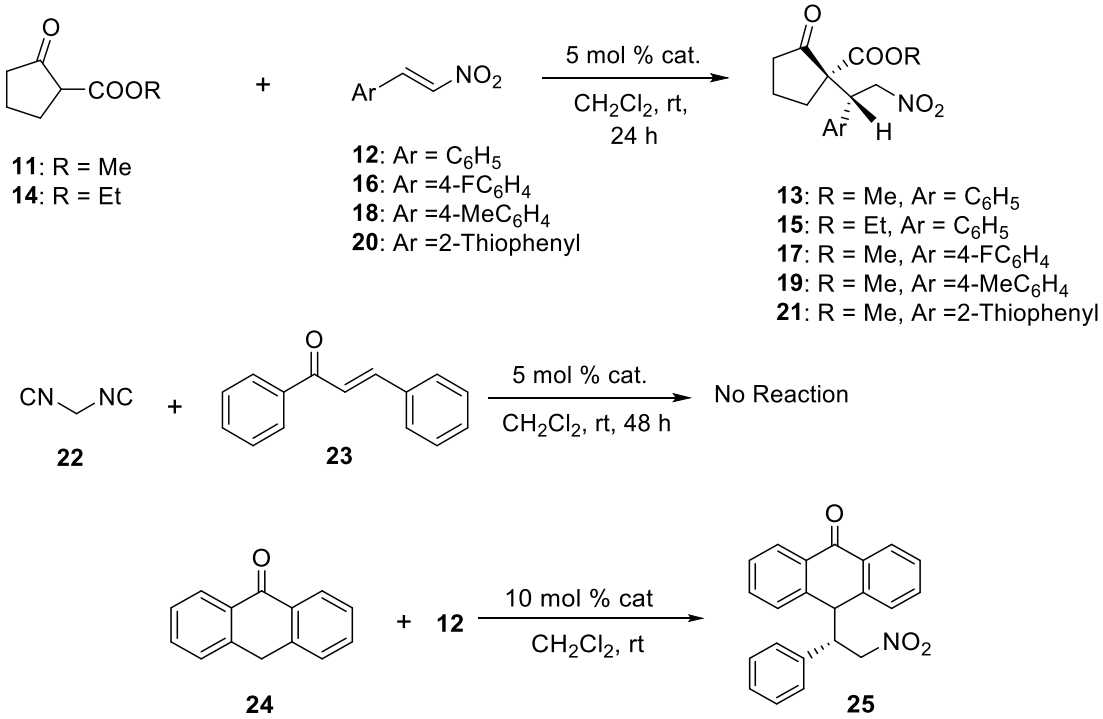

Scheme 2.8. Asymmetric Michael addition reaction using chiral HBP catalyst **P1aa**.

2.2.3.3 Michael addition reaction of other substrate combinations

Chiral HBP **P1aa** was applied to other Michael addition reactions as shown in Scheme 2.8. In the reaction with 2-oxocyclopentanecarboxylate **11** and **14**, a high level of enantioselectivity was obtained (Table 6 entries 1–4) with variety of nitroolifins. However, catalyst **P1aa** could not catalyze the reaction of malononitrile **22** and chalcone **23**.

Anthrone **24** was allowed to react with *trans*-β-nitrostyrene **12** in the presence of **P1aa** to give the Michael adduct **25** in good yield. Dimer **3c** and its corresponding hyperbranched polymer **P1ca** were applied in another Michael addition reaction of anthrone **24** to *trans*-β-nitrostyrene **12** (Scheme 6). Higher enantioselectivity 78% ee was observed in low molecular weight catalyst at room temperature with 93% yield (Table 2.7, entry 1). At -40°C, only 34% ee was observed (Table 2.7, entry 2). At 50°C, 72% ee was found with good yield (entry 3) and reaction time was short compared with room temperature and low temperature. For corresponding polymer **P1ca**, very low

ee was found 18% (entry 4). Other polymers **P1aa** and **P3ac** were also applied in this reaction. However, only low enantioselectivities were obtained with the chiral HBP catalysts. For efficient asymmetric reaction, suitable microenvironment may not be created by hyperbranched polymeric organocatalysts.

Table 2.6 The asymmetric Michael addition reaction using chiral HBP catalyst **P1aa.**

Entry	Michael donor	Michael acceptor	Product	Reaction time [h]	Yield[b] [%]	*dr*[c] [%]	*ee*[c] [%]
1	**14**	**12**	**15**	24	89	39:1	93
2	**11**	**16**	**17**	24	91	49:1	94
3	**11**	**18**	**19**	24	92	21:1	>99
4	**11**	**20**	**21**	24	94	27:1	96

[a] The asymmetric reactions were carried out at rt with **11,14** (0.50 mmol), *nitroolifins* **12** (0.55 mmol) and the monomeric and polymeric catalyst (5 mol%) in 2.5 mL CH_2Cl_2 in CH_2Cl_2 using the chiral HBP catalyst.
[b] Isolated yield of the product after column chromatography.
[c] The enantioselectivity (ee) was determined using HPLC (CHIRALCEL OD-H column at a flow rate of 1.0 mL/min)

Table 2.7 Asymmetric Michael addition reaction[a] of anthrone **24** and *trans* β-nitrostyrene **12** using dimer and different polymeric catalysts.

Entry	Catalyst	Reaction time [h]	Yield[b] [%]	*ee*[c] [%]
1	**3c**	24	93	78
2[d]	**3c**	48	48	34
3[e]	**3c**	12	95	72
4	**P1ca**	24	82	18
5	**P1aa**	17	85	9
6	**P3ac**	18	80	10

[a]Asymmetric reactions were carried out at *r*t with **anthrone 24** (0.24 mmol), *trans*- β-nitrostyrene **12** (0.20 mmol) and the monomeric and polymeric catalyst (10 mol%) in 2.5 mL CH_2Cl_2 with *S* configuration except entry **4**.[47]
[b]Isolated yield of the product after column chromatography
[c]Enantioselectivity (ee), determined by HPLC, (CHIRALPAK AS-H at a flow rate of 0.7 mL/min)
[d]Reaction was carried out at -40°C
[e]Reaction was carried out at 50°C

2.3. Conclusion

Chiral HBPs containing the cinchona squaramide moiety were successfully synthesized from cinchona squaramide dimer **3** and tri or tetrasubstituted aromatic iodide **6** via a Mizoroki–Heck polycondensation reaction. Chiral HBPs **P1**-**P3** were applied in the asymmetric Michael addition reaction and showed excellent enantioselectivity (>99% ee) in the Michael addition reaction of β-ketoesters to *trans*-β-nitrostyrene. Very high enantioselectivities were constantly obtained with **P1aa** in all solvents used in the asymmetric reaction. The HBPs can be easily separated and reused up to six times without losing their catalytic activity and enantioselectivity. This is the first example of chiral HBP organocatalyst successfully applied to the asymmetric Michael addition reaction.

2.4. Experimental

2.4.1. Materials and methods

All reagents and solvents used during the investigation were procured from Sigma Aldrich, Wako Pure Chemical Industries, Ltd., or Tokyo Chemical Industry (TCI) Co., Ltd. Thin layer chromatography (TLC) was carried out using pre-coated silica gel plates (Merck TLC silica gel,

60F254) to monitor the progress of the reactions. Column chromatography was performed to purify the as-synthesized compounds using a silica gel column (Wakogel C-200, 100–200 mesh). NMR spectroscopy was recorded on JEOL JNM-ECS400 and JEOL JNM-ECX500 spectrometers in $CDCl_3$ or DMSO-d_6 at room temperature operated at 400 MHz (^1H), 500 MHz (^1H), and 100 MHz ($^{13}C\{^1H\}$). Chemical shifts were reported in parts per million (ppm) using tetramethyl silane (TMS) as a reference and the *J* values were reported in Hertz (Hz). IR spectroscopy was recorded using KBR pellets on a JEOL JIR-7000 FTIR spectrometer and the wavenumbers were reported in cm^{-1}. HRMS (ESI) was recorded on a Bruker micro OTOF II HRMS instrument. High-performance liquid chromatography (HPLC) was carried out on a Jasco HPLC system composed of a DG-980-50 three-line degasser, a HPLC pump (PU-980), and a column oven CO-2065 equipped with a chiral column (Chiralpak OD-H, Daicel) using hexane/2-propanol as the eluent at a flow rate of 1.0 mL/min at room temperature. For peak detection, a Jasco UV-975 UV detector was used. Size exclusion chromatography (SEC) was performed using a Tosoh instrument with HLC 8020 UV (254 nm) or refractive index detector. Two polystyrene gel columns with a bead size of 10 µm were used and dimethylformamide (DMF) was used as the carrier solvent at a flow rate of 1.0 mL min^{-1} at 40 °C. A calibration curve was established to determine the number average molecular weight (M_n) and molecular weight distribution (M_w/M_n) values by comparison with polystyrene standards. Optical rotations were determined on a JASCO DIP-149 digital polarimeter using a 10 cm thermostatted microcell.

2.4.2. Synthesis of tris (4((4-iodobenzyl) oxy)phenyl)methane 6a [44]

Tris (4-hydroxy phenyl)methane **4** (292 mg, 1.0 mmol) and 4-iodo benzyl bromide **5** (979 mg, 3.3 mmol) were dissolved in 15.0 mL of CH_3CN in a 30 mL flask. After adding cesium carbonate Cs_2CO_3 (1.08 g, 3.3 mmol) to the resulting solution, the mixture was stirred at 60 ºC for 10 h under an Ar atmosphere. The reaction mixture was poured into CH_2Cl_2 (60 mL) and the organic solution was washed with water (2 × 30 mL) and brine (2 × 30 mL), and then dried over anhydrous magnesium sulfate. The solution was filtered and evaporated under reduced pressure to give the crude product, which was purified by column chromatography on silica gel (hexane:CH_2Cl_2; 55:45) to give **6a** (647 mg, 69%) as a white solid. R_f: 0.42 (CH_2Cl_2/hexane = 5.0/5.0); mp: 119–123 ºC; ^1H NMR (400 MHz, $CDCl_3$): δ 4.96 (s, 6H), 5.38 (s, 1H), 6.86 (d, J = 8.4 Hz, 6H), 6.98 (d, J = 8.4 Hz, 6H), 7.16 (d, J = 8.0 Hz, 6H), 7.70 (d, J = 8.0 Hz, 6H); ^{13}C NMR (100 MHz, $CDCl_3$): δ 54.5, 69.4, 93.5, 114.6, 129.3, 130.3, 136.9, 137.2, 137.7, 157.0; Elemental analysis: calcd C = 51.09% and H= 3.32%, found C = 51.01% and H = 3.30%.

2.4.3 Synthesis of squaramides 3

2.4.3.1 Synthesis of squaramides 3a and 3b[34]

To a stirred solution of the 9-amino (9-deoxy)epi cinchonidine **1a** (7.73 mmol) in methanol dimethylsquarate **2** (440 mg, 3.09 mmol) was added at room temperature. The reaction was

monitored by TLC. After stirring for 48 h at room temperature under argon gas, the precipitate was filtered, washed with cold methanol (2–3 times), and then dried in vacuo to afford the crude squaramide as a white solid. The solid compound was purified by silica gel (100–200 mesh) column chromatography with DCM/MeOH = 5/5 as an eluent to give the desired compound **3a** in 94% yield as white solid. ^{1}H NMR (400 MHz, DMSO-d_6, 25 °C) δ 8.97 (d, J = 3.2 Hz, 2H), 8.46 (d, J = 8 Hz, 2H),), 8.07 (d, J = 8 Hz, 2H), 7.79-7.91 (m, 2H), 7.61-7.73 (m, 2H), 7.63 (br, 2H) 5.8–6.05 (m, 4H), 4.89–5.00 (m, 4H), 3.03–3.25 (m, 8H), 2.57–2.66 (m, 2H), 2.17 (s, 2H), 1.27–1.50 (m, 8H), 0.50 (s, 2H) ppm. ^{13}C NMR (100 MHz, DMSO-d_6, 25 °C) δ 26.54, 27.73, 39.69, 55.93, 99.57, 114.76, 123.77, 126.79, 127.85, 130.10, 130.56, 142.65, 145.80, 148.65, 151.05, 166.88, 182.16 ppm. IR (KBr): v= 2945, 2921, 2861, 1797, 1667, 1623, 1587, 1541, 1512, 1474, 1245, 848, 693 cm^{-1}.

Squaramide **3b** was synthesized following same procedure.

2.4.3.2 Synthesis of squaramides 3c[36]

Quinine squaramide **3b** (500 mg, 0.690 mmol) was dissolved in dry CH_2Cl_2 and cooled to –78 ºC under an Ar atmosphere. 30 mL of 1 M BBr_3 in CH_2Cl_2 was added to the resulting solution at –78 ºC and stirred for 2 h. The reaction mixture was allowed to warm to room temperature and stirred for 48 h. Water was added to the reaction mixture to decompose the unreacted BBr_3, 10 wt% NaOH solution added to adjust the mixture to pH 12–13, and the organic phase was discarded. To the aqueous phase was added 2N HCl to adjust the solution to pH 7–8. The resulting precipitate was filtered, washed with CH_2Cl_2 and water and dried to give **3c** (471 mg, 98%) as a yellow solid. R_f: 0.74 (CH_2Cl_2/MeOH = 5.0/5.0; decomposition point: 262–277 ºC. ^{1}H NMR (500 MHz, DMSO-d_6): δ 0.82 (s, 1H), 1.45–1.65 (m, 4H), 1.83 (br s, 1H), 2.06 (m, 2H), 2.36 (m, 2H), 2.71 (s,1H), 3.71 (br s, 1H), 5.0–5.2 (m, 2H), 5.88–6.2 (m, 1H), 7.44 (d, J = 8.5, 1H), 7.55 (s, 1H), 7.79 (br s, 1H), 7.95 (d, J= 8.5 1H), 8.75 (s, 1H), 9.53 (s, 1H, NH) 10.36 (s, 1H, OH); ^{13}C NMR (100 MHz, DMSO-d_6): δ 24.4, 24.5, 39.9, 40.9, 41.5, 52.0,53.6,60.6, 104.7, 117.7, 123.4, 128.2, 132.6, 139.1, 144.4, 147.8, 147.9, 157.7, 157.8, 168, 183.1. IR (KBr): v = 3931, 3801, 3417, 3230, 2938, 2824, 2626, 2032, 1798, 1681, 1618, 1587, 1526, 1467, 1277, 1219, 1093, 992, 851, 691 cm^{-1}; HRMS (ESI) *m/z* for $C_{42}H_{44}N_6O_4$ [M^+H^+] calcd. 697.3502, found 697.3467; $[\alpha]^{25.8}_D$ = –139 (c 0.22, DMF).

2.4.4. Synthesis of cinchona-based chiral squaramide hyperbranched polymers using a Mizoroki–Heck polymerization reaction.

2.4.4.1 Synthesis of polymer P1aa

Squaramide **3a** (150 mg, 0.225 mmol) and tris(4((4-iodobenzyl)oxy)phenyl) methane **6a** (212 mg, 0.225 mmol) were added to a 20 mL flask and triethyl amine (66 µL, 0.450 mmol) was added to the mixture. After adding palladium acetate (10 mol%) and DMF (4 mL), the reaction mixture was stirred for 48 h at 100 ºC. The solvent was evaporated and the crude residue was precipitated using diethyl ether. The compound was dried in a vacuum oven to afford **P1aa** (355 mg, 62%) as a dark

brown solid. ^{1}H NMR (400 MHz, DMSO-d_6): δ 0.84, 1.23, 1.40–1.90, 2.08, 2.30 (quinuclidine H), 5.00 (6H,-CH_2 from monomer), 5.39 (-CH from monomer), 6.38 (vinylic H), 6.7–8.5 (aromatic H), 9.01 (NH); IR (KBr): v = 3931, 3852, 3710, 3688, 3420, 2930, 2870, 2360, 2041, 1793, 1682, 1602, 1586, 1506, 1454, 1419, 1361, 1299, 1221, 1110, 1013, 970, 824, 766, 697 cm^{-1}; $[\alpha]^{26.1}_D$ = +295 (c 0.085, DMF); M_n (SEC) = 72000; M_w/M_n = 2.10.

2.4.4.2 Synthesis of polymer P1ba

Squaramide **3b** (163.10 mg, 0.2250 mmol) and Tris (4((4-iodobenzyl)oxy)phenyl) methane **6a** (212 mg, 0.2250 mmol) were taken in a 20 mL flask and double amount of triethyl amine (66 µL, 0.4500 mmol) was added to the mixture. After adding palladium acetate (10 mol %) and DMF (4 mL) reaction mixture was stirred for 48 hours at 100 ºC. Then the solvent was evaporated, and crude residue was precipitated in diethyl ether. The compound was dried in a vacuum oven to afford 60% yield of the product **P1ba** (370 mg) as a dark brown solid. ^{1}H NMR (500 MHz, DMSO-d_6); δ 0.81, 1.28-2.0, 2.08, 2.36, 2.83 (quinuclidine H), 3.94 (-OCH_3), 5.02 (6H,-CH_2), 5.39 (-CH), 6.40 (vinylic H), 6.8-8.15 (aromatic H), 8.82(NH); IR (KBr); v = 3916, 3870, 3852, 3734, 3688, 3432, 2932, 2838, 2360, 2041, 1792, 1670, 1619, 1585, 1506, 1454, 1433, 1363, 1226, 1173, 1093, 1024, 970, 825, 777, 618 cm^{-1}. $[\alpha]^{24.9}_D$ = -49 (c 0.045, DMF). M_n (SEC) = 37000; M_w/M_n = 1.66.

2.4.4.3 Synthesis of polymer P1ca

Squaramide **3c** (157 mg, 0.225 mmol) and Tris (4((4-iodobenzyl)oxy)phenyl) methane **6a** (212 mg, 0.225 mmol) were taken in a 20 mL flask and double amount of triethyl amine (66 µL, 0.45 mmol) was added to the mixture. After adding palladium acetate (10 mol %) and DMF (4 mL) reaction mixture was stirred for 48 hours at 100 ºC. Then the solvent was evaporated, and crude residue was precipitated in diethyl ether. The compound was dried in a vacuum oven to afford 60% yield of the product **P1ca** (359 mg) as a dark brown solid. ^{1}H NMR (400 MHz, DMSO-d_6); δ 0.80, 1.10, 1.40-1.60, 2.32, 2.63, 2.89 (quinuclidine H), 5.02 (6H,-CH_2), 5.41 (-CH), 6.35 (vinylic H), 6.7-8.0 (aromatic H), 8.72 (NH), 10.24; IR (KBr); v = 3931, 3877, 3850, 3774, 3540, 3465, 3365, 3074, 2868, 2764, 2359, 2040, 1797, 1618, 1506, 1463, 1383, 1227, 1173, 1014, 934, 850, 737, 697 cm^{-1}. $[\alpha]^{25.7}_D$ = -55 (c 0.030, DMF). M_n (SEC) = 14000; M_w/M_n = 1.92.

2.4.4.4 Synthesis of polymer P2ab

Squaramide **3a** (150 mg, 0.225 mmol) and Benzene 1, 3, 5-triyl tris (4-iodo benzoate) **6b** (184 mg, 0.225 mmol) were taken in a 20 mL flask and double amount of triethyl amine (66 µL, 0.45 mmol) was added to the mixture. After adding palladium acetate (10 mol %) and DMF (4 mL) reaction mixture was stirred for 48 hours at 100 ºC. Then the solvent was evaporated, and crude residue was precipitated in diethyl ether and further washed with water. The compound was dried in a vacuum oven to afford 61% yield of the product **P2ab** (329 mg) as a dark brown solid. ^{1}H NMR (500 MHz, DMSO-d_6); δ 0.62, 1.14, 1.54, 2.24, 2.65, 2.96 (quinuclidine H), 6.13 (vinylic H), 6.41-9.0 (aromatic H), 9.61 (NH); IR (KBr); v = 3901, 3848, 3734, 3688, 3446, 3207, 3059, 2934, 2870,

2632, 2360, 1941, 1796, 1604, 1456, 1383, 1260, 1127, 1071, 973, 846, 766, 681 cm^{-1}. $[\alpha]^{25.2}_D$ = -63 (*c* 0.040, DMF). M_n (SEC) = 16000; M_w/M_n = 1.69.

2.4.4.5 Synthesis of polymer P3ac

Squaramide **3a** (200 mg, 0.301 mmol) and 1, 3, 5, 7 tetrakis (4-iodophenyl) adamantane **6c** (189 mg, 0.201 mmol) were taken in a 20 mL flask and double amount of triethyl amine (84 µL, 0.60 mmol) was added to the mixture. After adding palladium acetate (10 mol %) and DMF (4 mL) reaction mixture was stirred for 48 hours at 100 ºC. Then the solvent was evaporated, and crude residue was precipitated in diethyl ether. The compound was dried in a vacuum oven to afford 41% yield of the product **P3ac** (383 mg) as a dark brown solid. ^{1}H NMR (500 MHz, DMSO-d_6); δ 0.82, 1.22, 1.40-1.81 (quinuclidine H) 2.06 (-CH_2 from central adamantane), 2.62, 2.98 (quinuclidine H), 6.29 (vinylic H), 6.9-8.5 (aromatic H), 9.02 (NH); IR (KBr); ν = 3948, 3870, 3749, 3647, 3565, 3445, 3210, 2927, 2849, 2648, 2360, 1942, 1792, 1696, 1635, 1588, 1446, 1419, 1361, 1221, 1214, 1080, 970, 840, 765, 617 cm^{-1}. $[\alpha]^{26.1}_D$ = -66 (*c* 0.045, DMF). M_n (SEC) = 27000; M_w/M_n =1.72.

2.4.4.6 Synthesis of polymer PLa

Squaramide **3a** (150 mg, 0.2256 mmol) and 1,4-diiodo benzene (74.5 mg, 0.2250 mmol) were taken in a 20 mL flask and double amount of triethyl amine (66 µL, 0.4500 mmol) was added to the mixture. After adding palladium acetate (10 mol %) and DMF (3 mL) reaction mixture was stirred for 24 hours at 100 ºC. Then the solvent was evaporated, and crude residue was precipitated in diethyl ether. The compound was dried in a vacuum oven to afford 96% yield of the product **PLa** (160 mg) as a light brown solid. ^{1}H NMR (400 MHz, DMSO-d_6); δ 0.76, 1.33-1.99, 2.69, 2.94 (quinuclidine H), 5.86-6.52 (vinylic H), 6.95-8.51 (aromatic H), 9.03 (NH); M_n (SEC) = 15000; M_w/M_n = 1.85.

2.4.5. Representative procedure for the enantioselective Michael addition reaction of β-ketoesters to *trans*-β-nitrostyrene.

Trans-β-nitrostyrene **12** (82.1 mg, 0.55 mmol) and the HBP (5 mol%) were added to a reaction vessel with 2.5 mL of solvent. Methyl 2-oxocyclopentanecarboxylate **11** (63 µL, 0.50 mmol) was added via a syringe into the resulting solution. The reaction was stirred at room temperature and was monitored using TLC. The reaction mixture was then filtered, and the filtrate concentrated in vacuo. The crude compound was purified by column chromatography on silica gel (100–200 mesh) using hexane/EtOAc = 6.0/1.0 as the eluent to afford the addition product **13** as a colorless oil. The enantioselectivity (ee) and diastereomeric ratio (dr) were determined using HPLC on a Chiralcel OD-H column.

The other asymmetric Michael addition reactions were conducted using this procedure and the results summarized in Table 2.2 and 2.3 (Scheme 2.7).

2.4.6. Representative procedure for the Michael addition reaction of anthrone to *trans*-β-nitrostyrene.

Trans-β-nitrostyrene **12** (29.83 mg, 0.20 mmol) and the HBP catalyst (10 mol%) were added to reaction vessel with 2.5 mL of CH_2Cl_2. Anthrone **24** (46.62 mg, 0.24 mmol) was added to the resulting solution. The reaction was stirred at room temperature and was monitored using TLC. The reaction mixture was then filtered, and filtrate concentrated in vacuo. The crude product was purified by column chromatography on silica gel (100–200 mesh) using hexane/EtOAc = 5.0/1.0 as the eluent to afford **25** as a white solid. The enantioselectivity (ee) and diastereomeric ratio (dr) were determined using HPLC on a Chiralpak AS-H column.

2.5 Reference

1. Garfield, S. Mauve, Faber and Faber, London, **2000** pp 224.
2. *Boratyński, P. J. Mol. Diversity* **2015**, *19*, 385–422.
3. Jianga, L.; Chen, Y. -C. *Catal. Sci. Technol.* **2011**, *1*, 354–365.
4. Yeboah, E. M. O.; Yeboah, S. O.; Sing, G. S. *Tetrahedron* **2011**, *67*, 1725–1762.
5. Mercelli, T. *WIREs Comput. Mol. Sci.* **2011**, *1*,142–152.
6. Song, C. E. (Eds.), Cinchona Alkaloids in Synthesis & Catalysis, Wiley-VCH, Weinheim, **2009**.
7. (a) Dalko, P.I.; Moisan, L. *Angew. Chem. Int. Ed.* **2004**, *43*, 5138–5175.
(b) Mercelli, T. van Maarseveen J. H.; Hiemstra, H. *Angew. Chem. Int. Ed.* **2006**, *45*, 7496–7504.
(c) Dalko, P. I. (Eds.), Comprehensive Enantioselective Organocatalysis, 1, Wiley-VCH, Weinheim, **2013**.
8. Yoon, T. P.; Jacobsen, E. N. *Science* **2003**, *299*, 1691–1693.
9. Xiao, H.; Wu, F.; Shi, L.; Chen, Z.; Su, S.; Tang, C.; Wang, H.; Li, Z.; Li, M.; Shi, Q. *Molecules* **2014**, *19*, 3955–3972.
10. Lee, J.-W.; Ryu, T.-H.; Oh, J.-S.; Bae, H.-Y.; Jang, H.-B.; Song, C. E. *Chem. Commun*. **2009**, *46*, 7224–7226.
11. Yang, W.; Du, D.-M. *Org. Lett*. **2010**, *12*, 5450–5453.
12. Yang, W.; Du, D.-M. *Adv. Synth. Catal*. **2011**, *253*, 1241–1246.
13. Yang, W.; Du, D.-M. *Chem. Commun*. **2011**, *47*, 12706–12708.
14. Yang, W.; Jia, Y.; Du, D.-M. *Org. Biomol. Chem*. **2012**, *10*, 332–338.
15. Yang, W.; Du, D.-M. *Chem. Commun*. **2013**, *49*, 8842–8844.
16. Yang, W.; Yang, Y.; Du, D.-M. *Org. Lett*. **2013**, *15*, 1190–1193.
17. Rao, K.S.; Ramesh, P.; Chowhan, L.-R.; Trivedi, R. *RSC Adv*. **2016**, *6*, 84242–84247.
18. He, H.-X.; Du, D.-M. *RSC Adv*. **2013**, *3*, 16349–16358.
19. He, H.-X.; Du, D.-M. *Tetrahedron: Asymmetry* **2014**, *25*, 637–643.
20. Malerich, J. P.; Hagihara, K.; Rawal, V. H. *J. Am. Chem. Soc*. **2008**, *130*, 14416–14417.
21. Zhu, Y.; Malerich, J. P.; Rawal, V. H. *Angew. Chem. Int. Ed*. **2010**, *49*, 153–156.

22. Zhao, B.-L.; Du, D.-M. *Eur. J. Org. Chem*. **2015**, *24*, 5350–5359.

23. Konishi, H.; Lam, T. Y.; Malerich, J. P.; Rawal, V. H. *Org. Lett*. **2010**, *12*, 2028–2031.

24. Vakulya, B.; Varga, S.; Csámpai, A.; Soós, T. *Org. Lett*. **2005**, *7*, 1967–1969.

25. Song, C. E., *Cinchona alkaloids in synthesis and catalysis: ligands, immobilization and organocatalysis*; John Wiley & Sons: **2009**.

26. Itsuno, S., *Polymeric chiral catalyst design and chiral polymer synthesis*; John Wiley & Sons: **2011**.

27. Takata, S.; Endo, Y.; Ullah, M. S.; Itsuno, S. *RSC Advances* **2016**, *6*, 72300–72305.

28. Liang, J.; Deng, J. *Journal of Materials Chemistry B* **2016**, *4*, 6437–6445.

29. Ahamed, P.; Haque, M. A.; Ishimoto, M.; Parvez, M. M.; Haraguchi, N.; Itsuno, S. *Tetrahedron* **2013**, *69*, 3978–3983.

30. Itsuno, S.; Paul, D. K.; Ishimoto, M.; Haraguchi, N. *Chem. Lett*. **2010**, *39*, 86–87.

31. Parvez, M. M.; Haraguchi, N.; Itsuno, S. *Macromolecules* **2014**, *47*, 1922–1928.

32. Itsuno, S.; Paul, D. K.; Salam, M. A.; Haraguchi, N. *J. Am. Chem. Soc*. **2010**, *132*, 2864–2865.

33. Parvez, M. M.; Haraguchi, N.; Itsuno, S. *Org. Biomol. Chem*. **2012**, *101*, 2870–2877.

34. Ullah, M. S.; Itsuno, S. *Mol. Catal.* **2017**, *438*, 239–244.

35. Ullah, M. S.; Itsuno, S. *ACS Omega* **2018**, *3*, 4573–4582.

36. Kumpuga, B. T.; Itsuno, S. *J. Catal.* **2018**, *361*, 398–406.

37. Fréchet, J. M. J.; Tomalia, D. A. Dendrimers and other dendritic polymers, Wiley, Chichester, UK **2002**.

38. Gao, C.; Yan, D. *Progr. Polymer Sci.* **2004**, *29*, 183–275.

39. Yates, C. R.; Haye, S.W. *Eur. Polymer J.* **2004**, *40*, 1257–1281.

40. Yamanaka, K., Jikei, M.; Kakimoto, M. *Macromolecules* **2000**, *33,* 6937–6944.

41. Lee, J. -W.; Ryu, T. -H.; Oh, J. -S.; Bae, H. -Y.; Jang, H. -B.; Song, C. E. *Chem. Commun.* **2009**, *46*, 7224–7226.

42. Reviews on cinchona-substituted squaramides in asymmetric Michael-type reactions:

(a) Tsakos, M; Kokotos, C. G., *Tetrahedron* **2013**, *69*, 10199–10222.

(b) Rodriguez-Escrich, C.; Pericas, M. A., *Eur. J. Org. Chem.* **2015**, *2015*, 1173–1188.

43. Vakulya, B.; Varga, S.; Csampai, A.; Soos, T. *Org. Lett.* **2005**, *7*, 1967–1969.

44. Xia, Q.; Wang, Q.; Yan, C.; Dong, J.; Song, H.; Li, L.; Liu, Y.; Wang, Q.; Liu, X.; Song, H. *Chem. Eur J.* **2017**, *45*, 10871–10877.

45. Pigge F. C.; Vangala, V. R.; Swenson, D. C.; Rath, N. P. *Cryst Growth Des* **2010**, *10*, 224–231.

46. (a) Newman, H. *Synthesis* **1972**, *12*, 692– 693.

(b) Merkushev, E. B.; Simakhina, N. D.; Koveshnikova, G. M. *Synthesis* **1980**, *6*, 486 – 487.

(c) Reichert, V. R.; Mathias, L. J. *Macromolecules* **1994**, *27*, 7015–7023.

(d) Mathias, L. J.; Reichert, V. R.; Muir, A. V. G. *Chem. Mater.* **1993**, *5*, 4–5.

47. Zea, A.; Valero, G.; Alba, A-N. R.; Moyano, A.; Riosa, R. *Adv. Synth. Catal*. **2010**, *352*, 1102–1106.

Chapter 3

SYNTHESIS OF CINCHONA SQUARAMIDE BASED CHIRAL HYPERBRANCHED POLYMERS (AB_2 AND A_2B TYPES) AND THEIR APPLICATION IN ASYMMETRIC REACTIONS

3.1 Introduction

For the synthesis of chiral organic molecules, chiral organocatalysts including cinchona alkaloid derivatives have been recognized as powerful synthetic tool due to their multiple advantages such as their stability to moisture and oxygen, easy structure tuning and treatment, and environmentally benevolent.[1] Cinchona alkaloids contain diverse functionalities that are demonstrated to play important role in asymmetric catalysis,[1-7] including continuous flow asymmetric catalysis.[8]

Hyperbranched polymers (HBPs), which are highly branched three-dimensional macromolecules, have attracted significant attention for various applications.[9, 10] Compared to linear polymers, HBPs possess properties analogous to those of dendrimers, such as fragile molecular entanglement, higher viscosity, higher solubility, and large numbers of functional groups, because they have diverse branching points and terminal groups.[11-16] As dendrimers have precise molecular weights and exact numbers of repeating units, they require multistep synthesis with isolation and purification at each step.[11,17-19] Further, this process is time consuming and difficult to scale up. In contrast, the preparation of HBPs is suitable for large-scale production, even though the resulting HBPs constitute a mixture of chains with different molecular weights.[20] The highly branched tree-like structure is an important and unique characteristic of HBPs, which differentiates them from linear and cross-linked polymers.[9] Various kinds of achiral HBPs have been prepared.[9,10,21-29] Although these have promising potential in asymmetric reactions, the number of synthesized chiral HPBs is limited. We have previously prepared chiral branched polymers from A_2 and B_3 monomers.[30] In the $A_2 + B_3$ approach, network polymers may form by crosslinking and there is often very little control over the molar mass and topology.

In this study, we have focused on the AB_2 approach to prepare a novel type of chiral HBPs. The AB_2 monomer yields an HBP with A as the focal unit. The Mizoroki-Heck (MH) coupling is one of the most efficient C-C bond forming reactions.[31] It proceeds smoothly between olefinic compounds and an aromatic iodide. We have reported several types of cinchona-based linear polymers using MH polymerization.[32-34] The MH reaction was performed between an aryl or alkenyl halide and a terminal olefin of the cinchona-derived iodide and olefinic double bond in the presence of a Pd catalyst to produce a substituted olefin.[31] The reaction afforded high yields and showed high functional group selectivity.[31] Cinchona alkaloid derived organocatalysts possess a C3-vinyl group that can be used as a MH reactive site. Several types of cinchona-based chiral organocatalysts have been developed for asymmetric catalysis.[35] For example, cinchona squaramide derivatives have

shown excellent catalytic activities in asymmetric transformations. In this study, we chose the cinchona squaramide structure as the chiral catalyst site of the chiral HBPs.

Chiral HBP catalysts are different from the classical polymer-supported cinchona catalysts.[36-39] In this study, we designed the chiral AB_2 monomer using cinchona alkaloid squaramide. We applied MH polymerization technique to prepare chiral HBPs. Two iodophenyl groups were introduced into the cinchona squaramide derivative to obtain the AB_2 monomer. One component self-polycondensation of AB_2 monomer gives an HBP having focal site A and surface (terminal) functional groups B. The A_2B monomer can also be polymerized to give another type of chiral HBP, which possess focal site B and surface (terminal) functional groups A.

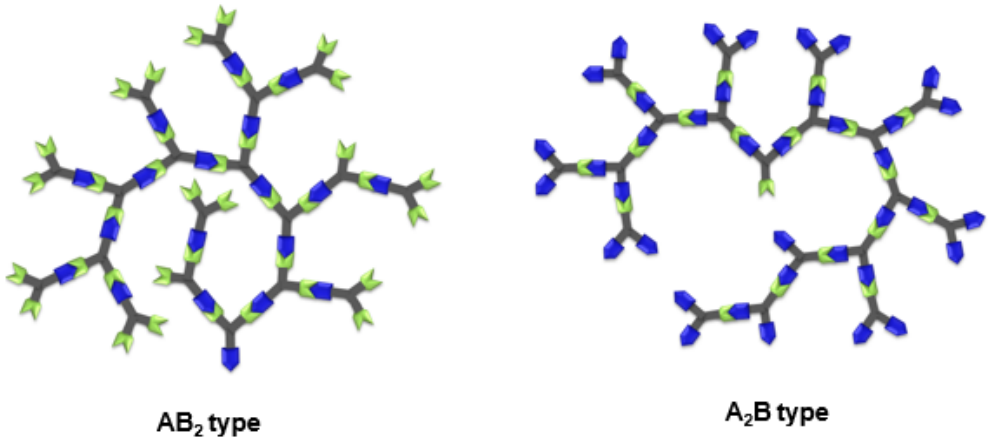

Figure 3.1. Different structure of hyperbranched polymer.

In both chiral HBPs derived from AB_2 and A_2B polymerization, each branching point involves a catalytic active site. The catalyst conformation in the interior branches may be uniform or different from that of the corresponding low molecular weight catalysts in homogeneous solution and the linear polymer catalysts. The interior cavities of HBP can provide a suitable microenvironment for asymmetric transformations. Based on this rationale, we synthesized novel chiral cinchona-based AB_2 and A_2B monomers and conducted their MH polymerization. We subsequently applied these chiral HBPs in asymmetric catalysis and evaluated their catalytic performance.

3.2 Results and discussions

Novel chiral HBPs containing cinchona squaramide moieties were designed and synthesized via the MH coupling polymerization. The monomer for the chiral HBPs was a cinchona squaramide derivative having an iodophenyl group.

3.2.1 Synthesis of AB_2 and A_2B types squaramides

Cinchona squaramide **4** having two iodophenyl groups was equivalent to an **AB_2**-type monomer for MH polymerization. Similarly, monomer **7** with two cinchona squaramide units and one iodophenyl group was an **A_2B**-type monomer. Polymerization of these monomers to HBPs is illustrated in Figure 3.1. One component and one step self-polycondensation is one of the easiest methods to obtain novel chiral HBPs.

For the synthesis of **AB_2** monomer **4**, a bis-iodophenyl component is required. Bis(4-iodobenzyl)amine **1** was synthesized from 4-iodobenzylamine via the Fukuyama secondary amine synthesis method.[33] Then, squaramide squarate **2** was synthesized by reacting **1** with an equimolar amount of diethyl squarate. **AB_2** monomer **4** was finally obtained by the reaction of **2** with 9-amino substituted cinchonidine **3** (Scheme 3.1).

The **A_2B** type squaramide **7** was synthesized by the reaction of (5-iodo-1,3-phenylene)dimethanamine **5** with cinchonidine squaramide **6** (Scheme 3.2). For comparison of the catalytic performances of the Chiral HBPs and a linear polymer, we also synthesized monoiodobenzyl squaramide **10** from 4-iodobenzyl amine **8** and **3** (Scheme 3.3).

3.2.2 Preparation of chiral cinchona-based squaramide HBPs

The synthesized chiral monomers contain both an iodophenyl group and an olefinic double bond. These functional groups are suitable for the MH reaction. In the presence of $Pd(OAc)_2$, monomer **4** underwent the MH reaction to give the corresponding chiral HBP **P1** in quantitative yield, as shown in Table 3.1. The MH polymerization conditions were established for the synthesis of chiral cinchona squaramide polymers using a two component polycondensation system.[24] We applied these polymerization conditions to the synthesis of chiral HBPs. Similarly, monomer **7** was polymerized under these MH conditions to give **P2**. Linear polymer **PL** was also prepared by the MH polymerization. The obtained chiral HBPs were soluble in DMF and DMSO, and insoluble in other commonly used organic solvents such as CH_2Cl_2, $CHCl_3$, MeOH, EtOAc, and THF. Figure 2 shows the structure of chiral HBP **P1** and **P2** and linear polymer **PL**. The yield and molecular weight of the HBPs and linear polymer are summarized in Table 3.1.

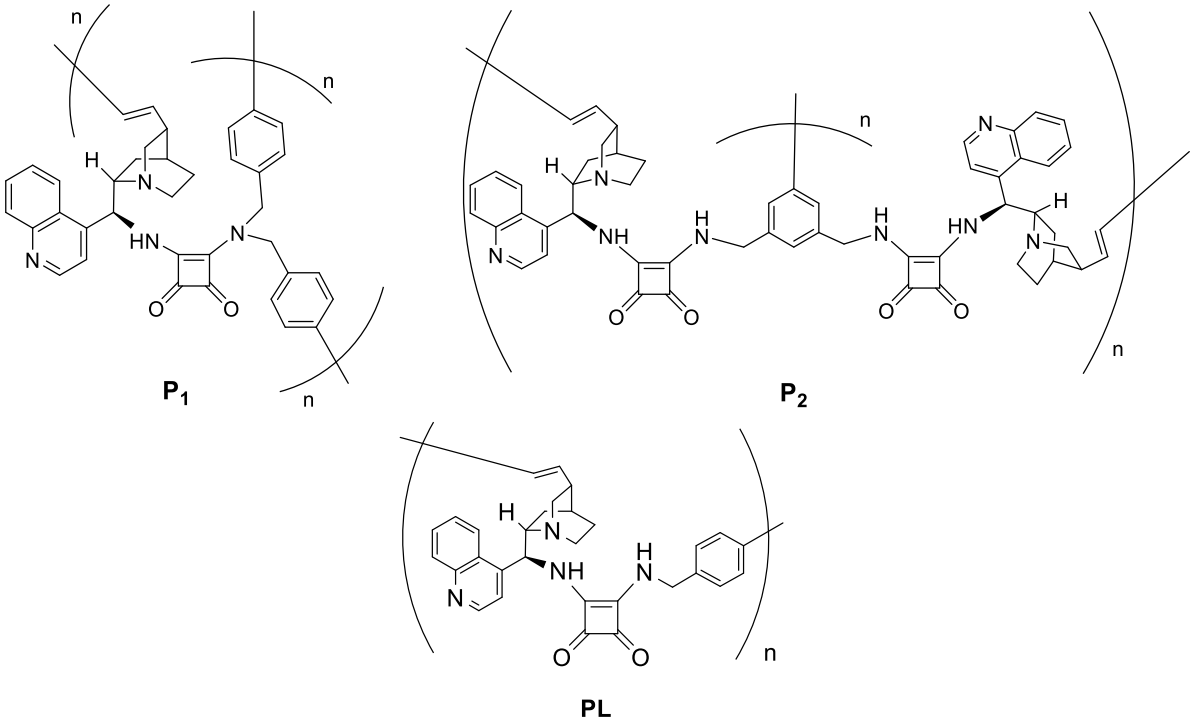

Figure 3.2. Structures of chiral HBPs, **P1** and **P2**, and chiral linear polymer **PL.**

Table 3.1. Synthesis of chiral HBPs **P1**, **P2** and linear polymer **PL** from cinchona squaramide **4, 7, 10** and their GPC data.[a]

Entry	Squaramide	Chiral HBP	Yield [%]	M_n[d]	M_w[d]	M_w/M_n[d]
1[a]	**4**	**P1**	99	20000	23000	1.14
2[b]	**7**	**P2**	99	88000	125000	1.43
3[c]	**10**	**PL**	99	10000	15000	1.48

[a] Polymerization was carried out with squaramide **4** (0.31 mmol), triethylamine (0.61 mmol) in DMF (3.5 mL) in the presence of 10 mol% $Pd(OAC)_2$.
[b] Polymerization was carried out with squaramide **7** (0.14 mmol), triethylamine (0.28 mmol) in DMF (3.0 mL) in the presence of 10 mol% $Pd(OAC)_2$.
[c] Polymerization was carried out with squaramide **10** (0.41 mmol), triethylamine (0.82 mmol) in DMF (4.0 mL) in the presence of 10 mol% $Pd(OAC)_2$.
[d] Determined by SEC using DMF as a solvent at a flow rate of 1.0 mL min^{-1} at 40 °C (polystyrene standard).

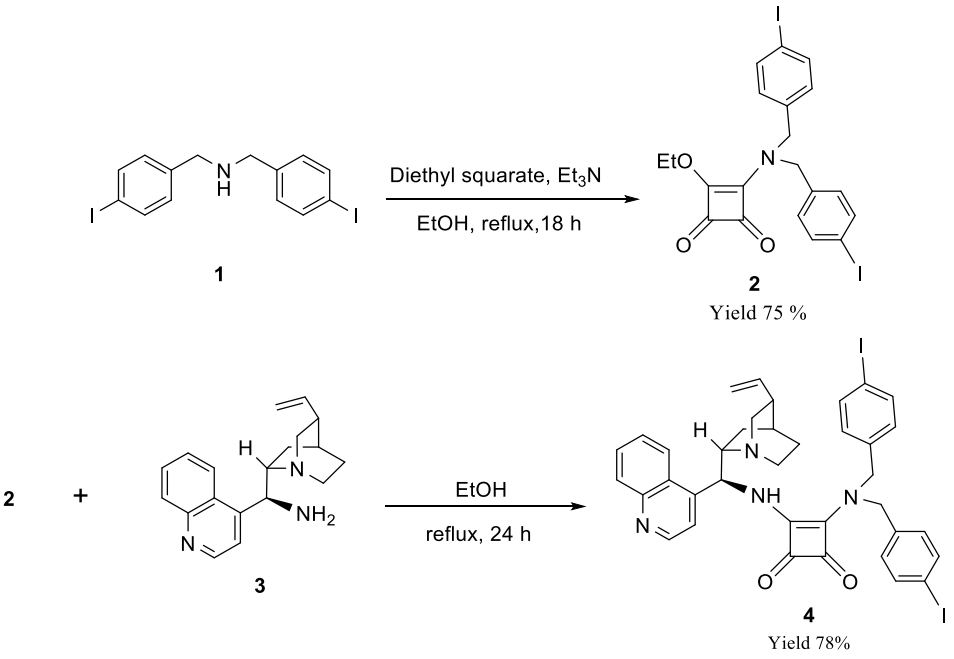

Scheme 3.1. Synthesis of squaramide **4**.

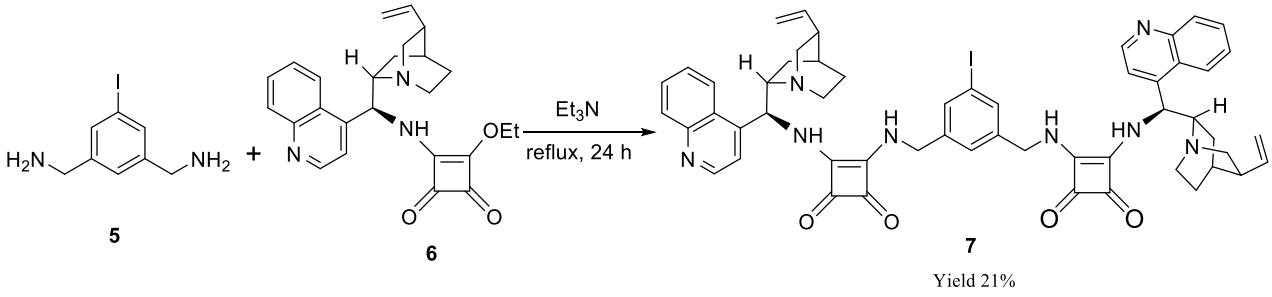

Scheme 3.2. Synthesis of squaramide **7**.

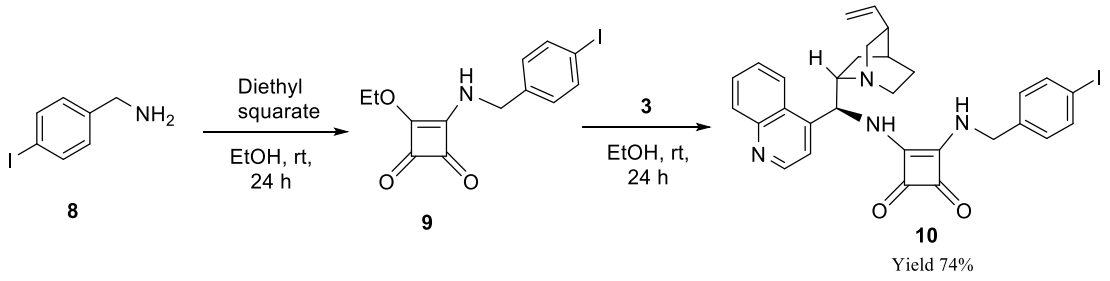

Scheme 3.3. Synthesis of squaramide **10**.

3.2.3 Catalytic performance of the cinchona squaramides and their polymers

3.2.3.1 Asymmetric Michael addition of methyl 2-oxocyclopentanecarboxylate to *trans*-β-nitrostyrene

We tested the catalytic activity of the chiral HBP catalyst **P1** (5 mol %) in the asymmetric Michael addition reaction of methyl 2-oxocyclopentanecarboxylate **11** and *trans*-β-nitrostyrene **12** (Scheme 3.4). Although **P1** was insoluble in solvent used for the asymmetric reaction, the reaction under the heterogeneous condition proceeded smoothly to give the corresponding Michael adduct **13** in 93% yield with excellent diastereoselectivity (diastereomer ratio (*dr*) >100:1). Enantioselectivity (in terms of enantiomeric excess, *ee*) of the major diastereomer was 98% (Table 3.2 entry 2). The results of the asymmetric reaction are summarized in Table 3.2. The catalytic activity of another HBP **P2** was almost equivalent to that of **P1** (entry 3). We also used a linear polymer catalyst **PL** for the same reaction. A similar result of high stereoselectivity was obtained with **PL** (entry 4). Further, all synthesized polymeric catalysts **P1**, **P2**, and **PL** showed excellent catalytic activity with higher stereoselectivity compared to the corresponding low molecular weight catalyst **4** (entry 1).

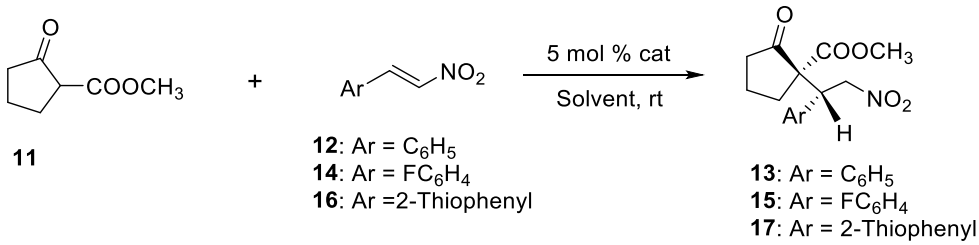

Scheme 3.4. Enantioselective Michael addition of methyl 2-oxocyclopentanecarboxylate **11** to *trans*-β-nitrostyrene **12**.

Table 3.2. Asymmetric Michael addition reaction of **11** with nitroolefins in different solvents using HBP catalysts.[a]

Entry	Catalyst	Solvent	Michael acceptor	Product	Reaction time [h]	Yield[b] [%]	*dr*[c] [%]	*ee*[c] [%]
1	**4**	CH_2Cl_2	12	13	48	85	56:1	98
2	**P1**	CH_2Cl_2	12	13	24	93	>100:1	98
3	**P2**	CH_2Cl_2	12	13	24	90	>100:1	98
4	**PL**	CH_2Cl_2	12	13	24	92	>100:1	98
5	**P1**	Hexane	12	13	48	64	34:1	99
6	**P1**	THF	12	13	24	91	51:1	>99
7	**P1**	MeOH	12	13	19	91	42:1	>99
8[d]	**P1**	MeOH	12	13	24	70	97:1	>99
9	**P1**	CH_2Cl_2	14	15	24	93	>100:1	98
10	**P1**	MeOH	14	15	24	90	54:1	91
11	**P1**	CH_2Cl_2	16	17	24	92	>100:1	98
12	**P1**	MeOH	16	17	24	89	36:1	94

[a]Asymmetric reaction was carried out with **11** (0.5 mmol), nitroolifin (0.55 mmol) and 5 mol% catalyst in solvent (2.0 mL) at room temperature.
[b]Isolated yield of the product after column chromatography.
[c] Enantioselectivity (*ee*) and *dr* value were determined using HPLC (Chiralcel OD-H column).
[d] Reaction was performed at 0 °C.

The effect of solvents on the catalytic performance was surveyed using **P1**. In hexane, both the yield and diastereoselectivity were low (entry 5). In contrast, both THF and methanol as solvents led

to high yields with low diastereoselectivity (entries 6 and 7). Interestingly, enantioselectivities higher than 99% *ee* were attained for the major diastereomer in these solvents (entries 5–7). Lowering the reaction temperature to 0 °C in methanol afforded somewhat higher diastereoselectivity compared to that obtained at room temperature (entry 8). Two other nitroolefins, **14** and **16**, were tested for the asymmetric reaction with **P1** in CH_2Cl_2 and methanol. Similar trends in the catalytic activity and stereoselectivity was observed in these cases (entries 9–12). The absolute configuration of the Michael adducts was assigned as (2*S*, 3*R*) by comparing the reported value in the literature.[40,41]

3.2.3.2 Recyclability of chiral HBPs

Chiral HBP catalysts were mostly insoluble in commonly used organic solvents, except for DMF and DMSO. In spite of the heterogeneous system, the asymmetric reaction with chiral HBP catalysts proceeded smoothly to give the product. The insoluble catalyst could be easily separated and recovered after completion of the reaction via simple filtration. Recovered polymeric catalyst **P1** was reused in the same reaction in methanol to examine its recyclability. **P1** could be recycled four times and the results of the recycling experiments are summarized in Table 3.3. Even after recycling for four catalytic runs, the catalytic activity and stereoselectivity were still maintained.

Table 3.3. Recyclability of chiral HBP **P1** in enantioselective Michael addition reaction of **11** and *trans*-β-nitrostyrene in methanol.[a]

Entry	Reaction time [h]	Yield[b] [%]	*dr*[c] [%]	*ee*[c] [%]
Fresh polymer	19	91	42:1	>99
Cycle 1	24	85	47:1	92
Cycle 2	24	86	39:1	94
Cycle 3	24	88	36:1	99
Cycle 4	24	86	30:1	99

[a]Asymmetric reaction was carried out with **11** (0.5 mmol), **12** (0.55 mmol) and 5 mol% catalyst in methanol (2.0 mL) at room temperature.
[b]Isolated yield of the product after column chromatography.
[c]Enantioselectivity (ee) and *dr* values were determined using HPLC (Chiralcel OD-H column).

3.2.3.3 Asymmetric Michael addition reaction of other active methylene compounds to *trans*-β-nitrostyrene

Other active methylene compounds (**18**, **20, 22** and **24**) were examined as Michael donors in the asymmetric addition reaction. In the presence of the low molecular weight cinchona squaramide catalysts **4**, **7**, and **10**, the reaction of acetylacetone **18** and **12** proceeded smoothly to give the chiral adduct **19** (Table 3.4, entries 1–3). Cinchona squaramide **10** gave the best enantioselectivity among these catalysts (entry 3). The corresponding chiral polymeric catalysts **P1**, **P2**, and **PL** were then applied in the same reaction. These chiral HBP catalysts showed excellent performance in the asymmetric reaction. When **P1** was used as a catalyst in CH_2Cl_2, chiral product **19** was obtained in 83% yield after 24 h even under heterogeneous conditions and gave high enantioselectivity (81%, entry 4). Enantioselectivity improved to 85% when this reaction was performed at 0 °C, although the reaction time was prolonged to 48 h (entry 7). At 50 °C, *ee* was reduced to 77% (entry 8).

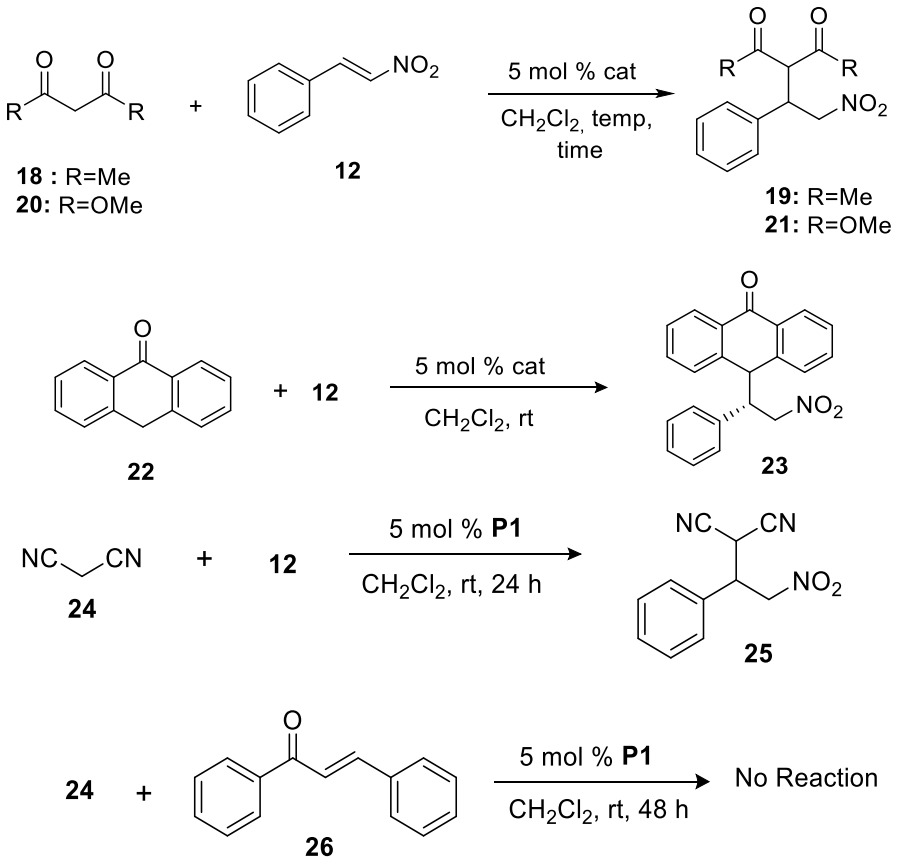

Scheme 3.5. Asymmetric Michael addition reaction using chiral HBP catalysts.

Table 3.4. Asymmetric Michael addition reaction using chiral low molecular weight catalysts and HBP catalysts.[a]

Entry	Catalyst	Michael donor	Product	Temperature [°C]	Reaction time [h]	Yield[b] [%]	*ee*[c][%]
1	**4**	**18**	**19**	rt	24	92	36
2	**7**	**18**	**19**	rt	24	91	76
3	**10**	**18**	**19**	rt	24	90	95
4	**P1**	**18**	**19**	rt	24	89	81
5	**P2**	**18**	**19**	rt	24	88	58
6	**PL**	**18**	**19**	rt	24	85	58
7	**P1**	**18**	**19**	0	48	77	85
8	**P1**	**18**	**19**	50	24	86	77
9[d]	**P1**	**20**	**21**	rt	96	55	33
10[d]	**P2**	**20**	**21**	rt	96	55	44
11[e]	**P1**	**22**	**23**	rt	20	82	61
12[e]	**P2**	**22**	**23**	rt	16	80	16
13[e]	**PL**	**22**	**23**	rt	16	79	47
14	**P1**	**24**	**25**	rt	24	90	14

[a]Asymmetric reaction was carried out with **18** (0.275 mmol), **12** (0.25 mmol) and 5 mol% catalyst in CH_2Cl_2 (2.0 mL).
[b]Isolated yield of the product after column chromatography.
[c] Enantioselectivity (*ee*) was determined using HPLC (Chiralpak AD-H and Chiralpak AS-H columns for entries 9–11).
[d] last 24 h carried out in 50 °C.
[e]Asymmetric reaction was carried out with **22** (0.24 mmol), **12** (0.20 mmol) and 5 mol% catalyst in CH_2Cl_2 (2.0 mL).

Using HBP **P2**, the reaction resulted in 88% yield with 58% *ee* (entry 5). The corresponding linear polymer catalyst **PL** gave the product **19** with almost similar catalytic activity and enantioselectivity (entry 6). A suitable microenvironment was created for the asymmetric reaction in

the chiral polymer network in the case of catalyst **P1**. The absolute configuration of the Michael adduct **19** was assigned as (*S*) by comparing the reported value in the literature.[42] The reaction of dimethyl malonate **20** and **12** was also catalysed by **P1** and **P2**. Same reaction time and yield was obtained in both cases, but little increased ee was found in case of **P2** than **P1**. The Michael addition of anthrone **22** to β-nitrostyrene **12** was also examined using the polymeric catalysts. The HBP **P1** catalyst showed higher enantioselectivity compared to other polymeric catalysts (entries 9–11). The absolute configuration of the Michael adduct **23** was assigned as (*S*) by comparing the reported value in the literature.[43]

3.2.3.4 Enantioselective aldol reaction of ketones with isatins[44]

Aldol reaction is one of the most important carbon-carbon bond formation reactions and, therefore, many asymmetric variants of this reaction have been developed in the past. Here, we examined catalyst **P1**and **P2** by using as a catalyst in the reaction of isatins with ketones. **P1**and **P2** chiral polymeric catalyst were applied to the reaction of isatin and ketone. **P1** gave 7% ee in the reaction of isatin **27** and acetophenone **28** (Table 3.6, entry 1) whereas 28 % ee was obtained with acetone **30** with good yield (entry 4). Decreasing the temperature to 0 °C, ee was not improved, only 4% ee was obtained (entry 2). **P2** catalyst was not good in these reactions. With acetone, it gave 6% ee with good yield (entry 5) whereas racemic product was found in the reaction with acetophenone (entry 3). Synthesized chiral HPBs can catalyze this reaction smoothly to give good yield but obtained ee is very poor.

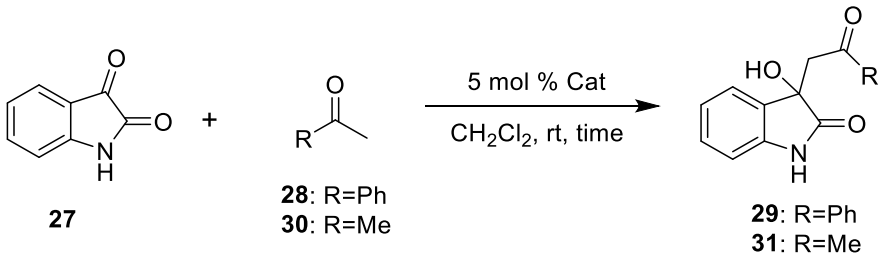

Scheme 3.6. Aldol condensation reaction using chiral HBP catalysts.

Table 3.5. Aldol condensation reaction using chiral HBP catalysts**.**

Entry	Catalyst	Ketone	Product	Temperature [°C]	Reaction time [day]	Yield[a] [%]	*ee*[b] [%]
1	**P1**	**28**	**29**	rt	3	87	7
2	**P1**	**28**	**29**	0	7	75	4
3	**P2**	**28**	**29**	rt	2	90	racemic
4	**P1**	**30**	**31**	rt	2.5	90	28
5	**P2**	**30**	**31**	rt	2	91	6

[a] Isolated yield of the product after column chromatography.
[b]Enantioselectivity (ee) was determined using HPLC (Chiralcel OD-H column for entry 1-3 and OJ-H column for entries 4,5).

3.3 Conclusion

We synthesized novel chiral HBPs from cinchona squaramide monomers **4** and **7** possessing both vinyl (**A**) and iodophenyl (**B**) groups in their structure. These **AB$_2$** and **A$_2$B** monomers were

successfully polymerized by the MH coupling reaction between the **A** and **B** functionalities to give chiral HBPs **P1** and **P2**, respectively. The chiral HBPs (**P1**, **P2**) prepared by one step MH polymerization were used as catalysts in asymmetric Michael reactions. The reactions occurred smoothly to give the corresponding chiral product. In case of the reaction between methyl 2-oxocyclopentanecarboxylate **11** and *trans*-β-nitrostyrene **12**, the HBP catalysts showed high catalytic activity with excellent diastereoselectivity and enantioselectivity. Reactions between some other substrate combinations also occurred smoothly with the HBP catalysts. **P1** exhibited superior selectivity in these reactions. Interestingly, the HBP catalysts gave higher diastereoselectivity compared to that obtained with the low-molecular-weight catalyst **4**. Somewhat higher catalytic activity was also observed with HBP catalyst. Precise control of the catalyst conformation may be possible in case of polymer catalyst. These results show that the design of chiral HBP catalyst may lead the development of high performance polymeric catalyst.The HBP catalysts were easily recovered from the reaction mixture and reused several times without any decrease in catalytic activity and stereoselectivity.

3.4 Experimental

3.4.1 Material and general consideration

All reagents and solvents were purchased from Sigma Aldrich, Wako Pure Chemical Industries, Ltd., or Tokyo Chemical Industry (TCI) Co., Ltd. To monitor the progress of the reactions, thin layer chromatography (TLC) was performed using pre-coated silica gel plates (Merck TLC silica gel, 60F254). To purify the synthesized compounds, column chromatography was performed using a silica gel column (Wakogel C-200, 100–200 mesh). NMR spectra were recorded on JEOL JNM-ECS400 and JEOL JNM-ECX500 spectrometers in $CDCl_3$ or DMSO-d_6 at room temperature operated at 400 MHz (^{1}H) and 500 MHz (^{1}H), and 400 MHz (^{13}C{^{1}H}) and 500 MHz (^{13}C{^{1}H}), respectively. Chemical shifts are reported in parts per million (ppm) using tetramethylsilane (TMS) as a reference and the *J* values are reported in Hertz (Hz). IR spectra were recorded using KBr pellets on a JASCO FT/IR-230 spectrometer and the wavenumbers are reported in cm^{-1}. HRMS (ESI and APCI) data was obtained using a Bruker micro OTOF II HRMS instrument. High-performance liquid chromatography (HPLC) was performed on a Jasco HPLC system composed of a DG-980-50 three-line degasser, an HPLC pump (PU-980), and CO-2065 column oven equipped with a chiral column (Chiralcel OD-H, Chiralpak AD-H, and Chiralpak AS-H, Daicel) using hexane/2-propanol as the eluent at a flow rate of 1.0 mL/min and 0.7 mL/min at room temperature. For peak detection, a Jasco UV-975 UV detector was used. Size exclusion chromatography (SEC) was performed using a Tosoh instrument with HLC 8020 UV (254 nm) or a refractive index detector. Two polystyrene gel columns with a bead size of 10 μm were used and dimethylformamide (DMF) was used as the carrier solvent at a flow rate of 1.0 mL min^{-1} at 40 °C. A calibration curve was established to determine the number average molecular weight (M_n) and molecular weight

distribution (M_w/M_n) values by comparison with polystyrene standards. Optical rotations were determined on a JASCO DIP-149 digital polarimeter using a 10 cm thermostatted microcell.

3.4.2 Synthesis of cinchona AB_2 type squaramide

For the synthesis of AB_2 type squaramide, starting compound **1** was necessary. So, this compound was synthesized first. Using 1, squaramide 2 was prepared and finally AB_2 type squaramide 4 was synthesized.

3.4.2.1 Synthesis and characterization of bis (4-iodo benzyl) amine 1

i) Step-1: 1.81g (7.77 mmol) 4-iodobenzyl amine and 1.08 ml (7.77 mmol) Et_3N is taken in a 50 mL volumetric flask with 18 mL CH_2Cl_2 under continuous N_2 flow. Mixture was stirred and cooled in an ice water bath while 1.57g (7.07 mmol) 2-nitrobenzene sulphonyl chloride was added over a period of 5 min. then after 10 min, ice bath was removed, reaction mixture allowed to warm room temp and stirred more 4 hr. After that mixture was quenched with 18 mL 1N HCl. Aq layer was extracted 2 times by DCM. Combined organic extract was washed with 20 mL brine, dried over $MgSO_4$, filtered, concentrated under reduced pressure to give crude product **A**. Then it was recrystallized from ethyl acetate hexane mixture. White crystal (2.75 g, 85%). R_f: 0.62 (hexane/EtOAc = 3.0/2.0). ^{1}H NMR (500 MHz, $CDCl_3$): δ 4.26 (d, J = 6.5 Hz, 2H), 5.77 (br, 1H), 6.97 (d, J = 8.5 Hz, 2H), 7.54 (d, J = 8.0 Hz, 2H), 7.63- 7.73 (m, 2H), 7.83 (d, J = 8 Hz, 1H), 7.95 (d, J = 8 Hz, 1H). ^{13}C NMR (500 MHz, $CDCl_3$): δ 47.39, 93.70, 125.40, 129.86, 131.04, 132.93, 133.59, 133.97, 135.63, 137.79, 147.83.

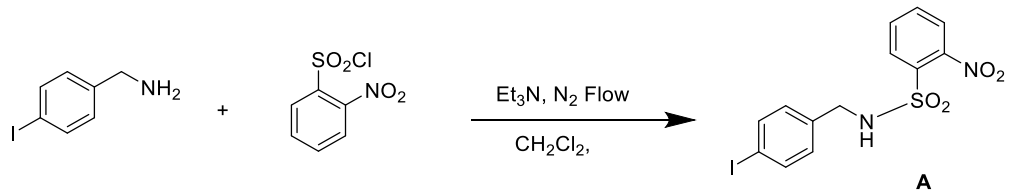

ii) Step-2: 2.70 g (6.46 mmol) compound **A**, 2.68 g (19.39 mmol) K_2CO_3 was taken with 9 mL dry DMF in a 50 mL volumetric flask with continuous N_2 flow. To the stirred solution 2.11 g (7.11 mmol) 4-iodo benzyl bromide was added over a period of 5 min and resulting mixture was heated in an oil bath at 65 ^{0}C for 6 h. Then reaction mixture allowed to cool at room temp. DMF was evaporated, quenched with 6 mL water, then 30 mL diethyl ether was added. White precipitate was formed. It was filtered, dried and dissolved in DCM, dried over $MgSO_4$, filtered and concentrated.

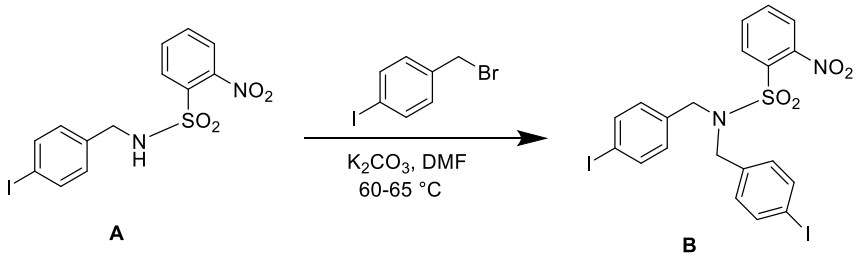

White solid (3.86 g, 94%). R_f: 0.45 (hexane/EtOAc = 2.0/1.0). ^{1}H NMR (500 MHz, $CDCl_3$): δ 4.36 (s, 4H), 6.79 (d, J = 8.5 Hz, 4H), 7.54 (d, J = 8.0 Hz, 4H), 7.60 (m, 1H), 7.70 (m, 2H), 7.93 (d, J = 8.0 Hz, 1H). ^{13}C NMR (500 MHz, $CDCl_3$): δ 50.38, 93.71, 124.51, 130.27, 131.23, 132.00, 133.79, 133.96, 134.75, 137.88, 147.73.

iii) Step-3: 21.6 mL (15.13 mmol) thiol was taken in a 50 mL flask with 5 mL acetonitrile under continuous N_2 flow. Mixture was cooled to ice bath and 10.9 M, 1400µL (15.13 mmol) aq. KOH solution was added over a period of 10 minutes. After 5 min, ice bath was removed and 3.84 g (6.05 mmol) of compound **B** (synthesized in step-2) was added over a period of 5 min. Reaction mixture was then heated for 55-60 ºC in oil bath for 6 hr. after cooling the mixture, DCM was added and extracted with water . Aq layer was again extracted with dichloromethane and combined organic layer was extracted with brine, dried over $MgSO_4$, filtered and concentrated. Crude mixture was purified by column chromatography by using Hex: EtOAc = 6:1 ratio. Off-white crystal (1.72 g, 63 %). mp: 77-81 ºC; R_f: 0.41 (hexane/EtOAc = 2.0/1.0); IR (KBr): ν = 3324, 3032, 3324,2920, 1562, 1479, 1229 cm^{-1}; HRMS (APCI) *m/z* for $C_{14}H_{14}I_2N$ [M^+H^+] calcd. 449.9215, found 449.9210. ^{1}H NMR (500 MHz, $CDCl_3$): δ 3.72 (s, 4H), 7.08 (d, J = 8.5 Hz, 2H), 7.64 (d, J = 8.5 Hz, 4H), ^{13}C NMR (500 MHz, $CDCl_3$): δ 52.50, 92.36, 130.21, 137.56, 139.87.

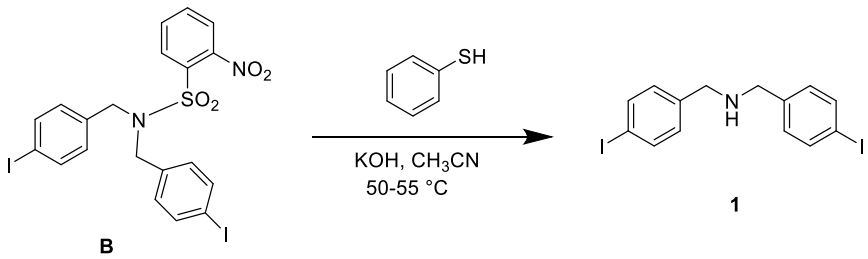

3.4.2.2 Synthesis of squaramide 2

In a 30 mL flask, 5.0 mmol (734 µL) of diethylsquarate and 15 mL of ethanol were mixed. Next, 2.0 mmol of triethyl amine was added and to the stirred solution, 1.0 mmol (449 mg) of bis(4-iodobenzyl)amine **1** was added slowly. The mixture was stirred at reflux for ~18 h under Ar. Subsequently, the solution was cooled to room temperature. Eventually, off-white crystals were formed, which were filtered and dried. Yield: 430 mg (75%). R_f: 0.43 (hexane/EtOAc = 2.0/1.0); mp: 145–149 ºC; ^{1}H NMR (400 MHz, $CDCl_3$): δ 1.44 (t, *J* = 7.2 Hz, 3H), 4.37 (s, 2H), 4.67 (s, 2H), 4.81 (q, *J* = 6.8 Hz, 2H), 6.95 (dd, *J* = 7.6 Hz and 14.4 Hz, 4H), 7.71 (dd, *J* = 8.4 Hz and 12.4 Hz, 4H); ^{13}C NMR (400 MHz, $CDCl_3$): δ 15.99, 50.58, 51.20, 70.32, 94.39, 130.05, 130.69, 134.25, 134.37, 138.27, 138.39, 171.95,176.79, 182.80, 188.68; IR (KBr): ν = 3076, 2979, 2880, 2081, 1908, 1800, 1702, 1562, 1460, 1383, 1282, 1183, 1069, 984, 889, 795, 719, 628, 532 cm^{-1}; HRMS (APCI) *m/z* for $C_{20}H_{18}I_2NO_3$ [M^+H^+] calcd. 573.9376, found 573.9371.

3.4.2.3 Synthesis of squaramide 4

Compound **2** (410 mg, 0.714 mmol) was mixed with 10 mL of ethanol in a 30 mL volumetric flask. To the stirred solution, 0.862 mmol (253 mg) of **3** in 10 mL ethanol was added slowly. The

mixture was stirring at reflux for ~24 h under Ar. A white precipitate was formed, and it was filtered, washed with ethanol, and dried to obtain **4** (460 mg, 78%) as a white solid. R_f: 0.48 (CH_2Cl_2/MeOH = 9.0/1.0; mp: 229–232 ºC. ^{1}H NMR (400 MHz, $CDCl_3$): δ 0.90 (m, 1H), 1.29 (m, 2H), 1.57 (m, 4H), 2.27 (br,1H), 2.57–3.14 (m, 4H), 4.59 (br, 4H), 4.93 (m, 2H), 5.63 (m, 1H), 6.95 (d, *J* = 8.0 Hz, 4H), 7.72 (m, 8H), 8.14 (d, *J* = 8.0 Hz, 1H), 8.86 (d, *J* = 4.4 Hz, 1H); ^{13}C NMR (500 MHz, $CDCl_3$): δ 25.9, 27.31, 27.69, 39.54, 40.77, 56.0, 94.20, 114.90, 123.57, 127.16, 129.56, 135.32, 138.41, 141.20, 149.99, 167.46, 168.0, 182.87, 183.50. IR (KBr): *v* = 3324, 3065, 2933, 2862, 1788, 1667, 1561, 1484, 1343, 1285, 1182, 1088, 981, 839, 771, 649, 564 cm^{-1}; HRMS (APCI) *m/z* for $C_{37}H_{35}I_2N_4O_2$ [M^+H^+] calcd. 821.0849, found 821.0844; $[\alpha]^{23.7}_D$ = –166 (*c* 0.22, DMF).

3.4.3 Synthesis of cinchona A_2B type squaramide

3.4.3.1 Synthesis and characterization of compound 7

0.631 mmol (165.4 mg) (5-iodo 1,3-phenylene) dimethanamine **5,** 1.30 mmol (542.8 mg) cinchonidine squaramide **6** and 1.32 mmol (184 µL) Et_3N were taken with 10 mL ethanol in a 30 mL volumetric flask. The mixture was stirring at reflux condition about 24 h under Ar gas. Brownish white precipitate was observed, and it was filtered, washed with ethanol and dried to give **7** (134 mg, 21%) as a brownish white solid. R_f: 0.38 (CH_2Cl_2/MeOH = 10.0/1.0; decomposition temp: 217-222 ºC. IR (KBr): *v* = 3500, 3235, 2939, 2864, 1797, 1671, 1589, 1531, 1458, 1344, 1240, 1164, 1091, 978, 767, 624 cm^{-1}; HRMS (ESI) *m/z* for $C_{54}H_{54}IN_8O_4$ [M^+H^+] calcd.1005.3312, found 1005.3307; $[\alpha]^{24.}_D$ =–70 (*c* 0.07, DMF). ^{1}H NMR (500 MHz, DMSO-d_6): *δ* 0.62 (m, 2H), 1.33 (m, 2H), 1.49 (m, 10H), 2.24 (br, 2H), 2.60 (m, 4H), 3.16 (m, 4H), 4.58 (s, 4H), 4.93 (m, 4H), 5.89 (m, 2H), 7.24 (s, 1H), 7.59-7.79 (m, 6H), 8.05 (d, J= 8 Hz, 4H), 8.46 (d, J= 8.0 Hz, 2H), 8.93 (d, J= 4.5 Hz, 2H). ^{13}C NMR (500 MHz, DMSO-d_6): *δ* 26.38, 27.74, 46.54, 56.09, 59.86, 96.94, 114.87, 124.00, 126.85, 127.66, 129.97, 130.47, 136.03, 142.08, 142.67, 148.61, 150.97, 167.33, 167.80, 182.59, 182.80.

3.4.4 Synthesis of cinchona AB type squaramide

3.4.4.1 Synthesis and characterization of compound 9

0.714 mmol (178.0 µL) diethyl squarate, 1.0 mmol Et_3N were taken with 5 mL ethanol in a 20 mL volumetric flask. To the stirred solution 1.0 mmol (233 mg) 4-iodo benzyl amine **8** was added slowly. The mixture was stirring at rt about 24 h under Ar. Reaction mixture was filtered and little concentrated. Yellowish crystal was found which was filtered, washed with ethanol and dried to give **9** (201 mg, 56%) as a yellowish crystal. R_f: 0.54 (CH_2Cl_2/MeOH = 9.0/1.0; mp: 120-125 ºC. IR (KBr): *v* = 3183, 3024, 2986, 1811, 1726, 1701, 1593, 1480, 1384, 1278, 1180, 1068, 955, 865, 785, 673, 506 cm^{-1}; HRMS (ESI) *m/z* for $C_{13}H_{13}INO_3$ [M^+H^+] calcd. 357.9940 found 357.9927. ^{1}H NMR (500 MHz, $CDCl_3$): *δ* 1.44 (t, J= 6.5 Hz, 3H), 4.56 (br, 2H), 4.78 (br, 2H), 7.05 (d, J= 6.5 Hz, 2H), 7.71 (d, J= 8.0 Hz, 2H). ^{13}C NMR (500 MHz, $CDCl_3$): *δ* 15.91, 48.13, 70.07, 93.99, 129.52, 138.23, 172.32, 177.91.

3.4.4.2 Synthesis and characterization of compound 10

1.0 mmol (357.15 mg) **9** was taken with 10 mL ethanol in a 30 mL volumetric flask. To the stirred solution 1.07 mmol (314.0 mg) cinchonidine amine in 10 mL ethanol was added slowly. The mixture was stirring at room temperature about 24 h under Ar. White precipitate was observed and it was filtered, washed with ethanol and dried to give **10** (450 mg, 74%) as a white solid. R_f: 0.74 (CH_2Cl_2/MeOH = 12.0/1.0; mp: 219-226 °C. IR (KBr): ν = 3193, 2944, 2863, 1793, 1661, 1566, 1459, 1343, 1285, 1181, 1059, 974, 814, 767, 625 cm^{-1}; HRMS (ESI) *m/z* for $C_{30}H_{30}N_4O_2$ [M^+H^+] calcd. 605.1413, found 605.1410; $[\alpha]^{21.7}_D$ = –53.95 (*c* 0.06, DMF). ^{1}H NMR (500 MHz, DMSO-d_6): δ 0.63 (m, 1H), 1.34 (m, 1H), 1.48 (m, 5H), 2.24 (br,1H), 2.61 (m, 2H), 3.14 (m, 2H), 4.61 (s, 2H), 4.95 (m, 2H), 5.89 (m, 1H), 7.09 (d, J= 8.0 Hz, 2H), 7.627-7.805 (m, 4H), 8.06 (d, J= 7.5 Hz, 2H), 8.47 (d, J= 8.0 Hz, 1H), 8.94 (d, J= 4.5 Hz, 1H). ^{13}C NMR (500 MHz, DMSO-d_6): δ 26.44, 27.76, 46.80, 56.09 59.86, 94.07, 114.83, 124.03, 126.88, 127.64, 129.97, 130.47, 130.58, 137.93, 139.02, 142.71, 146.11, 148.63, 150.96, 167.36, 167.72, 182.63, 182.80.

3.4.5 Synthesis of chiral cinchona-based squaramide hyperbranched polymers via the MH polymerization

3.4.5.1 Synthesis of polymer P1

In a 30 mL flask, squaramide **4** (250 mg, 0.305 mmol) and two equivalents of triethylamine (85.0 µL, 0.610 mmol) were mixed together. Next, palladium acetate (10 mol%) and DMF solvent (3.5 mL) were added and the reaction mixture was stirred for 48 h at 100 °C. Subsequently, the solution was concentrated by evaporation and poured into diethyl ether. The precipitated polymer was collected by filtration and washed with diethyl ether (3×60 mL) and water (40 mL). Next, the compounds were dried in a vacuum oven to afford the **P1** as a light brown solid. Yield: 245 mg; ^{1}H NMR (400 MHz, DMSO-d_6): δ 0.83, 1.20–2.00, 4.62, 6.38, 6.80–8.20, 8.92; IR (KBr): ν = 3586, 3470, 2933, 2862, 2385, 2114, 1790, 1673, 1582, 1431, 1319, 1257, 1143, 1059, 969, 844, 767, 620 cm^{-1}; $[\alpha]^{23.9}_D$ = −22.1(*c* 0.05, DMF); M_n (SEC) = 20000; M_w/M_n = 1.14.

3.4.5.2 Synthesis of polymer P2

Squaramide **7** (140 mg, 0.139 mmol) and double amount of triethyl amine (38 µL, 0.279 mmol) were taken in 20 mL flask. After adding palladium acetate (10 mol %) and DMF (3 mL) reaction mixture was stirred for 48 hours at 100 °C. Subsequently, the solution was concentrated by evaporation and poured into diethyl ether. The precipitated polymer was collected by filtration and washed with diethyl ether (3×60 mL) and water (40 mL). After that the compounds were dried over in vacuum oven to afford the **P2** as a light brown Solid. Yield: 138 mg; ^{1}H NMR (500 MHz, DMSO-d_6); δ 0.72-2.0, 2.95, 4.65, 5.01, 5.86, 6.39, 7.0-8.58, 8.98; IR (KBr); ν = 3470, 3223, 2936, 2866, 2128, 1797, 1671, 1619, 1530, 1428, 1240, 1084, 979, 814, 767, 619 cm^{-1}. $[\alpha]^{24.1}_D$ = –104 (*c* 0.02, DMF). M_n (SEC) = 88000; M_w/M_n = 1.43.

3.4.5.3 Synthesis of polymer PL

Squaramide **10** (250 mg, 0.414 mmol) and triethyl amine (115.8 µL, 0.828 mmol) were taken in a 20 mL flask and palladium acetate (10 mol %) and DMF (4 mL) were added in the reaction mixture and it was stirred for 48 hours at 100 ºC. Subsequently, the solution was concentrated by evaporation and poured into diethyl ether. The precipitated polymer was collected by filtration and washed with diethyl ether (3×60 mL) and water (40 mL). After that the compounds were dried over in vacuum oven to afford the **PL** as a light brown Solid. Yield: 248 mg; ^{1}H NMR (400 MHz, DMSO-d_6): δ 0.93-1.93, 2.95, 4.65, 6.41, 7.0–8.60, 8.44; IR (KBr): ν = 3469, 3222, 2935, 1797, 1673 1590, 1459, 1348, 1242, 973, 846, 768, 617, 529 cm^{-1}; $[\alpha]^{24.3}_{D} = -101$ (c 0.035, DMF); M_n (SEC) = 10000; M_w/M_n = 1.48

3.4.6 Representative procedure for the enantioselective Michael addition reactions.

3.4.6.1 Enantioselective Michael addition reaction of Methyl 2-oxocyclopentanecarboxylate to *trans*-β-nitrostyrene

Trans-β-nitrostyrene **12** (82.1 mg, 0.55 mmol) and the HBP (5 mol%, calculated from the unit molecular weight of the polymer catalyst) were added to a reaction vessel with 2.0 mL of solvent. Methyl 2-oxocyclopentanecarboxylate **11** (63 µL, 0.50 mmol) was added via a syringe into the resulting solution. The reaction was stirred at room temperature and its progress was monitored by TLC. The reaction mixture was then filtered, and the filtrate was concentrated in vacuo. The crude compound was purified by column chromatography on silica gel (100–200 mesh) using hexane/EtOAc = 6.0/1.0 as the eluent to afford the addition product **13** as a colorless oil. The enantioselectivity (*ee*) and diastereomeric ratio (*dr*) were determined using HPLC on a Chiralcel OD-H column using solvent mixture hexane:2-propanol=4:1. Experiments to understand the effect of the solvent, substrate scope, and recyclability were conducted according to this procedure.

3.4.6.2 Enantioselective Michael addition reaction between acetylacetone and *trans*-β-nitrostyrene

Trans-β-nitrostyrene **12** (37.3 mg, 0.25 mmol) and the HBP (5 mol%) were added to a reaction vessel with 1.0 mL of CH_2Cl_2. Next, acetylacetone **18** (30.6 µL, 0.275 mmol) was added using a syringe into the resulting solution. The reaction was stirred at room temperature and monitored using TLC. The reaction mixture was then filtered, and the filtrate was concentrated in vacuo. The crude compound was purified by column chromatography using hexane/EtOAc/CH_2Cl_2 = 6.0/1.0/1.0 as the eluent on silica gel (100-200 mesh) to afford the addition product **19** as a white solid. The *ee* values were determined using HPLC on a Chiralpak AD-H column using solvent mixture hexane:2-propanol=9:1.

3.4.6.3 Enantioselective Michael addition reaction between anthrone and *trans*-β-nitrostyrene

Trans-β-nitrostyrene **12** (29.8 mg, 0.20 mmol) and the HBP catalyst (5.0 mol%) were added to a reaction vessel with 2.0 mL of CH_2Cl_2. Anthrone **20** (46.6 mg, 0.24 mmol) was added to the

resulting solution. The reaction was stirred at room temperature and monitored using TLC. The reaction mixture was then filtered, and the filtrate was concentrated in vacuo. The crude product was purified by column chromatography on silica gel (100–200 mesh) using hexane/EtOAc = 5.0/1.0 as the eluent to afford **21** as a white solid. The *ee* was determined using HPLC on a Chiralpak AS-H column using solvent mixture hexane:2-propanol=5:1.

3.4.6.4 Enantioselective Michael addition reaction of malononitrile to *trans*-β-nitrostyrene [45]

Malononitrile **24** (39.64 mg, 0.6 mmol) was added to a solution of catalyst **P1** (5.0 mol %) and *trans*-β-nitrostyrene **12** (44.75 mg, 0.3 mmol) in CH_2Cl_2 (2 ml) at rt. After 24 h, the resulting mixture was evaporated to give the crude product, which was purified by column chromatography on silica gel (hexane/ethyl acetate) to afford the desired product **25** (90 % yield) as a white solid. The *ee* was determined using HPLC on a Chiralpak AD-H column using solvent mixture hexane:2-propanol=85:15.

3.4.6.5 Enantioselective aldol reaction of ketones with isatins [44,46]

A solution of catalyst **P1** (5 mol %) and isatin **27** (0.5 mmol) in CH_2Cl_2 (2 mL) were stirred for 10 min at rt. Then ketone (acetophenone **28**, 4 mmol; acetone **30**, 10 mmol) was added. The reaction mixture was stirred for appropriate time and the progress of the reaction monitored by TLC. After completion of the reaction, the volatile components were removed under reduced pressure and the residue was purified by column chromatography on silica gel (Hexane/EtOAc=5/4) to afford the Aldol product. The enantiomeric excess was determined by HPLC on chiralpak OD-H column [hexane/2-propanol 9:1].

3.5 References

1. Barrulas, P.; Benaglia, M.; Burke, A. J. *Tetrahedron: Asymmetry* **2014**, *25*, 923–935.

2. Takata, S.; Endo, Y.; Ullah, M. S.; Itsuno, S. *RSC Advances* **2016**, *6*, 72300–72305.

3. Endo, Y.; Takata, S.; Kumpuga, B. T.; Itsuno, S. *ChemistrySelect* **2017**, *2*, 10107–10111.

4. Ingemann, S.; Hiemstra, H. *Comprehensive Enantioselective Organocatalysis: Catalysts, Reactions, and Applications* **2013**, pp 117–160.

5. Song, C. E., *Cinchona alkaloids in synthesis and catalysis: ligands, immobilization and organocatalysis*; John Wiley & Sons: **2009**.

6. Itsuno, S., *Polymeric chiral catalyst design and chiral polymer synthesis*; John Wiley & Sons: **2011**.

7. Boratyński, P. J. *Molecular Diversity* **2015**, *19*, 385–422.

8. Zheng Y.; Li S.; Weng Z.; Gao C. *Chem. Soc. Rev.* **2015**, *44*, 4091–4130.

9. Yates C. R.; Hayes W. *Eur. Polym. J.* **2004**, *40*, 1257–1281.

10. Shi Y.; Nabae Y.; Hayakawa T.; Kobayashi H.; Yabushita M.; Fukuoka A.; Kakimoto M. *Polym. J.* **2014**, *46*, 722–727.

11. Tomalia, D. A.; Naylor, A. M.; Goddard, W. A. *Angew. Chem.*, *Int. Ed. Engl.* **1990**, *29*, 138–175.

12. Tomalia, D. A.; Durst ,H. D. *Top. Curr. Chem.* **1993**, *165*, 193–313.

13. Newkome, G. R.; Moorefield, C. N.; Baker, G. R.; Johnson, A. L.; Behera, R. K. *Angew. Chem.*, *Int. Ed. Engl*. **1991**, *30*, 1176–1178.

14. Voit B. I. *Acta Polym.* **1995***, 46*, 87–99.

15. Morikawa, A.; Kakimoto, M.; Imai, Y. *Macromolecules* **1991**, *24*, 3469–3474.

16. (a) Tomalia, D. A.; Baker, H.; Dewald, J.; Hall, M.; Kallos, G.; Martin, S.; Roeck, J.; Ryder, J.; Smith, P. *Polym. J.* **1985**, *17*, 117–132.

(b) Tomalia, D. A.; Baker, H.; Dewald, J.; Hall, M.; Kallos, G.; Martin, S.; Roeck, J.; Ryder, J.; Smith, P. *Macromolecules* **1986**, *19*, 2466–2468.

17. Newkome, G. R.; Yao, Z.; Baker, G. R.; Gupta, V. K. *J. Org. Chem*. **1985**, *50*, 2003–2004.

18. Morikawa, A.; Kakimoto, M.; Imai, Y. *Macromolecules* **1993**, *26*, 6324–6329.

19. Yan, D.; Gao, C.; Frey, H. *Hyperbranched Polymers. Synthesis, Properties, and Applications.* John Wiley & Sons, 2011.

20. Gao, C.; Yan, D. *Prog. Polym*. *Sci*. **2004**, *29*, 183–275.

21. Zimmerman, S. C.; Lawless, L. *Top. Curr. Chem.* **2001**, *217*, 95–120.

22. Vogtle, F.; Gestermann, S.; Hesse, R; Schwierz, H.; Windisch, B. *Prog. Polym. Sci.* **2000**, *25*, 987–1041.

23. Gong, L. -Z.; Hu, Q. -S.; Pu, L. *J. Org. Chem.* **2001**, *66*, 2358–2367.

24. Wyatt, S. R.; Hu, Q. -S.; Yan, X. -L.; Bare, W. D.; Pu, L. *Macromolecules* **2001**, *34*, 7983–7988.

25. Ma, L.; Lee, S. J.; Lin, W. *Macromolecules* **2002**, *35*, 6178–6184.

26. Satoh, N.; Nakashima, T.; Yamamoto, K. *J. Am. Chem. Soc.* **2005**, *127*, 13030–13038.

27. Imaoka, T.; Tanaka, R.; Arimoto, S.; Sakai, M.; Fujii, M.; Yamamoto, K. *J. Am. Chem. Soc*. **2005**, *127*, 13896–13905.

28. Yamanaka, K.; Jikei, M.; Kakimoto, M. *Macromolecules* **2000**, *33*, 6937–6944.

29. (a) Mizoroki, T.; Mori, K.; Ozaki, A. *Bull. Chem. Soc. Jpn.* **1971**, *44*, 581–581.

(b) Heck, R. F.; Nolley, J. P. *J. Org. Chem.* **1972,** *37*, 2320–2322.

(c) Heck, R. F. *Org. React.* **1982**, *27*, 345–390.

30. Ullah, M. S.; Itsuno, S. *Mol. Catal*. **2017**, *438*, 239–244.

31. Ullah, M. S.; Itsuno, S. *ACS Omega* **2018**, *3*, 4573–4582.

32. Kumpuga, B. T.; Itsuno, S. *J. Catal.* **2018**, *361*, 398–406.

33. Tian, S.-K.; Chen, Y.; Hang, J.; Tang, L.; Daid, P. M. C.; Deng, L. *Acc. Chem. Res.* **2004**, *37*, 621–631.

34. Kacprzak, K.; Gawronski, J. *Synthesis*, **2001**, *7*, 961–998.

35. Sykora, D.; Vozka, J.; Tesarova, E.; Kalikova, K.; Havlik, M.; Matejka, P.; Kral, V. *Electrophoresis*, **2017**, *38*, 1956–1963.

36. Fernandes, S. D.; Porta, R.; Barrulas, P. C.; Pugliusi, A; Burke, A. J.; Benaglia, M. *Molecules,* **2016**, *21*, 1–9.

37. Itsuno, S. *J. Syn. Org. Chem. Jpn.* **2016**, *74*, 710–719.

38. Jumde, R.P.; Di Pietro, A.; Manariti, A.; Mandoli, A. *Chem. Asian J.* **2015**, *10*, 397–404.

39. Kan, T.; Fukuyama, T. *Chem. Commun.* **2004**, *2004*, 353–359.

40. Begum, Z.; Sannabe, H.; Seki, C.; Kuyama, Y. O.; Kwon, E.; Uwai, K.; Tokiwa, M.; Tokiwa, S.; Takeshita, M.; Nakano, H. *RSC Adv*. **2021**, *211*, 203–209.

41. Togashi, R.; Chennapuram, M.; Seki, C.; Okuyama, Y.; Kwon, E.; Uwai, K.; Tokiwa, M.; Tokiwa, S.; Takeshita, M.; Nakano, H. *Eur. J. Org. Chem.* **2019**, *24*, 3882–3889.

42. Gao, P.; Wang, C.; Wu, Y.; Zhou, Z.; Tang, C. Eur. J. Org. Chem. **2008**, *27*, 4563–4566.

43. Zea, A.; Valero, G.; Alba, A-N. R.; Moyano, A.; Riosa, R. *Adv. Synth. Catal.* **2010**, *352*, 1102–1106.

44. Guo, Dr. Q.; Bhanushali, Dr. M.; Zhao, Dr. C.-G. *Angew. Chem. Int. Ed.* **2010**, *49*, 9460–9464.

45. Guo, H.; Li, J.-G.; Qu, G. R.; Zhang, X.-M.; Yuan, W.C. *Chirality*, **2011**, *23*, 514–518

46. Allu, S.; Molleti, N.; Panem, R.; Singh, V. K. *Tetrahedron Letters*, **2011**, *52*, 4080-4083.

Chapter 4

SYNTHESIS OF CINCHONA SQUARAMIDE POLYMERS BY YAMAMOTO COUPLING POLYMERIZATION AND THEIR APPLICATION IN ASYMMETRIC MICHAEL REACTIONS

4.1 Introduction

The utilization of chiral organocatalysts has depicted an important role in asymmetric synthesis because of their high performance and lack of toxic metal species and contributes to to green chemical processes. Cinchona alkaloids and their derivatives have been widely employed as chiral organocatalysts in diverse asymmetric synthesis, because of their outstanding catalytic activity for several asymmetric reactions.[1-6] Owing to their several functionalities such as secondary alcohols, quinoline rings, and quinuclidine and vinyl groups, cinchona alkaloids are useful for suitable modifications to versatile catalysts in asymmetric reactions. Several types of cinchona-based chiral organocatalysts have been developed that play significant roles in asymmetric catalysis.[7] Some cinchona alkaloid derivatives with catalytic activities were attached to various types of synthetic polymers[8-11] to act as polymeric organocatalysts in asymmetric reactions.[12-18] Modified cinchona alkaloids of with different functionalities such as hydroxyl, amino, urea and thiourea on position C9 and C6′ are used in asymmetric reactions.[19] Cinchona alkaloid–metal complexes were also efficient catalysts in some asymmetric reactions. Their polymeric counterparts were prepared and applied to asymmetric catalysis.[20, 21] Chiral cinchona-squaramide organocatalysts is important cinchona derivatives which were successfully explored in the pioneering work of Rawal.[22] Cinchona-derived squaramide possess an acidic NH and the tertiary nitrogen of the quinuclidine of cinchona alkaloids may serve as both an H-bond acceptor and a base in asymmetric Michael addition reactions.[23,24]

The C–C cross-coupling is one of the most powerful tools for the construction of complex organic compounds.[25] Transition metal complexes are used as catalysts for this purpose and have many advantages over the classical catalysts.[26] In this chapter, we designed new cinchona-based chiral polymers using Yamamoto coupling polymerization. A novel type of polymeric chiral catalyst can be synthesized via this polymerization. Cinchona squaramide derivative was selected as an efficient catalyst for the Michael addition reactions. For this purpose, a dibromophenyl group or two iodophenyl groups were introduced into the cinchona alkaloids. For the polymerization reaction, the original polymerization method reported by Yamamoto was followed.[27] In addition to the chiral homopolymers, the copolymers of these cinchona squaramide monomers with an achiral aromatic dihalide were synthesized. For the linear chiral polymer synthesis, the olefinic double bond (C3-vinyl group) in cinchona alkaloid was reduced to prevent the Mizoroki–Heck-type coupling reaction. In the presence of the C3-vinyl group in the cinchona squaramide monomer, both Yamamoto coupling and Mizoroki–Heck coupling occurred simultaneously to yield hyperbranched chiral polymers, which were also used as catalysts in asymmetric reactions.

Previously Mizoroki–Heck polymerization was developed for the synthesis of cinchona-derived polymeric catalysts.[14,15,28–30] Mizoroki–Heck reaction requires two components, an olefinic double bond and an aromatic halide. In contrast, Yamamoto coupling reaction occurs between aromatic halides. The homopolymerization of aromatic dihalides is possible using this coupling reaction. Yamamoto coupling is the nickel-catalyzed (most commonly used nickel catalyst is bis(cyclooctadiene)nickel(0):$Ni(COD)_2$) coupling reaction of organic halides in the presence of neutral ligands (e.g., PPh_3 and bipyridine).[31,32] This coupling reaction is particularly interesting when it is applied to polymer synthesis. Yamamoto coupling polymerization proceeds through reductive elimination from a diorganonickel(II) intermediate.[33–35] Aromatic dihalides in the presence of a Ni catalyst simply react to afford π-conjugated polymers.[36] Various types of π-conjugated polymers have been synthesized via Yamamoto coupling polymerization.[36]

Yamamoto coupling reaction is advantageous because only a single, halogen-functionalized monomer can be used to form polymer. Copolymerization can be carried out by using dihalogeno aromatic compound as a comonomer. Yamamoto reported the polycondensation of Br-Y-Br (Y=1,4-phenylene, 3-methyl-2,5-thienylene, etc) using $Ni(COD)_2$ catalysed cross-coupling of diaromatic compounds to give π-conjugated polymers (Scheme 4.1).[27]

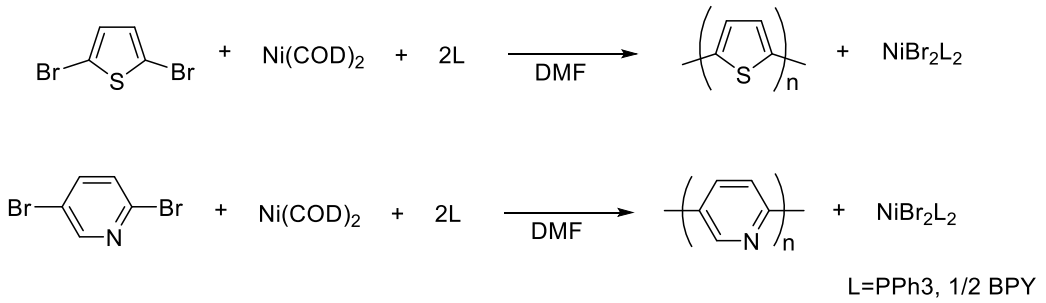

Scheme 4.1. Polymerization of dibromo derivatives.

However, to our knowledge, only one example of chiral polymer synthesis using Yamamotocoupling polymerization has been reported. Onimura et al. reported the Yamamoto coupling polymerization of chiral oxazoline monomers containing a diiodophenyl group.[38] They synthesized optically active poly(*m*-phenylene)s bearing chiral oxazoline at the side chains (Scheme 4.2). The structures and chiroptical properties were characterized using spectroscopic and thermal gravimetric analyses.[37]

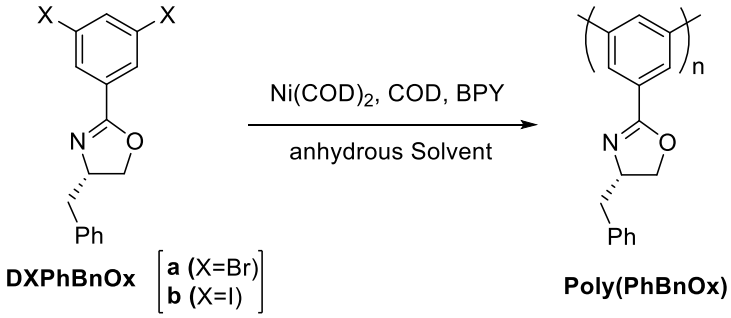

Scheme 4.2. Polymerization of 3,5-dihalidebenzene derivatives bearing chiral oxazoline group.

No application of the chiral polymers to asymmetric catalysis has been reported till date. In this chapter, the design and synthesis of monomers suitable for Yamamoto coupling polymerization and their reaction conditions are discussed. The chiral polymers obtained by this polymerization are applied to the asymmetric catalysis of Michael addition reactions. The catalytic activities and stereoselectivities of the chiral polymers are also described.

4.2 Results and discussions

4.2.1 Synthesis of cinchona squaramides

Cinchona squaramide derivatives **8**, **10**, **11**, and **12** were synthesized as monomers for the Yamamoto coupling polymerization. Scheme 1 describes the preparation of monosquaramides **3** and **6**, which contain two haloaryl moieties. These monosquaramides easily reacted with 9-amino (9-deoxy)epi cinchonidine **7** or 9-amino (9-deoxy) 3-ethyl epi cinchonidine[15] **9** to afford the corresponding cinchona squaramides **8**, **10**, **11**, and **12** (Scheme 4.4). These are chiral monomers for the Yamamoto coupling polymerization. Using these cinchona squaramide monomers (**8**, **10**, **11**, and **12**), the polymerization conditions of Yamamoto coupling polymerization were studied.

4.2.2 Preparation of chiral cinchona-based squaramide polymers using Yamamoto coupling

Since Onimura et al. reported the synthesis of chiral polymers using Yamamoto coupling polymerization[38], we used this procedure for the synthesis of cinchona squaramide polymers. First, this polymerization was applied to bis(4-iodobenzyl) derivative **10** of cinchona squaramide. Under standard conditions of Yamamoto coupling polymerization for aromatic dihalides,[35] cinchona squaramide monomer **10** was polymerized to afford polymer **P1**. The results are summarized in Table 4.1.

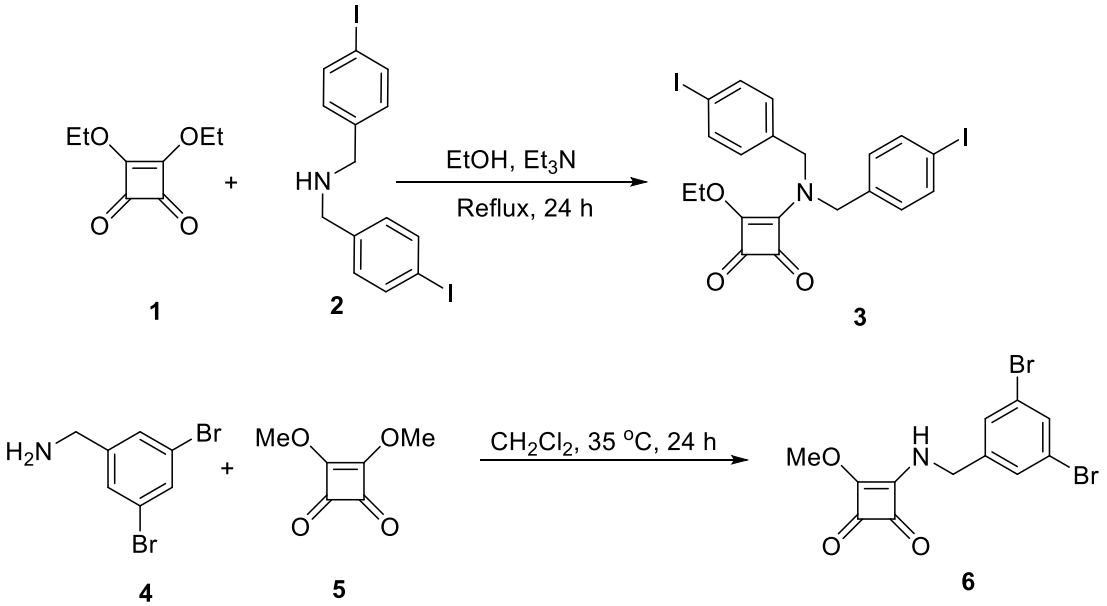

Scheme 4.3. Synthetic route to monosquaramides **3** and **6**.

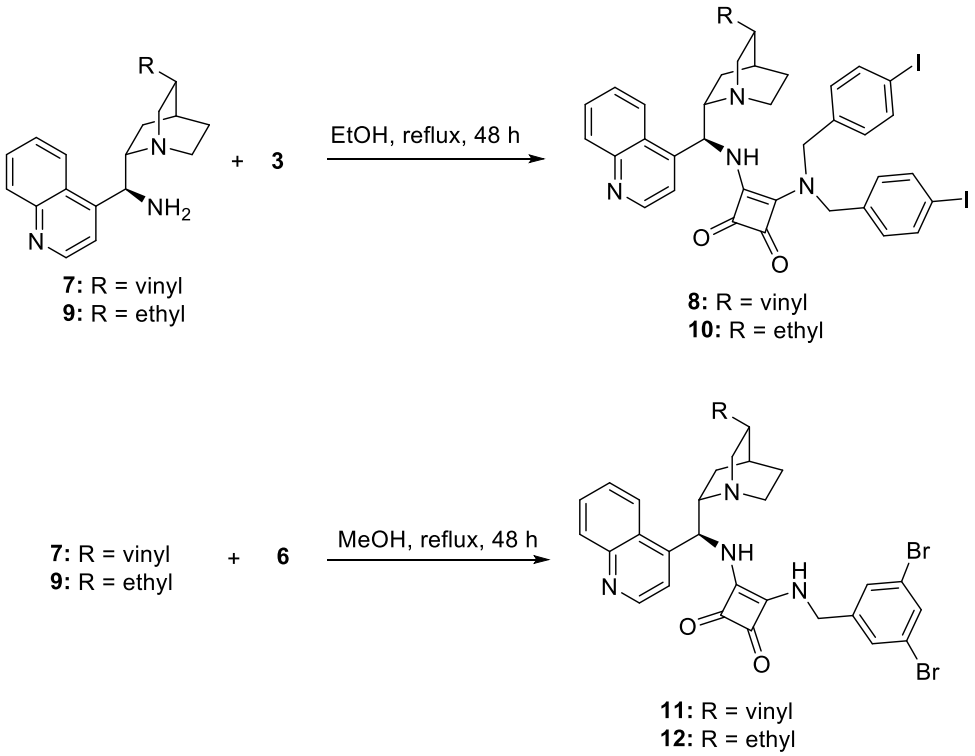

Scheme 4.4. Synthetic route to cinchona squaramide monomers **8**, **10**, **11** and **12**.

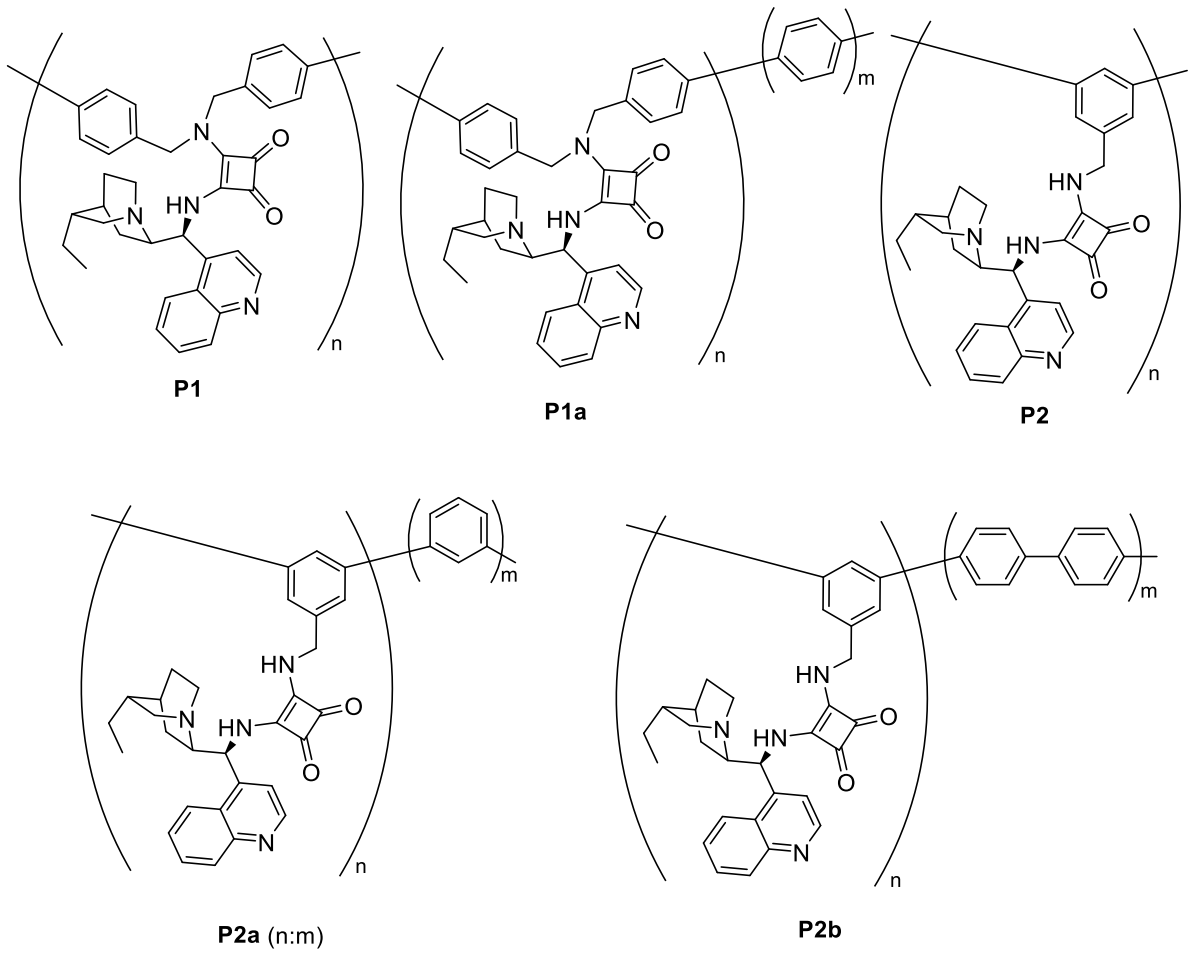

Figure 4.1. Cinchona squaramide linear homopolymers, **P1** and **P2**, and copolymers, **P1a**, **P2a** and **P2b**.

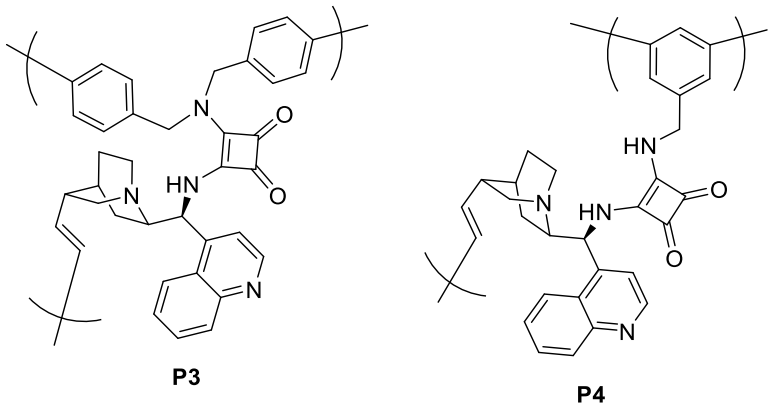

Figure 4.2. Cinchona squaramide branched polymers, **P3** and **P4**.

Table 4.1. Synthesis of chiral polymers **P1**–**P4** from cinchona squaramide **8**, **10**, **11**, and **12** and their SEC data.[a]

Entry	Monomer	Solvent	Chiral Polymers	Yield [%]	M_n[b]	M_w[b]	M_w/M_n[b]
1	**10**	DMF	**P1**	99	7400	14000	1.87
2	**10** + **13** (1:1)	DMF	**P1a** (1:1)	99	3900	4100	1.05
3	**12**	DMF	**P2**	99	8000	14000	1.74
4	**12**	DMSO	**P2**	92	4800	6000	1.23
5	**12**	Toluene	**P2**	55	6000	6100	1.02
6[c]	**12**	DMF	**P2**	97	4000	4600	1.15
7[d]	**12**	DMF	**P2**	98	4300	5000	1.14
8[e]	**12**	DMF	**P2**	95	7800	9300	1.20
9	**12** + **14** (1:1)	DMF	**P2a** (1:1)	99	12600	13000	1.03
10	**12** + **14** (1:1.5)	DMF	**P2a** (1:1.5)	98	5000	12000	2.46
11	**12** + **14** (1:0.7)	DMF	**P2a** (1:0.7)	98	4700	7000	1.48
12	**12** + **15** (1:1)	DMF	**P2b** (1:1)	91	3600	3700	1.03
13	**8**	DMF	**P3**	99	7500	13300	1.77
14	**8**	DMSO	**P3**	90	4900	6500	1.32
15	**8**	Toluene	**P3**	60	4400	5000	1.53
16[d]	**8**	DMF	**P3**	98	8000	8200	1.02
17	**11**	DMF	**P4**	98	4400	5000	1.13

[a]Reaction was carried out with 0.19 mmol monomers, 0.21 mmol 2, 2′ bipyridyl, 0.21 mmol 1,5-cyclooctadiene and 4.0 mL solvent for 48 h at 85°C.
[b]Determined by size exclusion chromatography (SEC) using DMF as the solvent at a flow rate of 1.0 mL/min at 40 °C (polystyrene standard).
[c]Reaction was carried out at 60 °C.
[d]Reaction was carried out at 110 °C.
[e]Reaction was carried out for 24 h.

In the presence of $Ni(COD)_2$, monomer **10** underwent a self-polycondensation reaction at 85 °C in dimethylformamide (DMF) to provide linear polymer P1 with a molecular weight of 7400 in quantitative yield (Table 4.1, entry 1). Copolymer **P1a** was also synthesized using cinchona squaramide **10** and 1,4-diiodobenzene **13** under the same Yamamoto coupling conditions (Scheme 4.5). Using squaramide **12** with a dibromobenzyl group, another linear polymer **P2** was synthesized. The polymerization conditions were investigated using **12** as a monomer. The polymerization of **12** in DMF at 85 °C for 24 h provided chiral polymer **P2** with a molecular weight of M_n = 7800 in 95% yield (Table 1, entry 8). The completion of polymerization required 48 h, and **P2** with a molecular weight of M_n = 8000 was obtained (entry 3). Other solvents including DMSO and toluene were used

for the polymerization of **12** at 85 °C for 48 h (entries 4 and 5). Low molecular weight and low yield in DMSO and toluene, respectively, were observed. At a low temperature (60 °C), polymerization occurred smoothly to afford polymer **P2** with a low molecular weight (M_n = 4000, entry 6). At a high temperature (110 °C), no increase in the molecular weight was observed (entry 7). We tested polymerization temperature from 60 to 110 °C (entries 6, 3, and 7). From these results, the suitable temperature for the polymerization may be 85 °C.

Under optimized conditions, copolymer **P2a** was synthesized from squaramide **12** and 1,3-dibromo benzene **14** (Figure 4.1) using different ratios of **12** and **14**. An equimolar ratio of **12** to **14** afforded the copolymer **P2a** (1:1). Polymers **P2a** (m:n) with different ratios of **12** and **14** were prepared using the same method. For copolymerization of **12** and **14**, depending on the comonomer ratio, the molecular weights varied from 4700 to 12600 (entries 3, 11, 9, and 10). The molecular weights were reproducible. However, no specific tendency was observed between the comonomer ratio and the molecular weight. An additional copolymer **P2b** was synthesized using **12** and 4,4′-dibromo biphenyl **15** (Figure 4.1). These cinchona squaramide polymers are synthesized via the Yamamoto coupling reaction for the first time. These chiral polymers were soluble in DMF, DMSO, CH_2Cl_2, and $CHCl_3$ and partly soluble in other commonly used organic solvents such as MeOH, EtOAc, and THF. These were insoluble in diethyl ether and hexane, and readily precipitated in diethyl ether. The transition-metal-catalyzed C–C coupling reaction between aryl halide and olefin is known as the Mizoroki–Heck coupling. Ni-catalyzed Mizoroki–Heck coupling is also possible.[39] In the presence of the Ni catalyst, both Yamamoto and Mizoroki–Heck coupling reactions occur simultaneously. For example, cinchona squaramide monomers **8** and **11** with a C3-vinyl group can be polymerized by either Yamamoto or Mizoroki–Heck coupling to yield hyperbranched polymers **P3** and **P4**, as shown in Figure 4.2.

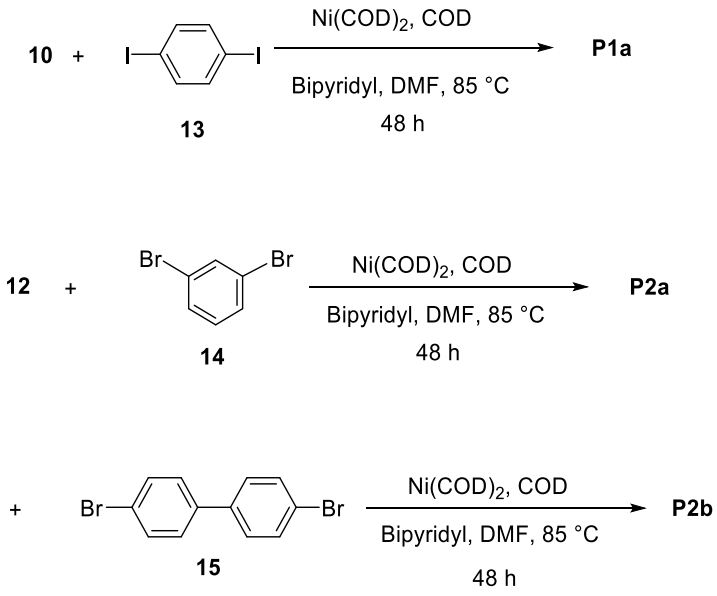

Scheme 4.5. Synthesis of polymers, **P1a**, **P2a** and **P2b**.

4.2.3 Catalytic performance of the cinchona squaramide polymers

4.2.3.1 Asymmetric Michael addition reaction of anthrone to *trans*-β-nitrostyrene

Polymeric catalysts **P1**−**P4** were studied as organocatalysts in the asymmetric Michael addition reaction of anthrone **16** and *trans*-β-nitrostyrene **17** (Scheme 4.6). The absolute configuration of the Michael adducts was assigned as (*S*) by comparing the reported value in the literature.[40] First, the catalytic activities of low-molecular-weight cinchona squaramides **10** and **12** were examined as model catalysts. Cinchona squaramides **10** and **12** showed excellent catalytic activities in the asymmetric Michael addition reaction of anthrone and *trans*-β-nitrostyrene to afford Michael adduct **18** in high yield with 58% ee and 84% ee (Table 4.2, entries 1 and 2). For linear polymer **P1**, 20% enantioselectivity was observed with good yield (Table 4.2, entry 3). The corresponding copolymer **P1a** afforded an almost racemic product in only 5% ee with a prolonged reaction time, but the yield was good (Table 4.2, entry 4). Linear polymer **P2** was then used as a catalyst for the same reaction. In the presence of **P2**, the asymmetric reaction was completed within 12 h at 25 °C. Michael adduct **18** was obtained in 90% yield with 66% ee (entry 5). The enantioselectivity increased to 78% ee using copolymer **P2a** (1:1) in the same asymmetric reaction (entry 6). By employing **P2a** (1:1), the reaction was completed in three hours, which was much faster than that with the low-molecular-weight catalyst **12**, which required 24 h. The faster reaction was observed because of its high substrate accumulation efficiency in the polymer microenvironment. The chiral polymer chain of **P2a** effectively solubilized the substrate molecule for the reaction. Low-molecular-weight catalyst **12** was not soluble in the solvent and a heterogeneous reaction occurred. **P2a** could be prepared using different molar ratios of **12** and **14**. When the molar ratio was changed from 1:1 to 1:1.5 or 1:0.7, the polymeric catalysts **P2a** (1:1.5) and **P2a** (1:0.7) afforded lower enantioselectivities (entries 7 and 8). The structure of the comonomer also affected the enantioselectivity, mainly due to the change in the polymer conformation. With the use of biphenyl comonomer **15** instead of **14**, a much lower enantioselectivity (25% ee) was obtained (entry 9). Similar to the linear polymers **P1** and **P1a**, the hyperbranched polymer **P3** provided an almost racemic product, and the reaction proceeded appropriately (entry 10). An additional hyperbranched polymer **P4** showed similar catalytic activity as **P2** (entries 5, 11).

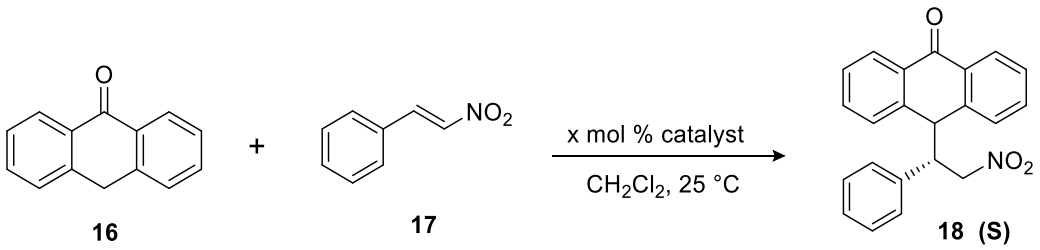

Scheme 4.6. Asymmetric Michael addition reaction of anthrone **16** to *trans*-β-nitrostyrene **17** using chiral polymeric catalysts**.**

The catalyst loading sometimes affects the catalytic performance in asymmetric reactions. Using **P2a**, different molar percentages of the catalyst were tested in the asymmetric reaction of anthrone **16** to *trans*-β-nitrostyrene **17**. Interestingly, even when the catalyst loading was decreased to 2.5 mol%, the reaction was completed in three hours (Table 4.2, entry 12).

Solvent screening was performed using **P2a**. The results are summarized in Table 4.3. Various types of solvents were tested, and dichloromethane afforded the best result in the asymmetric reaction with **P2a**. The polymeric catalyst **P2a** was insoluble and shrank in hexane, requiring a long time to complete the asymmetric reaction. Relatively polar solvents such as acetonitrile, THF, acetone, methanol, and ethyl acetate resulted in low enantioselectivities (entries 5–9). The temperature effect was also examined (Table 4.3). At high temperature (50 °C), the reaction time decreased, and it was completed in 1.5 h, affording a slightly low enantioselectivity of 72% (Table 4.3, entry 11). Decreasing the temperature to −20 °C resulted in high enantioselectivity (82% ee, entry 12). Increased enantiomeric excess of 84% was obtained when the reaction was performed at −40 °C, but a long time of 48 h was needed (entry 13).

Table 4.2. Reaction optimization: Asymmetric Michael addition reaction of anthrone **16** to *trans*-β-nitrostyrene **17** using polymeric catalysts.[a]

Entry	Catalyst	Catalyst loading (mol %)	Reaction time [h]	Yield[b] [%]	*ee*[c] [%]
1	**10**	5	7	93	58
2	**12**	5	24	89	84
3	**P1**	5	16	90	20
4	**P1a**	5	24	88	5
5	**P2**	5	12	90	66
6	**P2a** (1:1)	5	3	92	78
7	**P2a** (1:1.5)	5	6	91	61
8	**P2a** (1:0.7)	5	8	90	54
9	**P2b**	5	8	91	25
10	**P3**	5	24	82	2
11	**P4**	5	12	90	62
12	**P2a** (1:1)	2.5	3	92	75
13	**P2a** (1:1)	10	3	90	73
14	**P2a** (1:1)	15	3	92	72

[a]Asymmetric reaction was carried out using **16** (0.24 mmol), **17** (0.2 mmol), and 5 mol% cat. in CH_2Cl_2 (2.0 mL) at 25 °C.
[b]Isolated yield of the product after column chromatography.
[c]Enantioselectivity (ee) was determined using HPLC (CHIRALPAK AS-H column).

4.2.3.2 Substrate scope of chiral copolymer P2a (1:1)

Other phenyl-substituted *trans*-β-nitrostyrene derivatives were tested in the asymmetric reaction of anthrone **16** using **P2a** (1:1) in CH_2Cl_2 at −20 °C (Table 4). Good (89–91%) yields were obtained in all cases. Excellent enantioselectivity of 93% was obtained with the Michael acceptor *trans*-4-fluoro-β-nitrostyrene **19** (Table 4.4, entry 2). The electron-withdrawing group at the para position of the benzene ring favored the enantioselectivity; 84% ee was obtained using *trans*-4-methyl-β-nitrostyrene **21** (Table 4.4, entry 3). Decreased enantioselectivity of 55% ee was observed for *trans*-2-thiophenyl-β-nitrostyrene **23** (Table 4.4, entry 4).

Table 4.3. Asymmetric reaction of anthrone **16** and *trans*-β-nitrostyrene **17** using copolymer **P2a** (1:1).[a]

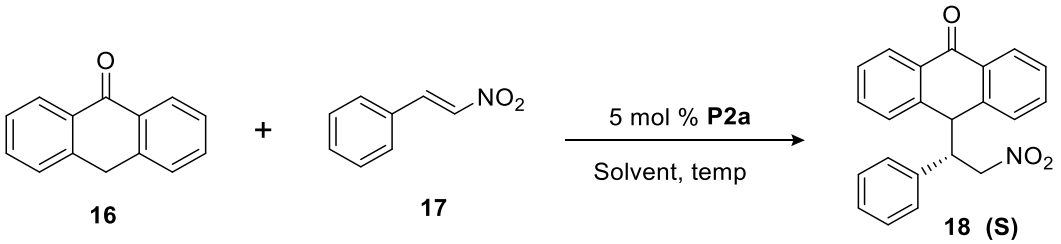

Entry	Solvent	Temperature [°C]	Reaction time [h]	Yield[b] [%]	*ee*[c] [%]
1	CH_2Cl_2	25	3	92	78
2	$CHCl_3$	25	9	91	70
3	Toluene	25	10	89	63
4	Hexane	25	48	83	42
5	Acetonitrile	25	9	90	6
6	THF	25	6	90	17
7	Acetone	25	4	92	9
8	MeOH	25	8	87	17
9	Ethyl acetate	25	5	89	17
10	Diethyl ether	25	27	88	57
11	CH_2Cl_2	50	1.5	92	72
12	CH_2Cl_2	−20	22	90	82
13	CH_2Cl_2	−40	48	89	84

[a]Asymmetric reaction was carried out using **16** (0.24 mmol), **17** (0.2 mmol), and 5 mol% **P2a** (1:1) in 2.0 mL solvent at different temperatures.
[b]Isolated yield of the product after column chromatography.
[c]Enantioselectivity (ee) was determined using HPLC (CHIRALPAK AS-H column)

Two possible isomers are formed in the asymmetric Michael addition reaction of anthrone **16** to *trans*-β-nitrostyrene **17**. The transition state leading to **18 (*S*)** may be the most stable configuration among them.

1. Major product **2. Minor product**

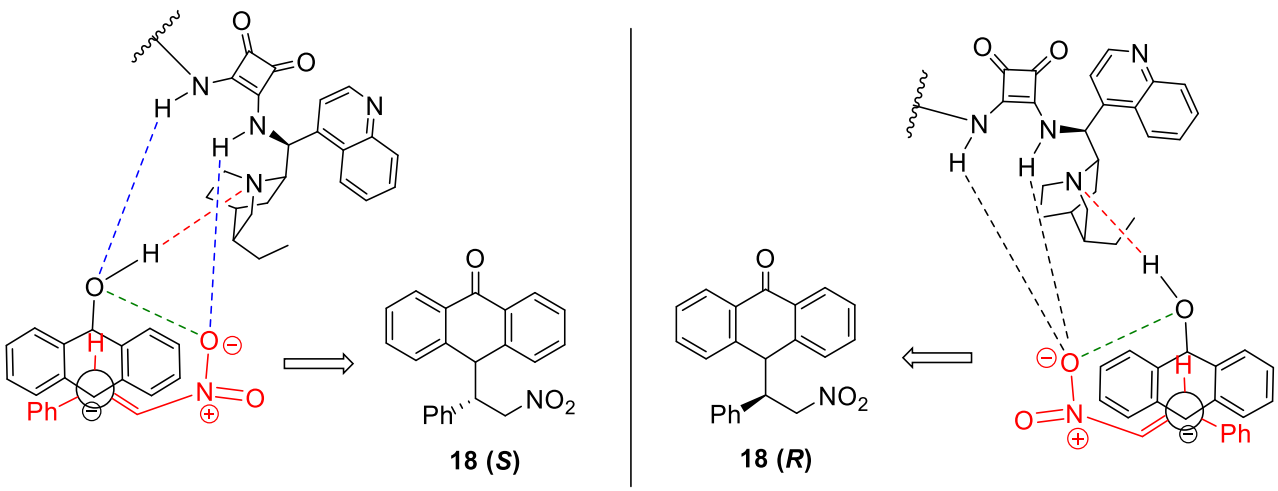

Figure 4.3. Possible Mechanistic view of the reaction of anthrone to *trans*-β-nitrostyrene.

Table 4.4. Substrate scope using copolymer catalyst **P2a** (1:1) in the reaction of anthrone **16** to nitroolifins.[a]

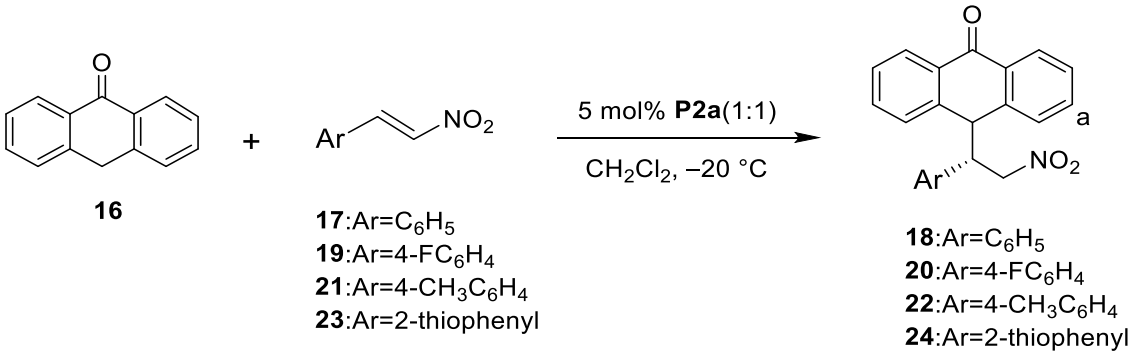

Entry	Michael acceptor	Product	Reaction time [h]	Yield[b] [%]	*ee*[c] [%]
1	**17**	**18**	22	90	82
2	**19**	**20**	36	90	93
3	**21**	**22**	30	91	84
4	**23**	**24**	24	89	55

[a]Asymmetric reaction was carried out using **16** (0.24 mmol), nitroolefin (0.2 mmol) and 5 mol% **P2a**(1:1) in CH_2Cl_2 (2.0 mL) at −20 °C.
[b]Isolated yield of the product after column chromatography.
[c]Enantioselectivity (ee) was determined using HPLC (CHIRALPAK AS-H column).

4.2.3.3 Recyclability of chiral copolymer P2a (1:1)

Chiral copolymer **P2a** (1:1) was completely soluble in CH_2Cl_2, and the asymmetric reaction occurred in a homogeneous system in this solvent. After completion of the reaction, the polymeric catalyst was precipitated in diethyl ether and then easily separated and recovered via simple filtration. The recovered polymeric catalyst **P2a** (1:1) was reused in the same reaction. The recyclability of **P2a** (1:1) was also examined, and in the recycling experiments, it could be used four times (Table 4.5); no significant differences in enantioselectivity were observed. The reaction was completed within 24 h using the reused polymeric catalyst **P2a** (1:1).

Table 4.5. Recyclability test of copolymer catalyst **P2a** (1:1) in the enantioselective reaction of anthrone **16** to *trans*-β-nitrostyrene **17** in CH_2Cl_2 at −20 °C.[a]

Entry	Reaction time [h]	Yield[b] [%]	*ee*[c] [%]
Fresh polymer	22	90	82
Cycle 1	24	82	84
Cycle 2	24	84	83
Cycle 3	24	85	84
Cycle 4	24	81	82

[a]Asymmetric reaction was carried out using **16** (0.24 mmol), **17** (0.2 mmol) and 5 mol% **P2a** (1:1) in CH_2Cl_2 (2.0 mL) at −20 °C.
[b]Isolated yield of the product after column chromatography.
[c]Enantioselectivity (ee) was determined using HPLC (CHIRALPAK AS-H column)

4.2.3.4 Michael addition reaction of other substrate combinations

An additional Michael donor, methyl 2-oxocyclopentanecarboxylate **25** was investigated. The chiral polymers **P1**–**P4** were used as organocatalysts in the reaction of **25** with **17** (Scheme 4.7). In all cases, the asymmetric reaction proceeded smoothly to provide chiral product **26** in good yield

and excellent enantioselectivity with **P1**, **P2**, and **P4** (Table 4.6). The absolute configuration of the Michael adducts **26** was assigned as (2*S*, 3*R*) by comparing the reported value in the literature.[41,42] Polymers **P1a** (1:1) and **P3** afforded low enantioselectivities (72% ee and 48% ee) in the prolonged reaction time of 48 h (entries 2 and 6). High diastereoselectivity (>100:1) was obtained with **P2a** (1:1), **P2b**, and **P4** catalysts (entries 4, 5, and 7).

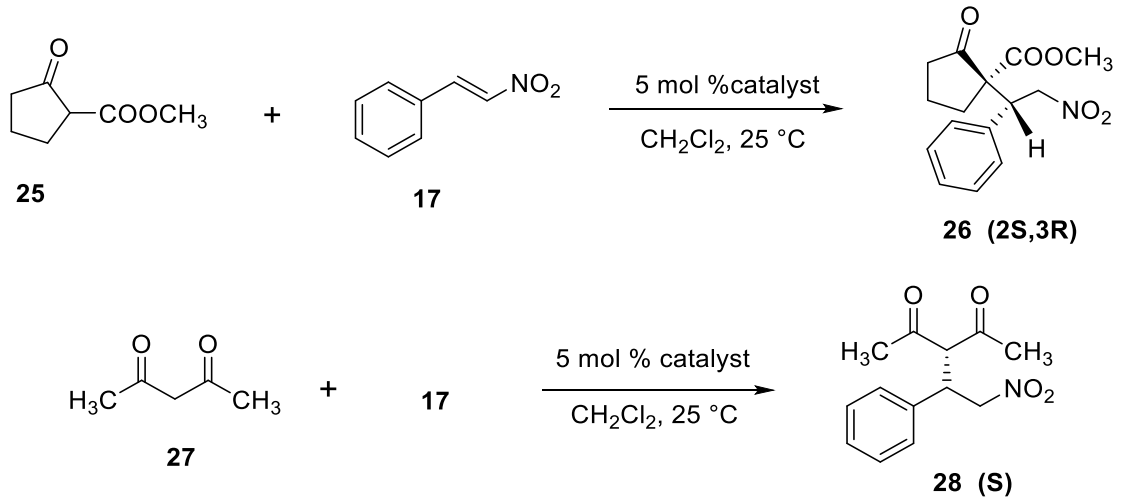

Scheme 4.7. Enantioselective Michael addition reaction using chiral polymers.

Table 4.6. Asymmetric Michael addition reaction using chiral polymeric catalysts.[a]

Entry	Catalyst	Michael donor	Product	Reaction time [h]	Yield[c] [%]	*dr*[d]	*ee*[d] [%]
1	**P1**	**25**	**26**	24	96	58:1	99
2	**P1a**	**25**	**26**	48	80	9:1	72
3	**P2**	**25**	**26**	24	95	92:1	98
4	**P2a** (1:1)	**25**	**26**	19	94	>100:1	98
5	**P2b**	**25**	**26**	24	92	>100:1	98
6	**P3**	**25**	**26**	48	85	6:1	48
7	**P4**	**25**	**26**	24	93	>100:1	99
8[b]	**P2a** (1:1)	**27**	**28**	18	82	–	78
9[b]	**P4**	**27**	**28**	23	80	–	65

[a]Asymmetric reaction was carried out using **25** (0.5 mmol), **17** (0.55 mmol) and 5 mol% cat. in CH_2Cl_2 (2.0 mL) at 25 °C.
[b]Asymmetric reaction was carried out using **27** (0.275 mmol), **17** (0.25 mmol) and 5 mol% catalyst in CH_2Cl_2 (2.0 mL) at 25 °C.
[c] Isolated yield of the product after column chromatography.
[c]Enantiomeric excess (ee) and diastereomeric ratio (dr) were determined using HPLC (CHIRALCEL OD-H column for entries 1-7 and CHIRAKPAK AD-H for entries 8 and 9).

Chiral polymers **P2a** (1:1) and **P4** were also used in the asymmetric reaction of acetylacetone **27** with *trans*-β-nitrostyrene **17**. The reaction occurred smoothly with polymer **P2a** (1:1) to provide chiral Michael adduct **28** in 78% enantioselectivity with 82% yield (Table 4.6, entry 8). With **P4** catalyst, the product was obtained in 65% ee with 80% yield (entry 9). The absolute configuration of the Michael adducts **28** was assigned as (*S*) by comparing the reported value in the literature.[43] Based on these results, a suitable microenvironment for the asymmetric reaction was created in the chiral polymer network of the polymeric catalyst **P2a** (1:1).

4.2.3.5 Enantioselective aldol reaction of ketones with isatins.

Here, we examined catalyst **P1**-**P4** by using as a catalyst in the reaction of isatins with ketones (Scheme 4.8). First, **P1** polymeric catalyst was applied to the reaction of isatin **29** with acetophenone **30**. 39% ee was obtained (Table 4.7, entry 1) whereas racemic product was obtained with acetone **32** (Table 4.7, entry 2). **P2** catalyst was not good in these reactions. With acetophenone **30**, it gave 6% ee with good yield (entry 3), whereas 23% ee was obtained by using corresponding copolymer **P2a** (entry 4). Almost no product was found in case of hyperbranched polymeric catalyst **P3** (entry 5). Another hyperbranched polymer **P4** gave only 5% ee with moderate yield (entry 6). Synthesized linear chiral polymers can catalyze this reaction to give good yield but enantioselectivity is not good.

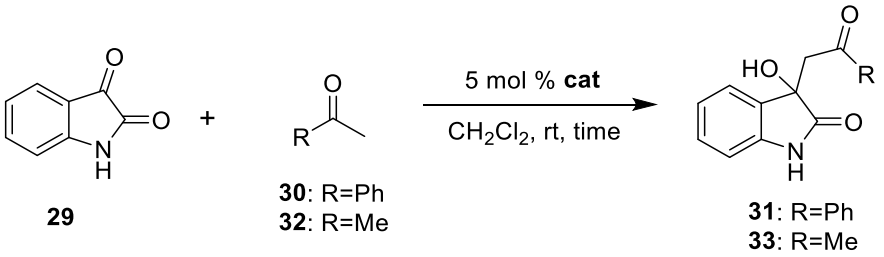

Scheme 4.8. Aldol condensation reaction using chiral HBP catalysts.

Table 4.7. Aldol condensation reaction using chiral HBP catalysts.

Entry	Catalyst	Ketone	Product	Reaction time [day]	Yield[a] [%]	ee[b] [%]
1	**P1**	**30**	**31**	2	87	39
2	**P1**	**32**	**33**	2.5	80	racemic
3	**P2**	**30**	**31**	2	79	5
4	**P2a**	**30**	**31**	2	83	23
5	**P3**	**30**	**31**	2.5	n.d	n.d
6	**P4**	**30**	**31**	2.5	56	6

[a] Isolated yield of the product after column chromatography.
[b] Enantioselectivity (ee) was determined using HPLC (CHIRALCEL OD-H column, [only for entry 2, CHIRALCEL OJ-H column was used]).

4.3 Conclusion

Cinchona squaramide-based chiral polymers **P1**−**P4** were successfully synthesized from monosquaramides **8, 10**, **11** and **12** via the Yamamoto coupling reaction. Copolymers **P1a**, **P2a**, **P2b** were synthesized from **10**, **12** with achiral diiodo or dibromo aromatic compounds **13**−**15**. Chiral polymers **P1**−**P4** were applied to the asymmetric Michael addition reactions and afforded good to excellent enantioselectivities. Interestingly, polymeric catalyst **P2a** (1:1) showed a high catalytic activity in the asymmetric reaction of anthrone **16** and *trans*-β-nitrostyrene **17**. The reaction was completed within three hours in CH_2Cl_2 at 25 °C in the presence of only 2.5 mol% catalyst **P2a** (1:1); a suitable catalyst conformation may be formed in the case of **P2a** (1:1). Solvent screening revealed that the asymmetric reaction in CH_2Cl_2 afforded high enantioselectivity and high reactivity. The polymeric catalyst was used in a wide temperature range (−40–50 °C), and high enantioselectivity was obtained at low temperatures. Polymeric catalyst **P2a** (1:1) showed good

performance in the asymmetric reactions for various combinations of the Michael donor and acceptor substrates. For 2-oxocyclopentanecarboxylate **25** and *trans*-β-nitrostyrene **17**, almost perfect diastereoselectivity with 98% ee was obtained with **P2a** (1:1). The polymeric catalyst was easily separated by precipitation into diethyl ether and recovered from the reaction mixture, allowing its reuse for the reaction. The recyclability of **P2a** (1:1) was determined in the asymmetric reaction of anthrone to *trans*-β-nitrostyrene for four cycles.

4.4 Experimental

4.4.1 Materials and general considerations

All reagents and solvents used during the investigation were purchased from Sigma–Aldrich, Wako Pure Chemical Industries, Ltd., or Tokyo Chemical Industry (TCI) Co., Ltd. To monitor the progress of the reactions, thin layer chromatography (TLC) was performed using pre-coated silica gel plates (Merck TLC silica gel, 60F254). To purify the synthesized compounds, column chromatography was performed using a silica gel column (Wakogel C-200, 100–200 mesh). The ^{1}H NMR spectra were recorded using JEOL JNM-ECS400 and JEOL JNM-ECX500 spectrometers operated at 400/500 MHz. The ^{13}C NMR spectra were recorded at 100/125 MHz in $CDCl_3$ or DMSO-d_6 at room temperature. The chemical shifts are reported in parts per million (ppm) using tetramethyl silane (TMS) as the reference, and the *J* values are reported in Hertz (Hz). Infrared (IR) spectroscopy was performed using "KBr" pellets on a JEOL JIR-7000 FTIR spectrometer, and the wavenumbers are reported in cm^{-1}. High-resolution mass spectrometry (HRMS; ESI and APCI) data were recorded on a Bruker micro OTOF II HRMS instrument. High-performance liquid chromatography (HPLC) was carried out using a Jasco HPLC system composed of a DG-980-50 three-line degasser, an Intelligent HPLC pump (PU-2080), and a UV/Vis detector (UV-2075). The instrument was equipped with a chiral column (Chiralpak AS-H, Daicel) and hexane/2-propanol were used as the eluent at a flow rate of 0.7 mL/min at room temperature. HPLC was also carried out on a Jasco HPLC system composed of an HPLC pump (PU-980), a UV/Vis detector (UV-975), and a column oven CO-2065 equipped with a chiral column (Chiralcel OD-H, Chiralpak AD-H, Daicel) using hexane/2-propanol as the eluent at a flow rate of 1.0 mL/min at room temperature. Size exclusion chromatography (SEC) was performed using a Tosoh instrument with HLC 8020 UV (254 nm) or refractive index detector. Two polystyrene gel columns with a bead size of 10 μm were used, and DMF was used as the carrier solvent at a flow rate of 1.0 mL/min at 40 °C. A calibration curve was established to determine the number average molecular weight (M_n) and molecular weight distribution (M_w/M_n) values by comparison with the polystyrene standards. Optical rotations were recorded on a JASCO DIP-149 digital polarimeter using a 10-cm thermostatted microcell.

4.4.2 Synthesis of cinchona squaramides

4.4.2.1 Synthesis and characterization of compound 3

Bis(4-iodo benzyl) amine **2** (449 mg, 1.0 mmol) was added slowly to a stirred solution of diethylsquarate **1** (734 μL, 5.0 mmol) and triethyl amine (2.0 mmol) in ethanol (15 mL) at room

temperature. The mixture was stirring at reflux condition about 18 h under Ar gas. Then the solution is allowed to cool in room temperature. The off-white crystal was observed which were filtered and dried. Yield: 430 mg (75%). R_f: 0.43 (hexane/EtOAc = 2.0/1.0); Off white crystal; mp: 145–149 °C; ; ^{1}H NMR (400 MHz, $CDCl_3$): δ 1.45 (t, J = 7.2 Hz, 3H), 4.37 (s, 2H), 4.67 (s, 2H), 4.81 (q, J = 6.8 Hz, 2H), 6.95 (dd, J = 7.6 Hz and 14.4 Hz, 4H), 7.71 (dd, J = 8.4 Hz and 12.4 Hz, 4H). ^{13}C NMR (400 MHz, $CDCl_3$): *d* 15.99, 50.58, 51.20, 70.32, 94.39, 130.05, 130.69, 134.25, 134.37, 138.27, 138.39, 171.95,176.79, 182.80, 188.68.; IR (KBr): ν= 3076, 2979, 2880, 2081, 1908, 1800, 1702, 1562, 1460, 1383, 1282, 1183, 1069, 984, 889, 795, 719, 628, 532 cm^{-1}; HRMS (APCI) *m/z* for $C_{20}H_{18}I_2NO_3$ [M^+H^+] calcd. 573.9376, found 573.9371.

4.4.2.2 Synthesis and characterization of compound 4

3,5-Dibromo benzylbromide (2.5 g, 7.60 mmol) and potassium phthalimide (1.39 g, 7.60 mmol) were taken in a 50 mL round bottom flask and dry DMF (15 mL) was added. The solution was heated at 55 °C for 24 h under N_2 flow. After reaction, DMF was evaporated and $CHCl_3$ was added and the solution was filtered. Then the solution was extracted with NaOH (0.2 M) solution (50 mL ´3 times) and dried over $MgSO_4$. After filtration $CHCl_3$ solvent was removed and white solid was found which was anhydride. Now hydrazine monohydrate (7.90 mmol) and ethanol (30 mL) were added into the solid and the reaction mixture was heated under reflux condition for 2.5 h. After reflux $CHCl_3$ was added and this solution was extracted with 20% NaOH solution. The organic phase was collected and washed 3 times with water. Then the $CHCl_3$ layer was dried over $MgSO_4$, filtered and evaporated to give white solid which was the product **4** (1.8 g, 89%). R_f: 0.16 (Hex/EtOAc = 1.0/3.0; mp: 62–65 °C; ^{1}H NMR (400 MHz, $CDCl_3$): δ *3*.84 (s, 2H), 7.41(s, 2H), 7.54 (s, 1H). ^{13}C NMR (500 MHz, $CDCl_3$): *d* 45.52, 123.08, 129.01, 132.43, 147.19.; IR (KBr): ν = 3316, 2992, 3065, 2183, 1647, 1560, 1498, 1094, 840, 685, 592 cm^{-1}; HRMS (APCI) *m/z* for $C_7H_8Br_2N$ [M^+H^+] calcd. 263.9032, found 263.9035.

4.4.2.3 Synthesis and characterization of compound 6

3,5-Dibromo benzylamine **4** (265 mg, 1.0 mmol) and dimethyl squarate **5** (142.11 mg, 1.0 mmol) with dichloromethane (8 mL) were taken in a 30 mL round bottom flask. The reaction was continued at 35 °C for 24 h under Ar gas. Then the solvent was decanted by a pipette and the mixture was washed three times with EtOAc/DCM=9/1 solvent mixture. Finally, all the solvent was evaporated and dried. The white solid was the desired product **6**. (240 mg, 64%). R_f: 0.48 (CH_2Cl_2/MeOH = 9.0/1.0; mp: 166–170 °C; ^{1}H NMR (400 MHz, $CDCl_3$): δ 4.28 (s, 3H), 4.49 (br, 1H), 4.67 (br, 1H), 7.54 (s, 2H), 7.79 (s, 1H). ^{13}C NMR (500 MHz, $CDCl_3$): *d* 46.09, 60.59, 123.14, 129.95, 132.97, 143.64, 172.90, 178.50, 183.2, 190.1; IR (KBr): ν = 3213, 2965, 2857, 1708, 1669, 1583, 1398, 1291, 1052, 923, 845, 581 cm^{-1}; HRMS (APCI) *m/z* for $C_{12}H_{10}Br_2NO_3$ [M^+H^+] calcd. 373.9027, found 373.9022.

4.4.2.4 Synthesis of squaramide 8 and 10

First, monosquaramide **3** (410 mg, 0.71mmol) and 10 mL of ethanol were added to a 30-mL volumetric flask. To the stirred solution, 0.86 mmol (253 mg) of 9-amino (9-deoxy)epi cinchonidine **7** in 10 mL ethanol was slowly added. The mixture was stirred under reflux for approximately 24 h in Ar atmosphere. A white precipitate was obtained, which was filtered, washed with ethanol, and dried to yield **8** (460 mg, 78%) as a white solid. R_f: 0.48 (CH_2Cl_2/MeOH = 9.0/1.0; mp: 229–231 °C. ^{1}H NMR (400 MHz, $CDCl_3$): δ 0.90 (m, 1H), 1.29 (m, 2H), 1.61 (m, 4H), 2.27 (br,1H), 2.53-3.14 (m, 4H), 4.59 (br, 4H), 4.93 (m, 2H), 5.63 (m, 1H), 6.95(d, J = 8.0 Hz, 4H), 7.72 (m, 8H), 8.14 (d, J = 8.0 Hz, 1H), 8.86 (d, J = 4.4 Hz, 1H); ^{13}C NMR (500 MHz, $CDCl_3$): δ 25.9, 27.31, 27.69, 39.54, 40.77, 56.0, 94.20, 114.90, 123.57, 127.16, 129.56, 135.32, 138.41, 141.20, 149.99, 167.46, 168.0, 182.87, 183.50. IR (KBr): ν = 3324, 3065, 2933, 2862, 1788, 1667, 1561, 1484, 1343, 1285, 1182, 1088, 981, 839, 771, 649, 564 cm^{-1}; HRMS (APCI) *m/z* for $C_{37}H_{35}I_2N_4O_2$ [M+H$^+$] calcd. 821.0849, found 821.0844; $[\alpha]^{23.7}_D$ = −166 (*c* 0.07, DMF).

Further, monosquaramide **3** (410 mg, 0.71 mmol) was added with 10 mL of ethanol to a 30-mL volumetric flask. To the stirred solution, 9-amino (9-deoxy) 3-ethyl epi cinchonidine **9** (255 mg, 0.86 mmol), 10 mL of ethanol was slowly added. The mixture was stirred under reflux for approximately 24 h in Ar atmosphere. A white precipitate was obtained, which was filtered, washed with ethanol, and dried to afford **10** (480 mg, 81%) as a white solid. R_f: 0.48 (CH_2Cl_2/MeOH = 9.0/1.0; mp: 224–226 °C. ^{1}H NMR (400 MHz, $CDCl_3$): δ 0.78 (t, J =7.6, 3H), 0.88 (m, 1H), 1.16 (m, 4H), 1.42-1.62 (m, 4H), 2.23 (br,1H), 2.52-3.14 (m, 4H), 4.59 (br, 4H), 6.95(d, J = 8.0 Hz, 4H), 7.72 (m, 8H), 8.15 (d, J = 7.6 Hz, 1H), 8.86 (d, J = 4.4 Hz, 1H); ^{13}C NMR (500 MHz, $CDCl_3$): δ 12.08, 24.97, 25.52, 27.60, 28.36, 37.31, 40.82, 57.69, 94.17, 123.63, 127.04, 129.46, 135.35, 138.41, 149.99, 167.82, 168.33, 182.89, 184.00. IR (KBr): ν = 3246, 2915, 2857, 1789, 1669, 1559, 1435, 1319, 1249, 1005, 839, 788, 673 cm^{-1}; HRMS (ESI) *m/z* for $C_{37}H_{37}I_2N_4O_2$ [M+H$^+$] calcd. 823.1006, found 823.1000; $[\alpha]^{16.7}_D$ = −190 (*c* 0.09, DMF).

4.4.2.5 Synthesis of squqrqmide 11 and 12

Monosquaramide **6** (198 mg, 0.53 mmol) and 9-amino (9-deoxy)epi cinchonidine **7** (171 mg, 0.58 mmol) were added to a 30-mL flask with 10 mL of MeOH and stirred at reflux temperature under Ar atmosphere for 48 h. White precipitate was obtained, which was filtered and washed with cold MeOH and finally dried in a vacuum oven to yield **11** (187 mg, 56%) as a white solid. R_f: 0.57 (CH_2Cl_2/MeOH = 1.0/1.0); mp: 296–298 °C. ^{1}H NMR (500 MHz, DMSO-d_6): δ 0.64 (m, 1H), 1.34 (m, 2H), 1.55 (m, 4H), 2.25 (br,1H), 2.66 (m, 2H), 3.12-3.32 (m, 2H), 4.64 (br, 2H), 4.96 (m, 2H), 5.90 (m, 1H), 7.53 (s, 1H), 7.63-7.80 (m, 4H), 8.07 (d, J = 8.5 Hz, 2H), 8.48 (d, J = 8.5 Hz, 1H), 8.95 (d, J = 4.0 Hz, 1H); ^{13}C NMR (500 MHz, DMSO-d_6): δ 26.40, 27.75, 39.9, 46.15, 56.09, 59.80, 114.85, 123.18, 124.01, 126.80, 127.64, 129.97, 130.28, 130.35, 132.94, 142.70, 143.98, 148.62, 150.95, 167.5, 182.63. IR (KBr): ν = 3196, 3067, 2952, 2864, 1799, 1638, 1512, 1474, 1342, 1207,

1132, 980, 814, 766, 682 cm^{-1}; HRMS (APCI) *m/z* for $C_{30}H_{29}Br_2N_4O_2$ [M+H^+] calcd. 637.0657, found 635.0652; $[\alpha]^{17.4}_D = -43$ (*c* 0.11, DMF).

Monosquaramides **6** (198 mg, 0.53 mmol) and 9-amino (9-deoxy) 3-ethyl epi cinchonidine **9** (173 mg, 0.58 mmol) were added to a 30-mL flask with 10 mL of MeOH and stirred under reflux conditions with Ar gas for 48 h. White precipitate was obtained, which was filtered and washed with cold MeOH and finally dried in a vacuum oven to afford **12** (185 mg, 55%) as a white solid. R_f: 0.57 (CH_2Cl_2/MeOH = 1.0/1.0); mp: 294–296 °C. ^{1}H NMR (400 MHz, DMSO-d_6): δ 0.61 (m, 1H), 0.78 (t, *J* = 7.6 Hz, 3H), 1.24-1.57 (m, 8H), 2.32-2.43 (m, 1H), 2.55-2.67 (m, 1H), 3.10-3.29 (m, 3H), 4.65 (br, 2H), 7.53 (s, 1H), 7.61-7.81 (m, 4H), 8.05 (d, *J* = 8.8 Hz, 2H), 8.48 (d, *J* = 8.4 Hz, 1H), 8.94 (d, *J* = 4.4 Hz, 1H); ^{13}C NMR (500 MHz, DMSO-d_6): δ 12.51, 25.49, 26.20, 27.49, 28.55, 37.32, 46.13, 57.68, 59.9, 123.18, 124.03, 127.61, 129.95, 130.27, 130.45, 132.94, 144.00, 148.85, 150.96, 167.50, 182.50. IR (KBr): ν = 3196, 3066, 2955, 2861, 1799, 1638, 1563, 1420, 1342, 1276, 1101, 958, 852, 766, 681 cm^{-1}; HRMS (APCI) *m/z* for $C_{30}H_{31}Br_2N_4O_2$ [M+H^+] calcd. 637.0814, found 637.0808; $[\alpha]^{17.1}_D = -34$ (*c* 0.06, DMF).

4.4.3 Synthesis of cinchona squaramide polymers by Yamamoto coupling polymerization

4.4.3.1 Synthesis of polymer P1

Squaramide **10** (100 mg, 0.12 mmol), 1, 5-cyclooctadiene (0.14 mmol), 2,2′-bipyridyl (0.14 mmol) and $Ni(COD)_2$ catalyst (0.18 mmol)were taken in a test tube with dry DMF (3.0 mL) and reaction was carried out at 85 °C under N_2 flow. After 48 h reaction, polymer was precipitated in diethyl ether and washed two times with diethyl ether. After that this polymer was washed with THF, then HCl acid and finally with EDTA solution. After filtration the compound was dried over in vacuum oven to afford the **P1** as a light brown Solid. Yield: 99 mg (99%); ^{1}H NMR (400 MHz, DMSO-d_6): δ 0.77, 1.20–1.60, 4.57, 6.40, 7.01–7.96, 8.57, 8.92; IR (KBr): ν = 3420, 2929, 1716, 1683, 1585, 1442, 1314, 1022, 768, 653 cm^{-1}; $[\alpha]^{18.0}_D = -15$ (*c* 0.085, DMF); M_n (SEC) = 7400; M_w/M_n = 1.87

4.4.3.2 Synthesis of polymer P1a

Squaramide **10** (100 mg, 0.12 mmol), 1,4-diiodo benzene **13** (40.12 mg, 0.12 mmol) 1, 5-cyclooctadiene (0.14 mmol), 2,2′-bipyridyl (0.14 mmol) and $Ni(COD)_2$ catalyst (0.18 mmol)were taken in a test tube with dry DMF (3.0 mL) and reaction was carried out at 85 °C under N_2 flow. After 48 h reaction, polymer was precipitated in diethyl ether and washed with diethyl ether two times. After that this polymer was washed with THF, then HCl acid and finally with EDTA solution. After filtration the compounds were dried over in vacuum oven to afford the **P1a** as a light brown Solid. Yield: 99 mg (99%); ^{1}H NMR (400 MHz, DMSO-d_6): δ 0.78, 1.20–1.58, 7.04, 7.20–8.10, 8.60, 8.90; IR (KBr): ν= 3412, 2852, 1644, 1598, 1442, 1313, 1156, 1023, 768, 653 cm^{-1}; $[\alpha]^{24.3}_D = -6$ (*c* 0.095, DMF); M_n (SEC) = 3900; M_w/M_n = 1.05

4.4.3.3 Synthesis of polymer P2

Squaramide **12** (100 mg, 0.16 mmol), 1, 5-cyclooctadiene (0.18 mmol), 2,2′-bipyridyl (0.18 mmol) and $Ni(COD)_2$ catalyst (0.24 mmol) were taken in a test tube with dry DMF (3.0 mL) and reaction was carried out at 85 °C under N_2 flow. After 48 h reaction, polymer was precipitated in diethyl ether and washed with diethyl ether two times. After that this polymer was washed with THF, then HCl acid and finally with EDTA solution. After filtration the compounds were dried over in vacuum oven to afford the **P2** as a light brown Solid. Yield: 99 mg (99%); ^{1}H NMR (400 MHz, DMSO-d_6): δ 0.74, 1.10–1.70, 4.50, 5.97, 7.22–8.43, 8.95; IR (KBr): ν = 3419, 3211, 2931, 2870, 1771, 1600, 1443, 1023, 768, 652 cm^{-1}; $[\alpha]^{18.4}_D$ = +38 (*c* 0.085, DMF); M_n (SEC) = 8000; M_w/M_n = 1.74

4.4.3.4 Synthesis of polymer P2a

Squaramide **12** (160 mg, 0.19 mmol), 1,3-dibromo benzene **14** (22.7 µL, 0.19 mmol), 1,5-cyclooctadiene (0.21 mmol), 2,2′-bipyridyl (0.21 mmol), and $Ni(COD)_2$ (0.28 mmol) were added to a test tube with DMF (4.0 mL), and the reaction was carried out at 85 °C under N_2 flow. After 48 h, the polymer was precipitated in diethyl ether and washed twice with this solvent. Then, this polymer was washed with THF, HCl, and EDTA solution. After filtration, the yellowish-brown product **P2a** was dried in a vacuum oven. Yield: 158 mg (99%). ^{1}H NMR (400 MHz, DMSO-d_6): δ 0.50–2.00, 4.69, 7.1–8.94; IR (KBr): ν = 3398, 3065, 2955, 2871, 1771, 1646, 1599, 1443, 1331, 1156, 1024, 969, 844, 768, 652 cm^{-1}; $[\alpha]^{18.8}_D$ = −9.0 (*c* 0.06, DMF); M_n (SEC) = 12600; M_w/M_n = 1.03

4.4.3.5 Synthesis of polymer P2b

Squaramide **12** (80 mg, 0.09 mmol), 4,4′- dibromo biphenyl **15 (**29.33 mg, 0.09 mmol), 1, 5-cyclooctadiene (0.11 mmol), 2,2′-bipyridyl (0.11 mmol) and $Ni(COD)_2$ catalyst (0.14 mmol) were taken in a test-tube with dry DMF (3.0 mL) and reaction was carried out at 85 °C under N_2 flow. After 48 h reaction, polymer was precipitated in diethyl ether and washed with diethyl ether two times. After that this polymer was washed with THF, then HCl acid and finally with EDTA solution. After filtration the compounds were dried over in vacuum oven to afford the **P2b** as a light brown Solid. Yield: 73 mg (91%); ^{1}H NMR (400 MHz, DMSO-d_6): δ 0.81, 1.25–1.65, 4.69, 5.78, 7.40–9.05; IR (KBr): ν = 3366, 3010, 2829, 1775, 1644, 1443, 1346, 1157, 1024, 854, 768, 633cm^{-1}; $[\alpha]^{27.1}_D$ = −43 (*c* 0.075, DMF); M_n (SEC) = 3600; M_w/M_n = 1.03

4.4.3.6 Synthesis of polymer P3

Squaramide **8 (**100 mg, 0.12 mmol), 1, 5-cyclooctadiene (0.14 mmol), 2,2′-bipyridyl (0.14 mmol) and $Ni(COD)_2$ catalyst (0.18 mmol) were taken in a test tube with dry DMF (3.0 mL) and reaction was carried out at 85 °C under N_2 flow. After 48 h reaction, polymer was precipitated in diethyl ether and washed with diethyl ether two times. After that this polymer was washed with THF, then HCl acid and finally with EDTA solution. After filtration the compounds were dried over

in vacuum oven to afford the **P3** as a light brown Solid. Yield: 99 mg (99%); ^{1}H NMR (400 MHz, DMSO-d_6): δ 0.83, 1.20–2.00, 4.62, 6.38, 6.80–8.20, 8.92; IR (KBr): ν = 3586, 3470, 2933, 2862, 2385, 2114, 1790, 1673 1582 1431, 1319, 1257, 1143, 1059, 969, 844, 767, 620 cm^{-1}; $[\alpha]^{17.6}_D = -44$ (c 0.08, DMF); M_n (SEC) = 7500; M_w/M_n = 1.77

4.4.3.7 Synthesis of polymer P4

Squaramide **11** **(**100 mg, 0.16 mmol), 1, 5-cyclooctadiene (0.18 mmol), 2,2′-bipyridyl (0.18 mmol) and Ni(COD)$_2$ catalyst (0.24 mmol) were taken in a test tube with dry DMF (3.0 mL) and reaction was carried out at 85 °C under N_2 flow. After 48 h reaction, polymer was precipitated in diethyl ether and washed with diethyl ether two times. After that this polymer was washed with THF, then HCl acid and finally with EDTA solution. After filtration the compounds were dried over in vacuum oven to afford the **P4** as a light brown Solid. Yield: 98 mg (98%); ^{1}H NMR (400 MHz, DMSO-d_6): δ 0.75, 1.10–1.70, 4.60, 4.97, 5.88, 7.20–9.01; IR (KBr): ν = 3421, 3210, 2943, 1771, 1600, 1443, 1341, 1156, 1023, 850, 737, 633 cm^{-1}; $[\alpha]^{18.6}_D = -18$ (c 0.095, DMF); M_n (SEC) = 4400; M_w/M_n = 1.13

4.4.4 Representative procedure for the enantioselective Michael addition reactions

4.4.4.1 Enantioselective Michael addition reaction between anthrone and *trans*-β-nitrostyrene

Trans-β-Nitrostyrene **17** (29.8 mg, 0.20 mmol) and the HBP catalyst (5.0 mol%) were added to a reaction vessel with 2.0 mL of CH_2Cl_2. Anthrone **16** (46.6 mg, 0.24 mmol) was added to the resulting solution. The reaction was stirred at room temperature and monitored using TLC. The reaction mixture was then filtered, and the filtrate was concentrated in vacuo. The crude product was purified by column chromatography on silica gel (100–200 mesh) using hexane/EtOAc = 5.0/1.0 as the eluent to afford **18** as a white solid. The *ee* was determined using HPLC on a Chiralpak AS-H column using solvent mixture hexane:2-propanol=5:1.

4.4.4.2 Enantioselective Michael addition reaction of Methyl 2-oxocyclopentanecarboxylate to *trans*-β-nitrostyrene

Trans-β-Nitrostyrene **17** (82.1 mg, 0.55 mmol) and the HBP (5 mol%, calculated from the unit molecular weight of the polymer catalyst) were added to a reaction vessel with 2.0 mL of solvent. Methyl 2-oxocyclopentanecarboxylate **25** (63 µL, 0.50 mmol) was added via a syringe into the resulting solution. The reaction was stirred at room temperature and its progress was monitored by TLC. The reaction mixture was then filtered, and the filtrate was concentrated in vacuo. The crude compound was purified by column chromatography on silica gel (100–200 mesh) using hexane/EtOAc = 6.0/1.0 as the eluent to afford the addition product **26** as a colorless oil. The enantioselectivity (*ee*) and diastereomeric ratio (*dr*) were determined using HPLC on a Chiralcel OD-H column using solvent mixture hexane:2-propanol=4:1. Experiments to understand the effect of the solvent, substrate scope, and recyclability were conducted according to this procedure.

4.4.4.3 Enantioselective Michael addition reaction between acetylacetone and *trans*-β-nitrostyrene

Trans-β-Nitrostyrene **17** (37.3 mg, 0.25 mmol) and the HBP (5 mol%) were added to a reaction vessel with 1.0 mL of CH_2Cl_2. Next, acetylacetone **27** (30.6 μL, 0.275 mmol) was added using a syringe into the resulting solution. The reaction was stirred at room temperature and monitored using TLC. The reaction mixture was then filtered, and the filtrate was concentrated in vacuo. The crude compound was purified by column chromatography using hexane/EtOAc/CH_2Cl_2 = 6.0/1.0/1.0 as the eluent on silica gel (100-200 mesh) to afford the addition product **28** as a white solid. The *ee* values were determined using HPLC on a Chiralpak AD-H column using solvent mixture hexane:2-propanol=9:1.

4.4.4.4 Enantioselective aldol reaction of ketones with isatins [44,45]

A solution of catalyst **P1** (5 mol %) and isatin **27** (0.5 mmol) in CH_2Cl_2 (2 mL) were stirred for 10 min at rt. Then ketone (acetophenone **28**, 4 mmol; acetone **30**, 10 mmol) was added. The reaction mixture was stirred for appropriate time and the progress of the reaction monitored by TLC. After completion of the reaction, the volatile components were removed under reduced pressure and the residue was purified by column chromatography on silica gel (Hexane/EtOAc=5/4) to afford the Aldol product. The enantiomeric excess was determined by HPLC on chiralpak OD-H column [hexane/2-propanol 9:1].

4.5 Reference

1. Yeboah, E. M. O.; Yeboah, S. O.; Singh, G. S. *Tetrahedron* **2011**, *67*, 1725–1762.
2. Jiang, L.; Chen, Y.-C. *Catal. Sci. Technol*. **2011**, *1*, 354–365.
3. Song, C. E. *Cinchona Alkaloids in Synthesis and Catalysis,* Wiley-VCH: Weinheim; Ed., **2009**.
4. Ingemann, S.; Hiemstra, H. *In Comprehensive Enantioselective Organocatalysis*, Dalko, P. I., Ed.; Wiley-VCH: Weinheim, **2013**; p 119–160.
5. Marcelli, T.; Hiemstra, H. *Synthesis* **2010**, *8*, 1229–1279.
6. Marcelli, T. *WIREs Comput Mol Sci*. **2011**, *1*, 142–152.
7. Tian, S. K.; Chen, Y.; Hang, J.; Tang, L.; McDaid, P. M. C.; Deng, L. *Acc. Chem. Res.* **2004**, *37*, 621–631.
8. Kacprzak, K.; Gawronski, J. *Synthesis* **2001**, *7*, 0961–0998.
9. Fernandes, S. D.; Porta, R.; Barrulas, P. C.; Pugliusi, A.; Burke, A. J.; Benaglia, M. *Molecules* **2016**, *21*, 1-9.
10. Itsuno, S. *J. Syn. Org. Chem. Jpn.* **2016**, *74*, 710–719.
11. Jumde, R. P.; Di Pietro, A.; Manariti, A.; Mandoli, A. *Chem. Asian J.* **2015**, *10*, 397–404.
12. Itsuno, S., (ed.) Polymeric Chiral Catalyst Design and Chiral Polymer Synthesis, John Wiley & Sons, Hoboken, New Jersey, **2011**.
13. Itsuno, S.; Hassan, M. M. *RSC Adv.* **2014**, *4*, 52023–52043.

14. Parvez, M. M.; Haraguchi, N.; Itsuno, S. *Macromolecules* **2014**, *47*, 1922–1928.

15. Ullah, M. S.; Itsuno, S. *Mol. Catal.* **2017**, *438*, 239–244.

16. Itsuno, S.; Parvez, M. M.; Haraguchi, N. *Polym. Chem.* **2011**, *2*, 1942–1949.

17 Chinchilla, R.; Mazon, P.; Najera, C. *Adv. Synth. Catal.* **2004**, *346*, 1186–1194.

18. Arakawa, Y.; Haraguchi, N.; Itsuno, S. *Angew. Chem. Int. Ed.* **2008**, *47*, 8232–-235.

19. Singh, G.S.; Eboah, E. M. *Dove press, Reports in org. Chem.* **2016**, *6*, 47–75

20. Gałęzowska, J.; Boratyński, P. J.; Kowalczyk, R.; Lipke, K.; Czapor-Irzabek, H. *Polyhedron* **2017**, *121*, 1–8.

21. Lewinski, J.; Kaczorowski, T.; Prochowicz, D.; Lipinska, T.; Justyniak, I.; Kaszkur, Z.; Lipkowski, J. *Angew. Chem. Int. Ed.* **2010**, *49*, 7035–7039.

22. Malerich, J. P.; Hagihara, K.; Rawal, V. H. *J. Am. Chem. Soc*. **2008**, *130,* 14416–14417.

23. Lee, J. W.; Ryu, T. H.; Oh, J. S.; Bae, H. Y.; Jang, H. B. Song, C. E. *Chem. Commun*. **2009**, *0*, 7224–7226.

24. (a) Tsakos, M.; Kokotos, C. G. *Tetrahedron* **2013**, *69*, 10199–10222.
(b) Zhao, B.-L.; Du, D.-M. *Eur. J. Org. Chem*. **2015**, *2015*, 5350–5359.

25. Meijere, A. D.; Brase, S.; Oestreich M. (ed.) Metal-Catalyzed Cross-Coupling Reactions and more, Wiley-VCH, Weinheim, **2014**.

26. Khosravi, E.; Yagci, Y.; Savelyev, Y., (ed.) New Smart Materials via Metal Mediated Macromolecular Engineering, Springer, Dordrecht, **2009**.

27. Yamamoto, T.; Wakabayashi, S.; Osakada, K., *J. Organomet. Chem.* **1992**, *428,* 223–237.

28. Kumpuga, B. T.; Itsuno, S. *J. Catal.* **2018**, *361*, 398–406.

29. Kumpuga, B. T.; Itsuno, S. *Catal. Commun.* **2019**, *118*, 5–9.

30. Ullah, M. S.; Itsuno, S. *ACS Omega,* **2018**, *3*, 4573–4582.

31. Powell, D. A.; Maki, T.; Fu, G. C. *J. Am. Chem. Soc.* **2005**, *127*, 510–511.

32. Everson, D. A.; Shrestha, R.; Weix, D. J. *J. Am. Chem. Soc.* **2010**, *132*, 920–921.

33. Yamamoto, T.; Koizumi, T. *Polymer* **2007**, *48*, 5449–5472.

34. Tsou, T. T.; Kochi, J. K. *J. Am. Chem. Soc.* **1979**, *101*, 7547–7560.

35. Yamamoto,T.; Yamamoto, A.; Ikeda, S. *J. Am. Chem. Soc.* **1971**, *93*, 3350–3359.

36. Yamamoto, T.; Morita, A.; Miyazaki, Y.; Maruyama, T.; Wakayama, H.; Zhou, Z. H.; Nakamura, Y.; Kanbara, T.; Sasaki, S.; Kubota, K. *Macromolecules* **1992**, *25*, 1214-1223.

37. Yamamoto, T. *Chem. Soc. Jpn.* **2010**, *83*, 431–455.

38. Rattanatraicharoen, P.; Tanaka, Y.; Shintaku, K.; Kawaguchi, T.; Yamabuki, K.; Oishi, T.; Onimura, K. *J. Polym. Sci. part A Polym. Chem.* **2013**, *51*, 1315–1322.

39. Lin, Liu, L.; Fu, Y.; Luo, S. -W.; Chen, Q.; Guo, Q. -X. *Organometallics* **2004**, *23*, 2114–2123.

40. Zea, A.; Valero, G.; Alba, A-N. R.; Moyano, A.; Riosa, R. *Adv. Synth. Catal.* **2010**, *352*, 1102–1106.

41. 41. Begum, Z.; Sannabe, H.; Seki, C.; Okuyama, Y.; Kwon, E.; Uwai, K.; Tokiwa, M.; Tokiwa, S.; Takeshita, M.; Nakano, H. *RSC Adv.* **2021**, *11*, 203–209.

42. Togashi, R.; Chennapuram, M.; Seki, C.; Okuyama, Y.; Kwon, E.; Uwai, K.; Tokiwa, M.; Tokiwa, S.; Takeshita, M.; Nakano, H. Eur. *J. Org. Chem.* **2019**, *24*, 3882–3889.

43.Gao, P.; Wang, C.; Wu, Y.; Zhou, Z.; Tang, C. *Eur. J. Org. Chem.* **2008**, *27*, 4563–4566.

44. Guo, Dr. Q.; Bhanushali, Dr. M.; Zhao, Dr. C.-G. *Angew. Chem. Int. Ed.* **2010**, *49*, 9460–9464.

45. Allu, S.; Molleti, N.; Panem, R.; Singh, V. K. *tetrahedron Letters*, 2011, *52*, 4080-4083.

Chapter 5

GENERAL CONCLUSION

5.1 Introduction

Owing to the easy separation from the reaction mixture, chiral polymeric catalysts have drawn significant attention to the researchers. Chiral polymeric organocatalysts as a class of chiral organocatalysis which is advantageous because of being derived from a metal free catalyst and their recyclability. This allows a clean and safe alternative to conventional methods of asymmetric processes. Polymeric catalyst creates specific microenvironment in a polymer network which make them lucrative for using in organic reactions especially in enantioselective synthesis. Although polymeric organocatalysts, sometimes show poor reactivity in asymmetric synthesis due to their heterogeneity in the reaction mixture. But a well-designed polymeric chiral organocatalyst can possess sufficient reactivity along with higher enantioselectivity in asymmetric synthesis.

Cinchona alkaloids and their derivatives have been widely employed as chiral organocatalysts in diverse asymmetric synthesis, because of their outstanding catalytic activity for several asymmetric reactions.[1-8] Cinchona alkaloids are functional for suitable modifications to versatile catalysts in asymmetric reactions due to their several functionalities such as secondary alcohols, quinoline rings, and quinuclidine and vinyl groups.[4,6,9-11] Cinchona alkaloids have found part in chiral polymeric organocatalysts design as a privileged class of chirality inducers. The polymeric catalyst design is an essential tool to understand the efficient catalytic process in asymmetric transformations. For this purpose, cinchona derived squaramide were used for the design of chiral polymeric organocatalysts in this work. Because of possessing an acidic NH which can act as H-bond donor and the tertiary nitrogen of the quinuclidine of cinchona squaramides may serve as both an H-bond acceptor and a base in asymmetric Michael addition reactions.[12-24]

In this work, we synthesized hyperbranched and linear polymers using cinchona derived squaramide by using Mizoroki-Heck reaction and Yamamoto coupling reaction.

5.3 Hyperbranched polymer

Highly branched tree-like macromolecules bearing unique three-dimensional structures are called Hyperbranched polymers (HBPs), have attracted a lot of attention in various applications. Chiral HBPs containing chiral catalytic moieties are potential polymer catalysts in asymmetric catalysis.[25-27] Mizoroki-Heck (MH) coupling reaction was used for the preparation of hyperbranched chiral polymers of cinchona alkaloids derivatives in chapter 2 and 3. We have reported, the design and synthesis of chiral polymers of cinchona squaramides and their application as catalysts in asymmetric reactions. Our design of chiral HBPs involves the use of C3 olefinic double bond of the cinchona squaramide dimer (A2) through Mizoroki-Heck (MH) coupling reaction of aryl tri or tetra substituted aromatic odides (B3) and we called the approach as two components polycondensation

which was described in chapter 2. Another approach was one-component polycondensation where AB_2 and A_2B type squaramide synthesized firstly from the reaction of cinchona squaramide and aryl iodo compounds. Then using this monomer which contains both C3 olefinic double bond and aromatic iodo group in its molecule, chiral HBPs were synthesized via Mizoroki-Heck polymerization reaction.

In the preparation of hyperbranched chiral polymers, first cinchonidine was used as a starting material in the preparation of monomeric or dimeric cinchona alkaloid derivatives. Then these were used for polymerization by MH coupling reaction. General characterization methods for the main-chain chiral polymers in this work involves;

i) Proton-NMR analysis

ii) Size exclusion (SEC) measurements analysis

iii) Specific rotation measurements

iv) FT-IR spectrum analysis

5.3 Synthesis of chiral hyperbranched polymers containing cinchona squaramide moieties by Mizoroki-Heck polymerization and their catalytic activity in the asymmetric Michael addition reaction

5.3.1 Synthesis of chiral hyperbranched polymers of cinchona squaramide (two component polycondensation) by Mizoroki-Heck polymerization

In this chapter we designed and synthesized cinchona derived squaramide chiral HBPs. Cinchona squaramides dimers, such as **1**, was used for the synthesis of three chiral HBPs. One of the simple HBPs can be prepared via the combination of bifunctionalized (**A2**) and trifunctionalized (**B3**) compounds, as shown in Scheme 5.1 by Mizoroki-Heck reaction. A quantitative reaction between functionalities **A** and **B** is necessary to prepare HBPs. Cinchona alkaloid possesses an olefinic double bond at the C3 position, therefore the reaction between cinchona alkaloid dimer (**A2**) and trisubstituted aromatic iodide (**B3**) may give rise to chiral hyperbranched polymers. This is a new type of polymeric chiral organocatalyst.

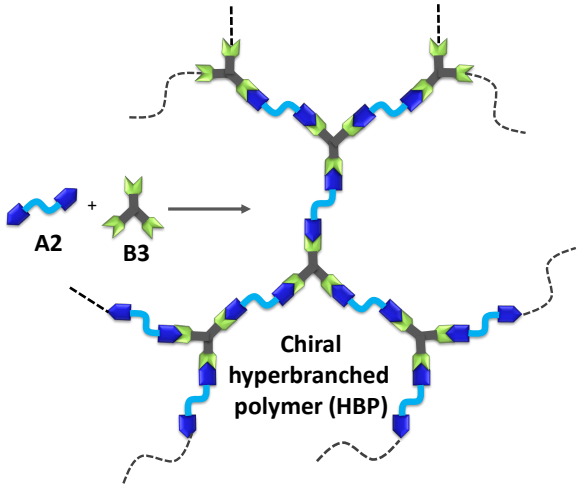

Scheme 5.1. Synthesis of chiral hyperbranched polymers (HBPs)

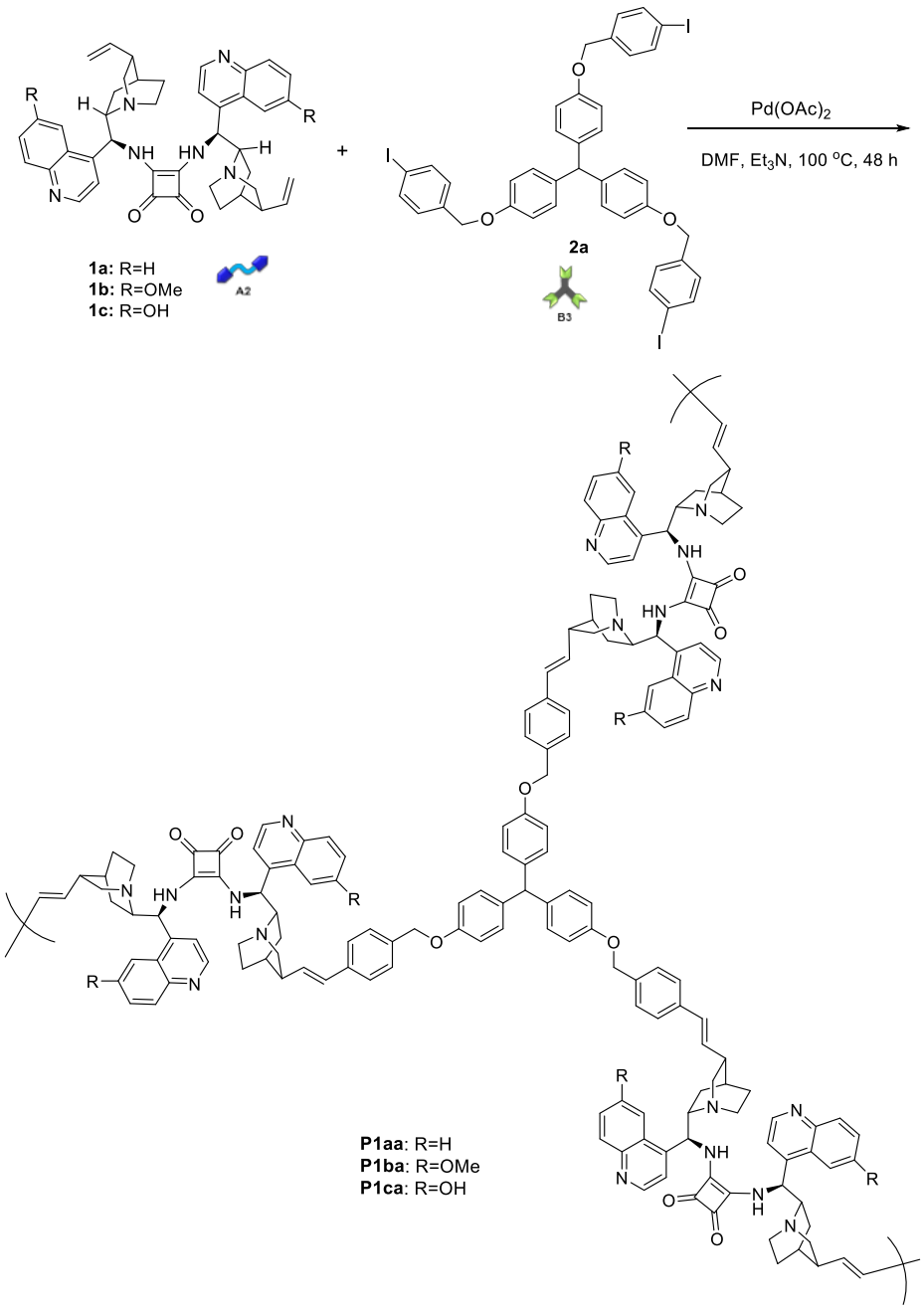

Scheme 5.2. Synthesis of Polymers **P1aa**, **P1ba** and **P1ca**

Using other trisubstituted aromatic iodide **2b** and tetra substituted aromatic iodides **2c** gave hyperbranched polymer **P2ab** and **P3ac** with cinchona squaramide dimer **2a** by MH coupling. All polymers gave moderate yield.

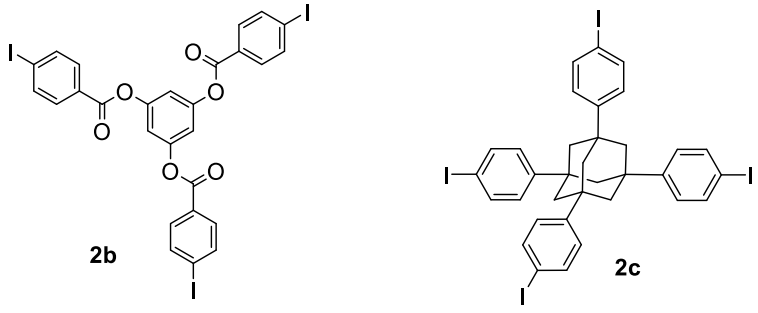

Figure 5.1. Other two aromatic tri- and tetrasubstituted iodides

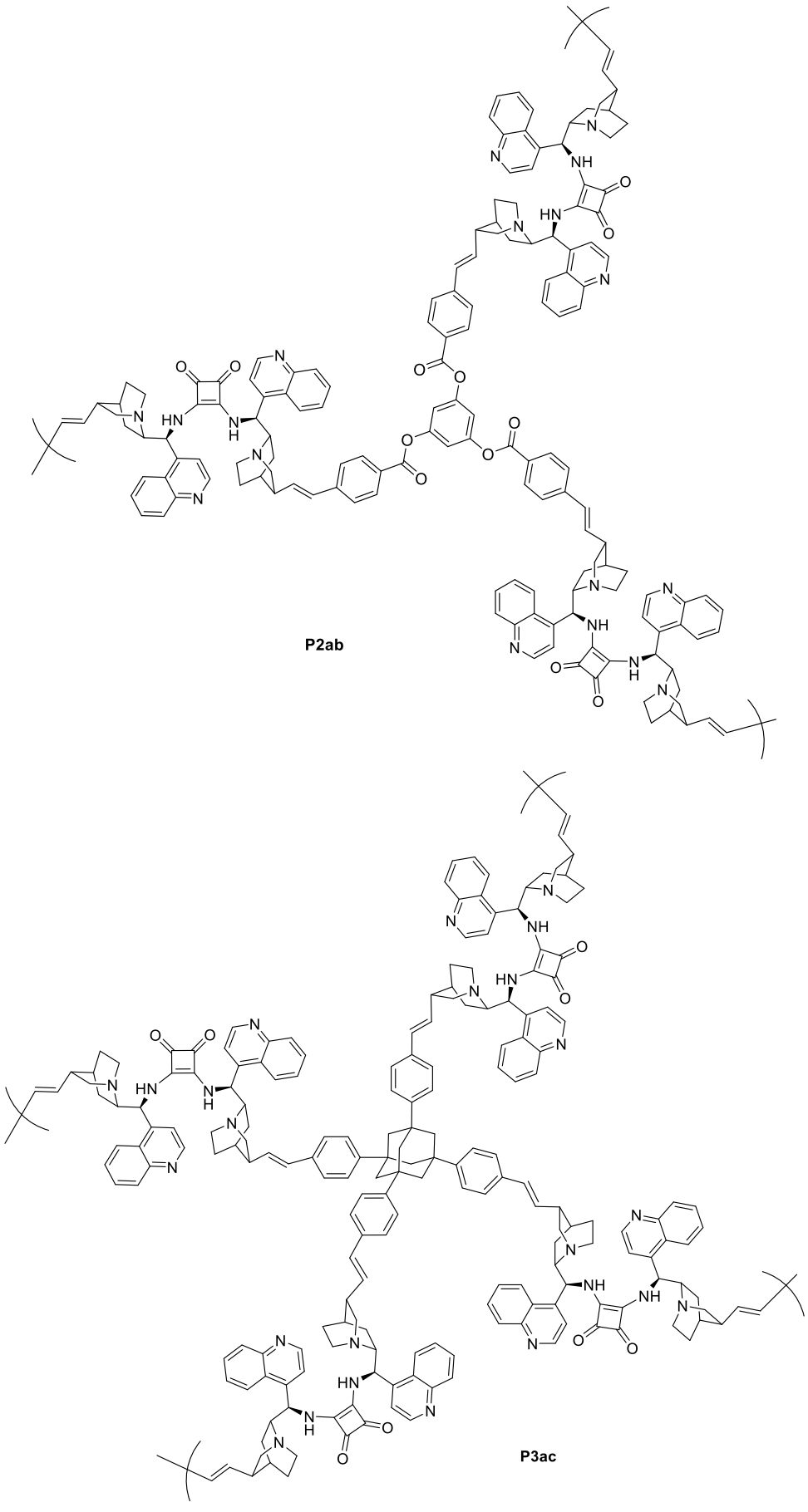

Figure 5.2. Structure of polymers **P2ab** and **P3ac**

5.3.2 Catalytic activity of HPBs in the asymmetric Michael addition reaction

The obtained chiral HBPs were applied in asymmetric catalysis and their catalytic performance were evaluated in the asymmetric Michael addition reaction of methyl 2-oxocyclopentanecarboxylate to β-nitrostyrene as well as the addition of anthrone to β-nitrostyrenes. The following parameters were used for their evaluation in asymmetric synthesis.

i) The effect of C6'-substituent group Dimeric and polymeric structure effects: Dimeric cinchona squaramide **1a** (R=H), **1b** (R=OMe) and **1c** (R=OH) was first examined as an organocatalyst in the asymmetric Michael addition reaction of methyl 2-oxocyclopentanecarboxylate **3** and *trans*-β-nitrostyrene **4** (scheme 5.3). In the presence of **1a**, the asymmetric reaction smoothly occurred to give chiral product **5** in 95% yield and 98% ee with high diastereoselectivity (>100:1). Good result was obtained with dimer **1a**. Then the corresponding chiral HBPs (**P1**–**P3**) were applied as organocatalysts in the same reaction. These chiral HBP catalysts showed excellent performance in the asymmetric reaction. When **P1aa** was used as a catalyst in CH_2Cl_2, chiral product **5** was obtained in 90% yield even under heterogeneous conditions, although the diastereoselectivity decreased to some extent (dr 27:1), the enantioselectivity (>99% ee) of the major diastereomer was almost perfect with **P1aa.**

The other chiral HBPs showed excellent enantioselectivity (>99% ee) except for the result obtained using **P1ca** bearing a C6'-OH group (dr 2:1, ee 40%). The corresponding dimeric catalyst **3c** also gave lower stereoselectivity (dr 2:1, ee 71%).). The structural difference between iodides **6a**, **6b**, and **6c** had almost no effect on the catalytic activity of their corresponding chiral HBPs.

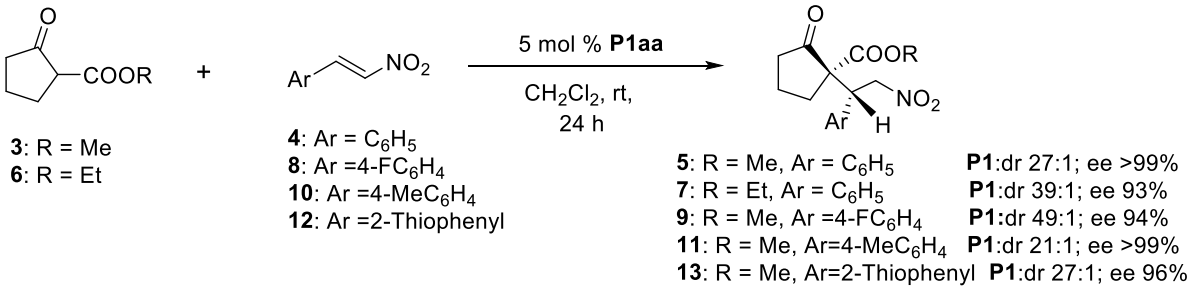

Scheme 5.3. Enantioselective Michael addition reaction of β-keto ester to nitroolifins.

ii) Solvent effect: The solvent effect on the asymmetric reaction was examined using **P1aa**. Except for hexane as a solvent, high levels of enantioselectivity (>99% ee) were found for the major diastereomer. The diastereoselectivity varied with the solvent used. The reaction of **P1aa** in dichloromethane gave the desired product with the highest diastereoselectivity (dr 27:1, >99% ee).

iii) Catalyst loading and reacting substrate effect: 2.5 mol% and 5 mol % catalyst was applied during the reaction. There is no big change in enantioselectivity. Chiral HBP **P1aa** was applied to other Michael addition reactions as shown in Scheme 5.3. In the reaction with 2-

oxocyclopentanecarboxylate **3** and **6**, a high level of enantioselectivity was obtained with variety of nitroolifin.

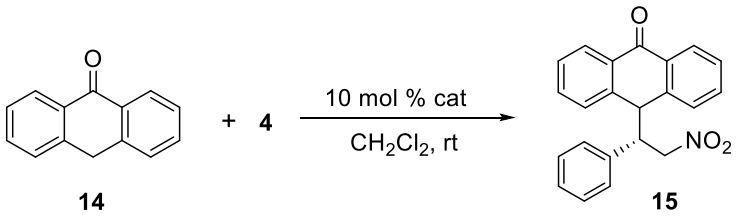

1c: ee78%; **P1ca**: ee 18%
[a]**1c**: ee 34%; **P1aa**: ee 9%
[b]**1c**: ee 72%; **P3ac**: ee 10%
a=reaction carried out at –40 °C
b=reaction carried out at 50 °C

Scheme 5.4. Enantioselective Michael addition reaction of anthrone to *trans*-β-nitrostyrene **4.**

Dimer **1c** and its corresponding hyperbranched polymer **P1ca** were applied in another Michael addition reaction of anthrone **14** to *trans*-β-nitrostyrene **4** (Scheme 5.4). Higher enantioselectivity 78% ee was observed in low molecular weight catalyst at room temperature with 93% yield with dimer **1c**. For corresponding polymer **P1ca**, very low ee was found 18%. Other polymers **P1aa** and **P3ac** were also applied in this reaction. However, only low enantioselectivities were obtained with the chiral HBP catalysts.

iv) Recyclability evaluation: Recovered polymeric catalysts **P1aa** and **P3ac** were reused in the same reaction to examine their recyclability. **P1aa** was recycled six times and **P3ac** four times. Both these chiral HBP catalysts maintained a high level of catalytic activity without any decrease in the diastereoselectivity and enantioselectivity.

Each of the evaluated parameters showed different catalytic effect in the enantioselective synthesis of Michael products with chiral polymeric organocatalysts of cinchona alkaloids derivatives. We found that the obtained chiral HBPs show excellent catalytic activity in the asymmetric Michael reaction. Almost perfect enantioselectivity (>99% ee) was achieved in the reaction of β-ketoester and *trans*-β-nitrostyrene. The three-dimensional network structure of the chiral HBPs is structurally robust and can be reused for further reaction without any loss in their catalytic activity.

5.4 Synthesis of cinchona squaramide based hyperbranched polymers (AB_2 and A_2B types) and their application in Asymmetric reactions

5.4.1 Synthesis of cinchona squaramide chiral hyperbranched polymers (one component polycondensation, AB_2 and A_2B types) by Mizoroki-Heck polymerization

In this study, we designed the chiral AB_2 and A_2B monomer using cinchona alkaloid squaramide. We applied MH polymerization technique to prepare chiral HBPs. Two iodophenyl groups were introduced into the cinchona mono squaramide derivative to obtain the AB_2 monomer.

The A_2B monomer contained two cinchona squaramide moieties. In both chiral HBPs derived from AB_2 and A_2B polymerization, each branching point involves a catalytic active site. For comparison, corresponding linear polymer was also synthesized.

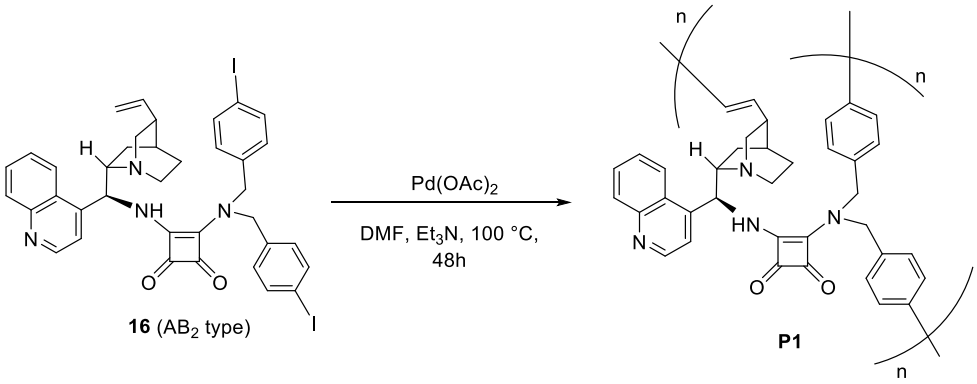

Scheme 5.5. Synthesis of polymer **P1** by MH polymerization.

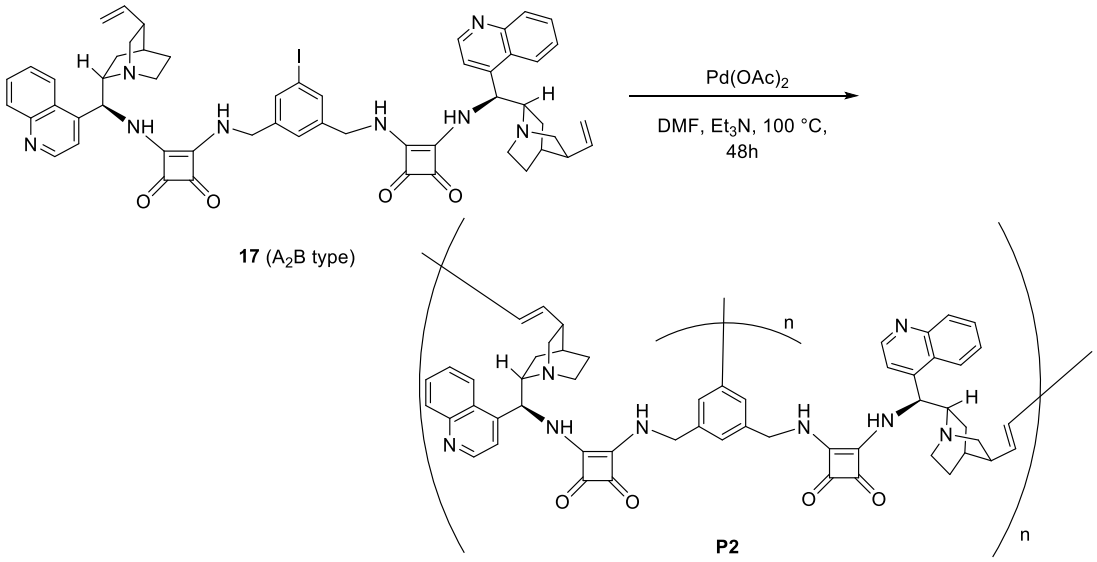

Scheme 5.6. Synthesis of polymer **P2** by MH polymerization.

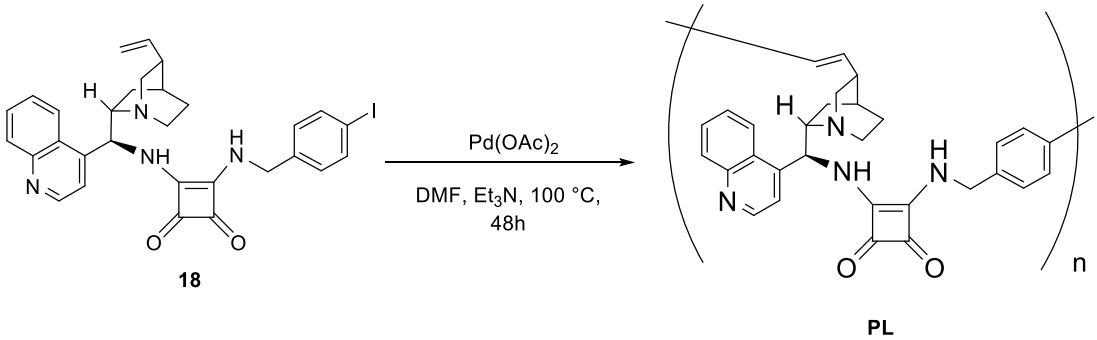

Scheme 5.7. Synthesis of polymer **PL**.

5.4.2 Catalytic application of HBPs in asymmetric reactions

HBPs obtained by MH polymerization were evaluated their catalytic performance in the asymmetric Michael addition reactions of methyl 2-oxocyclopentanecarboxylate **3** to *trans* β-

nitrostyrene **4** as well as the addition of acetylacetone **19** to β-nitrostyrenes **4**. The following parameters were used for their evaluation in asymmetric synthesis.

i) Polymeric structure effects: Chiral HBP catalyst **P1** (5 mol%) was first applied in the asymmetric Michael addition reaction of methyl 2-oxocyclopentanecarboxylate **3** and *trans*-β-nitrostyrene **4** (Scheme 5.8). The reaction proceeded smoothly to give the corresponding Michael adduct **13** in 93% yield with excellent enantioselectivity (98% ee) and diastereoselectivity (*dr* >100:1) in heterogeneous condition. Other HBPs **P2** and **PL** gave almost same results in this reaction.

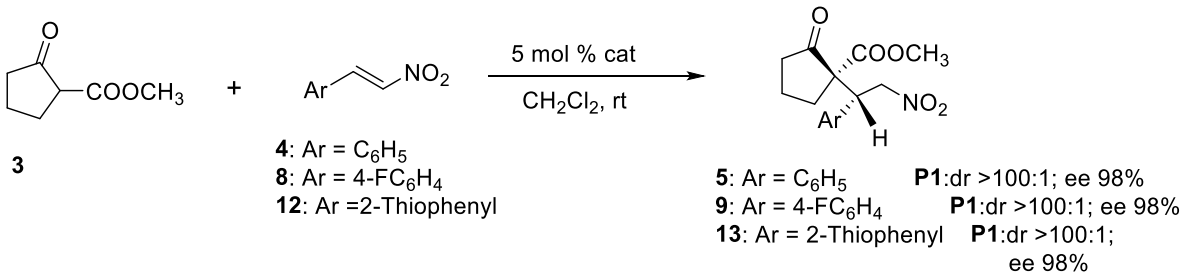

Scheme 5.8. Asymmetric Michael addition of methyl 2-oxocyclopentanecarboxylate **3** to nitroolifins

ii) Solvent effect and reacting substrates effect: The effect of solvents on the catalytic performance was surveyed using **P1**. In both THF and methanol solvents, **P1** led to high yields with low diastereoselectivity (51:1 dr; >99% ee and 42:1 dr; >99% ee). Lowering the reaction temperature to 0 °C in methanol afforded somewhat higher diastereoselectivity compared to that obtained at room temperature (97:1 dr; >99% ee). Two other nitroolefins, **8** and **12**, were also tested for the asymmetric reaction with **P1** in CH_2Cl_2 and methanol. Similar trends in the catalytic activity and stereoselectivity was observed in these cases.

iii) Recyclability evaluation: The insoluble catalyst could be easily separated and recovered after completion of the reaction via simple filtration. Recovered polymeric catalyst **P1** was reused in the same reaction in methanol to examine its recyclability. Even after recycling for four catalytic runs, the catalytic activity and stereoselectivity were still maintained.

iv) Asymmetric reaction of other active methylene compounds to trans-β-nitrostyrene: Other active methylene compounds were examined as Michael donors in the asymmetric addition reaction (scheme 5.9). The chiral polymeric catalysts **P1**, **P2**, and **PL** were applied in the reaction of acetylacetone **19** to *trans*-β-nitrostyrene. These chiral HBP catalysts showed excellent performance in the asymmetric reaction. Best result was observed by using **P1** as a catalyst in CH_2Cl_2, chiral product **20** was obtained in 83% yield after 24 h even under heterogeneous conditions with high enantioselectivity (81% ee). Enantioselectivity improved to 85% when this reaction was performed at 0 °C, although the reaction time was prolonged to 48 h. The reaction of dimethyl malonate **21** and

4 was also catalysed by **P1** and **P2**. The Michael addition of anthrone **14** to β-nitrostyrene **4** was also examined using the polymeric catalysts **P1** and **P2**. Another aMichael adduct **23** also obtained by using catalyst **P1.**

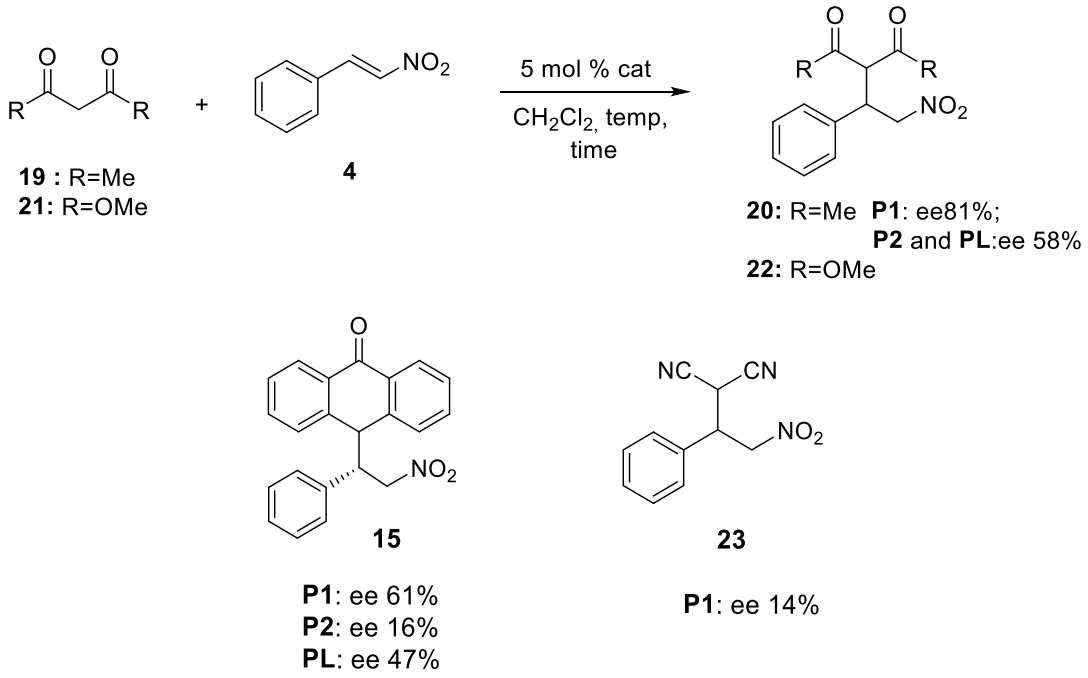

Scheme 5.9. Asymmetric Michael addition reaction using chiral HBP catalysts.

v) Enantioselective aldol reaction of ketones with isatins: Polymeric catalysts **P1** and **P2** were applied in aldol reaction (scheme 5.10). Chiral HBPs could catalyze the reaction of isatins with ketones smoothly, although enantioselectivity was very poor. **P1** gave 7% ee in the reaction of isatin **24** and acetophenone **25** whereas 28 % ee was obtained with acetone **27** with good yield. Decrease of temperature to 0 °C, could not improve ee (4% ee). With **27**, **P2** gave only 6% ee with good yield whereas racemic product was found in the reaction with acetophenone **25.**

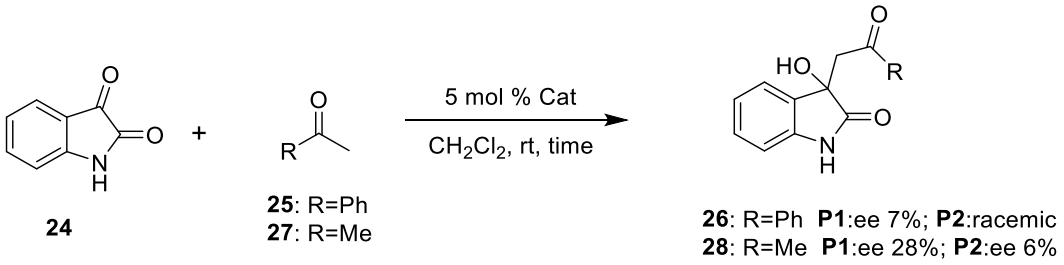

Scheme 5.10. Aldol condensation reaction using chiral HBP catalysts.

Each of the evaluated parameters showed different catalytic effect in the enantioselective synthesis of Michael products with chiral polymeric organocatalysts of cinchona alkaloids derivatives.

5.5 Synthesis of cinchona squaramide polymers by Yamamoto coupling polymerization and their application in Asymmetric Michael reactions

We have reported on the design and synthesis of linear main-chain chiral polymers of cinchona alkaloids as catalysts for their application in asymmetric reactions in chapter 4. We designed new cinchona-based chiral polymers using Yamamoto coupling polymerization.

5.5.1 Synthesis of cinchona squaramide polymers by Yamamoto polymerization

Yamamoto coupling is the nickel-catalyzed coupling reaction of organic halides in the presence of neutral ligands, eg. bipyridine. The most commonly used nickel catalyst for the Yamamoto coupling reaction is bis(cyclooctadiene)nickel(0) ($Ni(COD)_2$). This coupling reaction is particularly interesting when it is applied to polymer synthesis. A novel type of polymeric chiral catalyst can be synthesized via this polymerization. Yamamoto coupling reaction is advantageous because only a single, halogen-functionalized monomer can be used to form polymer. Copolymerization can be carried out by using dihalogeno aromatic compound as a comonomer.

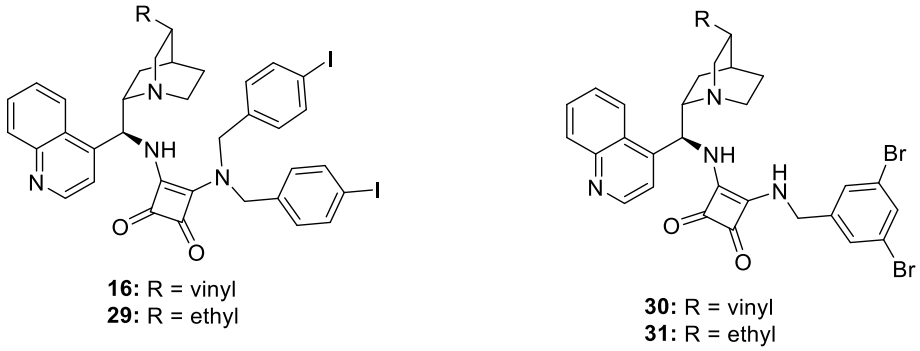

Figure 5.3. Cinchona squaramide monomers.

Chiral cinchona squaramides monomer **16**, **29**, **30**, and **32** (Figure 5.3) were first synthesized. Using these cinchona squaramide monomers, the polymerization conditions of Yamamoto coupling polymerization were studied. Best condition for polymerization was found in DMF for 48 h at 85°C. Linier polymers and copolymers were synthesized first.

Under optimized conditions, copolymer **P2a** was synthesized from squaramide **31** and 1,3-dibromo benzene **33** (Figure 5.4; Scheme 5.11) using different ratios of **31** and **33**. An equimolar ratio of **12** to **14** afforded the copolymer **P2a** (1:1). Polymers **P2a** (m:n) with different ratios of **31** and **33** were prepared using the same method. Depending on the comonomer ratio, the molecular weights varied from 4700 to 12600. The transition-metal-catalyzed C–C coupling reaction between aryl halide and olefin is known as the Mizoroki–Heck coupling. Ni-catalyzed Mizoroki–Heck coupling is also possible. In the presence of the Ni catalyst, both Yamamoto and Mizoroki–Heck coupling reactions occur simultaneously. For example, cinchona squaramide monomers **16** and **30** with a C3-vinyl group can be polymerized by either Yamamoto or Mizoroki–Heck coupling to yield hyperbranched polymers **P3** and **P4**, as shown in Figure 5.5.

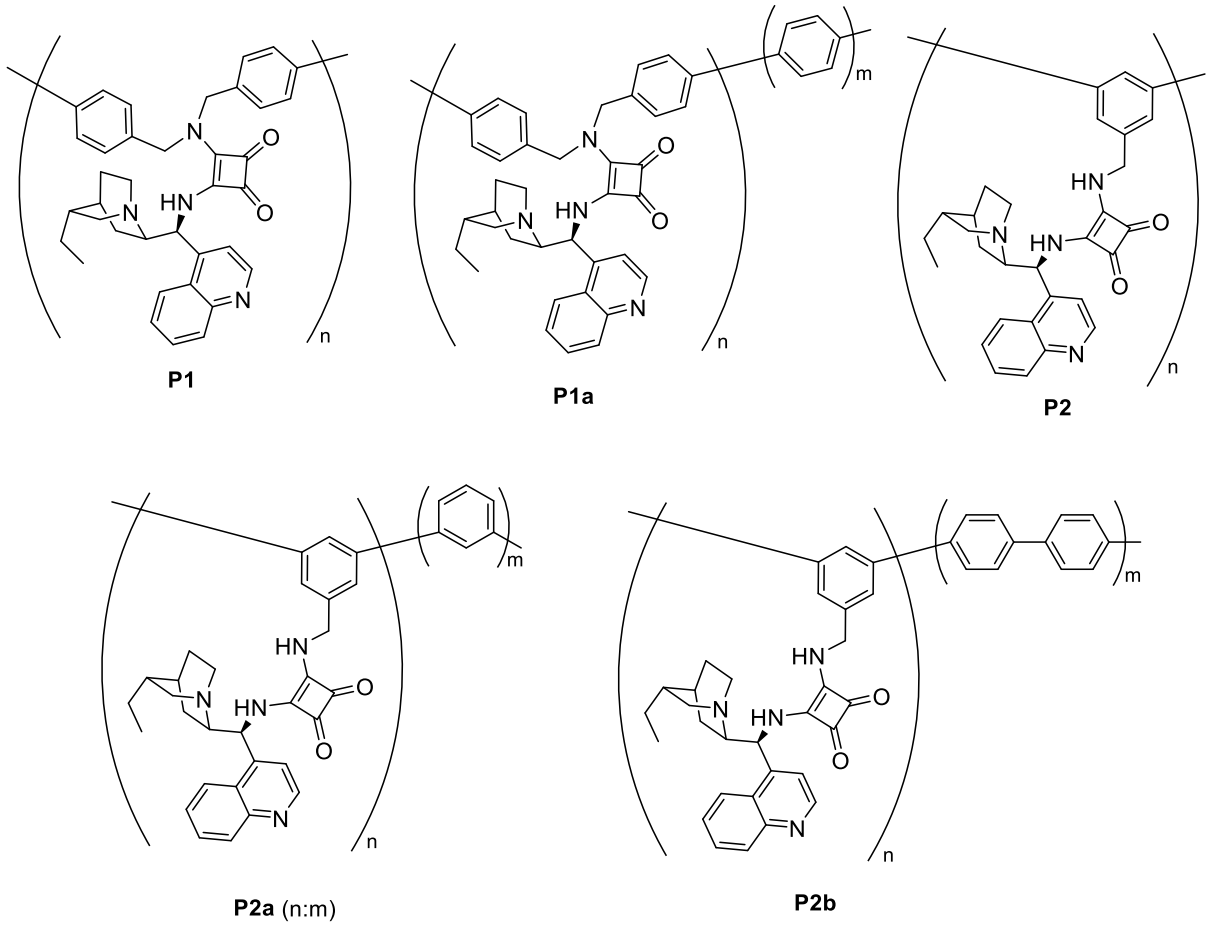

Figure 5.4. Cinchona squaramide linear homopolymers and copolymers.

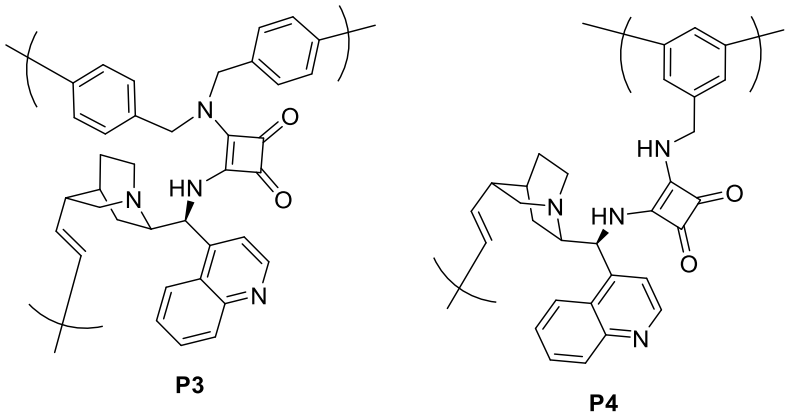

Figure 5.5. Cinchona squaramide branched polymers.

5.5.2 Catalytic performance of the cinchona squaramide polymers

Chiral polymers obtained by Yamamoto coupling, were evaluated their catalytic performance in the asymmetric Michael addition reactions of anthrone **14** to β-nitrostyrene **4.** The following parameters were used for their evaluation in asymmetric synthesis.

i) Polymeric structure effects and effect of comonomer: Polymeric catalysts **P1**−**P4** were applied in the asymmetric Michael addition reaction of anthrone **14** and *trans*-β-nitrostyrene **4** (Scheme 5.12).

First, the catalytic activities of low-molecular-weight cinchona squaramides **29** and **31** were examined as model catalysts. These cinchona squaramides showed excellent catalytic activities reaction of anthrone and *trans*-β-nitrostyrene to afford Michael adduct **15** in high yield with 58% ee and 84% ee (Table 5.1, entries 1 and 2). Linear polymer **P1** showed 20% enantioselectivity with good yield. The corresponding copolymer **P1a** afforded an almost racemic product with a prolonged reaction time, with good yield. In the presence of **P2**, Michael adduct **15** was obtained in 90% yield with 66% ee (entry 5). The enantioselectivity increased to 78% ee using copolymer **P2a** (1:1) in the same asymmetric reaction (entry 6). By employing **P2a** (1:1), the reaction was completed in three hours, which was much faster than that with the low-molecular-weight catalyst **31**, which required 24 h. When the molar ratio was changed from 1:1 to 1:1.5 or 1:0.7, the polymeric catalysts **P2a** (1:1.5) and **P2a** (1:0.7) afforded lower enantioselectivities (entries 7 and 8).

The structure of the comonomer also affected the enantioselectivity, mainly due to the change in the polymer conformation. With the use of biphenyl comonomer **34** instead of **33**, a much lower enantioselectivity (25% ee) was obtained (entry 9). Similar to the linear polymers **P1** and **P1a**, the hyperbranched polymer **P3** provided an almost racemic product, and the reaction proceeded appropriately (Table 2, entry 10). An additional hyperbranched polymer **P4** showed similar catalytic activity as **P2** (entries 5, 11).

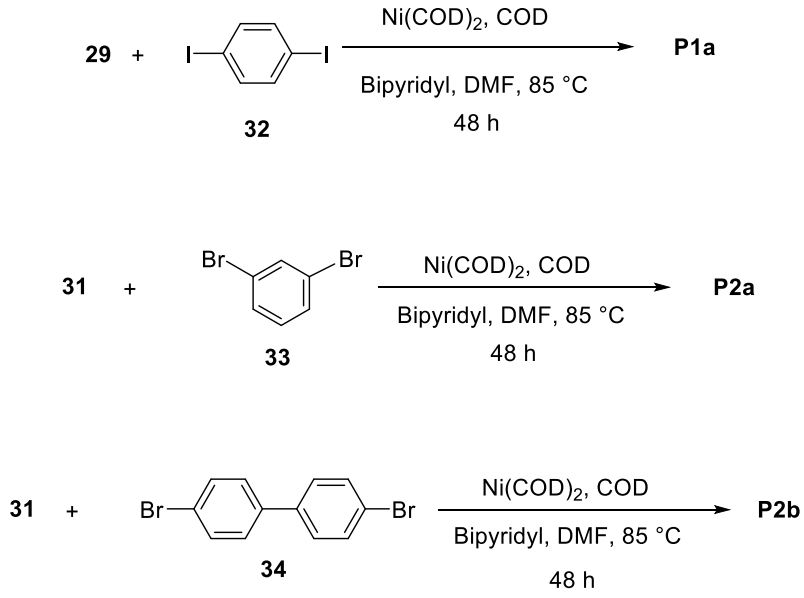

Scheme 5.11. Synthesis of copolymers, **P1a**, **P2a** and **P2b**.

ii) Reaction condition effect such as catalyst loading, sovent effect and temperature effect: The catalyst loading sometimes affects the catalytic performance in asymmetric reactions. Using **P2a**, different molar percentages of the catalyst were tested in the asymmetric reaction of anthrone **14** to *trans*-β-nitrostyrene **4**. Interestingly, even when the catalyst loading was decreased to 2.5 mol%, the reaction was completed in three hours (Table 2, entry 12).

Solvent screening was performed using **P2a**. Various types of solvents were tested, and dichloromethane afforded the best result in the asymmetric reaction with **P2a**.

At high temperature (50 °C), the reaction time decreased, and it was completed in 1.5 h, affording a slightly low enantioselectivity of 72%. Decreasing the temperature to −20 °C resulted in high enantioselectivity (82% ee). Increased enantiomeric excess of 84% was obtained when the reaction was performed at −40 °C, but a long time of 48 h was needed

Table 5.1. Reaction optimization: Asymmetric Michael addition reaction of anthrone **14** to *trans*-β-nitrostyrene **4** using polymeric catalysts.[a]

Entry	Catalyst	Catalyst loading (mol %)	Reaction time [h]	Yield[b] [%]	*ee*[c] [%]
1	**29**	5	7	93	58
2	**31**	5	24	89	84
3	**P1**	5	16	90	20
4	**P1a**	5	24	88	5
5	**P2**	5	12	90	66
6	**P2a** (1:1)	5	3	92	78
7	**P2a** (1:1.5)	5	6	91	61
8	**P2a** (1:0.7)	5	8	90	54
9	**P2b**	5	8	91	25
10	**P3**	5	24	82	2
11	**P4**	5	12	90	62
12	**P2a** (1:1)	2.5	3	92	75
13	**P2a** (1:1)	10	3	90	73
14	**P2a** (1:1)	15	3	92	72

[a]Asymmetric reaction was carried out using **14** (0.24 mmol), **4** (0.2 mmol), and 5 mol% cat. in CH_2Cl_2 (2.0 mL) at 25 °C.
[b]Isolated yield of the product after column chromatography.
[c]Enantioselectivity (ee) was determined using HPLC (CHIRALPAK AS-H column).

iii) *Reacting substrates effect*: Other phenyl-substituted *trans*-β-nitrostyrene derivatives were tested in the asymmetric reaction of anthrone **14** using **P2a** (1:1) in CH_2Cl_2 at −20 °C. Good (89–91%) yields and ee were obtained in all cases.

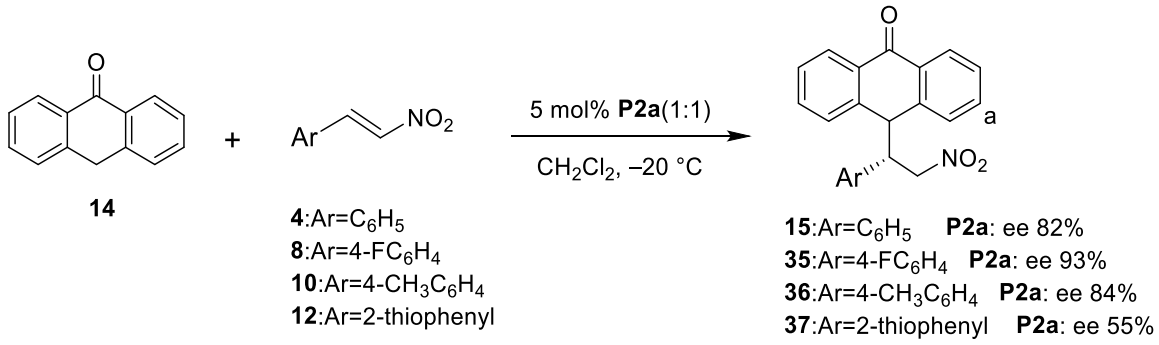

Scheme 5.12. Asymmetric reaction of anthrone to different nitroolifins.

iv) Recyclability evaluation: Chiral copolymer **P2a** (1:1) was completely soluble in CH_2Cl_2, and the asymmetric reaction occurred in a homogeneous system in this solvent. After completion of the reaction, the polymeric catalyst was precipitated in diethyl ether and then easily separated and

recovered via simple filtration. The recovered polymeric catalyst **P2a** (1:1) was reused in the same reaction. no significant differences in enantioselectivity were observed after four times recyclation. The reaction was completed within 24 h using the reused polymeric catalyst **P2a** (1:1).

v) Michael addition reaction of other substrate combinations: An additional Michael donor, methyl 2-oxocyclopentanecarboxylate **3** was investigated. The chiral polymers **P1**–**P4** were used as organocatalysts in the reaction of **3** with **4**. In all cases, the asymmetric reaction proceeded smoothly to provide chiral product **5** in good yield and excellent enantioselectivity. High diastereoselectivity (>100:1) was obtained with **P2a** (1:1), **P2b**, and **P4** catalysts (Figure 5.6).

Chiral polymers **P2a** (1:1) and **P4** were also used in the asymmetric reaction of acetylacetone **19** with *trans*-β-nitrostyrene **4**. Chiral Michael adduct **28** was obtained with good yield and ee in both cases.

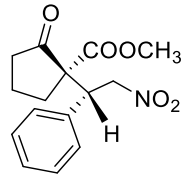

5 (2*S*, 3*R*)

P1: dr 58:1; ee 99%
P1a: dr 9:1; ee 72%
P2: dr 92:1; ee 98%
P2a: dr >100:1; ee 98%
P2b: dr >100:1; ee 98%
P3: dr 6:1; ee 48%
P4: dr >100:1; ee 99%

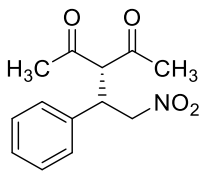

20 (*S*)

P2a: ee 78%
P4: ee 65%

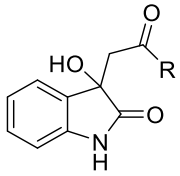

26: R=Ph **P1**:ee 39%;
P2: ee 6%
P2a: ee 23%
P3: ee n.d;
P4: ee 5%
28: R=Me **P1**:racemic

Figure 5.6. Enantioselective Michael addition and aldol reaction using chiral polymers

vi) Enantioselective aldol reaction of ketones with isatins: Polymeric catalysts **P1**-**P4** were applied in aldol reaction. **P1** gave highest ee 39% ee in the reaction of isatin and acetophenone whereas 23 % ee was obtained with catalyst **P2a** with good yield. Racemic product **28** was found in the reaction with isatin and acetone with catalyst **P1**.

Each of the evaluated parameters showed different catalytic effect in the enantioselective synthesis of Michael products with chiral polymeric organocatalysts of cinchona alkaloids derivatives.

5.6 Conclusion

In this work, cinchona squaramide-based chiral hyperbranched polymers by Mizoroki-Heck reaction and linear and hyperbranched polymers by Yamamoto coupling were successfully synthesized. The summary of each work on chiral polymeric catalysts of cinchona alkaloids are as explained below:

i) Chiral HBPs **P1**-**P3** were successfully synthesizes by MH polymerization and these polymers were applied in the asymmetric Michael addition reaction and showed excellent enantioselectivity (>99% ee) in the Michael addition reaction of β-ketoesters to *trans*-β-nitrostyrene. Very high enantioselectivities were constantly obtained with **P1aa** in all solvents used in the asymmetric reaction. The HBPs can be easily separated and reused up to six times without losing their catalytic activity and enantioselectivity. This is the first example of chiral HBP organocatalyst successfully applied to the asymmetric Michael addition reaction.

ii) We synthesized novel chiral HBPs from cinchona squaramide monomers **4** and **7**. These were successfully polymerized by the MH coupling reaction between the **A** and **B** functionalities to give chiral HBPs **P1** and **P2**, respectively. The reactions occurred smoothly to give the corresponding chiral product. In case of the reaction between methyl 2-oxocyclopentanecarboxylate **11** and *trans*-β-nitrostyrene **12**, the HBP catalysts showed high catalytic activity with excellent diastereoselectivity and enantioselectivity. Reactions between some other substrate combinations also occurred smoothly with the HBP catalysts. **P1** exhibited superior selectivity in these reactions. Interestingly, the HBP catalysts gave higher diastereoselectivity compared to that obtained with the low-molecular-weight catalyst **4**. Somewhat higher catalytic activity was also observed with HBP catalyst. Precise control of the catalyst conformation may be possible in case of polymer catalyst. These results show that the design of chiral HBP catalyst may lead the development of high performance polymeric catalyst.

Cinchona squaramide based chiral hyperbranched polymers (HBPs) **P1** and **P2** were designed and successfully synthesized from cinchona squaramide monomers possessing both vinyl (**A**) and iodophenyl (**B**) groups in their structure by using Mizoroki–Heck (MH) coupling reaction. This kind of polymeric catalysts are contemporary which are not reported before. The chiral HBPs (**P1**, **P2**) prepared by one step MH polymerization from $\mathbf{AB_2}$ and $\mathbf{A_2B}$ monomers, and HBPs were used as catalysts in asymmetric Michael reactions. Excellent enantioselectivity was observed in different types of asymmetric Michael reactions. In case of the reaction between methyl 2-oxocyclopentanecarboxylate **3** and *trans*-β-nitrostyrene **4**, the HBP catalysts showed high catalytic activity with excellent diastereoselectivity and enantioselectivity. Reactions between some other substrate combinations also occurred smoothly with the HBP catalysts. **P1** exhibited superior selectivity in these reactions. Interestingly, the HBP catalysts gave higher diastereoselectivity compared to that obtained with the low-molecular-weight catalyst **4**. Somewhat higher catalytic activity was also observed with HBP catalyst. Precise control of the catalyst conformation may be possible in case of polymer catalyst. Because of three-dimensional network structure of the chiral HBPs, these are structurally robust and easily recovered from the reaction mixture and reused several times without any decrease in catalytic activity and stereoselectivity.

iii) Chiral polymers containing squaramide moieties **P1**−**P4** were successfully synthesized from monosquaramides via the Yamamoto coupling reaction. Copolymers **P1a**, **P2a**, **P2b** were synthesized from monosquaramides **29** and **31** with achiral diiodo or dibromo aromatic compounds **32**−**34**. These polymers were applied to the asymmetric Michael addition reactions and afforded good to excellent enantioselectivities. Interestingly, polymeric catalyst **P2a** (1:1) showed a high catalytic activity in the asymmetric reaction of anthrone and *trans*-β-nitrostyrene. The reaction was completed within three hours in CH_2Cl_2 at 25 °C in the presence of only 2.5 mol% catalyst **P2a** (1:1); a suitable catalyst conformation may be formed in the case of **P2a** (1:1). Polymeric catalyst **P2a** (1:1) showed good performance in the asymmetric reactions for various combinations of the Michael donor and acceptor substrates. For methyl 2-oxocyclopentanecarboxylate **3** and *trans*-β-nitrostyrene **4**, almost perfect diastereoselectivity with 98% ee was obtained with **P2a** (1:1). The polymeric catalyst was easily separated by precipitation into diethyl ether and recovered from the reaction mixture, allowing its reuse for the reaction. The recyclability of **P2a** (1:1) was determined in the asymmetric reaction of anthrone to *trans*-β-nitrostyrene for four cycles.

5.7 Reference

1. Garfield, S. Mauve, Faber and Faber, London, **2000** pp 224.
2. Boratyński, P. J. *Mol. Diversity* **2015**, *19*, 385–422.
3. Jianga, L.; Chen, Y. -C. *Catal. Sci. Technol.* **2011**, *1*, 354–365.
4. Yeboah, E. M. O.; Yeboah, S. O.; Sing, G. S. *Tetrahedron* **2011**, *67*, 1725–1762.
5. Mercelli, T. *WIREs Comput. Mol. Sci.* **2011**, *1*, 142–152.
6. Song, C. E. (Eds.), Cinchona Alkaloids in Synthesis & Catalysis, Wiley-VCH, Weinheim, **2009**.
7. (a) Dalko, P.I.; Moisan, L. *Angew. Chem. Int. Ed.* **2004**, *43*, 5138–5175.
(b) Mercelli, T. van Maarseveen J. H.; Hiemstra, H. *Angew. Chem. Int. Ed.* **2006**, *45*, 7496–7504.
(c) Dalko, P. I. (Eds.), Comprehensive Enantioselective Organocatalysis, 1, Wiley-VCH, Weinheim, **2013**.
8. Yoon, T. P.; Jacobsen, E. N. *Science* **2003**, *299*, 1691–1693.
9. Rabe, P.; Ackerman, E.; Schneider, W. *Chem. Ber*. **1907**, *40*, 3655–3658.
10. Ye, J.; Dixon, D. J.; Hynes, P. S. *Chem. Commun.* **2005**, *324*, 4481–4483.
11. Ingemann, S.; Hiemstra, H. *Comprehensive Enantioselective Organocatalysis: Catalysts, Reactions, and Applications* **2013**, 117–160.
12. Lee, J.-W.; Ryu, T.-H.; Oh, J.-S.; Bae, H.-Y.; Jang, H.-B.; Song, C. E. *Chem. Commun*. **2009**, *46*, 7224–7226.
13. Yang, W.; Du, D.-M. *Org. Lett*. **2010**, *12*, 5450–5453.
14. Yang, W.; Du, D.-M. *Adv. Synth. Catal*. **2011**, *253*, 1241–1246.
15. Yang, W.; Jia, Y.; Du, D.-M. *Org. Biomol. Chem*. **2012**, *10*, 332–338.
16. Yang, W.; Du, D.-M. *Chem. Commun*. **2013**, *49*, 8842–8844.

17. Yang, W.; Yang, Y.; Du, D.-M. *Org. Lett*. **2013**, *15*, 1190–1193.
18. Rao, K.S.; Ramesh, P.; Chowhan, L.-R.; Trivedi, R. *RSC Adv*. **2016**, *6*, 84242–84247.
19. He, H.-X.; Du, D.-M. *RSC Adv*. **2013**, *3*, 16349–16358.
20. He, H.-X.; Du, D.-M. *Tetrahedron: Asymmetry* **2014**, *25*, 637–643.
21. Malerich, J. P.; Hagihara, K.; Rawal, V. H. *J. Am. Chem. Soc*. **2008**, *130*, 14416–14417.
22. Zhu, Y.; Malerich, J. P.; Rawal, V. H. *Angew. Chem. Int. Ed*. **2010**, *49*, 153–156.
23. Zhao, B.-L.; Du, D.-M. *Eur. J. Org. Chem*. **2015**, *24*, 5350–5359.
24. Konishi, H.; Lam, T. Y.; Malerich, J. P.; Rawal, V. H. *Org. Lett*. **2010**, *12*, 2028–2031.
25. Gao, C.; Yan, D. *Progr. Polymer Sci.* **2004**, *29*, 183–275.
26. Yates, C. R.; Haye, S.W. *Eur. Polymer J.* **2004**, *40*, 1257–1281.
27. Yamanaka, K., Jikei, M.; Kakimoto, M. *Macromolecules* **2000**, *33*, 6937–6944.

Appendix A

List of Publications:

A1. Journal papers:

J.1. Sadia Afrin Chhanda and Shinichi Itsuno "Design and synthesis of chiral hyperbranched polymers containing cinchona squaramide moieties and their catalytic activity in the asymmetric Michael addition reaction," *Journal of Catalysis*, **2019**, 377, 543-549 (7 pages).

J.2 Sadia Afrin Chhanda and Shinichi Itsuno "Design and synthesis of cinchona-based chiral hyperbranched polymers and their application in asymmetric reactions," *Tetrahedron*, **2020**, 76 (24), 131247 (8 pages).

J.3. Sadia Afrin Chhanda and Shinichi Itsuno "Synthesis of Cinchona Squaramide Polymers by Yamamoto Coupling Polymerization and their Application in Asymmetric Michael Reaction," *Reactive and Functional Polymers*, **2021**, 164, 104913 (10 pages).

A2. Conference presentations:

C.1. **Sadia Afrin Chhanda**, Naoki Haraguchi and Shinichi Itsuno "Design and synthesis of chiral polymeric organocatalyst having controlled nanospace for asymmetric catalysis." 49th Annual meeting of Union of Chemistry-Related Societies in Chubu Area, Nagoya, Japan, November-**2018.**

C.2. **Sadia Afrin Chhanda**, Naoki Haraguchi and Shinichi Itsuno, "Design and synthesis of cinchona based chiral hyperbranched polymeric organocatalyst for asymmetric catalysis." 68th Symposium on Macromolecules, Fukui, Japan, September 26, **2019**

C.3. **Sadia Afrin Chhanda** "Design and synthesis of cinchona squaramide polymeric organocatal yst and its application to asymmetric synthesis," 3rd G′L′owing Polymer Symposium in KANTO (on-line International Symposium), November 28, **2020**.

Appendix B

Supporting Information for Chapter 2

B.1 ^{1}H and ^{13}C NMR data for monomers and polymers

^{1}H NMR of 3a in DMSO-*d*$_6$

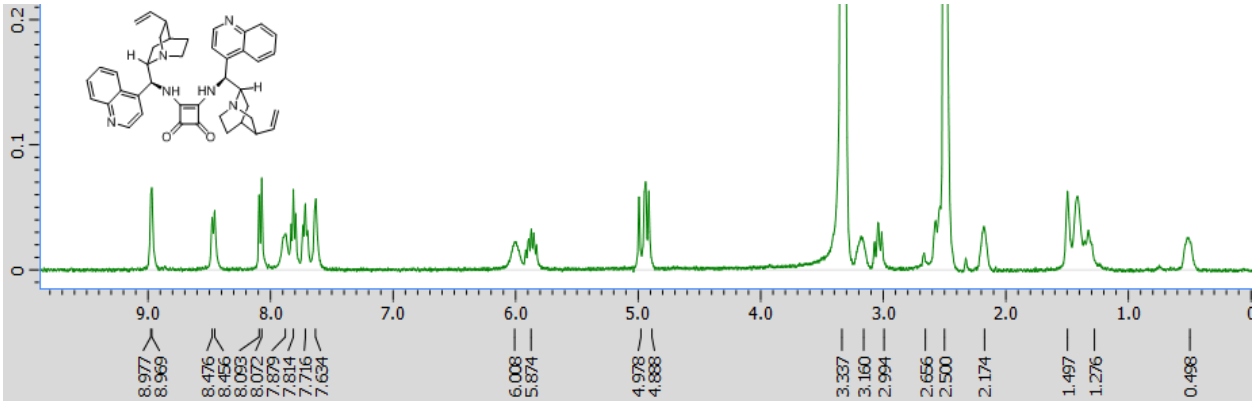

^{13}C NMR of 3a in DMSO-*d*$_6$

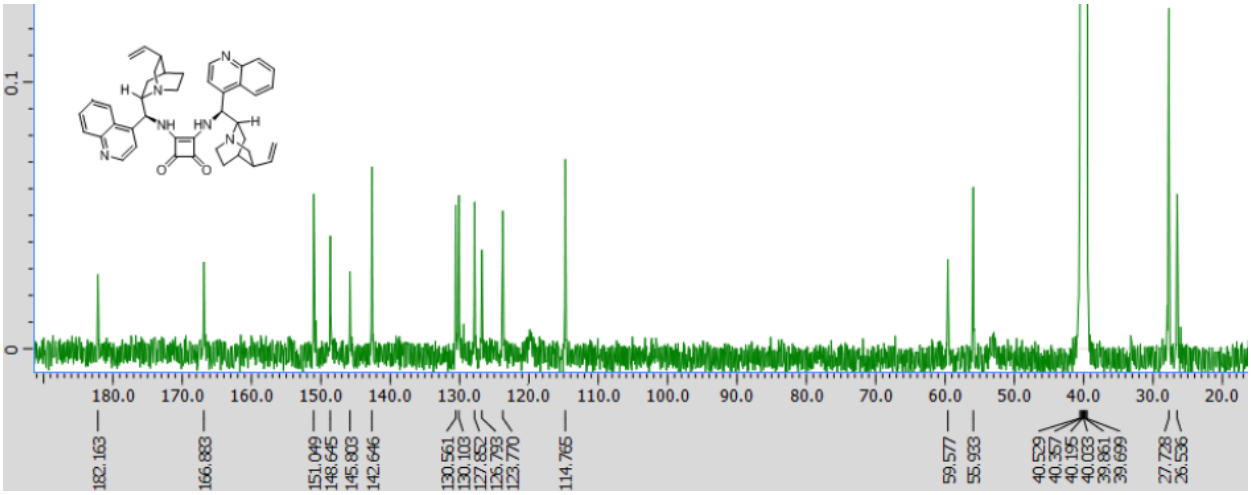

^{1}H NMR of 3c in DMSO-*d*$_6$

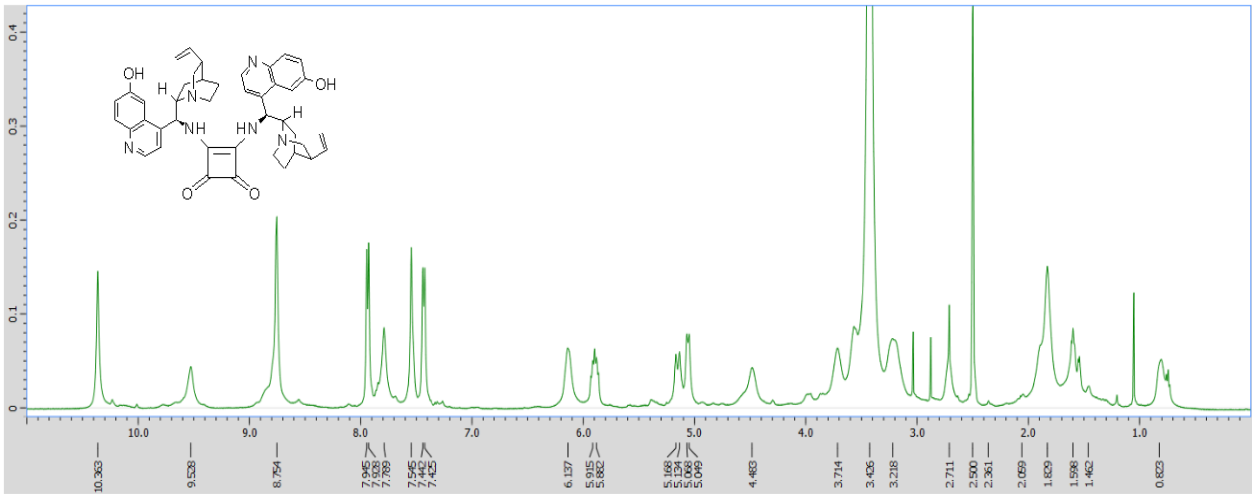

^{13}C NMR of 3c in DMSO-d_6

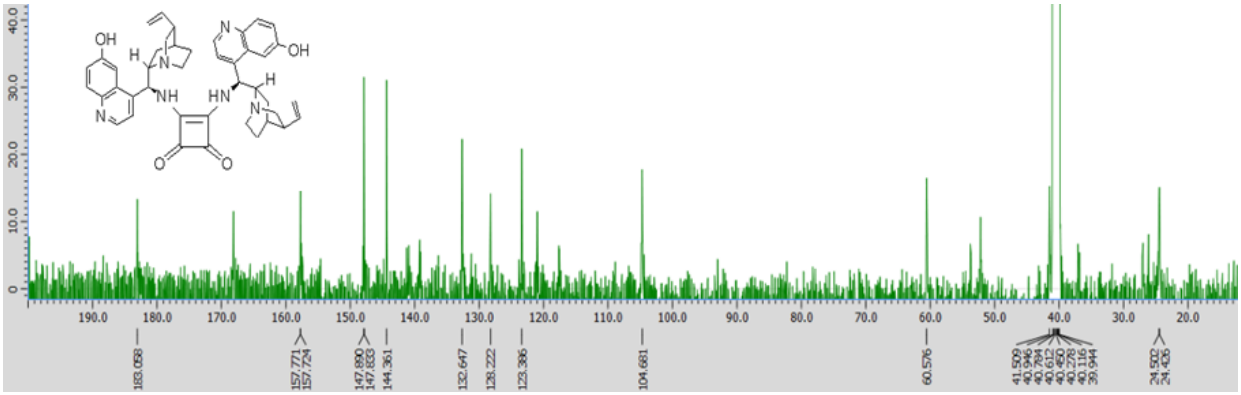

^{1}H NMR of 6a in $CDCl_3$

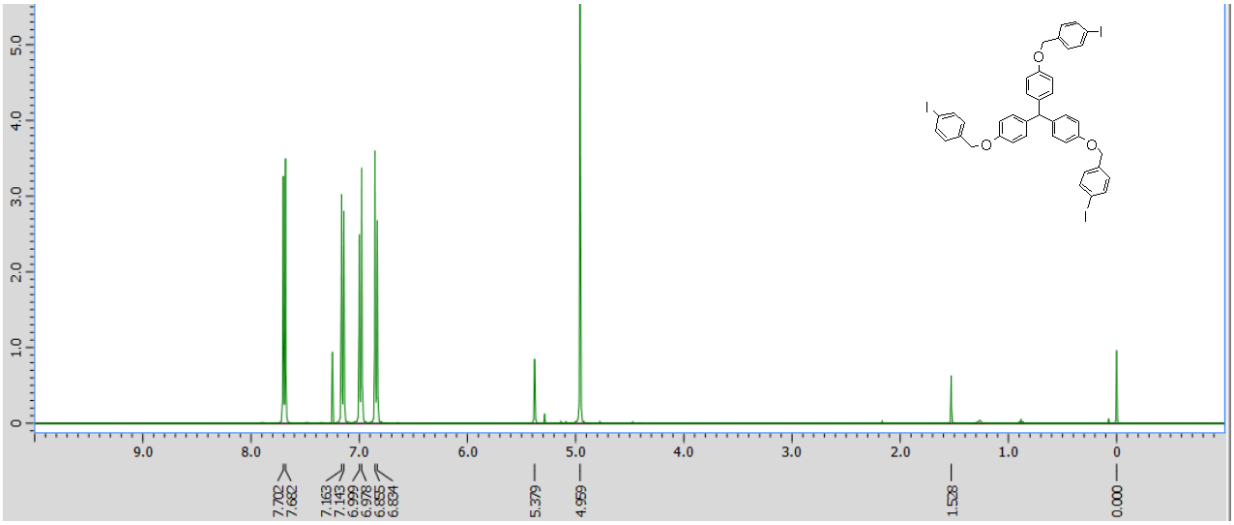

^{13}C NMR of 6a in $CDCl_3$

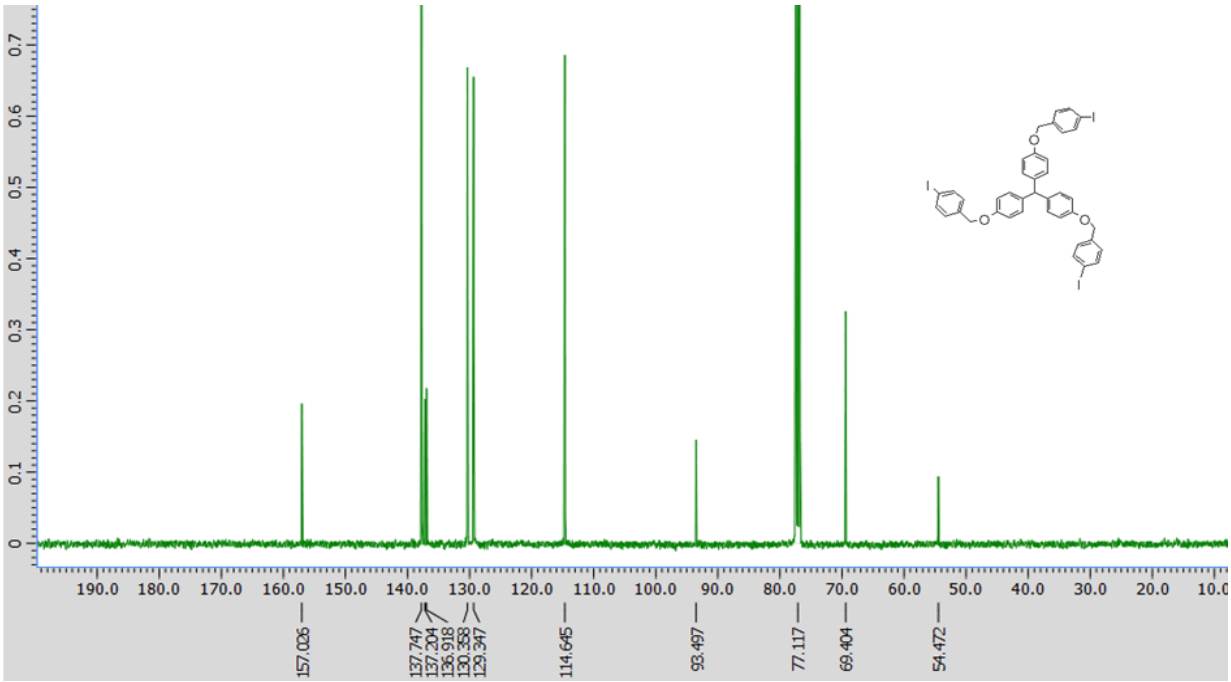

^{1}H NMR of polymer PLa in DMSO-d_6

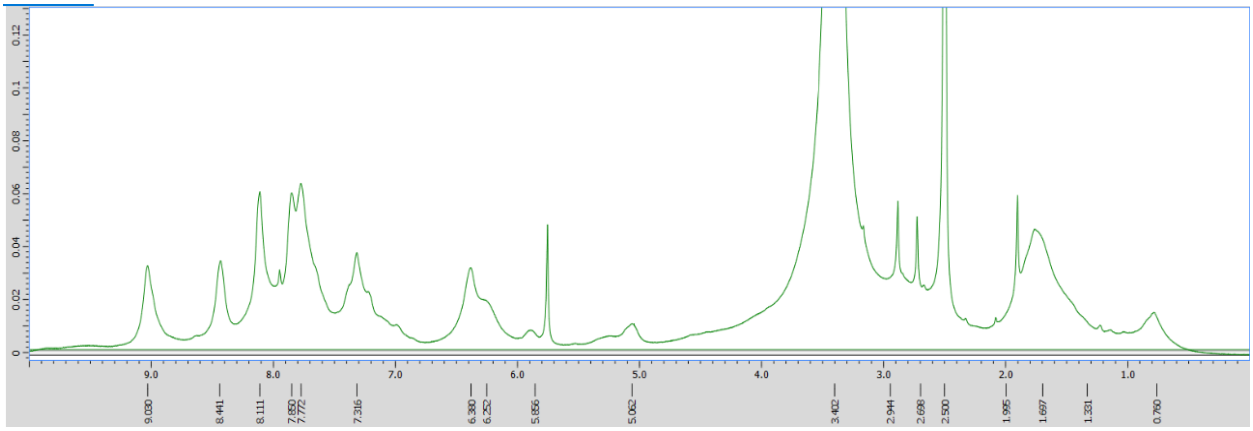

^{1}H NMR of polymer P1aa in DMSO-d_6

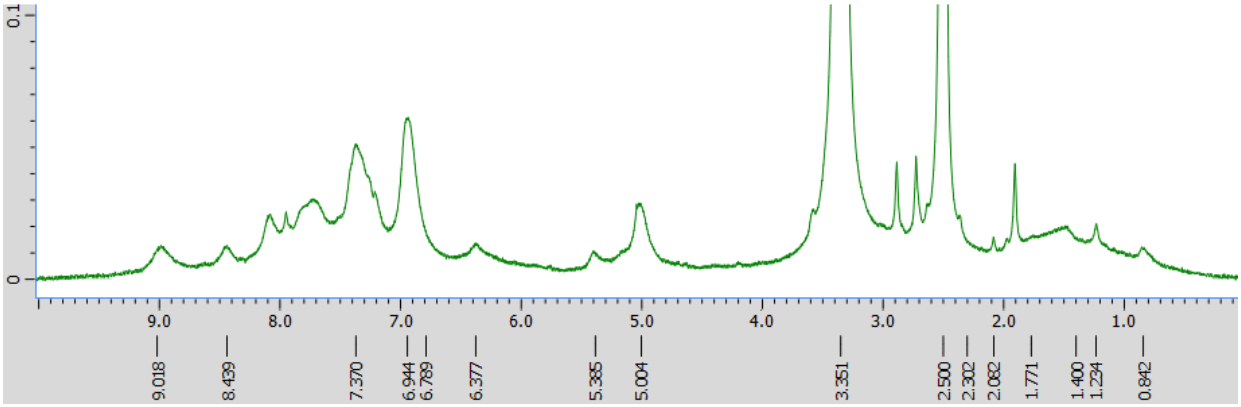

^{1}H NMR of polymer P1ba in DMSO-d_6

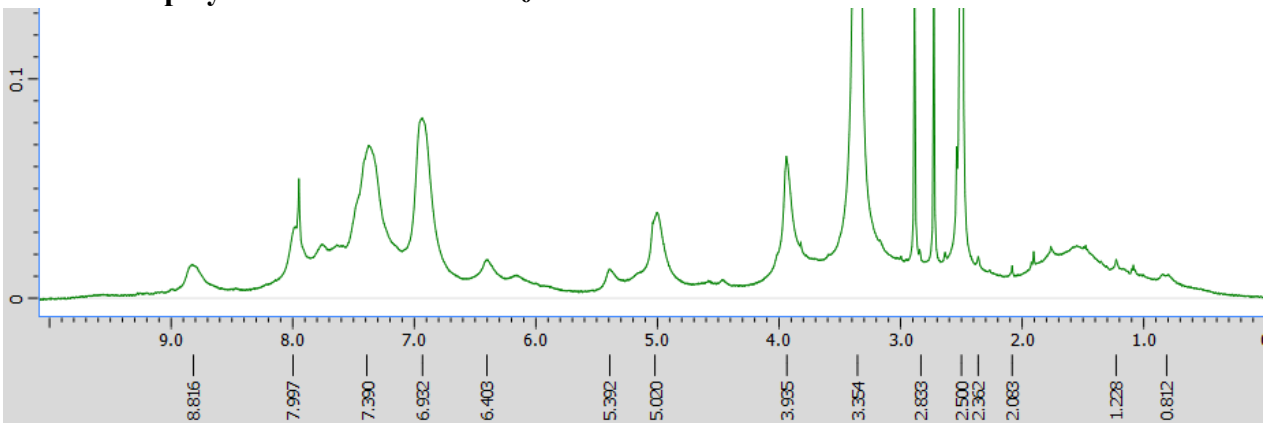

^{1}H NMR of polymer P1ca in DMSO-d_6

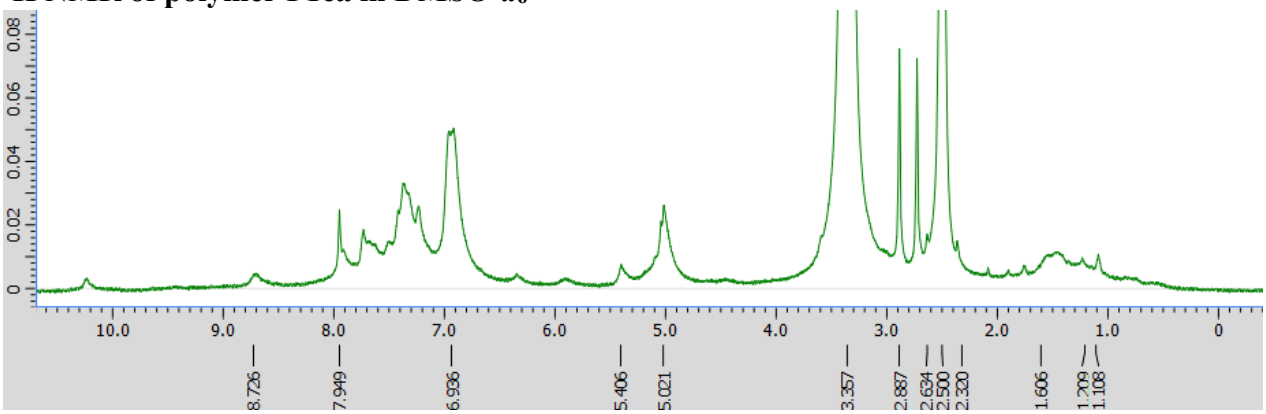

^{1}H NMR of polymer P2ab in DMSO-d_6

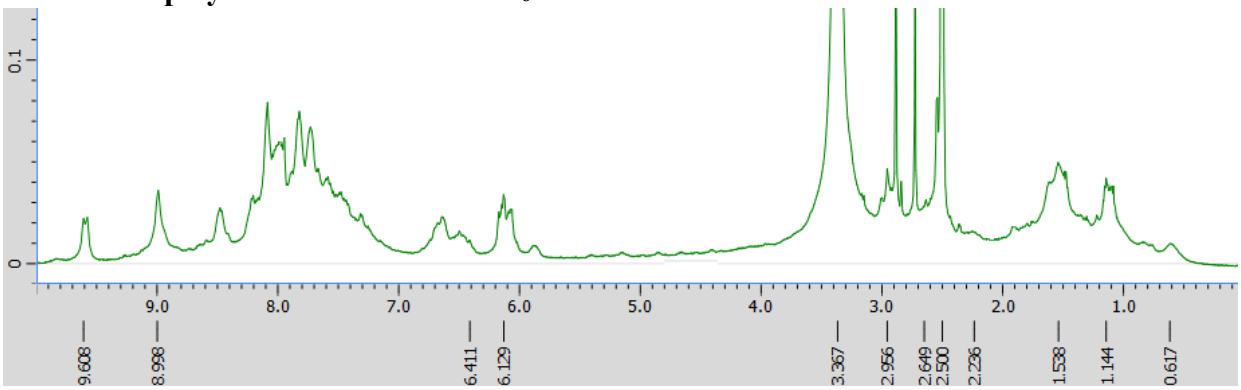

^{1}H NMR of polymer P3ac in DMSO-d_6

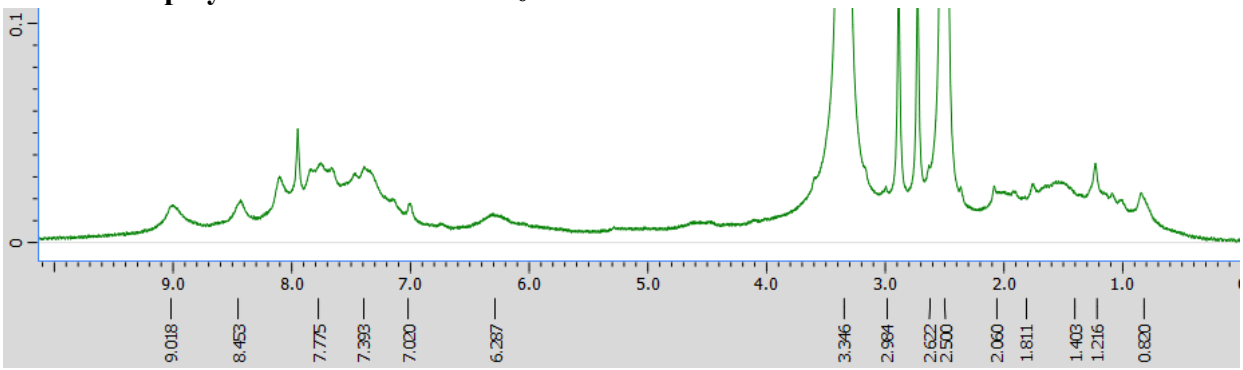

B.2 FT-IR Spectrum for monomers and polymers

1. **IR spectrum of 3c**

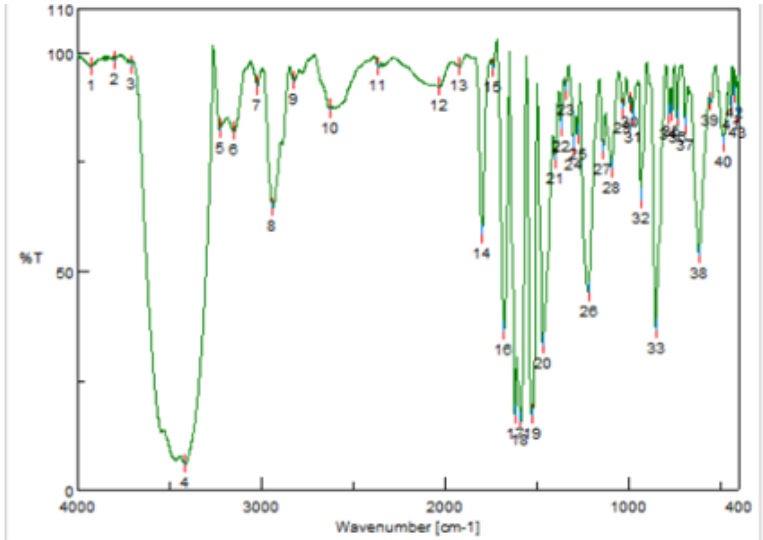

[ピーク検出結果]

No.	位置	強度	No.	位置	強度
1	3931.18	95.7184	2	3801.01	98.1197
3	3710.37	97.046	4	3417.24	6.05822
5	3230.18	82.4768	6	3151.11	82.0589
7	3024.8	92.3813	8	2938.98	64.6555
9	2824.24	93.5183	10	2626.57	87.0963
11	2366.23	96.6958	12	2002.6	92.1277
13	1921.72	96.6553	14	1798.3	58.6129
15	1737.55	96.3903	16	1681.62	36.4295
17	1618.95	17.3025	18	1587.13	15.7763
19	1526.38	17.2838	20	1467.56	33.2954
21	1399.1	75.6305	22	1365.35	82.8809
23	1340.28	91.3109	24	1299.79	78.7082
25	1277.61	81.1842	26	1219.76	45.2949
27	1139.72	77.5906	28	1093.44	73.5974
29	1031.73	87.1853	30	992.196	88.5543
31	974.84	85.0014	32	933.378	66.412
33	851.418	36.7914	34	779.101	85.708
35	762.709	85.2269	36	735.71	84.8976
37	691.355	83.2748	38	617.109	53.7285
39	553.47	88.681	40	480.188	79.2752
41	443.547	87.783	42	426.191	90.3964

2. IR spectrum of P1aa

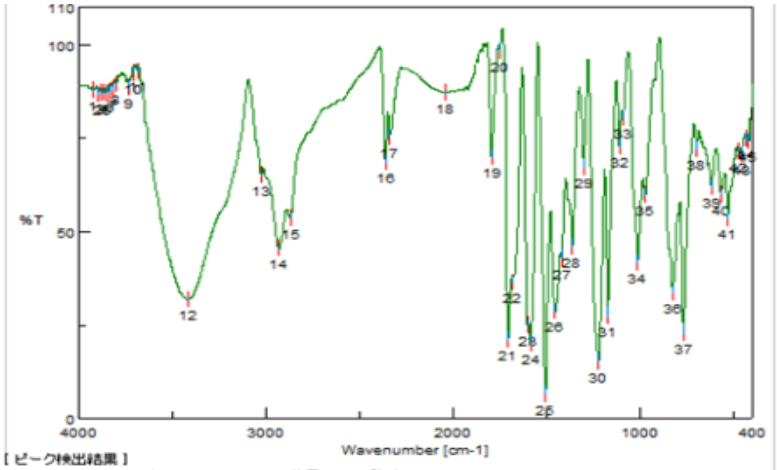

[ピーク検出結果]

No.	位置	強度	No.	位置	強度
1	3931.18	87.7962	2	3901.29	86.6367
3	3882.97	87.2028	4	3869.47	87.1425
5	3852.11	86.7373	6	3837.65	87.5473
7	3819.33	88.1296	8	3800.04	89.4174
9	3734.48	88.4227	10	3710.37	92.3944
11	3688.19	92.882	12	3420.14	31.8001
13	3026.73	65.0882	14	2930.31	45.5737
15	2870.52	53.5852	16	2360.44	68.426
17	2341.16	75.2705	18	2041.28	87.058
19	1793.47	69.87	20	1749.12	98.2578
21	1704.76	21.1759	22	1682.59	36.3115
23	1602.56	24.9125	24	1586.16	20.2148
25	1506.13	6.57128	26	1454.06	28.7419
27	1419.35	42.8143	28	1361.5	45.9822
29	1299.79	67.0713	30	1221.68	15.3206
31	1173.47	27.3915	32	1110.8	72.6729
33	1080.55	80.2528	34	1013.41	41.5734
35	970.983	59.78	36	824.42	33.5647
37	766.566	22.841	38	697.141	72.0669
39	617.109	61.7362	40	566.969	59.9901
41	530.328	53.5012	42	470.546	71.4047
43	459.939	70.5465	44	434.869	74.8757
45	419.442	74.0038			

3. IR spectrum of P1ba

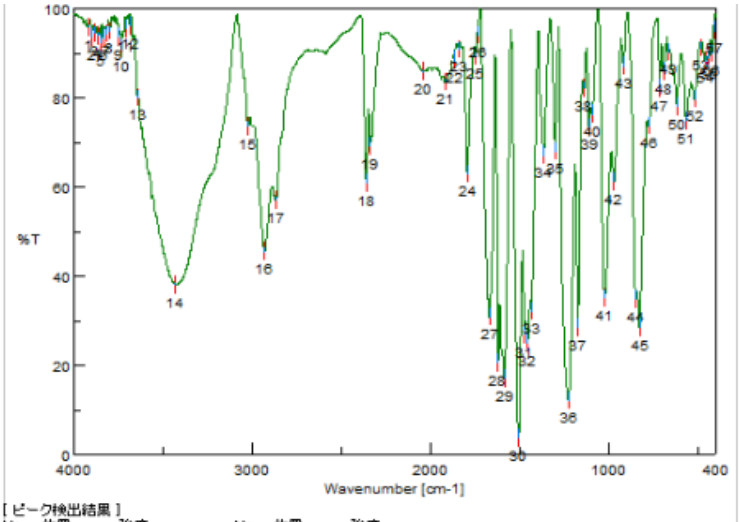

[ピーク検出結果]

No.	位置	強度	No.	位置	強度
1	3916.72	95.7134	2	3901.29	93.506
3	3882	94.4538	4	3870.43	93.8003
5	3852.11	92.2597	6	3838.51	93.3863
7	3819.33	94.2455	8	3800.04	94.8394
9	3748.94	93.531	10	3734.48	90.9367
11	3710.37	95.4335	12	3688.19	96.0754
13	3647.7	80.0006	14	3432.67	38.0395
15	3024.8	73.5634	16	2932.23	45.517
17	2868.59	57.0086	18	2360.44	60.7964
19	2341.16	69.0587	20	2041.28	85.7474
21	1918.82	83.441	22	1868.68	88.3994
23	1844.58	90.7828	24	1792.51	62.8501
25	1748.16	89.2052	26	1732.73	93.9307
27	1670.05	30.7863	28	1619.91	20.5432
29	1585.2	17.0625	30	1506.13	3.70425
31	1473.35	26.9146	32	1455.99	24.9865
33	1433.82	32.0211	34	1363.43	67.1041
35	1299.79	67.9773	36	1226.5	12.1763
37	1173.47	28.489	38	1137.8	82.0488
39	1109.83	73.3572	40	1083.44	76.2842
41	1024.98	35.1708	42	970.019	61.1517
43	916.022	87.0411	44	848.525	34.8736
45	826.348	28.45	46	777.172	73.5079
47	715.461	82.0505	48	692.32	85.8655
49	668.214	90.1163	50	618.074	78.0026
51	566.969	74.8108	52	517.793	79.5596
53	484.045	91.0425	54	458.975	88.1589
55	435.834	89.3945	56	419.442	89.8164

4. IR spectrum of P1ca

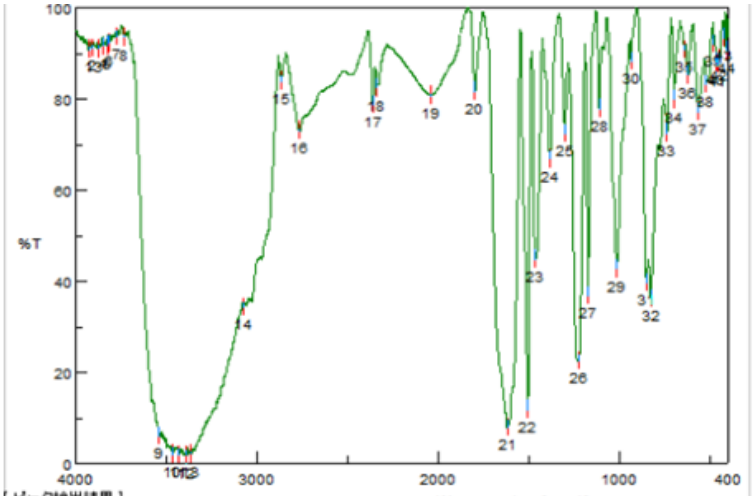

[ピーク検出結果]

No.	位置	強度	No.	位置	強度
1	3931.18	90.8848	2	3909.97	91.0922
3	3877.18	91.018	4	3850.18	91.405
5	3829.94	91.6135	6	3816.44	92.2517
7	3774.01	93.6837	8	3735.44	93.4662
9	3540.67	6.12719	10	3465.46	2.08086
11	3433.64	1.93056	12	3389.28	1.87552
13	3365.17	2.2084	14	3074.94	34.307
15	2868.59	83.8904	16	2764.46	73.1049
17	2359.48	78.6775	18	2341.16	82.3792
19	2040.32	80.7749	20	1797.33	81.5647
21	1618.95	8.02887	22	1506.13	11.3132
23	1463.71	44.8585	24	1383.68	66.8281
25	1299.79	72.3946	26	1227.47	22.5843
27	1173.47	35.7988	28	1110.8	77.8957
29	1014.37	42.7466	30	934.342	88.1614
31	850.454	39.7187	32	825.384	36.1647
33	737.639	72.4623	34	697.141	79.8609
35	636.394	90.8051	36	621.931	85.253
37	565.041	77.271	38	521.65	83.1844
39	478.26	92.0023	40	461.868	88.015
41	454.154	87.5319	42	445.476	88.8439
43	423.298	93.4143	44	408.835	90.5999

5. IR spectrum of P2ab

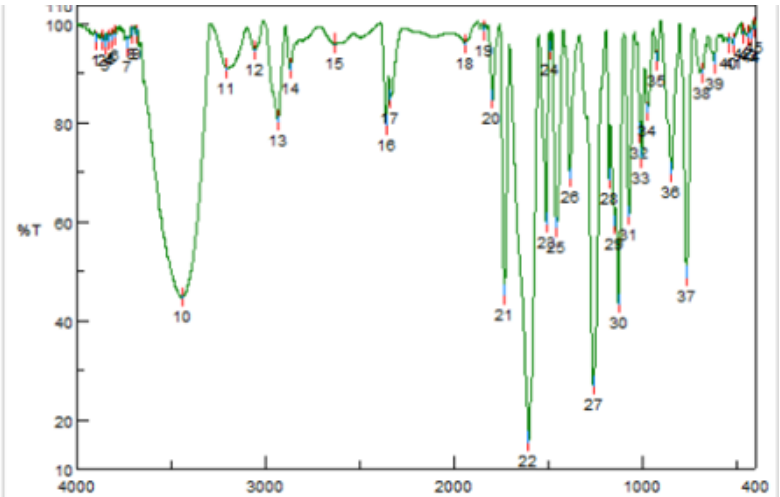

[ピーク検出結果]

No.	位置	強度	No.	位置	強度
1	3901.29	95.372	2	3870.43	96.4595
3	3852.11	95.5147	4	3838.61	96.4074
5	3819.33	96.7704	6	3800.04	97.3579
7	3734.48	95.1624	8	3710.37	97.5371
9	3688.19	97.6273	10	3446.17	44.6025
11	3207.04	90.7583	12	3059.51	94.4069
13	2934.16	80.2763	14	2870.52	90.751
15	2632.36	95.8274	16	2360.44	79.3957
17	2341.16	84.5324	18	1941.97	95.7138
19	1840.61	98.4731	20	1796.37	84.5797
21	1731.76	45.1272	22	1604.48	15.5691
23	1509.99	59.6844	24	1487.81	94.4044
25	1456.96	58.7701	26	1383.68	68.6953
27	1260.25	26.842	28	1178.29	68.5454
29	1147.44	59.282	30	1127.19	43.4172
31	1071.26	61.0562	32	1014.37	77.86
33	1004.73	72.7571	34	973.876	82.0825
35	919.879	92.4282	36	846.597	69.7934
37	766.566	48.8374	38	681.713	89.8873
39	617.109	91.8158	40	541.899	95.9352
41	517.793	95.7982	42	467.653	97.7423
43	440.655	97.4291	44	422.334	96.9295
45	400.05	98.922			

6. IR spectrum of P3ac

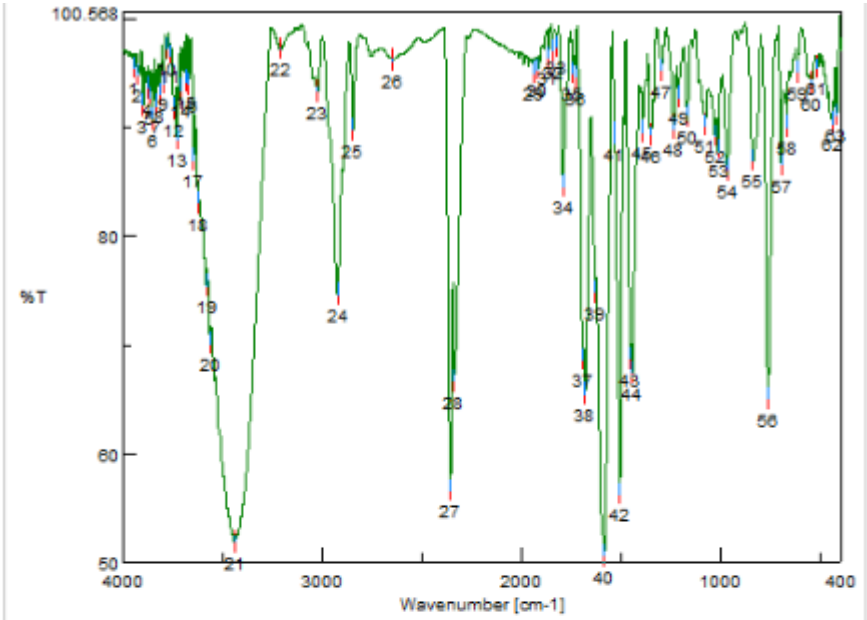

[ピーク検出結果]

No.	位置	強度	No.	位置	強度
1	3948.54	95.4063	2	3931.18	94.8024
3	3902.25	91.966	4	3882	93.6039
5	3870.43	92.6617	6	3853.08	90.7327
7	3838.61	91.928	8	3819.33	92.9677
9	3800.04	94.046	10	3778.83	97.1813
11	3768.22	96.5669	12	3749.3	91.6353
13	3734.48	88.8979	14	3710.37	93.3989
15	3689.16	94.1847	16	3674.69	93.903
17	3647.7	86.9594	18	3627.45	83.0226
19	3585.98	75.4278	20	3565.74	70.1069
21	3445.21	51.9041	22	3210.9	97.1723
23	3026.73	93.2767	24	2927.41	74.6285
25	2849.31	89.7535	26	2648.75	96.1203
27	2360.44	56.6235	28	2341.16	66.645
29	1942.93	94.9983	30	1921.72	95.2539
31	1867.72	96.3621	32	1844.58	96.9432
33	1828.19	97.3457	34	1792.51	84.5733
35	1748.16	94.9553	36	1732.73	94.5566
37	1696.09	68.6412	38	1682.59	65.5058
39	1635.34	74.8432	40	1588.09	50.6276
41	1539.88	89.441	42	1509.03	56.2726
43	1455.99	68.7143	44	1446.35	67.4302
45	1395.25	89.5374	46	1352.82	89.264
47	1299.79	95.2274	48	1240	89.8337
49	1214.93	92.7339	50	1171.54	91.0206
51	1080.91	90.1834	52	1032.69	89.1574
53	1016.3	87.8457	54	970.019	86.0817
55	840.812	86.9401	56	765.601	65.0438
57	700.034	86.521	58	669.178	90.0363
59	617.109	95.0528	60	546.72	94.076
61	517.793	95.4605	62	444.512	90.3226

B.3 HPLC analysis for asymmetric Michael adducts

1. Chromatogram data for asymmetric product 12 in Table 2.2

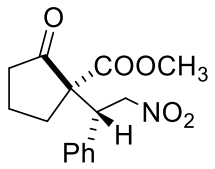

12 (2*S*, 3*R*)

Table 2.2, entry 1: 98% ee

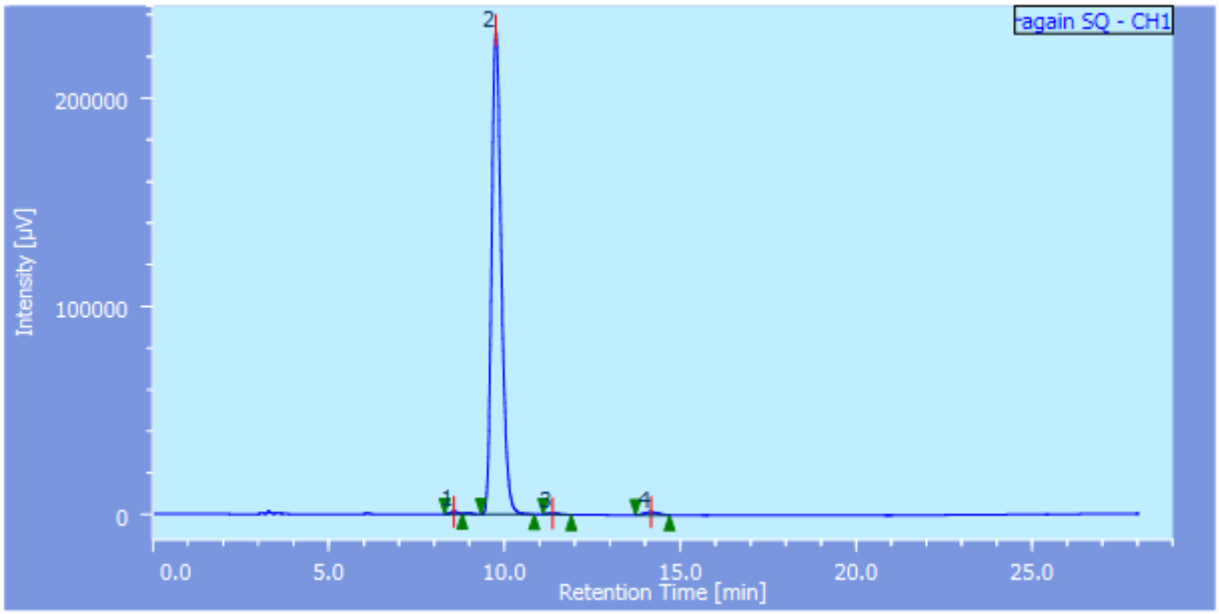

Table 2.2, entry 3: 71% ee

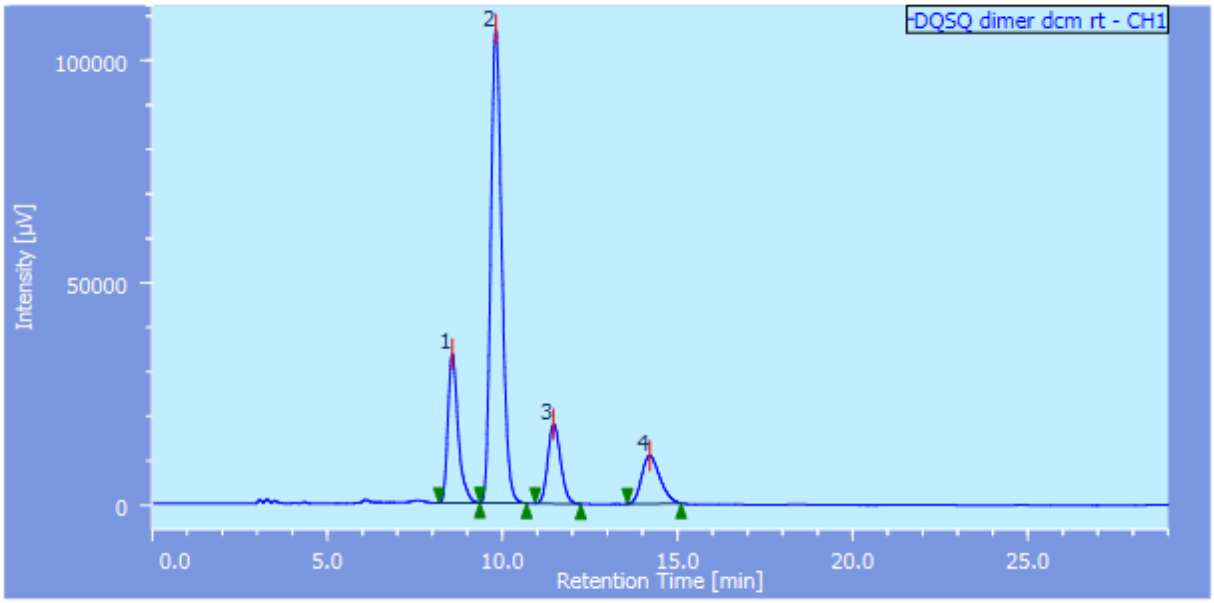

Table 2.2, entry 4: 98% ee

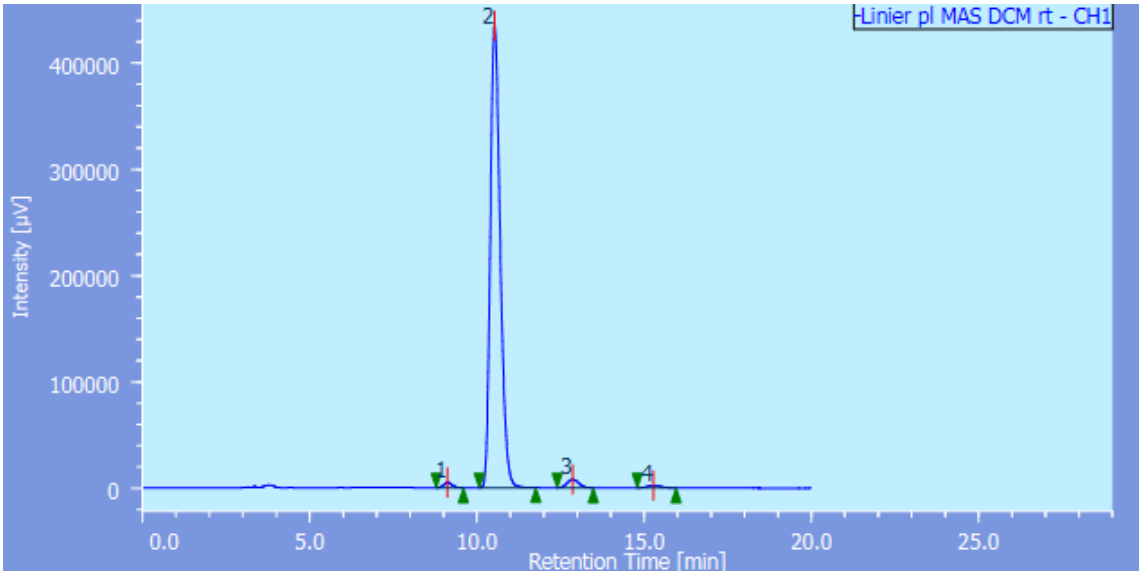

Table 2.2, entry 6: >99% ee

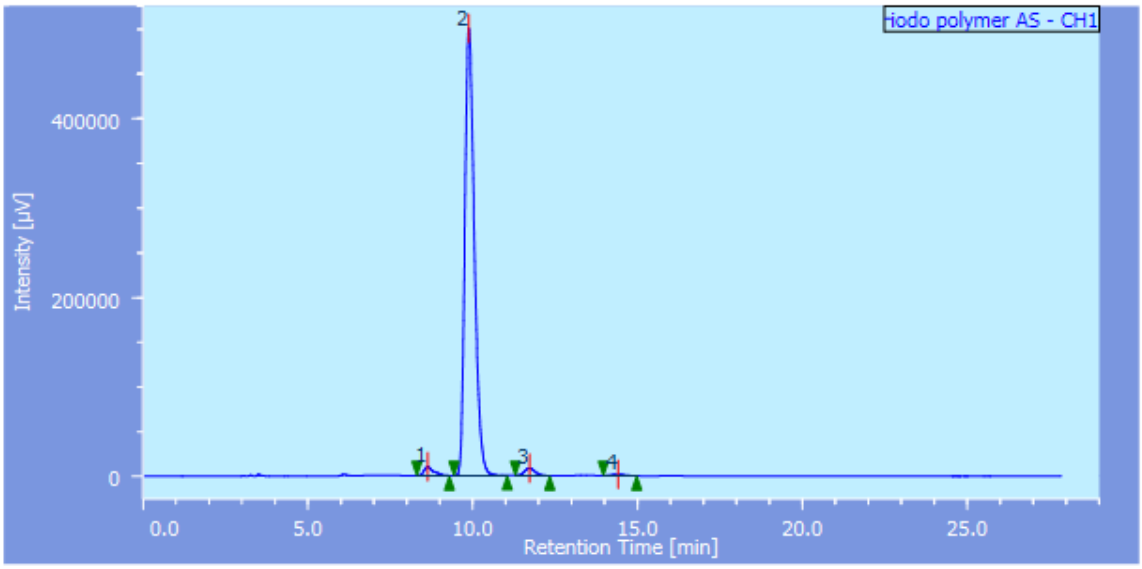

Table 2.2, entry 7: 99% ee

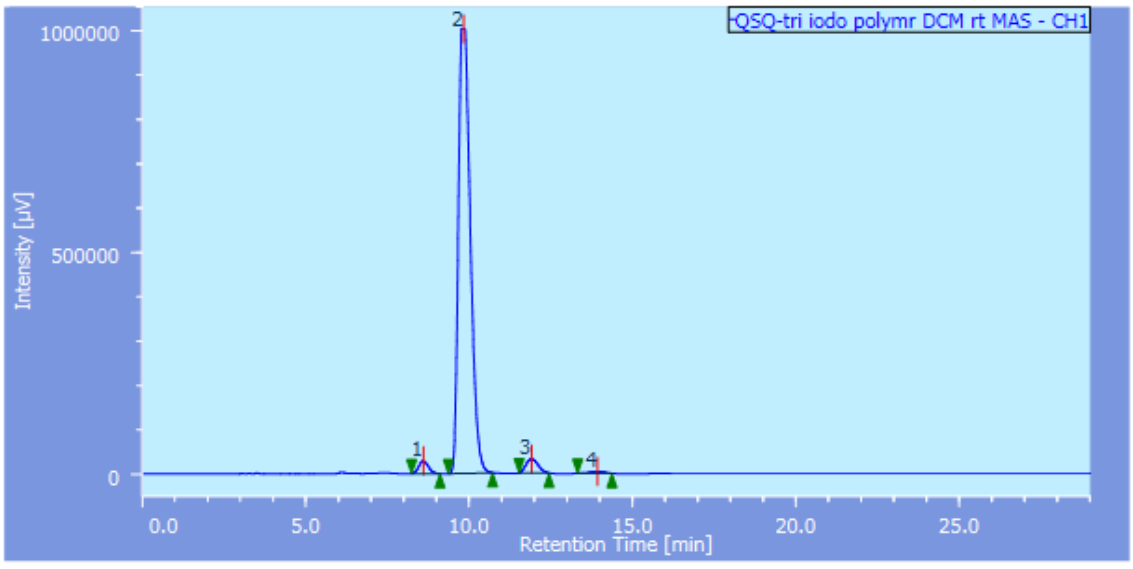

Table 2.2, entry 8: 40% ee

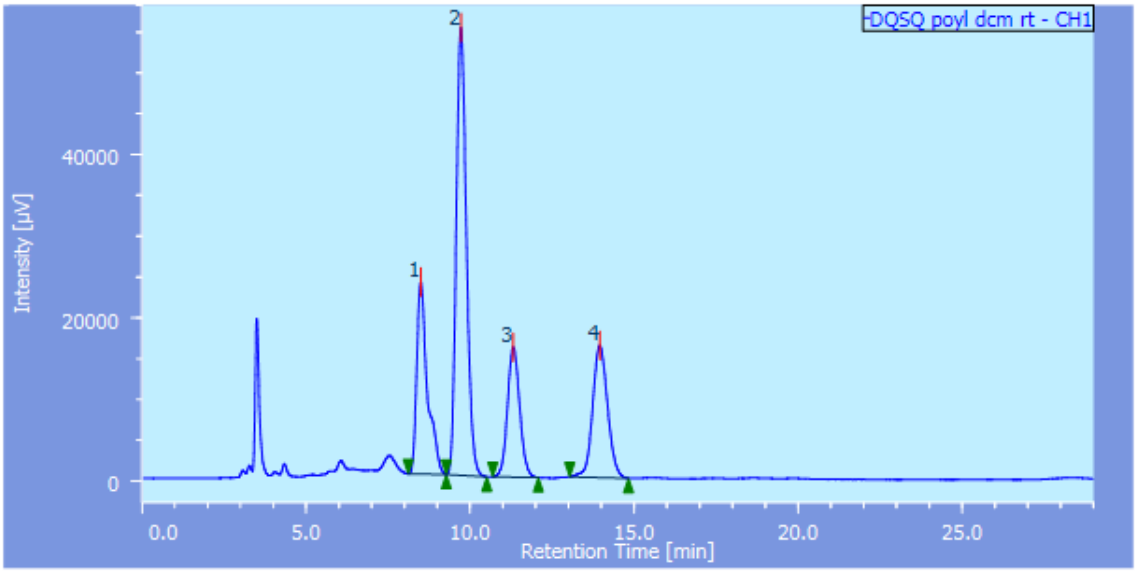

Table 2.2, entry 9: >99% ee

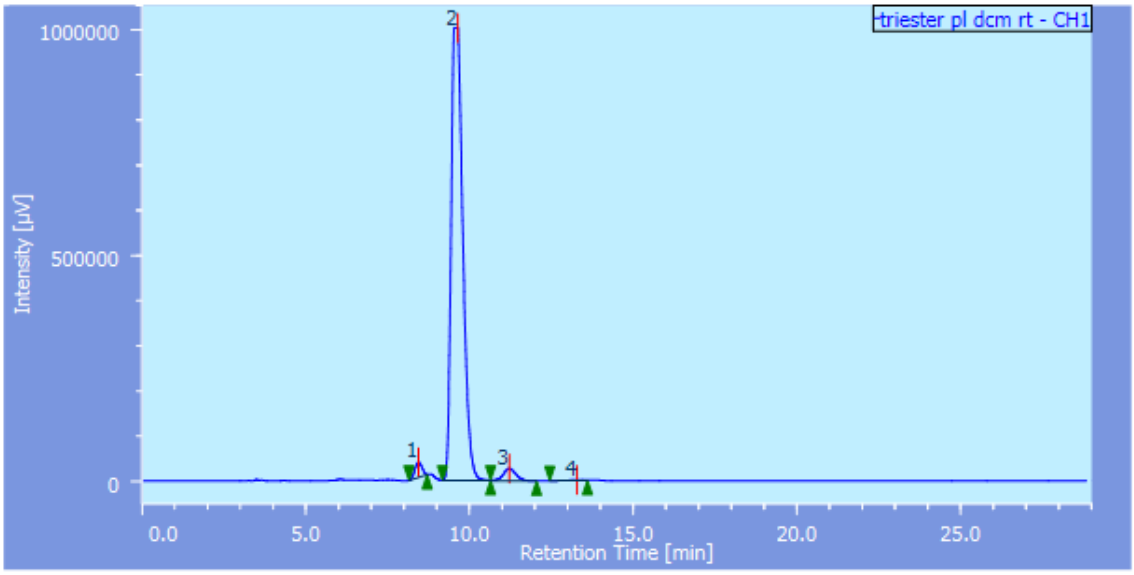

Table 2.2, entry 10: 99% ee

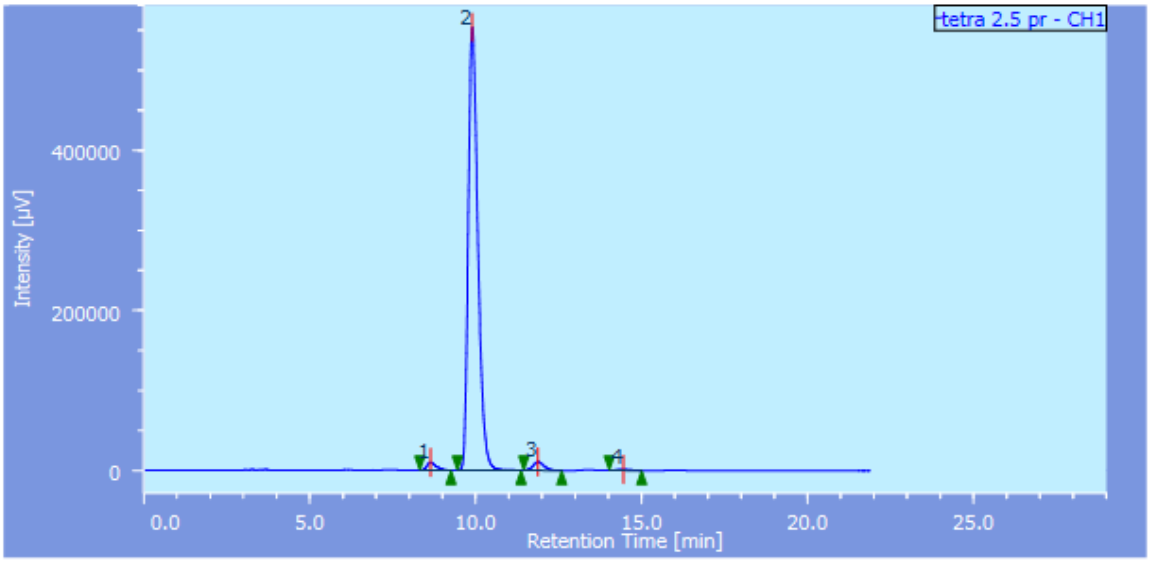

Table 2.2, entry 11: >99% ee

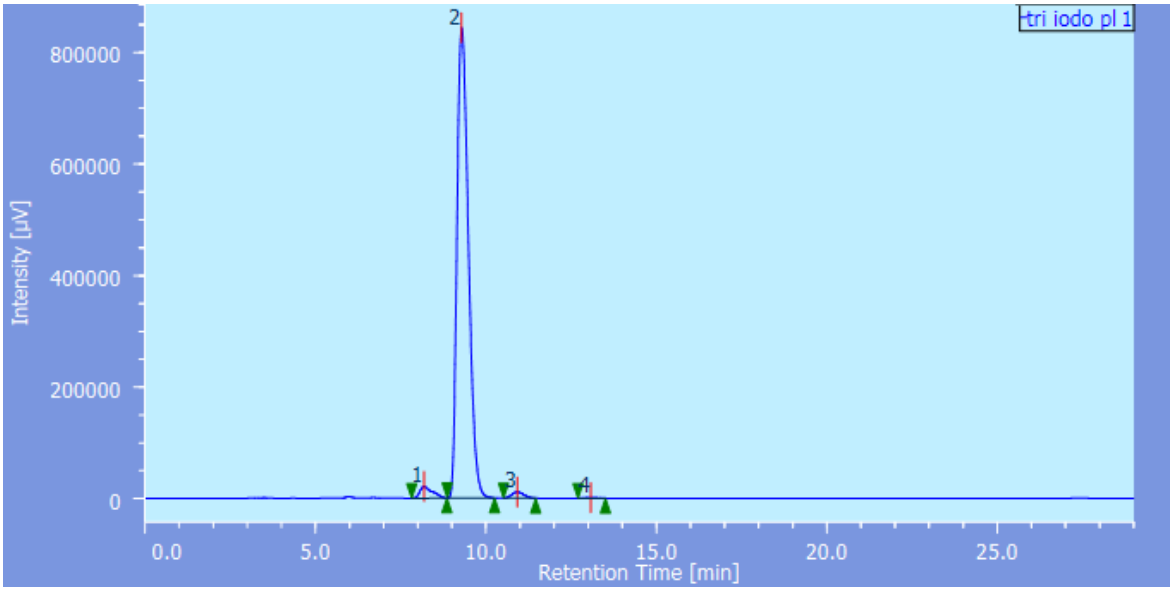

2. Chromatogram data on solvent screening for catalyst P1aa (Table 2.3)

Table 2.3, entry 1: >99% ee

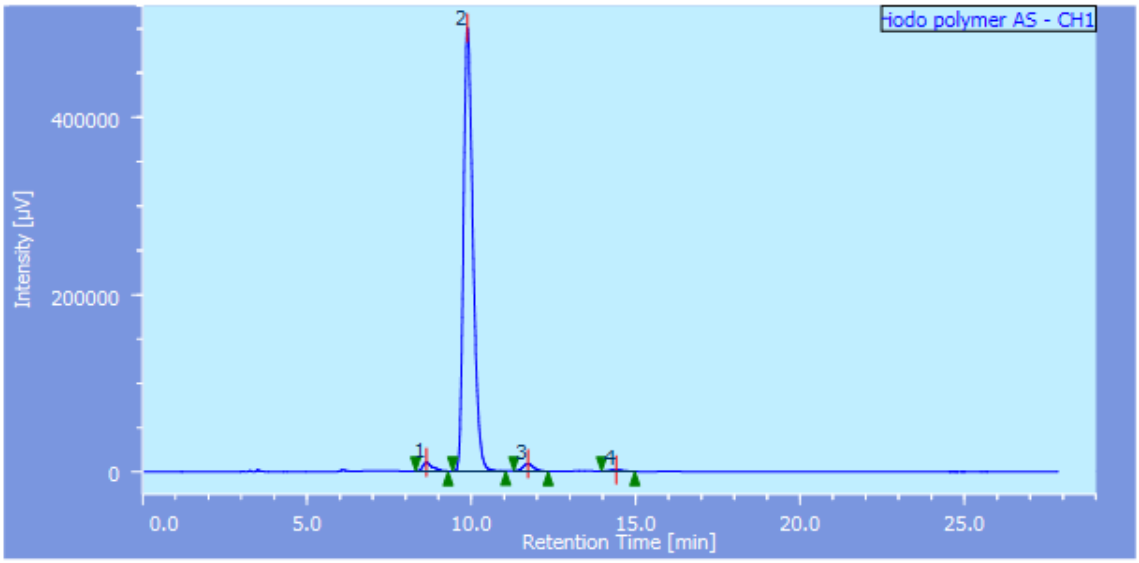

Table 2.3, entry 2: 99% ee

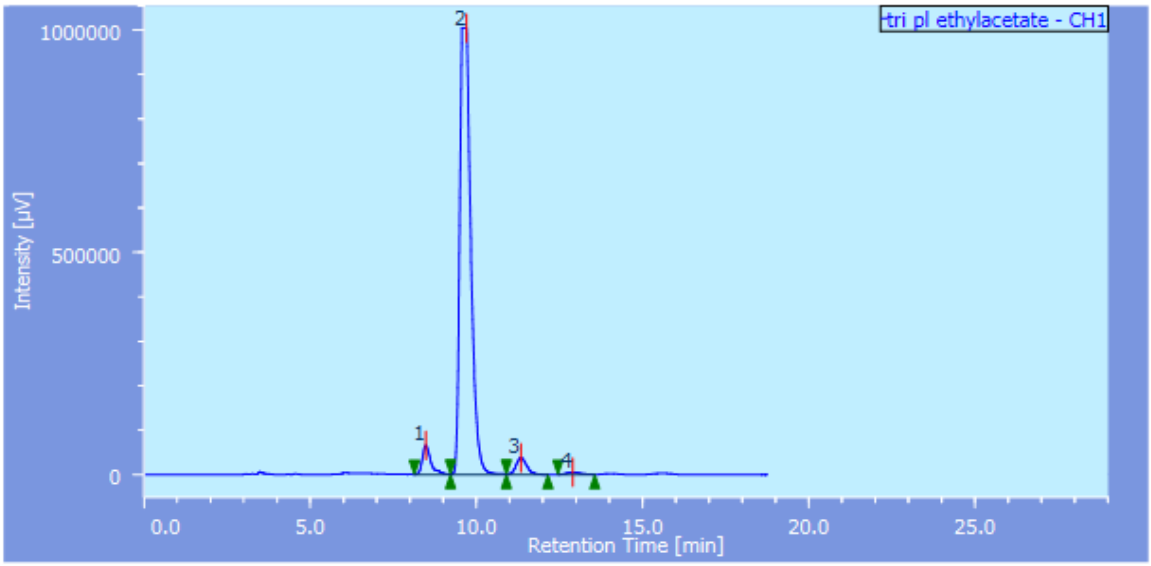

Table 2.3, entry 3: >99% ee

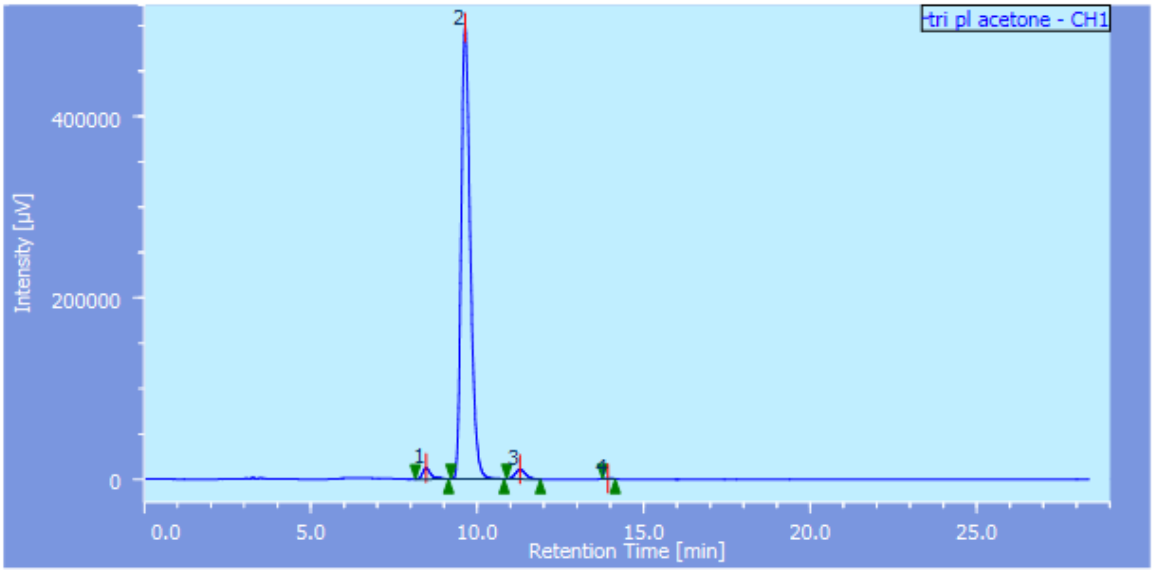

Table 2.3, entry 4: >99% ee

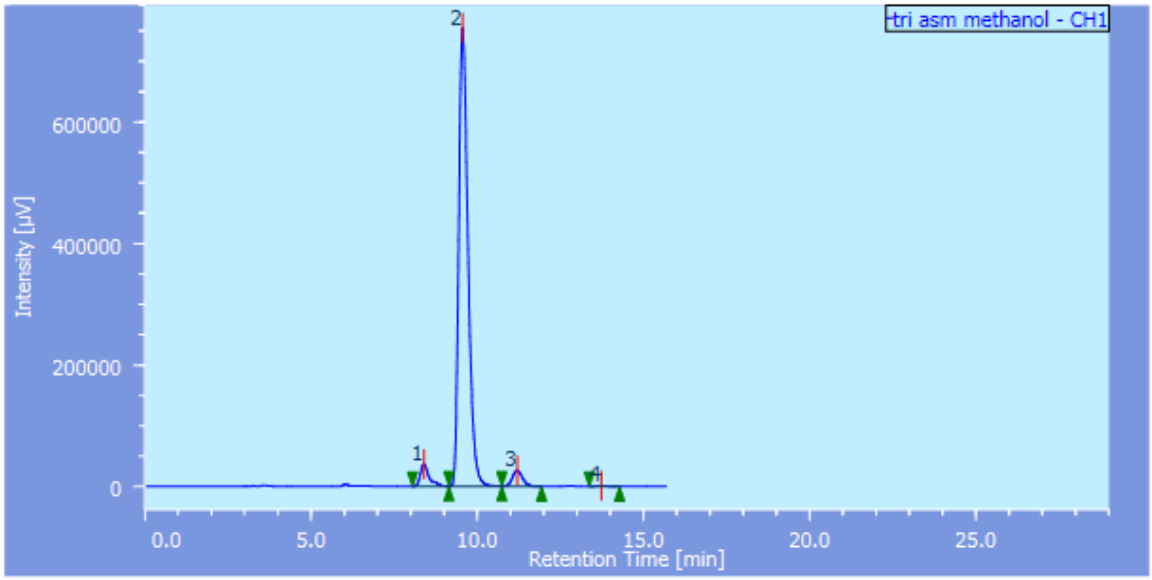

Table 2.3, entry 5: 99% ee

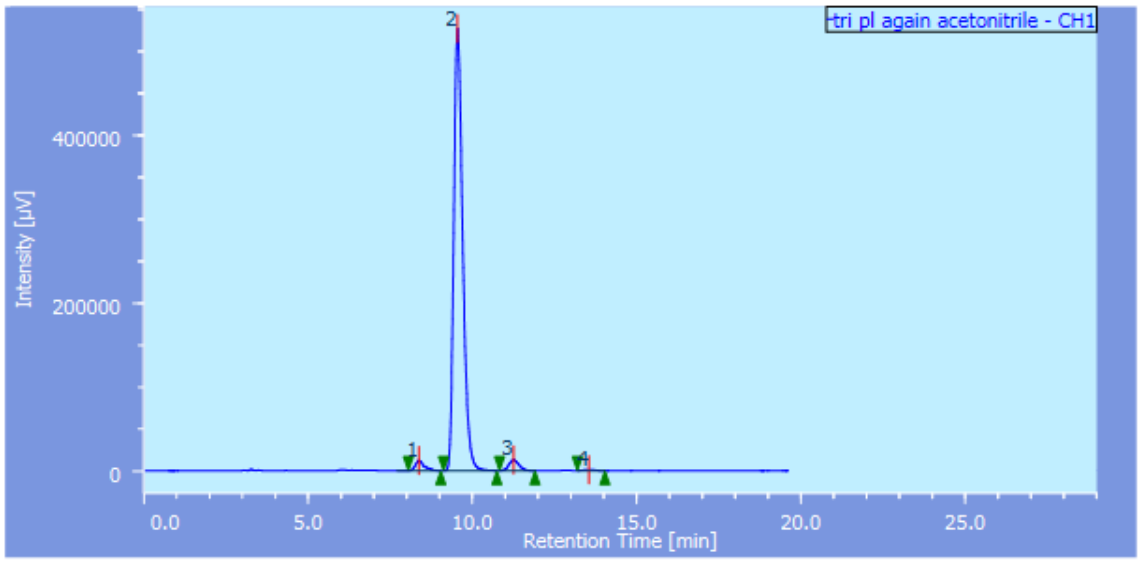

Table 2.3, entry 6: 99% ee

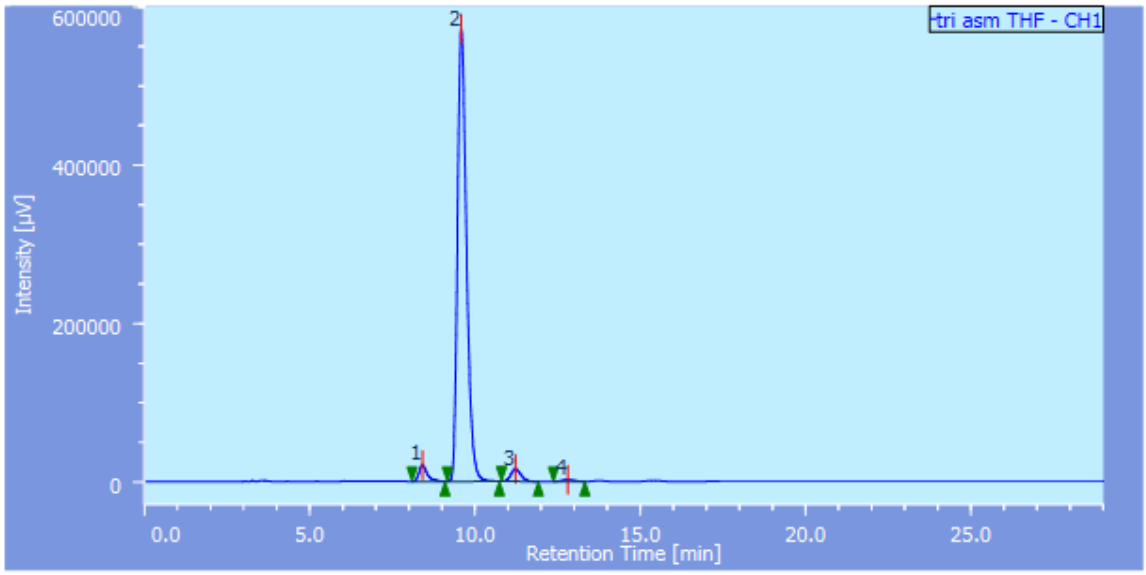

Table 2.3, entry 7: >99% ee

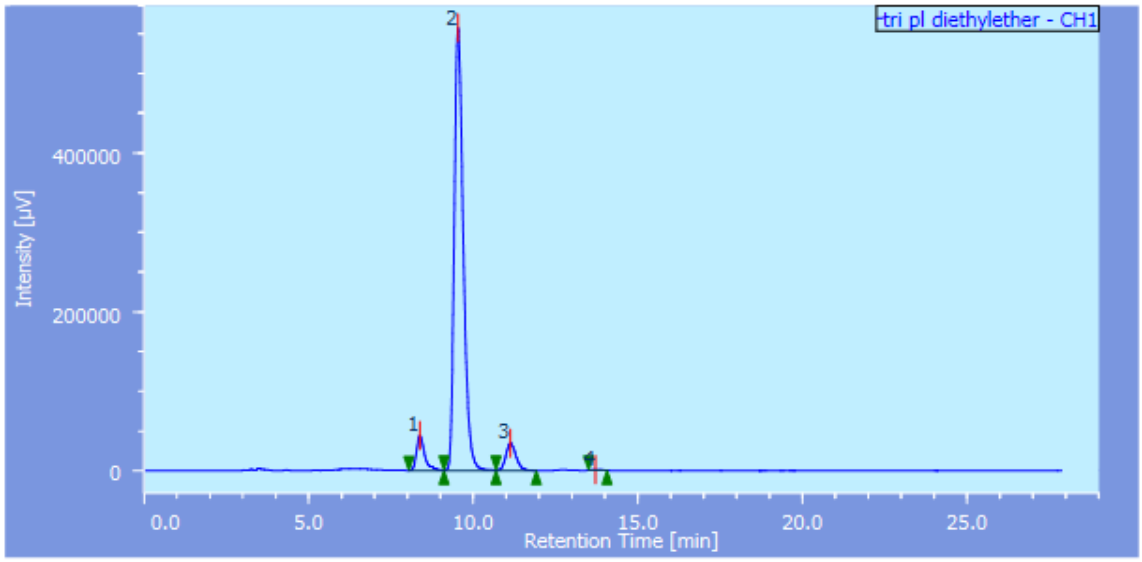

Table 2.3, entry 8: 99% ee

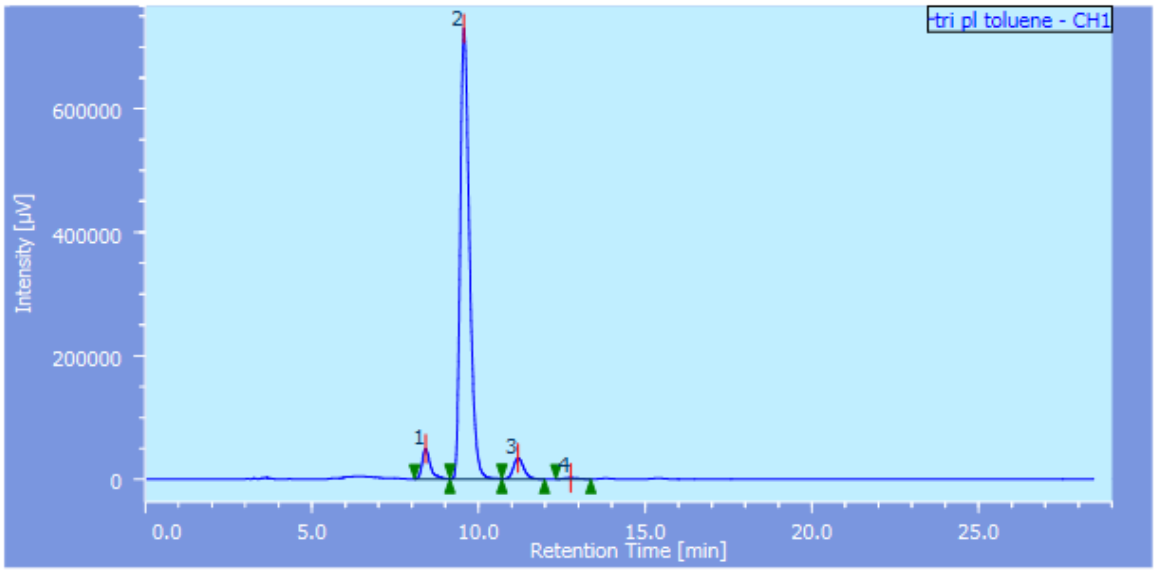

Table 2.3, entry 9: 97% ee

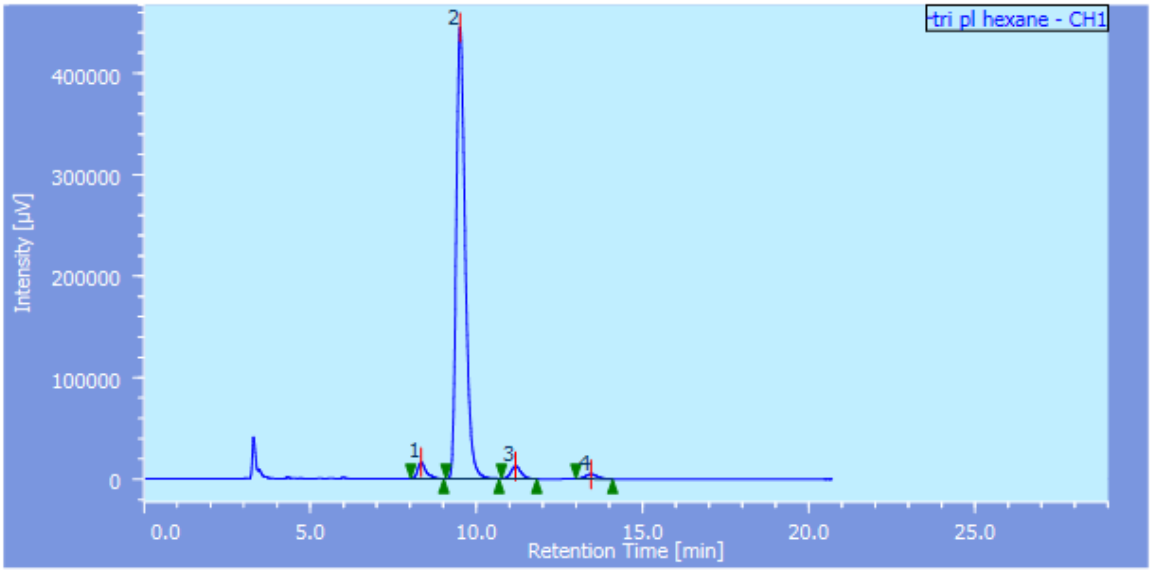

3. Chromatogram data on recyclability for catalyst P1aa (Table 2.4)

Table 2.4, Fresh polymer P1aa: >99% ee

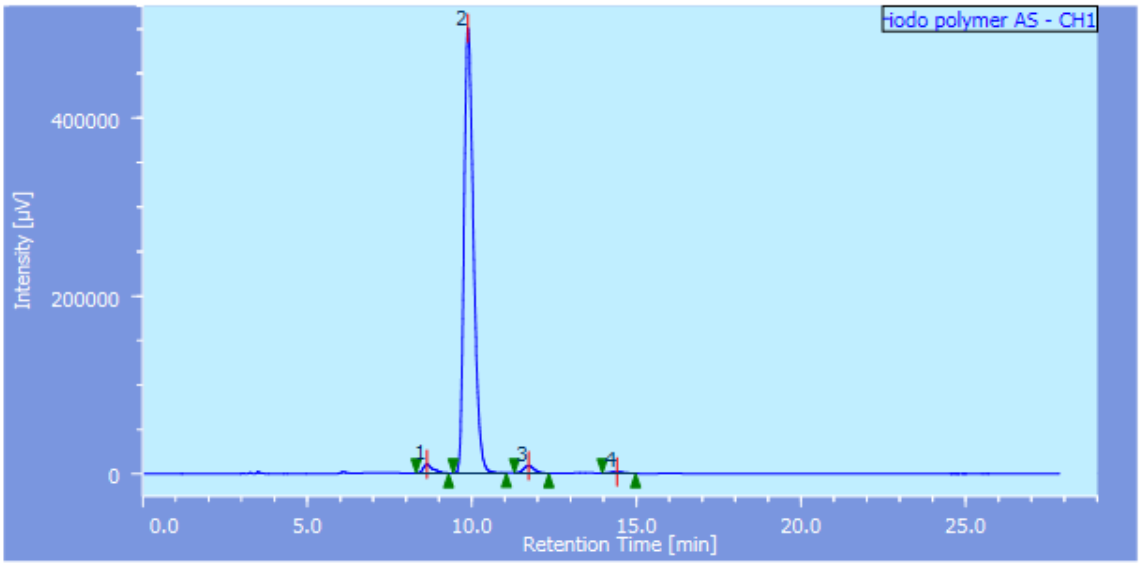

Table 2.4, Cycle 1: >99% ee

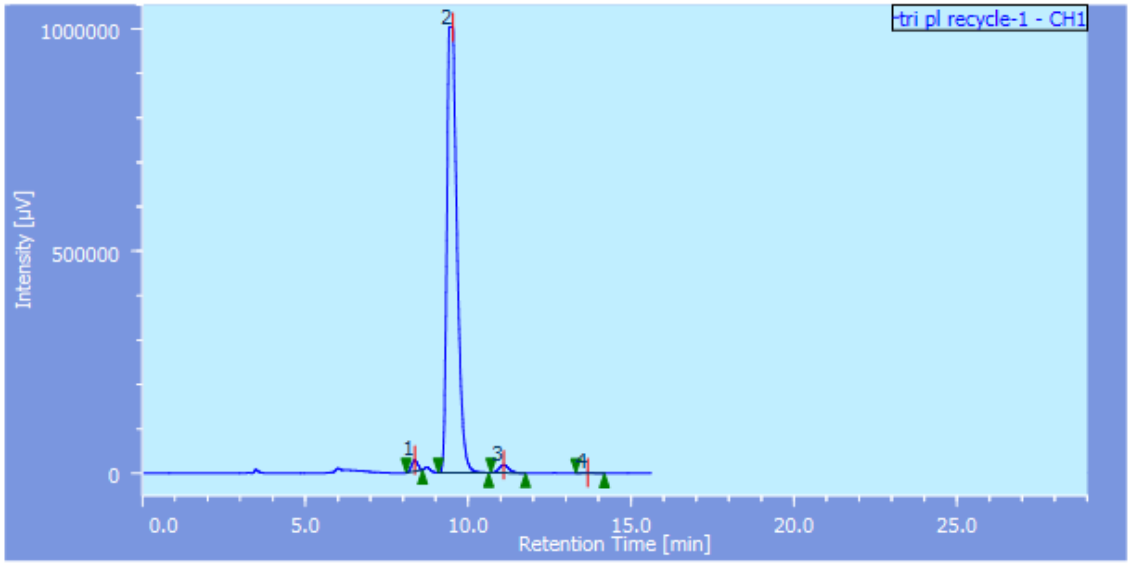

Table 2.4, Cycle 2: 99% ee

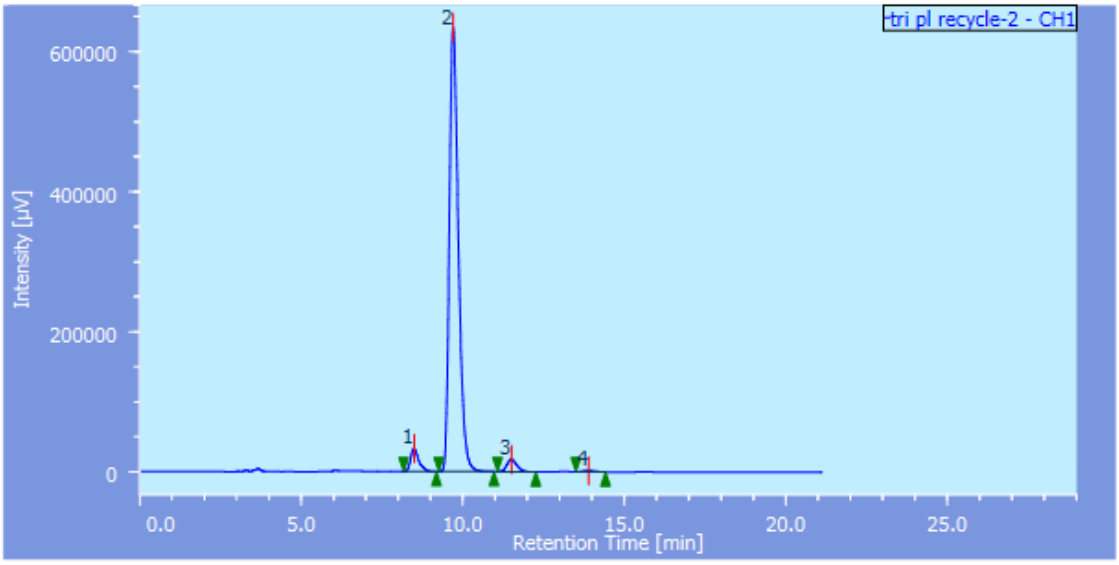

Table 2.4, Cycle 3: >99% ee

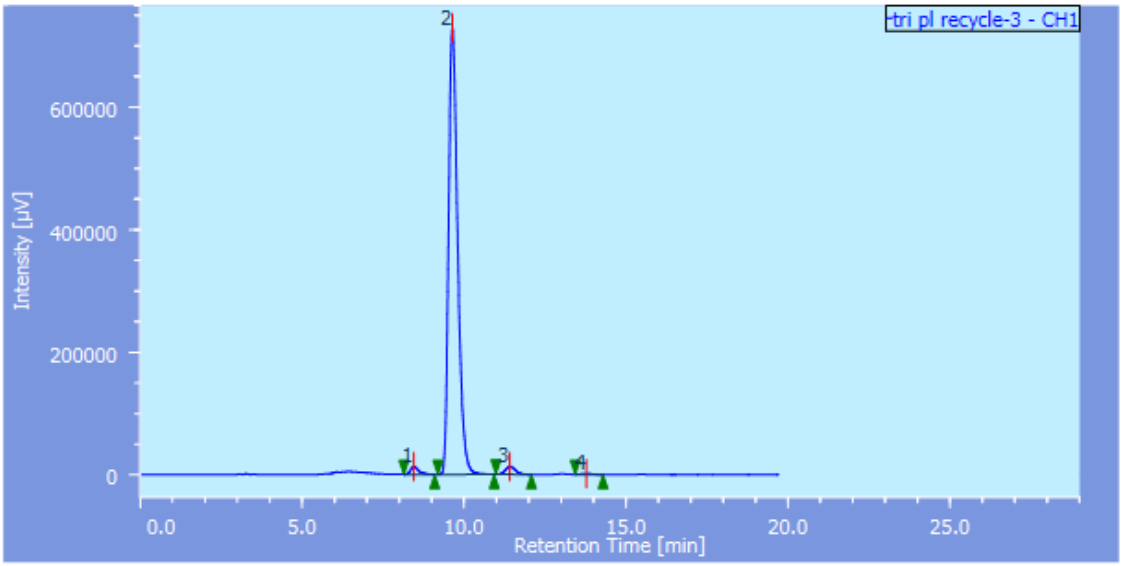

Table 2.4, Cycle 4: 99% ee

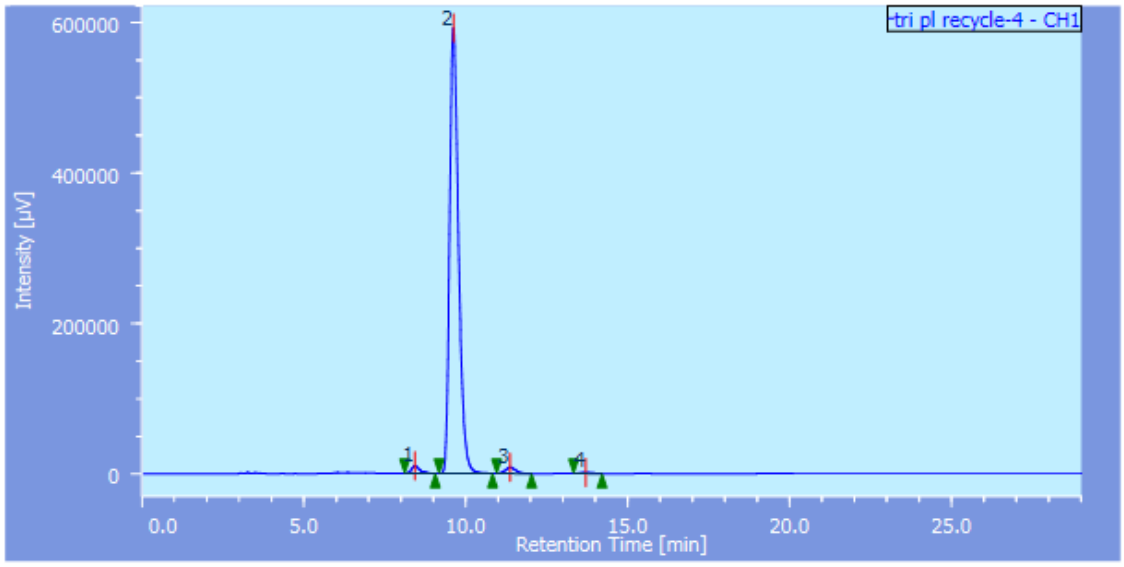

Table 2.4, Cycle 5: >99% ee

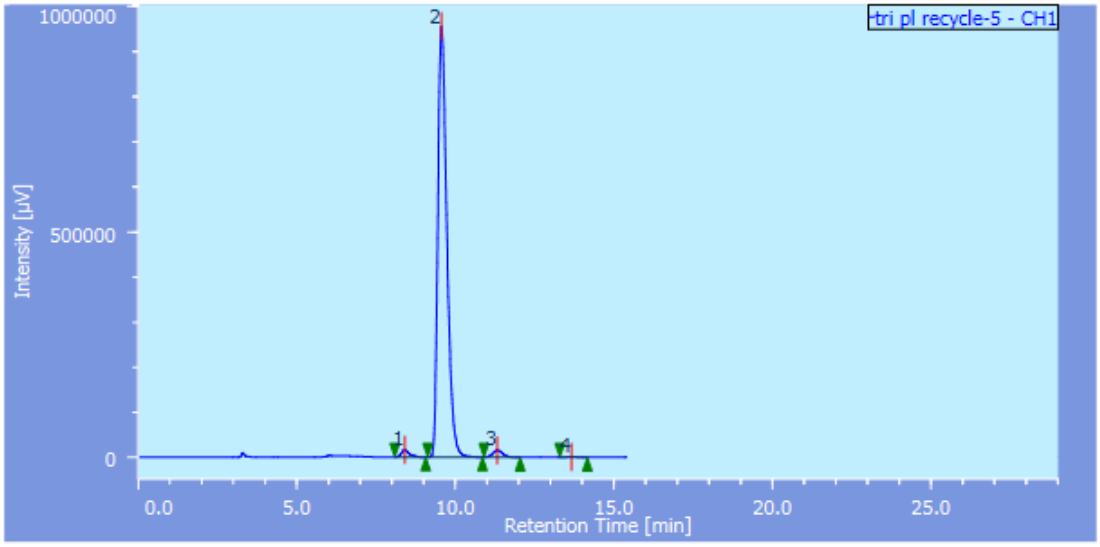

Table 2.4, Cycle 6: >99% ee

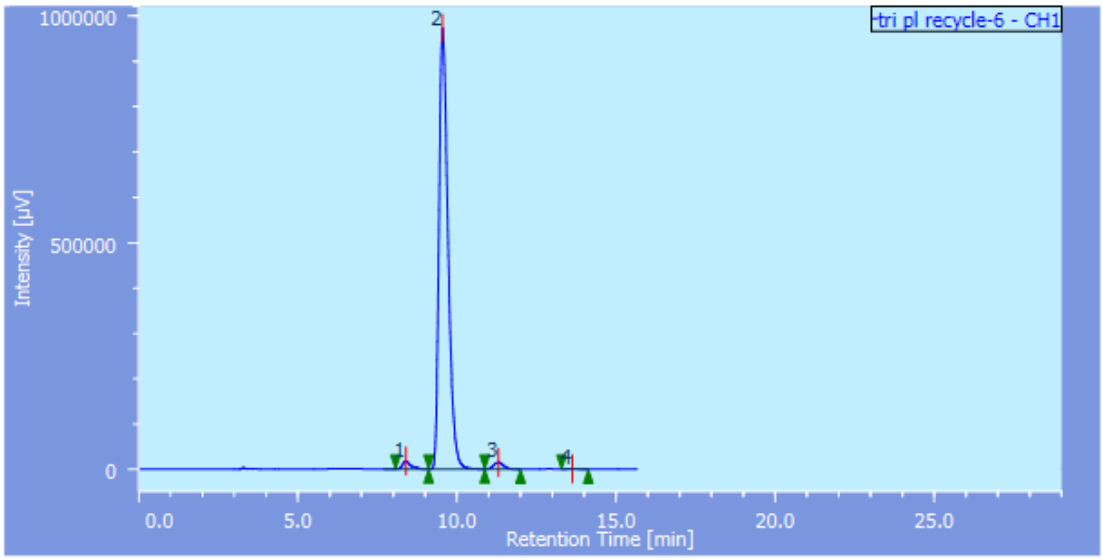

4. Chromatogram data on recyclability for catalyst P3ac (Table 2.5)

Table 2.5, Fresh polymer P3ac: 99% ee

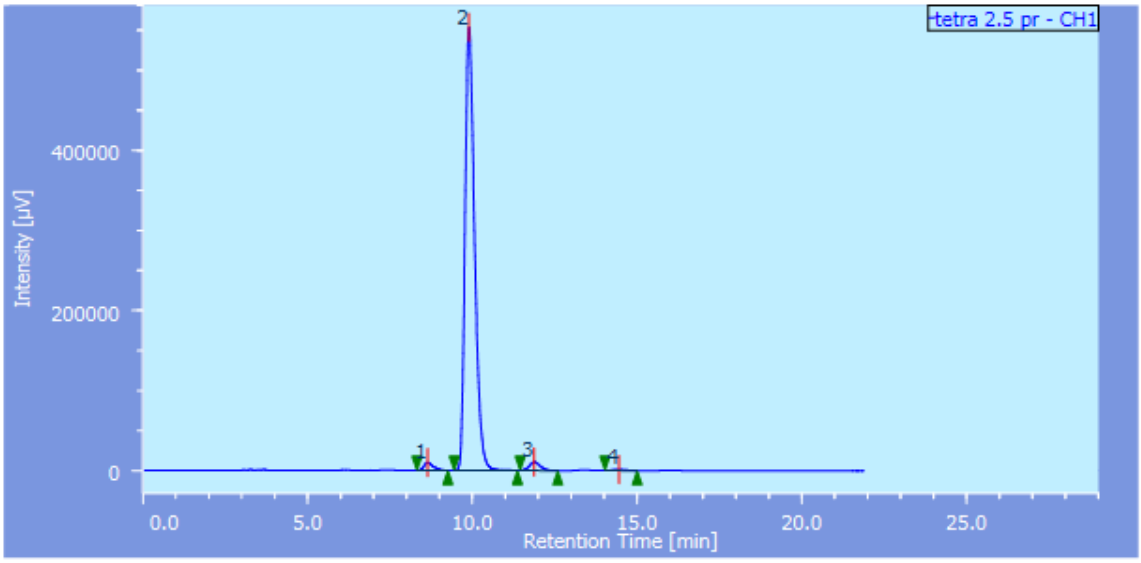

Table 2.5, Cycle 1: 99% ee

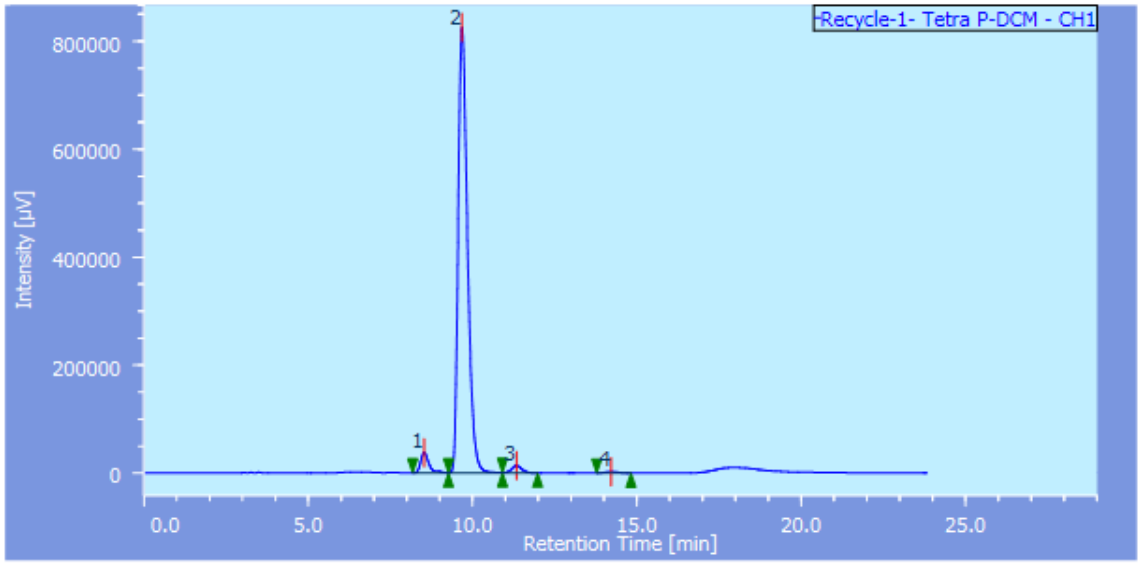

Table 2.5, Cycle 2: 99% ee

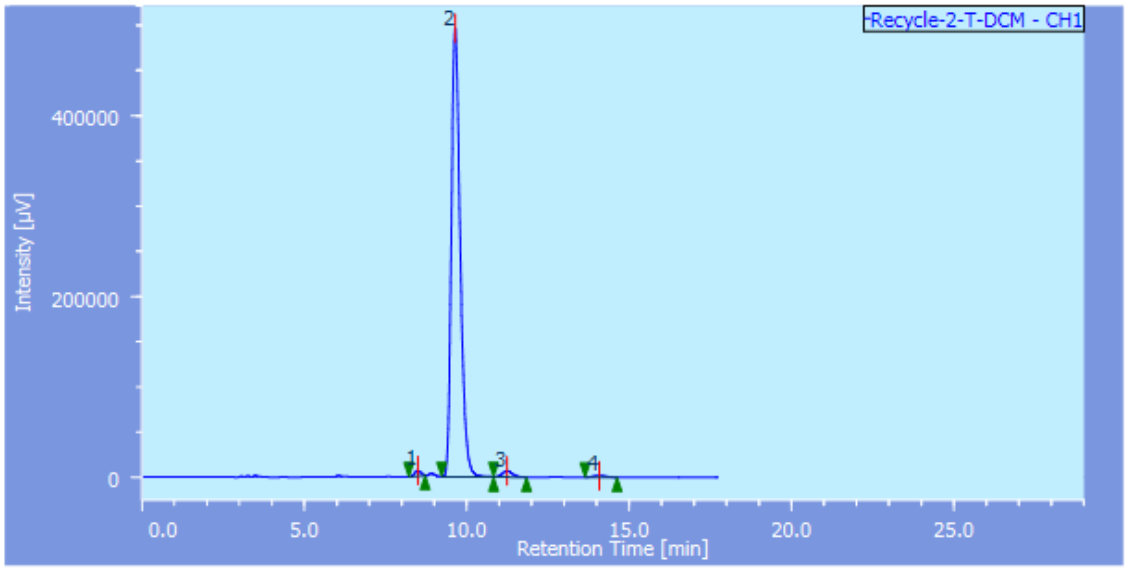

Table 2.5, Cycle 3: >99% ee

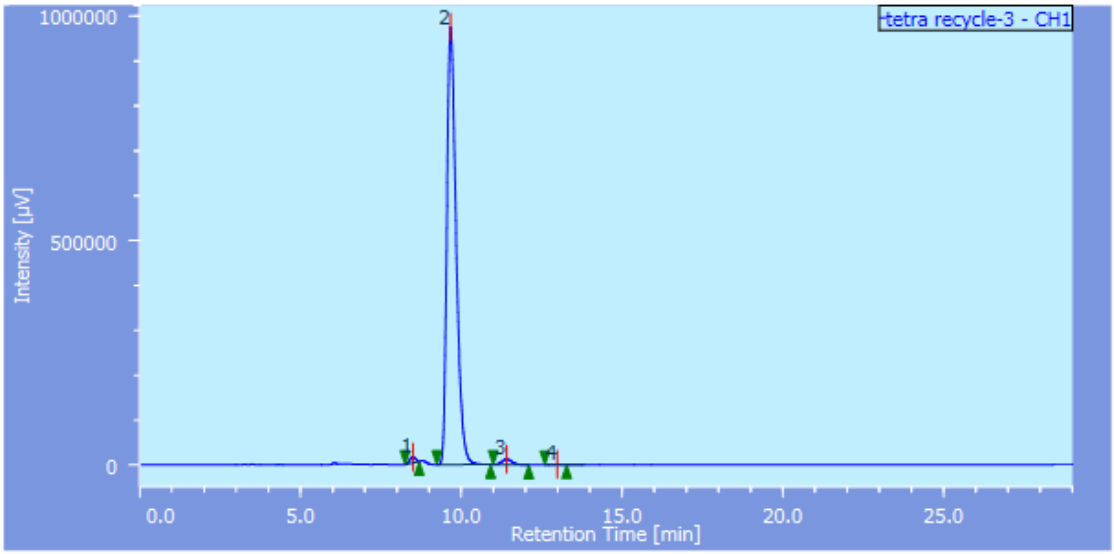

Table 2.5, entry cycle 4: 99% ee

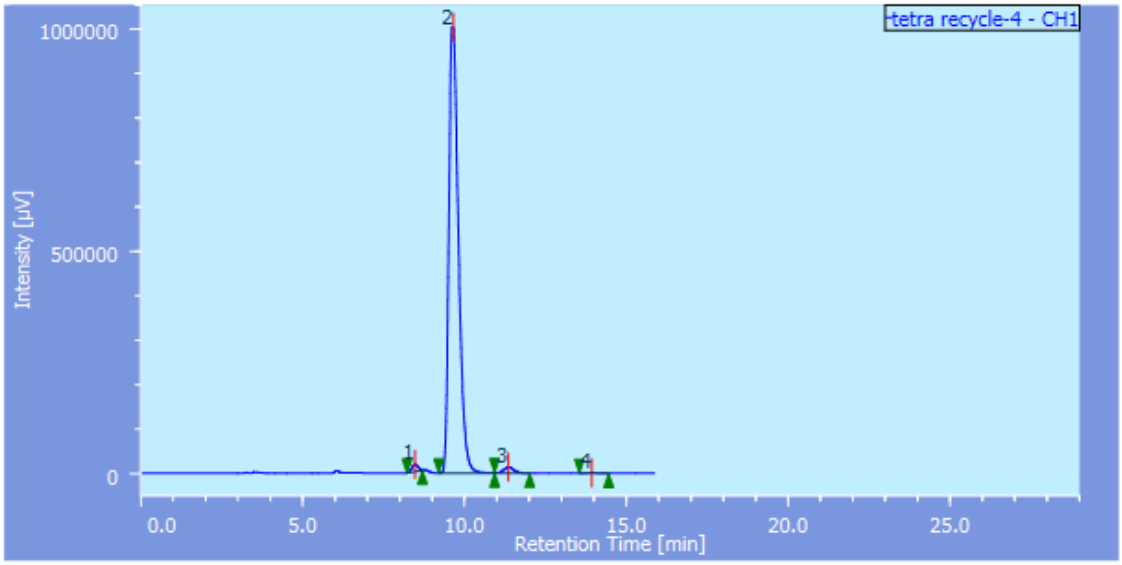

5. Chromatogram data for different Michael adduct using P1aa (Table 6)

Table 2.6, entry 1, 93% ee

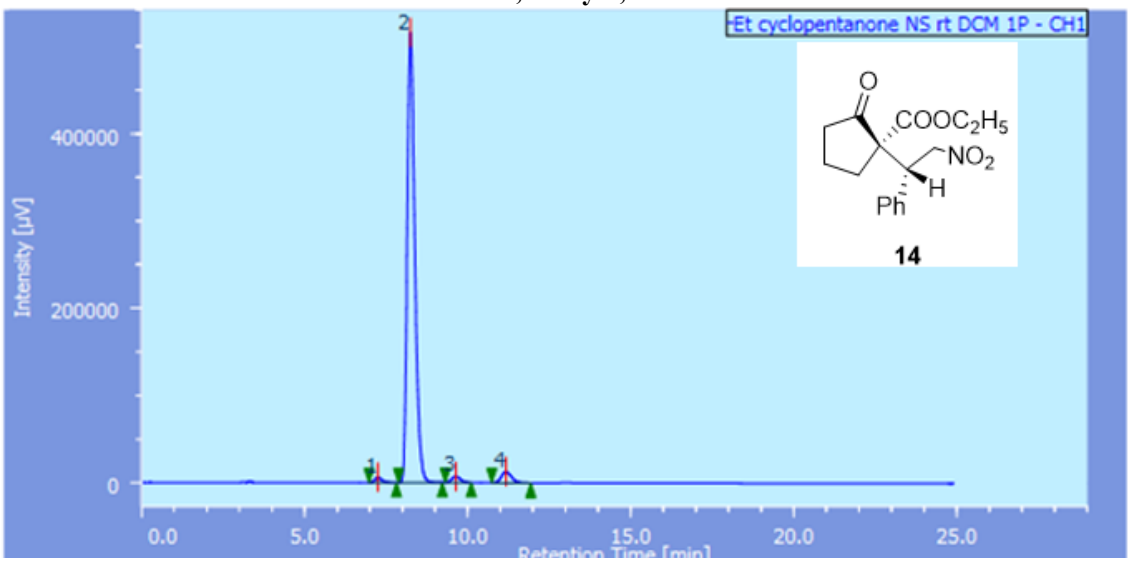

Table 2.6, entry 2, 94% ee

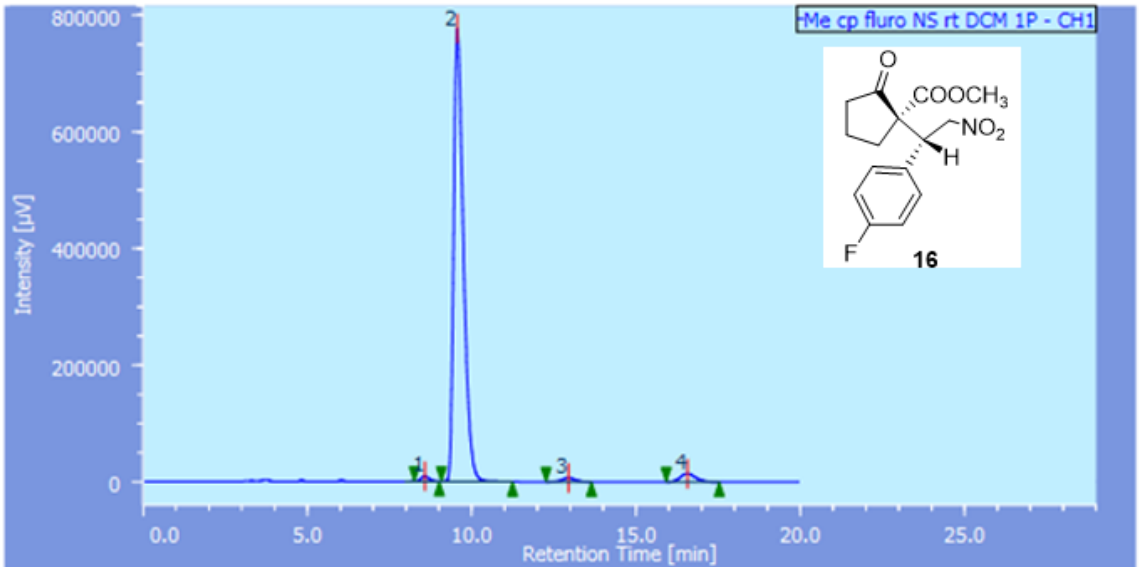

Table 2.6, entry 3, >99% ee

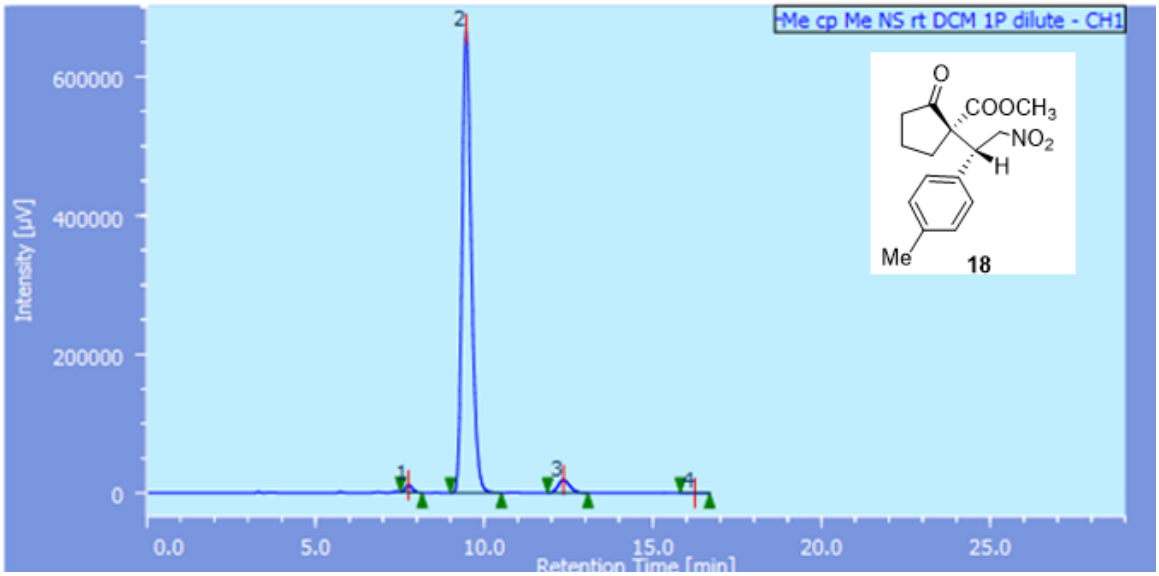

Table 2.6, entry 4, 96% ee

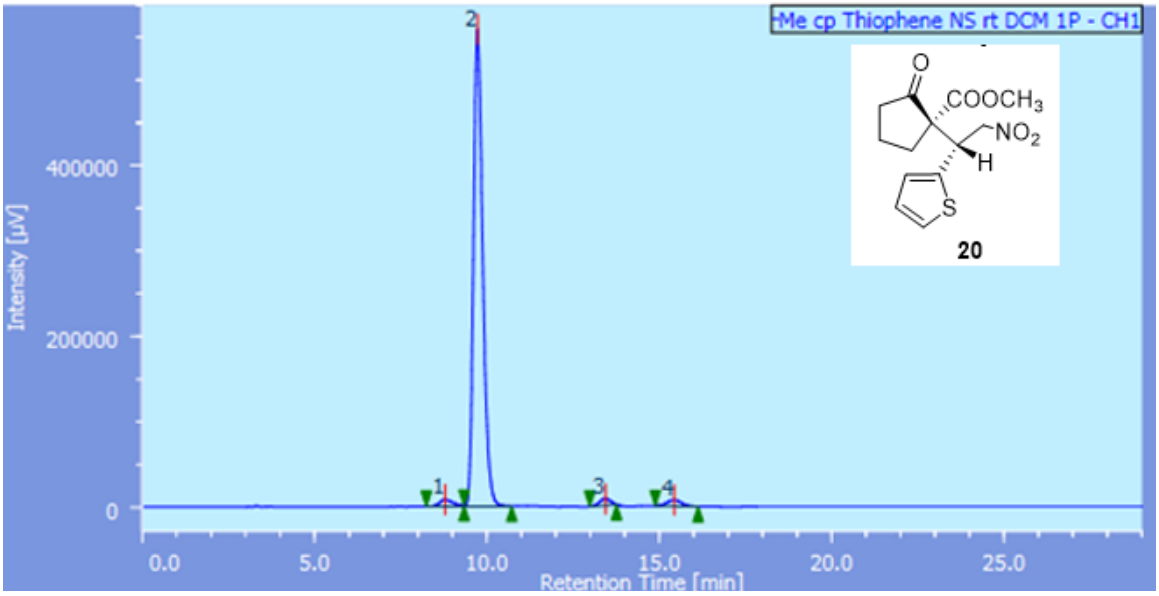

6. Chromatogram data for asymmetric reaction of anthrone to β-nitro styrene (Table 2.7).

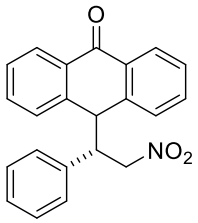

24 (*S*)

Table 2.7, entry 1: 78% ee

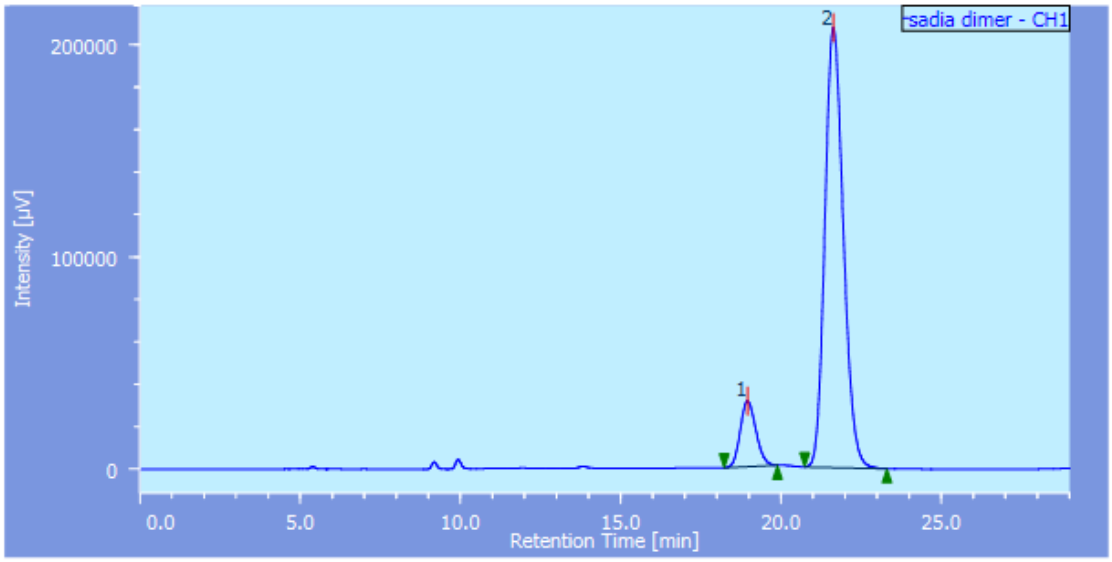

Table 2.7, entry 2, 34% ee

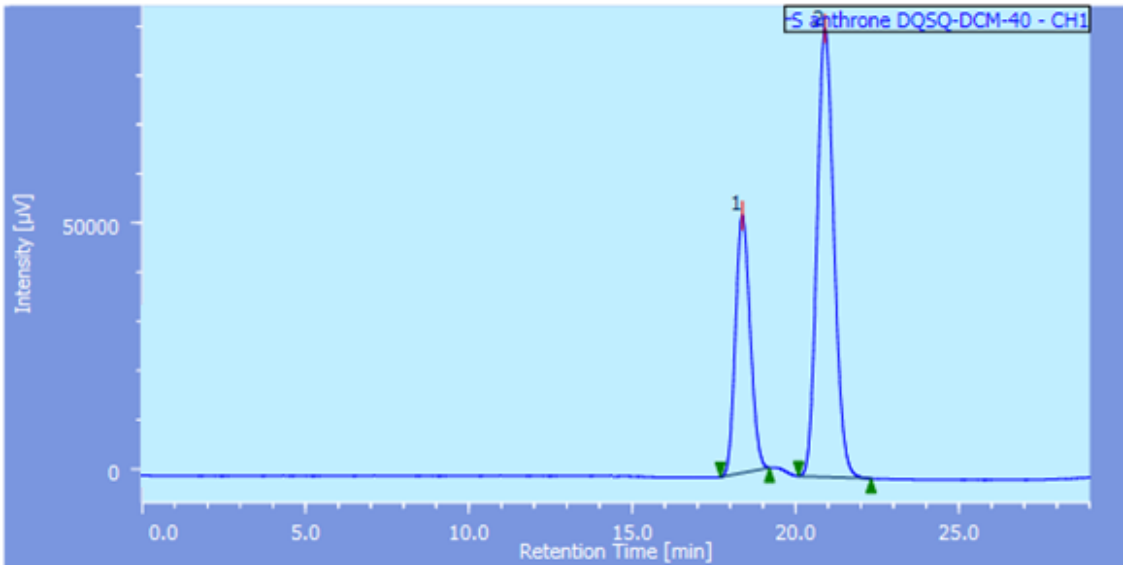

Table 2.7, entry 3, 72% ee

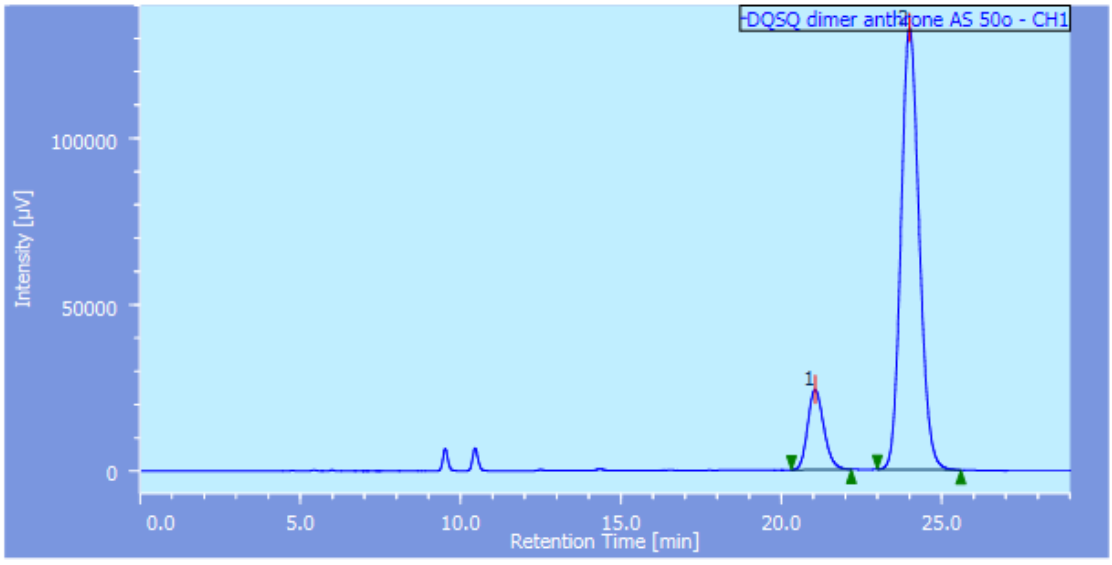

Table 2.7, entry 4: 18% ee

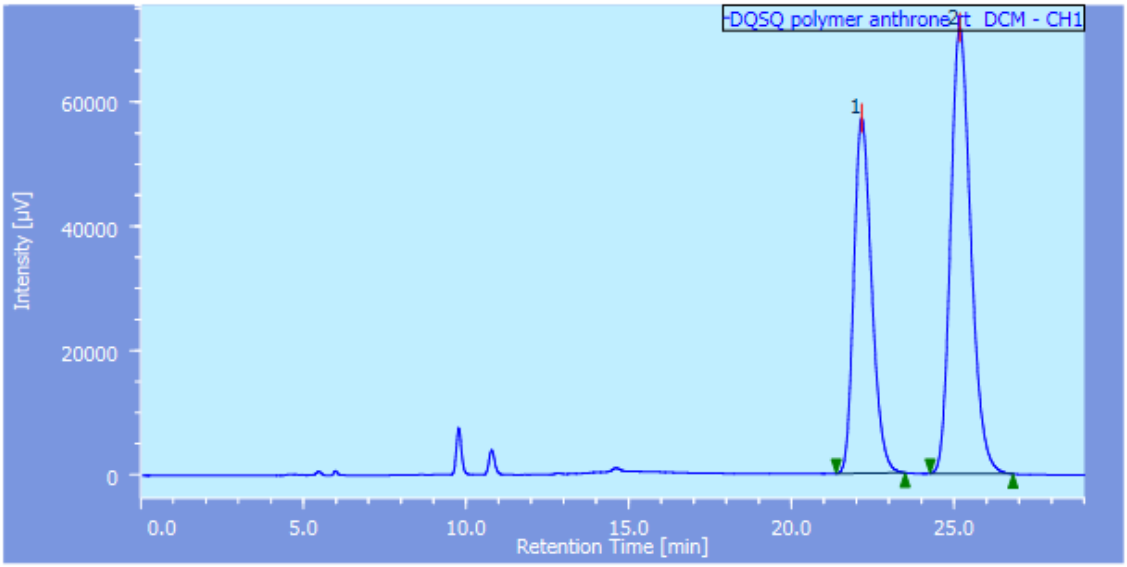

Table 2.7, entry 5: 9% ee

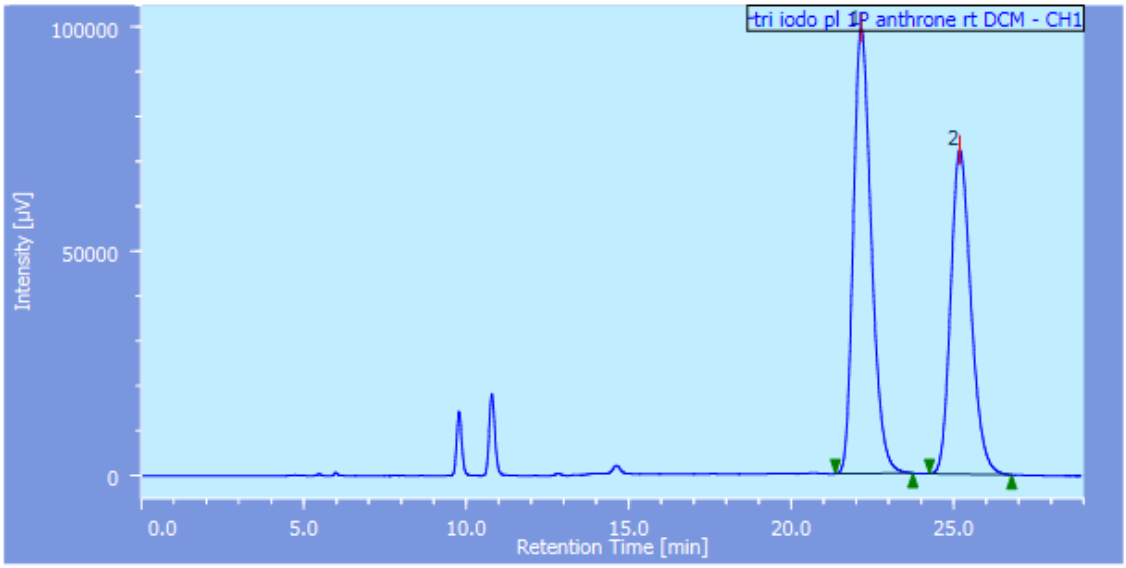

Table 2.7, entry 6: 10% ee

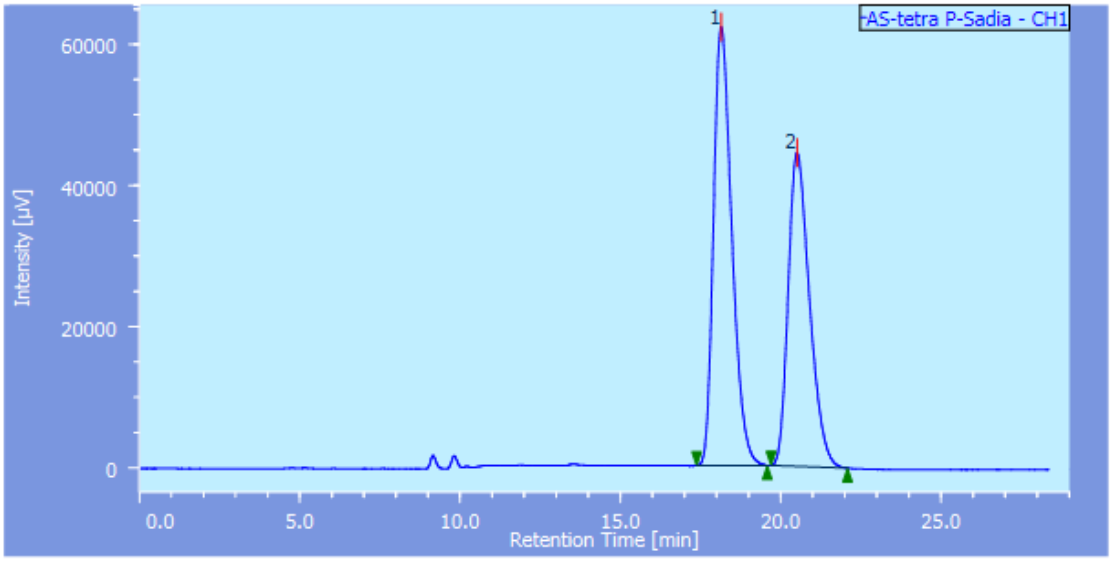

Appendix C

Supporting Information for Chapter 3

C.1 ^{1}H and ^{13}C NMR data for monomers and polymers

^{1}H NMR spectrum of A in $CDCl_3$

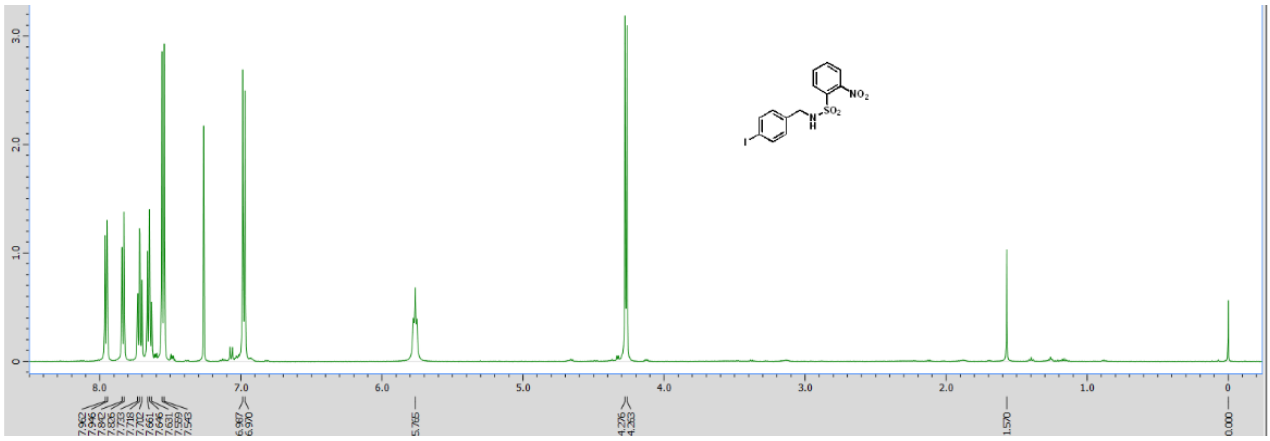

^{13}C NMR spectrum of A in $CDCl_3$.

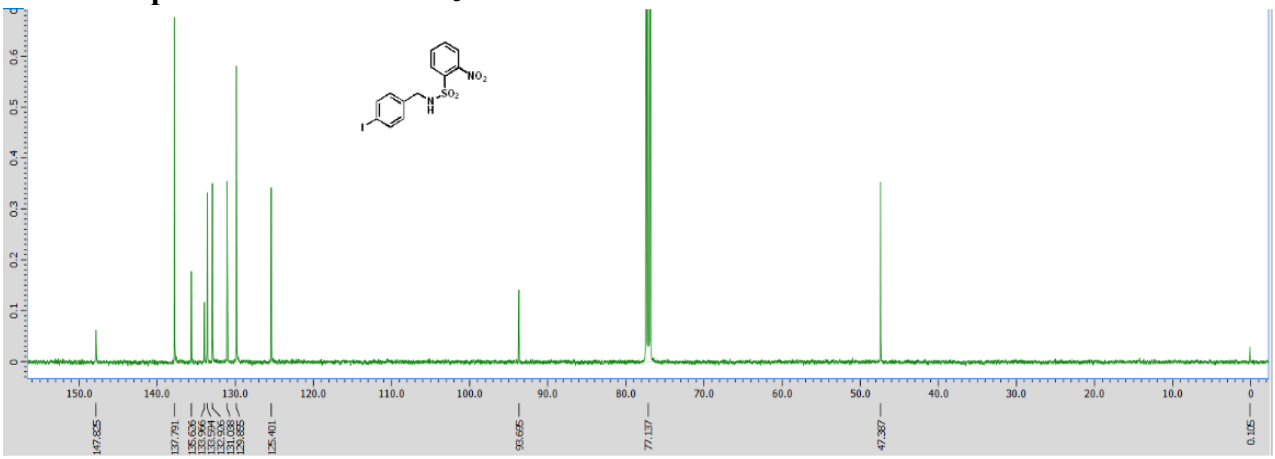

^{1}H NMR spectrum of B in $CDCl_3$

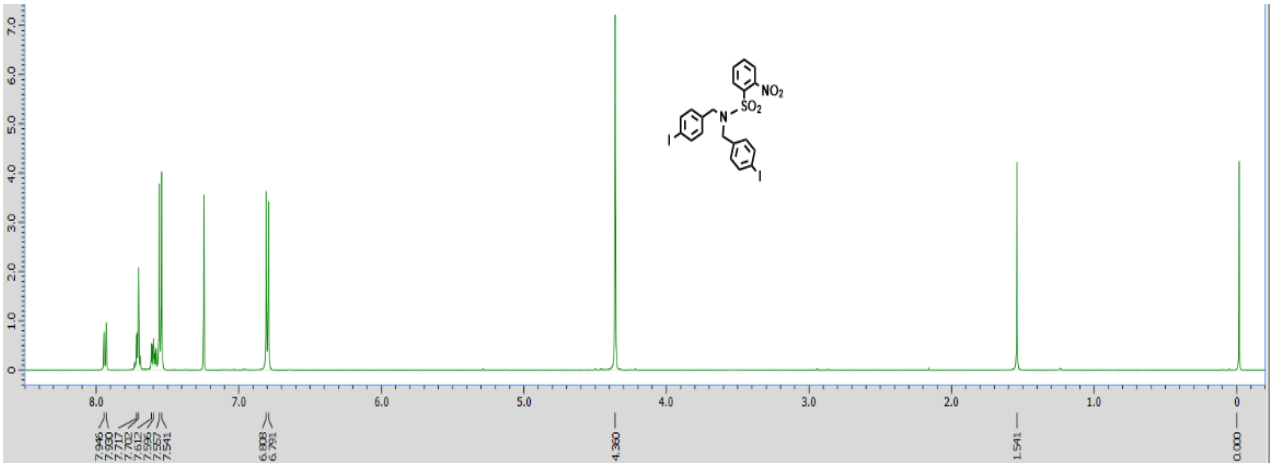

^{13}C NMR spectrum of B in $CDCl_3$.

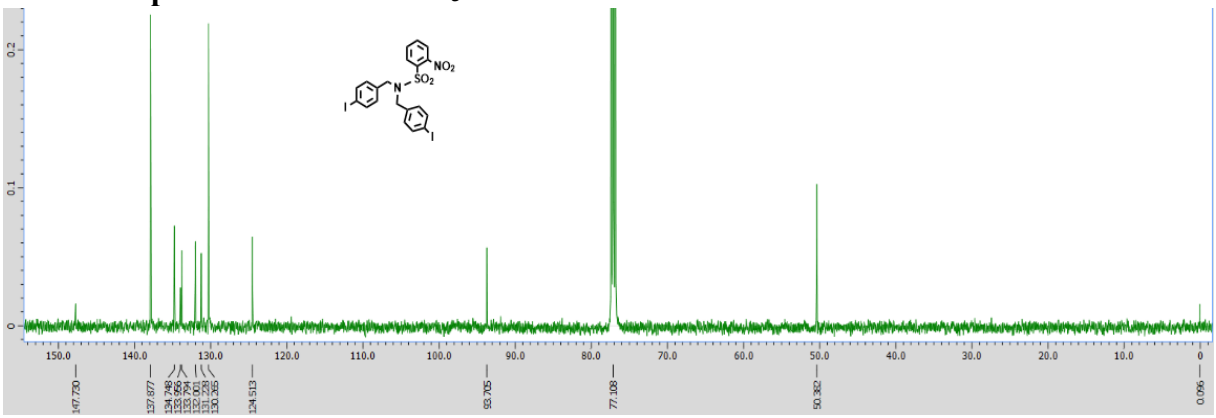

^{1}H NMR spectrum of 1 in $CDCl_3$.

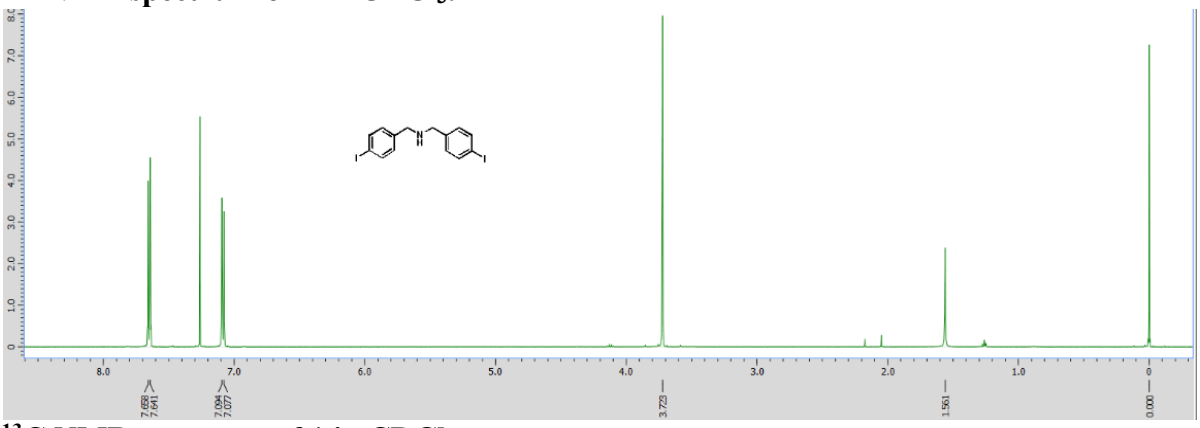

^{13}C NMR spectrum of 1 in $CDCl_3$.

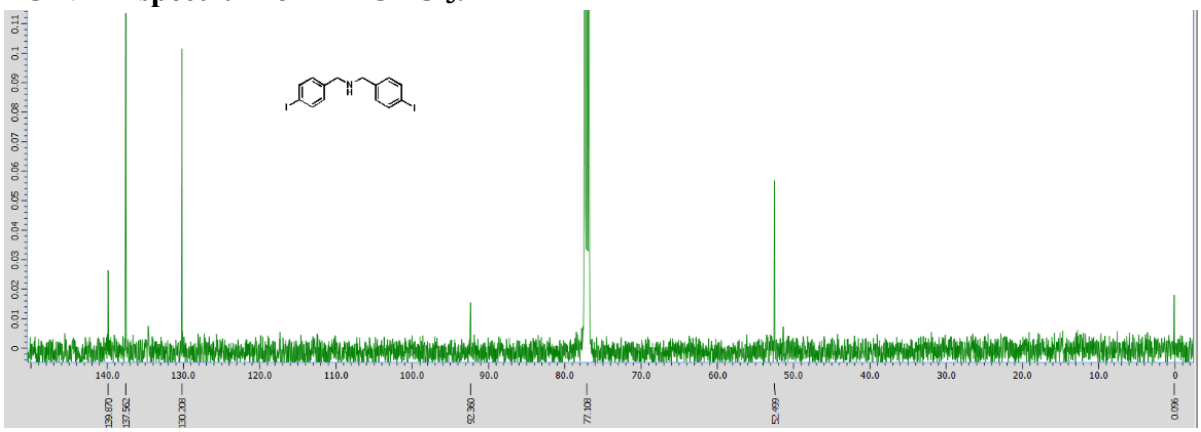

^{1}H NMR spectrum of 2 in $CDCl_3$.

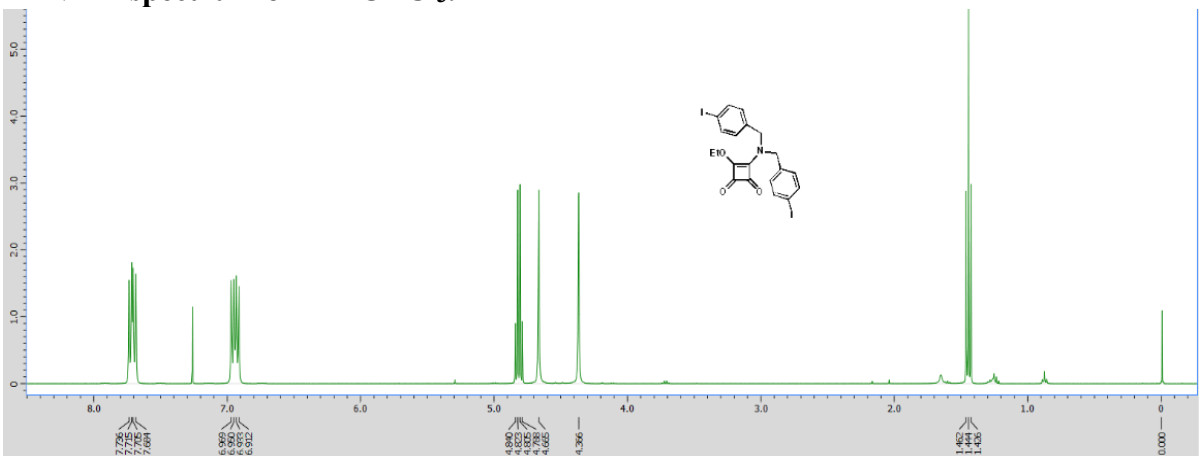

^{13}C NMR spectrum of 2 in $CDCl_3$.

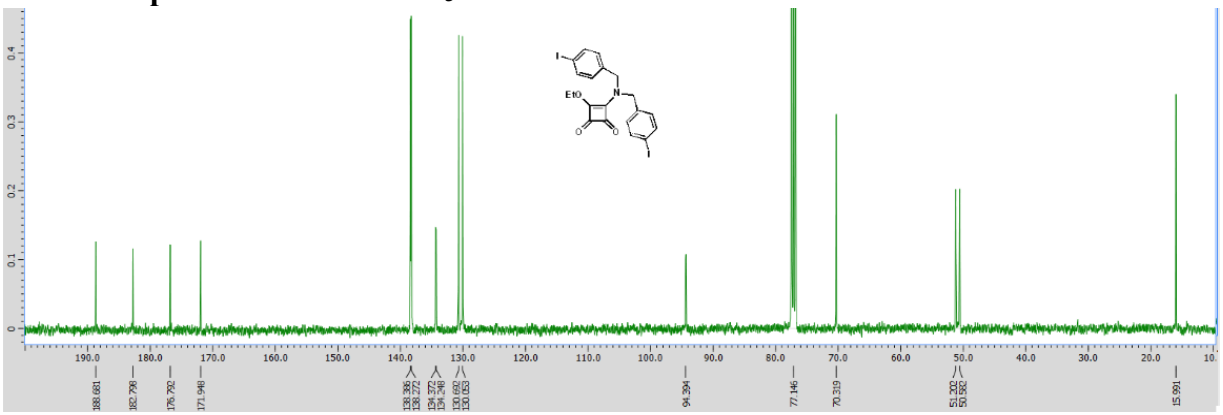

^{1}H NMR spectrum of 3 in $CDCl_3$.

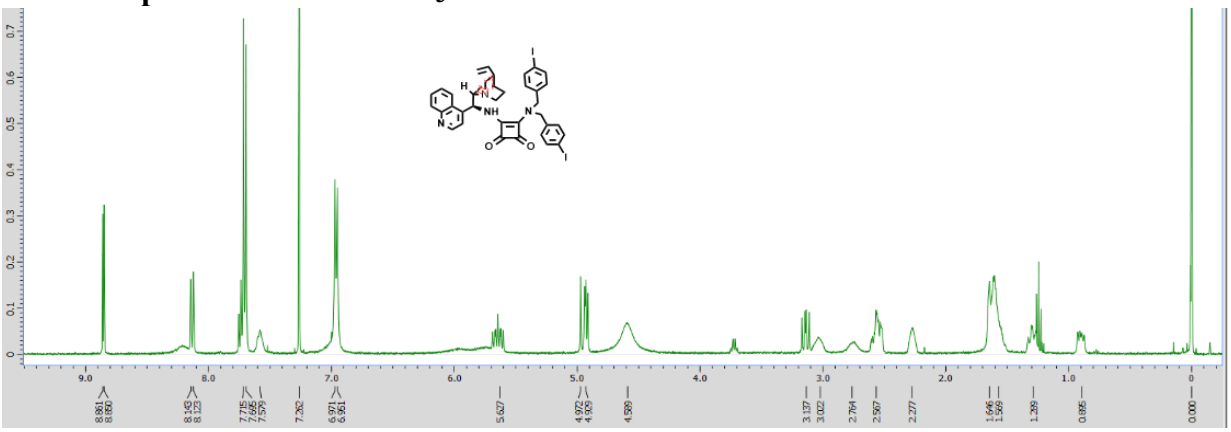

^{13}C NMR spectrum of 3 in $CDCl_3$.

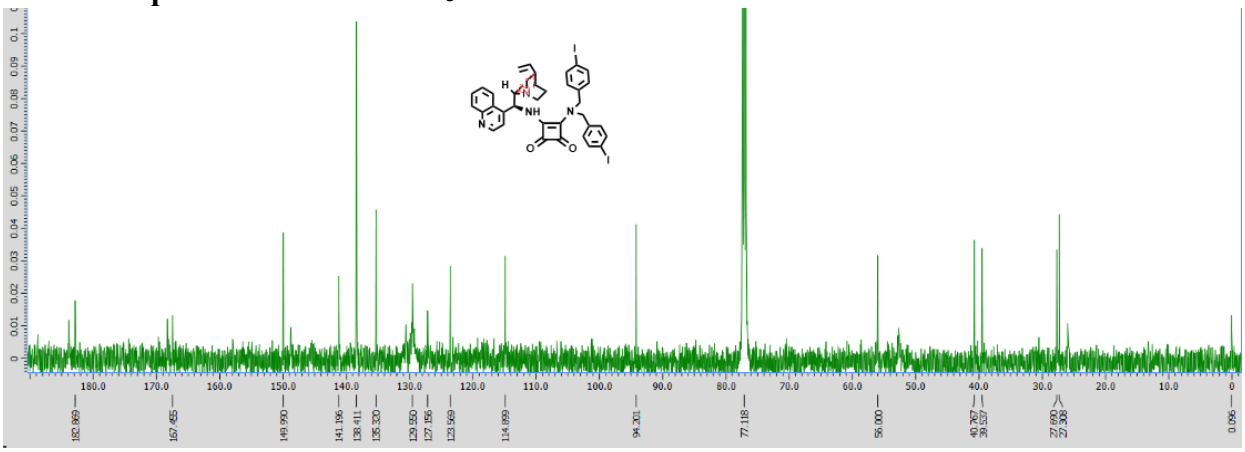

^{1}H NMR spectrum of 6 in DMSO-*d_6*.

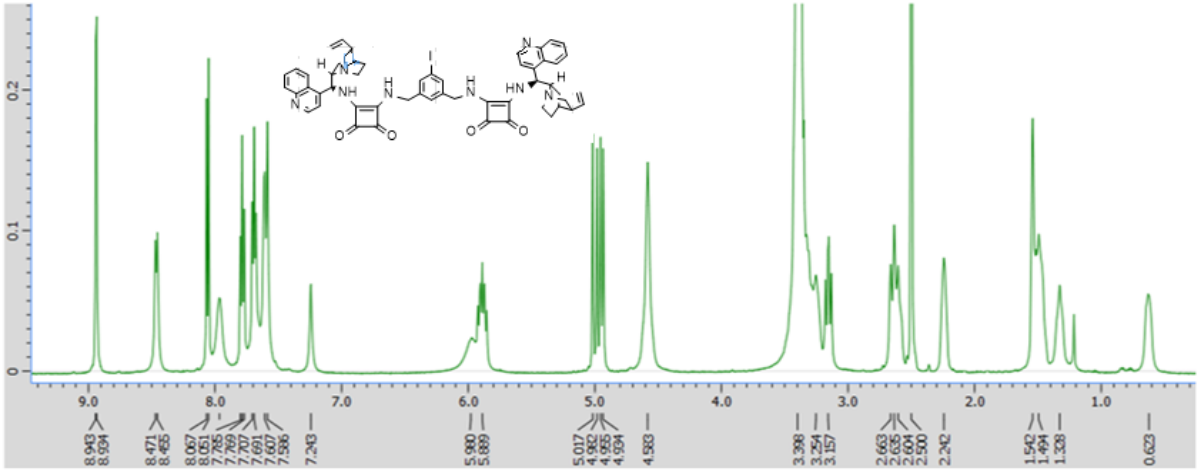

^{13}C NMR spectrum of 6 in DMSO-*d*$_6$.

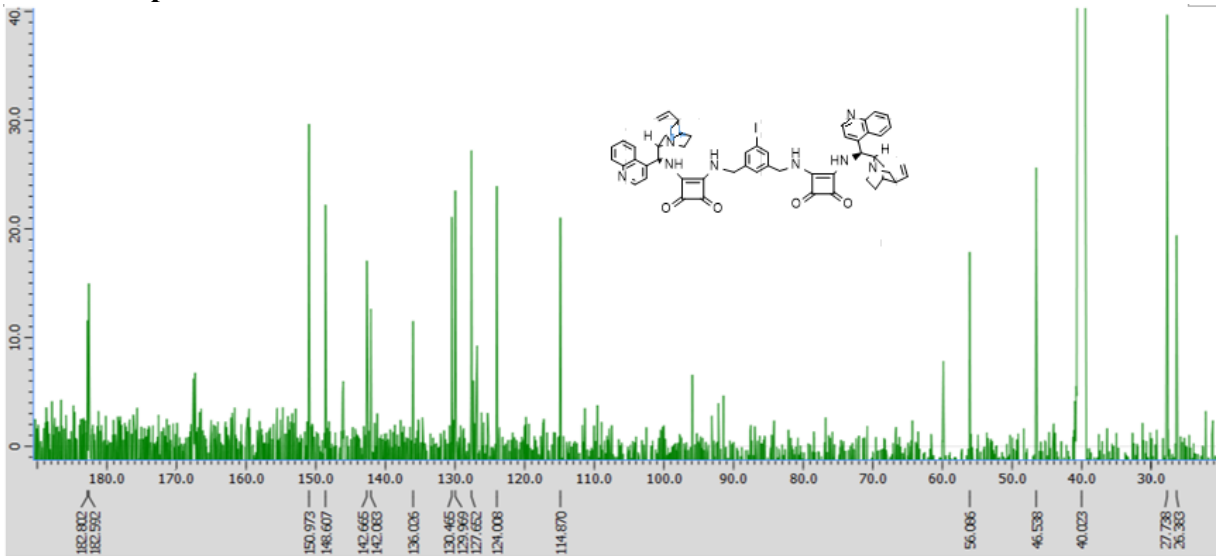

^{1}H NMR spectrum of 8 in $CDCl_3$.

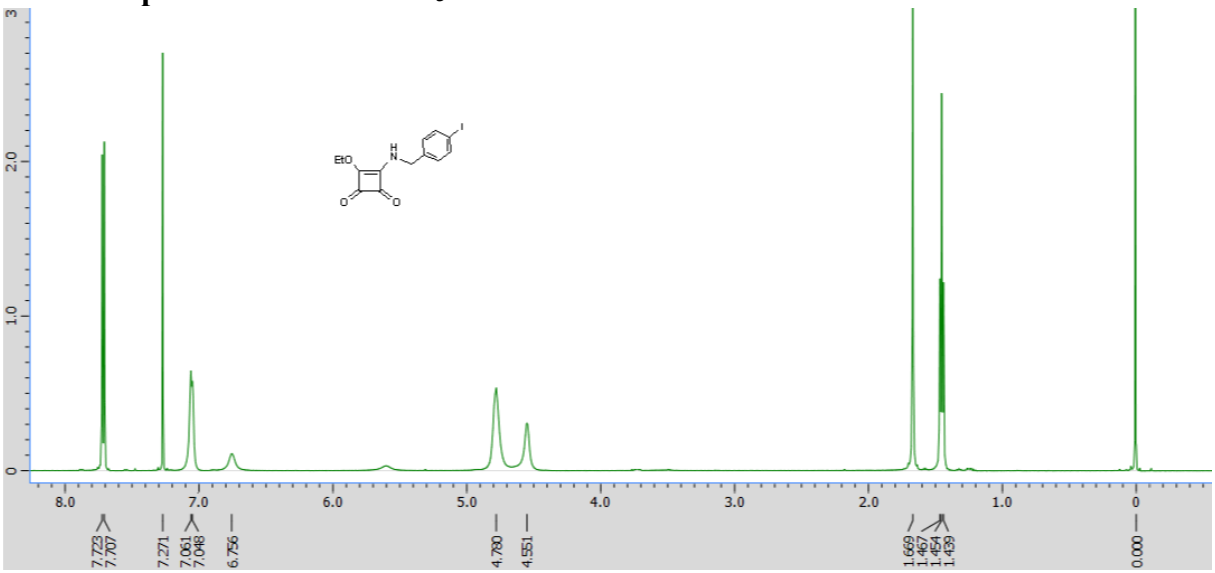

^{13}C NMR spectrum of 8 in $CDCl_3$.

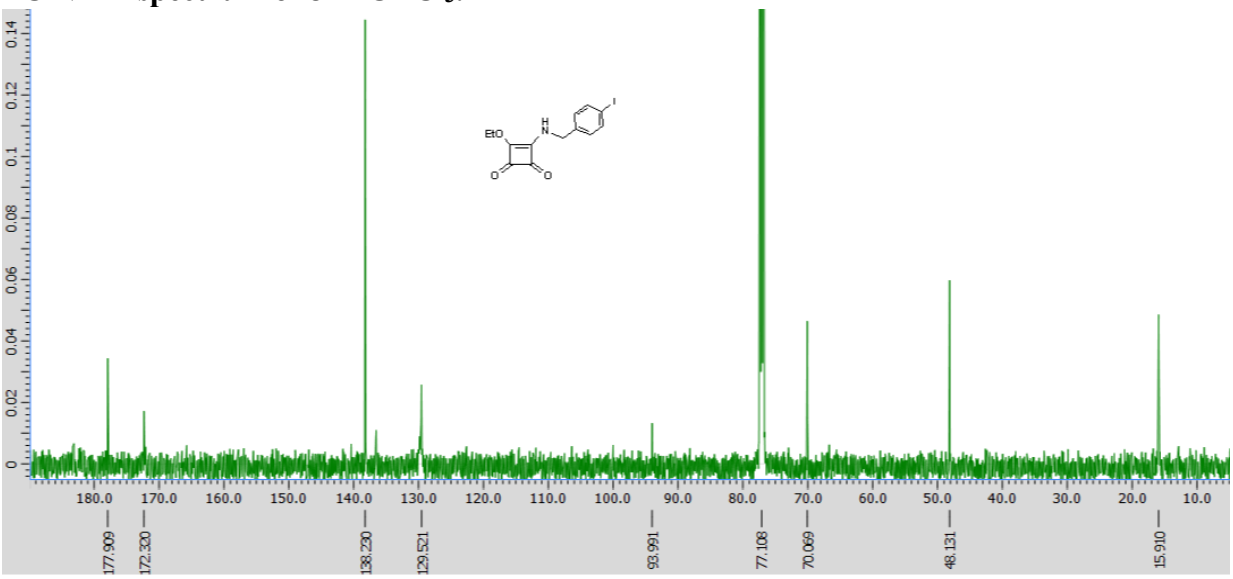

^{1}H NMR spectrum of 9 in DMSO-*d*$_6$.

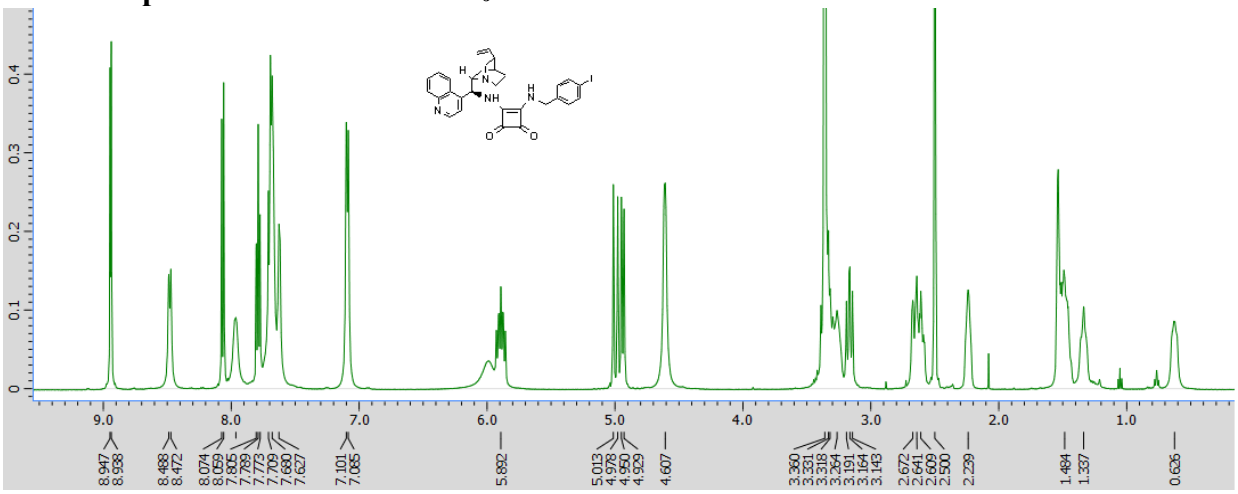

^{13}C NMR spectrum of 9 in DMSO-*d*$_6$.

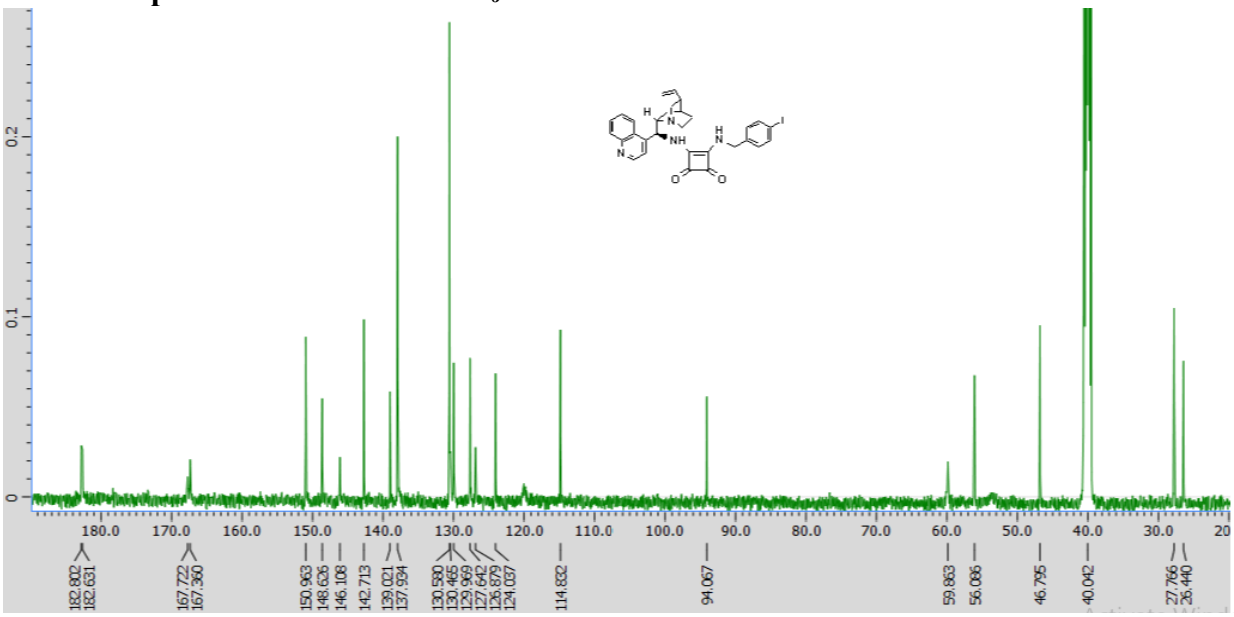

^{1}H NMR of P1 polymer in DMSO-*d*$_6$

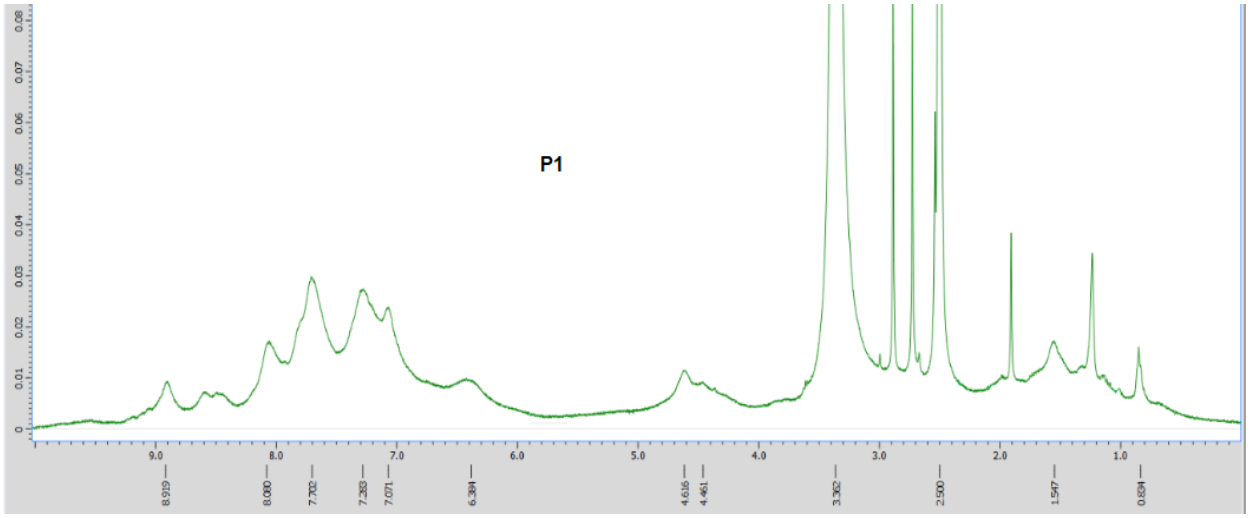

^{1}H NMR of P2 polymer in DMSO-*d*$_6$

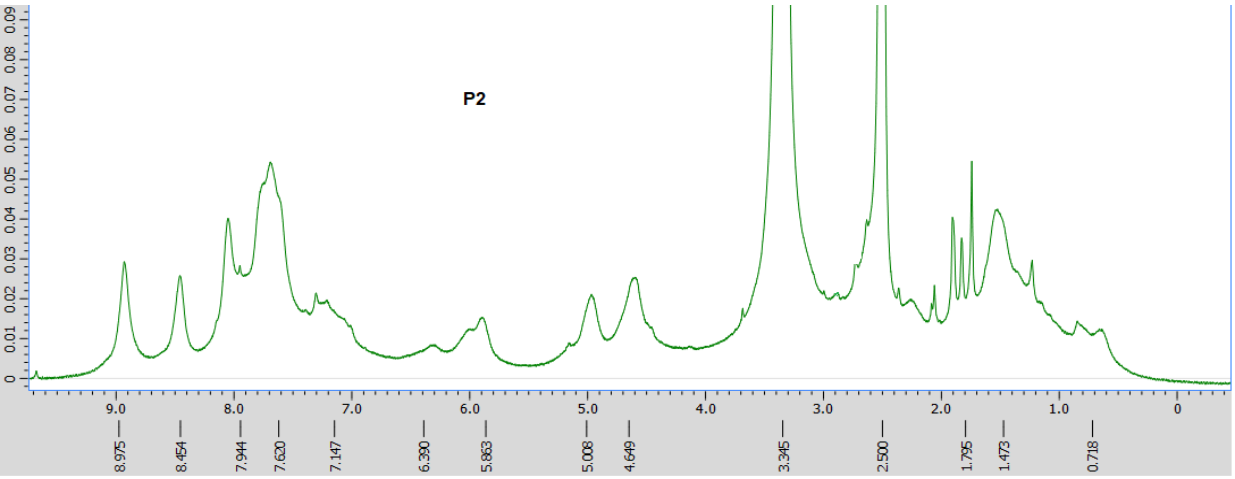

^{1}H NMR spectrum of PL polymer in DMSO-*d*$_6$

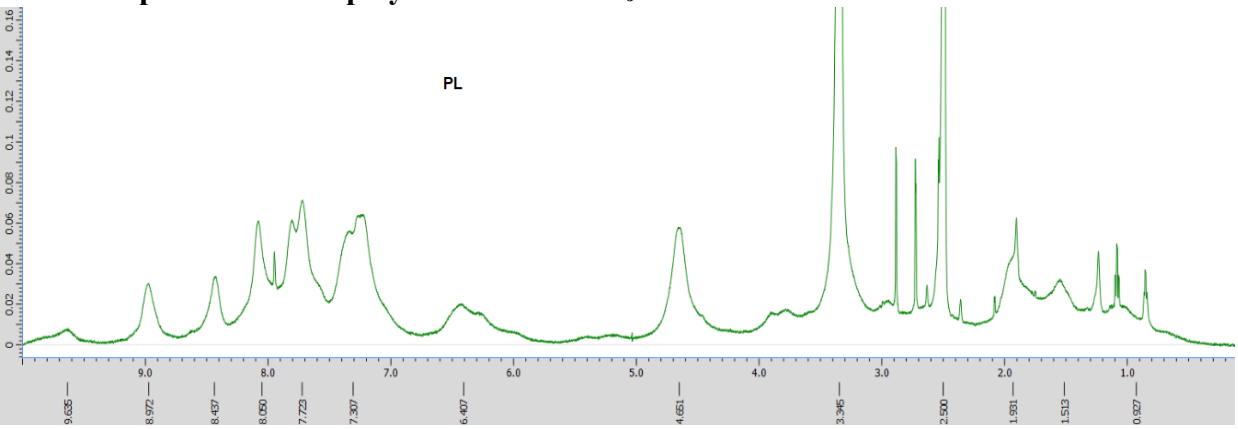

C.2 FT-IR Spectrum for monomers and polymers

1. IR spectrum of 1

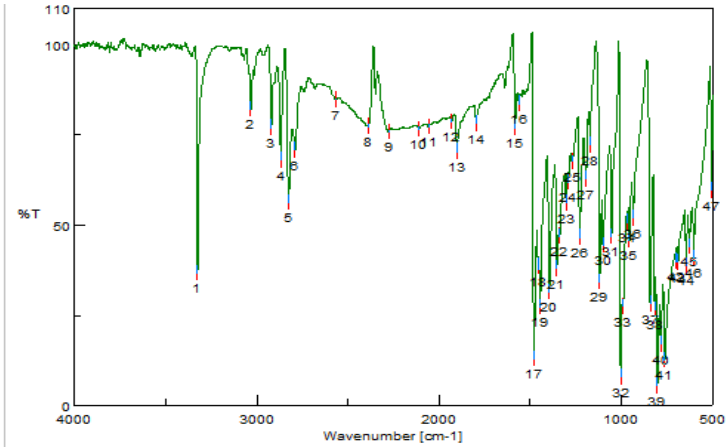

[ピーク検出結果]

No.	位置	強度	No.	位置	強度
1	3324.68	36.5864	2	3032.51	82.0391
3	2920.66	76.858	4	2867.63	67.8861
5	2825.2	56.2812	6	2789.53	70.7571
7	2567.75	84.6818	8	2391.3	77.3095
9	2276.56	75.7994	10	2109.74	76.4308
11	2059.6	77.1922	12	1931.36	78.5413
13	1902.43	70.34	14	1795.4	78.0185
15	1583.27	76.7528	16	1562.06	83.5202
17	1479.13	13.0072	18	1456.96	38.595
19	1446.35	27.2271	20	1396.21	31.4027
21	1354.75	38.0015	22	1339.32	46.9328
23	1303.64	56.092	24	1292.07	61.7925
25	1271.82	67.635	26	1229.4	46.5943
27	1194.69	62.7057	28	1172.51	72.1262
29	1119.48	34.1715	30	1102.12	44.2874
31	1053.91	46.7928	32	1003.77	7.9143
33	991.232	27.4441	34	969.055	50.7836
35	956.52	45.7358	36	936.271	51.9197
37	841.776	28.139	38	817.67	26.5161
39	803.206	5.45061	40	783.922	16.987
41	761.744	12.6365	42	702.926	39.9119
43	689.427	39.6977	44	645.072	38.8176
45	627.716	43.9353	46	603.61	40.86

2. IR spectrum of 2

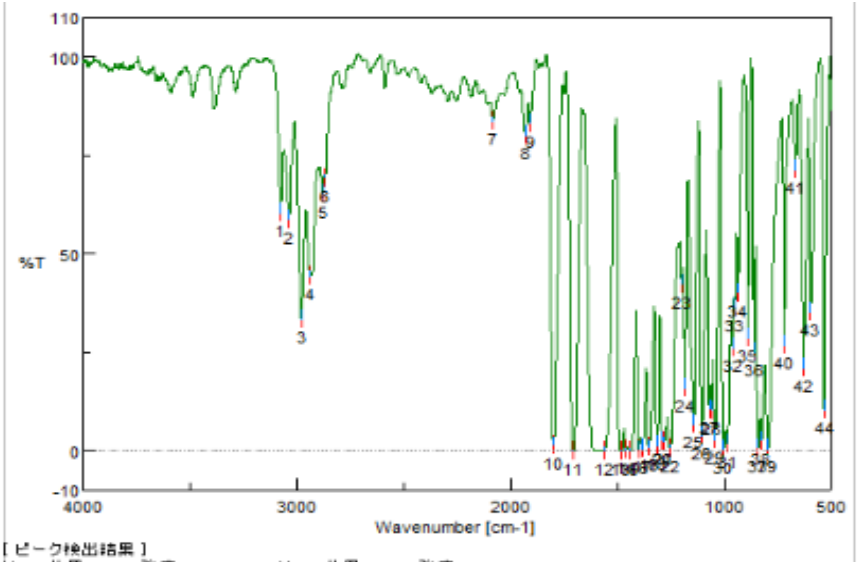

[ピーク検出結果]

No.	位置	強度	No.	位置	強度
1	3075.87	60.3428	2	3036.37	58.7257
3	2979.48	33.3668	4	2936.09	44.2815
5	2880.17	65.3301	6	2867.63	69.3224
7	2081.78	83.7729	8	1930.4	80.19
9	1908.22	83.2559	10	1800.22	1.38041
11	1702.84	0	12	1562.06	-2.65193E-038
13	1481.06	0.0205595	14	1460.81	0.10781
15	1442.49	0.0143659	16	1402	0.248361
17	1383.68	0.584781	18	1354.75	0.901117
19	1313.29	1.21233	20	1292.07	2.57737
21	1282.43	2.38703	22	1254.47	0.730828
23	1198.54	42.2445	24	1183.11	15.8051
25	1142.62	6.63404	26	1104.05	3.79962
27	1069.33	10.559	28	1057.76	10.1528
29	1043.3	2.52958	30	1005.7	0.298708
31	984.482	1.70842	32	961.341	26.1157
33	949.77	36.2522	34	934.342	40.147
35	889.987	28.6534	36	861.06	25.0308
37	840.812	0.727783	38	825.384	2.46314
39	795.493	0.504599	40	719.318	26.743
41	666.285	71.2823	42	629.58	20.9171
43	594.932	35.1161	44	532.257	10.3352

3. IR spectrum of 3

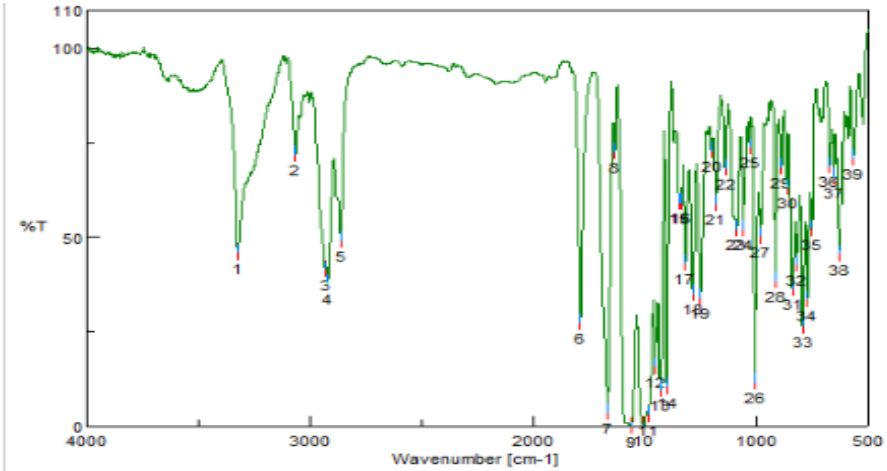

[ピーク検出結果]

No.	位置	強度	No.	位置	強度
1	3324.68	45.9368	2	3065.3	71.8537
3	2933.2	41.6177	4	2921.53	37.8765
5	2862.81	49.0609	6	1788.65	27.3444
7	1667.16	3.64877	8	1633.41	72.5971
9	1561.09	0.11898	10	1504.2	0.183657
11	1484.92	2.90841	12	1452.14	15.8523
13	1429.96	9.60268	14	1402	10.5323
15	1343.18	59.2317	16	1336.43	59.2598
17	1318.11	43.1467	18	1285.32	35.1391
19	1249.65	34.107	20	1200.47	72.8808
21	1182.15	58.8697	22	1139.72	68.173
23	1088.62	52.1204	24	1059.59	52.0745
25	1031.73	73.8042	26	1006.66	11.5558
27	981.59	50.3208	28	914.093	38.4857
29	888.059	68.4862	30	862.025	63.1225
31	839.847	36.3253	32	819.598	42.8195
33	793.564	26.5327	34	771.387	33.5211
35	749.209	52.2972	36	671.106	68.9036
37	649.893	65.7692	38	625.788	45.5131
39	564.077	70.9567			

4. IR spectrum of 6

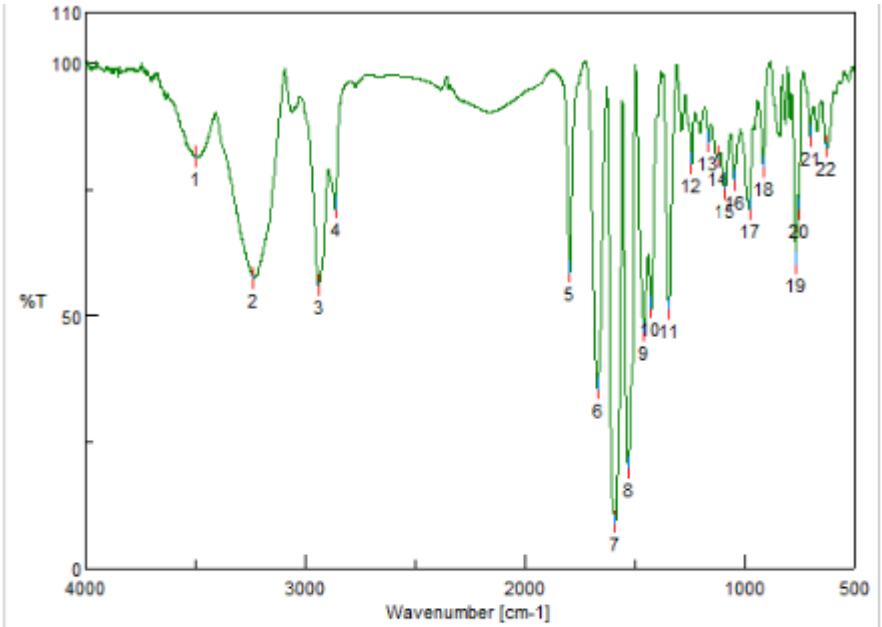

[ピーク検出結果]

No.	位置	強度	No.	位置	強度
1	3500.17	81.232	2	3235	57.3246
3	2939.95	55.9041	4	2864.74	71.2199
5	1797.33	58.5138	6	1671.02	35.4445
7	1589.06	9.05001	8	1531.2	19.8363
9	1458.89	46.704	10	1426.1	51.3973
11	1344.14	51.2788	12	1240.97	80.1072
13	1164.79	84.3256	14	1124.3	81.2283
15	1091.51	75.0166	16	1045.23	76.7005
17	978.597	71.072	18	915.058	79.4939
19	767.53	60.1795	20	753.066	71.0168
21	701.962	85.3675	22	624.823	83.1985

5. IR spectrum of 8

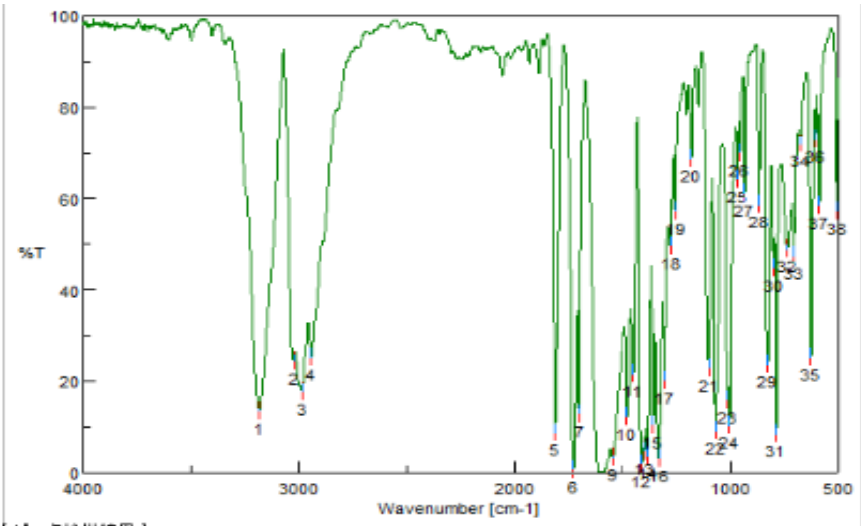

[ピーク検出結果]

No.	位置	強度	No.	位置	強度
1	3183.9	13.4243	2	3024.8	24.4453
3	2986.23	17.7465	4	2943.8	25.1934
5	1811.79	8.56892	6	1726.94	0.569715
7	1701.87	12.8288	8	1593.88	0.00219288
9	1544.7	3.21478	10	1480.1	12.2342
11	1449.24	21.4811	12	1410.67	1.92974
13	1399.1	4.56546	14	1384.64	3.53715
15	1357.64	10.3795	16	1332.57	3.08218
17	1305.57	20.1314	18	1278.57	49.6266
19	1255.43	57.2394	20	1180.22	58.6849
21	1089.23	22.8735	22	1058.37	9.0496
23	1012.45	15.8942	24	1003.77	10.2525
25	967.126	64.3411	26	955.555	70.0276
27	932.414	61.1238	28	865.882	58.6246
29	825.384	23.6139	30	799.35	44.7777
31	765.85	8.41047	32	735.71	48.01
33	704.855	47.4521	34	673.999	71.9759
35	624.823	25.1336	36	602.546	72.9362
37	587.218	58.5232	38	505.223	57.2564

6. IR spectrum of 9

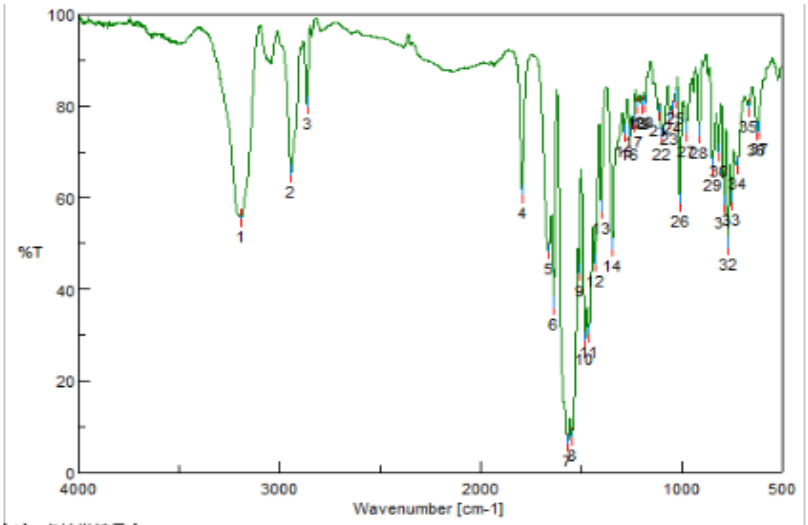

[ピーク検出結果]

No.	位置	強度	No.	位置	強度
1	3193.54	55.4459	2	2944.77	65.1008
3	2863.77	80.0067	4	1793.47	60.6537
5	1651.37	48.2263	6	1635.34	36.1302
7	1566.88	6.35557	8	1545.67	7.61067
9	1509.99	43.4401	10	1481.06	28.6307
11	1459.85	30.2499	12	1431.89	45.5713
13	1400.07	57.1614	14	1343.18	48.8866
15	1285.32	73.8955	16	1256.4	73.3845
17	1240	76.1969	18	1221.68	79.863
19	1197.58	80.0814	20	1181.19	80.2766
21	1115.62	78.5084	22	1097.3	73.3225
23	1059.69	76.7908	24	1045.23	79.205
25	1029.8	81.2097	26	1008.59	58.77
27	974.84	74.015	28	914.093	73.5433
29	844.669	66.6037	30	814.777	69.7719
31	789.707	58.4566	32	767.53	48.1936
33	751.138	59.191	34	724.139	67.0518
35	685.321	79.5248	36	625.788	74.3615
37	614.217	74.5273			

7. IR spectrum of P1

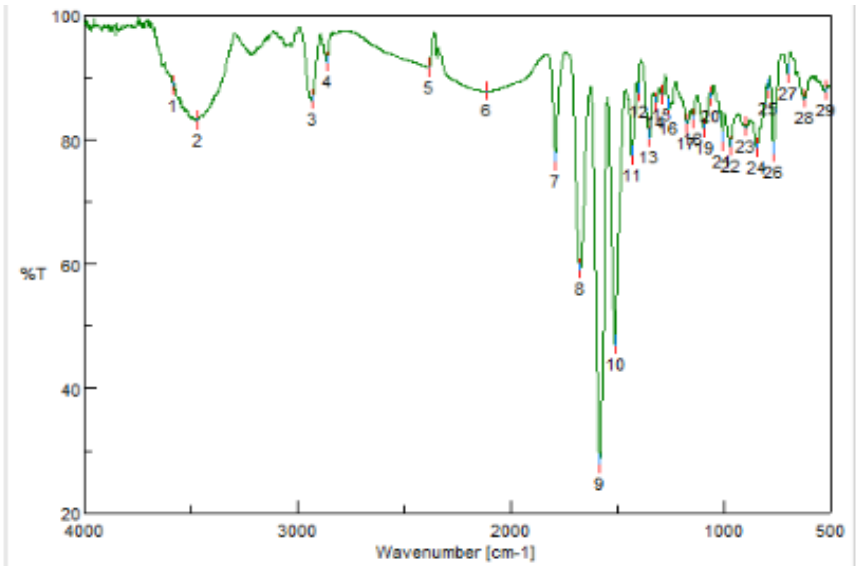

[ピーク検出結果]

No.	位置	強度	No.	位置	強度
1	3586.96	88.5795	2	3470.28	83.1437
3	2933.2	86.3396	4	2862.81	92.4678
5	2385.51	91.5877	6	2114.56	87.8046
7	1790.58	76.5266	8	1673.91	59.1902
9	1582.31	27.8646	10	1509.99	45.9173
11	1431.89	77.4815	12	1402	87.5495
13	1346.96	80.3171	14	1319.07	86.07
15	1289.18	87.1923	16	1257.36	85.0717
17	1174.44	82.5185	18	1143.58	83.4175
19	1093.44	81.8672	20	1059.69	86.3111
21	1006.56	79.5725	22	969.055	78.9316
23	895.773	81.9826	24	844.669	78.7426
25	793.564	88.1229	26	767.53	77.9247
27	701.952	90.5244	28	620.966	86.5721
29	523.579	87.8294			

8. IR spectrum of P2

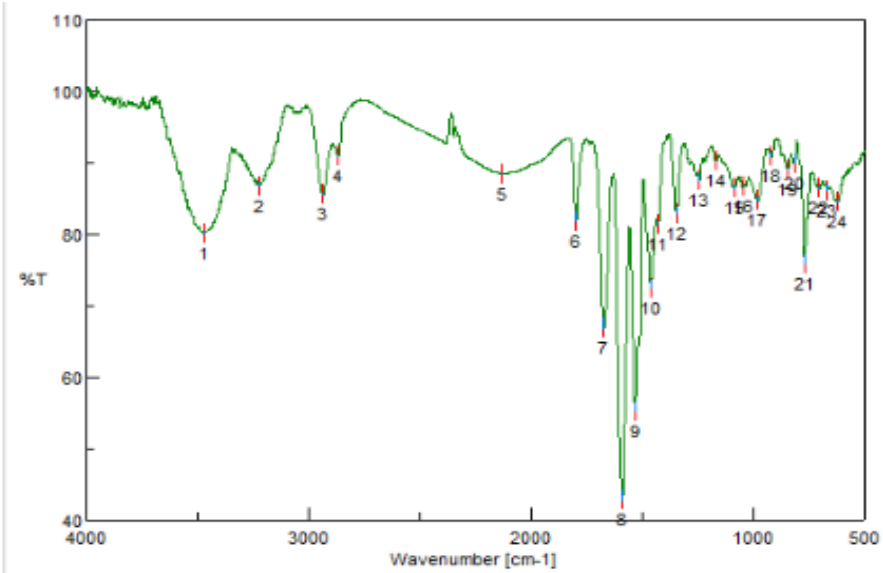

[ピーク検出結果]

No.	位置	強度	No.	位置	強度
1	3470.28	80.0691	2	3223.43	86.5718
3	2936.09	85.5384	4	2866.67	90.805
5	2128.06	88.3724	6	1797.33	81.8277
7	1671.98	66.8286	8	1589.06	42.7466
9	1530.24	55.1743	10	1458.89	72.4563
11	1428.03	81.3997	12	1345.11	82.8846
13	1240.97	87.4672	14	1169.65	90.1889
15	1084.76	86.3884	16	1043.3	86.5627
17	979.661	84.639	18	917.95	90.8766
19	843.704	89.0147	20	814.777	89.8904
21	767.53	75.8393	22	702.926	86.3912
23	665.321	86.019	24	619.038	84.4789

9. IR spectrum of PL

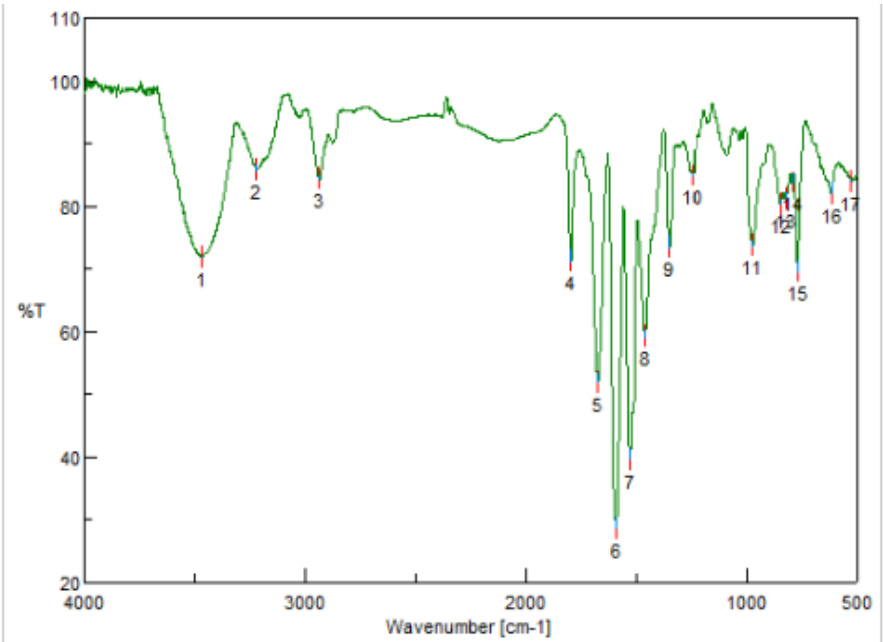

[ピーク検出結果]

No.	位置	強度	No.	位置	強度
1	3469.31	71.8357	2	3222.47	85.6919
3	2935.13	84.3337	4	1797.33	71.1919
5	1673.91	51.7856	6	1590.02	28.6055
7	1529.27	39.4755	8	1459.85	59.1267
9	1348.96	73.2865	10	1242.9	84.7687
11	973.876	73.6627	12	846.597	80.3105
13	823.455	81.1206	14	793.564	83.6658
15	768.494	69.5388	16	617.109	81.9132
17	529.364	83.8095			

C.3 HPLC analysis for asymmetric Michael adducts

1. Chromatogram data for different Michael adducts in Table 3.2

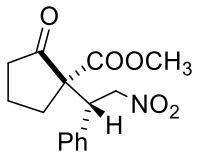

13 (2*S*, 3*R*)

Table 3.2, entry 1: 98% ee

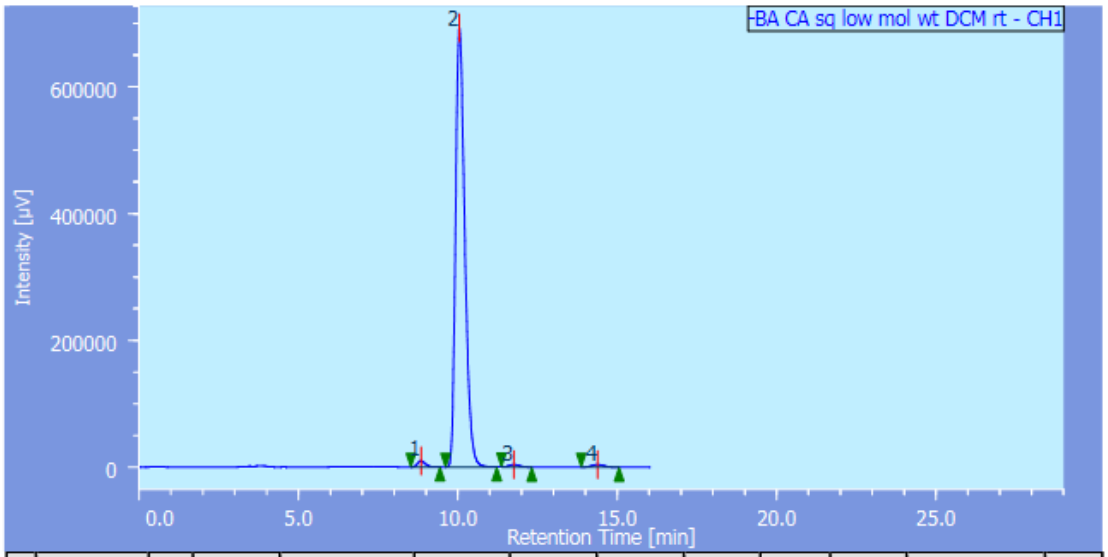

#	ピーク名	CH	tR [min]	面積 [μV·sec]	高さ [μV]	面積%	高さ%	定量値	NTP	分離度	シンメトリー係数	警告
1	Unknown	1	8.842	167078	9779	1.167	1.377	N/A	6453	2.491	1.313	
2	Unknown	1	10.042	13952506	692198	97.424	97.463	N/A	5835	3.113	1.362	
3	Unknown	1	11.758	85532	3927	0.597	0.553	N/A	6576	4.041	1.128	
4	Unknown	1	14.375	116268	4310	0.812	0.607	N/A	6407	N/A	1.124	

Table 3.2, entry 2: 98% ee

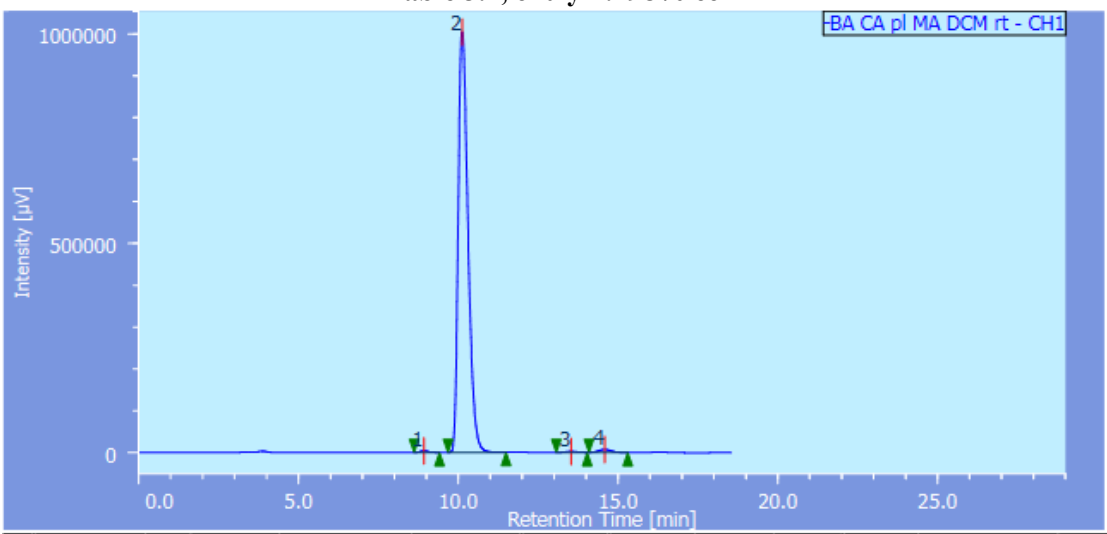

#	ピーク名	CH	tR [min]	面積 [μV·sec]	高さ [μV]	面積%	高さ%	定量値	NTP	分離度	シンメトリー係数	警告
1	Unknown	1	8.925	67752	4031	0.312	0.396	N/A	6625	2.403	1.256	
2	Unknown	1	10.117	21373749	1003501	98.484	98.645	N/A	5301	5.435	1.422	
3	Unknown	1	13.525	63084	2433	0.291	0.239	N/A	5945	1.482	1.060	
4	Unknown	1	14.575	198072	7316	0.913	0.719	N/A	6566	N/A	1.130	

Table 3.2, entry 3: 98% ee

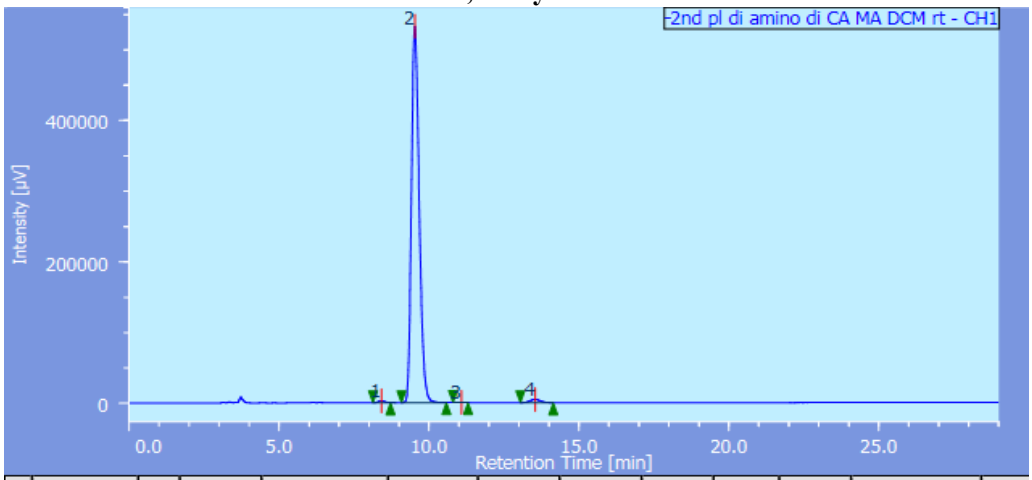

#	ピーク名	CH	tR [min]	面積 [μV·sec]	高さ [μV]	面積%	高さ%	定量値	NTP	分離度	シンメトリー係数	警告
1	Unknown	1	8.408	39884	2694	0.410	0.499	N/A	7150	2.580	1.113	
2	Unknown	1	9.525	9564741	532161	98.319	98.548	N/A	6565	3.292	1.267	
3	Unknown	1	11.075	7765	475	0.080	0.088	N/A	8732	4.361	0.922	
4	Unknown	1	13.533	115902	4672	1.191	0.865	N/A	6800	N/A	1.091	

Table 3.2, entry 4: 98% ee

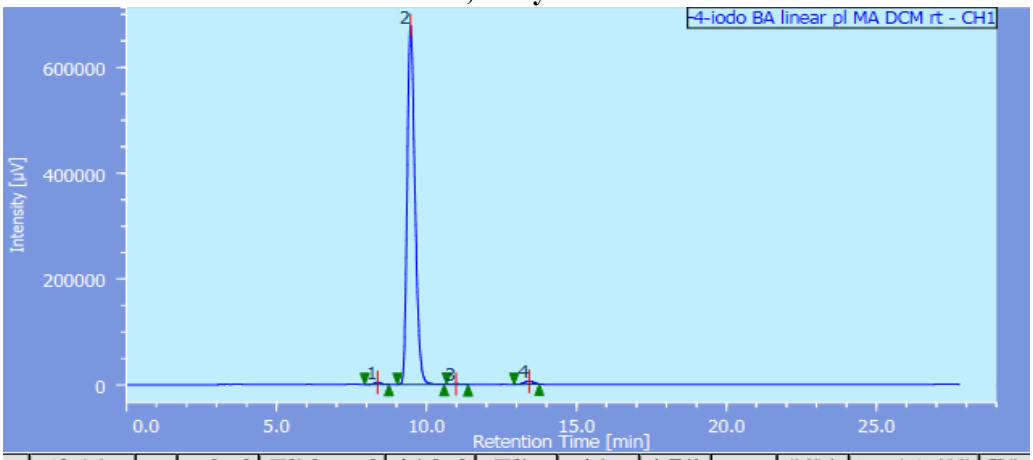

#	ピーク名	CH	tR [min]	面積 [μV·sec]	高さ [μV]	面積%	高さ%	定量値	NTP	分離度	シンメトリー係数	警告
1	Unknown	1	8.367	60919	4070	0.490	0.591	N/A	7284	2.552	1.111	
2	Unknown	1	9.467	12236881	678051	98.335	98.419	N/A	6430	3.088	1.272	
3	Unknown	1	10.975	20334	1079	0.163	0.157	N/A	7493	4.417	1.133	
4	Unknown	1	13.417	125899	5744	1.012	0.834	N/A	7963	N/A	0.949	

Table 3.2, entry 5: 99% ee

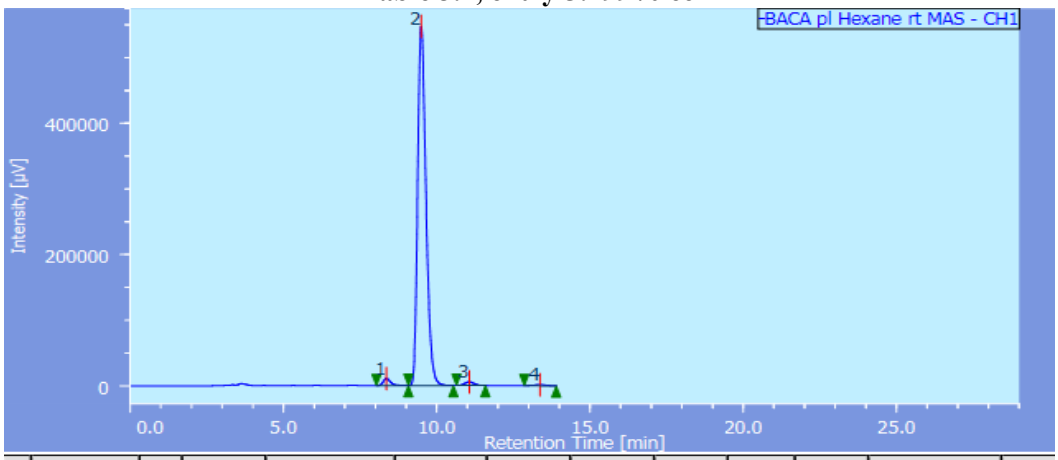

#	ピーク名	CH	tR [min]	面積 [μV·sec]	高さ [μV]	面積%	高さ%	定量値	NTP	分離度	シンメトリー係数	警告
1	Unknown	1	8.358	190423	10863	1.788	1.924	N/A	6164	2.480	1.709	
2	Unknown	1	9.492	10300765	546489	96.717	96.798	N/A	5988	3.013	1.308	
3	Unknown	1	11.058	116970	5570	1.098	0.987	N/A	6416	3.741	1.103	
4	Unknown	1	13.358	42243	1643	0.397	0.291	N/A	6162	N/A	1.002	

Table 3.2, entry 6: >99% ee

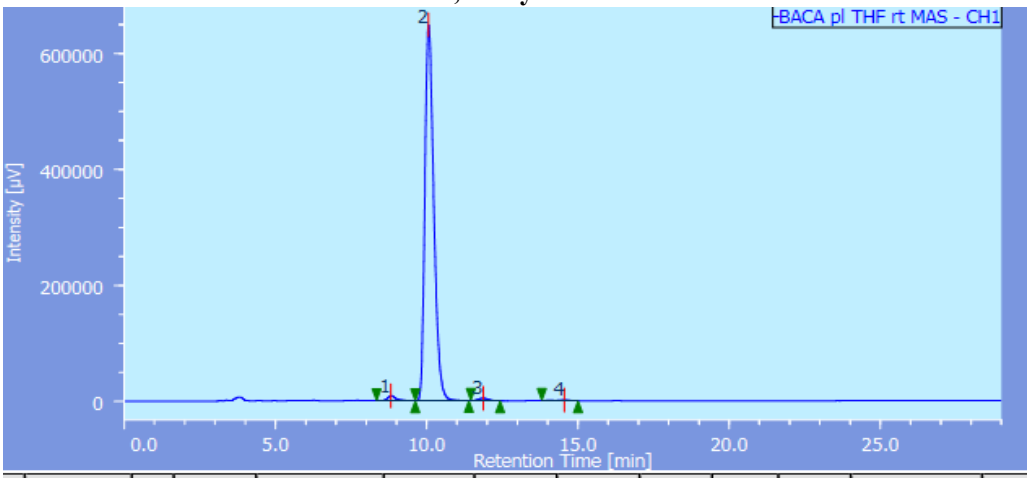

#	ピーク名	CH	tR [min]	面積 [μV·sec]	高さ [μV]	面積%	高さ%	定量値	NTP	分離度	シンメトリー係数	警告
1	Unknown	1	8.817	166578	8595	1.226	1.298	N/A	5974	2.513	1.441	
2	Unknown	1	10.058	13279435	647949	97.736	97.865	N/A	5665	3.223	1.349	
3	Unknown	1	11.867	96283	4313	0.709	0.651	N/A	6458	2.916	1.111	
4	Unknown	1	14.550	44703	1227	0.329	0.185	N/A	2153	N/A	0.782	

Table 3.2, entry 7 : >99% ee

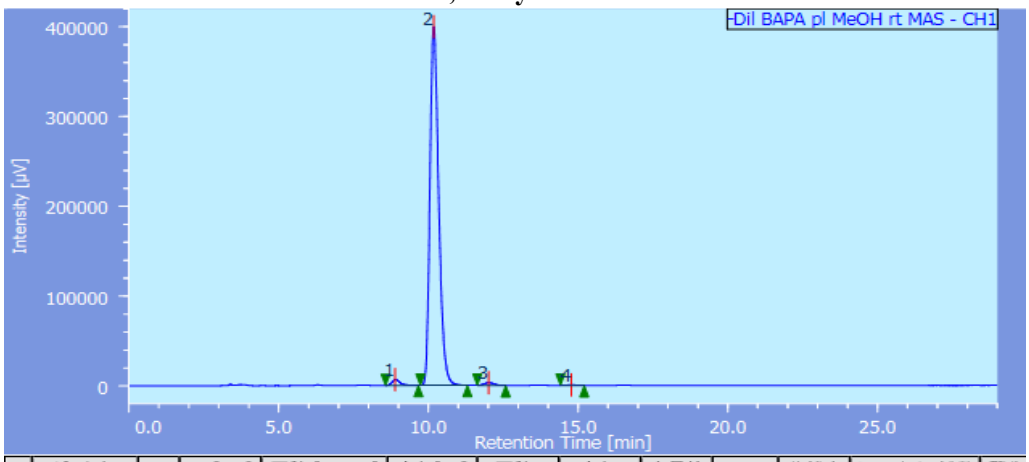

#	ピーク名	CH	tR [min]	面積 [μV·sec]	高さ [μV]	面積%	高さ%	定量値	NTP	分離度	シンメトリー係数	警告
1	Unknown	1	8.892	123750	6591	1.485	1.611	N/A	5966	2.600	1.512	
2	Unknown	1	10.175	8126711	399026	97.517	97.502	N/A	5908	3.244	1.299	
3	Unknown	1	12.008	67909	3007	0.815	0.735	N/A	6327	4.304	1.160	
4	Unknown	1	14.767	15300	625	0.184	0.153	N/A	7513	N/A	1.085	

Table 3.2, entry 8 : >99% ee

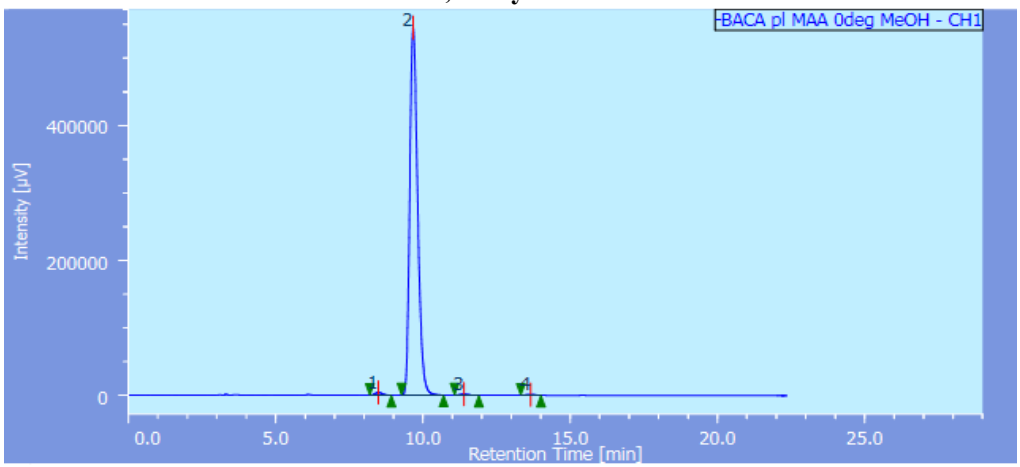

#	ピーク名	CH	tR [min]	面積 [μV·sec]	高さ [μV]	面積%	高さ%	定量値	NTP	分離度	シンメトリー係数	警告
1	Unknown	1	8.483	69014	4240	0.670	0.769	N/A	6533	2.619	1.267	
2	Unknown	1	9.667	10164480	544388	98.729	98.693	N/A	6321	3.352	1.278	
3	Unknown	1	11.392	35759	1765	0.347	0.320	N/A	6974	3.968	1.179	
4	Unknown	1	13.658	26079	1202	0.253	0.218	N/A	8292	N/A	0.996	

Table 3.2, entry 9: 98% ee

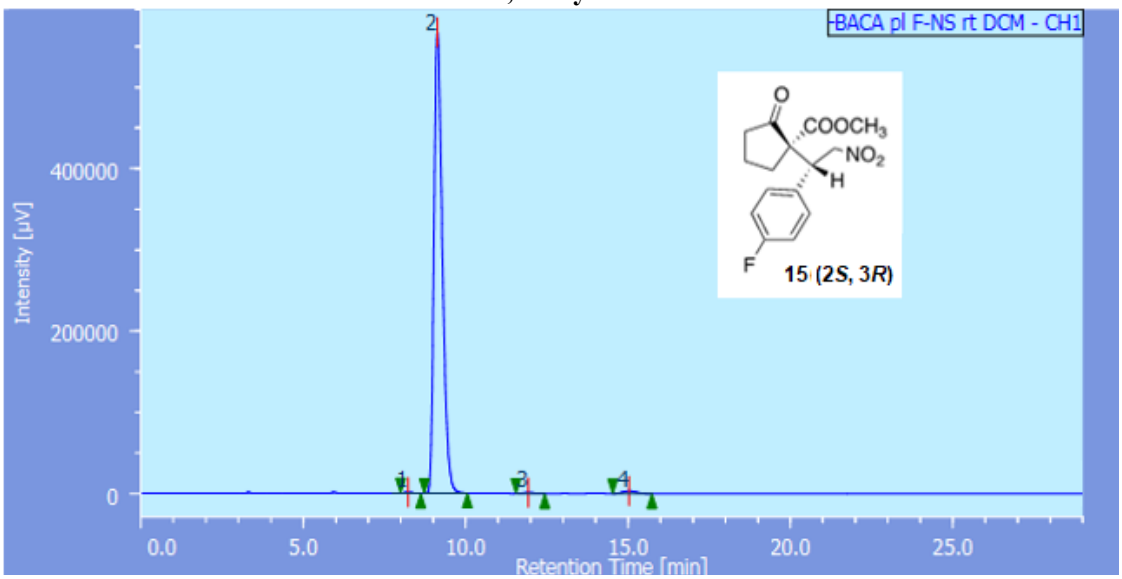

Table 3.2, entry 10 : 91% ee

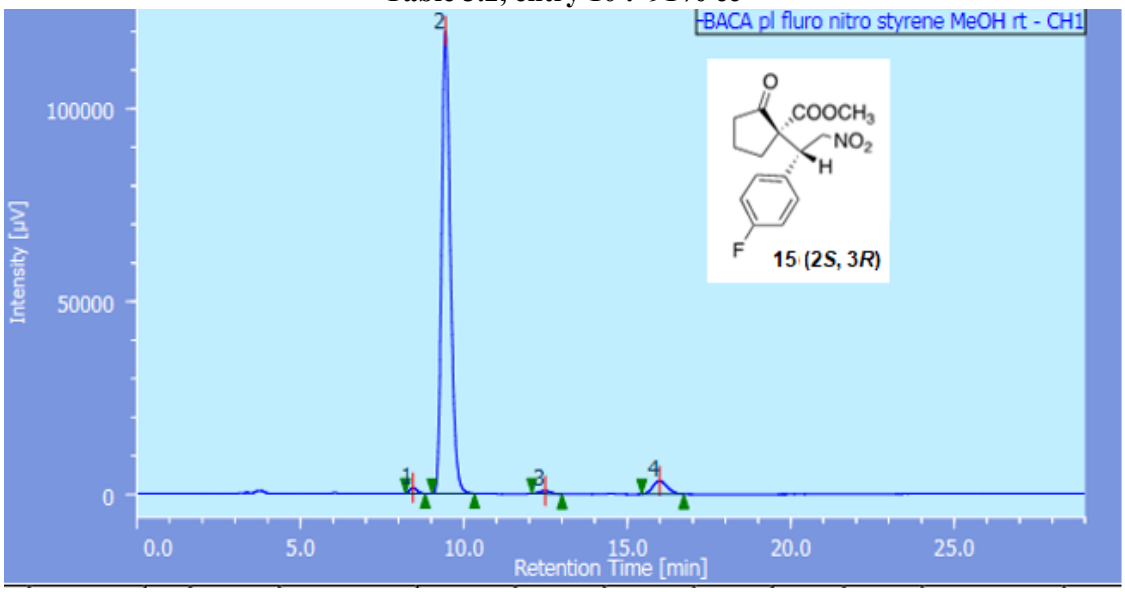

Table 3.2, entry 11: 98% ee

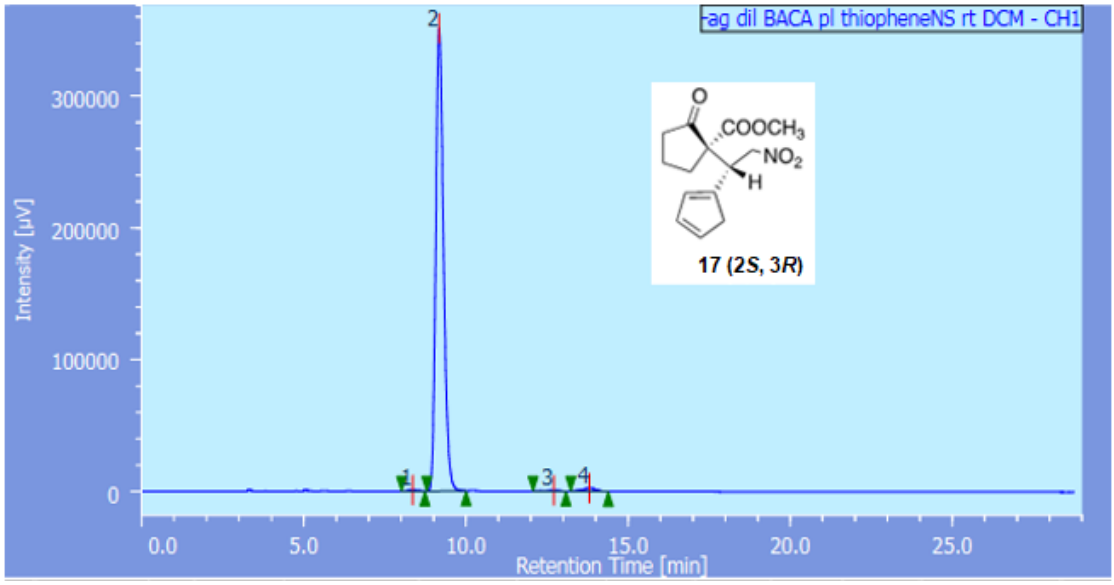

Table 3.2, entry 12: 94% ee

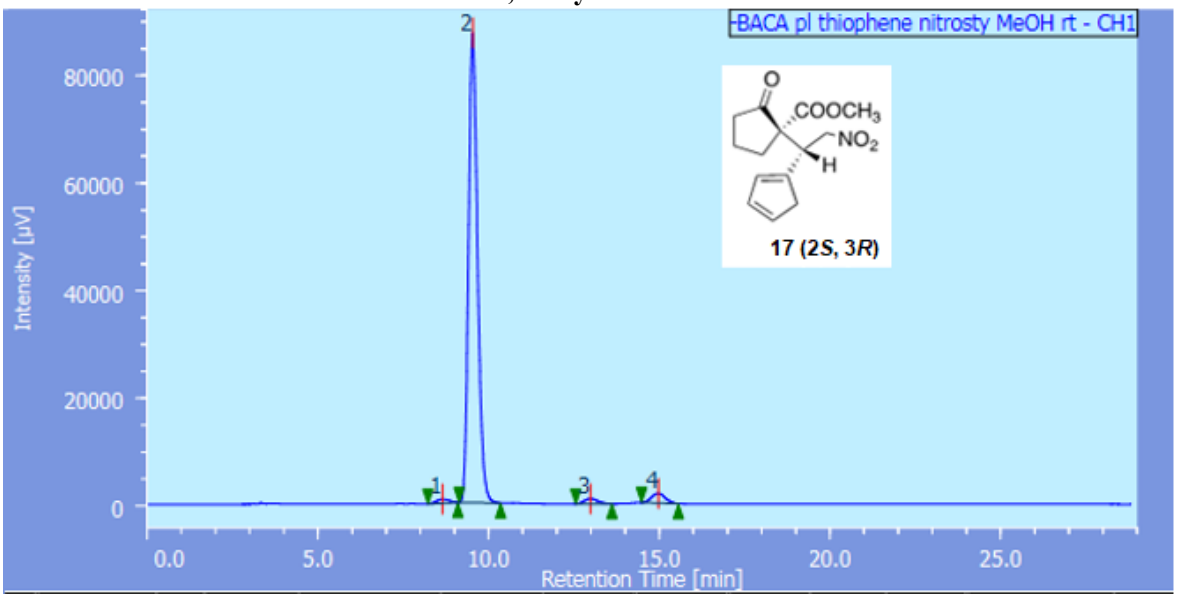

2. Chromatogram data for 13 in recyclability evaluation of P1 (Table 3.3)

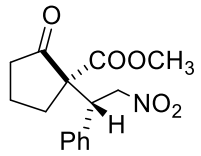

13 (2*S*, 3*R*)

Table 3.3, fresh polymer: >99% ee

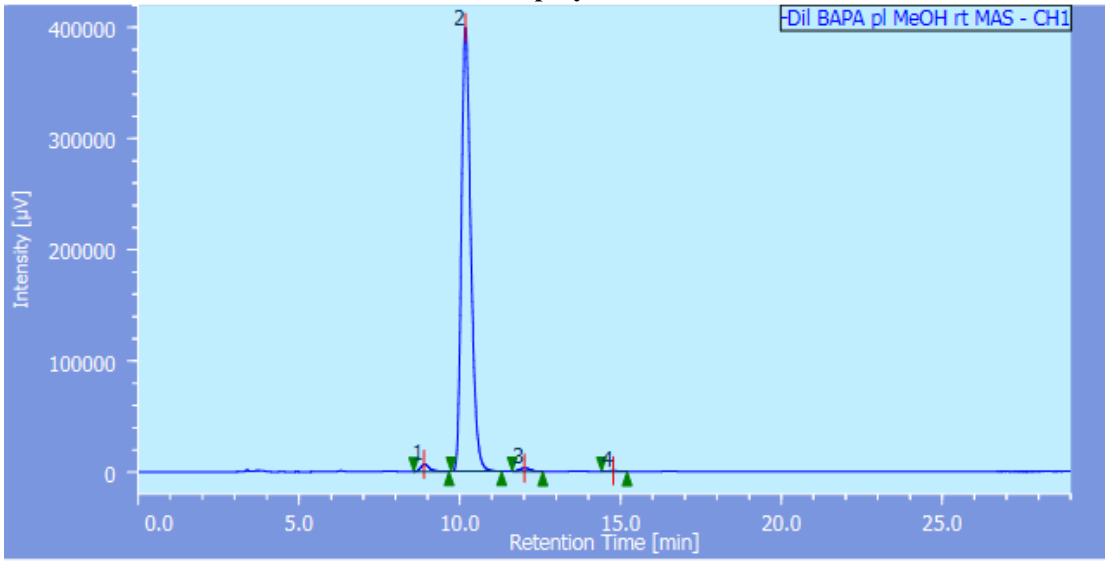

#	ピーク名	CH	tR [min]	面積 [μV·sec]	高さ [μV]	面積%	高さ%	定量値	NTP	分離度	シンメトリー係数	警告
1	Unknown	1	8.892	123750	6591	1.485	1.611	N/A	5966	2.600	1.512	
2	Unknown	1	10.175	8126711	399026	97.517	97.502	N/A	5908	3.244	1.299	
3	Unknown	1	12.008	67909	3007	0.815	0.735	N/A	6327	4.304	1.160	
4	Unknown	1	14.767	15300	625	0.184	0.153	N/A	7513	N/A	1.085	

Table 3.3, cycle 1: 92% ee

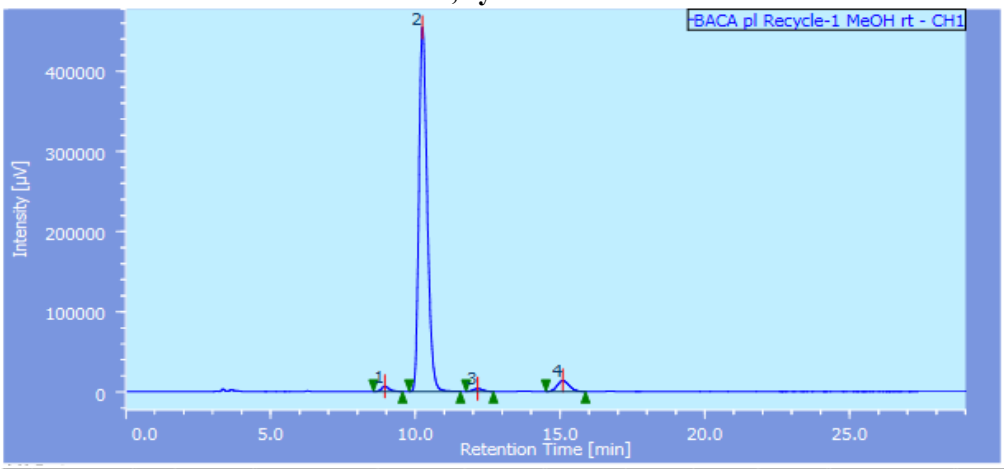

#	ピーク名	CH	tR [min]	面積 [μV·sec]	高さ [μV]	面積%	高さ%	定量値	NTP	分離度	シンメトリー係数	警告
1	Unknown	1	8.942	120392	6585	1.251	1.379	N/A	6190	2.676	1.321	
2	Unknown	1	10.242	9035887	453656	93.882	95.013	N/A	6216	3.454	1.295	
3	Unknown	1	12.150	79448	3573	0.825	0.748	N/A	6821	4.406	1.127	
4	Unknown	1	15.092	388998	13653	4.042	2.860	N/A	6469	N/A	1.135	

Table 3.3, cycle 2: 94% ee

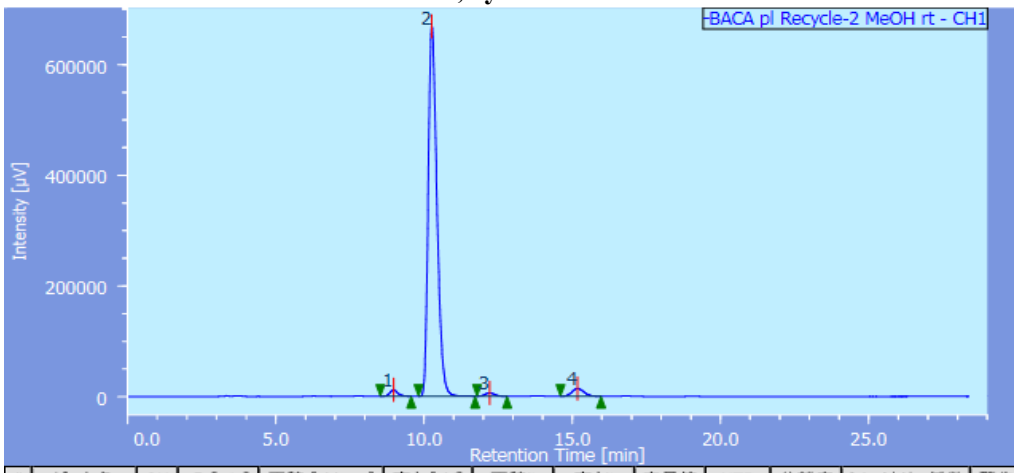

#	ピーク名	CH	tR [min]	面積 [μV·sec]	高さ [μV]	面積%	高さ%	定量値	NTP	分離度	シンメトリー係数	警告
1	Unknown	1	8.967	221463	11955	1.535	1.707	N/A	6025	2.601	1.205	
2	Unknown	1	10.258	13660153	667990	94.682	95.389	N/A	5909	3.460	1.347	
3	Unknown	1	12.208	137384	6105	0.952	0.872	N/A	6703	4.394	1.132	
4	Unknown	1	15.175	408378	14230	2.831	2.032	N/A	6420	N/A	1.128	

Table 3.3, cycle 3: 99% ee

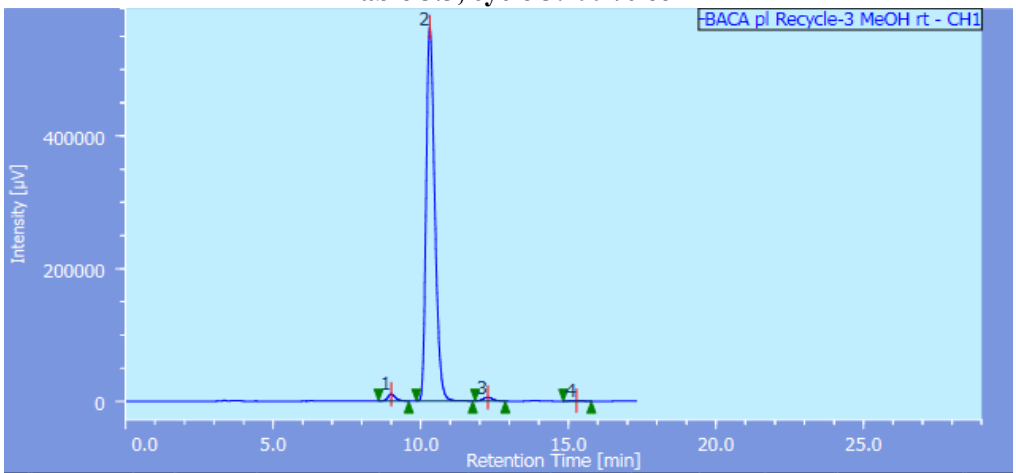

#	ピーク名	CH	tR [min]	面積 [μV·sec]	高さ [μV]	面積%	高さ%	定量値	NTP	分離度	シンメトリー係数	警告
1	Unknown	1	9.000	192160	10462	1.629	1.803	N/A	6085	2.627	1.238	
2	Unknown	1	10.300	11449018	563152	97.029	97.031	N/A	6026	3.500	1.332	
3	Unknown	1	12.267	128032	5668	1.085	0.977	N/A	6774	4.468	1.113	
4	Unknown	1	15.275	30318	1099	0.257	0.189	N/A	6568	N/A	1.055	

Table 3.3, cycle 4: 99% ee

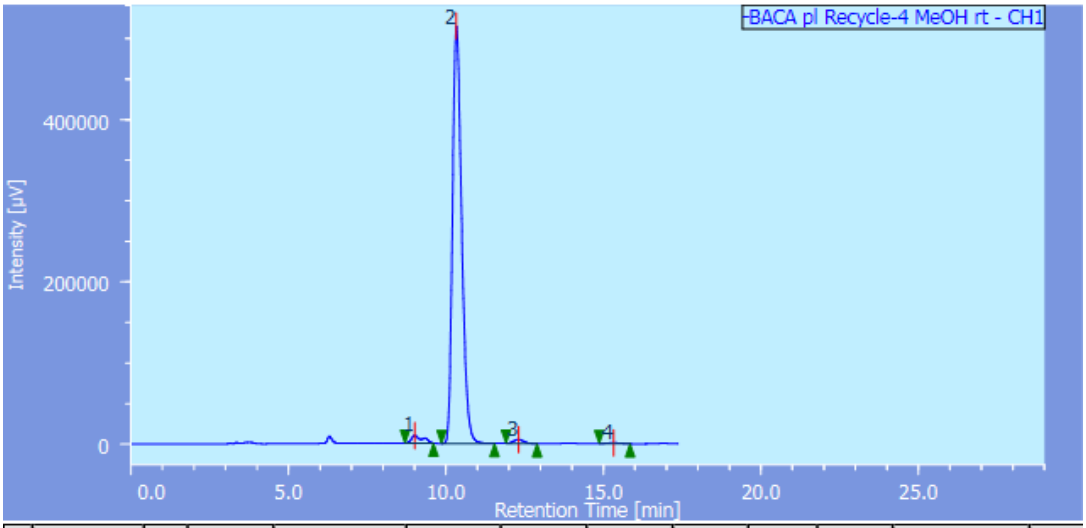

#	ピーク名	CH	tR [min]	面積 [μV·sec]	高さ [μV]	面積%	高さ%	定量値	NTP	分離度	シンメトリー係数	警告
1	Unknown	1	9.008	238080	9313	2.203	1.757	N/A	1688	1.877	1.600	
2	Unknown	1	10.325	10425282	514424	96.459	97.066	N/A	6090	3.537	1.316	
3	Unknown	1	12.300	111563	5034	1.032	0.950	N/A	6942	4.492	1.123	
4	Unknown	1	15.317	33065	1202	0.306	0.227	N/A	6566	N/A	1.058	

3. Chromatogram data for asymmetric adduct 18, 20 in Table 4

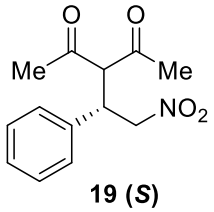

19 (*S*)

Table 3.4, entry 1: 36% ee

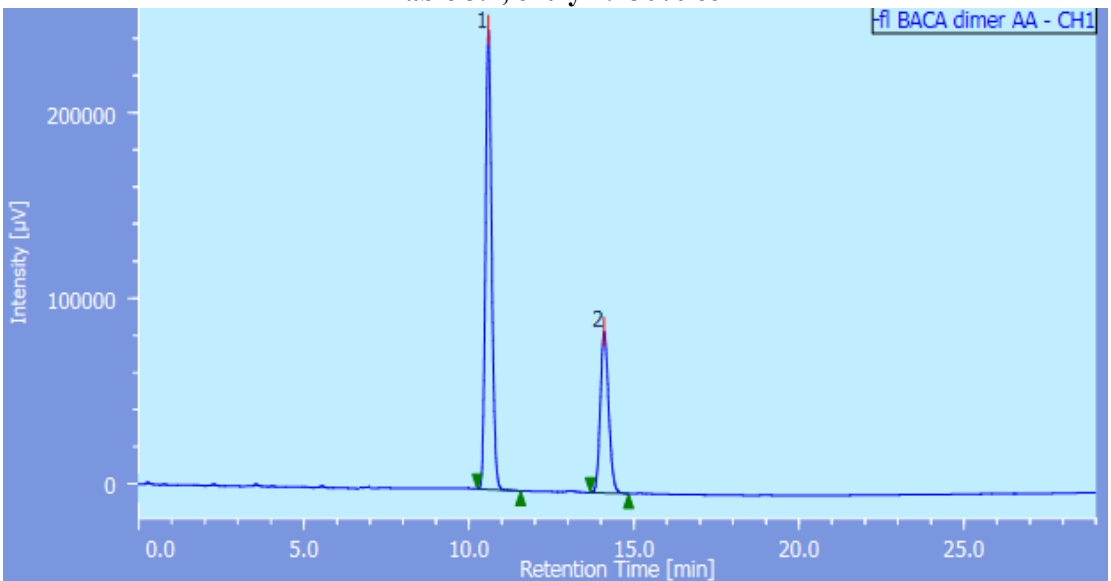

#	ピーク名	CH	tR [min]	面積 [μV·sec]	高さ [μV]	面積%	高さ%	定量値	NTP	分離度	シンメトリー係数	警告
1	Unknown	1	10.583	3254810	247529	68.048	74.082	N/A	15165	8.729	1.163	
2	Unknown	1	14.092	1528291	86599	31.952	25.918	N/A	14873	N/A	1.156	

Table 3.4, entry 2: 76% ee

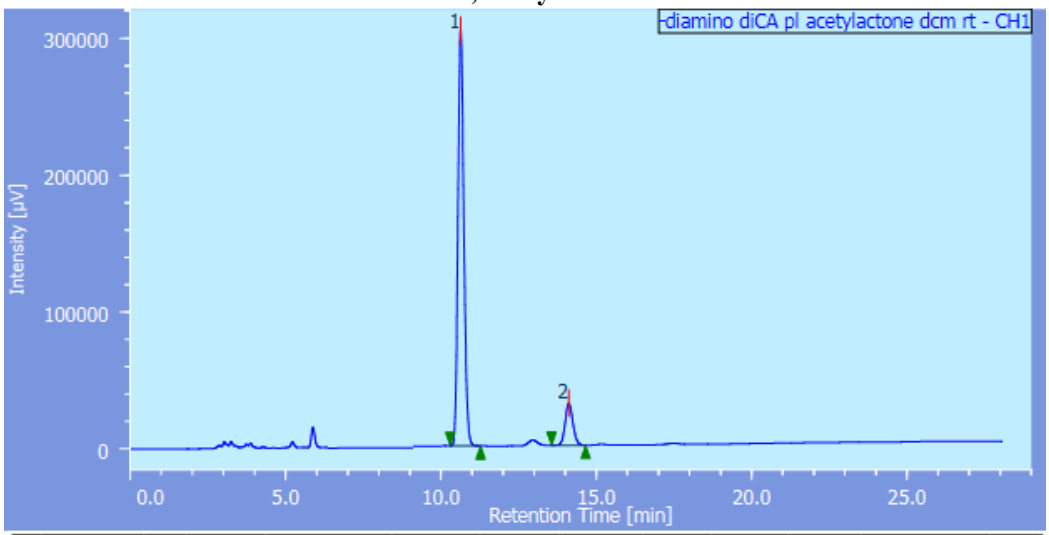

#	ピーク名	CH	tR [min]	面積 [μV·sec]	高さ [μV]	面積%	高さ%	定量値	NTP	分離度	シンメトリー係数	警告
1	Unknown	1	10.633	3989399	303841	88.132	90.811	N/A	15363	8.733	1.140	
2	Unknown	1	14.108	537195	30744	11.868	9.189	N/A	15395	N/A	1.118	

Table 3.4, entry 3: 95% ee

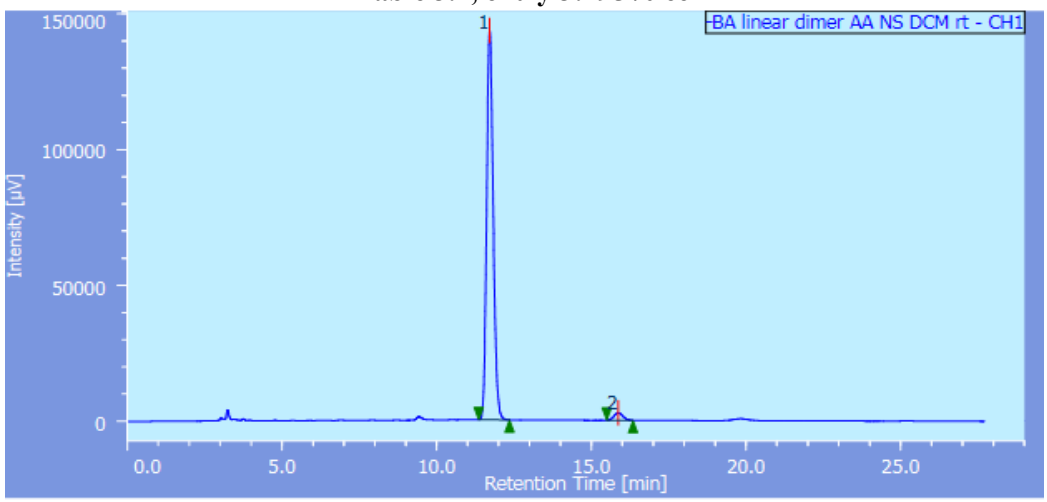

#	ピーク名	CH	tR [min]	面積 [μV·sec]	高さ [μV]	面積%	高さ%	定量値	NTP	分離度	シンメトリー係数	警告
1	Unknown	1	11.708	2113046	143265	97.491	98.123	N/A	14794	9.136	1.169	
2	Unknown	1	15.867	54374	2741	2.509	1.877	N/A	14462	N/A	1.099	

Table 3.4, entry 4: 81% ee

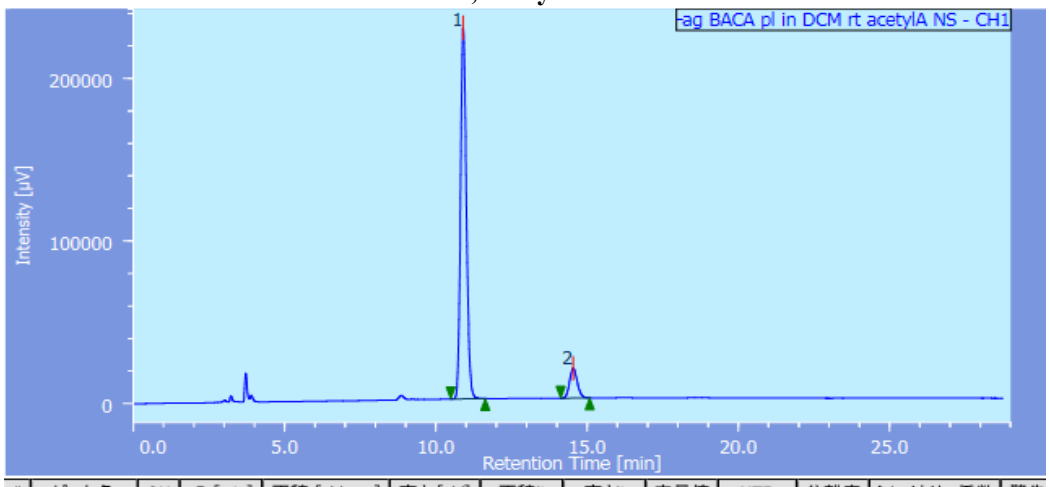

#	ピーク名	CH	tR [min]	面積 [μV·sec]	高さ [μV]	面積%	高さ%	定量値	NTP	分離度	シンメトリー係数	警告
1	Unknown	1	10.900	3060703	228311	90.350	92.573	N/A	15540	8.914	1.159	
2	Unknown	1	14.533	326893	18317	9.650	7.427	N/A	15456	N/A	1.144	

Table 3.4, entry 5: 58% ee

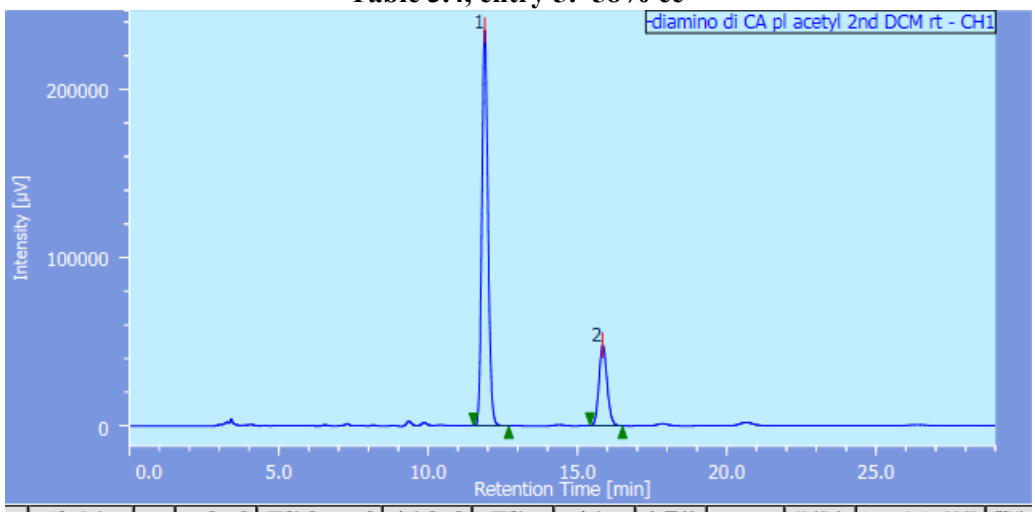

#	ピーク名	CH	tR [min]	面積 [μV·sec]	高さ [μV]	面積%	高さ%	定量値	NTP	分離度	シンメトリー係数	警告
1	Unknown	1	11.892	3371712	235191	78.777	83.115	N/A	16135	9.073	1.142	
2	Unknown	1	15.842	908377	47780	21.223	16.885	N/A	16152	N/A	1.147	

Table 3.4, entry 6: 58% ee

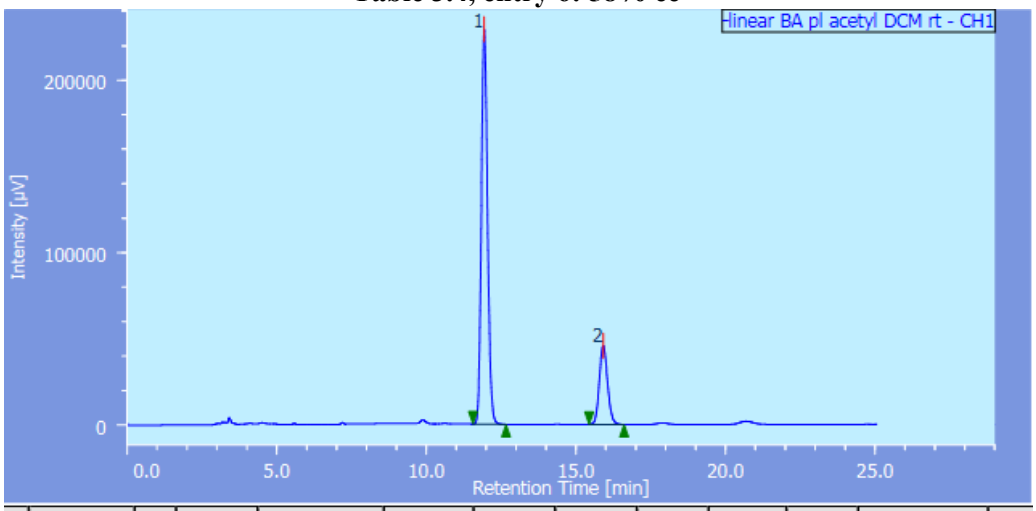

#	ピーク名	CH	tR [min]	面積 [μV·sec]	高さ [μV]	面積%	高さ%	定量値	NTP	分離度	シンメトリー係数	警告
1	Unknown	1	11.933	3300312	229050	79.047	83.368	N/A	16096	9.086	1.132	
2	Unknown	1	15.908	874835	45696	20.953	16.632	N/A	16128	N/A	1.120	

Table 3.4, entry 7: 85% ee

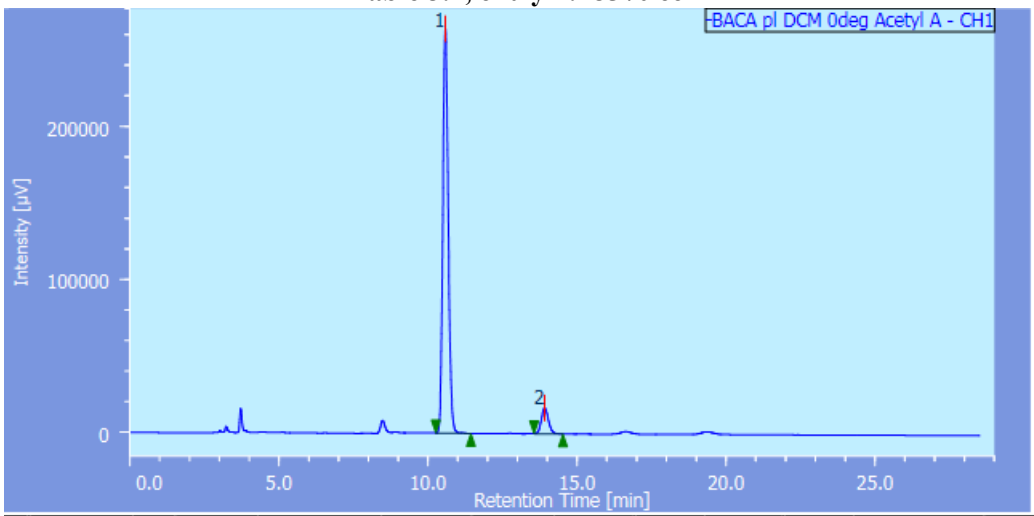

#	ピーク名	CH	tR [min]	面積 [μV·sec]	高さ [μV]	面積%	高さ%	定量値	NTP	分離度	シンメトリー係数	警告
1	Unknown	1	10.575	3345619	264293	92.293	94.002	N/A	16381	8.752	1.171	
2	Unknown	1	13.908	279375	16865	7.707	5.998	N/A	16487	N/A	1.153	

Table 3.4, entry 8: 77% ee

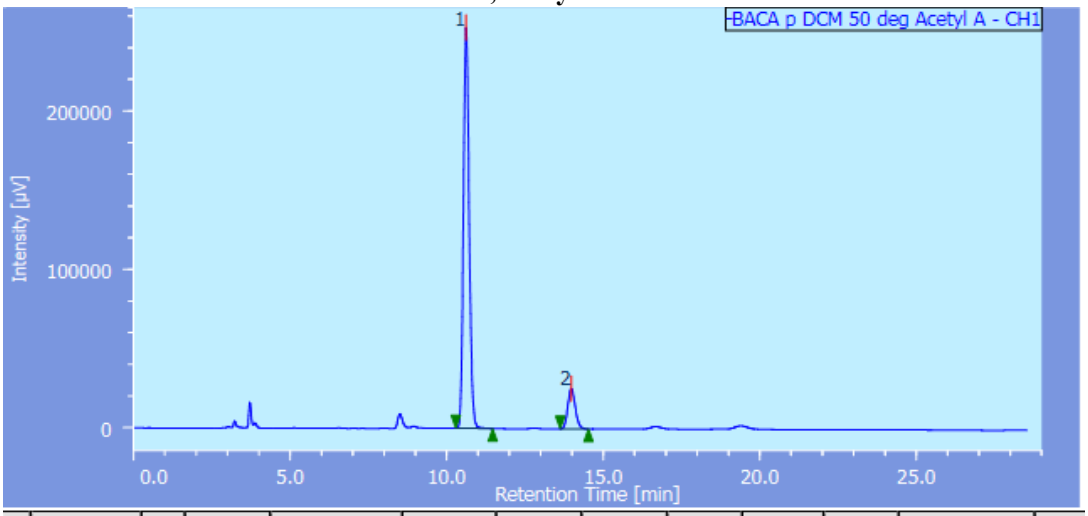

#	ピーク名	CH	tR [min]	面積 [μV·sec]	高さ [μV]	面積%	高さ%	定量値	NTP	分離度	シンメトリー係数	警告
1	Unknown	1	10.617	3215072	252918	88.347	90.834	N/A	16379	8.777	1.141	
2	Unknown	1	13.975	424070	25523	11.653	9.166	N/A	16478	N/A	1.137	

Table 3.4, entry 9: 33% ee

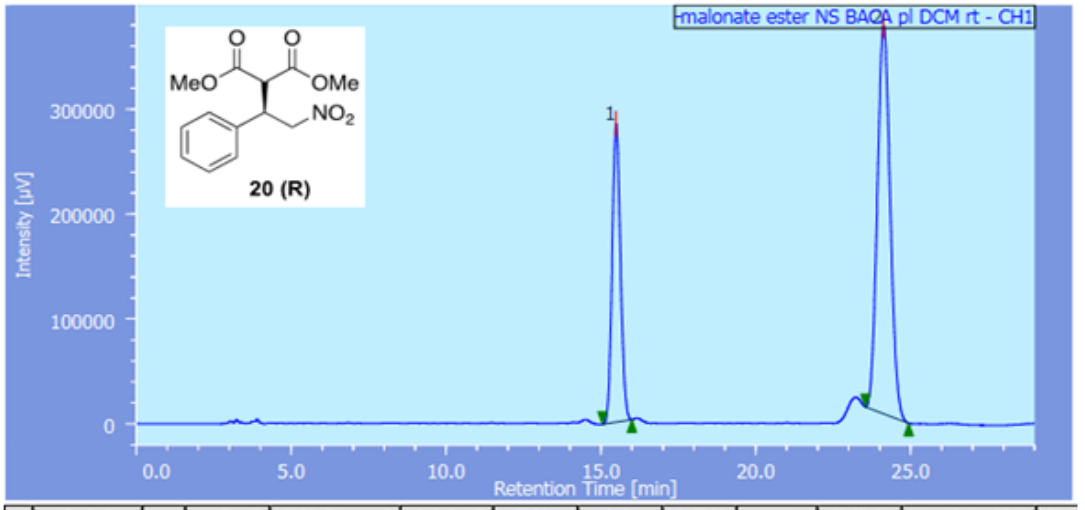

#	ピーク名	CH	tR [min]	面積 [μV·sec]	高さ [μV]	面積%	高さ%	定量値	NTP	分離度	シンメトリー係数	警告
1	Unknown	1	15.483	5325953	284457	33.302	43.456	N/A	15635	13.714	1.108	
2	Unknown	1	24.117	10666923	370125	66.698	56.544	N/A	15814	N/A	1.086	

Table 4, entry 10: 44% ee

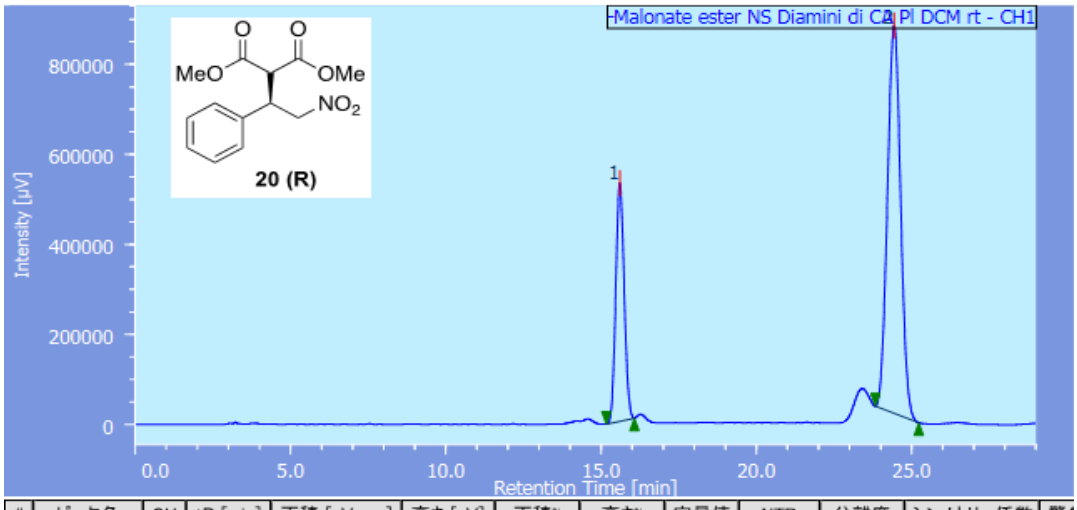

#	ピーク名	CH	tR [min]	面積 [μV·sec]	高さ [μV]	面積%	高さ%	定量値	NTP	分離度	シンメトリー係数	警
1	Unknown	1	15.600	9950436	528997	28.201	38.048	N/A	15575	13.767	1.074	
2	Unknown	1	24.425	25333360	861341	71.799	61.952	N/A	15471	N/A	1.037	

Table 3.4, entry 11: 61% ee

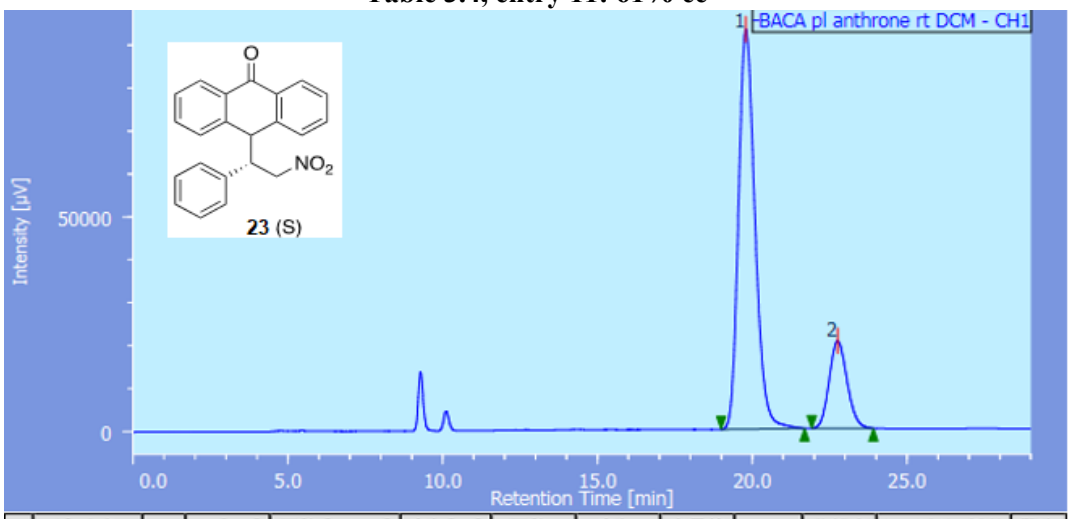

#	ピーク名	CH	tR [min]	面積 [μV·sec]	高さ [μV]	面積%	高さ%	定量値	NTP	分離度	シンメトリー係数	警告
1	Unknown	1	19.783	3437517	93134	80.693	82.051	N/A	6865	2.945	1.244	
2	Unknown	1	22.750	822474	20373	19.307	17.949	N/A	7301	N/A	1.129	

Table 3.4, entry 12: 16% ee

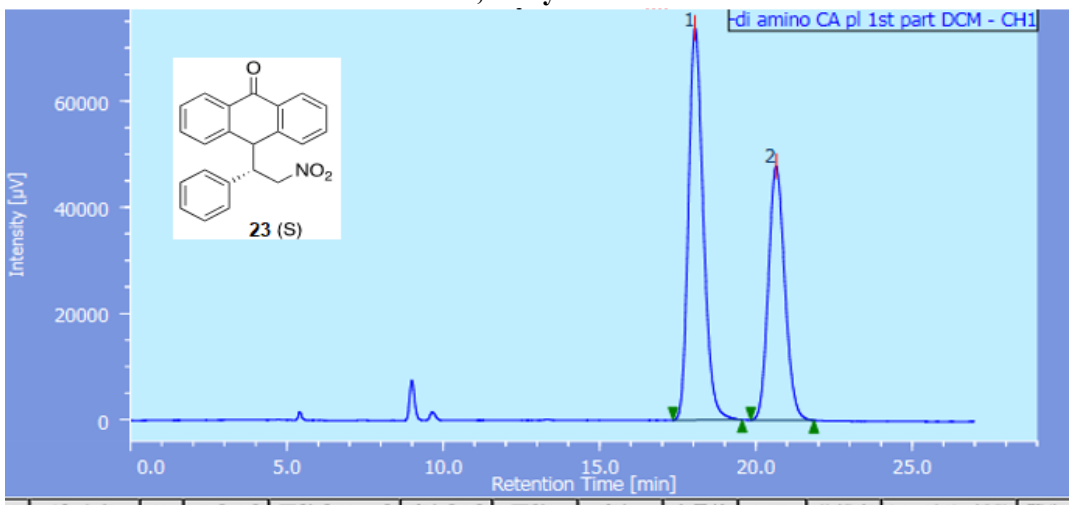

#	ピーク名	CH	tR [min]	面積 [μV·sec]	高さ [μV]	面積%	高さ%	定量値	NTP	分離度	シンメトリー係数	警告
1	Unknown	1	18.050	2433644	73802	58.157	60.696	N/A	7133	2.858	1.228	
2	Unknown	1	20.642	1750942	47790	41.843	39.304	N/A	7344	N/A	1.131	

Table 3.5, entry 13: 47% ee

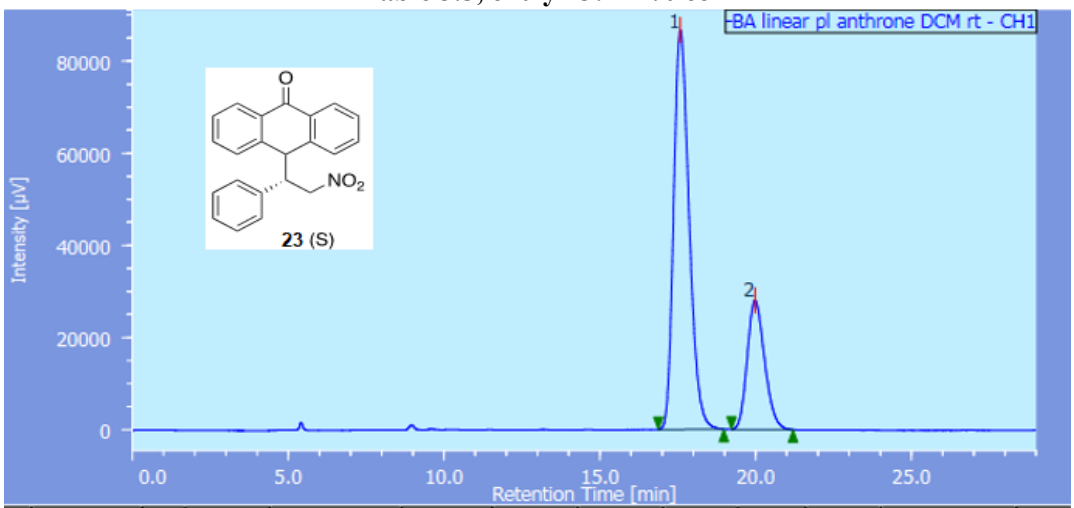

#	ピーク名	CH	tR [min]	面積 [μV·sec]	高さ [μV]	面積%	高さ%	定量値	NTP	分離度	シンメトリー係数	警告
1	Unknown	1	17.575	2996827	86697	73.366	75.569	N/A	6063	2.502	1.285	
2	Unknown	1	19.975	1087952	28029	26.634	24.431	N/A	6125	N/A	1.207	

Table 3.4, entry 14: 14% ee

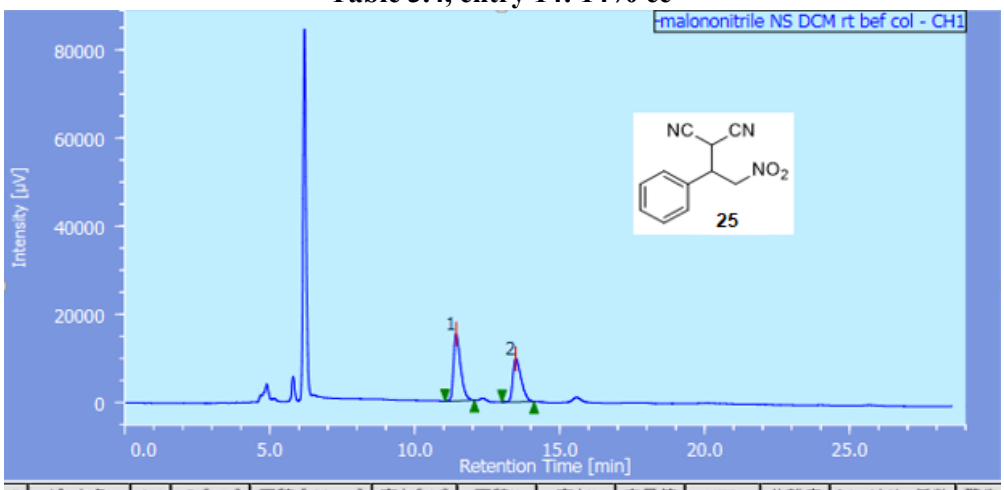

#	ピーク名	CH	tR [min]	面積 [μV·sec]	高さ [μV]	面積%	高さ%	定量値	NTP	分離度	シンメトリー係数	警告
1	Unknown	1	11.425	259765	15199	56.917	60.794	N/A	10790	4.272	1.543	
2	Unknown	1	13.483	196629	9802	43.083	39.206	N/A	10505	N/A	1.564	

5. Chromatogram data for Table 3.5

Table 3.5, entry 1: 7 % ee

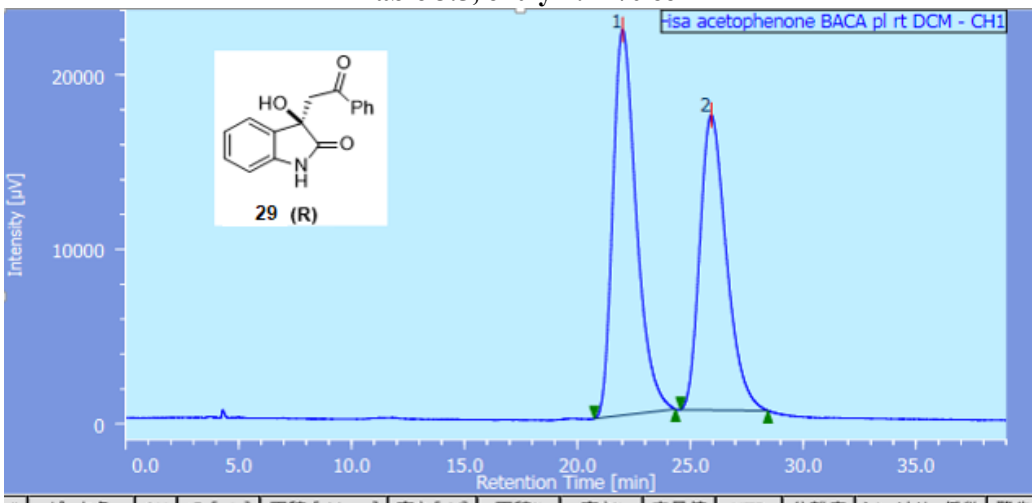

#	ピーク名	CH	tR [min]	面積 [μV·sec]	高さ [μV]	面積%	高さ%	定量値	NTP	分離度	シンメトリー係数	警告
1	Unknown	1	22.000	1597859	22085	53.609	56.676	N/A	2238	1.971	1.403	
2	Unknown	1	25.925	1382704	16882	46.391	43.324	N/A	2365	N/A	1.332	

Table 3.5, entry 2 : 4 % ee

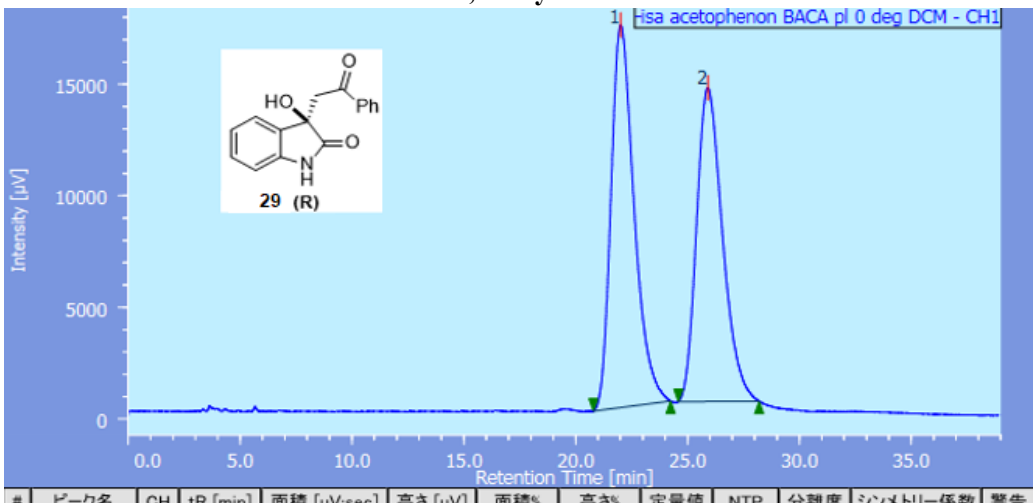

#	ピーク名	CH	tR [min]	面積 [μV·sec]	高さ [μV]	面積%	高さ%	定量値	NTP	分離度	シンメトリー係数	警告
1	Unknown	1	22.000	1235646	17139	52.104	54.943	N/A	2238	1.967	1.382	
2	Unknown	1	25.900	1135859	14055	47.896	45.057	N/A	2399	N/A	1.301	

Table 3.5, entry 3: Racemic

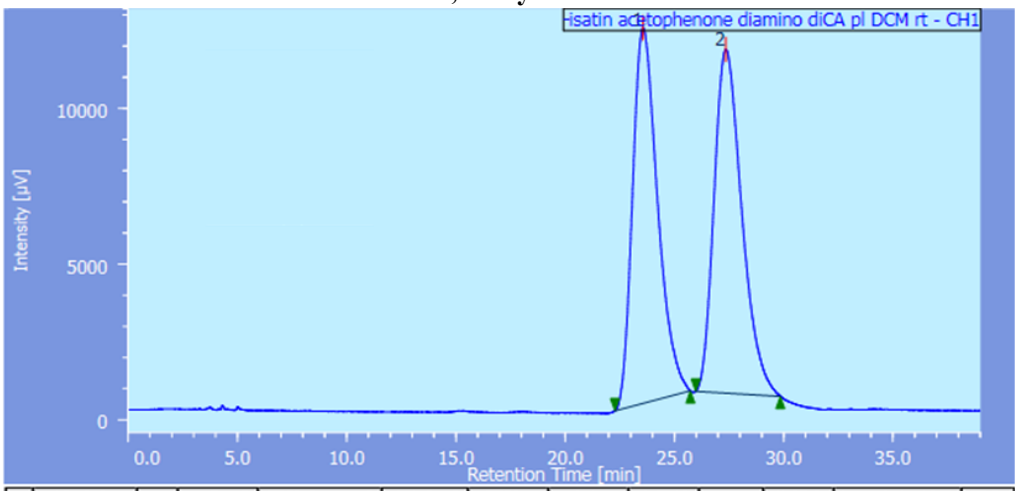

#	ピーク名	CH	tR [min]	面積 [μV·sec]	高さ [μV]	面積%	高さ%	定量値	NTP	分離度	シンメトリー係数	警告
1	Unknown	1	23.558	961579	12054	49.634	52.205	N/A	2050	1.727	1.355	
2	Unknown	1	27.342	975776	11036	50.366	47.795	N/A	2237	N/A	1.350	

Table 3.5, entry 4: 28% ee

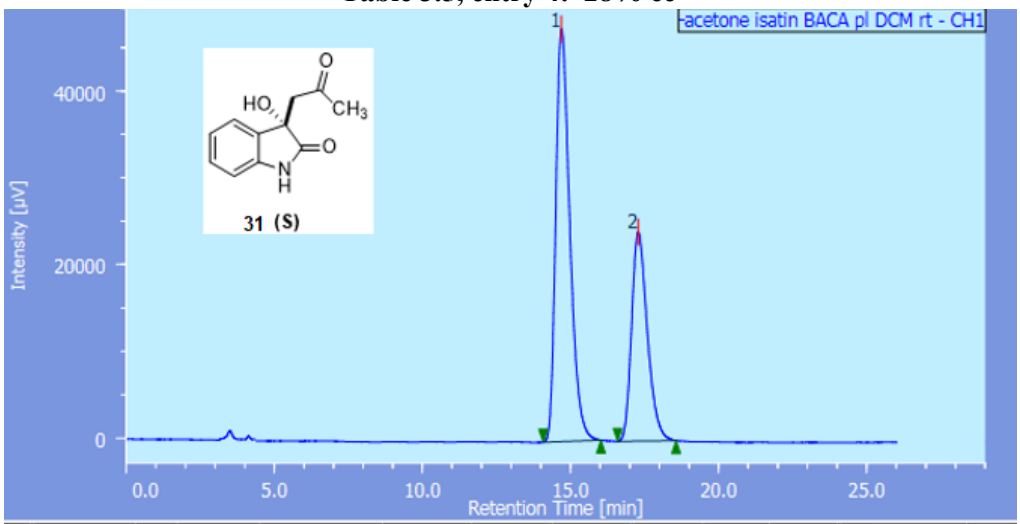

#	ピーク名	CH	tR [min]	面積 [μV·sec]	高さ [μV]	面積%	高さ%	定量値	NTP	分離度	シンメトリー係数	警告
1	Unknown	1	14.692	1566369	47523	63.749	66.394	N/A	4753	2.868	1.394	
2	Unknown	1	17.283	890710	24054	36.251	33.606	N/A	5187	N/A	1.320	

Table 6, entry 5: 6 % ee

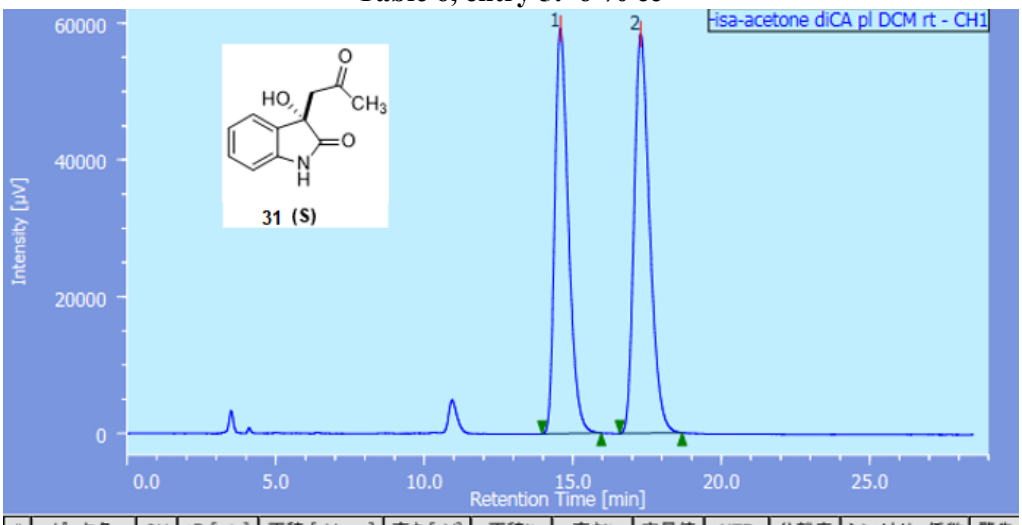

#	ピーク名	CH	tR [min]	面積 [μV·sec]	高さ [μV]	面積%	高さ%	定量値	NTP	分離度	シンメトリー係数	警告
1	Unknown	1	14.583	1894551	59229	47.115	50.384	N/A	4942	3.045	1.361	
2	Unknown	1	17.283	2126551	58327	52.885	49.616	N/A	5316	N/A	1.321	

Appendix D

Supporting Information for Chapter 4

D.1 ^{1}H and ^{13}C NMR data for monomers and polymers

^{1}H NMR spectrum of 3 in $CDCl_3$

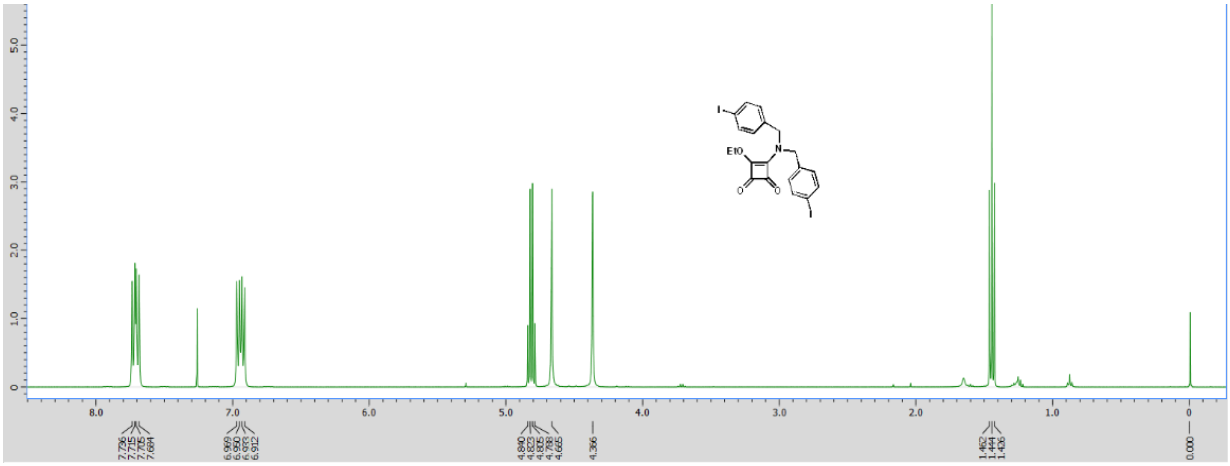

^{13}C NMR spectrum of 3 in $CDCl_3$

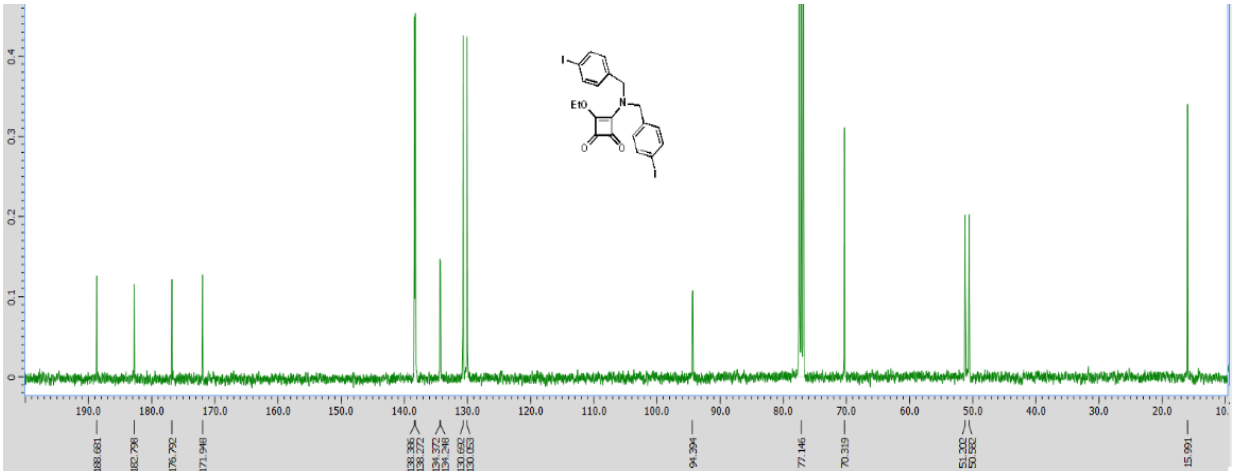

^{1}H NMR spectrum of 4 in $CDCl_3$

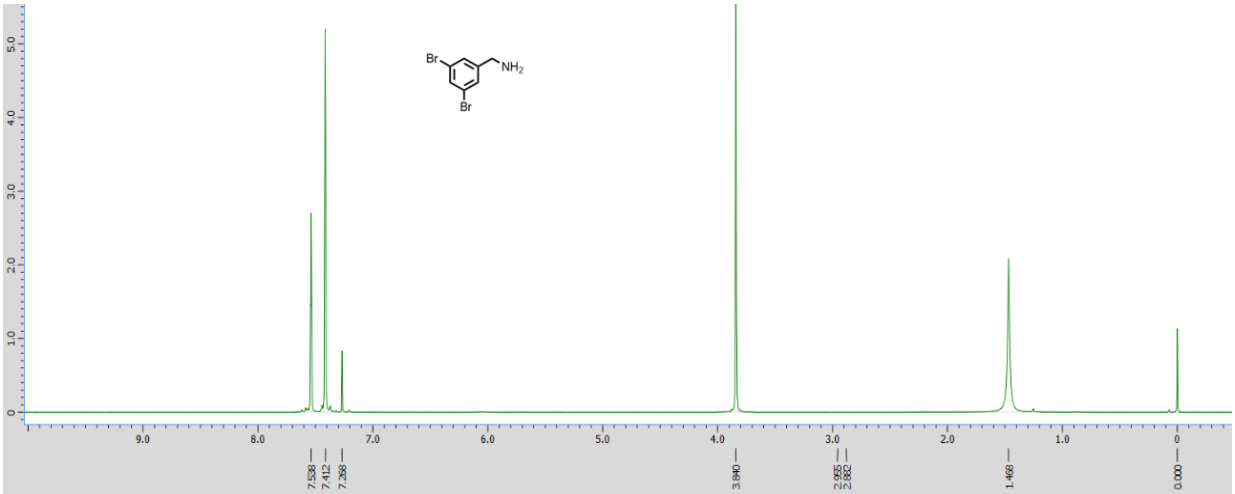

^{13}C NMR spectrum of 4 in $CDCl_3$

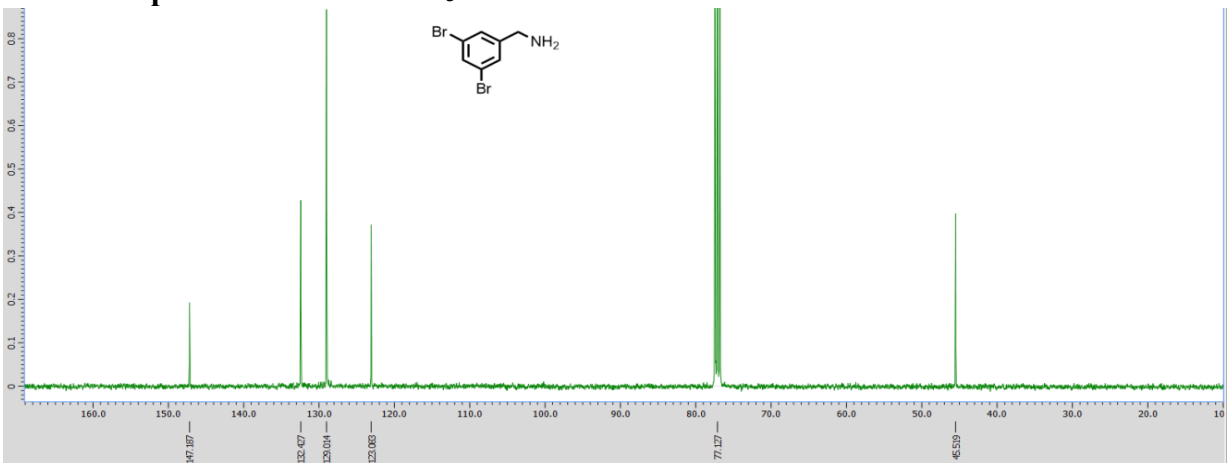

^{1}H NMR spectrum of 6 in DMSO-*d*$_6$

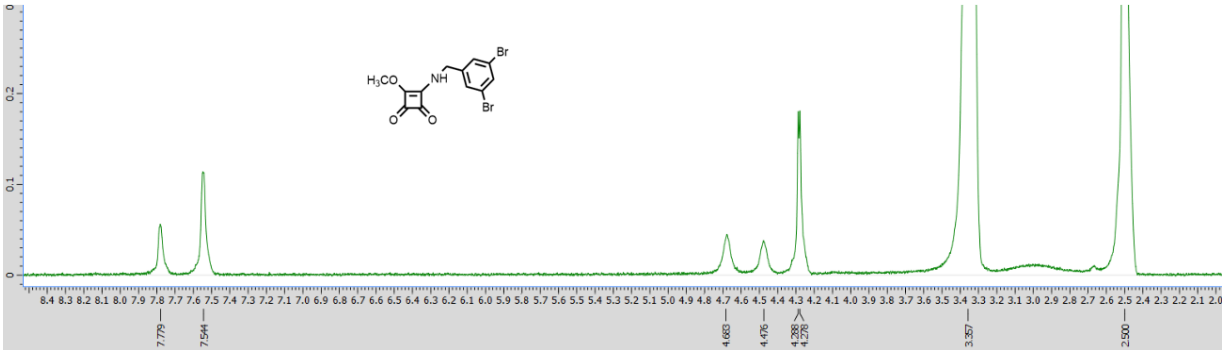

^{13}C NMR spectrum of 6 in DMSO-*d*$_6$

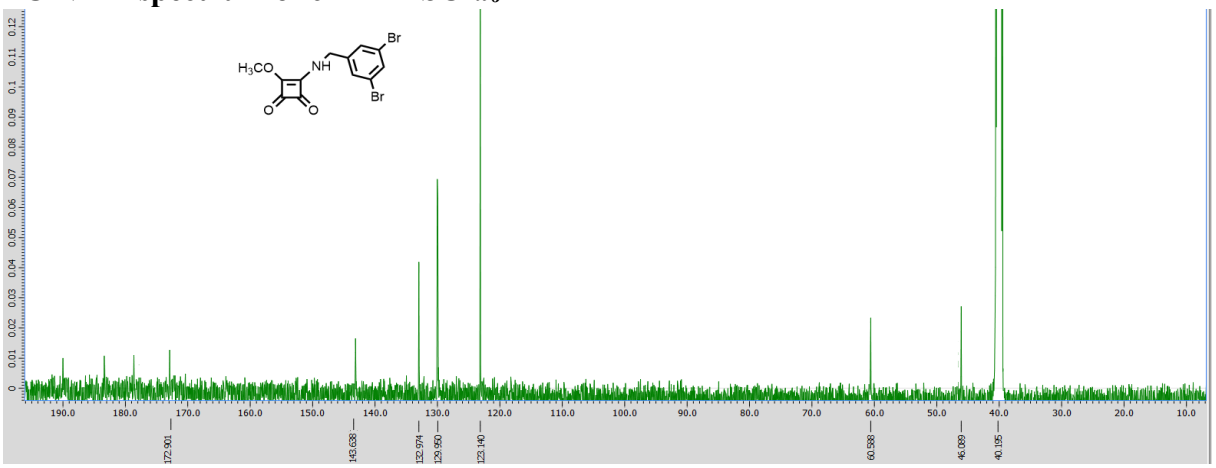

^{1}H NMR spectrum of 8 in $CDCl_3$

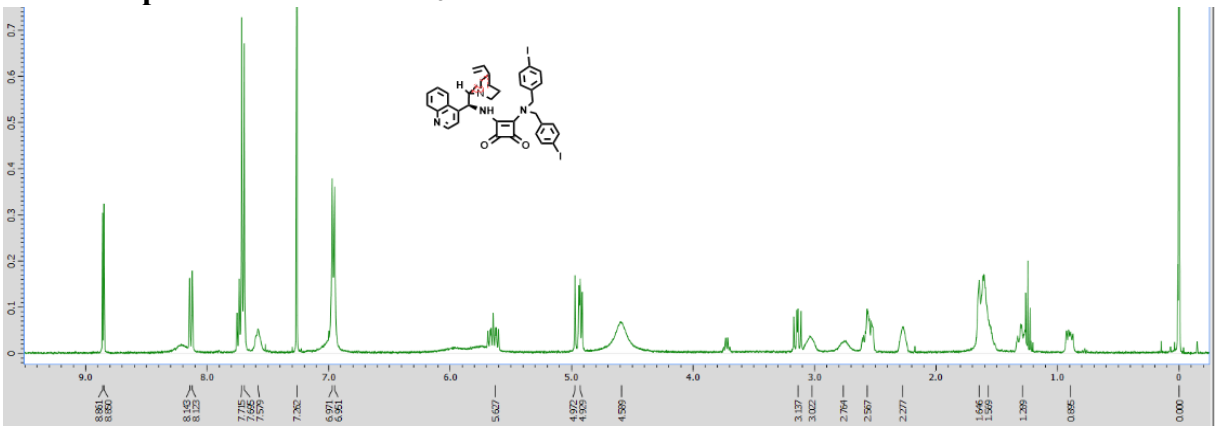

^{13}C NMR spectrum of 8 in $CDCl_3$

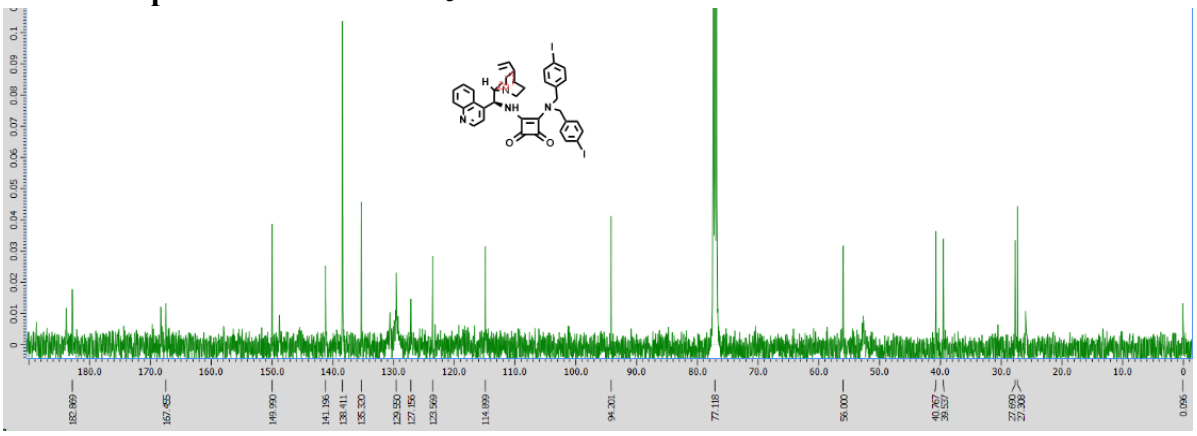

^{1}H NMR spectrum of 10 in $CDCl_3$

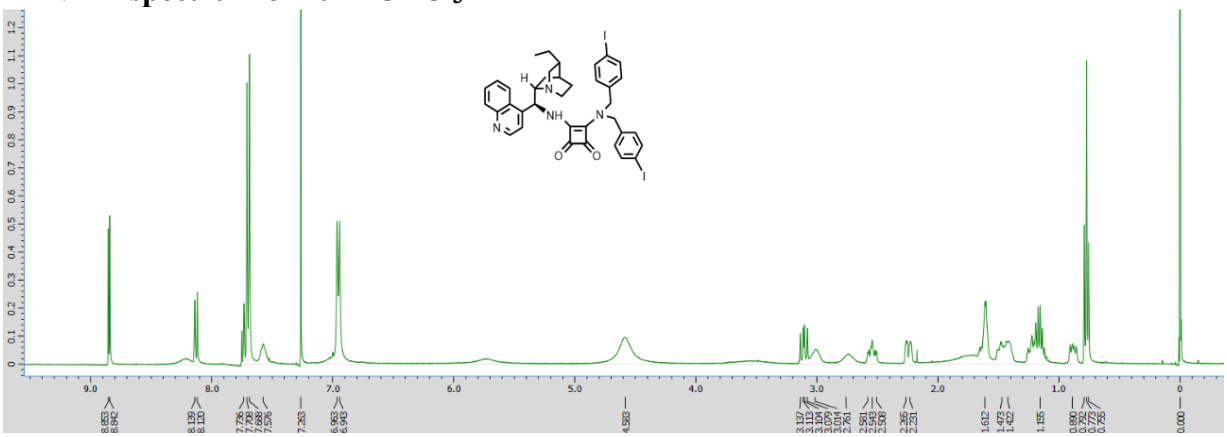

^{13}C NMR spectrum of 8 in $CDCl_3$

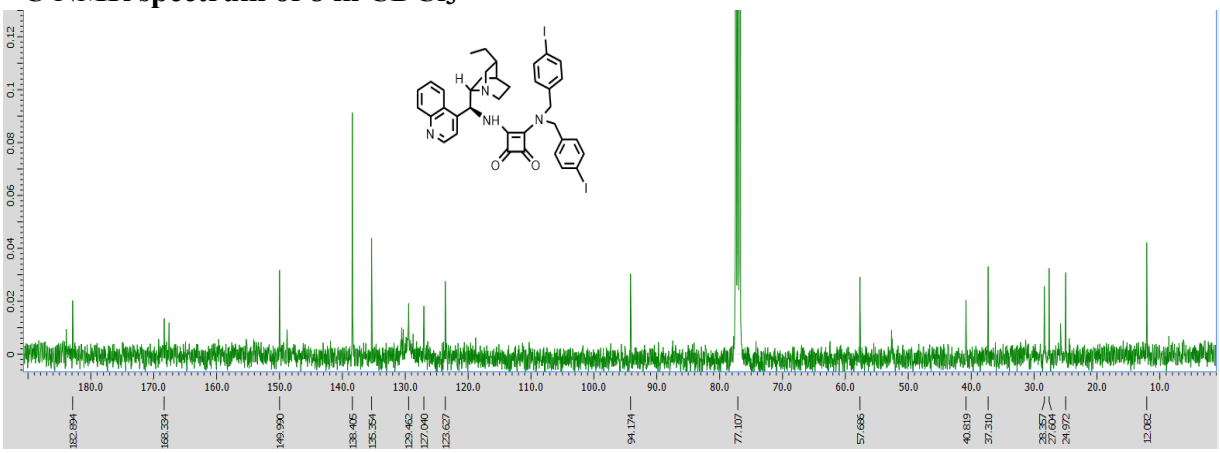

^{1}H NMR spectrum of 11 in DMSO-*d_6*

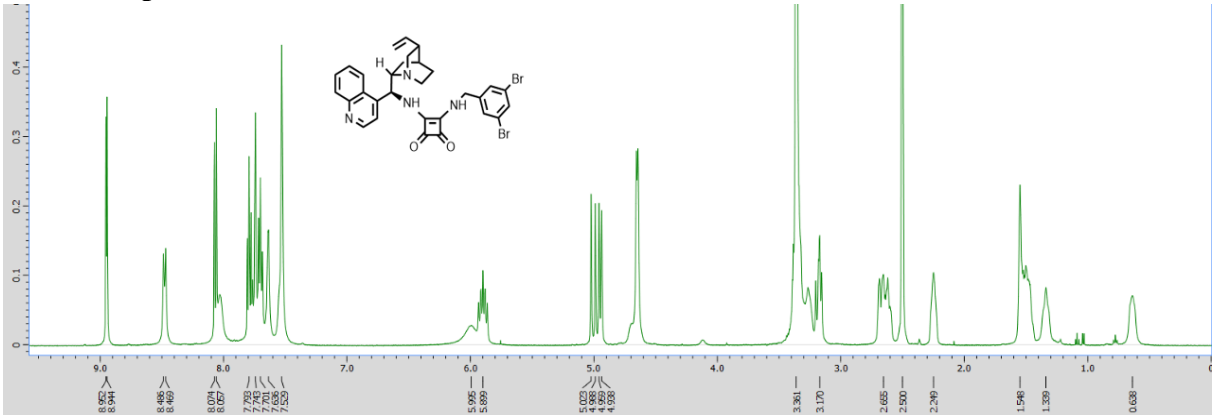

^{13}C NMR spectrum of 11 in DMSO-*d*$_6$

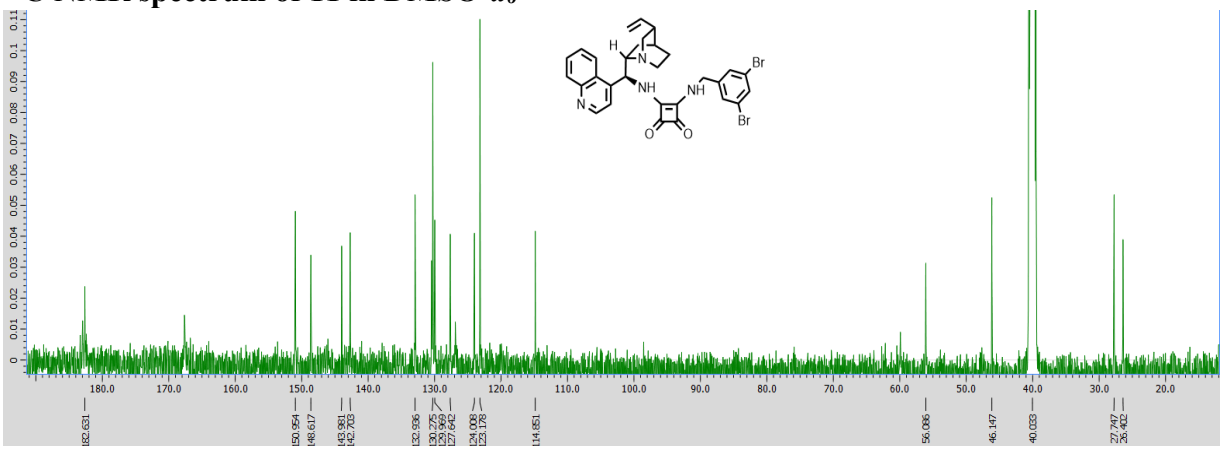

^{1}H NMR spectrum of 12 in DMSO-*d*$_6$

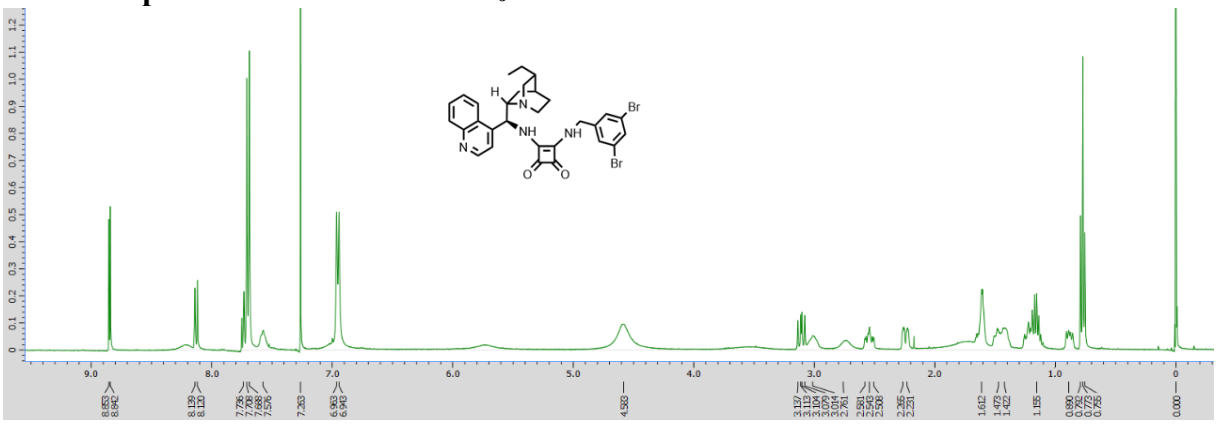

^{13}C NMR spectrum of 12 in DMSO-*d*$_6$

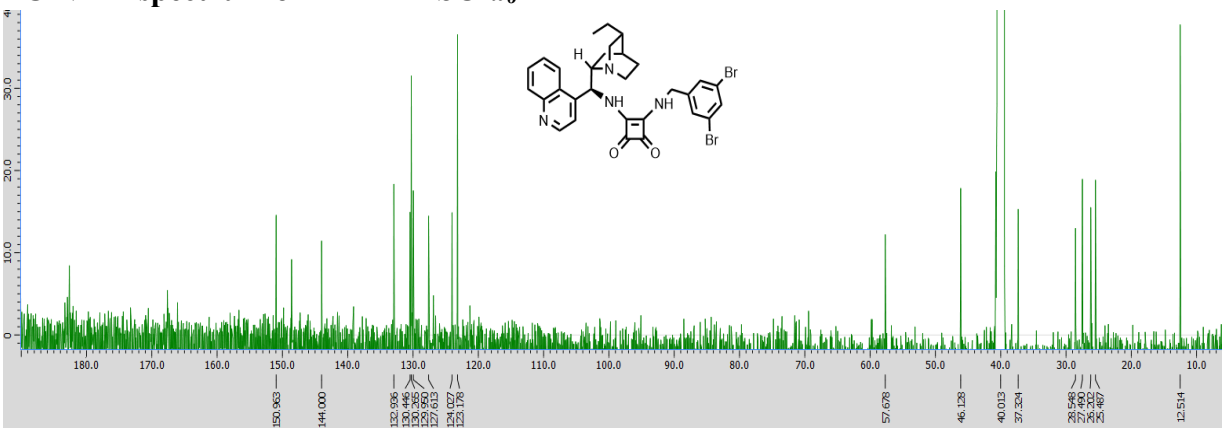

^{1}H NMR spectrum of polymer P1 in DMSO-*d*$_6$

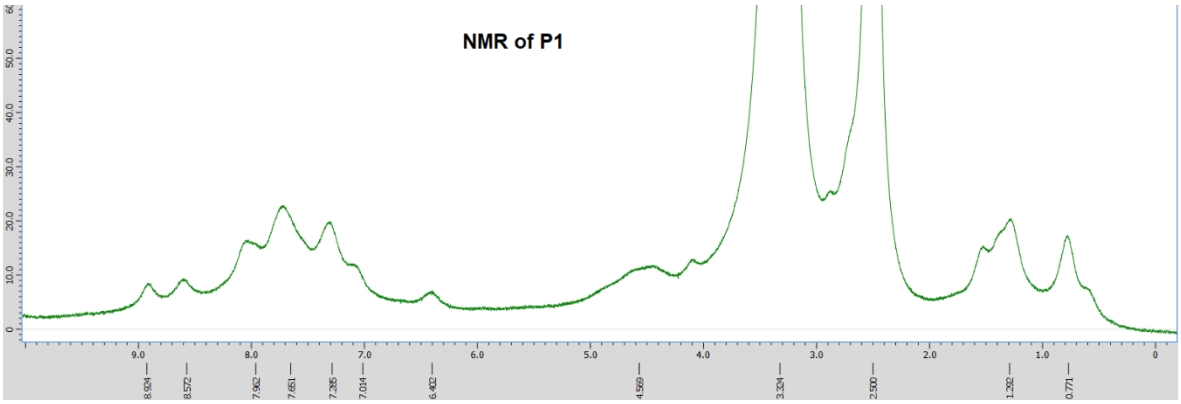

^{1}H NMR spectrum of polymer P1a in DMSO-*d*$_6$

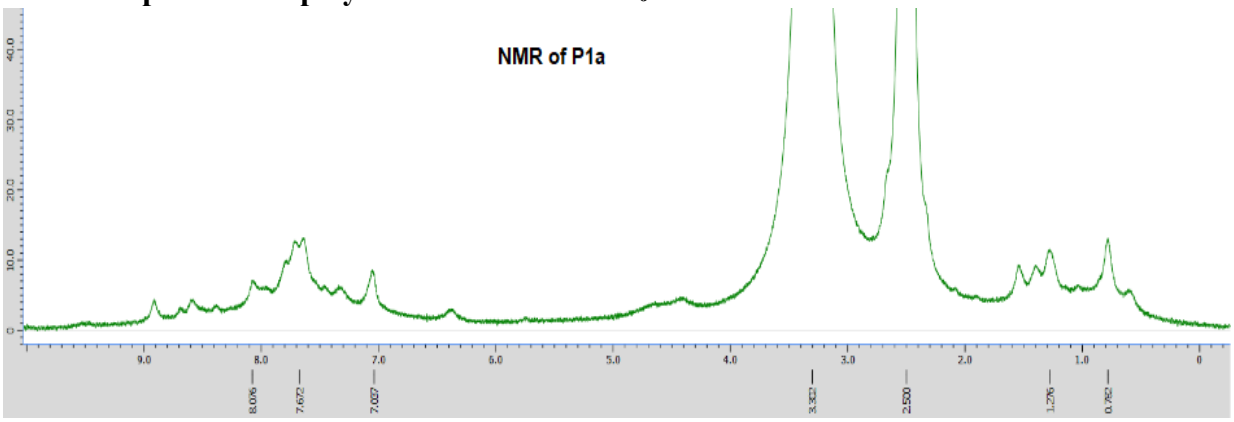

^{1}H NMR spectrum of polymer P2 in DMSO-*d*$_6$

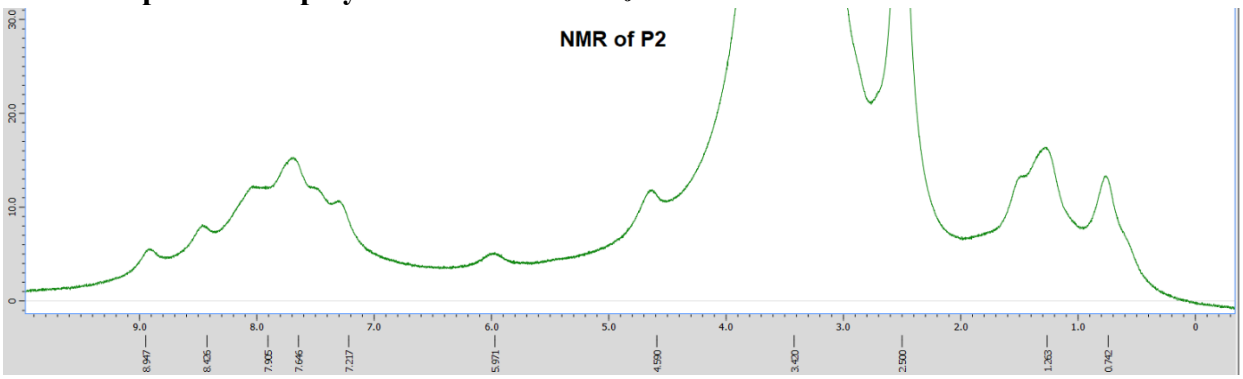

^{1}H NMR spectrum of polymer P2a in DMSO-*d*$_6$

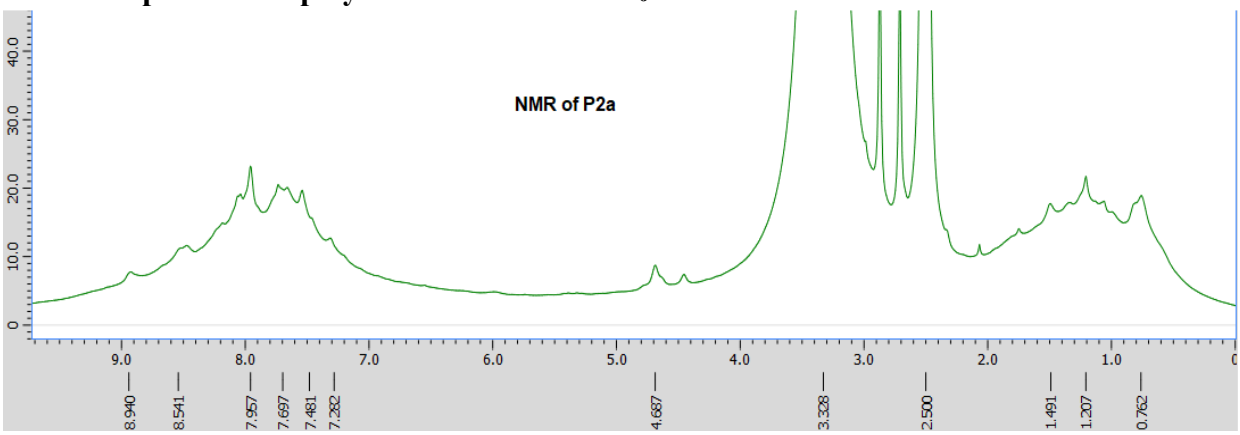

^{1}H NMR spectrum of polymer P2b in DMSO-*d*$_6$

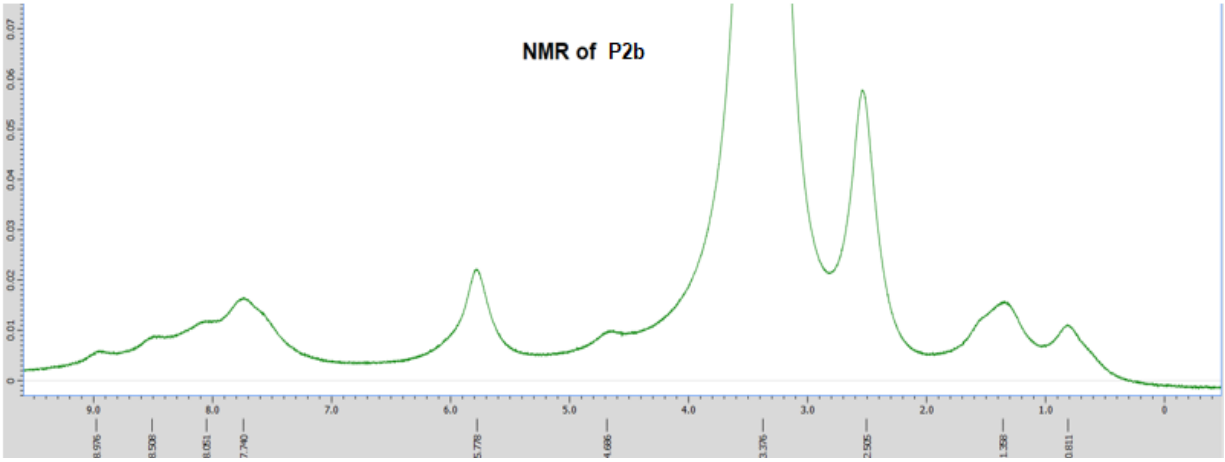

^{1}H NMR spectrum of polymer P3 in DMSO-*d*$_6$

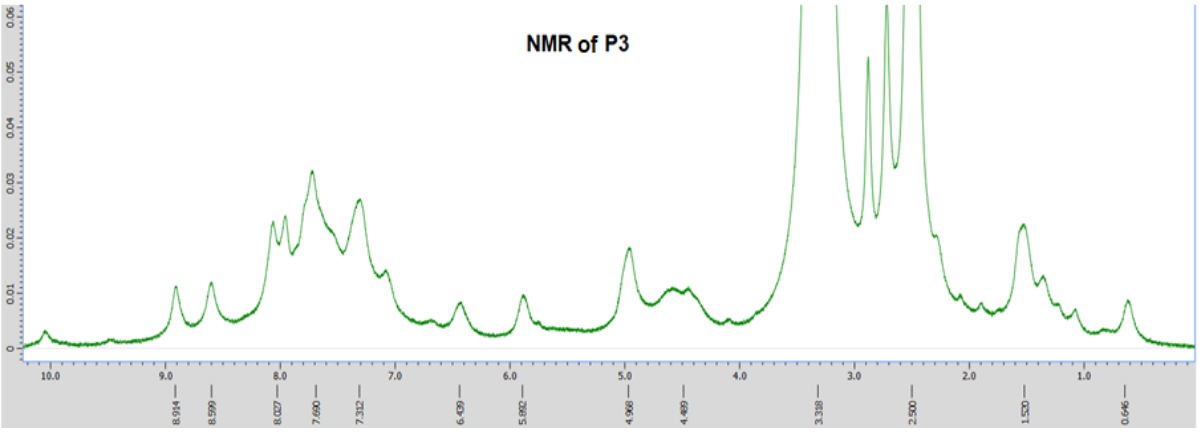

^{1}H NMR spectrum of polymer P4 in DMSO-*d*$_6$

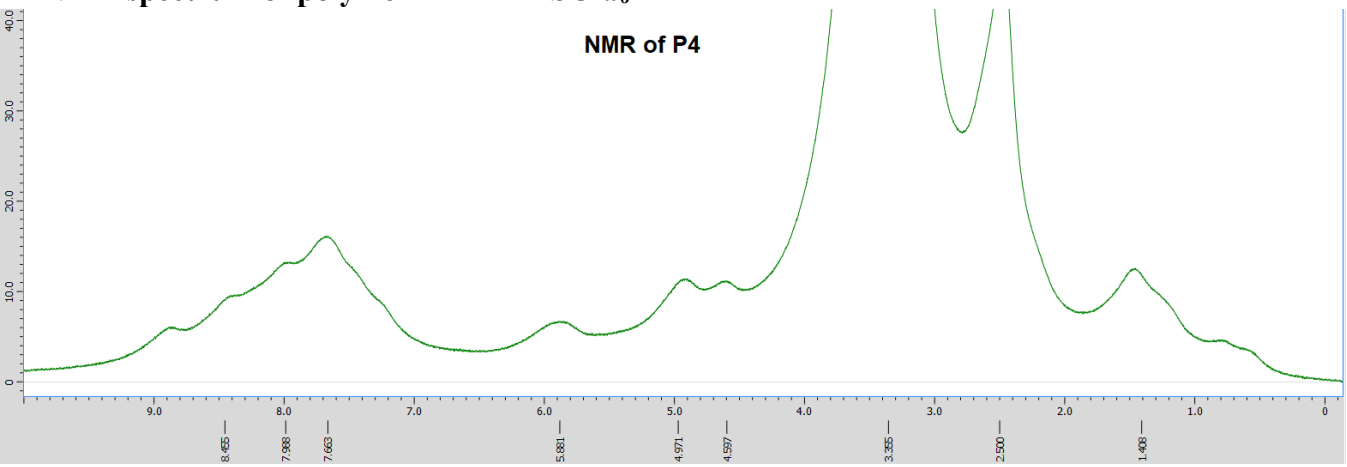

D.2 FT-IR Spectrum for monomers and polymers

1. IR spectrum of 3

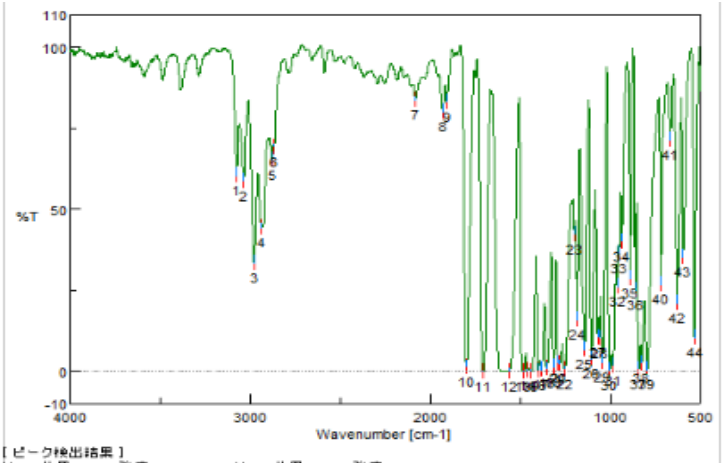

[ピーク検出結果]

No.	位置	強度	No.	位置	強度
1	3076.87	60.3428	2	3036.37	58.7257
3	2979.48	33.3668	4	2936.09	44.2815
5	2880.17	65.3301	6	2867.63	69.3224
7	2081.78	83.7729	8	1930.4	80.19
9	1908.22	83.2559	10	1800.22	1.38041
11	1702.84	0	12	1562.06	-2.65193E-038
13	1481.05	0.0205595	14	1460.81	0.10781
15	1442.49	0.0143659	16	1402	0.248361
17	1383.68	0.584781	18	1354.75	0.901117
19	1313.29	1.21233	20	1292.07	2.57737
21	1282.43	2.38703	22	1254.47	0.730828
23	1198.54	42.2445	24	1183.11	15.8051
25	1142.62	6.63404	26	1104.05	3.79862
27	1069.33	10.859	28	1057.76	10.1528
29	1043.3	2.62358	30	1005.7	0.298708
31	984.482	1.70842	32	961.341	26.1157
33	949.77	36.2522	34	934.342	40.147
35	889.987	28.6534	36	861.06	25.0308
37	840.812	0.727783	38	825.384	2.46314
39	795.493	0.504599	40	719.318	26.743
41	566.285	71.2823	42	628.58	20.9171
43	594.932	35.1161	44	532.257	10.3352

2. IR spectrum of 4

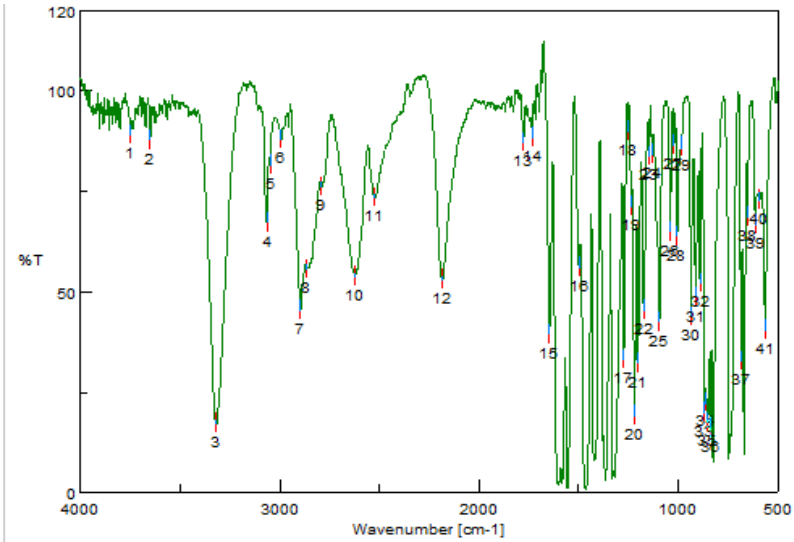

[ピーク検出結果]

No.	位置	強度	No.	位置	強度
1	3749.9	89.0387	2	3649.62	87.8499
3	3316.96	17.3412	4	3065.3	67.2829
5	3048.91	81.5719	6	2992.02	87.9293
7	2895.59	45.4422	8	2864.74	55.5619
9	2789.53	76.187	10	2623.68	53.8061
11	2523.4	73.4979	12	2183.99	53.0839
13	1779.97	87.2623	14	1732.73	88.451
15	1647.88	39.4955	16	1498.42	56.065
17	1273.75	33.0691	18	1250.61	89.9581
19	1236.15	71.3296	20	1219.76	19.1994
21	1201.43	32.2172	22	1174.44	45.4362
23	1147.44	83.7511	24	1132.01	84.2703
25	1094.4	42.5944	26	1040.41	64.9489
27	1022.09	86.6106	28	1005.7	63.8869
29	984.482	86.2775	30	937.235	43.7866
31	912.165	48.6208	32	890.952	52.2122
33	868.774	19.9639	34	861.06	22.5625
35	853.347	17.4914	36	840.812	16.2076
37	685.57	32.7891	38	652.786	68.7141
39	613.252	66.7432	40	592.039	72.9071
41	564.077	40.548			

3. IR spectrum of 6

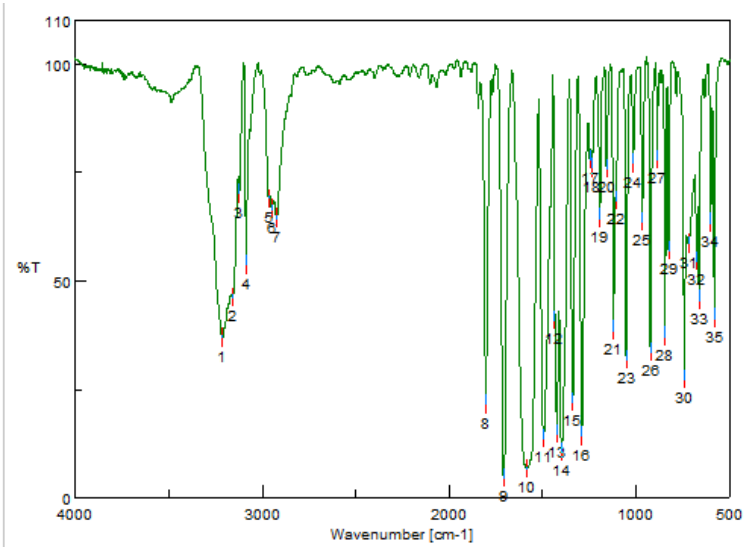

[ピーク検出結果]

No.	位置	強度	No.	位置	強度
1	3213.79	36.8943	2	3159.79	46.1507
3	3123.15	70.0065	4	3086.51	53.6027
5	2965.02	68.7338	6	2948.63	66.4971
7	2922.59	64.3636	8	1804.08	21.5954
9	1708.62	4.61637	10	1583.27	6.70859
11	1495.53	13.665	12	1434.78	40.9254
13	1425.14	14.7215	14	1398.14	10.4529
15	1340.28	22.0429	16	1291.11	14.2303
17	1247.72	77.7915	18	1235.18	75.9606
19	1193.72	64.3623	20	1158.04	75.759
21	1120.44	38.588	22	1107.9	68.3694
23	1052.94	31.8081	24	1015.34	77.0103
25	967.126	63.5899	26	923.736	33.4943
27	887.095	77.8903	28	845.633	37.1449
29	826.348	56.8454	30	742.46	27.306
31	720.282	58.511	32	675.928	54.4638
33	662.428	45.4945	34	601.682	63.3049
35	581.433	41.2611			

4. IR spectrum of 8

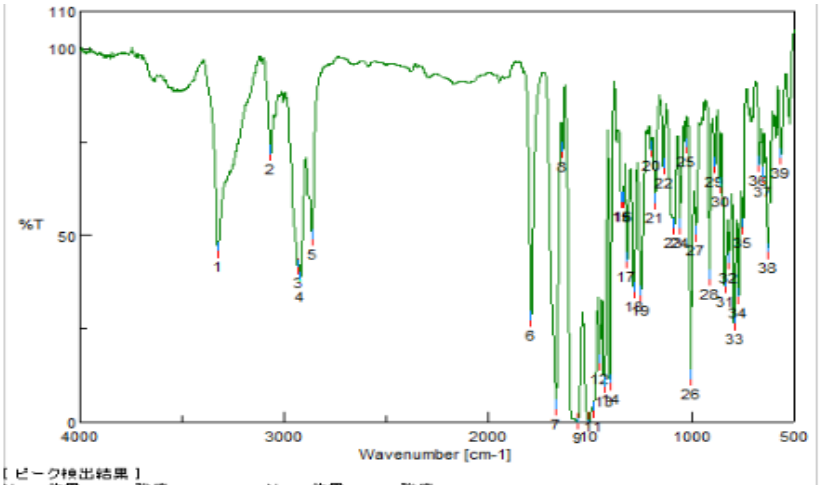

[ピーク検出結果]

No.	位置	強度	No.	位置	強度
1	3324.68	45.9368	2	3065.3	71.8537
3	2933.2	41.6177	4	2921.53	37.8765
5	2862.81	49.0609	6	1788.55	27.3444
7	1667.16	3.64877	8	1633.41	72.5971
9	1561.09	0.11898	10	1504.2	0.183657
11	1484.92	2.90841	12	1452.14	15.8523
13	1429.96	9.60268	14	1402	10.5323
15	1343.18	59.2317	16	1336.43	59.2598
17	1318.11	43.1467	18	1285.32	35.1391
19	1249.55	34.107	20	1200.47	72.8808
21	1182.15	58.8697	22	1139.72	68.173
23	1088.62	52.1204	24	1059.59	52.0745
25	1031.73	73.8042	26	1006.56	11.5558
27	981.59	50.3208	28	914.093	38.4857
29	888.059	68.4862	30	862.025	63.1225
31	839.847	36.3253	32	819.598	42.8195
33	793.564	26.5327	34	771.387	33.5211
35	749.209	52.2972	36	671.106	68.9036
37	649.893	65.7692	38	625.788	45.6131
39	564.077	70.9567			

5. IR spectrum of 10

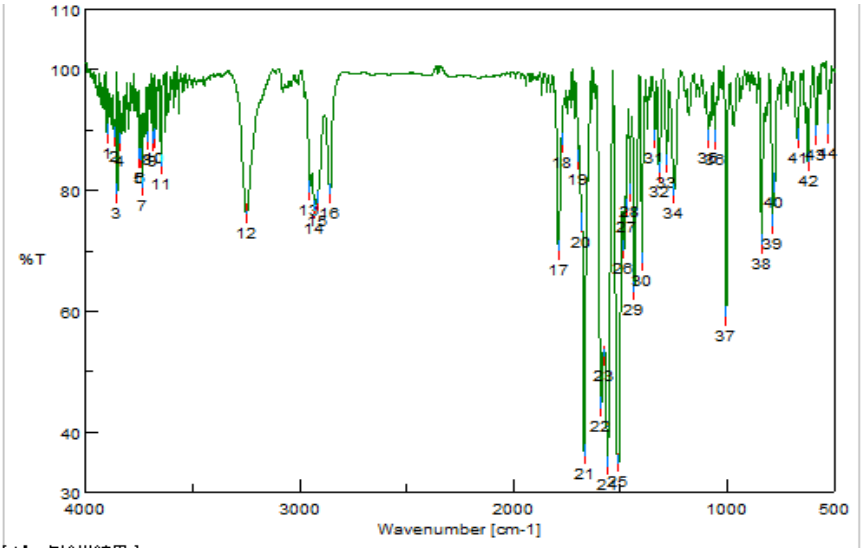

[ピーク検出結果]

No.	位置	強度	No.	位置	強度
1	3900.32	89.2679	2	3862.72	88.7822
3	3852.11	79.436	4	3836.68	87.9142
5	3749.9	85.2847	6	3743.15	85.1555
7	3733.51	80.4929	8	3709.41	88.1214
9	3688.19	87.948	10	3674.69	88.526
11	3647.7	84.1627	12	3246.57	76.0799
13	2952.48	79.8437	14	2931.27	76.7447
15	2915.84	78.0834	16	2857.02	79.4403
17	1789.62	70.0513	18	1772.26	87.6976
19	1697.05	84.9483	20	1682.59	74.4917
21	1669.09	36.2152	22	1590.99	44.0691
23	1575.56	52.525	24	1559.17	34.3492
25	1509.03	34.8853	26	1483.96	70.1155
27	1474.31	77.0199	28	1455.99	79.5287
29	1435.74	63.2503	30	1399.1	68.1229
31	1339.32	88.4212	32	1319.07	82.951
33	1284.36	84.306	34	1249.65	79.3517
35	1089.58	88.3775	36	1058.73	88.2124
37	1005.7	59.0719	38	839.847	71.0104
39	788.743	74.2459	40	779.101	81.1482
41	673.035	88.4513	42	623.859	84.7535
43	586.254	89.062	44	529.364	89.3163

6. IR spectrum of 11

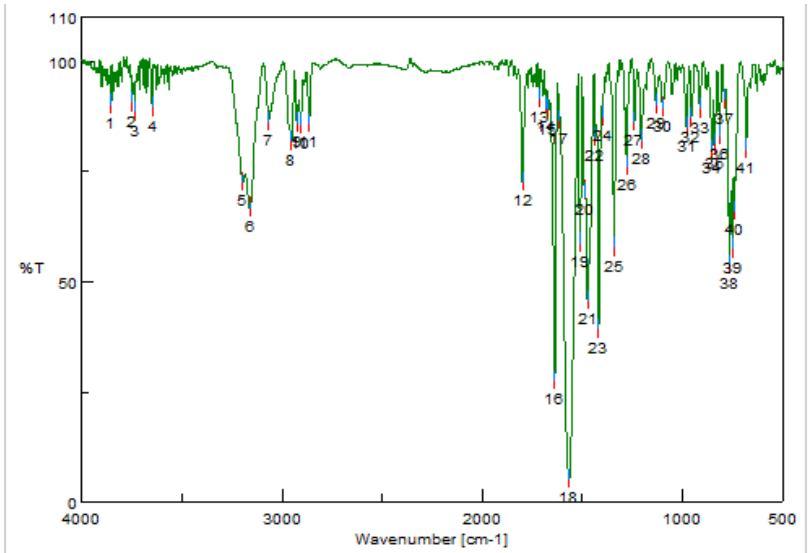

[ピーク検出結果]

No.	位置	強度	No.	位置	強度
1	3852.11	90.1188	2	3749.9	90.6146
3	3734.48	88.5106	4	3648.66	89.5928
5	3196.43	72.5805	6	3160.76	66.7967
7	3067.23	86.281	8	2952.48	81.8791
9	2925.48	86.0076	10	2907.16	85.6633
11	2864.74	85.8276	12	1799.26	72.6177
13	1716.34	91.4128	14	1683.55	89.494
15	1670.05	88.828	16	1638.23	27.6468
17	1615.09	86.5275	18	1566.88	5.26591
19	1512.88	58.7416	20	1489.74	70.7793
21	1474.31	45.7237	22	1434.78	82.7809
23	1419.35	39.3467	24	1398.14	87.4229
25	1342.21	57.8513	26	1278.57	76.0747
27	1240.97	86.266	28	1207.22	82.1158
29	1132.97	90.1916	30	1098.26	89.4538
31	980.625	84.9268	32	956.52	87.0911
33	913.129	89.1895	34	852.382	80.0122
35	837.919	81.2006	36	814.777	83.1814
37	791.636	91.3349	38	766.566	53.7757
39	752.102	57.4638	40	740.531	65.9527
41	682.677	80.0306			

7. IR spectrum of 12

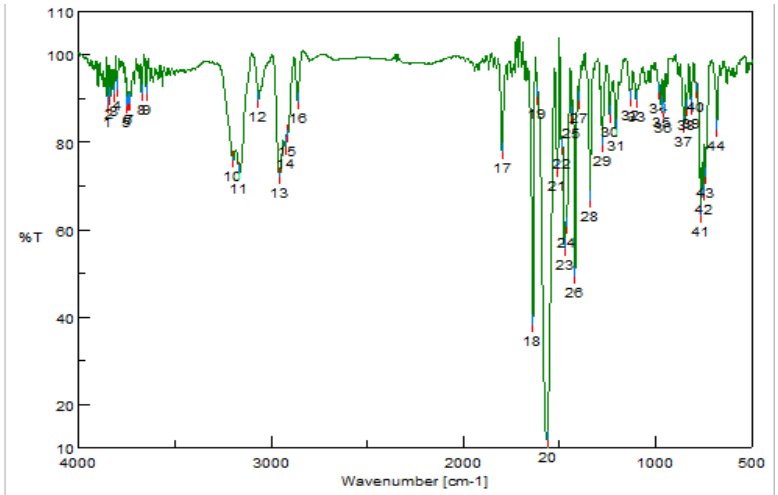

[ピーク検出結果]

No.	位置	強度	No.	位置	強度
1	3850.18	88.59	2	3835.72	90.5007
3	3818.36	91.0977	4	3799.08	92.2493
5	3747.98	88.4349	6	3741.23	89.0085
7	3732.55	89.0945	8	3672.77	91.2632
9	3646.73	91.1558	10	3196.43	75.9809
11	3162.69	73.2956	12	3066.26	89.6374
13	2955.38	72.2001	14	2925.48	79.0611
15	2911.99	81.7864	16	2861.84	89.334
17	1799.26	77.9235	18	1638.23	38.3944
19	1615.09	90.4646	20	1563.02	11.8019
21	1511.92	74.0119	22	1489.74	78.8123
23	1473.35	55.8264	24	1464.67	60.7551
25	1436.71	86.0485	26	1420.32	49.3261
27	1398.14	89.4991	28	1342.21	66.847
29	1276.65	79.6008	30	1240	86.3998
31	1207.22	83.1896	32	1130.08	90.0775
33	1101.15	89.5879	34	983.518	91.5828
35	971.947	88.5805	36	958.448	87.0309
37	852.382	83.9214	38	837.919	87.7468
39	815.742	88.1414	40	790.671	91.838
41	766.566	63.4114	42	753.066	68.4394
43	740.531	72.1461	44	681.713	83.1052

8. IR spectrum of P1

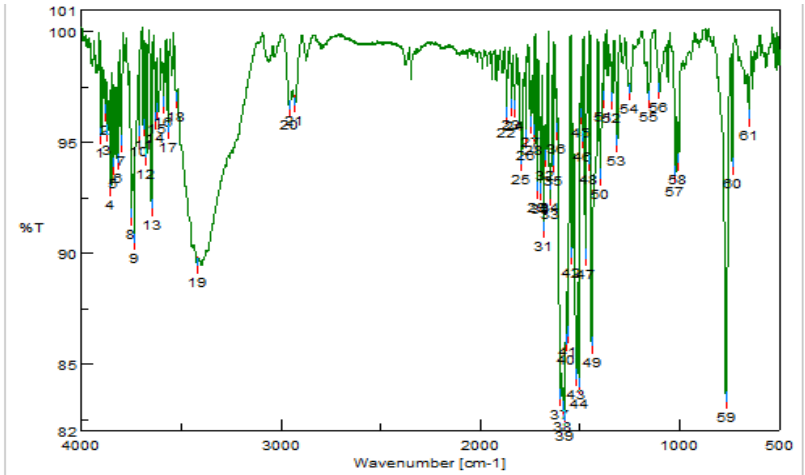

[ピーク検出結果]

No.	位置	強度	No.	位置	強度
1	3901.29	95.2984	2	3882	96.3262
3	3869.47	95.43	4	3852.11	92.9623
5	3837.65	93.9074	6	3819.33	94.1251
7	3800.04	94.92	8	3748.94	91.623
9	3734.48	90.5037	10	3711.33	95.3433
11	3689.16	95.6515	12	3674.69	94.3365
13	3648.66	92.0438	14	3628.41	95.9563
15	3617.8	96.3876	16	3586.95	96.674
17	3566.7	95.4996	18	3523.31	96.8978
19	3420.14	89.4526	20	2956.34	96.5237
21	2929.34	96.7243	22	1868.68	96.1789
23	1844.58	96.558	24	1829.15	96.5086
25	1792.51	94.0581	26	1772.26	95.1952
27	1749.12	95.7678	28	1733.69	95.3945
29	1716.34	92.8262	30	1698.02	92.7645
31	1683.55	91.0541	32	1671.02	94.2664
33	1652.7	92.4826	34	1646.91	92.8294
35	1636.3	94.0103	36	1616.06	95.4789
37	1597.73	83.4829	38	1585.2	82.9514
39	1577.49	82.5093	40	1568.81	85.9394
41	1559.17	86.3158	42	1540.85	89.8612
43	1519.63	84.3741	44	1508.06	83.9741
45	1497.45	96.1653	46	1488.78	95.1041
47	1473.35	89.7977	48	1456.96	94.0528
49	1442.49	85.8487	50	1397.17	93.417
51	1386.57	96.9317	52	1339.32	96.8767
53	1314.25	94.9134	54	1248.58	97.2593
55	1156.12	96.9241	56	1103.08	97.3044
57	1022.09	93.5384	58	1006.66	94.0882
59	768.494	83.3598	60	736.674	93.9187
61	653.75	96.0857			

9. IR spectrum of P1a

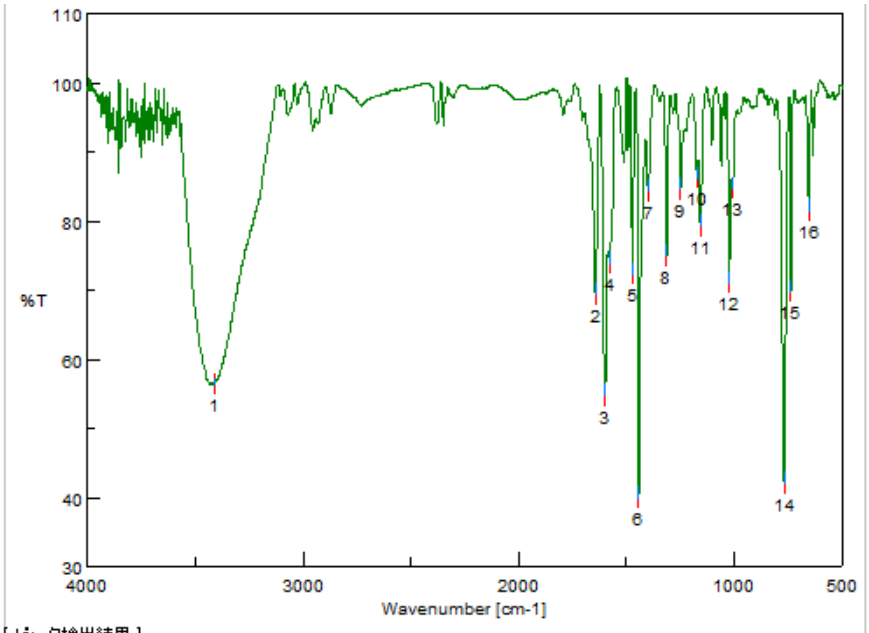

[ピーク検出結果]

No.	位置	強度	No.	位置	強度
1	3412.42	56.3169	2	1644.02	69.4423
3	1598.7	54.7057	4	1576.52	73.8918
5	1472.38	72.264	6	1442.49	39.928
7	1399.1	84.3409	8	1313.29	75.0291
9	1247.72	84.6547	10	1172.51	86.2184
11	1156.12	79.281	12	1023.05	71.0156
13	1006.66	84.7449	14	768.494	42.0491
15	736.674	69.809	16	653.75	81.5321

10. IR spectrum of P2

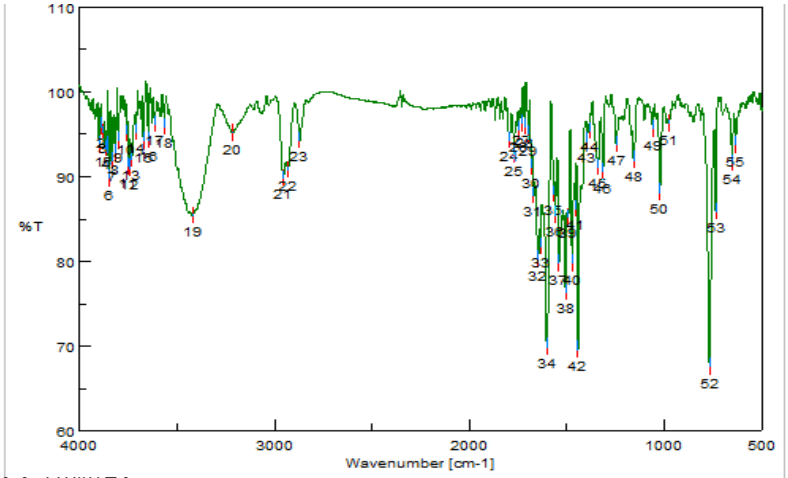

[ピーク検出結果]

No.	位置	強度	No.	位置	強度
1	3898.4	93.7536	2	3888.75	95.9224
3	3882	95.2377	4	3867.54	93.3052
5	3858.86	93.762	6	3850.18	89.7759
7	3834.76	91.8553	8	3818.36	92.8015
9	3799.08	94.1885	10	3754.73	95.0664
11	3747.98	91.1897	12	3740.26	91.0052
13	3731.58	92.0285	14	3708.44	95.24
15	3672.77	94.2239	16	3646.73	94.3001
17	3614.91	96.1677	18	3564.77	95.8874
19	3419.17	85.3714	20	3211.86	95.1541
21	2954.41	89.8518	22	2931.27	90.7995
23	2870.52	94.286	24	1793.47	94.2651
25	1771.3	92.6123	26	1749.12	95.4811
27	1733.69	96.3043	28	1716.34	95.8681
29	1698.02	95.0287	30	1682.59	91.0808
31	1670.05	87.7293	32	1646.91	80.1938
33	1636.3	81.7503	34	1600.63	69.9009
35	1567.84	87.9152	36	1559.17	85.4607
37	1540.85	79.7705	38	1508.06	76.3289
39	1497.45	85.2153	40	1473.35	79.7664
41	1457.92	86.2016	42	1443.46	69.5944
43	1396.21	94.1548	44	1386.57	95.3871
45	1340.28	91.0681	46	1314.25	90.5921
47	1247.72	93.7727	48	1157.08	91.9548
49	1059.69	95.6421	50	1023.05	88.1331
51	980.625	96.2509	52	768.494	67.5811
53	736.674	85.8896	54	652.786	91.544
55	633.501	93.7594			

11. IR spectrum of P2a

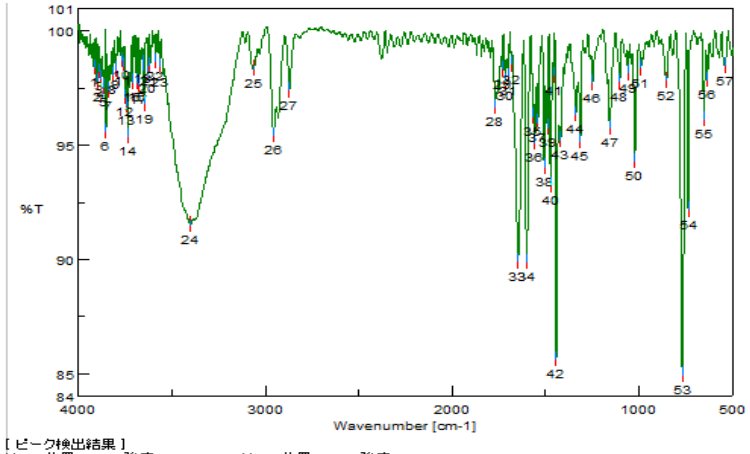

[ピーク検出結果]

No.	位置	強度	No.	位置	強度
1	3915.75	98.3978	2	3900.32	97.7792
3	3890.68	98.2471	4	3880.08	97.8946
5	3862.72	97.5488	6	3852.11	95.6029
7	3837.65	97.4055	8	3814.51	98.069
9	3800.04	98.3184	10	3768.22	98.7217
11	3757.62	98.4826	12	3749.9	97.1153
13	3743.15	96.7398	14	3734.48	95.3945
15	3710.37	97.7759	16	3688.19	97.7727
17	3674.69	97.6676	18	3656.37	98.5757
19	3647.7	96.8242	20	3627.45	98.1267
21	3617.8	98.4868	22	3585.38	98.6685
23	3565.74	98.4468	24	3398.92	91.5288
25	3065.3	98.3665	26	2955.38	95.4323
27	2871.49	97.4092	28	1771.3	96.6728
29	1733.69	98.331	30	1716.34	97.8102
31	1698.98	98.0255	32	1683.55	98.5513
33	1646.91	89.9212	34	1599.66	89.8804
35	1566.88	96.2714	36	1558.2	95.1067
37	1540.85	95.9885	38	1508.06	94.0442
39	1490.7	95.7764	40	1473.35	93.2705
41	1457.92	98.0526	42	1443.46	85.6202
43	1420.32	95.2373	44	1339.32	96.3532
45	1314.25	95.17	46	1248.68	97.7373
47	1156.12	95.751	48	1105.01	97.7954
49	1059.69	98.1771	50	1024.02	94.2919
51	990.268	98.3773	52	855.275	97.8397
53	768.494	84.9435	54	736.674	92.1794
55	652.786	96.1271	56	634.466	97.8613
57	542.863	98.4945			

12. IR spectrum of P2b

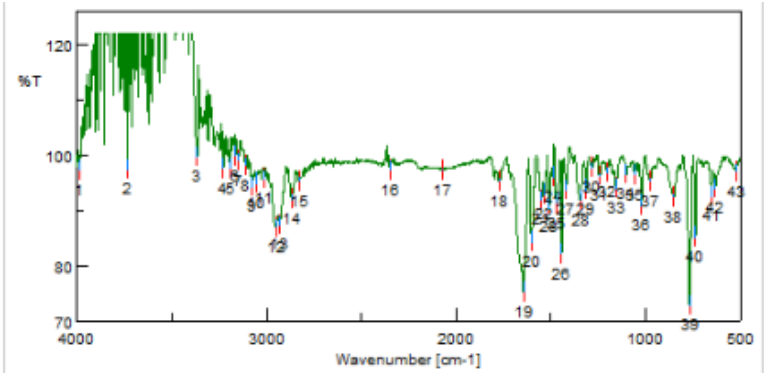

[ピーク検出結果]

No.	位置	強度	No.	位置	強度
1	3984.21	97.3702	2	3735.44	97.4455
3	3366.14	99.6824	4	3227.29	97.5837
5	3192.58	97.5784	6	3164.51	99.8866
7	3151.11	99.0928	8	3111.58	98.1438
9	3076.87	94.2982	10	3052.76	94.9522
11	3010.34	95.7967	12	2950.55	87.0422
13	2929.34	87.4508	14	2868.59	92.116
15	2829.06	95.321	16	2348.87	97.3719
17	2074.07	97.3683	18	1775.15	95.3407
19	1644.98	75.3325	20	1600.53	84.4502
21	1551.45	92.0052	22	1535.06	92.9941
23	1509.03	90.6421	24	1491.57	96.0836
25	1473.35	91.3212	26	1443.46	82.232
27	1421.28	93.7439	28	1346.07	91.9356
29	1313.29	93.818	30	1281.47	97.8248
31	1245.79	96.2351	32	1204.33	95.9269
33	1157.08	94.1406	34	1103.08	95.6063
35	1059.69	96.463	36	1024.02	90.9428
37	976.769	95.3591	38	854.311	92.445
39	768.494	72.8887	40	737.639	85.31
41	692.786	92.557	42	633.501	94.046
43	523.579	97.0116			

13. IR spectrum of P3

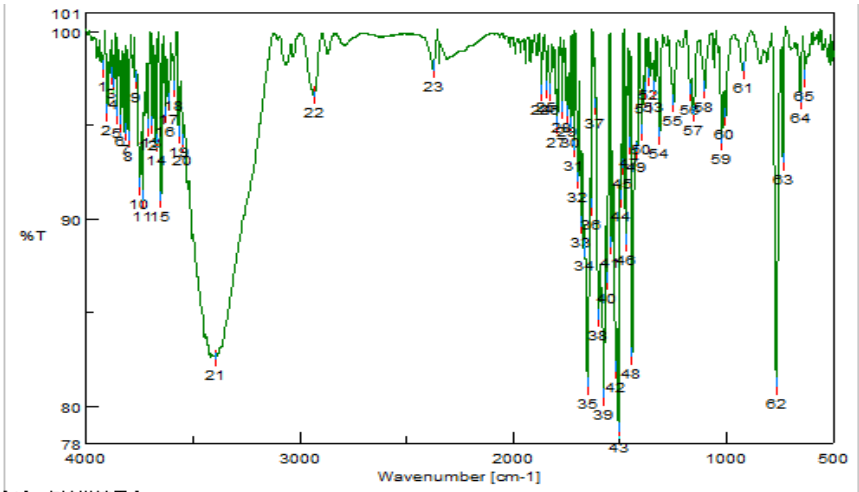

[ピーク検出結果]

No.	位置	強度	No.	位置	強度
1	3919.61	97.9704	2	3903.22	95.6303
3	3882.97	97.577	4	3871.4	97.0202
5	3855.01	95.4865	6	3838.61	95.0523
7	3819.33	94.5906	8	3801.97	94.1857
9	3769.19	97.3598	10	3747.01	91.7011
11	3736.4	91.0122	12	3712.3	94.8373
13	3690.12	94.9752	14	3671.8	94.0232
15	3649.62	90.9968	16	3630.34	95.5176
17	3613.95	96.1965	18	3587.91	96.9129
19	3566.7	94.4494	20	3545.49	94.0127
21	3394.1	82.5412	22	2932.23	96.5602
23	2373.94	97.954	24	1868.68	96.6893
25	1844.58	96.8732	26	1829.15	96.7016
27	1792.51	94.9627	28	1772.26	95.7677
29	1748.12	95.5293	30	1733.69	94.9277
31	1716.34	93.6995	32	1698.02	92.0215
33	1683.55	89.6319	34	1669.09	88.413
35	1652.7	81.0572	36	1637.27	90.6098
37	1616.06	95.9441	38	1599.66	84.672
39	1576.52	80.4635	40	1559.17	86.6276
41	1540.85	88.5245	42	1519.63	81.8876
43	1508.06	78.6625	44	1498.42	91.0407
45	1489.74	92.7432	46	1473.35	88.687
47	1456.96	93.8648	48	1443.46	82.647
49	1420.32	93.6133	50	1397.17	94.5516
51	1386.57	96.7821	52	1362.46	97.5395
53	1339.32	96.8463	54	1314.25	94.3993
55	1249.65	96.1297	56	1171.54	96.7198
57	1156.12	95.5752	58	1104.05	96.8457
59	1024.98	94.0439	60	1005.7	95.405
61	921.807	97.8908	62	767.53	81.0488

14. IR spectrum of P4

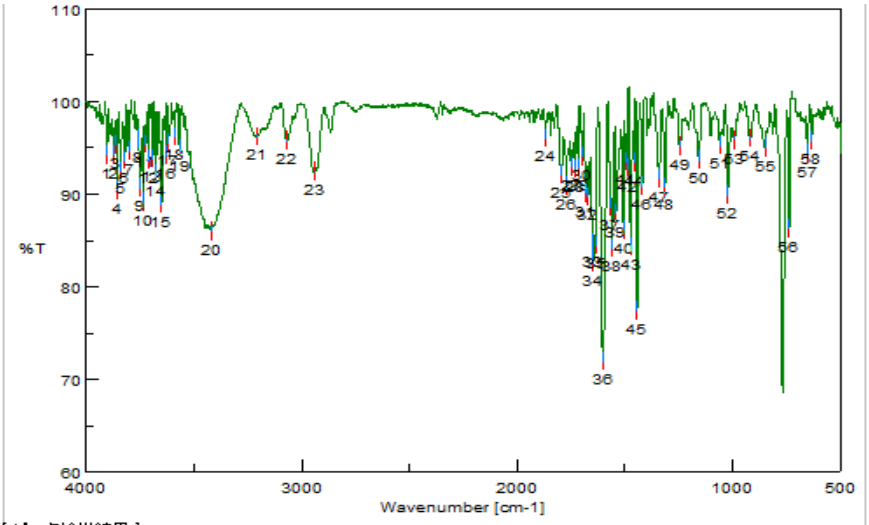

[ピーク検出結果]

No.	位置	強度	No.	位置	強度
1	3903.22	94.2094	2	3871.4	94.2053
3	3864.65	95.3101	4	3854.04	90.4246
5	3839.58	92.5516	6	3821.26	93.6342
7	3801.97	94.6315	8	3759.55	95.9676
9	3750.87	90.6856	10	3735.44	89.0864
11	3724.83	95.3612	12	3711.33	93.6717
13	3690.12	93.7841	14	3676.62	92.2383
15	3649.62	88.8684	16	3629.37	94.1556
17	3619.73	95.5415	18	3587.91	96.1945
19	3566.7	94.9319	20	3421.1	85.9821
21	3210.9	96.1504	22	3068.19	95.733
23	2943.8	92.4108	24	1868.68	96.0369
25	1792.51	92.1007	26	1771.3	90.8719
27	1749.12	92.9376	28	1732.73	92.6687
29	1716.34	92.848	30	1698.02	94.0586
31	1682.59	90.0628	32	1670.05	89.703
33	1651.73	84.6545	34	1645.95	82.6229
35	1637.27	84.4321	36	1600.63	71.9163
37	1566.88	88.5774	38	1558.2	84.0909
39	1540.85	87.8921	40	1508.06	86.143
41	1496.49	93.4618	42	1490.7	92.7406
43	1473.35	84.2575	44	1457.92	93.4114
45	1443.46	77.4195	46	1419.35	90.8243
47	1341.25	91.6841	48	1314.25	90.7866
49	1246.75	95.146	50	1156.12	93.6703
51	1059.69	95.2415	52	1023.05	89.8759
53	992.196	95.801	54	920.843	96.0235
55	850.454	95.0219	56	737.639	86.3078
57	652.786	94.3319	58	633.501	95.7619

D.3 HPLC analysis for asymmetric Michael adducts

1. Chromatogram data for Michael adduct 18 in Table 2 for different polymers.

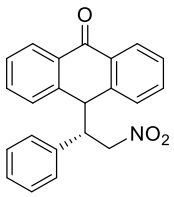

18 (S)

Table 4.2, entry 1: 58% ee

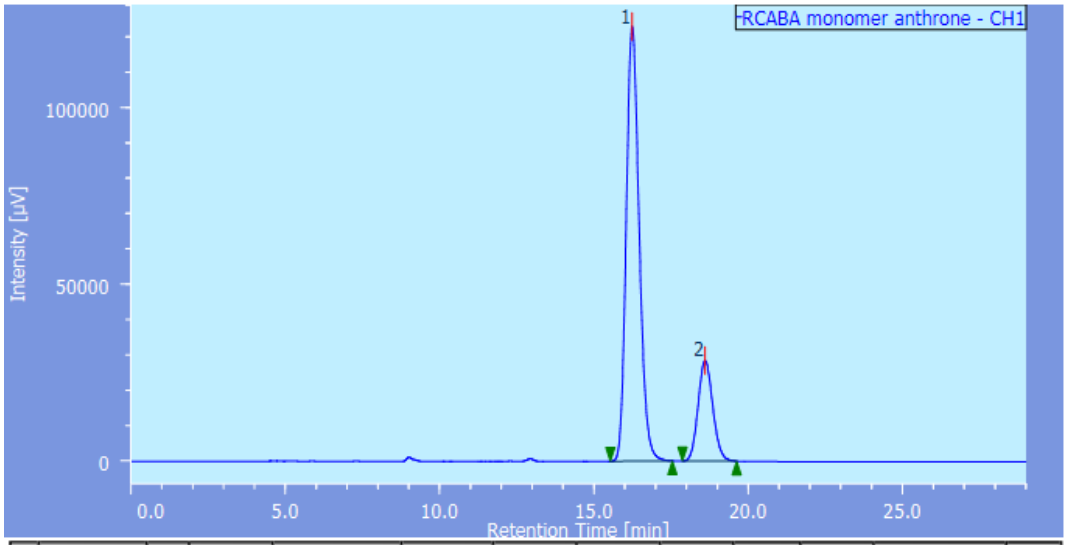

#	ピーク名	CH	tR [min]	面積 [μV·sec]	高さ [μV]	面積%	高さ%	定量値	NTP	分離度	シンメトリー係数	警告
1	Unknown	1	16.233	3591337	122970	79.140	81.205	N/A	7278	2.902	1.196	
2	Unknown	1	18.600	946631	28462	20.860	18.795	N/A	7241	N/A	1.111	

Table 4.2, entry 2: 84% ee

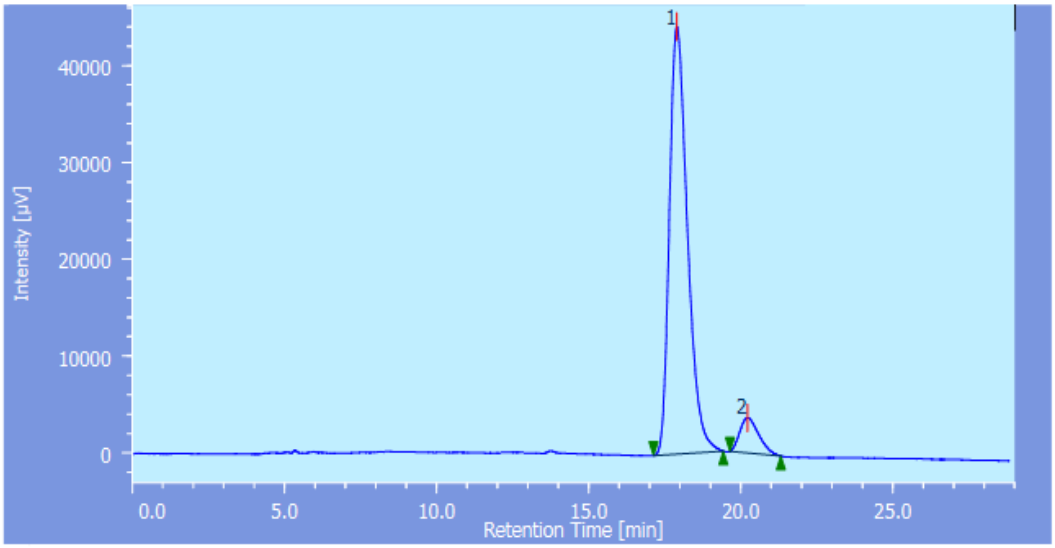

#	ピーク名	CH	tR [min]	面積 [μV·sec]	高さ [μV]	面積%	高さ%	定量値	NTP	分離度	シンメトリー係数	警告
1	Unknown	1	17.892	1818677	44142	91.970	92.397	N/A	4482	2.077	1.383	
2	Unknown	1	20.217	158796	3632	8.030	7.603	N/A	4729	N/A	1.358	

Table 4.2, entry 3: 20% ee

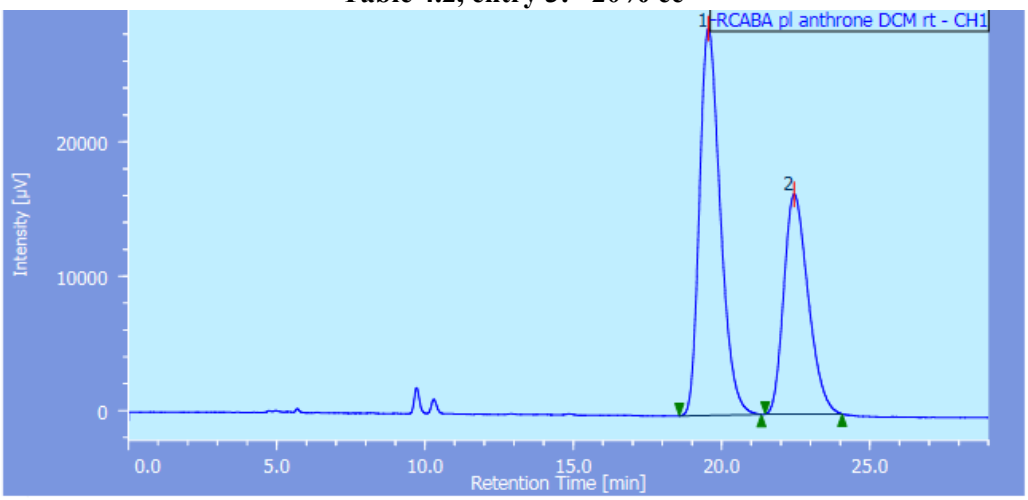

#	ピーク名	CH	tR [min]	面積 [μV·sec]	高さ [μV]	面積%	高さ%	定量値	NTP	分離度	シンメトリー係数	警告
1	Unknown	1	19.550	1405757	28777	60.030	63.759	N/A	3759	2.083	1.307	
2	Unknown	1	22.442	936018	16357	39.970	36.241	N/A	3541	N/A	1.295	

Table 4.2, entry 4: 5% ee

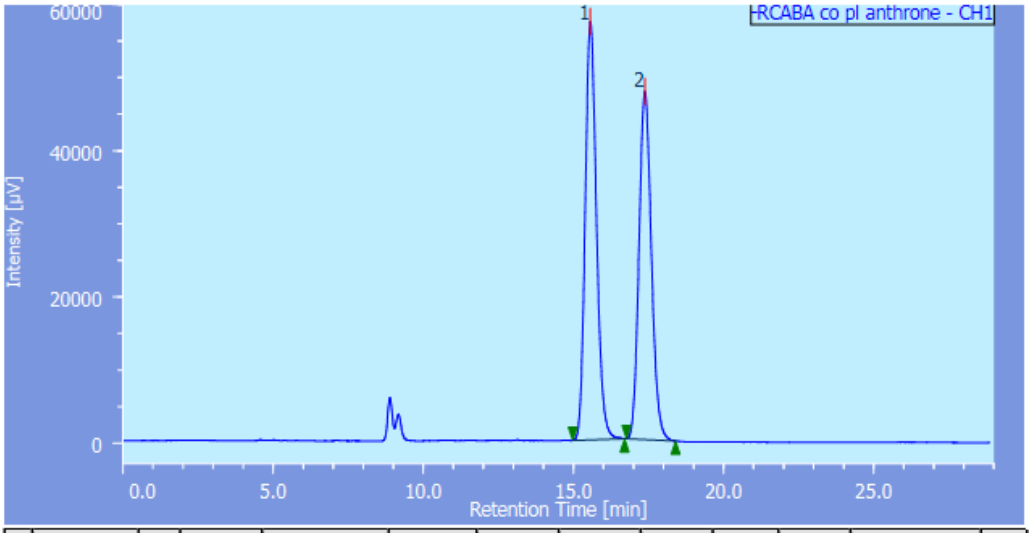

#	ピーク名	CH	tR [min]	面積 [μV·sec]	高さ [μV]	面積%	高さ%	定量値	NTP	分離度	シンメトリー係数	警告
1	Unknown	1	15.558	1493112	57204	52.285	54.591	N/A	8432	2.551	1.179	
2	Unknown	1	17.375	1362628	47582	47.715	45.409	N/A	8582	N/A	1.132	

Table 4.2, entry 5: 66% ee

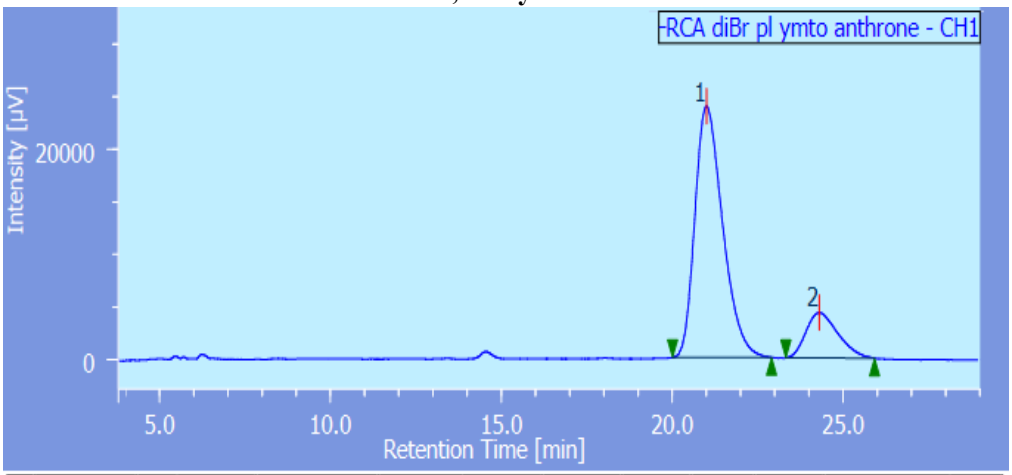

#	ピーク名	CH	tR [min]	面積 [μV·sec]	高さ [μV]	面積%	高さ%	定量値	NTP	分離度	シンメトリー係数	警告
1	Unknown	1	21.000	1352197	23908	82.772	84.733	N/A	3237	2.052	1.346	
2	Unknown	1	24.292	281439	4308	17.228	15.267	N/A	3117	N/A	1.325	

Table 4.2, entry 6: 78% ee

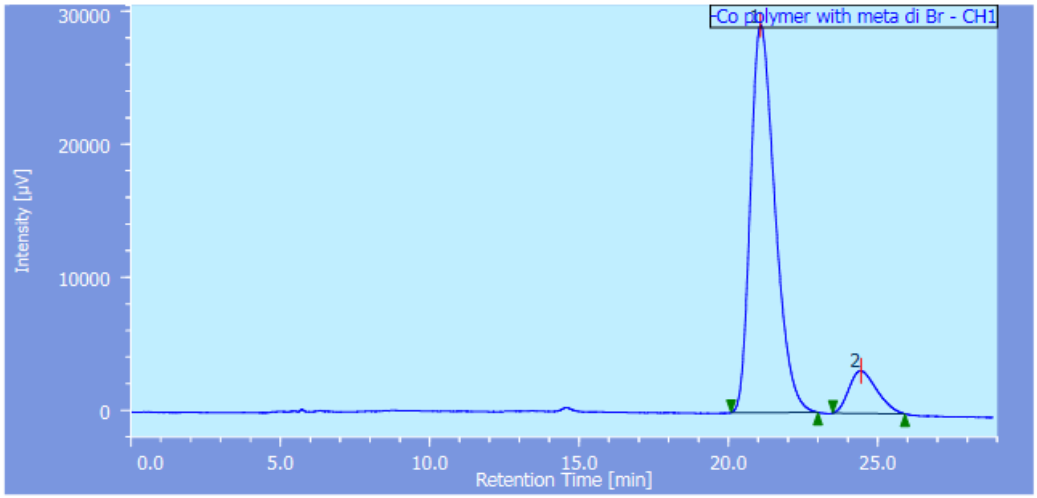

#	ピーク名	CH	tR [min]	面積 [μV·sec]	高さ [μV]	面積%	高さ%	定量値	NTP	分離度	シンメトリー係数	警告
1	Unknown	1	21.075	1663963	29140	88.899	90.095	N/A	3172	2.077	1.355	
2	Unknown	1	24.433	207785	3203	11.101	9.905	N/A	3134	N/A	1.281	

Table 4.2, entry 7: 61% ee

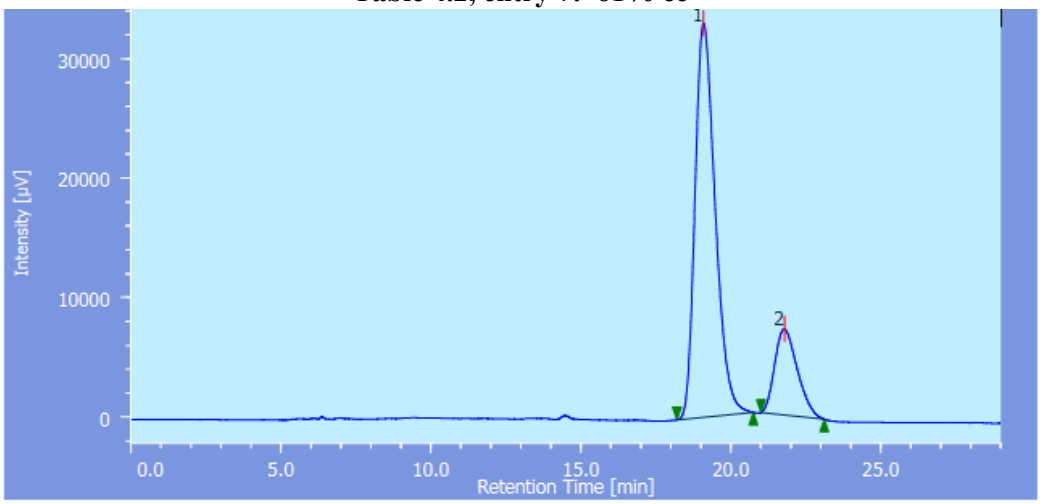

#	ピーク名	CH	tR [min]	面積 [μV·sec]	高さ [μV]	面積%	高さ%	定量値	NTP	分離度	シンメトリー係数	警告
1	Unknown	1	19.083	1540246	32972	80.241	82.067	N/A	3907	2.062	1.329	
2	Unknown	1	21.783	379275	7205	19.759	17.933	N/A	3850	N/A	1.287	

Table 4.2, entry 8: 54% ee

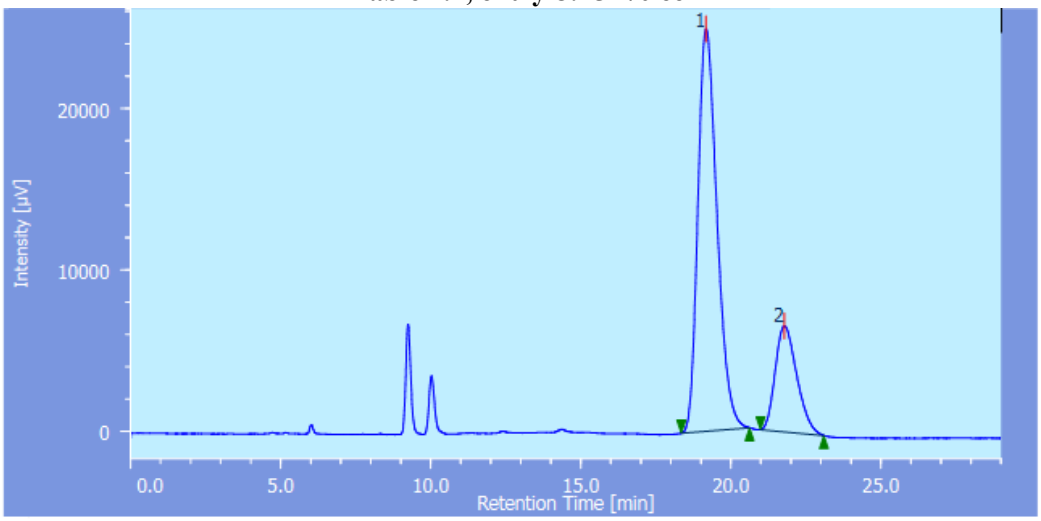

#	ピーク名	CH	tR [min]	面積 [μV·sec]	高さ [μV]	面積%	高さ%	定量値	NTP	分離度	シンメトリー係数	警告
1	Unknown	1	19.167	1104165	24903	77.095	79.152	N/A	4348	2.100	1.300	
2	Unknown	1	21.775	328057	6559	22.905	20.848	N/A	4300	N/A	1.295	

Table 4.2, entry 9: 25% ee

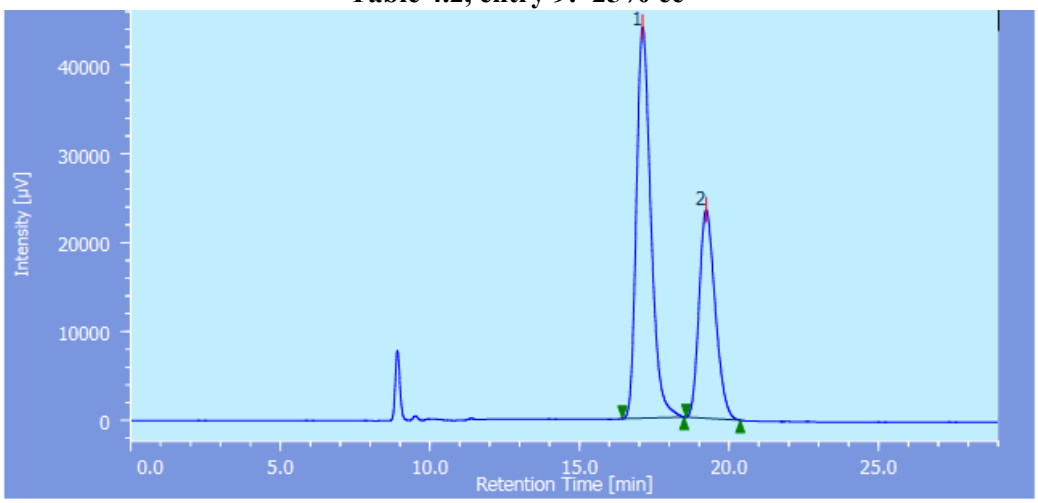

#	ピーク名	CH	tR [min]	面積 [μV·sec]	高さ [μV]	面積%	高さ%	定量値	NTP	分離度	シンメトリー係数	警告
1	Unknown	1	17.108	1473054	43974	62.677	65.209	N/A	6308	2.308	1.313	
2	Unknown	1	19.233	877192	23461	37.323	34.791	N/A	6103	N/A	1.245	

Table 4.2, entry 10: 2% ee

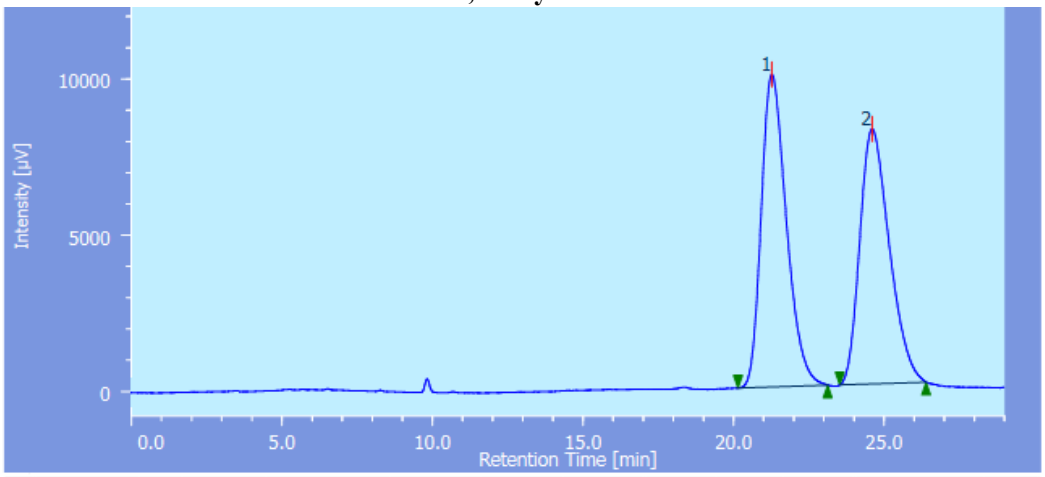

#	ピーク名	CH	tR [min]	面積 [μV·sec]	高さ [μV]	面積%	高さ%	定量値	NTP	分離度	シンメトリー係数	警告
1	Unknown	1	21.267	579425	9995	51.005	55.068	N/A	3153	2.013	1.324	
2	Unknown	1	24.600	556587	8155	48.995	44.932	N/A	2972	N/A	1.322	

Table 4.2, entry 11: 62% ee

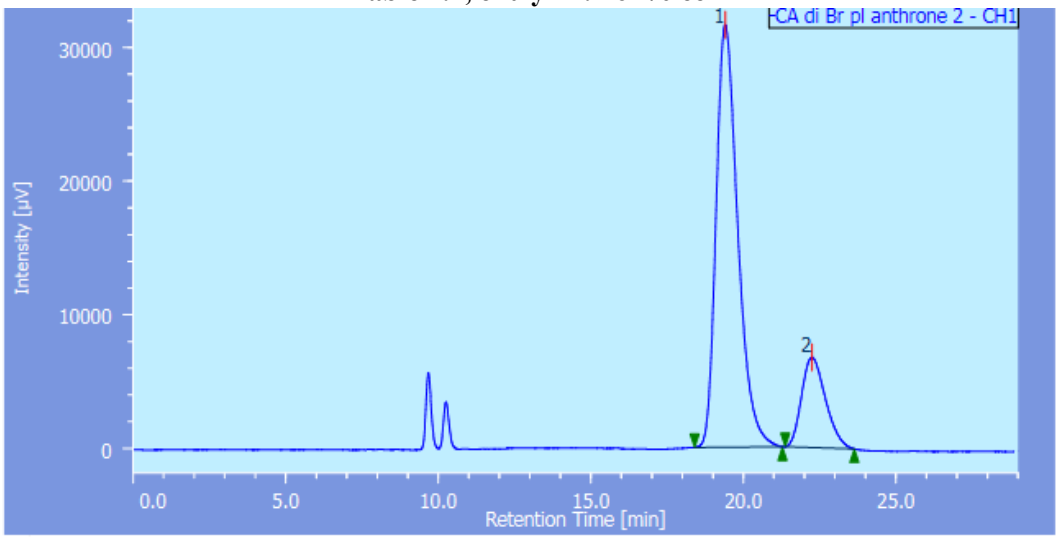

#	ピーク名	CH	tR [min]	面積 [μV·sec]	高さ [μV]	面積%	高さ%	定量値	NTP	分離度	シンメトリー係数	警告
1	Unknown	1	19.400	1561425	31610	80.863	82.391	N/A	3716	2.090	1.366	
2	Unknown	1	22.242	369520	6756	19.137	17.609	N/A	3743	N/A	1.270	

Table 4.2, entry 12: 75%ee

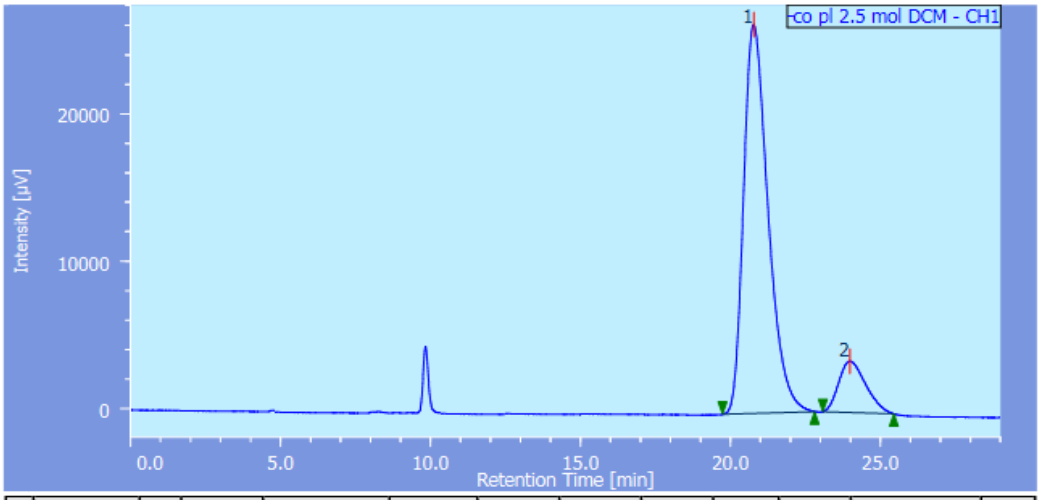

#	ピーク名	CH	tR [min]	面積 [μV·sec]	高さ [μV]	面積%	高さ%	定量値	NTP	分離度	シンメトリー係数	警告
1	Unknown	1	20.767	1499001	26380	87.268	88.343	N/A	3191	2.037	1.404	
2	Unknown	1	23.975	218692	3481	12.732	11.657	N/A	3227	N/A	1.312	

Table 4.2, entry 13: 73% ee

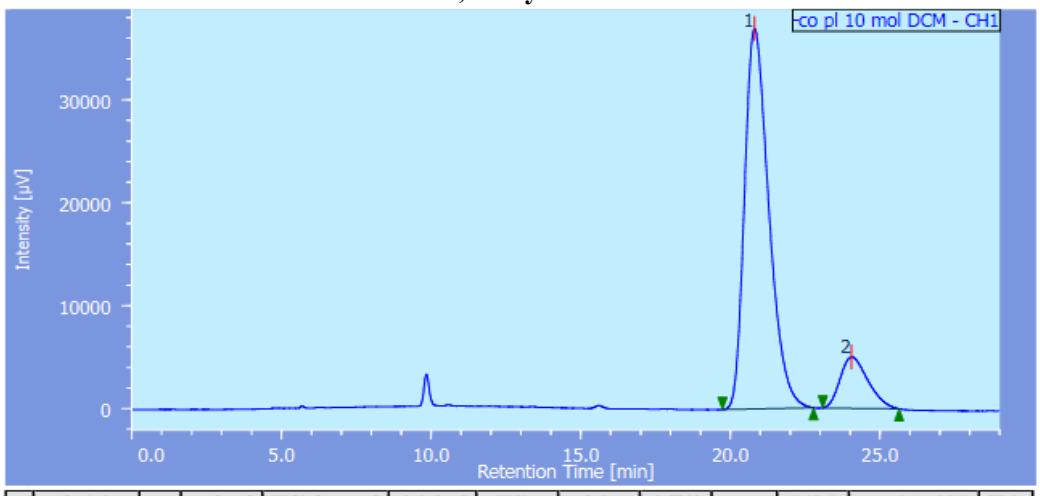

#	ピーク名	CH	tR [min]	面積 [μV·sec]	高さ [μV]	面積%	高さ%	定量値	NTP	分離度	シンメトリー係数	警告
1	Unknown	1	20.800	2085768	36947	86.598	88.102	N/A	3187	2.034	1.379	
2	Unknown	1	24.042	322807	4990	13.402	11.898	N/A	3117	N/A	1.325	

Table 4.2, entry 14: 72% ee

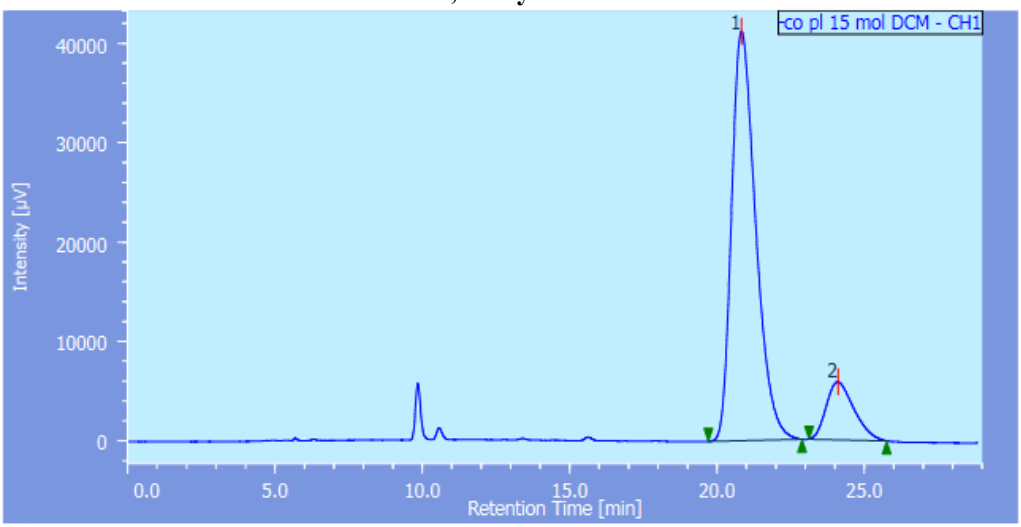

#	ピーク名	CH	tR [min]	面積 [μV·sec]	高さ [μV]	面積%	高さ%	定量値	NTP	分離度	シンメトリー係数	警告
1	Unknown	1	20.825	2344480	41188	86.045	87.621	N/A	3153	2.040	1.386	
2	Unknown	1	24.100	380245	5819	13.955	12.379	N/A	3083	N/A	1.319	

2. Chromatogram data for 18 using P2a in different solvent and temperature (Table 4.3)

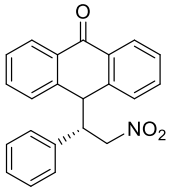

18 (S)

Table 4.3, entry 1: 78% ee

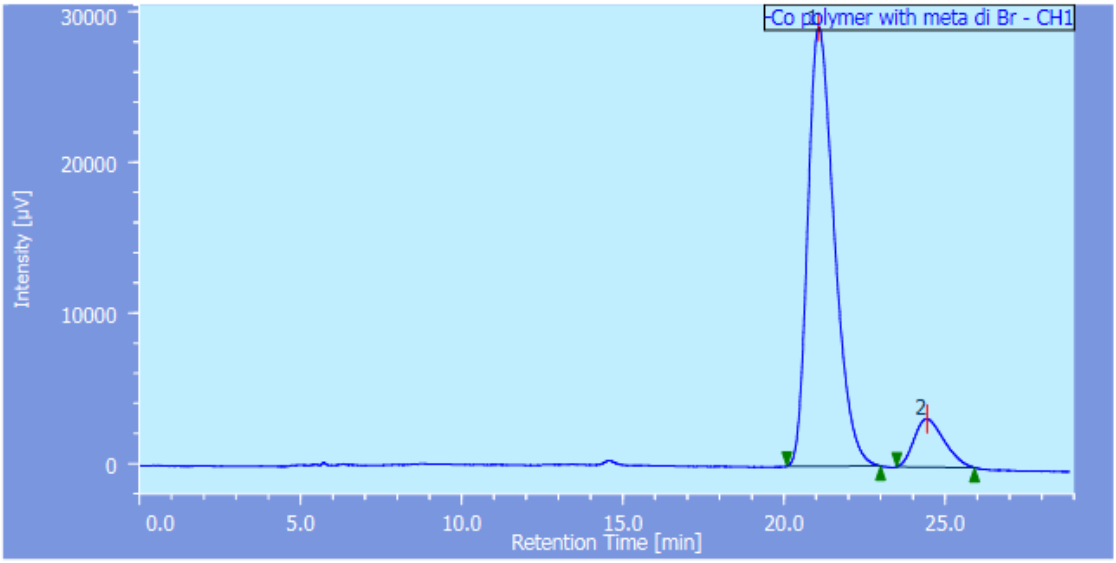

#	ピーク名	CH	tR [min]	面積 [μV·sec]	高さ [μV]	面積%	高さ%	定量値	NTP	分離度	シンメトリー係数	警告
1	Unknown	1	21.075	1663963	29140	88.899	90.095	N/A	3172	2.077	1.355	
2	Unknown	1	24.433	207785	3203	11.101	9.905	N/A	3134	N/A	1.281	

Table 4.3, entry 2: 70% ee

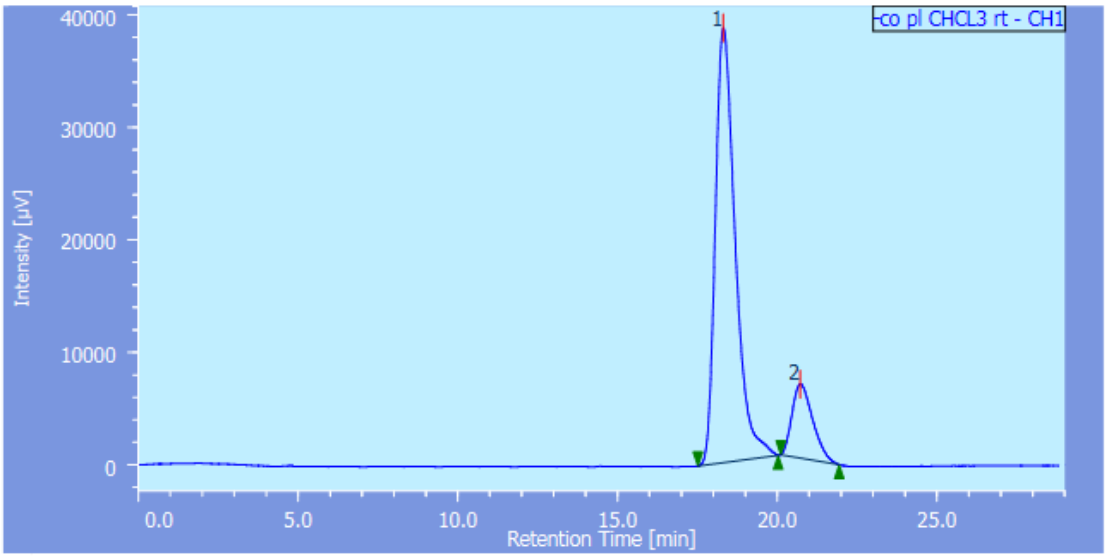

#	ピーク名	CH	tR [min]	面積 [μV·sec]	高さ [μV]	面積%	高さ%	定量値	NTP	分離度	シンメトリー係数	警告
1	Unknown	1	18.308	1670388	38610	84.823	85.452	N/A	4423	2.090	1.473	
2	Unknown	1	20.717	298864	6573	15.177	14.548	N/A	4697	N/A	1.388	

Table 4.3, entry 3: 63% ee

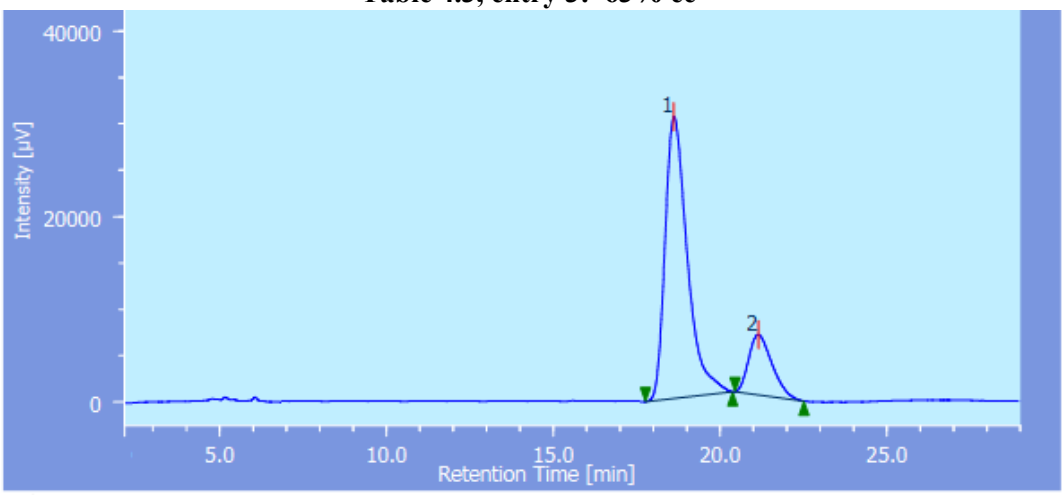

#	ピーク名	CH	tR [min]	面積 [μV·sec]	高さ [μV]	面積%	高さ%	定量値	NTP	分離度	シンメトリー係数	警告
1	Unknown	1	18.608	1409377	30355	81.597	82.355	N/A	4033	2.054	1.590	
2	Unknown	1	21.142	317866	6504	18.403	17.645	N/A	4224	N/A	1.346	

Table 4.3, entry 4: 42% ee

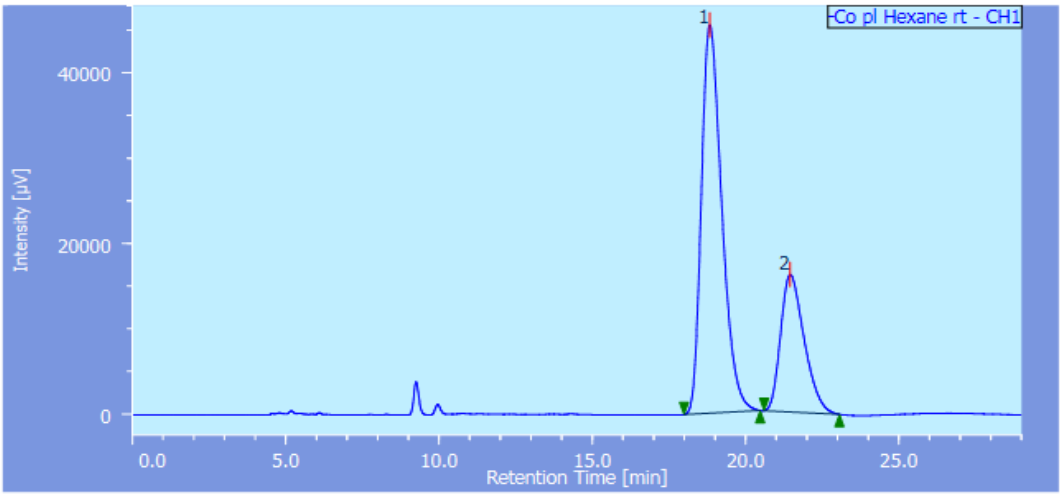

#	ピーク名	CH	tR [min]	面積 [μV·sec]	高さ [μV]	面積%	高さ%	定量値	NTP	分離度	シンメトリー係数	警告
1	Unknown	1	18.825	2112288	45500	71.006	73.843	N/A	3858	2.009	1.380	
2	Unknown	1	21.450	862502	16118	28.994	26.157	N/A	3715	N/A	1.361	

Table 4.3, entry 5: 6% ee

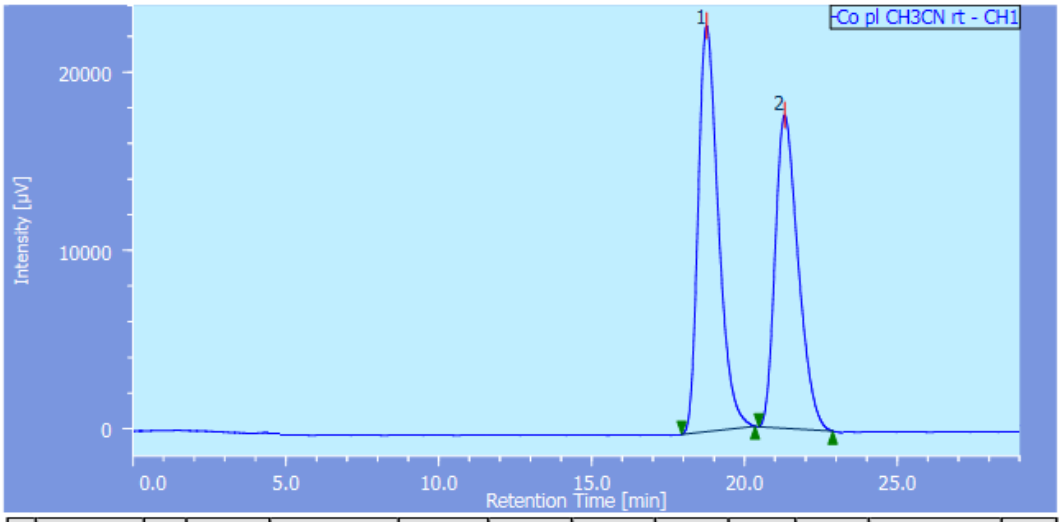

#	ピーク名	CH	tR [min]	面積 [μV·sec]	高さ [μV]	面積%	高さ%	定量値	NTP	分離度	シンメトリー係数	警告
1	Unknown	1	18.758	1046345	22763	53.229	56.462	N/A	3961	1.989	1.375	
2	Unknown	1	21.308	919405	17553	46.771	43.538	N/A	3820	N/A	1.348	

Table 4.3, entry 6: 17% ee

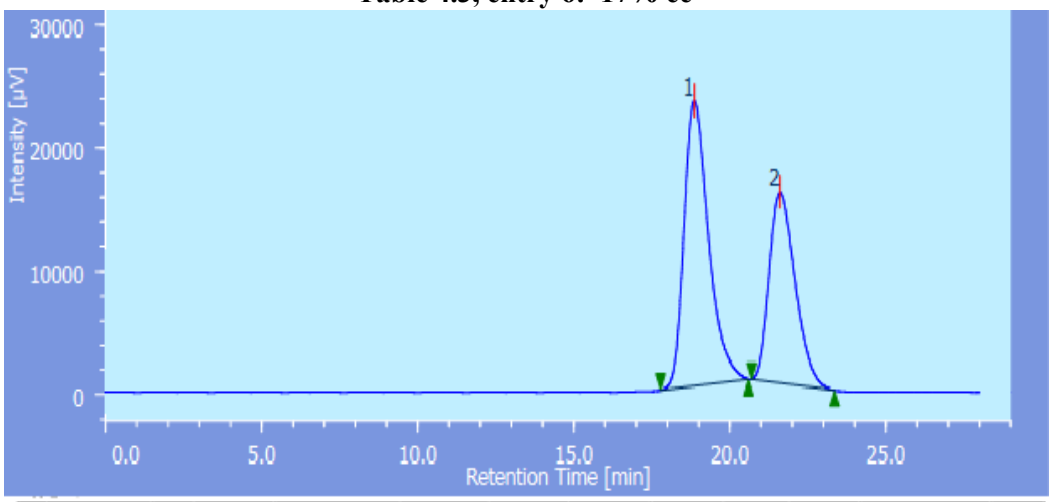

#	ピーク名	CH	tR [min]	面積 [μV·sec]	高さ [μV]	面積%	高さ%	定量値	NTP	分離度	シンメトリー係数	警告
1	Unknown	1	18.858	1268568	23137	58.528	59.911	N/A	2900	1.869	1.398	
2	Unknown	1	21.600	898905	15482	41.472	40.089	N/A	3143	N/A	1.321	

Table 4.3, entry 7: 9% ee

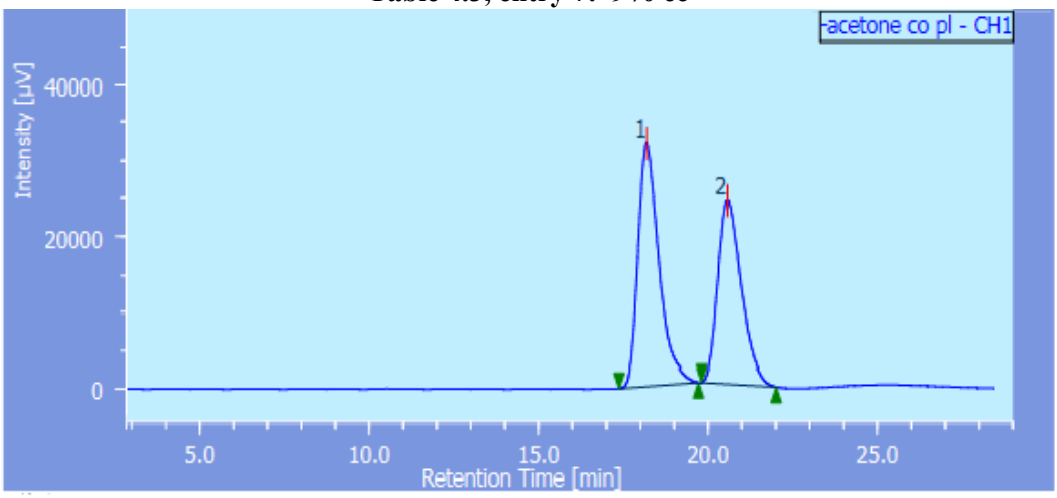

#	ピーク名	CH	tR [min]	面積 [μV·sec]	高さ [μV]	面積%	高さ%	定量値	NTP	分離度	シンメトリー係数	警告
1	Unknown	1	18.183	1403749	31957	54.437	57.039	N/A	4205	1.984	1.468	
2	Unknown	1	20.567	1174929	24069	45.563	42.961	N/A	4084	N/A	1.349	

Table 4.3, entry 8: 17% ee

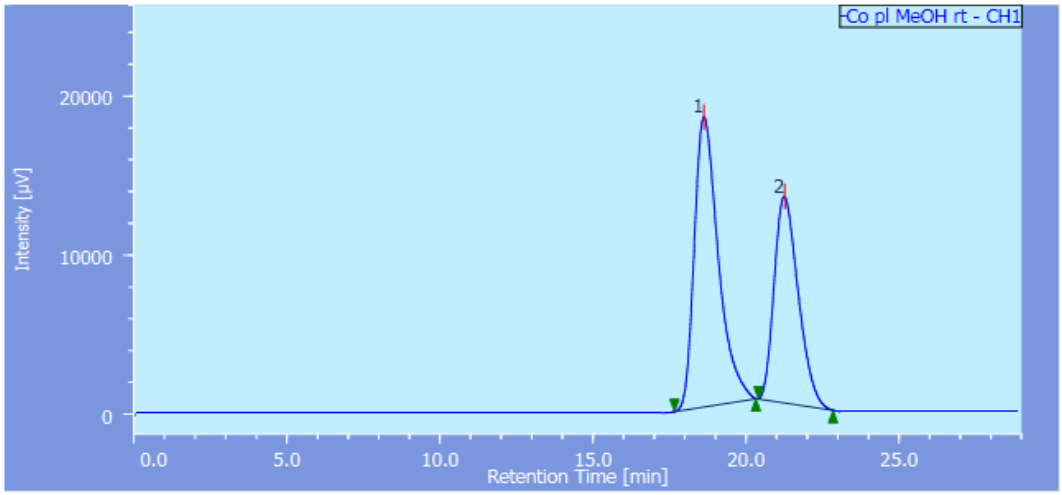

#	ピーク名	CH	tR [min]	面積 [μV·sec]	高さ [μV]	面積%	高さ%	定量値	NTP	分離度	シンメトリー係数	警告
1	Unknown	1	18.617	996983	18224	58.403	58.396	N/A	2857	1.857	1.504	
2	Unknown	1	21.250	710085	12984	41.597	41.604	N/A	3432	N/A	1.301	

Table 4.3, entry 9: 17% ee

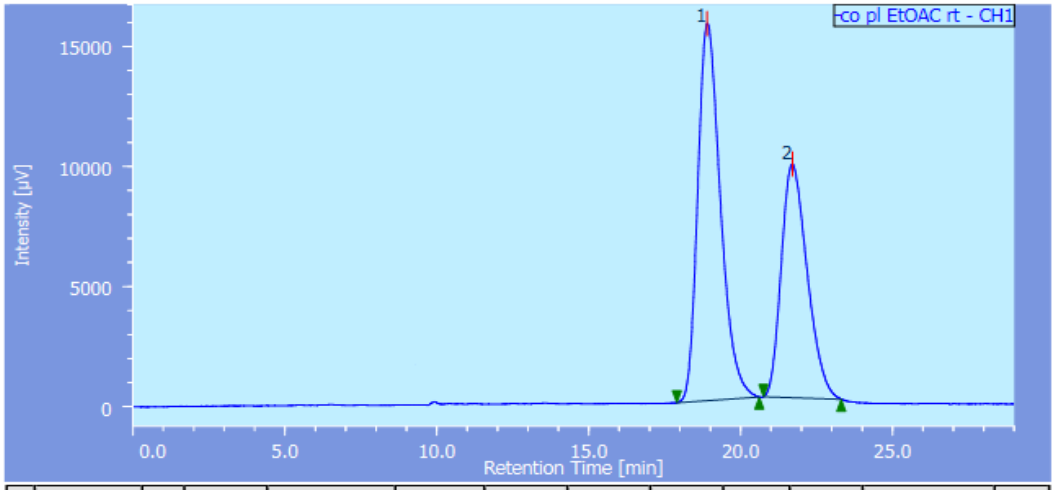

#	ピーク名	CH	tR [min]	面積 [μV·sec]	高さ [μV]	面積%	高さ%	定量値	NTP	分離度	シンメトリー係数	警告
1	Unknown	1	18.892	816548	15697	58.623	61.740	N/A	3133	1.927	1.356	
2	Unknown	1	21.700	576327	9728	41.377	38.260	N/A	3050	N/A	1.288	

Table 4.3, entry 10: 57% ee

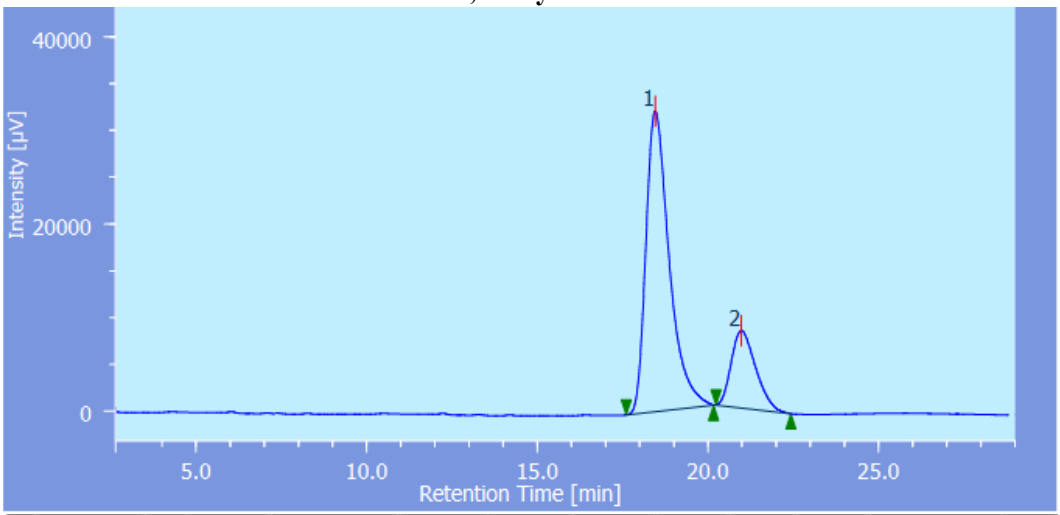

#	ピーク名	CH	tR [min]	面積 [μV·sec]	高さ [μV]	面積%	高さ%	定量値	NTP	分離度	シンメトリー係数	警告
1	Unknown	1	18.450	1526204	32092	78.720	79.555	N/A	3779	2.002	1.542	
2	Unknown	1	20.975	412568	8247	21.280	20.445	N/A	3984	N/A	1.325	

Table 4.3, entry 11: 72% ee

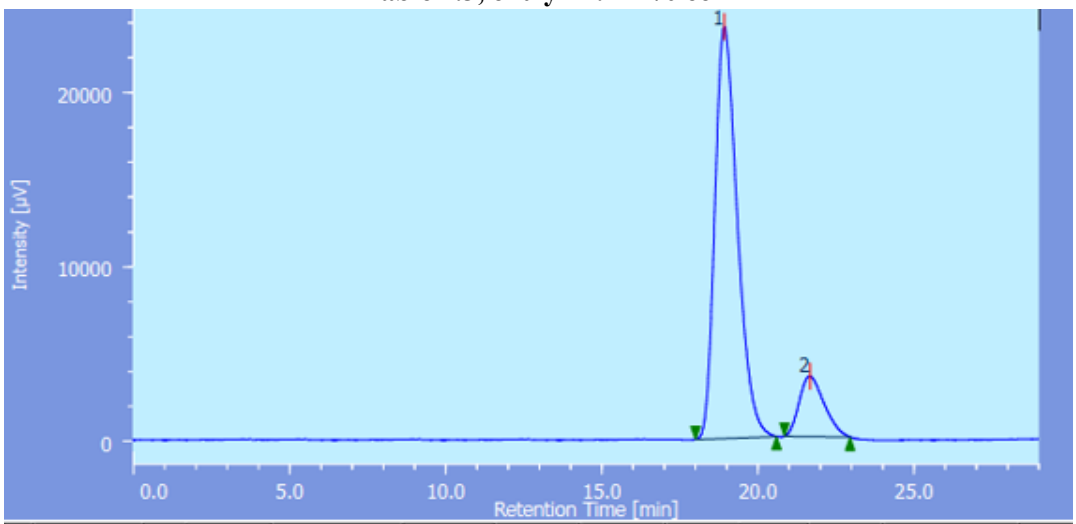

#	ピーク名	CH	tR [min]	面積 [μV·sec]	高さ [μV]	面積%	高さ%	定量値	NTP	分離度	シンメトリー係数	警告
1	Unknown	1	18.917	1180234	23596	85.966	87.219	N/A	3342	1.966	1.343	
2	Unknown	1	21.667	192672	3458	14.034	12.781	N/A	3356	N/A	1.271	

Table 4.3, entry 12: 82% ee

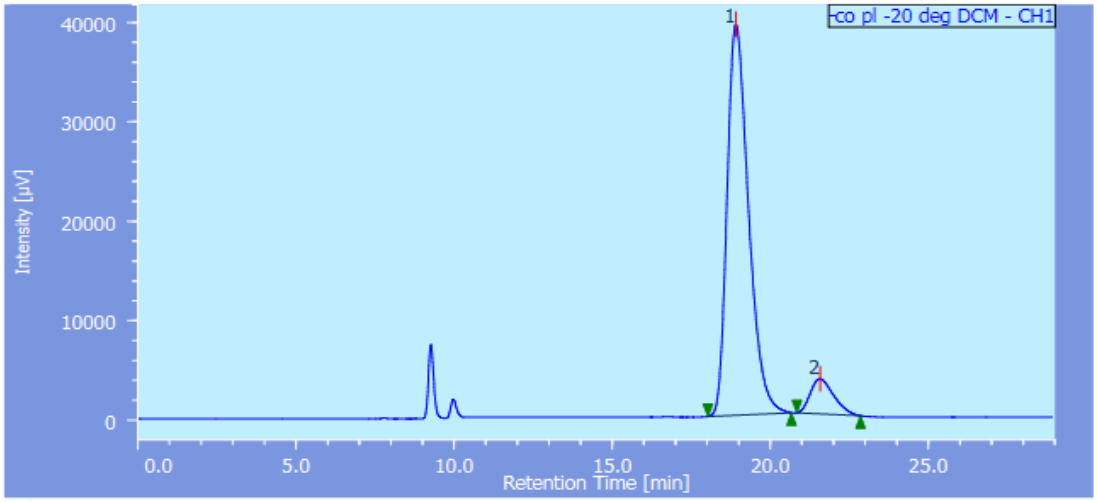

#	ピーク名	CH	tR [min]	面積 [μV·sec]	高さ [μV]	面積%	高さ%	定量値	NTP	分離度	シンメトリー係数	警告
1	Unknown	1	18.908	1852918	39301	91.069	91.750	N/A	3814	2.060	1.383	
2	Unknown	1	21.575	181724	3534	8.931	8.250	N/A	3961	N/A	1.323	

Table 4.3, entry 13: 84% ee

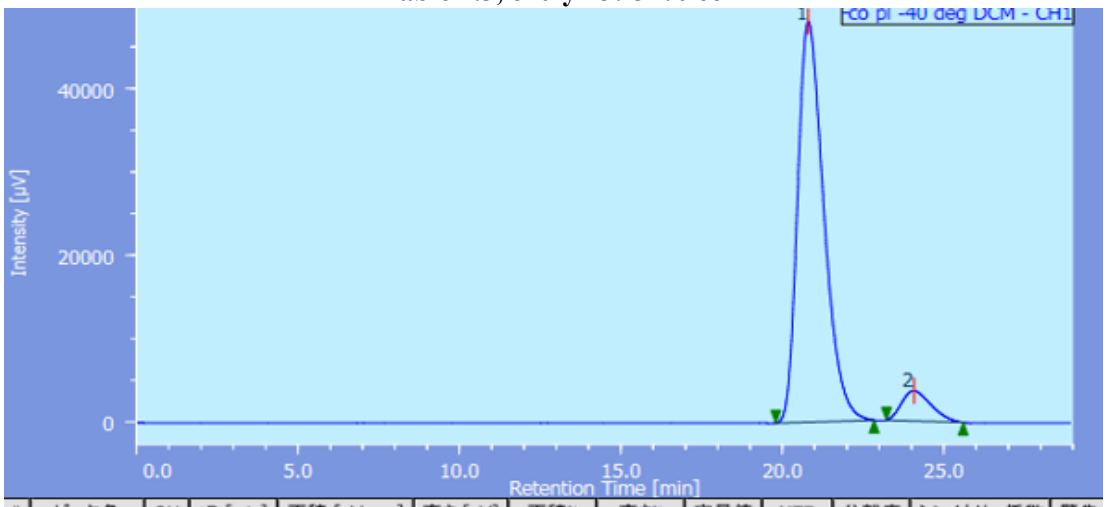

#	ピーク名	CH	tR [min]	面積 [μV·sec]	高さ [μV]	面積%	高さ%	定量値	NTP	分離度	シンメトリー係数	警告
1	Unknown	1	20.800	2719452	48057	92.195	92.963	N/A	3170	2.061	1.388	
2	Unknown	1	24.075	230229	3638	7.805	7.037	N/A	3176	N/A	1.325	

3. Chromatogram data for substrate scope evaluation of P2a (Table 4.4)

Table 4.4, entry 1: 82% ee

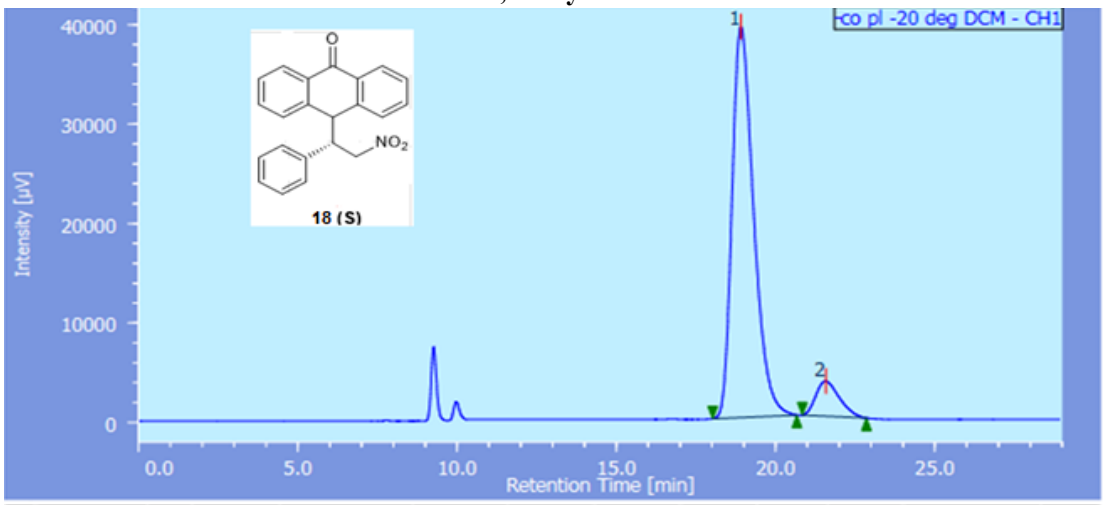

#	ピーク名	CH	tR [min]	面積 [μV·sec]	高さ [μV]	面積%	高さ%	定量値	NTP	分離度	シンメトリー係数	警告
1	Unknown	1	18.908	1852918	39301	91.069	91.750	N/A	3814	2.060	1.383	
2	Unknown	1	21.575	181724	3534	8.931	8.250	N/A	3961	N/A	1.323	

Table 4.4, entry 2: 93% ee

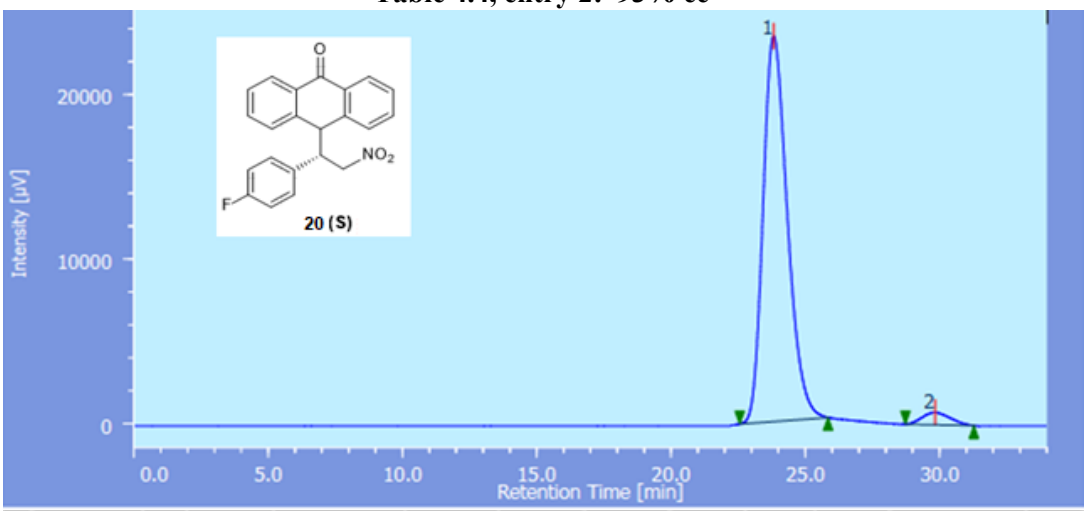

#	ピーク名	CH	tR [min]	面積 [μV·sec]	高さ [μV]	面積%	高さ%	定量値	NTP	分離度	シンメトリー係数	警告
1	Unknown	1	23.817	1471021	23425	96.418	96.890	N/A	3359	3.308	1.280	
2	Unknown	1	29.825	54657	752	3.582	3.110	N/A	3561	N/A	1.173	

Table 4.4, entry 3: 84% ee

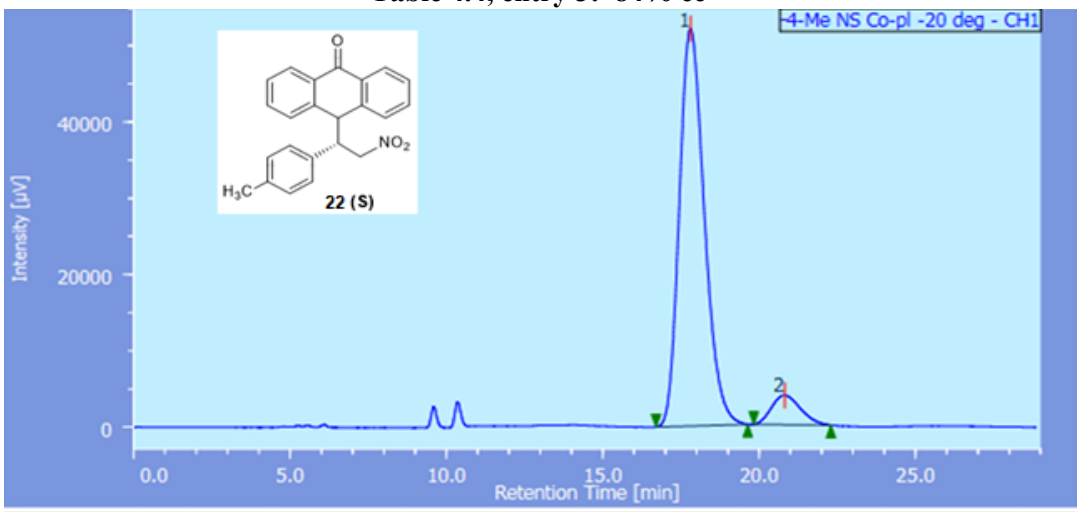

#	ピーク名	CH	tR [min]	面積 [μV·sec]	高さ [μV]	面積%	高さ%	定量値	NTP	分離度	シンメトリー係数	警告
1	Unknown	1	17.800	2893886	52090	92.095	93.112	N/A	2388	1.896	1.240	
2	Unknown	1	20.817	248381	3853	7.905	6.888	N/A	2306	N/A	1.208	

Table 4.4, entry 4: 55% ee

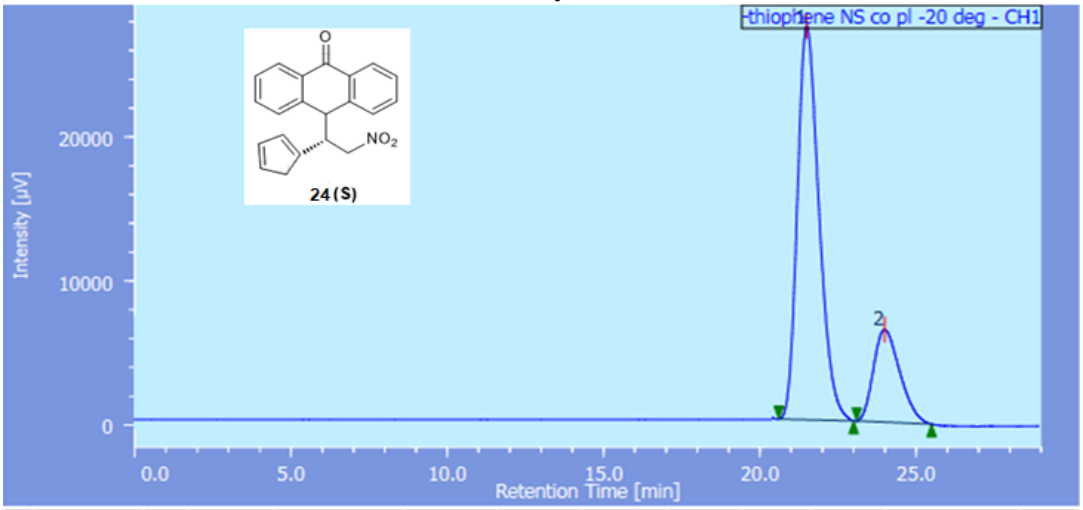

#	ピーク名	CH	tR [min]	面積 [μV·sec]	高さ [μV]	面積%	高さ%	定量値	NTP	分離度	シンメトリー係数	警告
1	Unknown	1	21.492	1313841	27358	77.672	80.990	N/A	4669	1.765	1.280	
2	Unknown	1	23.983	377676	6422	22.328	19.010	N/A	3721	N/A	1.308	

4. Chromatogram data for 18 in recyclability evaluation of P2a (Table 4.5)

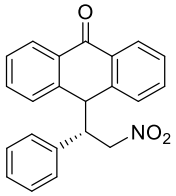

18 (S)

Table 4.5, fresh polymer: 82% ee

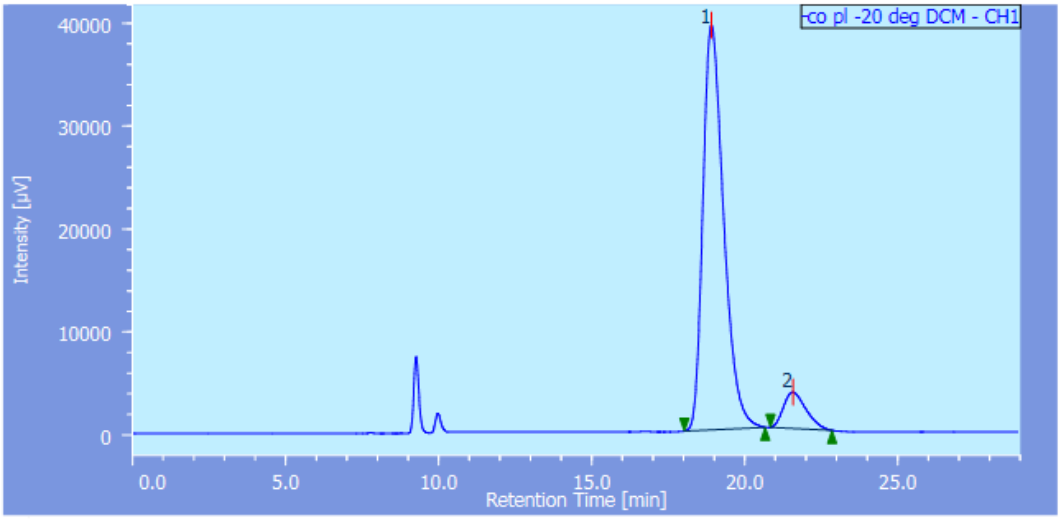

#	ピーク名	CH	tR [min]	面積 [μV·sec]	高さ [μV]	面積%	高さ%	定量値	NTP	分離度	シンメトリー係数	警告
1	Unknown	1	18.908	1852918	39301	91.069	91.750	N/A	3814	2.060	1.383	
2	Unknown	1	21.575	181724	3534	8.931	8.250	N/A	3961	N/A	1.323	

Table 4.5, cycle 1: 84% ee

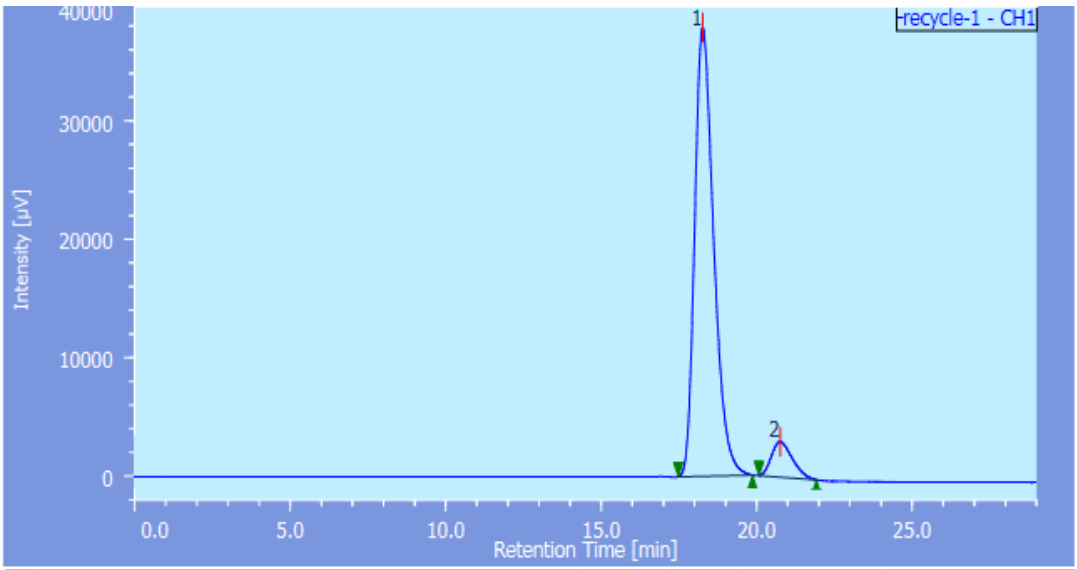

#	ピーク名	CH	tR [min]	面積 [μV·sec]	高さ [μV]	面積%	高さ%	定量値	NTP	分離度	シンメトリー係数	警告
1	Unknown	1	18.258	1612890	37899	92.003	92.684	N/A	4371	2.117	1.350	
2	Unknown	1	20.750	140202	2992	7.997	7.316	N/A	4367	N/A	1.311	

Table 4.5, cycle 2: 83% ee

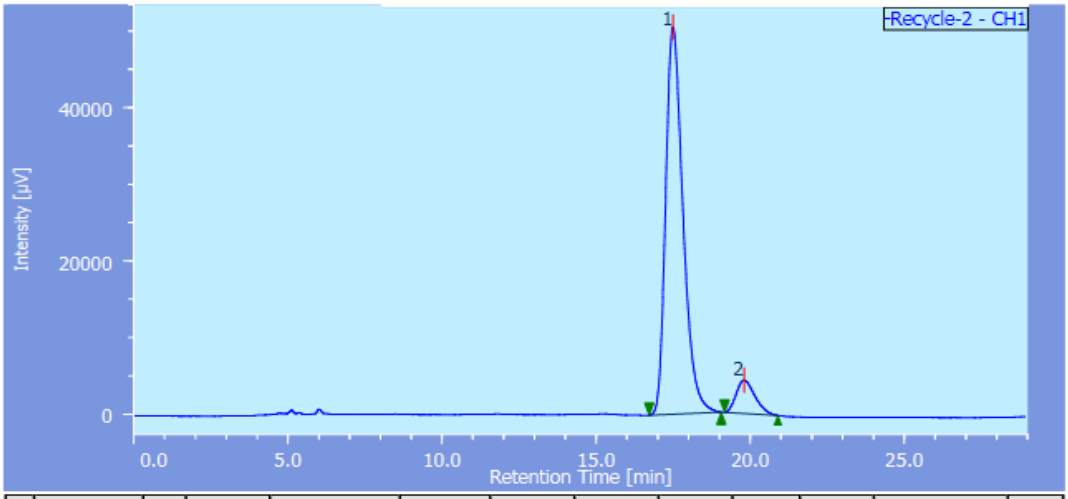

#	ピーク名	CH	tR [min]	面積 [μV·sec]	高さ [μV]	面積%	高さ%	定量値	NTP	分離度	シンメトリー係数	警告
1	Unknown	1	17.492	1976352	50507	91.472	92.081	N/A	4810	2.169	1.351	
2	Unknown	1	19.800	184259	4344	8.528	7.919	N/A	4956	N/A	1.298	

Table 4.5, cycle 3: 84% ee

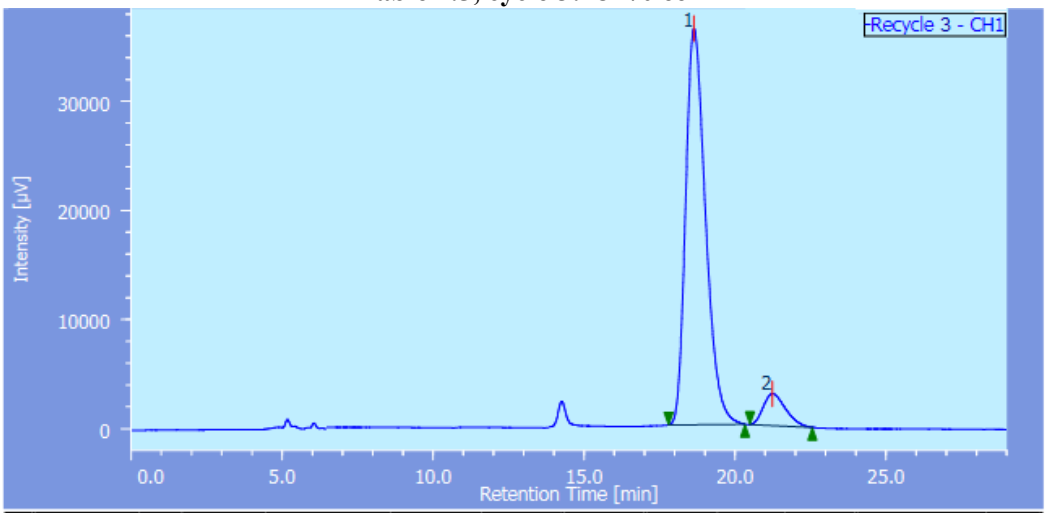

#	ピーク名	CH	tR [min]	面積 [μV·sec]	高さ [μV]	面積%	高さ%	定量値	NTP	分離度	シンメトリー係数	警告
1	Unknown	1	18.633	1665471	36302	91.757	92.585	N/A	3893	2.020	1.350	
2	Unknown	1	21.225	149620	2907	8.243	7.415	N/A	3795	N/A	1.347	

Table 4.5, cycle 4: 82% ee

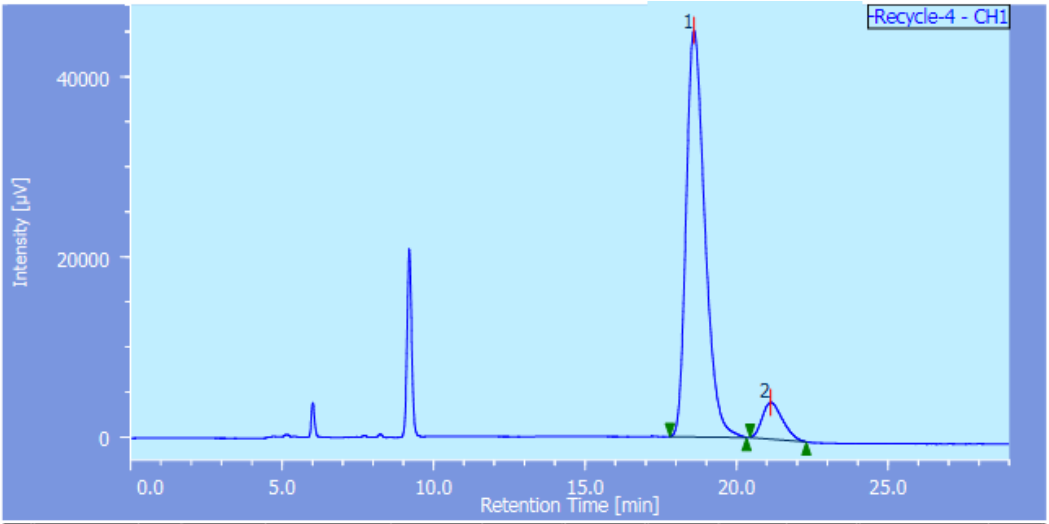

#	ピーク名	CH	tR [min]	面積 [μV·sec]	高さ [μV]	面積%	高さ%	定量値	NTP	分離度	シンメトリー係数	警告
1	Unknown	1	18.592	1930321	45097	91.006	91.724	N/A	4479	2.138	1.341	
2	Unknown	1	21.117	190764	4069	8.994	8.276	N/A	4514	N/A	1.329	

5. Chromatogram data for Table 4.6

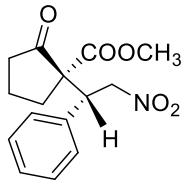

26 (S,R)

Table 4.6, entry 1: 99% ee

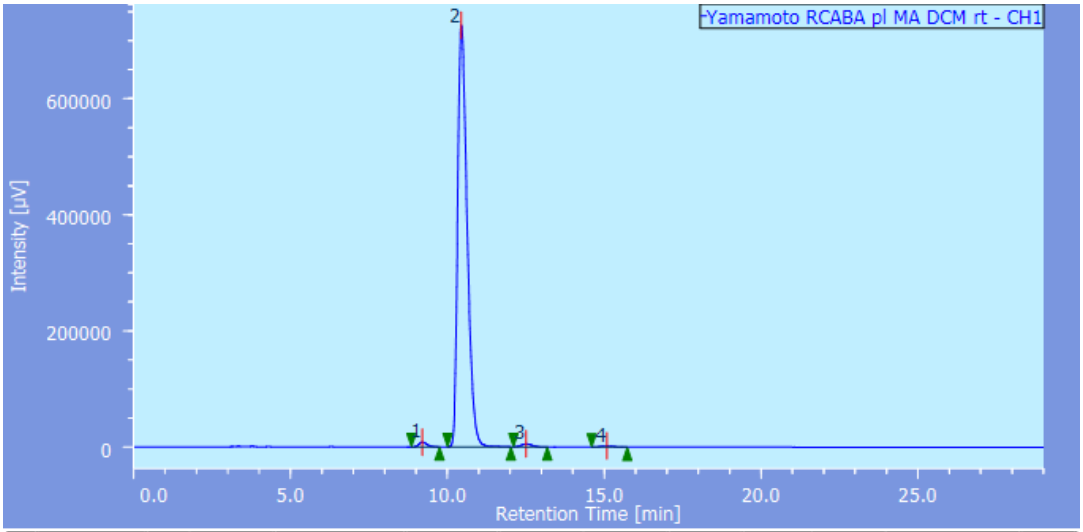

#	ピーク名	CH	tR [min]	面積 [μV·sec]	高さ [μV]	面積%	高さ%	定量値	NTP	分離度	シンメトリー係数	警告
1	Unknown	1	9.200	148472	8140	0.951	1.098	N/A	5914	2.419	1.282	
2	Unknown	1	10.442	15284558	725786	97.928	97.934	N/A	5748	3.567	1.458	
3	Unknown	1	12.508	118349	5129	0.758	0.692	N/A	6705	3.817	1.153	
4	Unknown	1	15.083	56650	2045	0.363	0.276	N/A	6617	N/A	1.121	

Table 4.6, entry 2: 72% ee

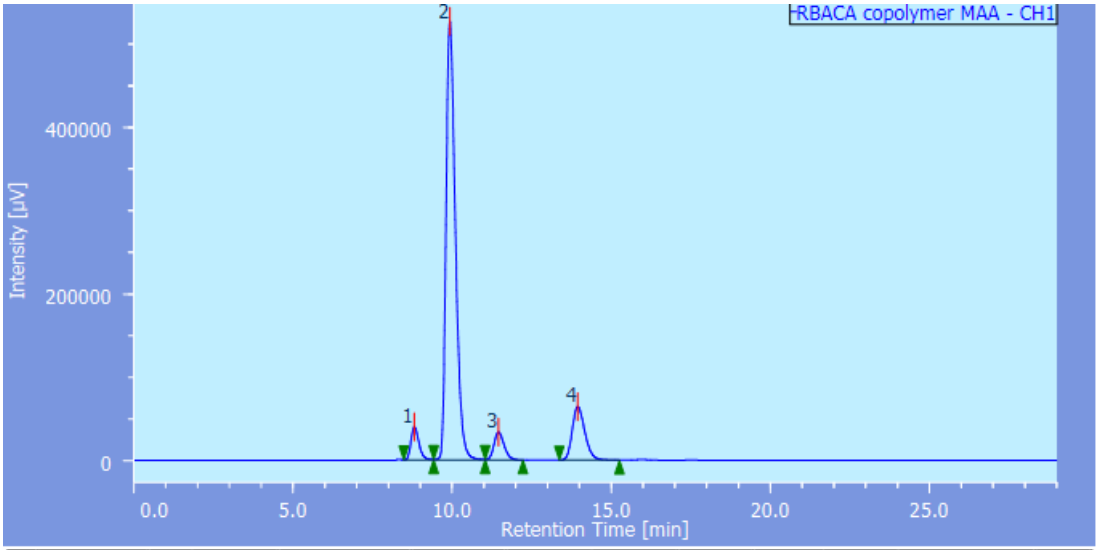

#	ピーク名	CH	tR [min]	面積 [μV·sec]	高さ [μV]	面積%	高さ%	定量値	NTP	分離度	シンメトリー係数	警告
1	Unknown	1	8.808	691530	39554	4.963	5.964	N/A	6124	2.287	1.340	
2	Unknown	1	9.925	10722422	526126	76.957	79.333	N/A	5638	2.753	1.396	
3	Unknown	1	11.450	744471	33355	5.343	5.030	N/A	6188	3.832	1.215	
4	Unknown	1	13.942	1774636	64151	12.737	9.673	N/A	5971	N/A	1.255	

Table 4.6, entry 3: 98% ee

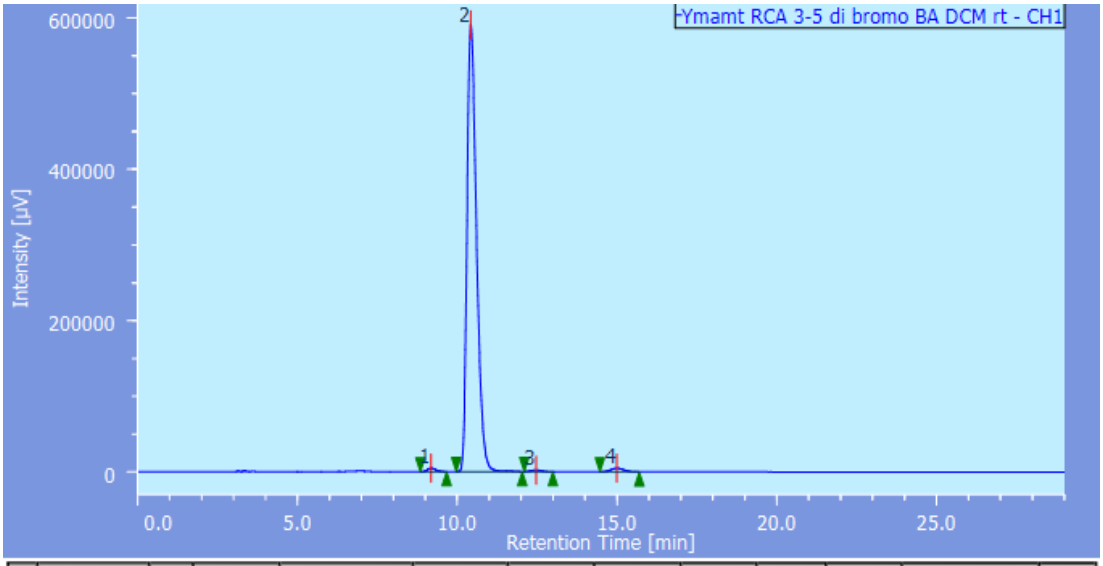

#	ピーク名	CH	tR [min]	面積 [μV·sec]	高さ [μV]	面積%	高さ%	定量値	NTP	分離度	シンメトリー係数	警告
1	Unknown	1	9.183	86463	4846	0.694	0.805	N/A	6154	2.471	1.219	
2	Unknown	1	10.425	12192491	589969	97.798	98.009	N/A	5975	3.612	1.386	
3	Unknown	1	12.467	46910	2115	0.376	0.351	N/A	7045	3.786	1.096	
4	Unknown	1	14.992	141157	5024	1.132	0.835	N/A	6509	N/A	1.148	

Table 4.6, entry 4: 98% ee

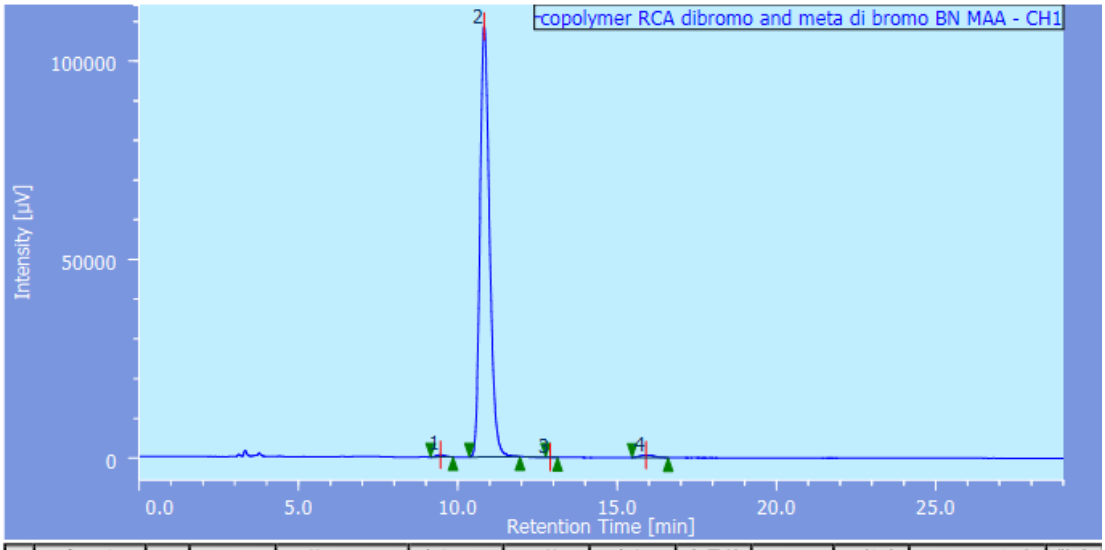

#	ピーク名	CH	tR [min]	面積 [μV·sec]	高さ [μV]	面積%	高さ%	定量値	NTP	分離度	シンメトリー係数	警告
1	Unknown	1	9.450	9874	552	0.431	0.503	N/A	6374	2.717	1.189	
2	Unknown	1	10.825	2261132	108392	98.693	98.880	N/A	6398	4.143	1.248	
3	Unknown	1	12.900	223	18	0.010	0.017	N/A	12421	4.826	1.222	
4	Unknown	1	15.900	19839	658	0.866	0.600	N/A	6589	N/A	1.228	

Table 4.6, entry 5: 98% ee

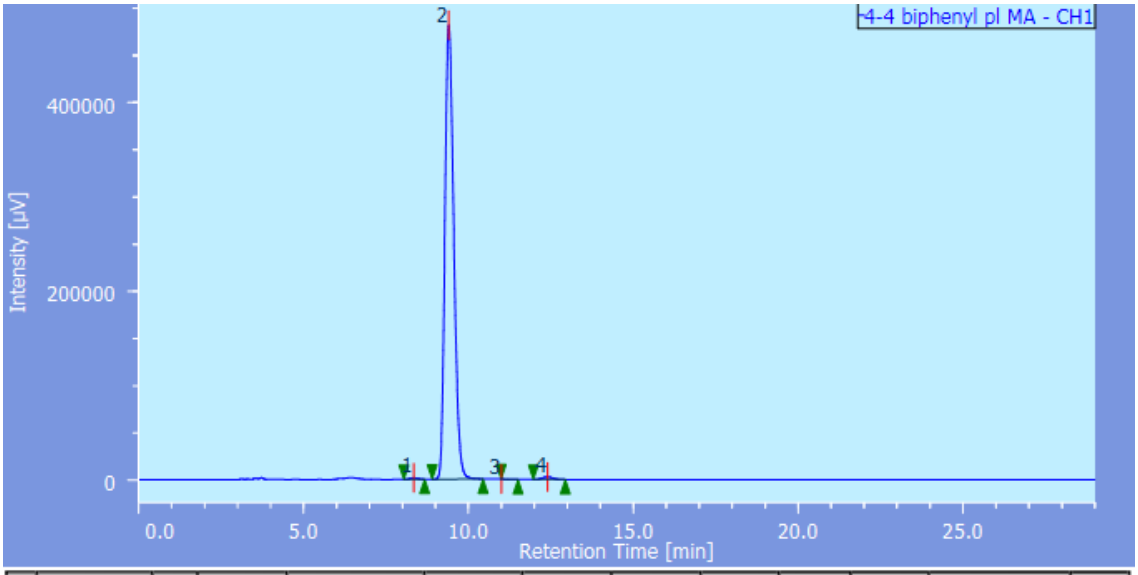

#	ピーク名	CH	tR [min]	面積 [μV·sec]	高さ [μV]	面積%	高さ%	定量値	NTP	分離度	シンメトリー係数	警告
1	Unknown	1	8.342	27013	1641	0.298	0.338	N/A	5704	2.269	1.083	
2	Unknown	1	9.400	8978290	480476	98.956	99.072	N/A	5801	N/A	1.254	
3	Unknown	1	11.000	2	3	0.000	0.001	N/A	N/A	N/A	N/A	
4	Unknown	1	12.392	67715	2856	0.746	0.589	N/A	6061	N/A	1.099	

Table 4.6, entry 6: 48% ee

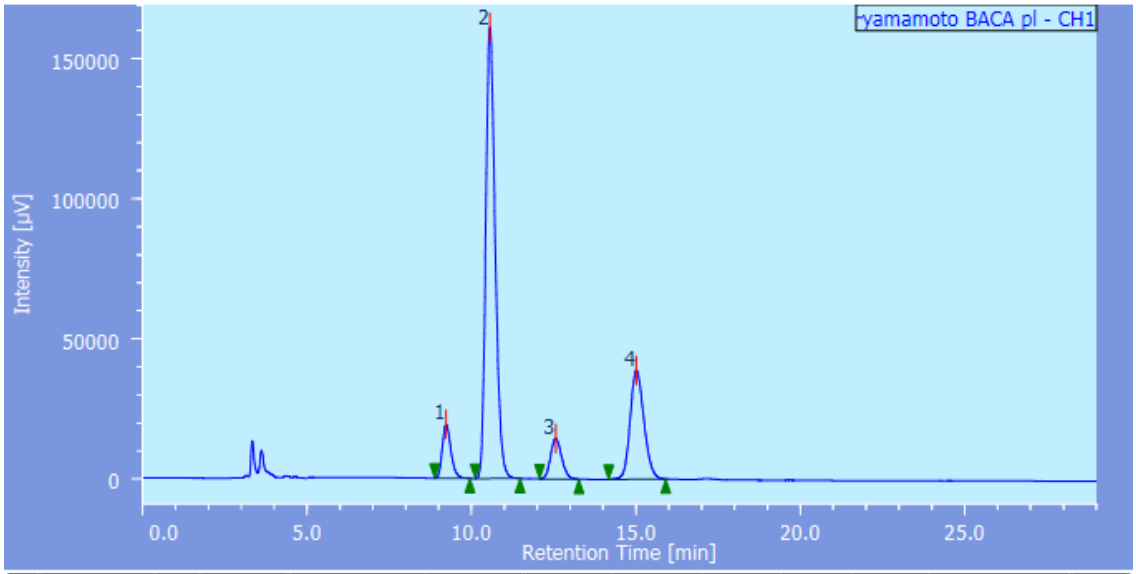

#	ピーク名	CH	tR [min]	面積 [μV·sec]	高さ [μV]	面積%	高さ%	定量値	NTP	分離度	シンメトリー係数	警告
1	Unknown	1	9.225	352923	19291	7.021	8.267	N/A	6074	2.691	1.265	
2	Unknown	1	10.558	3202126	160815	63.699	68.913	N/A	6596	3.521	1.234	
3	Unknown	1	12.558	340312	14451	6.770	6.193	N/A	6581	3.554	1.152	
4	Unknown	1	15.008	1131571	38801	22.510	16.627	N/A	6188	N/A	1.170	

Table 4.6, entry 7: 99% ee

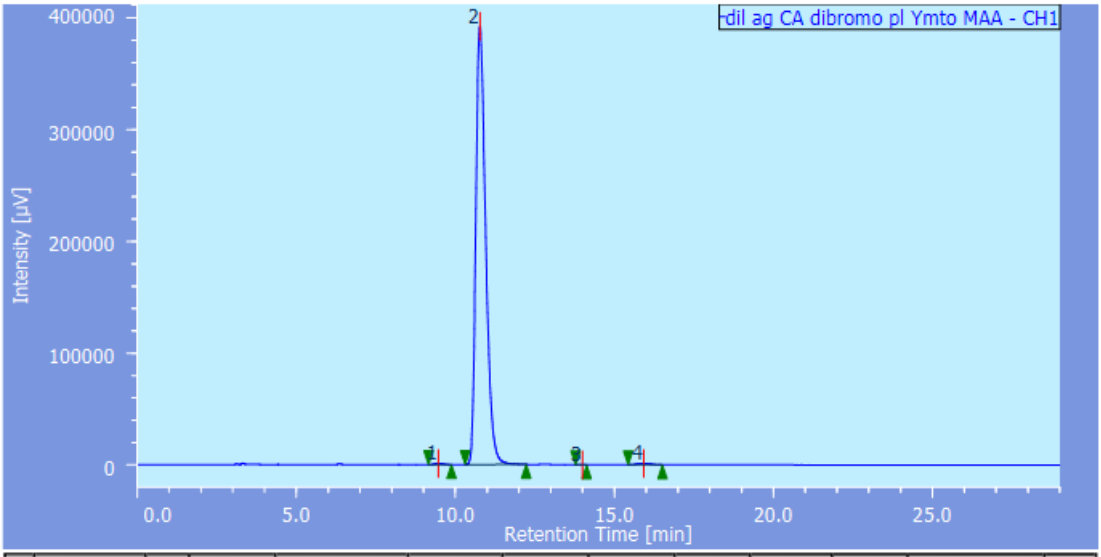

#	ピーク名	CH	tR [min]	面積 [μV·sec]	高さ [μV]	面積%	高さ%	定量値	NTP	分離度	シンメトリー係数	警告
1	Unknown	1	9.458	20882	1106	0.246	0.281	N/A	5614	2.467	1.236	
2	Unknown	1	10.767	8434270	391919	99.277	99.371	N/A	5943	5.960	1.378	
3	Unknown	1	13.992	26	11	0.000	0.003	N/A	11302	2.904	0.805	
4	Unknown	1	15.917	40526	1363	0.477	0.346	N/A	6286	N/A	1.104	

Table 4.6, entry 8: 78% ee

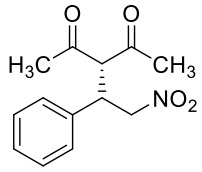

28 (S)

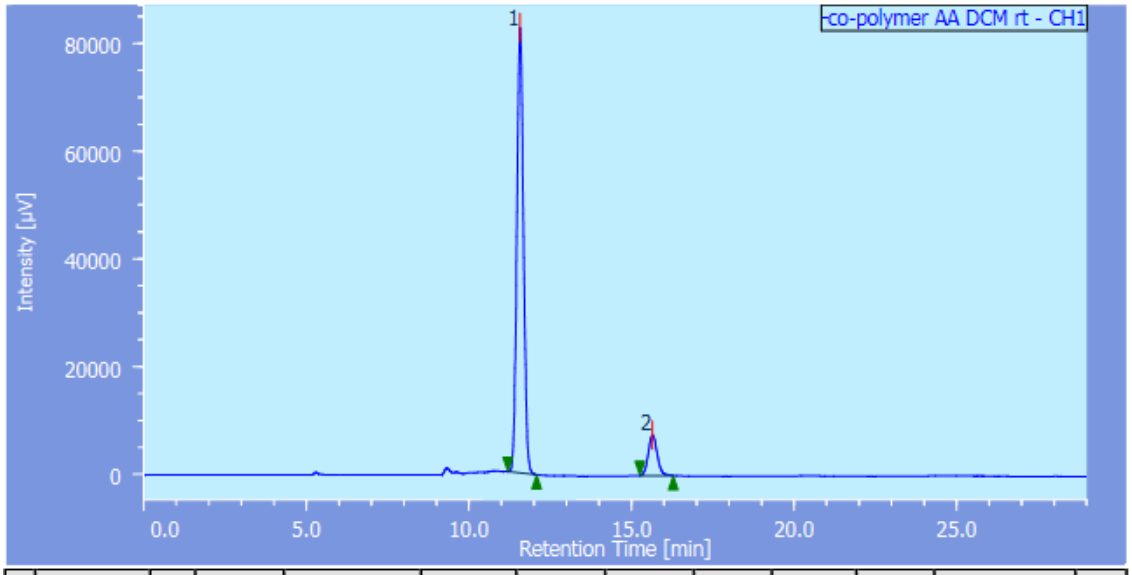

#	ピーク名	CH	tR [min]	面積 [μV·sec]	高さ [μV]	面積%	高さ%	定量値	NTP	分離度	シンメトリー係数	警告
1	Unknown	1	11.567	1137838	81572	88.784	91.566	N/A	15845	9.431	1.090	
2	Unknown	1	15.642	143745	7513	11.216	8.434	N/A	15727	N/A	1.112	

Table 4.6, entry 9: 65% ee[[

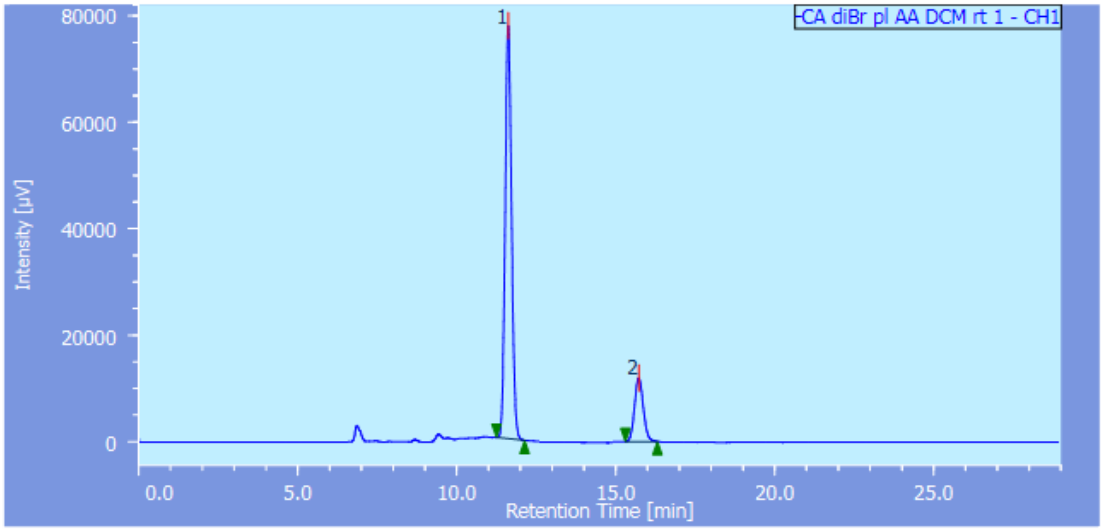

#	ピーク名	CH	tR [min]	面積 [μV·sec]	高さ [μV]	面積%	高さ%	定量値	NTP	分離度	シンメトリー係数	警告
1	Unknown	1	11.617	1086664	77548	82.549	86.641	N/A	15911	9.437	1.085	
2	Unknown	1	15.717	229716	11957	17.451	13.359	N/A	15629	N/A	1.112	

6. Chromatogram data for Table 4.7

Table 4.7, entry 1: 39% ee

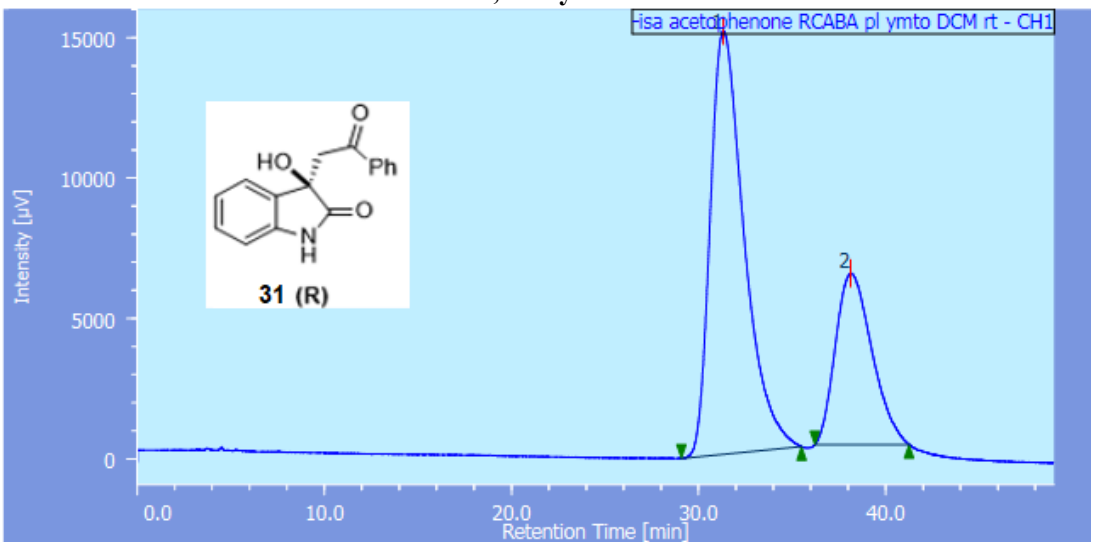

Table 4.7, entry 2: racemic

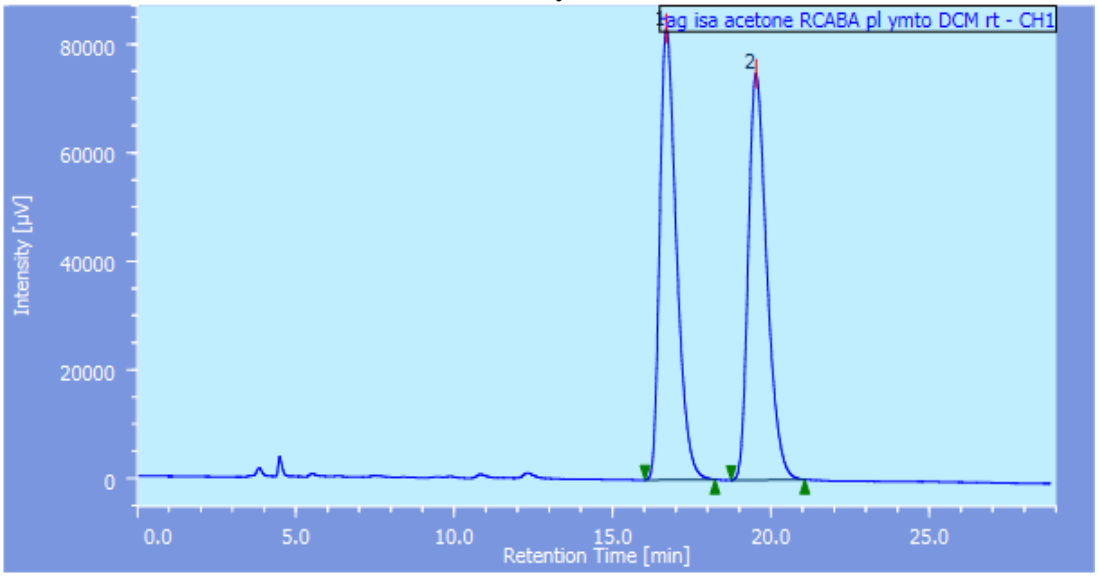

Table 4.7, entry 3: 5% ee

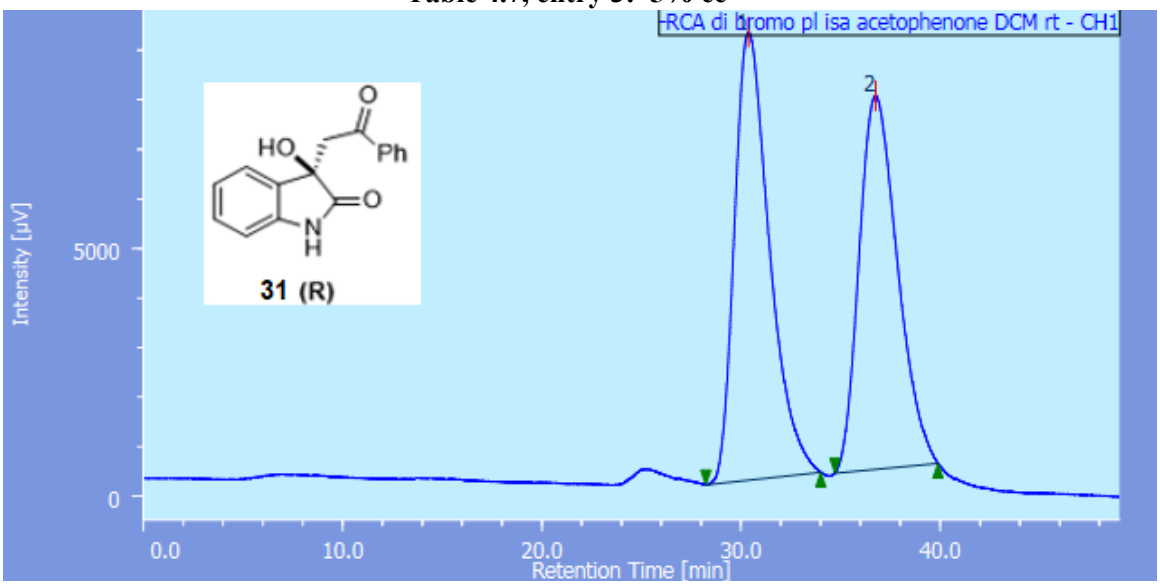

Table 4.7, entry 4: 23% ee

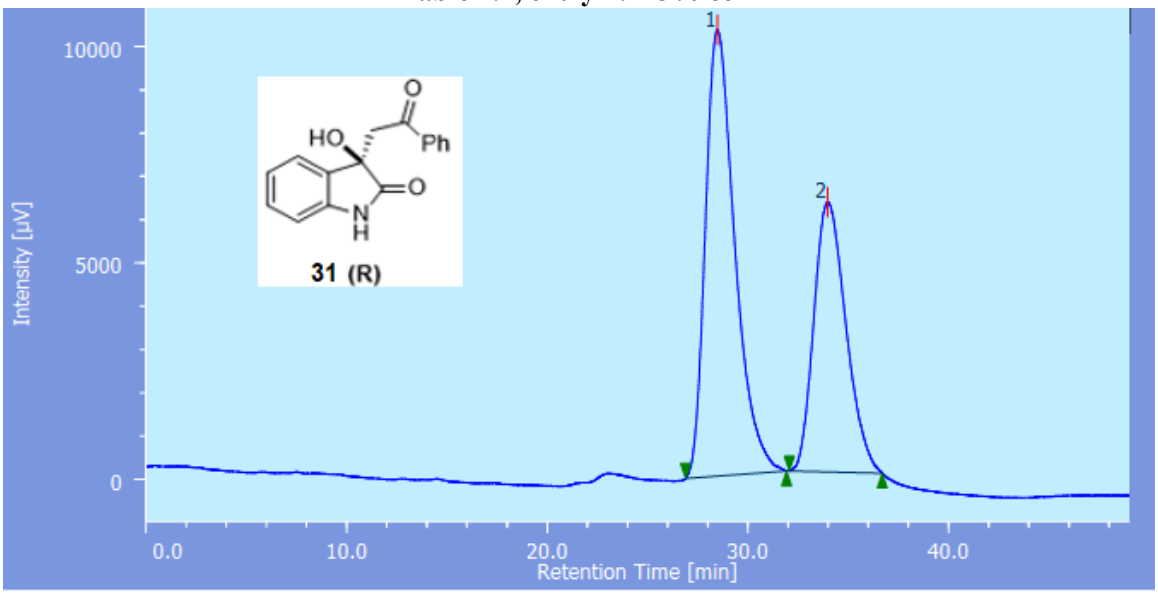

Table 4.7, entry 6: 6 % ee